Maternal Immune Activation: exploring the interaction of IL-6 and 22q11.2DS in an hiPSC model of neurodevelopment.

Couch, Amalie

Awarding institution:
King's College London

Maternal Immune Activation: exploring the interaction of IL-6 and 22q11.2DS in an hiPSC model of neurodevelopment

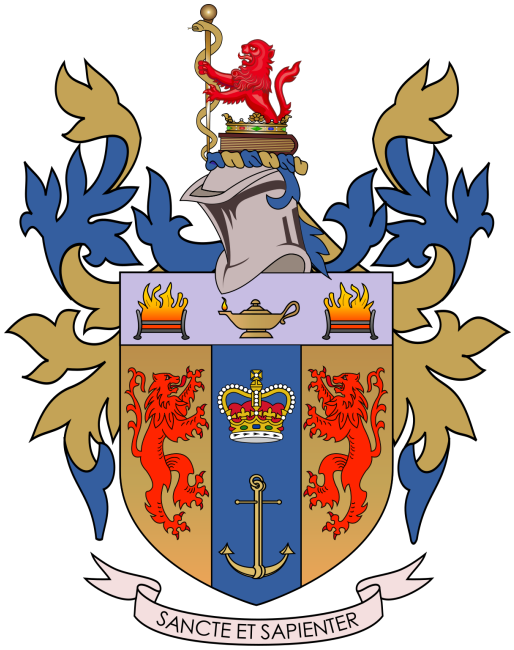

Amalie C. M. Couch

Thesis submitted for the degree of

Doctor of Philosophy

at King's College London

2023

Department of Basic and Clinical Neuroscience

Insitute of Psychiatry, Psychology and Neuroscience

Abstract

Maternal immune activation (MIA) as a consequence of either infectious or non-infectious stimuli is an environmental risk factor associated with increased risk for psychiatric disorders with a putative neurodevelopmental origin in the offspring. At least in part, this association is driven by elevations in cytokines in the foetal brain downstream of the maternal immune response. Although this likely involves many such molecules, there is evidence to suggest that elevations in the levels of maternal and foetal interleukin (IL)-6 is specifically associated with higher risks for schizophrenia (SZ), bipolar disorder (BD), and autism spectrum condition (ASC) in the offspring. In this context, IL-6 appears to act as sensor, transducer, and effector. Consistent with this view, blocking IL-6 signalling in pregnant mice after induction of MIA prevents the development of behavioural phenotypes relevant for ASC and SZ. However, our understanding of the cellular and molecular mechanisms specific to human physiology that drive these relationships is limited, particularly in non-neuronal cells such as microglia that are implicated in the neurobiology of psychiatric disorders. In part this reflects a lack of access to human brain tissue at early developmental stages. To bridge this gap, we have developed a novel human induced pluripotent stem cell (iPSC)-derived model, to study the impact of IL-6 exposure on both neurons and microglia. By using hiPSC to retrain the donor's genetic background, we can explore connections between genetic risk and environmental factors that can be modelled *in vitro*, such as IL-6. This is crucial for studying underlying mechanisms, given the known interactions between genetic and environmental factors in the context of psychiatric disorders, which is currently challenging to achieve using mouse models.

First, we characterized the effect of acute IL-6 exposure on iPSC-derived microglia-like cells (MGL) and cortical neural progenitor cells (NPC) in monoculture. Human forebrain NPCs did not respond to acute IL-6 exposure in monoculture due to the absence of IL-6Ra expression and sIL-6Ra secretion. The addition of recombinant IL-6Ra however, enabled NPCs to respond to IL-6 in dose-dependent manner via trans-signalling as measured by phosphorylation of STAT3. By contrast, MGLs express IL-6Ra and secrete sIL-6Ra, hence acute IL-6 exposure resulted in rapid STAT3 phosphorylation and increased expression of genes downstream of STAT3. Transcriptomic analysis of MGLs following acute IL-6 exposure revealed overlapping changes between gene sets and pathways identified using

post-mortem brain tissue of individuals with SZ, with no effect on the expression of risk genes for SZ as measured by GWAS. Live imaging showed increased MGL cytoplasm ruffling, consistent with observations in rodent MIA models. Finally, MGLs exhibited elevated levels of cytokines and chemokines, consistent with observations MIA rodent models such as MIP-1α.

Having provided evidence for cell-specific responses to acute IL-6 exposure in vitro, we proceeded to evaluate how this interacts with a known genetic risk profile for psychiatric disorders. To achieve this, we used hiPSC cell lines donated by individuals with 22q.11 deletion syndrome (DS), one of the most penetrant genetic risk factors for ASC and SZ. To study how the MGL response to IL-6 might influence the development of cortical neurons, a trans-well culture system was developed that allows communication between these cell types without direct physical interaction, so the responses of each cell type may be assessed. Cytokine secretion and transcriptomic RNAseq analysis revealed a robust response by MGLs to IL-6 exposure and differed in 22q11.2DS cells which associated with the "regulation of vasculature development" consistent with the upregulation of VEGFA expression that was not noted in control cells, which is consistent with a dysfunctional endothelial cells and blood-brain barrier in 22q11.2DS. Separately, staining of mature cortical neurons, that were exposed to acute IL-6 during their NPC development stage in combination with microglia, showed a decrease in vGlut1 synaptic puncta in 22q11.2DS neurons but not in control cells which is consistent with data from post-mortem studies and in vivo PET imaging for reduced pre-synaptic proteins in SZ.

In summary, this thesis aimed to develop a human gene (22q11.2DS) by environment (IL-6) model to investigate the effects of acute IL-6 exposure on microglia and cortical neuron development. The findings enhance our understanding of NDD mechanisms by: (1) identifying that NPCs are unable to respond to IL-6 by cis-signalling; (2) the MGL transcriptome response overlaps with post-mortem SZ transcriptome; and (3) acute IL-6 reduces vGlut1 expression in mature neurons with the 22q11.2 deletion. The findings were validated against previously published data from both human and mouse MIA models, demonstrating cell-specific changes relevant to NDDs. Further investigation with additional cell types, such as endothelial cells, is necessary to study this complex interaction in a human iPSC model. Taken together, these results emphasize the importance of studying gene-environment interactions in a human-specific context using multiple cell types.

Acknowledgements

It really takes a village to complete a project like this. I would like to acknowledge and thank those of you who have contributed intellectually, emotionally, and financially towards my PhD to make it the extraordinary journey it has been. First and foremost, thank you to my primary supervisor and leader of the doughnut revolution, **Anthony Vernon**. You might possibly the most wonderfully English man I've ever known; with your love of cricket and distinct hatred for British politics, but also with your humbleness. Throughout these awesome three and a half years, I don't believe you given yourself enough credit, so perhaps I'll do it here for you. You've been a brilliant supervisor, a great support and friend, and a future Professor who always has the right ideas before anyone else has even begun to consider them. Thank you so much for choosing me to do this project with you, and getting to the end of it with me. We did it! Thank you also to my secondary supervisor **Deepak Srivastava**, you have been the extra dimension to the mega supervisory team. Thank you for teaching me everything I need to know about hiPSCs and synapses and thank you for your patience with me and for including the Vernon lab into your NCND family. In addition, without the funding and support from the **NC3Rs**, this project would never have been given its wings, thank you for supporting me through the PhD process at King's.

To my Daily Quordle crew, **Rugile Matuleviciute** and **Shiden Solomon**, thank you. You've lifted me up when I've been down, celebrated my wins harder than I ever could have imagined and donated your thoughts for scientific sound boarding whenever it was asked for, thank you both so much for everything. I echo the fact that you, **Laura Sichlinger**, are my science sister. You are a genuine inspiration to me with how you live your life, run your science, and continue to support the women around you. I quite often find myself asking, "what would Laura do?"; thank you for being around from Day 1 all the way through to Day 1368 when we can finish this together. **Amelia Brown**, you were my sprint finish that came from the science gods. You gave me the motivation and help with key experiments right when I needed it, I cannot thank you enough for those final lab moments. I can't wait to see where your own PhD journey will take you. **Bjørn Hanger,** you welcomed me to the Vernon Lab and taught me how to make these alien factories and handle hiPSCs, without you I wouldn't have

known where to start. To all the other members of both Vernon and Srivastava labs past and present: **Lucia, Rodrigo, Adam**, **Pooja**, **Nick**, **Deep**, **Rolo**, and **Deborah**, your questions during lab meetings, your high scientific standards, lunchtime chats and lockdown calls will form some of the most important memories and scientific developments for me during these times. Lastly from the lab, all our MSc and BSc students, **Carlotta**, **Alessia**, **Chloe**, **Karin**, **Yiqian**, **Sophie**, and **Morgan**, supervising you all has been a dream, and you have all taught me things about my own data and I thank you all for it.

From home, **Mama** and **Papa**, thank you for raising me to a point where I'm submitting a PhD thesis. You were my first teachers, not only did you teach me to read and write but you taught me how to navigate the world and raised me to be curious through ups and downs, thank you both for your incredibly hard work, I am forever grateful. Mama, thank you also for teaching me about the power of the semi-colon. To my **Borjita**, you've stitched up my self-doubt and set me on the path to belief in myself. I mean it when I say that you've been a massive contributing factor in creating a stable foundation for me to get up and do this PhD. Gracias y te quiero, from the bottom of my heart, even if you are little bit bored of listening to me nerd out about cells during a river walk. To **Martino**, thank you for always including me as one of your own in your thoughts and actions, no matter where you are in the world. Thank you to my teachers at Latymer: **Mrs Bilderbeck**, **Mrs Sellars**, **Jackie Hayward** and **Ceri Ellis**, you started the PhD spark… who knew it would get me this far? Thank you also to **Gris**, **Ottie**, **Grace**, **Ella**, **Jack**, **Rosie**, and **Pogo**, you all checked in with me and got me out of the house when I needed it most. And last but by no means least, to **Oma** and **Opa**, who would have loved to celebrate this moment.

"SCIENCE, FOR ME, GIVES A PARTIAL EXPLANATION FOR LIFE. IN SO FAR AS IT GOES, IT IS BASED ON FACT, EXPERIENCE, AND EXPERIMENT."

— ROSALIND FRANKLIN

Statement of Work

All work in this thesis was carried out by myself, Amalie Couch (AC), other than the following:

Chapter 3:

- Neuralisation of hiPSCs to the relevant cell types and collection of RNA samples for Figures 3.4B and 3.4D was carried out by Laura Sichlinger and Lucia Dutan Polit respectively and shared with AC for cDNA synthesis and qPCR analysis.

Chapter 4:

- RNAseq library preparation and NovaSeq sequencing of all RNAseq samples was carried out by Genewiz Inc (South Plainfield, NJ), who provided AC with the generated FASTQ files.
- The gene set enrichment analysis presented in Figures 4.4A and 4.4C was aided by Rodrigo Duarte (RD). Firstly, both the Fischer's overlap test analysis and MAGMA analysis scripts were written by RD. The MAGMA analysis was performed by RD, and the Fischer's overlap test was performed by AC using RD's script in R.
- Ingenuity pathway analysis presented in Figure 4.3E was carried out by Alessia Marrocu as part of her rotation project in collaboration with Shahram Kordasti.
- As presented in Figure 4.5, microglial motility assay live imaging data collection on the OperaPhenix was carried out by Shiden Solomon.
-

Chapter 5:

- As in chapter 4, RNAseq library preparation and NovaSeq sequencing of all RNAseq samples presented throughout chapter 5 was carried out by Genewiz Inc (South Plainfield, NJ).
- Also as in chapter 4, the Fischer's overlap test was performed by AC using RD's script in R.
- Finally, as part of Amelia Brown's (AB) rotation project, analysis of the co-culture media by the sIL-6Ra ELISA in Figure 5.6, and the XL Proteome Profiler and MSD plate analysis both presented in Figure 5.7, were all performed by AB, supervised by AC.

Declaration of Competing Interest

I declare that I have no known competing financial interests or personal relationships that could have appeared to influence the work reported in this thesis.

Funding Acknowledgement

Amalie Couch, Anthony Vernon and Deepak Srivastava acknowledge financial support for this study from the National Centre for the Replacement, Refinement and Reduction of Animals in Research (NC/S001506/1). The work (at King's College, London) was also supported in part by the Medical Research Council (MRC) Centre grant (MR/N026063/1).

Table of Contents

Word Count: 66,919 (From chapter 1 to the end of chapter 7)

List of Figures

List of Tables

Abbreviations

IN ALPHABETICAL ORDER

22q11.2DS	22q11.2 DELETION SYNDROME
ADHD	ATTENTION-DEFICIT/HYPERACTIVITY DISORDER
ANOVA	ANALYSIS OF VARIANCE
ASC	AUTISM SPECTRUM CONDITION
AUC	AREA UNDER THE CURVE
BBB	BLOOD BRAIN BARRIER
BD	BIPOLAR DISORDER
BDNF	BONE DERIVED NEUROTROPHIC FACTOR
BH	BENJAMINI-HOCHBERG
bRGC	BASAL RADIAL GLIAL CELL
cIN	CORTICAL INTERNEURON
CNS	CENTRAL NERVOUS SYSTEM
CNV	COPY NUMBER VARIATION
CP	CORTICAL PLATE
CSF	CEREBROSPINAL FLUID
Ct	CYCLE THRESHOLD
D	DAY
DA	DOPAMINERGIC
DEG	DIFFERENTIALLY EXPRESSED GENE
DMEM	DULBECCO'S MODIFIED EAGLE MEDIUM
DMSO	DIMETHYL SULFOXIDE
DNA	DEOXYRIBOSE NUCLEIC ACID
EB	EMBRYOID BODY
ECM	EXTRACELLULAR MATRIX
ELISA	ENZYME-LINKED IMMUNOSORBENT ASSAY
EMA	EARLY MARKERS FOR AUTISM STUDY
EMP	ERYTHOMYELOID PROGENITOR
FACS	FLUORESCENCE-ACTIVATED CELL SORTING
FC	FOLD CHANGE
FDR	FALSE DISCOVERY RATE
FE	FOLD ENRICHMENT
FISH	FLUORESCENCE IN SITU HYBRIDIZATION
GAD67	GLUTAMIC ACID DECARBOXYLASE 67
GD	GESTATIONAL DAY
GFAP	GLIAL FIBRILLARY ACIDIC PROTEIN
GluN1	NMDA RECEPTOR SUBUNIT 1
GM-CSF	GRANULOCYTE MACROPHAGE COLONY-STIMULATING FACTOR
GSEA	GENE SET ENRICHMENT ANALYSIS

GW	Gestation week
GWAS	Genome-wide association studies
GxE	Gene by environment interactions
HBSS	Hanks' Balanced Salt Solution
HCMV	Human cytomegalovirus
hiPSC	Human induced pluripotent stem cell
HLA	Human leukocyte antigen
HPC	Hippocampus
HSP	Heat shock protein
ICM	Inflammatory cytokine mixture
IFN-γ	Interferon-gamma
IL-	Interleukin
IL-6Rα	IL-6 receptor alpha
IL-6ST	IL-6 signal transducer
IPA	Ingenuity pathway analysis
IPC	Intermediate progenitor cell
IVF	In vitro fertilisation
JAK/STAT	Janus kinase/signal transducer and activator of transcription
LOD	Limit of detection
LPS	Lipopolysaccharide
LUHMES	Lund human mesencephalic
MAP2	Microtubule-associated protein 2
MCP-1	Monocyte Chemoattractant Protein-1
MDD	major depressive disorder
MEA	Multi-electrode array
MGL	Microglia-like cell
MHC	Major histocompatibility complex
MIA	Maternal immune activation
MIP-1α	Macrophage inflammatory protein alpha
MR	Mendelian randomization
MSN	Medium spiny neuron
NC3Rs	National Council for the Reduction, Refinement and Replacement of the use of animals in biological research
NDDs	Neurodevelopmental disorders
NGS	Normalised goat serum
NPC	Neural progenitor cell
OCD	obsessive-compulsive disorder
OD	Optical density
OR	Odds ratio
ORA	Over representation analysis
oSVZ	Outer subventricular zone
PANSS	Positive and Negative Syndrome Scale

PBS	Phosphate-buffered saline
PCA	Principle component analysis
PDL	Poly-D-Lysine
PFC	Prefrontal cortex
PiNDs	Patient iPSCs for Neurodevelopmental Disorders study
PND	Postnatal day
Poly I:C	Polyinosinic-polycytidylic acid
PSD95	Postsynaptic density protein 95
qPCR	Quantitative polymerase chain reaction
RGC	Radial glial cell
rIL-6Ra	Recombinant soluble IL-6Ra
RIPA	Radioimmunoprecipitation assay
RNA	Ribonucleic acid
ROS	Reactive oxygen species
RT	Room temperature
SDS-PAGE	Sodium dodecyl sulphate–polyacrylamide gel electrophoresis
sgp130	Soluble IL-6ST
sIL-6Ra	Soluble IL-6 receptor alpha
SLaM	South London and Maudsley
SMAD	Suppressor of Mothers against Decapentaplegic
SNP	Single nucleotide polymorphism
SV2A	synaptic vesicle glycoprotein 2A
SVZ	Subventricular zone
SZ	Schizophrenia
TBI	Traumatic brain injury
TBS	Tris-buffered saline
TGF-β	Transforming growth factor beta
TLR	Toll-like receptor
TNFα	Tumour necrosis factor alpha
TUJ1	b-tubulin III
VEGF	Vascular endothelial growth factor
vGlut1	Vesicular glutamate transporter 1
VZ	Ventricular zone

Chapter 1

General Introduction

NOTE: SOME OF THE CONCEPTS AND FIGURES FROM THIS CHAPTER WERE FIRST PUBLISHED IN BRAIN, BEHAVIOR AND IMMUNITY, IN 2023, ENTITLED "ACUTE IL-6 EXPOSURE TRIGGERS CANONICAL IL-6RA SIGNALING IN HIPSC MICROGLIA, BUT NOT NEURAL PROGENITOR CELLS" (COUCH *ET AL.*, 2023) (APPENDIX 1) AND IN 2021, ENTITLED "MATERNAL IMMUNE ACTIVATION PRIMES DEFICIENCIES IN ADULT HIPPOCAMPAL NEUROGENESIS" (COUCH *ET AL.*, 2021) (APPENDIX 2).

1.1 Neurodevelopmental Disorders

Neurodevelopment refers to the biological and environmental processes that shape the development and maturation of the central nervous system (CNS). This includes the growth differentiation and migration of a diverse range of cell types, the colonisation of the brain by microglia, the formation of neural circuits, and the establishment of functional connections between different regions of the brain (Khodosevich and Sellgren, 2023). Neurodevelopmental Disorders (NDDs) are a group of conditions that arise as a result of abnormal neurodevelopmental processes such as neurogenesis, neuronal migration, axonogenesis, synaptogenesis, myelination, and synaptic pruning that occur from prenatal stages to early adolescence and can impair normal brain and nervous system functioning, potentially lasting into late adulthood (Francés *et al.*, 2022; Dubois *et al.*, 2014). As such, they are characterized by developmental deficits verbal communication, social interactions, cognition, and in both internalising and externalising behaviours associated with various cortico-amygdalar networks (Anholt *et al.*, 2010; Havdahl *et al.*, 2016; Vijayakumar *et al.*, 2017; Chahal *et al.*, 2021; Umbach and Tottenham, 2021; Nakua *et al.*, 2022). NDDs encompass various conditions such as Autism Spectrum Condition (ASC), obsessive–compulsive disorder (OCD), Attention-Deficit/Hyperactivity Disorder (ADHD), Schizophrenia (SZ), and Bipolar Disorder (BD).

Importantly, the classification of SZ as a neurodevelopmental disorder has sparked an ongoing debate (Murray et al., 2022; Stone et al., 2022). Several key points and metrics contribute to the argument that SZ may not fall clearly into the category of NDDs. Firstly, unlike typical neurodevelopmental disorders that manifest in early childhood, SZ can emerge during childhood, late adolescence and through adulthood (Coulon et al., 2020). The age at onset varies widely among individuals with SZ, indicating a heterogeneous developmental trajectory (Coulon et al., 2020). It is possible that some individuals may experience neurodevelopmental

challenges that surface later in life, or that the summative make-up of non-neurodevelopmental factors such as psychosocial factors can contribute to SZ onset in later life (Howard et al., 2000). The implication of social adversity pathways in the onset of SZ, including childhood trauma, migration, and adverse life events, suggest that the aetiology of SZ may not solely originate from inherent developmental factors, emphasizing the ongoing role of environmental and psychosocial influences in later life that influence the onset of the disorder (Howard et al., 2000). Therefore, the concept of "late-onset" neurodevelopmental disorders is derived to recognise that SZ encompasses a spectrum of aetiologies and onset age (Khodosevich and Sellgren, 2023; Howard et al., 2000). Secondly, not all individuals with SZ exhibit neurodevelopmental characteristics, such as copy number variations (CNVs), high polygenic risk scores (PRS) or low IQ (Beilen et al., 2002; Jones et al., 2016; Kirov et al., 2014). Although these traits are associated with some cases of SZ, the disorder's diverse nature suggests that it cannot be solely attributed to neurodevelopmental pathways. Third, SZ-like symptoms can be induced in individuals through the application of N-methyl-D-aspartate receptors (NMDR) antagonists (Farber, N. 2003; Newcomer et al., 1999). This indicates that the disorder can occur without any inherent developmental differences, further challenging the neurodevelopmental categorization. In light of these challenges in categorizing SZ as a neurodevelopmental disorder, there is a growing acknowledgment of distinct subgroups within the SZ population, necessitating a more nuanced perspective (Murray et al., 2022). This recognition underscores the complexity and multifaceted nature of SZ, where developmental, genetic, environmental, and social factors interact in various ways to contribute to the disorder's onset.

In any case, NDDs are typically lifelong conditions that require ongoing support and management, and can have a significant impact on an individual's quality of life. According to a recent systematic review carried out to estimate the global frequency of NDDs according to

the Diagnostic and Statistical Manual of Mental Disorders, 5th Edition classification (American Psychiatric Association, 2022) in individuals under the age of 18 years old, the following NDD prevalence rates were reported: ADHD, 5–11%; specific learning disorder, 3–10%; ASC, 0.70–3%; Communication Disorders, 1–3.42%; Motor Disorders, 0.76–17%; and Intellectual Disability, 0.63% (Francés *et al.*, 2022). With regards to adolescent and early adulthood onset disorders, a Finnish registers study estimated 0.87% of the population are affected by SZ and 0.35% by Major Depressive Disorder (MDD) with psychotic features (Perälä *et al.*, 2007; Kahn *et al.*, 2015). The worldwide prevalence of BD type 1 is estimated to be 1.06%, and type 2 1.57% (Clemente *et al.,* 2015). These disorders are considered chronic, heterogeneous and comorbidity of multiple NDDs at once is likely (Francés *et al.*, 2022). Importantly, early onset neurodevelopmental disorders such as ASC manifest along a continuum and impact individuals to varying extents, and these disorders currently lack well-established treatment options (Francés *et al.*, 2022). On the other hand, treatment options do exist for conditions like SZ and BD but they are not comprehensive in addressing all symptoms and are often accompanied by significant side effects, particularly in the case of antipsychotics (Huhn *et al.*, 2019). As a result, it is critical to uncover the largely unknown molecular mechanisms of human NDD aetiology, allowing for the future development of treatments that will improve the quality of life for individuals diagnosed with NDDs while decreasing the current economic cost to society.

1.1.1 The Genetics of Neurodevelopmental Disorders

Both early and late-onset neurodevelopmental disorders are highly heritable and linked with the expression of numerous common risk variants with low penetrance; hence they are classified as polygenic diseases (Jansen *et al.*, 2020). Exome sequencing has successfully identified at least 10 high confidence genes that are associated with increased risk for SZ (Singh

et al., 2022). Genome-wide association studies (GWAS) have found evidence for single nucleotide polymorphisms (SNPs) in 240 gene loci linked with an elevated risk of SZ, with the top 41 risk genes being highly expressed in neurons (Ma *et al.*, 2018; Trubetskoy *et al.*, 2022). Furthermore, recent research has revealed that many of the genes related with SZ and ASC are also strongly expressed, and in a cell-specific manner, throughout neurodevelopment (O'Brien *et al.*, 2018; Cameron *et al.*, 2023). Indeed, mapping of GWAS data to a brain single cell sequencing database, these top frequent risk variants appear to be elevated in expression in pyramidal cells, medium spiny neurons (MSNs), and specific interneurons (Skene *et al.*, 2018). However, the use of GWAS studies to establish how risk loci affect NDD onset has limits because many risk loci are abundant in non-coding enhancer regions, making molecular function difficult to explore (Ripke *et al.*, 2014). Although *post-mortem* tissue can be used to study the genetic influence on protein expression, the results of such research can be skewed due to confounding factors such as age, sickness, and therapy (D. Liu *et al.*, 2022). Novel human methods for studying neurodevelopment are thus necessary.

The 22q11.2 Deletion Syndrome

On the other hand, vulnerability to NDDs may also be increased via inheritance of rare, but highly penetrant copy number variation (CNVs). One example is deletions at chromosome 22q11.2, distinguished by the loss of a portion of DNA from the long arm of chromosome 22 (q) at the 11.2 locus (McDonald-McGinn *et al.*, 2015; Khan *et al.*, 2020). This is the most frequent microdeletion syndrome in humans, affecting 1 in every 3,000 to 6,000 live births (Du Montcel *et al.*, 1996; Óskarsdóttir, Vujic and Fasth, 2004; McDonald-McGinn *et al.*, 2015; Zinkstok *et al.*, 2019). 22q11.2 deletion syndrome (22q11.2DS), also referred to as DiGeorge syndrome, or velocardiofacial syndrome is associated with an elevated, if variable, risk of both developing either SZ or ASC (Bassett and Chow, 2008). Specifically, it is estimated that one

in every four people with the 22q11.2DS polymorphism will develop psychosis, representing a considerable 20-fold increase in risk and accounting for 1-2% of all instances of SZ, which makes 22q11.2DS one of the greatest known risk factors for SZ (Murphy, Jones and Owen, 1999; Arinami, 2006; Monks *et al.*, 2014; Schneider *et al.*, 2014). Furthermore, this microdeletion increases the likelihood of ASC by 30-40% (Vorstman *et al.*, 2006; Olsen *et al.*, 2018). Aside from an elevated incidence of NDDs, 22q11.2DS is characterised by heart defects, cleft palate or other facial deformities, immune system disorders, developmental delays, and learning challenges (McDonald-McGinn *et al.*, 2015). Although, the intensity and exact symptoms of the condition might vary greatly across individuals. Some may have only modest symptoms and have relatively typical lives, whilst others may face more serious medical and developmental issues. Genetic testing, such as a microarray or Fluorescence in situ hybridization (FISH) analysis, is commonly used to determine the missing fragment of chromosome 22 in 22q11.2 deletion syndrome (Scambler *et al.*, 1991; McDonald-McGinn *et al.*, 2001; Botto *et al.*, 2003). Early diagnosis is critical because it enables for adequate medical treatment and early interventions to address any health concerns and developmental requirements.

The typical ~3Mb A-D 22q11.2 region deletion is known to result in the loss of approximately 40 coding genes (Morrow *et al.*, 2018). Nevertheless, there is considerable variation in the size of the deleted area among individuals, and the region may also exhibit duplications, contributing to a significant level of genetic heterogeneity among individuals diagnosed with 22q11.2DS (McDonald-McGinn *et al.*, 2015; Nehme *et al.*, 2022; Morrow *et al.*, 2018). Despite this heterogeneity, many genes on the 22q11.2 arm that are impacted by the deletion are involved in key developmental processes during embryogenesis. Most 22q11.2 deletions occur *de novo* during early foetal development, with 5-10% of cases directly inherited from a parent

who has the deletion (Scambler, 2000). When compared to *de novo* 22q11.2 CNVs, inherited cases generally have a less severe penetrance of affected region (McDonald-McGinn *et al.*, 2015). One example of an affected gene located on the 22q arm is the leukaemia inhibitory factor (LIF) gene. Polymorphic variations of the gene (rs929271, rs737812, and rs929273) are associated with hebephrenic SZ (Okahisa *et al.*, 2010). Interestingly, LIF has a role in coordinating microglial function, implying that disruption of immune and microglial function is one of several plausible mechanisms to explain this connection.

1.1.2 Influence of genes and environmental factors on the innate immune system and their relevance for NDD pathophysiology

The available data suggest that the bulk of common genetic risk factors for SZ are primarily enriched in their expression within neurons. This does not however, rule out the potential contribution of "non-neuronal" cell types, including microglia. This is supported by data linking common genetic abnormalities in genes that cluster into immune pathways to an elevated risk of psychiatric disorders (Sekar *et al.*, 2016; Ma *et al.*, 2018; Skene *et al.*, 2018). Several genes in these top 41 SNPs (including ATP2A2, PSMA4, PBRM1, SERPING1, and VRK2) are also expressed in microglia (Ma *et al.*, 2018). Whilst the impact of genetic in these genes on microglia form and function remains unknown, they raise the possibility that microglia could play a role in SZ pathophysiology. In support of this view, there is a strong GWAS link between SZ and genetic variance within the human leukocyte antigen (HLA) gene, which codes for proteins that form the major histocompatibility complexes (MHCs) (Mokhtari and Lachman, 2016). Specifically, variations within the MHC class-II gene locus, such as the gene encoding complement factor 4 A/B (C4A/B), are strongly linked to an increased risk of SZ. Moreover, whether through targeted overexpression manipulation of C4A specifically in the prefrontal cortex of mice or through overall overexpression achieved by genetic

manipulation, both scenarios result in an increase of synaptic pruning (Druart *et al.*, 2021). Consequently, this leads to impaired neuronal communication and the manifestation of SZ-related behaviours, encompassing cognitive and social deficits (Druart *et al.*, 2021). Additionally, in rodents with a global knockout of C4A/B, there is an observed increase in synaptic engulfment in the visual thalamus, a process in which various glial cells, including microglia, play a significant role (Sekar *et al.*, 2016). It is also worth mentioning that C4A is strongly expressed in astrocytes and vascular leptomeningeal cells, in addition to microglia (Skene *et al.*, 2018). As a result, while not all cell types are enriched in the expression of common SZ risk alleles, it is possible that other cell types, including microglia, may play a role in the pathogenesis of SZ associated with unique genotypes.

By taking into account the genetic association between the pathogenesis of NDDs and the presence of the 22q11.2 region CNV, a valuable opportunity arises to delve into the heterogeneous nature of NDDs and unveil their specific molecular mechanisms of which the CNS immune system appears to be involved. This is particularly relevant because CNVs, known for their capacity to capture genomic structural variations, serve as a valuable model for investigating heterogeneity (Khan *et al.*, 2020). However, aside from genetic risk, environmental variables are responsible for 30-40% of the risk of neurodevelopmental disorders (Cattane, Richetto and Cattaneo, 2020). Given the complexity and heterogeneity of neurodevelopmental processes, a wide range of environmental and genetic perturbations at different timepoints throughout critical neurodevelopmental phases can change any of these processes. Such obstacles in the regular track of brain development have the potential to result in atypical neurodevelopment, a deviation from typical brain and nervous system functioning that can last into adulthood (Khodosevich and Sellgren, 2023; Dubois *et al.*, 2014). The more an individual's exposure to these barriers and disruptions, the greater the danger of developing

psychopathology (Bayer, Falkai and Maier, 1999; Meyer, 2019; Couch *et al.*, 2021). Identification of the most significant risk factors for NDDs requires a detailed understanding of each of these risk variables, both separately and in combination. In the following section, we will explore this concept within the framework of an exposure to inflammatory events during prenatal development. However, we must also acknowledge the potential influence of other environmental factors, both during the prenatal and postnatal stages, in elevating the risk of NDDs (Meyer, 2019).

1.2 The Immune System, Maternal Immune Activation and Neurodevelopmental Disorders

Exposure to infections during early life has been repeatedly linked by epidemiological studies to an increased risk for the manifestation of psychiatric disorders with a putative neurodevelopmental origin in the affected offspring (Kępińska *et al.*, 2020). The concept of the "psychoses of influenza" was first established in the 18th century (Kraepelin, 1890; Kendler and Jablensky, 2011). Ensuing epidemiological data collected during the 1918 Spanish H1N1 influenza pandemic conferred increased risk of psychosis with infection (Menninger, 1919; Kępińska *et al.*, 2020). Subsequently, during the early 1970s, Edwin Fuller Torrey developed an interest in viral infections, specifically *Toxoplasma gondii,* and demonstrated them to be potential factors contributing to the onset of SZ and BD (Torrey and Peterson, 1976). More recently, a Danish register cohort study conducted on data collected from individuals between 1981 and 1996 (n = 843,390) revealed that those who had a hospital contact with infection were 1.41 times (relative risk) more likely to develop SZ (Nielsen, Benros and Mortensen, 2014). Today, we have unfortunately yet conceivably seen a repeat of history with the SARS-CoV-2 pandemic (Garrido-Torres *et al.*, 2022). A study of 214 hospitalised Coronavirus Disease 2019

patients in Wuhan cited 36.4% of patients presented with neuropsychiatric symptoms from various aetiologies (Mao *et al.*, 2020), plus an additional study reported 58 out of 64 patients had neurological symptoms (Helms *et al.*, 2020). Taken together, these studies demonstrate that an immune response to infectious agents at any stage of life, such as SARS-CoV-2, could be a key environmental factor causing the precipitation of psychiatric disorders at any life stage, with a putative neurodevelopmental origin.

In addition, non-infectious stimuli that lead to immune activation have also been associated with psychosis in patients. Clinical observations note patients with auto-antibody-mediated encephalitis present with an increased risk for psychosis, supported by the identification of auto-antibodies against antigens on the neuronal cell surface in individuals with SZ (Graus, Saiz and Dalmau, 2010; Zandi *et al.*, 2011). Even non-neurological autoimmune diseases confer risk for schizophrenia, with additional infections increasing psychosis risk in a dose-dependent rate (Benros *et al.*, 2011; Cullen *et al.*, 2019). It is therefore suitable to theorise a heightened immune response can precipitate the psychiatric symptoms we see in individuals with neurodevelopmental disorders. The epidemiological correlations laid out here lead us to two questions: what are the molecular mechanisms carried out by the immune system that cause alterations to brain function, and can these be primed for during vulnerable prenatal neurodevelopmental stages?

1.2.1 Maternal Immune Activation

Maternal immune activation (MIA) during pregnancy has been reported to increase the risk of the offspring developing neurodevelopmental disorders later in life, namely SZ, BD and ASC (Estes and McAllister, 2016; Mondelli *et al.*, 2017). MIA is a broad term that encompasses a range of environmental agents that convey risk for NDDs, including insults from both

infectious and non-infectious agents, with activation of the maternal immune system as a common downstream mechanism (Meyer, 2019). The maternal biochemical response to environmental MIA-derived insults during the perinatal period is considered to be a risk factor capable of diverting the offspring's neurodevelopment from its typical path. Findings from both human epidemiological studies and animal models of MIA provide causal support to suggest that exposure to these MIA-derived insults during both prenatal and postnatal periods give rise to an increased NDD risk for the offspring (Meyer, 2019; Potter *et al.*, 2023; Lydholm *et al.*, 2019). Several birth cohort studies have shown that prenatal stress from non-infectious agents, such as bereavement (Huttunen and Niskanen, 1978) and socio-economic disadvantage (Gilman *et al.*, 2017), are also risk factors for NDDs in the offspring (Malaspina *et al.*, 2008; Brown and Conway, 2019). With regards to infectious agents, specific viral infections with maternal-foetus vertical transmission, such as Zika, Rubella, and Human Cytomegalovirus (HCMV) (Claus, Jung and Hübschen, 2020) can confer NDD risk by direct infection of the foetus via the placenta. However, it is generally believed that the majority of infectious MIA cases do not transfer NDD risk in this way. Rather, the maternal immune response at a systemic level effects neurodevelopment (Meyer, 2014). Returning to the topic of SARS-CoV-2, a recent study of 18,355 infants born after February 2020 found that male offspring, but not female offspring, of mothers who tested positive for SARS-CoV-2 during pregnancy were more likely to receive a neurodevelopmental diagnosis within the first 12 months after birth, even when preterm delivery was accounted for (Edlow *et al.*, 2023). As a result, there is a notion that the risk of NDDs may be heightened when the insult occurs during a vulnerable period. This could either reveal underlying psychopathology due to genetics, sex or establish a hidden disturbance that interacts with other environmental risk factors, such as stress.

Key questions, however, remain unanswered by human studies regarding the associations between MIA and the risk for psychiatric disorders with a putative neurodevelopmental origin (Brown and Meyer, 2018). Chiefly, MIA is a fairly common occurrence, with 285 out of 686 pregnant women (41.5%) in a cohort tested serologically positive for influenza infection during pregnancy (Mahic et al., 2017). Yet, there is considerable heterogeneity in its impact on the developing foetus in utero. For instance, following the aforementioned example, only 139 of the 285 (48.8%) prenatally influenza-infected mothers went on to have children diagnosed with ASC (Mahic et al., 2017). Hence, the issue lies in our lack of understanding of the specific factors that elucidate why only some offspring exposed to MIA proceed to develop NDDs and why the specific diagnosis of NDD varies within this subgroup. Typically, human MIA model studies primarily focus on observable outcomes like social behaviour, leaving the underlying mechanisms less explored. Additionally, human MIA models tend to overlook postnatal effects and genetic factors. These limitations identify a need for better experimental design when it comes to correlating MIA to NDD diagnosis outcome in humans (Brown and Meyer, 2018). Without this, current human MIA model literature has left a gap in our understanding of the molecular basis for NDD risk transmission from mother to foetus after MIA. Consequently, a more integrated analysis and the development of human-led models, incorporating genetic variance based on robust human epidemiology, would be beneficial. Brynge and colleagues (2022) demonstrated, for example, that MIA is not a specific risk factor for ASC, but rather, the risk is driven by inherited factors using a sibling design (Brynge et al., 2022). Overall, these critiques underscore the need for a more comprehensive approach to MIA research in addition to human models that consider the complexity of factors influencing MIA outcomes. Therefore, *in vitro* and *in vivo* MIA models are therefore essential for establishing the cellular and molecular mechanisms by which psychiatric risk is conferred, since the mechanistic link underpinning this association remains unclear.

1.2.2 Maternal Immune Activation Evidence Gained from Animal Models

Animal models have been essential in establishing causality for the link between MIA and NDD onset in the offspring. As previously extensively reviewed (Meyer and Feldon, 2010; Meyer, 2014; Brown and Meyer, 2018), preclinical investigation of MIA in animals is achieved by exposing pregnant dams to either infectious or non-infectious risk factors to trigger a maternal and foetal immune response. These factors include live infectious agents such as influenza (Fatemi *et al.*, 1999, 2012), viral or bacterial infection mimetics, such as agonists for toll-like receptor (TLR) 3 (polyinosinic-polycytidylic acid (Poly I:C)) or TLR4 (lipopolysaccharide (LPS)) respectively (Meyer, 2019), or direct exposure to specific pro-inflammatory cytokines such as interleukin (IL-)6 (Smith *et al.*, 2007), IL-17 (Choi *et al.*, 2016) and IL-1β (Girard *et al.*, 2010).

These MIA exposure animal models, which typically cause a brief, but high intensity acute activation of the maternal immune system demonstrate causation for the relationship between a MIA and increased NDD risk in the offspring. Specifically, behavioural, neurotransmitter systems, neurogenesis, morphological, and epigenetic changes relevant to SZ and ASC have been reported in offspring following prenatal Poly I:C, LPS, or cytokine stimulation of the mother during gestation (Meyer, 2014, 2019). The specifics of each study and how these changes are relevant for NDDs are outlined in Table 1.1. Firstly, abnormalities in sensorimotor gating and low latent inhibition are indicative of behavioural changes identified in rodent MIA models also found in those with NDDs (Meyer *et al.*, 2006; Borçoi *et al.*, 2015; Ding *et al.*, 2019). Localised disruption to neurotransmitter systems including GABAergic, glutamatergic, seratonergic and dopaminergic transmission are highlighted by differences in key receptor expressions in these MIA models (Nyffeler *et al.*, 2006; Samuelsson *et al.*, 2006; U. Meyer *et*

al., 2008; Holloway *et al.*, 2013; Richetto *et al.*, 2014; Canetta *et al.*, 2016; Rahman *et al.*, 2020). Furthermore, aberrant development of $CTIP2^{+}$ cells, GABAgeric interneuron connections, midbrain and substantia nigra dopaminergic cell number, impaired neuron-microglial signalling and increased astrogliosis as a result of differential expression in key regulatory pathways leading to morphological abnormalities in overall brain volume, hippocampal structure and white matter connectivity are noted in the MIA animal models (Carvey *et al.*, 2003; Vuillermot *et al.*, 2010; Deng *et al.*, 2011; Willette *et al.*, 2011; Cotel *et al.*, 2015; Giovanoli *et al.*, 2015; Crum *et al.*, 2017; da Silveira *et al.*, 2017; Richetto *et al.*, 2017; Schaafsma *et al.*, 2017; Lee *et al.*, 2018; Nakamura *et al.*, 2019; Vasistha *et al.*, 2020; Ben-Reuven and Reiner, 2021). Finally, epigenetic alterations to DNA methylation and decreased histone acetylation at influential loci for neurogenesis and signalling pathways could present a possible source for the widespread phenotypes revealed as a result of prenatal MIA exposure in animal models (Tang *et al.*, 2013; Richetto *et al.*, 2017; Basil *et al.*, 2018). Taken together, these animal MIA models show that immune activation in the maternal system at critical moments in an offspring's prenatal brain development results in abnormal brain development trajectories with effects on epigenetic, morphological, neurogenic, neurotransmitter and behavioural systems. As mentioned earlier, the prevailing notion is that most cases of MIA that result from infections do not directly transmit the risk of NDDs through viral tropism but instead, it is the systemic impact of the maternal immune response that affects neurodevelopment by the transduction of signalling indirectly to the foetus, implicating both chemokines and cytokines as the key messengers of the immune system (Meyer, 2014).

Table 1.1 - Evidence of offspring atypical neurodevelopment after maternal immune activation from animal models prenatally exposed to either LPS or Poly I:C. GD = gestation day exposure to stimulant.

Theme	Observation in Offspring	Human NDD Relevance	Stimulant	GD	Model	Citation
Behavioural	Decreased prepulse inhibition	Decreased sensorimotor gating and inability to filter out irrelevant information, found in SZ	Poly I:C	9	Mice	Ding *et al.*, 2019
	Decreased latent inhibition	Shows an inability to learn from a stimulus with reward or adverse consequences, associated with psychosis	Poly I:C	9	Mice	Meyer *et al.*, 2006
	Increased response to amphetamines	Epidemiology links SZ with vulnerability to drug use	Poly I:C	9	Mice	Borçoi *et al.*, 2015
Neuro-transmitter Systems	Increased NMDA receptor binding in cingulate and male striatum	Glutamate neurotransmission changes found in SZ	Poly I:C	9-9.5	Mice	Rahman *et al.*, 2017
	Decreased paravalbumin-GABAergic transmission to pyramidal cells in the prefrontal cortex	GABAergic transmission abnormal in those with SZ, BD and depression due to GAD67 expression reduction in humans; the enzyme responsible for GABA production	Poly I:C	9-9.5	Mice	Canetta *et al.*, 2016
	Increased $GABA_A$ alpha 2 receptor expression in ventral dentate gyrus and basolateral amygdala		Poly I:C	9	Mice	Nyffeler *et al.*, 2006
	Further maturation-dependent alterations in prefrontal GABAergic gene expression		Poly I:C	17	Mice	Richetto *et al.*, 2013
	Reduced D1 and D2 receptors in male prefrontal cortex	Receptors responsible for regulating sensorimotor gating, something that is impaired in those with NDDs	Poly I:C	9	Mice	Meyer *et al.*, 2008
	Increased 5-HT_{2A} and decreased mGluR2 receptor density in frontal cortex	Antipsychotics target 5-HT_{2A} such as clozapine, causing internalisation and therefore reduction. mGlu2 is necessary to induce some 5-HT_{2A} antipsychotic behaviours	Poly I:C	9-9.5	Mice	Holloway *et al.*, 2013
Morphology and Neurogenesis	Excess $CTIP2^+$ neuron formation	Excess cortical neurons found in the cortex of patients with ASC	Poly I:C	12.5	Mice	Ben-Reuven and Reiner, 2019
	Disrupted cortical GABAergic interneuron development	As above, GABAergic transmission abnormal in those with SZ, BD and depression	Poly I:C	9	Mice	Vasistha *et al.*, 2019
	Reduced BDNF expression in hippocampal microglia	BDNF important in learning and memory processes	LPS	15,16 and 17	Mice	Schaafsma *et al.*, 2017

	Significant white matter changes	White matter hyperintensities have been associated with BD and depression	Poly I:C	9-9.5	Rhesus Monkey	Willette *et al.*, 2011
	Decreased HSP60 expression and increased HSP90 expression in prefrontal cortex	HSPs such as HSP90 overexpressed in patients with SZ	Poly I:C	9-9.5	Mice	Deng *et al.*, 2011
	Reduced Arx expression in the forebrain	Arx essential to PV interneuron development and GABAergic function, both of which found abnormal in patients with psychosis	Poly I:C	17	Mice	Nakamura *et al.*, 2019
	Reduced midbrain dopaminergic cell number	As above, dopaminergic transmission responsible for regulating sensorimotor gating, something that is impaired in those with NDDs	LPS	9-14	Rats	Carvey *et al.*, 2003
	Increased TH-positive dopaminergic cells in the substantia nigra		Poly I:C	9	Mice	Vuillermot *et al.*, 2010
	Long-term reactive astrogliosis	Found in SZ and ASC patients *post-mortem*	LPS	15 and 16	Mice	Yin *et al.*, 2015
	Decreased BBOX1 expression	SNPs found in the 5'-near region of BBOX1 in SZ patients	Poly I:C	9	Mice	Lee *et al.*, 2018
	Decreased in brain volume, especially in posterior structures	Reduced volume of posterior corpus callosum found in children with ADHD	Poly I:C	9-9.5	Mice	da Silveira *et al.*, 2017
Epigenetic	Decreased DNA methylation in hippocampus and prefrontal cortex	Some evidence for dysregulated methylation in patients with SZ, including altered expression of epigenetic enzymes and abnormal chromatic state	Poly I:C	9	Mice	Basil *et al.*, 2018
	Decreased histone acetylation in cortex and hippocampus regions		Poly I:C	9	Mice	Tang *et al.*, 2013
	Hyper- and hypomethylated CpGs at numerous loci including genes relevant for GABAergic differentiation and signalling		Poly I:C	9 and 17	Mice	Richetto *et al.*, 2017

1.2.3 Cytokines and Chemokines: The Risk Mediators of Maternal Immune Activation

The previous section summarises the evidence for potential cellular and molecular mechanisms that underlie the development of behavioural deficits relevant for human neurodevelopmental disorders. Whether these mechanisms are conserved in human model systems remains uncertain, as does the means through which the signal is transmitted from a mother's immune

system to the child's developing brain. Plainly, if maternal immune response is the critical determinant of risk outcome following prenatal agent exposure, then understanding the specific mediators involved in this maternal-foetal risk transfer is beneficial for the development of mitigation strategies. Given that cytokine and chemokine signals are essentially the immune system's communication structure, both human birth cohort and animal MIA model studies have attempted to attribute changes in specific maternal serum cytokine levels with an offspring's NDD risk (Gilmore and Jarskog, 1997; Jarskog *et al.*, 2005). One example of a human cohort study by Allswede and colleagues reported increased concentrations of the pro-inflammatory cytokines tumour necrosis factor (TNF)α, IL-1β, and IL-6 in the maternal serum of offspring who subsequently developed psychosis (Allswede *et al.*, 2020). There is also evidence to suggest that the risk of offspring developing NDDs was greater when prenatal infection occurs earlier, for example in the first trimester, indicating that the developing brain is susceptible to environmental influences that can disrupt its normal developmental trajectory (Meyer *et al.*, 2006; Vuillermot *et al.*, 2010; Adam, 2012; Knuesel *et al.*, 2014; Giovanoli *et al.*, 2015; Allswede *et al.*, 2020). However, while human birth cohort studies can only establish a correlation between increased levels of maternal cytokines and the prevalence of NDDs in the offspring, animal models and *in vitro* studies have the capability to offer evidence supporting the causality and underlying mechanism.

Animal models demonstrate elevated cytokines in the foetal brain in response to MIA (Gilmore, Jarskog and Vadlamudi, 2005; Meyer *et al.*, 2006; Fatemi *et al.*, 2008; Urs Meyer *et al.*, 2008; Arrode-Brusés and Brusés, 2012; Garay *et al.*, 2013). For example, the injection of Poly I:C during mid- or late gestation causes IL-1β, IL-6, IL-10, TNFα, IL-17, MCP-1, and MIP-1α levels in the mother's serum to significantly increase in rodent models (Gilmore, Jarskog and Vadlamudi, 2005; Meyer *et al.*, 2006; Koga *et al.*, 2009; Arrode-Brusés and

Brusés, 2012), thereby giving mechanistic causality to the aforementioned human birth cohort study by Allswede *et al.* (2020) to present the concept that maternal infection raises cytokine levels in the foetal brain is a risk factor for NDD. Furthermore, in terms of specific cytokine influence, increased maternal IL-17A or IL-6 alone have also been sufficient shown to influence neurodevelopment and give risk to NDD-relevant behaviours (Smith *et al.*, 2007; Choi *et al.*, 2016). A study of control and pregnant dams pre-treated with IL-17A-blocking antibodies revealed that IL-17A is an influencing factor for alteration of cortical lamination in offspring following maternal Poly I:C exposure at GD14.5, as shown in ASC patients (Choi *et al.*, 2016). In addition, according to Smith *et al.* (2007), IL-6 plays a crucial role in mediating the effects of the maternal immune response on the foetus, and the subsequent risk for NDD development in the offspring. This study will be discussed in detail in later sections. Collectively, data from animal MIA models demonstrate the heightened cytokine response observed in maternal serum during pregnancy is adequate to induce alterations in cytokine levels within the foetal brain. However, it has remained unclear whether MIA leads to changes in brain cytokines in postnatal offspring.

In terms of studying mechanistic links between cytokines and MIA within a human context, human cell *in vitro* models are valuable for studying cell-specific responses to various cytokines. Demonstrating this practicality, the Lund human mesencephalic (LUHMES) cell line was used to simulate the effects of MIA-associated cytokines on neurodevelopment (Matelski *et al.*, 2021). The LUHMES cell line is an immortalised human mesencephalic neural progenitor cell line; it is a subclone of the tetracycline-controlled, v-myc-over-expressing human mesencephalic-derived cell line MESC2.10 with dopaminergic characteristics (Scholz *et al.*, 2011). This *in vitro* model was exposed to groups of various cytokine mixtures, including cytokines increased in maternal mid-gestational serum collected from the Early Markers for

Autism study (EMA) (Jones *et al.*, 2017), an inflammatory cytokine mixture (ICM) of five cytokines elevated in experimental MIA models, and individual cytokines (Table 1.2). The EMA cytokines were applied at physiologically matched "biologically plausible" concentrations from the Early Markers for Autism study (Jones *et al.*, 2017), whereas ICM and individual cytokine concentrations were applied at the same concentrations as EMA, with an additional increasing factor of 10 (Matelski *et al.*, 2021). In these three distinct MIA modelling circumstances, apoptosis, neurite outgrowth, and synapse quantity were all assessed. Changes in cytokine receptor expression, synaptic density, and neurite outgrowth were seen in an ICM cytokine dose- and age-dependent way, with only 1000X the concentration phenocopying EMA (Matelski *et al.*, 2021). Preclinical rodent MIA models (Coiro *et al.*, 2015) and *post-mortem* brain tissue samples from diagnosed people with SZ (Glantz and Lewis, 2000) and ASC (Martínez-Cerdeño, 2017) have shown such synaptic alterations to dendritic spine density and spine dynamics. Maximum dosages of both the EMA and ICM cytokine groups caused apoptosis in LUHMES cells, but individual cytokines had little effect on cell survival or neurite outgrowth (Matelski *et al.*, 2021). These findings show that a combination of cytokines, rather than a single cytokine, have the capacity to affect critical neurodevelopmental phenotypes of human neuron-like cells in a dose- and age-dependent manner. Having said this, although the combined effect of cytokines was found to have a stronger impact than that of any individual cytokines, the specific cytokine or cytokines accountable for these effects remain unclear from this study alone.

Table 1.2 – Groups of cytokines examined for MIA-associated phenotype risk mediation by Matelski et al. (2021). ECM = Cytokines increased in maternal mid-gestational serum samples of children with autism and intellectual disability. ICM = inflammatory cytokine mixture of five cytokines heightened in experimental MIA models. Abbreviations as follows: IL = interleukin, IFN = interferon, TNF = tumour necrosis factor, GM-CSF = granulocyte-monocyte colony-stimulating factor, MCP = monocyte chemoattractant protein, MIP = macrophage inflammatory protein.

Group	Cytokines
EMA	IFN-γ, IL-4, IL-17A, TNFα, IL-1α, IL-1β, IL-6, IL-10, GM-CSF, IL-8, MCP-1, MIP-1α
ICM	TNFα, IL-1β, IL-6, IFN-γ, IL-17A

Overall, these studies reveal that, at least in part, the prenatal maternal peripheral cytokine profile underlies the elevated risk for NDD pathology in the offspring or stimulated cells (Meyer, 2014; Careaga, Murai and Bauman, 2017; Graham *et al.*, 2018; Rudolph *et al.*, 2018; Rasmussen *et al.*, 2019, 2021; Allswede *et al.*, 2020; Matelski *et al.*, 2021; Mueller *et al.*, 2021; Potter *et al.*, 2023). While these findings are not always consistent, there is mounting evidence that IL-6 may function on the prenatal brain as a sensor, effector, and transducer of environmental risk factors (Ozaki *et al.*, 2020; Allswede *et al.*, 2020). This point of view is compatible with genetic and blood biomarker studies that show elevated IL-6 expression in a range of mental diseases, and it is crucial to note that it is not limited to prenatal timepoints (Smith *et al.*, 2007; Graham *et al.*, 2018; Rudolph *et al.*, 2018; Rasmussen *et al.*, 2019, 2021; Ozaki *et al.*, 2020; Perry *et al.*, 2021). Specifically, in Mendelian randomization (MR) studies, genetically predicted IL-6 is associated with increased risk for SZ in univariable MR (Perry *et al.*, 2021). Having said this, and returning to the prenatal MIA context, the mechanisms by which prenatal and postnatal MIA exposure confers NDD risk are likely to be explained by unique cellular and/or molecular processes. These findings raise a few questions: why IL-6 is so commonly detected in these investigations, and can maternal IL-6 influence the prenatal MIA risk for NDDs in the offspring?

1.2.4 Interleukin-6 Function and Signalling Mechanisms

Interleukin 6 (IL-6) is a pleiotropic cytokine that is secreted by various types of cells in the body, including immune cells, endothelial cells, and some types of tumour cells (Rose-John *et al.*, 2009; Hunter and Jones, 2015). It is a small protein that acts as a signalling molecule in the immune system, involved in a wide range of biological processes such as inflammation, immune response and hematopoiesis (Peters *et al.*, 1997). It has both pro-inflammatory and anti-inflammatory effects, depending on the context in which it is produced, and the target cells it interacts with (Scheller *et al.*, 2011).

The IL-6 receptor is composed of two subunits: a ligand-binding subunit called IL-6Ra (also known as gp80) and a signalling subunit called the IL-6 signal transducer (IL-6ST, also known as gp130) (Rose-John, 2001). The binding of IL-6 to IL-6Ra induces a conformational change in the receptor that allows it to associate with IL-6ST. This dimerization of the receptor complex activates the intracellular domain of IL-6ST, which then recruits and activates various intracellular signalling molecules (Wolf, Rose-John and Garbers, 2014). Yet, the IL-6 signalling pathway can be activated by two distinct mechanisms: cis-signalling and trans-signalling (Wolf, Rose-John and Garbers, 2014). These mechanisms differ in the way IL-6Ra is expressed on the surface of target cells (Figure 1.1).

Cis-signalling occurs when IL-6Ra is expressed on the cell surface membrane as a transmembrane receptor. In this case, IL-6 binds to the IL-6Ra on the cell surface, which is then associated IL-6ST (Figure 1.1) (Wolf, Rose-John and Garbers, 2014). On the other hand, trans-signalling occurs in cells which do not express IL-6Ra on the cell surface but do express IL-6ST. In this case, IL-6 binds to soluble forms of the IL-6 receptor (sIL-6Ra), which can be produced by proteolytic cleavage of the transmembrane domain of IL-6Ra by a disintegrin and

metalloprotease 17 (ADAM17), or by alternative splicing of the *IL6R* gene by cells that express this receptor (Figure 1.1) (Müllberg *et al.*, 1999). The soluble receptor can then bind to IL-6 and activate cells that do not express the full receptor complex, including endothelial cells, fibroblasts, and immune cells in peripheral tissues (Rose-John, 2001, 2012; Wolf, Rose-John and Garbers, 2014). IL-6Ra is found to be mostly highly expressed by microglia and in part by astrocytes in both the foetal and adult human brain, but not neurons (Zhang *et al.*, 2016). Both cis- and trans-signalling can contribute to the overall effects of IL-6 in the body. An important distinction, however, is evidence that suggests trans-signaling via sIL6R is a mechanism for pathogenic IL-6 action on non-glial cell types (Campbell *et al.*, 2014). This was demonstrated by blocking trans-signalling with soluble IL-6ST in mice, resulting in a reduction of various neuropathological changes typically observed in the mice with induced overexpression of IL-6 in the CNS (Campbell *et al.*, 2014). These changes included astrogliosis and microgliosis, blood-brain barrier leakage, vascular proliferation, neurodegeneration, as well as the restoration of impaired neurogenesis (Campbell *et al.*, 2014). Furthermore, the initiation of either IL-6 trans- or classic signalling is considered to be solely dependent on the expression ratios of the receptor complex's subunits (Reeh *et al.*, 2019).

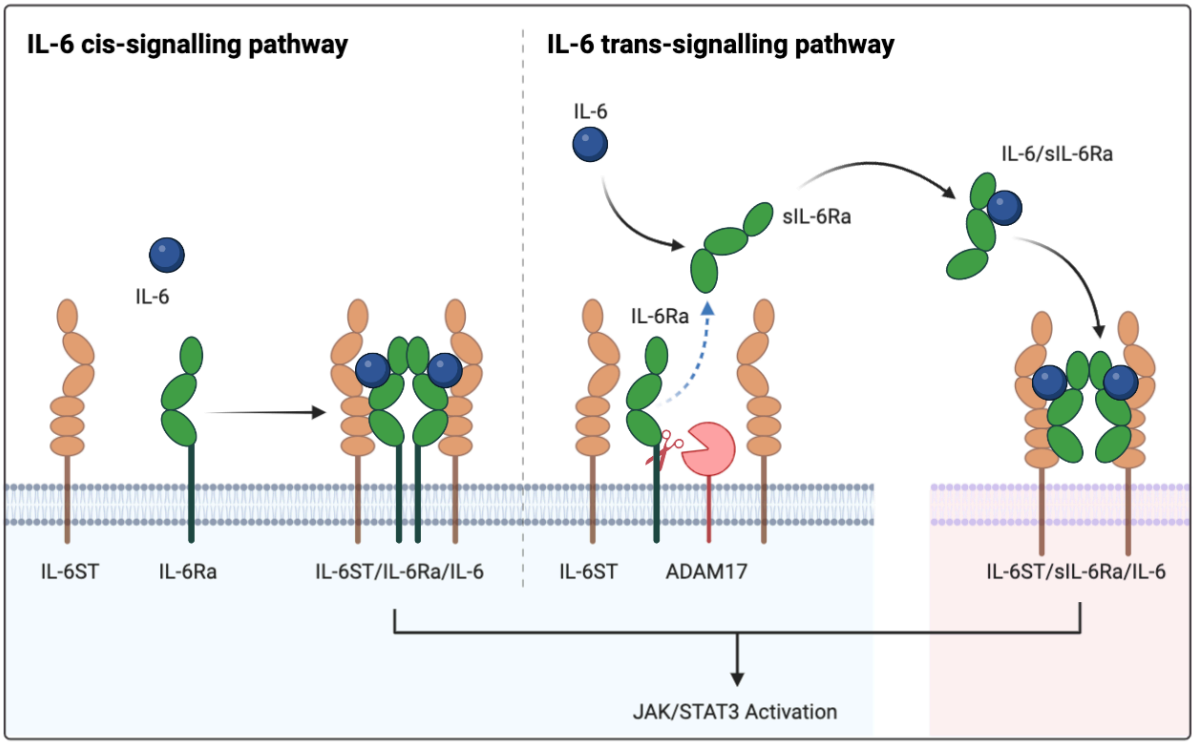

Figure 1.1 – The two distinct mechanisms of IL-6 signalling: cis-signalling and trans-signalling. When IL-6Ra is expressed as a transmembrane receptor on the cell surface membrane, cis-signalling takes place. In this instance, IL-6 binds to the cell's IL-6Ra, which is connected to the IL-6ST. Trans-signalling, on the other hand, takes place in cells that express IL-6ST but not IL-6Ra on their cell surfaces. In this instance, IL-6 binds to soluble versions of the IL-6 receptor (sIL-6Ra), which can be created by alternative splicing of the IL6R gene by cells that express this receptor or by proteolytic cleavage of the transmembrane domain of IL-6Ra by ADAM17. Cells that don't express the entire receptor complex can then be activated by the soluble receptor binding to IL-6. Initiation of the IL-6ST dimerization leads to STAT3 phosphorylation and the activation of the JAK/STAT3 pathway activation.

One of the primary signalling pathways activated by IL-6 is the Janus kinase/signal transducer and activator of transcription (JAK/STAT) pathway. This pathway involves the activation of the JAK family of tyrosine kinases, which then phosphorylate and activate the STAT family of transcription factors (Rose-John, 2001, 2012; Scheller *et al.*, 2011; Wolf, Rose-John and Garbers, 2014). The activated STAT proteins then translocate to the nucleus, where they regulate the expression of specific target genes involved in immune response and inflammation.

In both IL-6-induced trans- and classic signalling, classical intracellular JAK/STAT signalling is indifferent (Reeh *et al.*, 2019).

The Correlation of Increased Maternal IL-6 and Neurodevelopmental Disorder Risk in the Offspring

An increasing number of human and animal model studies have been conducted to determine a clearer causal relationship between elevated prenatal IL-6 concentrations and an increased risk of NDDs in the offspring (Table 1.3). Human birth cohort data show that higher levels of maternal serum steady-state IL-6 concentrations during pregnancy are associated with larger right amygdala volume and stronger bilateral amygdala connectivity in the offspring, which influences both network development and some externalising behaviours (Graham *et al.*, 2018; Rudolph *et al.*, 2018; Rasmussen *et al.*, 2019, 2021). Using machine learning it is also possible to estimate the mean maternal IL-6 concentration from functional connectivity patterns, as measured from resting state fMRI scans of the offspring (Rudolph *et al.*, 2018). In support of maternal IL-6's critical function in foetal development, an ex vivo isolated cotyledon human placental perfusion model revealed that IL-6, but not IL-1α or TNFα, is transferred bidirectionally between mother and foetus (Zaretsky *et al.*, 2004). This supports the notion that IL-6 is a potential mediator for the transduction of MIA risk to offspring, leading to NDDs.

In animal models, several studies have found that IL-6 may play a more important role than other cytokines in shaping long-term phenotypes in offspring than other cytokines such as IL-1α or TNFα (Samuelsson *et al.*, 2006; Smith *et al.*, 2007; Ozaki *et al.*, 2020; Mirabella *et al.*, 2021). *IL6* transcripts are persistently raised in the maternal liver, placenta, and foetal microglia following MIA induction by Poly I:C in mice at GD12 and GD15 (Ozaki *et al.*, 2020). Furthermore, acute prenatal IL-6 administration into pregnant mice on GD12.5 mimics

influenza and Poly I:C-induced behavioural phenotypes with relevance for NDDs in rodent MIA models (Smith *et al.*, 2007) (Table 1.3). By blocking IL-6 signalling through genetic modifications to knockout IL-6 itself in pregnant mice or pharmacological means using an anti-IL-6 antibody administered at the time of stimulation, the detrimental effects of MIA on the foetal rodent brain and subsequent behavioural abnormalities in the adult animal were be eliminated (Smith *et al.*, 2007) (Table 1.3). This provides crucial evidence indicating that IL-6 plays a mediating role in transmitting the effects following immune system activation. Furthermore, IL-6 administration also promotes glutamatergic synapse development, resulting in overall brain hyperconnectivity and behavioural deficits relevant to human SZ and ASC phenotypes in adult offspring (Mirabella *et al.*, 2021) (Table 1.3). One pro-inflammatory function of IL-6 is to promote T_H17 cell development, resulting in the production of IL-17A (Lee *et al.*, 2012), another cytokine that is notably also believed to lead to behavioural deficits of relevance for ASC and SZ (Choi *et al.*, 2016). Finally, peripheral IL-6 levels remain increased in adult mouse offspring with behavioural abnormalities relevant for SZ and ASC following MIA exposure compared to offspring with no such deficits despite MIA in utero exposure (Mueller *et al.*, 2021).

Taken together, these data from human cohort, blood biomarker, genetic and animal model studies suggest that IL-6 plays an important role in modulating MIA risk for NDD in children, as IL-6 appears to be a critical sensor, effector, and transducer of the mother immune response to the foetus (Table 1.3). Identifying the mechanisms through which prenatal maternal IL-6 increases this risk could assist in the reduction of an offspring's NDD risk by identifying techniques to block its detrimental mechanisms. The current limitations of animal MIA models could be hindering this progression and are outlined in the following section.

Table 1.3 – Evidence from human birth cohorts, animal and in vitro models of atypical neurodevelopment after heightened prenatal maternal IL-6.

Theme	Observation	Relevance for Human NDD	Model	Citation
Behavioural	Decreased prepulse inhibition in offspring	Decreased sensorimotor gating and inability to filter out irrelevant information, found in SZ	Pregnant mice exposed to IL-6 on GD12.5	Smith *et al.*, 2007
	Decreased latent inhibition in offspring	Shows an inability to learn from a stimulus with reward or adverse consequences, associated with psychosis	Pregnant mice exposed to IL-6 on GD12.5	Smith *et al.*, 2007
	Increased maternal IL-6 concentrations associated with lower impulse control in 2 years old children	Individuals with NDDs are found to have lower impulse control	Human maternal-child correlation cohort	Graham *et al.* 2018
Neuro-transmitter Systems	Increased $GABA_A$ alpha 5 receptor and NDMA-receptor NR1 subunit expression in hippocampus of offspring	As in table 1.1, GABAergic transmission abnormal in those with SZ, BD and depression due to GAD67 expression reduction in humans; the enzyme responsible for GABA production	Pregnant dams exposed to IL-6 on GD8-12 or GD16-20	Samuelsson *et al.*, 2006
	Increased glutamatergic synapse development in hippocampal cells in offspring	Glutamate neurotransmission changes found in SZ	Pregnant mice exposed to IL-6 on GD15	Mirabella et al 2021
Morphology and Neurogenesis	Abnormal hippocampal structural and morphology in offspring	The hippocampus is responsible for learning and cognition, with morphological abnormalities identified by MRI in children with ASC, foetal alcohol spectrum disorders, Rett and Fragile C syndromes	Pregnant dams exposed to IL-6 on GD8-12 or GD16-20	Samuelsson *et al.*, 2006
	Larger right amygdala volume in offspring	MRI reports of amygdala differences in children with ASC and Fragile X syndrome, adolescents and adults with ASC, SZ, paediatric BD and William's and Fragile X Syndrome	Human maternal-child correlation cohort	Graham *et al.* 2018
	Stronger bilateral amygdala connectivity in offspring		Human maternal-child correlation cohort	Graham *et al.* 2018
	Average maternal IL-6 concentration during pregnancy inversely associated with main frontolimbic fibre tract volume in the neonates, proximal to the amygdala, and through the first year of life		Human maternal-child correlation cohort	Rasmussem *et al.*, 2019
	Early-childhood pars triangularis volume jointly linked with maternal IL-6 and childhood nonverbal fluid intelligence	Fluid intelligence describes abstract thinking and adaptability. It is positively corelated with individuals with high-functioning ASC and developmental language disorders	Human maternal-child correlation cohort	Rasmussen *et al.*, 2021

	Modelling the functional connectivity within and between multiple new-born neural networks can estimate maternal IL-6 concentrations during pregnancy	Functional connectivity is aberrant in infants with impaired language skills, ADHD and ASC	Human maternal-child correlation cohort	Rudolph *et al.*, 2018
	Increased IL6 expression in maternal liver, maternal placenta and primary foetal microglia	IL-6 consistently up-regulated through these tissues identify it as a transducer of MIA from mother to foetus	Pregnant mice exposed to Poly I:C on GD12 or GD15	Ozaki *et al.*, 2020

1.2.4 The Current Limitations in the Maternal Immune Activation Field

Animal MIA Model Limitations

Animal MIA models are essential to determine the relationship between MIA and altered offspring neurodevelopment. Yet, such models are also associated with important caveats. First, the animal brain development differs from human brain development in terms of gene regulatory networks as well as cellular proliferation mechanisms (Fougerousse *et al.*, 2000; Hansen *et al.*, 2010; Yokoyama, Zhang and Ma, 2014; Rockowitz and Zheng, 2015). Second, humans have a much longer developmental timeline than animal models, which causes significant disparities in complicated spatiotemporal developmental networks (Zhao and Bhattacharyya, 2018). Third, distinct human genetics result in differences in molecular pathway regulations between humans and animals (Zeng *et al.*, 2012). Conclusions achieved in animal MIA models might therefore be questioned in terms of their applicability to human physiology.

It should also be noted that findings from animal MIA models published in the literature are often contradictory, raising concerns about reproducibility (Smolders *et al.*, 2018; Mueller *et al.*, 2019). This is most likely due to variation in maternal immune responses across rodent strains, as well as variation in gestational timing, dose, frequency, route of administration across laboratories, and batch differences in TLR3 or 4 agonist potency from different vendors (Smolders *et al.*, 2018; Mueller *et al.*, 2019). Poly I:C molecular weight may even be used to

predict rat maternal IL-6 response and litter size, as well as placental weight and male-specific reductions in foetal brain weights (Kowash *et al.*, 2019). As a result, concerns have been expressed about comparing Poly I:C animal MIA model results from different labs, emphasising the necessity of Poly I:C quality control for effective animal MIA models (Mueller *et al.*, 2018, 2019). Recent revisions to animal MIA model reporting requirements have pushed researchers to focus on specifics associated with individual techniques rather than variations in methodology themselves, in order to find more precise reasons impacting MIA result heterogeneity (Kentner *et al.*, 2019).

It may also be suggested that current practices in the use of animals to study MIA are not in lines with guidance put forward by the National Council for the Reduction, Refinement and Replacement of the use of animals in biological research (NC3Rs). Specifically, in multiparous species such as rats, after exposure of the dam to a stimulus to induced MIA, it is common practise to select 1-2 offspring from each litter at random for participation in an experimental group to control for within-litter effects (Mueller *et al.*, 2021). Although experimental evidence suggests this is a valid strategy, since the variance in the presence or absence of a phenotype is greater within, than between litters (Mueller *et al.*, 2021), this has the potential to lead to inclusion of animals without a phenotype in experimental groups and may result in large numbers of offspring going unused depending on the study design. Furthermore, the bulk of studies have focused solely on males, with the female offspring often culled – not only is this inherently wasteful and not in line with NC3Rs policy, it also has resulted in a paucity of understanding concerning the role of biological sex on MIA traits. As a consequence of these practices, a significant number of dams and litters are often necessary to produce sufficient power and statistically valid data, resulting in the waste of many animals. Data from our own surveys of the literature suggest that on average, the MIA research community uses roughly

200 rats for this purpose each year, and the Vernon Lab's collaborators utilise at least 300 mice per year to model MIA (Mueller *et al.*, 2021; Meyer, 2014). Approximately 25-50% of this research use molecular or cellular techniques that, ideally, might be replaced by a human *in vitro* model (Richetto *et al.*, 2017; Notter *et al.*, 2018). It is crucial to note, however, that animal models of MIA are still absolutely required for behavioural and systems-level studies, such as neuroimaging. As a result, decreasing the use of animals is a more attainable goal than replacing the, all together. Transitioning from animal models to a human-based *in vitro* system could result in a future reduction of 50 to 100 rats per year, or 25 to 50%, in upcoming studies.

Importantly, MIA models are used most frequently to investigate changes to behavioural and neurogenesis phenotypes in adult endpoints. Only a small number of animal studies have investigated the proximal cellular or molecular phenotypes that are specifically downstream of the maternal immune response in the foetal brain. This is significant because understanding the most proximal molecular steps underlying MIA may provide key treatment strategies for preventing subsequent disease. As a result, our understanding of the effects of MIA on human neurodevelopment, particularly at the molecular functional level, is limited (Schepanski *et al.*, 2018).

The Lack of Neurodevelopmental Disorder Models that Combine Both Environmental and Genetic Risk Factors

Clearly, the research presented in section 1.1.2 of this chapter indicates that NDD risk factors can arise from both genetic and environmental sources. Yet, the majority of these studies look specifically at one individual risk agent. It is improbable that a person would be exposed to only one of these risk variables in typical human physiological settings. Both genetic and environmental risk factors might present in unique combinations to an individual, resulting in

various risk levels to commence disorder precipitation, or not, depending on the scenario. To more properly predict and understand the development of NDDs, it is necessary to consider both types of risk sources; genetic and environmental.

Importantly, a person's unique genetic background might result in distinct responses to environmental risk factors for NDDs. For example, foetal loci for immune function were identified to independently impact maternal immune mediators in a genome-wide association analysis (Traglia *et al.*, 2018), the response to MIA by maternal and neonate cytokine serum concentrations could therefore be argued to be genetically programmed. Thus, particular cytokines contribute to the risk of neurodevelopmental disorders through altering neurodevelopment, as dictated by genetic variables. Such studies give evidence for the need for NDD models to integrate both environmental and genetic factors in order to better comprehend the aetiology of NDDs by studying their risk interaction.

The immune system plays a crucial role in mediating the interaction between the external environment and internal physiological and biochemical processes (Rook, 2013). As a result, environmental influences on the immune system during critical developmental periods of prenatal programming can potentially "pre-set" an individual's susceptibility to future behavioural or psychiatric disorders. However, it is evident that not all mothers who experience an immune response during pregnancy have children with NDDs. These concepts raise fundamental questions regarding the mechanisms that define vulnerability or resilience in the face of prenatal and postnatal environmental risk factors, MIA, and stress. Moreover, it urges us to contemplate the most effective approaches for modelling and studying these factors in our research. Notably, certain infants who are exposed to prenatal genetic and environmental risks show resilience to neurodevelopmental disorders and healthy until adulthood (Meyer, 2019). However, a subsequent exposure to high-risk environmental stimuli, like drug exposure

or systemic infection, can trigger the onset of neurodevelopmental disorders in later stages of life (Bayer, Falkai and Maier, 1999; Giovanoli *et al.*, 2015; Meyer, 2019). Therefore, MIA exposure may lead to a "latent insult" that predisposes infants to develop psychopathology in adulthood only after further environmental "hits". The interaction between offspring sensitivity and resilience to MIA is now being studied, with the idea that risk variables reach a tipping point during a sensitive stage of development, prior to the onset of neurodevelopmental abnormalities (Meyer, 2019; Mueller *et al.*, 2021). Studies such as these must be built on by including both genetic and environmental risk sources.

Many of the concerns raised in this section might be addressed by using human induced pluripotent stem cell (hiPSC) technologies to create a novel *in vitro* MIA model. Complementary to epidemiological and animal MIA models, implementing a human based system to more closely mimic human neurodevelopment at relevant timepoints with both genetic and environmental risk factors would be valuable. Such a model can also be used to determine the extent to which animal MIA model conclusions can be translated to human physiology, particularly at the molecular and cellular levels.

1.2 Building a Human *in vitro* Model for Neurodevelopmental Disorders

1.2.1 Human Induced Pluripotent Stem Cells

Human induced pluripotent stem cells (hiPSCs) are a type of stem cell that can be generated via transforming adult somatic cells back into an embryonic-like pluripotent state. The discovery of hiPSCs is a relatively recent one, with the first successful creation of mouse iPSCs reported in 2006 by Shinya Yamanaka's group at Kyoto University in Japan (Takahashi and

Yamanaka, 2006). Yamanaka and his colleagues were able to convert mouse fibroblast cells into pluripotent stem cells by exposing them to a cocktail of four transcription factors known as the "Yamanaka factors": Oct3/4, Sox2, Klf4, and c-Myc (Takahashi and Yamanaka, 2006). These variables were chosen based on their known involvement in sustaining embryonic stem cell pluripotency (Qi and Pei, 2007). Yamanaka and his colleagues were encouraged by the success of this mouse work to attempt the same feat in human cells. They revealed in 2007 that they could create hiPSCs from human fibroblasts using the same four transcription factors (Takahashi *et al.*, 2007). This was a ground-breaking advance, since it provided a method for producing pluripotent stem cells without the use of human embryos, which had previously been the principal source of human embryonic stem cells.

Researchers have continued to improve the methods used to generate and characterise hiPSCs since their discovery. The landmark discovery of hiPSC technology has now spread to various areas of research (Takahashi and Yamanaka, 2006; Hoffman *et al.*, 2019). HiPSCs may develop into numerous types of cells in the body, making them an attractive research, drug discovery, and regenerative medicine tool. In addition, hiPSCs have since been created from a wide range of somatic cell types, including keratinocytes (Aasen *et al.*, 2008) and blood cells (Loh *et al.*, 2009), in addition to fibroblasts. The technology is also being used in disease models and drug development, with researchers studying a wide range of diseases, from genetic abnormalities (Yamasaki, Panopoulos and Belmonte, 2017) to neurological diseases (Saporta, Grskovic and Dimos, 2011) and cancer (Marin Navarro *et al.*, 2018). More than a decade later, there is potential for hiPSC applications in drug discovery and screening, *in vitro* disease aetiology modelling, personalised medicine, and cell replacement therapy (Yamanaka, 2012). Given the basic limitations of animal models, using hiPSC for *in vitro* disease modelling in combination with animal models can assist to minimise and refine animal models.

To this end, one significant feature of hiPSC-derived model systems in this regard is their application for pathological exploration of cellular and molecular dysfunction with human relevance, particularly in completely inaccessible organs such as the human embryonic developing brain. Outside of hiPSCs, investigations in mimicking human neurodevelopment are severely limited, with the earliest developmental tissues available for examination being IVF embryos that can be cultured *in vitro* for no more than 14 days (Pera, 2017; Deglincerti *et al.*, 2016). As a result, hiPSC-derived systems are presently the *in vitro* model choice, capable of demonstrating the complex early neurodevelopment processes predicted during human embryogenesis.

Arguably, the key benefit of hiPSCs when modelling polygenic disorders is their capacity to differentiate into various neuronal and glial lineages whilst retaining the unique genetic background of the donor which could be contributing to the mechanism behind their diagnosis. This enables the study of genetic variations across a diverse range of cell types, all with the same genetic background. Crucially, the inclusion of genetic variations allows for the modelling of polygenic diseases or conditions involving CNVs using donor lines that accurately mimic heritable traits, thereby surpassing the limitations of animal models in replicating such conditions. Taken together, hiPSC-derived cell models appear to be a well-suited choice to attempt to understand both gene and environmental mechanisms, and their interaction, which give risk for NDDs.

Examples of using Human Induced Pluripotent Stem Cells to Study the Influence of Immune Activation on Neurodevelopmental

Neurodevelopmental investigations on human tissue have seldom ventured beyond the analysis on individuals with specific NDD diagnoses *post-mortem*, as categorised by information according to the DSM-5 (Ishii and Hashimoto-Torii, 2015; Francés *et al.*, 2022). However, with the improvement of differentiation techniques to both neural and glial lineages in recent years (Hoffman *et al.*, 2019), investigators have elected to employ hiPSC-derived models in their neurodevelopmental studies. Considering the clinical and animal evidence presented in section 1.2.3 regarding specific cytokines or signalling pathways, it is logical to examine these agents in a simplified manner by introducing them externally to cells *in vitro* setting to observe the resulting effects on neurodevelopment. An example demonstrating this approach effectively is provided by Matelski *et al.* (2021), as mentioned earlier in section 1.2.3. However, it is important to note that a significant limitation of this study was the utilization of an immortalized cell line, which poses a challenge as it fails to replicate the genetic interactions since these cells are genetically manipulated to be immortalized. Thus, highlighting the importance and advantages of utilizing hiPSC models in such investigations.

Yet, only a few studies have attempted to investigate the effects of specific cytokines such as interferon (IFN-)γ (Warre-Cornish *et al.*, 2020; Bhat *et al.*, 2022) and IL-6 (Zuiki *et al.*, 2017; Kathuria *et al.*, 2022; Couch *et al.*, 2023; Sarieva *et al.*, 2023), or TLR3-agonists (Ritchie *et al.*, 2018; Park *et al.*, 2020) on neurodevelopment in a hiPSC-derived *in vitro* model. First, one of the earliest works to employ human neural aggregates to mimic the effects of MIA-related cytokine response on neurodevelopment was aimed at elucidating the molecular function of IL-6 (Zuiki *et al.*, 2017). Aggregates were subjected to a high dosage of IL-6 (100ng/ml) for 24 hours, and STAT3 phosphorylation demonstrated IL-6 pathway activation. IL-6 treatment

increased astrocyte (GFAP+) area ratio while decreasing neural progenitor cell (NPC; TBR1+ or CTIP2+) area ratio, implying a shift in cell fate differentiation or enhanced cell-specific death (Zuiki *et al.*, 2017). The observed increase in astrogliosis reflects the phenotype described in investigations into *post-mortem* human tissue from both control individuals and individuals with ASC aged between 4-21 years old, which similarly show evidence of increased expression of astrocyte markers in the prefrontal cortex and decreased expression of neuron specific markers were decreased in both the prefrontal cortex and cerebellum of individuals with ASC (Edmonson, Ziats and Rennert, 2014). These findings provide evidence of that the atypical gene expression specific to glial cells found in the brains of individuals with ASC could be mediated by IL-6.

Second, given the importance of IFN-γ in viral infection response, the effect of IFN-γ investigated in cortical neurons generated from hiPSCs (Warre-Cornish *et al.*, 2020; Bhat *et al.*, 2022). NPC monocultures were stimulated with the pro-inflammatory cytokine at a developmental time point corresponding to the late first to early second trimester. This resulted in widespread transcriptional changes that overlap with gene expression signatures measured in human *post-mortem* brain tissue from ASC and SZ, as well as increased neurite outgrowth, a hallmark phenotype of human neurons derived from donors with ASC genetic risk factors like Shank-3 deletion (Bhat *et al.*, 2022; Kathuria *et al.*, 2018a; Warre-Cornish *et al.*, 2020).

Third, LPS and Poly I:C pre-activated immortalised mouse microglia (BV2) cells grown on top of mesh inserts within the same well as hiPSC-derived cortical interneurons (cINs) disrupted metabolic pathways, arborization, synapse formation, and synaptic GABA release in the cINs (Park *et al.*, 2020). This metabolic change was not observed in SZ hiPSCs or glutamatergic neurons, and it lasted longer, indicating a possible link between SZ genetic

backgrounds and environmental risk factors, with glial activation possibly playing a causal role (Park *et al.*, 2020).

Together, these studies not only demonstrate the value of hiPSCs for exploring both neurons and microglia in co-culture, but also supports the concept of using an hiPSC-derived cellular model that incorporates control and high-risk genetic backgrounds to understand the effects of cytokines and specifically IL-6 on neurodevelopment.

Considerations for the use of Human induced pluripotent Stem Cells

Experiments employing hiPSC-derived model systems certainly give proof-of-concept for MIA. However, there are a few considerations to bear in mind when working with them, given the presence of heterogenicity seen within and across studies (Volpato and Webber, 2020; Anderson *et al.*, 2021; Dutan Polit *et al.*, 2023). Importantly, when using hiPSC models to address potential molecular mechanisms linking prenatal viral infections to increased risk for NDDs, methodological-specific influences should be discussed. A Zika virus study found lower brain organoid size due to a decrease in NPC number after 5 days of viral treatment, which resulted in TLR3 activation in NPCs, encouraging apoptosis (Dang *et al.*, 2016). A further investigation three years later, however, found no TLR3 signalling activity in ZIKV infection (Liu *et al.*, 2019). The distinction between both investigations was in the method of differentiation employed, with Dang and colleagues (2016) employing an organoid system and Liu and colleagues (2019) simply culturing NPCs in a 2D system. Specific hiPSC-derived tissues may not always fully exemplify the physiological process of MIA as well as animal models, as demonstrated by Liu and colleges using only NPCs to model Zika virus while ignoring potential pathophysiological contributions from other cell types and Matelski and colleges (2021) using conditionally immortalised LUHMES cells to model the developing

brain (Matelski *et al.*, 2021). As a result, the variability of 2D, 3D, or organoid culture limits the ability to compare research employing hiPSC-derived systems (Claus, Jung and Hübschen, 2020).

Keeping these caveats in mind, it may be suggested that overall, hiPSC-derived neurodevelopment models are ideally adapted to supplement animal models in the search of improved understanding of the aetiology of NDD caused by MIA. Although they are still in their early stages of use in the field of MIA research, their ability to bridge gaps in molecular information left by animal MIA models has already been demonstrated. So far, hiPSC-derived MIA systems have revealed the following: NPCs at the epicentre of MIA sensitivity, region- and cell-specific responses to MIA immunostimulants, and the relevance of cytokines such as IL-1β, IL-6, and IFN-γ in mediating the MIA-associated molecular phenotypes first identified in animal models and *post-mortem* tissue from individuals with NDDs (Ritchie *et al.*, 2018; Park *et al.*, 2020; Warre-Cornish *et al.*, 2020; Mirabella *et al.*, 2021; Bhat *et al.*, 2022; Couch *et al.*, 2023; Sarieva *et al.*, 2023). Furthermore, patient-specific hiPSC-derived MIA systems have enabled unique inquiry methodologies into genetic particular risk variables or disease diagnoses, by using hiPSCs donated from individuals with risk genotypes (Warre-Cornish *et al.*, 2020; Adhya *et al.*, 2021; Bhat *et al.*, 2022; Reid *et al.*, 2022). As a result, researchers may now look at how genetic and environmental risk factors combine to influence neurodevelopment. Therefore, prospective application of hiPSC-derived systems within the field of NDD research should be responsible for understanding the interaction of genetic and environment risk factors, with particular focus on understanding the translation of animal MIA model conclusions to human physiology. The data presented in the preceding sections clearly indicate that there is a distinct regulation of the immune system in individuals diagnosed with NDDs compared to those without a diagnosis. However, it is rather surprising that, apart from

animal models, there is a scarcity of studies investigating the glial immune response specifically within the context of NDDs using *in vitro* systems derived from hiPSCs. Existing studies have primarily emphasized the examination of neurons, neglecting an essential aspect, which is the role of microglia and thereby creating a gap of knowledge. Therefore, it is also crucial to shift focus towards studying microglial responses within models for NDDs.

1.2.2 Microglia and Neurodevelopmental Disorders

Microglia Ontogeny

Microglia are the resident immune cell of the CNS, and account for 10-20% of all cells in the CNS. Uniquely, microglia are thought to be derived from C-KIT$^+$/CD41$^+$ erythromyeloid progenitor (EMP) cells of the mesoderm's hematopoietic yolk sac (Ginhoux *et al.*, 2010; Hanger *et al.*, 2020; Kierdorf *et al.*, 2013; Menassa *et al.*, 2022), as opposed to a neuron's ontogeny originating in the ectoderm. These EMP cells are reliant on PU.1 and Irf8 for fate selection and survival, respectively, and vary from haematopoietic monocyte and macrophage development in that they lack Myb (Kierdorf *et al.*, 2013; Kierdorf and Prinz, 2013; Schulz *et al.*, 2012). Data from animals indicate that a subset of these EMPs begin to exhibit the chemokine receptor for fractalkine (CX3CR1$^+$ cells), which move to the brain between rodent GD9.5 and GD10.5 (Kierdorf *et al.*, 2013). Following the formation of the blood-brain barrier between GD13.5-14.5, microglia begin to self-renew and spread throughout the CNS (Ginhoux *et al.*, 2010; Gomez Perdiguero *et al.*, 2015). In humans, microglia migration into the developing brain occurs around gestation week (GW) 4-5, where microglia have been seen in the forebrain (Bloom and Bartelmez, 1940; Menassa *et al.*, 2022). Following peak haematopoiesis, microglia are discovered in the hindbrain metencephalon at GW6. This is followed by additional microglia identified in the spinal cord at GW9, and ultimately microglia

in the midbrain at GW19 (Choi and Lapham, 1978; Cho *et al.*, 2013; Hanger *et al.*, 2020; Menassa *et al.*, 2022).

The Array of Microglial Functions

Microglia are highly dynamic cells that may adopt a variety of functional and morphological states, resulting in considerable intra- and inter-regional variability in the brain (Lawson *et al.*, 1990; Grabert *et al.*, 2016; Eggen, Boddeke and Kooistra, 2019; Hanger *et al.*, 2020; Sharma and Tremblay, 2020). Transcriptional profiling investigations has demonstrated that various microglial states, each with potentially diverse functions, co-exist in the same tissue (Lawson *et al.*, 1990; Grabert *et al.*, 2016; Ransohoff, 2016; Eggen, Boddeke and Kooistra, 2019). These functions exist beyond the traditional M1 and M2 paradigms (Paolicelli *et al.*, 2022). Microglia can shift between various functional states by integrating genomic and genetic alterations with microenvironment and systemic signals, and thus play key roles in several brain processes such as brain development and synaptic plasticity, in addition to their traditional roles in mitigating tissue injury, infection, or disease (Wright-Jin and Gutmann, 2019; Mondelli *et al.*, 2017). Particularly, microglia have significant roles in both the developing and adult brains, with an ability to influence CNS development through a variety of mechanisms, including axon formation/guidance regulation and neural circuit refinement (Table 1.4). Within the context of the developing brain, microglia are thought to play a role in determining the appropriate number of synapses by controlling both synapse production and elimination, as well as moderating the proliferation and differentiation of neural progenitor cells (Squarzoni *et al.*, 2014; Wright-Jin and Gutmann, 2019). As a result, microglial activity must strike a balance between defending the brain from immune-based signals and sculpting the growing brain's neuronal networks. It should also be noted that astrocytes have a similar function in the establishment of synapses and neural progenitor cells (Matias, Morgado and Gomes, 2019).

Data from the mouse brain imply that microglia acquire these roles in a sequential way, owing to the activation of various transcriptional programmes and chromatin structure throughout microglia development from embryonic beginnings through to adulthood (Matcovitch-Natan *et al.*, 2016). Three distinct phases of microglial regulation are proposed to emerge during mouse brain development, each with potentially distinct functional effects: early microglia (cell cycle), pre-microglia (synaptic pruning and development), and adult microglia (immune surveillance and homeostasis) (Matcovitch-Natan *et al.*, 2016). Changes in histone modifications, chromatin accessibility, and expression programmes with unique indicators cause transitions between these phases (Matcovitch-Natan *et al.*, 2016). Early microglia, for example, are related with the expression of Dab2, Mcm5, and Lyz2, progressing to pre-microglia expression of Crybb1, Csf1, and Cxcr2, and eventually MafB, Cd14, and Mef2a in mature microglia (Matcovitch-Natan *et al.*, 2016). Changes to this stepwise programme have the evident potential to result in deleterious impacts in microglial function, impairing brain development, homeostasis, and immune defence. The evident disruption of microglia function caused by MIA during early stages carries the potential to increase an individual's susceptibility to the onset of neurodevelopmental disorders in later life. In fact, Matcovitch-Natan *et al.* (2016) demonstrated this phenomenon by showing that MIA negatively affected the developmental programming of microglia, compromising their intended developmental function (Matcovitch-Natan *et al.*, 2016).

Table 1.4 - The Numerous Functions of Microglia. Microglia functions are broadly classified as immunological, developmental, and homeostatic. These functions are further distinguished by the spectrum of microglial transformation states, which have either gain or loss of function impacts on the CNS.

Function	Neurotoxic	Neuroprotective
Immunological	Phagocytosis	
Developmental	Synaptic Elimination Targeted Neuron Cell Death	Synaptogenesis Neurite Formation Astrocyte Growth and Activation Myelinogenesis Axon Fasciculation NPC Growth and Differentiation Dendritogenesis
Homeostatic		Neuronal Surveillance Function

Evidence for the Role of Microglia in Neurodevelopmental Disorders

As previously extensively reviewed, microglia and the innate immune system are implicated in the pathogenesis of NDDs (Mondelli *et al.*, 2017; Coomey *et al.*, 2020). Animal model microglial depletion studies lend additional credence to the notion that microglia play a role in neurodevelopmental diseases. In particular, prenatal microglia reduction in mice alters the density and function of fast-spiking Parvalbumin inhibitory interneurons in a bi-phasic way from the juvenile to the adult phase of life (Thion *et al.*, 2019; Schalbetter *et al.*, 2022). This result is especially intriguing considering the long-standing data foundation for PV impairments in SZ (Bitanihirwe *et al.*, 2009), as well as ASC (Lauber, Filice and Schwaller, 2018). The growing evidence for microglia's multifaceted roles in brain development, as well as the findings from depletion studies, point to the possibility that manipulating microglia form and function during critical periods of brain development can induce a behavioural state in the animal that has some potential relevance for NDDs.

As previously mentioned, microglia are also essential in regulating neurodevelopment and the central immune response in order maintain homeostasis (Paolicelli *et al.*, 2011; Hanger *et al.*, 2020). Given that MIA has the greatest influence on microglial neurodevelopmental function

in early life (Matcovitch-Natan *et al.*, 2016), but also primes the immune system to respond more strongly to stress (Giovanoli *et al.*, 2013), malfunctioning microglia might result in atypical neurodevelopment (Knuesel *et al.*, 2014). Of importance, in offspring exposed to MIA, microglia exhibited reduced innate immune reactivity throughout their developmental trajectory, which is believed to be associated with the absence of an inflammatory state typically observed in microglia, as revealed by single-cell RNA-sequencing (Hayes *et al.*, 2022). The same dataset revealed enhanced fatty acid metabolism and a reduction of oxidative phosphorylation, suggesting a functional change to the respiratory and mitochondrial pathways in MIA microglia, which are often associated with regulation of shifts in functional state (Hayes *et al.*, 2022). These MIA microglia may therefore sensitise an individual to an altered immunological response after subsequent stress exposure, therefore having a hidden latent effect on the precipitation of phenotypes important for NDDs, such as synaptic engulfment.

However, it should be noted that the role of microglial activation in SZ remains debated, especially since much of the literature on the subject is derived from *post-mortem* studies. Specifically, it remains unclear whether microglial activation is a cause of SZ pathogenesis or if it's a secondary response to factors such as illness duration, antipsychotic medication, suicide, *post-mortem* delay, or patient age, since incidental lesions and microglial activation are more common in elderly patients (Cotel *et al.,* 2015; Steiner *et al.,* 2006, 2008; Kenk *et al.,* 2015). In addition, methodological challenges persist in studies that look to identify microglial activation in patients with SZ, in particular the lack of specific neuroimaging techniques with which to study microglia in the living human brain (Nutma et al., 2023). Importantly, there are notable problems with markers that are commonly used to assess microglial activation, such as translocator protein (TSPO) ligands in positron emission tomography (PET)-imaging. From these cross-species assessments, it appears that TSPO PET-imaging can reliably measure the

abundance of microglia (Matuleviciute *et al.,* 2023). However, it does not offer insights into the functional status of microglia, making it challenging to conclusively determine their role in the disease process of SZ, irrespective of whether it's related to maintaining homeostasis or causing harm. Furthermore, a recent study by Nutma et al. (2023) underscored that TSPO only reliably indicates microglial activation in rodents, not in humans (Nutma *et al.,* 2023; Notter *et al.,* 2018), making it even more challenging to identify the functional status of microglia in individuals with SZ. Overall, the current circumstantial evidence of microglial activation in patients with SZ lacks solid mechanistic inference, making it difficult to attribute SZ-related changes solely to microglial activation.

Currently, a few studies have utilized hiPSCs to investigate the involvement of neuron-microglia interactions in the context of SZ. Notably, in co-culture experiments with neurons, hiPSC-derived microglia from individuals diagnosed with SZ have exhibited a higher capacity for uptake of human synaptosomes compared to those derived from healthy donors (Schwieler *et al.*, 2015; Sellgren *et al.*, 2019; Breitmeyer *et al.*, 2023). These findings take on significant importance when considering the research conducted by Druart *et al.* (2021), discussed in section 1.1.2, which demonstrated that increased synaptic engulfment mediated by C4A led to impaired neuronal communication and the manifestation of SZ-related behaviours. Thus, these results suggest that microglia derived from SZ patients play a role in inducing a SZ phenotype. Moreover, these findings highlight the potential of utilizing hiPSCs to model the molecular mechanisms underlying SZ.

However, studies that have used hiPSC-derived *in vitro* to specifically mimic prenatal MIA risk for NDDs have focused solely on neurons or astrocytes, at the cost of human microglia with no studies to date (Russo *et al.*, 2018; Park *et al.*, 2020; Warre-Cornish *et al.*, 2020; Bhat

et al., 2022). Importantly, none of the studies employing organoids to understand the role of MIA in neurodevelopment incorporated microglia in their studies, given current methods for generating human cerebral organoid cultures from hiPSCs do not include the generation of microglia due to their differences in ectoderm and mesoderm differentiation lineages (Zhang *et al.*, 2023). However, new methods for changing this have only recently been developed (Zhang *et al.*, 2023). As a result, there is a scarcity of evidence on the effect of IL-6 on these crucial immune-effector cells in a human-relevant paradigm. To examine the impact of immune activation on neurodevelopment, it is therefore critical to include human microglia into hiPSC models or add hiPSC-derived microglia into developed organoids (Gonzalez, Gregory and Brennand, 2017; Russo *et al.*, 2018).

1.4 Project Aims, Objectives and Hypotheses

In summary, several important points can be highlighted from the literature reviewed in this chapter. Markedly, there exists a correlation between MIA and an elevated susceptibility of offspring to NDDs. However, there is a scarcity of research examining the immediate effects in models that closely resemble humans. Additionally, while the involvement of microglia in this context has been implicated, their role remains understudied. Nevertheless, there is promise in utilizing hiPSCs for further investigation, as they possess the ability to incorporate the genetic background of the donor and can be differentiated into various cell types. By leveraging this potential, researchers can gain valuable insights into the mechanisms underlying MIA-related NDDs and pave the way for future advancements in the field. Hence, this thesis has the following overall and specific aims, and hypotheses for investigation.

1.4.1 Project Aim

To develop, validate and utilise a human induced pluripotent stem cell model to capture 22q11.2 deletion genotype by IL-6 interactions, in both neurons and microglia, with human-relevance for studying the pathophysiology of neurodevelopmental disorders.

1.4.2 Specific Objectives and Sub-Aims

Objective 1: Develop and phenotype a multi-cell type hiPSC model to study IL-6 response mechanisms as a proxy for prenatal maternal immune activation.

Aim 1: to determine the optimal dose, timing, and length of IL-6 cytokine exposure, starting with monocultures of neural progenitor cells and microglial like cells derived from human induced pluripotent stem cells, and then progressing to co-cultures of both neural progenitor cells and microglial like cells.

Aim 2: to examine the effects of IL-6 exposure on human-induced pluripotent stem cell cultures differentiated into neural and microglial cells, both in the short and long term. This will be accomplished by analysing changes in gene expression through RNAseq and observing cellular markers for GABAergic and glutamatergic cells in confocal imaging of long-term differentiated cortical neurons.

Objective 2: Use the hiPSC Model to Study if the effect of IL-6 is distinct on a 22q11.2 deletion region genotype background.

Aim 3: to apply the established hiPSC-derived model to explore the interaction between high-risk genes and environmental stimuli. This investigation will involve comparing the endpoints mentioned in Aim 2 in NPC-MGL co-cultures derived from hiPSCs obtained from healthy

donors and those carrying a specific genetic risk for neurodevelopmental disorders, in this case the 22q11.2 deletion, that are also exposed to IL-6.

1.4.3 Hypotheses under investigation

Hypothesis 1: comprehensive and physiologically relevant hiPSC-derived models of maternal immune activation are currently lacking. Therefore, the first hypothesis is that the exposure of forebrain neuronal cultures to IL-6 will lead to atypical development of GABAergic and glutamatergic synapses in mature cortical neurons, as well as gene expression patterns in neurons and microglia that will resemble data obtained from *post-mortem* brain tissue of individuals with Autism Spectrum Condition and Schizophrenia.

Hypothesis 2: Individuals carrying certain high-risk gene variants, such as the 22q11.2 deletion, have an increased likelihood of developing psychiatric symptoms. Based on this, the second hypothesis is that mimicking maternal immune activation with an IL-6 stimulation will interact with a pre-existing genetic risk factor, the 22q11.2DS genotype, to induce a wider range and greater severity of cellular and molecular phenotypes in the derived hiPSC model.

Chapter 2

General Methods

2.1 Cell Culture

2.1.1 Human induced pluripotent stem cell culture

Participants were recruited and methods carried out in accordance with the 'Patient iPSCs for Neurodevelopmental Disorders (PiNDs) study' (REC No 13/LO/1218). Informed consent was obtained from all subjects for participation in the PiNDs study. Ethical approval for the PiNDs study was provided by the NHS Research Ethics Committee at the South London and Maudsley (SLaM) NHS R&D Office. Human induced pluripotent stem cells (hiPSCs) were derived from keratinocytes donated by both males and females ranging from 17-60 years old, with and without 22q11.2 deletions (Table 2.1). The hiPSC lines were reprogramed by introducing C-MYC, KLF4, OCT4 and SOX2 TF in a polycistronic excisable vector, transformed with CytoTune-iPS 2.0 Sendai Reprogramming Kit (ThermoFisher, A16517). Reprogramming and quality control or reprogrammed hiPSC lines was carried out by previous members of the Price and Srivastava Labs (Adhya *et al.*, 2021; Deans *et al.*, 2017; Kathuria *et al.*, 2018a; Reid *et al.*, 2022; Shum *et al.*, 2015).

Table 2.1 - Characteristics of donor lines used throughout this thesis.

Donor	Line Clone	Genotype	Reprogramming	Cohort	Age	Sex
014_CTM	014_CTM_02	Control	CytoTune™ Sendai	LEAP / StemBANCC	18-30	Male
	014_CTM_03					
	014_CTM_04					
M3_CTM	M3_CTM_36S	Control	CytoTune™ Sendai	EU-AIMS	18-30	Male
	M3_CTM _37S					
	M3_CTM _38S					
127_CTM	127_CTM_01	Control	CytoTune™ Sendai	EU-AIMS	51 - 60	Male
	127_CTM_03					
	127_CTM_04					
069_CTF	069_ CTF_01	Control	CytoTune™ Sendai	EUAIMS / StemBANCC	31-50	Female
287_SZM	287_SZM_01	22q11.2DS	CytoTune™ Sendai	LEAP / StemBANCC	18-30	Male
509_CXF	509_CXF_05	22q11.2DS	CytoTune™ Sendai	GQAIMS / StemBANCC	11-17	Female

Table 2.2 - The 22q11.2 region and its correlation with the donor's clinical status. The table provides information about the overall number of affected genes in this region for each of the 22q11.2DS donor used, including the count of deleted and duplicated genes. Analysis carried out by Bjørn Hanger from the Vernon Lab. Data for 287_SZM_01 published by Reid et al. 2022 and data for 509_CXF_05 is currently in preparation for publication.

Donor	Altered Genes	Deletions	Duplications	Total CNVs	Diagnosis
287_SZM_01	126	126	0	1	22q11.2 deletion: ASC, mild LD, developed psychosis with no family history
509_CXF_05	155	88	67	3	22q11.2 deletion: Atypical ASC

Thawing of hiPSCs

hiPSCs were thawed from cell banks kept in liquid nitrogen onto Geltrex coated 6-well plates, with one 1ml cryovial per well. The vial was thawed in a 37ºC water bath quickly, until a small amount of ice remained. 1ml of pre-warmed DMEM was added to a 1ml cell cyrovial to complete the ice thawing, and then the cell suspension was transferred to a 15ml falcon containing 6ml pre-warmed DMEM. Cells were pelleted by centrifugation at 300 x *g* for 2 minutes at room temperature (RT), supernatant removed, and cells resuspended in 3ml StemFlex per well, supplemented with RevitaCell (Gibco; A2644501) to mitigate cell death. One vial equated to the plating density of one well of a 6-well plate. Media was exchanged 100% for StemFlex without RevitaCell 24h after plating.

Maintenance of hiPSC Cultures

hiPSCs were incubated under hypoxic conditions (37°C; 5% CO_2; 5% O_2) and cultured on Geltrex™ (Life Technologies; A1413302) coated 6-well NUNC™ plates in StemFlex medium (Gibco; A3349401), exchanged every 48 hours. For passaging, once cells reached about 80% confluency, they were washed with HBSS (Invitrogen; 14170146) and then incubated with 1ml/well Versene (Gibco; 15040066) for 4 minutes at 37ºC (Lonza; BE17-711E). Versene was then removed, and cells were dislodged using a p1000 to pipette StemFlex up and down. Cells

were then diluted up to 1:8 before being plated onto fresh Geltrex-coated 6-well NUNC™ plates. After cells were added to each well and placed in the incubator, plates were slide gently front-to-back and side-to-side, not in a circular motion, so that cells are evenly distributed across wells.

Freezing of hiPSCs

To maintain frozen cell banks, hiPSC cells grown to 80-100% confluency in a 6-well plate were frozen into one cryovial per well. The culture media was removed, cells washed with HBSS and incubated for 4 mins with Versene at 37ºC. Cells were then dislodged by pipetting the Versene up and down with a p1000 and spun down in 1ml/well DMEM at 300 x *g* for 2 minutes at RT. The supernatant was removed, and cell pellets were resuspended in StemFlex + 10% sterile dimethyl sulfoxide (DMSO) at 1ml/well of cells and transferred to a cryovial, labelled with the information of line name, date of freezing, passage number and name of individual who froze the cells. The cryovials were moved rapidly to a mister frosty™ and quickly frozen at -80ºC for 24h before being moved to liquid nitrogen for long-term storage. In an attempt to reduce variance in experiments using these frozen cells (Dutan Polit *et al.*, 2023), frozen cell banks were created in batches with a low passage number (between 19 to 23). Once live cultures reached a passage number 30, these cultures were discarded. Where this was not possible, it should be mentioned that this is a possible source of variance when culturing hiPSCs.

2.1.2 Microglia like cell differentiation and culture

Myeloid progenitor factory generation

Microglia like cell (MGL) culture was performed following a previously published protocol (van Wilgenburg *et al.*, 2013; Haenseler *et al.*, 2017) (Figure 2.2). Individual hiPSC lines were

collected by passaging, pelleted by centrifugation at 300 x *g* for 2 minutes at RT, and resuspended in StemFlex + 10μM Y-27632 (Rock inhibitor; Sigma; Y0503) to a final concentration which gave approximately 100,000 cells/well of a 96-well low adherent plate (Fisher Scientific; 174927). Over the following three days, embryoid bodies (EBs) developed (Figure 2.1), which were cultured in hypoxic conditions (as per the maintenance of hiPSC cultures) and underwent daily 75% medium exchanges with EB medium (Figure 2.2 and Table 2.3). The EBs were then harvested, first by washing individual wells with HBSS to dislodge the EBs from their wells, then taken up by a 10ml stripette and resuspended in factory medium (Figure 2.2 and Table 2.3). Approximately 75 EBs were added to one T75 flask and incubated in factory medium under normoxic conditions (37°C; 5% CO_2; 20% O_2). Once a week, 5ml factory medium was added to the flask. After 5 weeks, factories began to release macrophage/microglia progenitors into the factory supernatant (Figure 2.1). To avoid disturbing the factories during their 5-week maturation period, quality inspection may only be done visually. This requires evaluating the growing EBs to ensure that sufficient cysts containing progenitor cells are forming on the sides of the EBs (Figure 2.1). Furthermore, the initial factory harvest at 5 weeks may be evaluated for the quantity of cells generated and their viability.

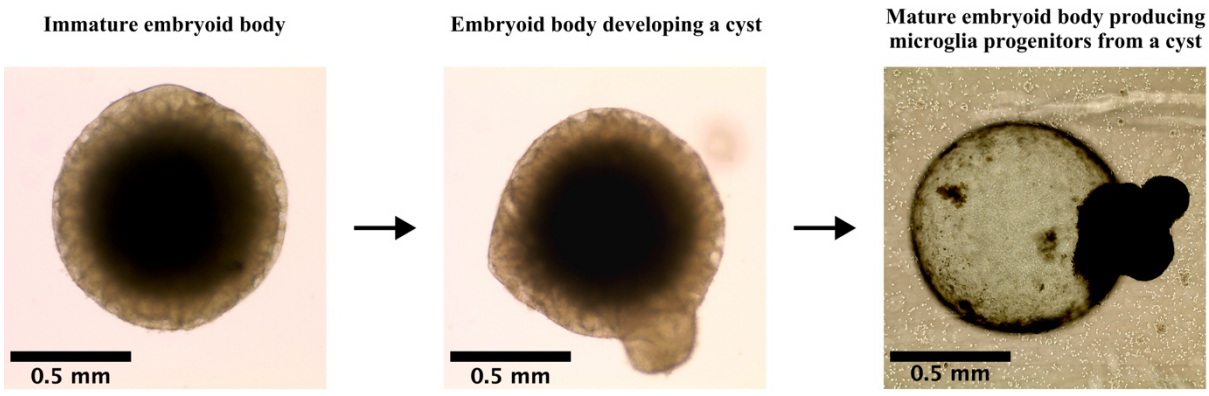

Figure 2.1 – Brightfield images representing the sequential development of microglial progenitors in cyst lobes from embryoid bodies during the 5-week embryoid body maturation in factories. Progenitors are then released into the factory supernatant, ready for harvest and terminal differentiation into microglia-like cells.

Table 2.3 - Culture medias used during microglial cell type differentiation.

Medium	Reagent	Final Concentration
Embryoid Body	StemFlex (Gibco; A3349401)	1X
	BMP-4 (Gibco; PHC9534)	50ng/ml
	SCF (Miltenyi; 130-093-991)	20ng/ml
	VEGF (Peprotech; 100-20-10UG)	50ng/ml
Factory	X-VIVO 15 (Lonza; BE04-418F)	1X
	Glutamax (Life Technologies; 35050-038)	2mM
	IL-3 (Invitrogen; 34-8038-82)	25ng/ml
	M-CSF (Gibco; PHC9501)	100ng/ml
	2-Mercaptoethanol (Gibco; 31350)	50μM
Microglia	DMEM (Sigma; D6421)	1X
	N2 Supplement (Life Technologies; 17502-048)	1%
	Glutamax (Life Technologies; 35050-038)	2mM
	IL-34 (BioLegend; 577906)	100ng/ml
	GM-CSF (BioLegend; 572903)	10ng/ml

Myeloid progenitor cell harvest and differentiation into microglia-like cells

Cells were harvested weekly by removing factory supernatant and replenishing the factory with factory medium replacements of the same volume (Figure 2.2). Unless otherwise stated, 80% (20ml) of supernatant was taken from factories each week, ensuring 20% of the total factory media volume remained in the factory flask. On days where fewer cells were required, a smaller volume of supernatant could be harvested. On day 0, the supernatants containing harvests of erythromyeloid progenitors from the factories were pelleted at 300 x *g* for 2 minutes at room temperature, supernatant removed, and the cell pellet resuspended in Microglia medium (Table 2.3). The myeloid progenitor suspension was seeded at a density that corresponded to the well size (Table 2.4) and cultured under normoxic conditions with 50% medium exchanges every 4 days until day 14 (Figure 2.2). It should be noted that the concentrations and growth factors used throughout this thesis to generate MGLs follows the originally published protocol, which was revised in 2022 with the only modification being the addition of TGF-β to the culture media (Washer *et al.*, 2022). Given this updated protocol was published once the experiments

of this thesis were already underway, it was decided that the project would continue to follow the originally published protocol.

Table 2.4 – Microglia seeding densities that correspond to plate well size. The 6-well plating density is based on the protocol by Haenseler et al. (2017), and subsequent densities calculated based on well surface area ratio to cells seeded.

Plate	Seeding Density (Cells/well)
6-well NUNC™	$1.5x10^6$
12-well NUNC™	$0.5x10^6$
96-well Perkin Elmer CellCarrier Ultra	$0.3x10^5$

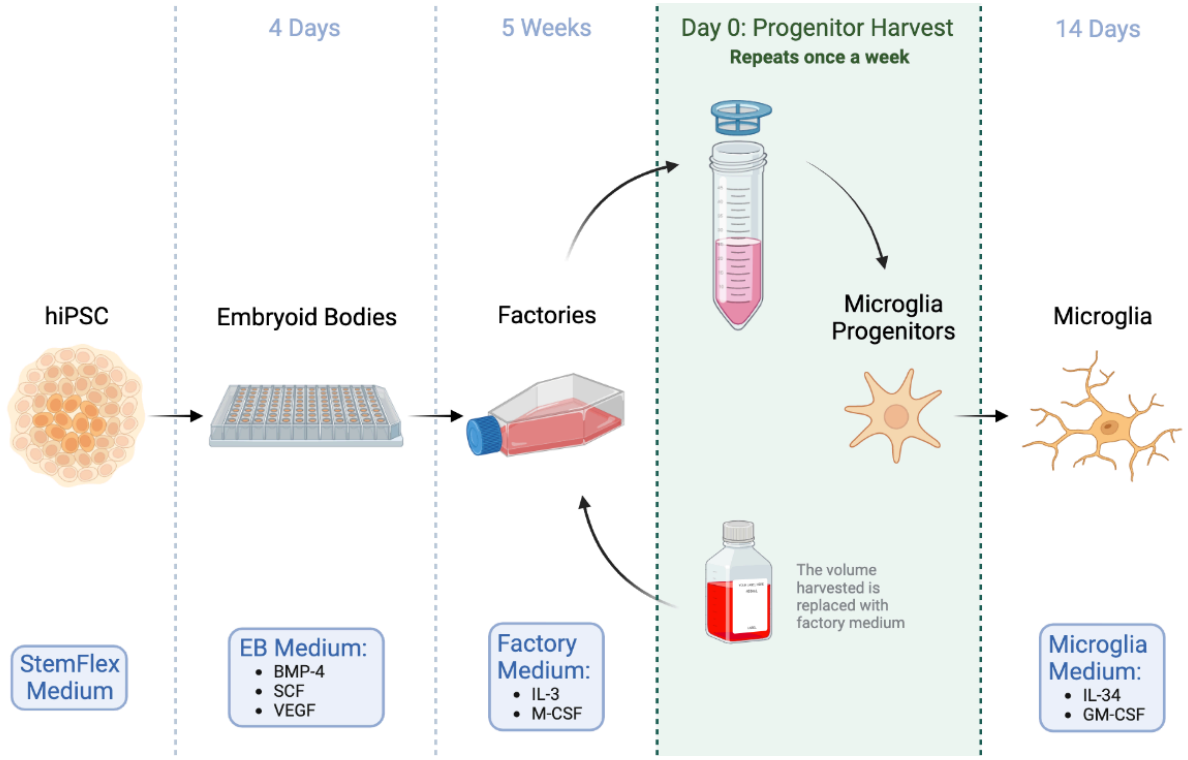

Figure 2.2 – Differentiation of microglia like cells from hiPSCs following the Haenseler et al. 2017 protocol. iPSCs are cultured in StemFlex until confluent, when they are seeded into a 96-well plate for embryoid body (EB) formation. Media is exchanged every day for EB medium for the following 3 days. Then, EBs are moved into a T75 flask and grown in Factory media for 5 weeks, adding factory media every week. Then, microglia progenitors are harvested on day 0 when factory supernatant is passed through a strainer to remove large clumps of cells and the removed supernatant volume is replaced with factory medium. This is a process that can be repeated once a week. Microglia progenitors are then seeded and terminally differentiated into mature microglia-like cells for 14 days in microglia medium.

2.1.3 Forebrain cortical neural progenitor cell differentiation and culture

Cultures of individual hiPSC lines were neuralised towards neural progenitor cells (NPCs) using a modified dual SMAD inhibition protocol as previously defined to develop a mixture of excitatory and inhibitory forebrain neuronal subtypes (Adhya *et al.*, 2021; Bhat *et al.*, 2022; Shi *et al.*, 2012a; Warre-Cornish *et al.*, 2020) (Figure 2.3). To commence neuralisation (day 0), hiPSC cultures were washed with HBSS, neuralised with induction medium (Table 2.5) and moved to normoxic conditions (37°C; 5% CO_2; 20% O_2). Neuralisation media was changed daily. By day 7, a uniform neuroepithelial sheet appeared. These neuroepithelial cells were then collected and passaged to new plate. To passage the neuroepithelial layer (neural passage), neuroepithelial cells were washed with HBSS and then incubated at 37ºC for 4 mins with Versene. The neuroepithelial sheet was then gently broken down into aggregates by slowly pipetting up and down with a p1000, collected in Versene and transferred to 2ml DMEM at RT. Cells were pelleted at 300 x *g* for 2 minutes at RT and supernatant discarded. The resulting pellet was resuspended and plated 1:1 on Geltrex coated plates in 2ml per well of neural induction medium + 10µM Rock inhibitor to prevent apoptosis, by gently pipetting up and down with a 10ml stripette. Hereafter, from day 8, SMAD inhibitors were omitted from the culture medium was exchanged daily until cady 28 of neuralisation (Table 2.5). Neural maintenance medium was changed daily until day 18 of neuralisation. Further neural passages were performed on day 12, 15 and 21 of neuralisation as described (Figure 2.3).

2.1.4 Mature cortical neuron differentiation and culture

NPCs to be terminally differentiated into post-mitotic cortical neurons were passaged on D21 into 50ng/ml poly-l-ornithine (Gibco; A3890401) and 20ng/ml laminin (Sigma; L2020) coated 96-well Perkin Elmer CellCarrier Ultra plates, at a density of 100,000 cells/well in 1X B27 +

10µM DAPT + 10µM Rock inhibitor and incubated (37°C; 5% CO_2; 20% O_2) (Figure 2.3). After 24 hours, medium was replaced with Rock inhibitor excluded medium every 24 hours until D28. After this time frame, the notch inhibitor DAPT was removed from the medium as continued half medium exchanges every 7 days with 1X B27 only occurred (Figure 2.3).

Table 2.5 - Culture medias used during forebrain cortical neural progenitor cell and mature neuron differentiation.

Medium	Reagent	Final Concentration
N2	DMEM (Sigma; D6421)	1X
	N2 Supplement (Life Technologies; 17502-048)	1%
	Glutamax (Life Technologies; 35050-038)	2mM
B27	Neurobasal Medium (Life Technologies; 21103-049)	1X
	B27 Supplement (Life Technologies; 17504-044)	2%
	Glutamax (Life Technologies; 35050-038)	2 mM
Neuralisation	B27:N2 (as above)	1:1 mixture
	SB431542 (Cambridge Bioscience; ZRD-SB-50)	10µM
	LDN193189 (Sigma; SML0559)	1µM
Maintenance	B27:N2 (as above)	1:1 mixture

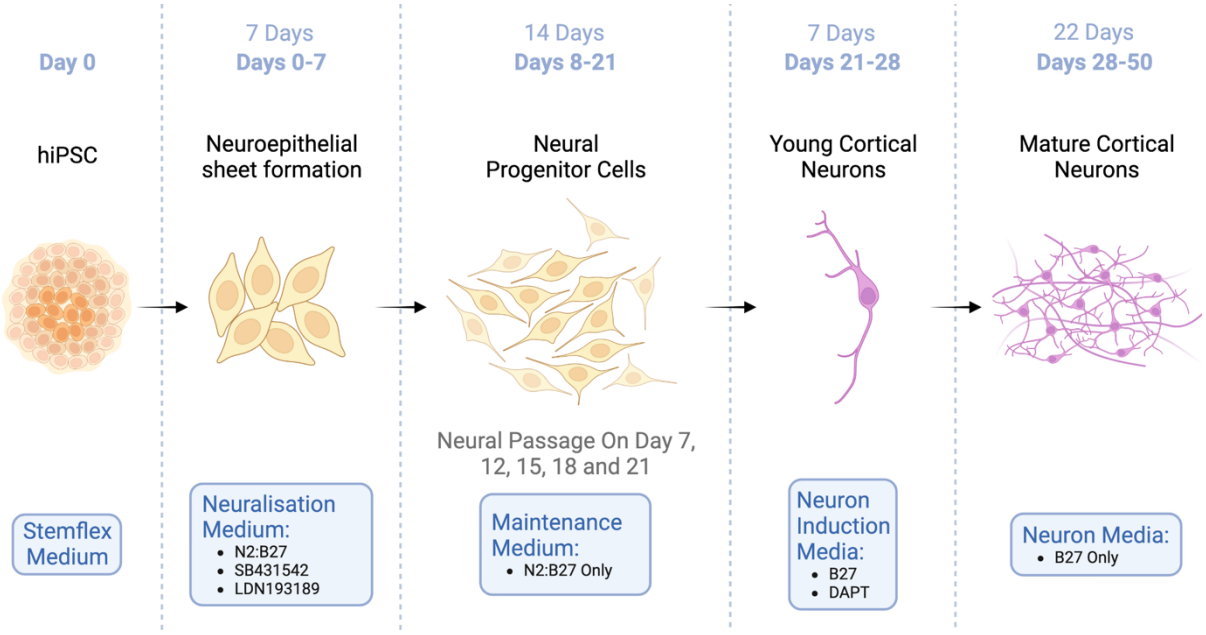

Figure 2.3 - Differentiation of cortical neural progenitor cells and mature neurons from hiPSCs following the Shi et al. 2012 dual SMAD inhibition protocol. hiPSCs were neuralised on D0 with neuralisation medium until neuroepithelial sheet formation around day 7. In the following 14 days, neural progenitor cells were formed and passaged on days 7, 12, 15, 18 and 21. On day 21, neural progenitor cells were treated with DAPT for 7 days to indue post-mitotic differentiation of cortical neurons until finally, mature cortical neurons were cultured for up to 50 days.

2.1.5 BV2 cell culture

BV2 Maintenance

BV2 cells, the immortalised mouse microglia line, were kindly provided by the Mitchell lab in the Department for Basic and Clinical Neuroscience. These cells were cultured under hypoxic conditions in DMEM (Sigma; D6421) supplemented with 10% foetal calf serum (FCS, ThermoFisher; A4768801). Cells were expanded in T75 Nunc™ EasYFlask™ or T175 Nunc™ EasYFlask™ flasks, and assays were carried out in 12-well NUNC™ plates. The 12-well NUNC™ plates were coated with 0.1mg/ml poly-l-ornithine (Sigma; P3655).

BV2 Splitting

Cultures were split when they reached 80-100% confluency. The media was removed, and cultures washed with HBSS. 1ml of trypsin (ThermoFisher; 25300054) was added to each well and incubated for 3mins at 37ºC to detach the cells. DMEM with 10% FCS was added to inactivate the trypsin and cells were scraped into suspension. Cells were then spun down at 300 x *g* for 2mins, counted and seeded at densities and volumes found in Table 2.6.

Table 2.6 – Seeding densities and media volumes during BV2 cell culture.

Plate or Flask	Seeding Density (cells/well)	Media Volume (ml/well)
T75 Nunc™ EasYFlask™	1:10 from T75	10
T175 Nunc™ EasYFlask™	1:10 from T75	20
12-well NUNC™	150,000	1

2.1.6 Cell Culture Stimulation with Interleukin-6

Human recombinant Interleukin-6 (Gibco; PHC0066) was reconstituted to a stock concentration of 100µg/ml in 100nM acetic acid, as per the manufacturer's instructions, as a 1000X stock concentration. Cell cultures were exposed directly to recombinant human IL-6 at a 1:1000 dilution from the frozen stock, or it's corresponding vehicle (sterile water with 100

picomolar acetic acid) for the length of time described in each experiment. Before stimulation, cell culture media was removed, and cells were washed in 1x HBSS. Fresh media was returned to the cells and then stimulated with 100ng/ml IL-6 or it's corresponding vehicle by pipetting the correct amount into each individual well.

2.2 Molecular Biology

2.2.1 RNA extraction

Cells cultured for RNA extraction were collected at RT in TRI Reagent™ Solution (Invitrogen; AM9738) by splashing the cells with TRI Reagent™ Solution using a p1000, after removing media and stored at -80ºC. 1ml of TRI Reagent™ Solution per 6-well was used for NPCs, and 0.5ml of TRI Reagent™ Solution per 6-well was used for MGLs. RNA was extracted from each sample by centrifugation with 200µl of 100% Chloroform (10,000 x *g* for 5 minutes at 4ºC). The top aqueous layer was moved to a new 1.5ml tube with 500µl of 100% isopropanol and mixed 10 times by inversion and incubated 15 minutes at RT. Then, RNA was precipitated by centrifugation (17,000 x *g*, 15 minutes at 4ºC). The supernatant was removed, and the pellet was washed in 1ml of 80% ethanol followed by centrifugation (20,000 x *g*, 5 minutes at 4ºC). The ethanol was then removed, the pellet air dried for 15 minutes at RT and then dissolved in 30µl of nuclease free water. Precipitation of RNA by 0.3M Sodium-acetate and 100% ethanol at -80ºC overnight was done to clean samples further, before resuspension in 30µl RNAse-free water. Nucleic acid content was measured using NanoDrop™ One.

2.2.2 cDNA synthesis

Reverse transcription of RNA to complementary DNA was carried out according to manufacturer's instruction (SuperScript™ III Reverse Transcriptase, Invitrogen 18080093).

Briefly, up to 1µg RNA was incubated with 2.5µM Oligo $(dT)_{20}$ primers (Invitrogen; 18418020) and 0.5µM dNTPs (Invitrogen; 18427013) for 5 minutes at 65ºC and then cooled on ice for 1 minute. Subsequently, 5X First-Strand Buffer, 5mM DTT, 200 U SuperScriptTM III Reverse Transcriptase (all Invitrogen; 18080093) and 40 U RNaseOUT (Invitrogen; 10777019) were added to the reaction mixture and incubated for 60 min at 50 ºC. The reaction was inactivated by a 15 min incubation at 70 ºC and diluted by a factor of 5 with RNAse-free water and stored long term at -20ºC.

2.2.3 Quantitative PCR

Quantitative PCR (qPCR) was carried out using Forget-Me-Not™ EvaGreen® qPCR Master Mix (Biotium; 31041-1) in the QuantStudio 7 Flex Real-Time PCR System (Fisher), according to cycling parameters described in Table 2.7. Briefly, 2µM of forward and reverse primers (Table 2.8) were mixed with 2µl of diluted copy (c)DNA and Forget-Me-Not™ EvaGreen® qPCR Master Mix to a final volume of 11µl per well reaction of a 384-well plate. Technical repeats of each reaction were plated three times in the same plate, and an average Cycle threshold value (Ct) was calculated for each primer/sample combination. Melt curve analysis was performed from 60ºC to 95ºC with readings every 1ºC. Ct data were normalized to an average of *GADPH, SDHA* and *RPL13* housekeeper expression Ct values, both of which had been previously characterized in the Vernon and Srivastava groups (Warre-Cornish *et al.*, 2020; Adhya *et al.*, 2021; Bhat *et al.*, 2022; Couch *et al.*, 2023). Gene expression fold change analysis was calculated following the $2^{-\Delta\Delta Ct}$ method (Livak and Schmittgen, 2001), using the following formulas:

$$\Delta Ct = Ct_{Gene\ of\ interest} - Ct_{Housekeeping\ gene\ average}$$

$$\Delta\Delta Ct = \Delta Ct_{Sample} - \Delta Ct_{Control\ average}$$

$$Fold\ change\ from\ control = 2^{-\Delta\Delta Ct}$$

Table 2.7 – Cycling parameters used during qPCR.

Step	Temperature (ºC)	Time	Cycle
Initial denaturation	95	10 mins	1
Denaturation	95	15 sec	40
Annealing	60	30 sec	
Extension	72	30 sec	

Table 2.8 – List of primers used for qPCR.

Gene	Forward primer	Reverse primer
Nanog	CCAACATCCTGAACCTCAGCTAC	GCCTTCTGCGTCACACCATT
TMEM119	AGTCCTGTACGCCAAGGAAC	GCAGCAACAGAAGGATGAGG
MERTK	ACTTGCTGGTGGATGTTCC	ACTTGCTGGTGGATGTTCC
CX3CR1	ACTTGCTGGTGGATGTTCC	ACTTGCTGGTGGATGTTCC
P2RY12	GACAGGAGCTGCAGAACAGA	GTTGCCAAACCTCTTTGTGA
GP80 (IL6R)	ACTTGCTGGTGGATGTTCC	ACTTGCTGGTGGATGTTCC
GP130 (IL-6ST)	GGCCTGAGTGAAACCCAAT	GGCCTGAGTGAAACCCAAT
IFNGR1	GGTCTGTGAAGAGCCGTTGTC	GGTCTGTGAAGAGCCGTTGTC
IFNGR2	GGTCTGTGAAGAGCCGTTGTC	GGTCTGTGAAGAGCCGTTGTC
TNFRSF1A	ACTTGCTGGTGGATGTTCC	ACTTGCTGGTGGATGTTCC
TNFRSF1B	GCCAGTGCGTTGGACAGAAG	CCACCAGGGGAAGAATCTGAG
IL17Ra	TGCGACTCCTGGACCAC	GTCAGGTTTCGAGGGTGAATC
TLR4	CCCTGAGGCATTTAGGCAGCTA	AGGTAGAGAGGTGGCTTAGGCT
IL6	GCGCTTGTGGAGAAGGAGT	TGGAGATGTCTGAGGCTCATT
JMJD3	CCTTCTCACCTGTCCTGCTG	GGTCTTGGTGGAGAAGAGGC
IL10	GTGGCGCTCCTGAGGTATGG	GTGGTACAGGTCCAAGGTCAC
TNF	ACCAAGCCCGTGGTGAAG	TGACATCCTTGATGAAGAGCA
GADPH	GCAGCAACAGAAGGATGAGG	AACGTACTCAGCGCCAGCAT
RPL13	CCCGTCCGGAACGTCTATAA	CCCGTCCGGAACGTCTATAA
IRF8	ATCAAAAGGAGCCCTTCCCC	TAGGTGGTGTACCCCGTCAC
ZEB2	GTACCTTCAGCGCAGTGACA	CAGGTGGCAGGTCATTTTCT
TBR1	ACACTGGGGCTCACTGGAT	AAAACCACCATCTGCCCATT
PAX6	GCCAGAGCCAGCATGCAGAACA	CCTGCAGAATTCGGGAAATGTCG
SDHA	TGGGAACAAGAGGGCATCTG	CCACCACTGCATCAAATTCATG

2.2.4 RNAseq

RNA library preparation and NovaSeq sequencing

Total RNA was submitted for sequencing at Genewiz Inc (South Plainfield, NJ). The following library reparations and RNA sequencing was carried out by Genewiz. Libraries were prepared using a polyA selection method using the NEBNext Ultra II RNA Library Prep Kit for Illumina following manufacturer's instructions (NEB, Ipswich, MA, USA) and quantified using Qubit

4.0 Fluorometer (Life Technologies, Carlsbad, CA, USA). RNA integrity was checked with RNA Kit on Agilent 5300 Fragment Analyzer (Agilent Technologies, Palo Alto, CA, USA). The sequencing libraries were multiplexed and loaded on the flowcell on the Illumina NovaSeq 6000 instrument according to manufacturer's instructions. The samples were sequenced using a 2x150 Pair-End configuration v1.5. Image analysis and base calling were conducted by the NovaSeq Control Software v1.7 on the NovaSeq instrument.

Upon receipt of FASTQ files from Genewiz, the subsequent bioinformatic analysis began. Files were quality controlled using Fastqc (Wingett and Andrews, 2018) and aligned to the human reference genome (GRCh38) with STAR (Dobin *et al.*, 2013), then sorted and duplicates removed with samtools version 1.13 (Li *et al.*, 2009) and Picard version 2.26.2 respectively, all within the King's CREATE and Rosalind high performance computing systems (King's College London, 2022). Downstream gene expression analyses were carried out in R version 4.0.2 (R Core Team, 2020). A count table was prepared and filtered for counts ≥ 1 using featureCounts (Liao *et al.*, 2014) from the Rsubread (Liao, Smyth and Shi, 2019) package, version 2.4.3. Differential gene expression analysis was carried out using DESeq2 (Love, Huber and Anders, 2014) version 1.30.1 and the default Wald test. Subsequently, using the Benjamini-Hochberg (BH) method, only genes with adjusted $P < 0.05$ were considered differentially expressed and submitted for downstream analyses.

Over Representation Analysis

Over representation analysis (ORA) was carried out using WebGestalt (Liao *et al.*, 2019), where differentially expressed genes were tested for over representation of non-redundant cellular component, biological process and molecular function gene ontology terms. This analysis used as a background list all genes considered expressed in our model, according to

DESeq2s's internal filtering criteria (i.e., adjusted p ≠ NA). Enrichment p-values were corrected for multiple testing using the BH method, and only terms with adjusted $p < 0.05$ were considered significant.

To complement the ORA, outcomes from differential expression analysis from DESeq2 were uploaded into the Qiagen Ingenuity Pathway Analysis (IPA) software (QIAGEN Inc., https://digitalinsights.qiagen.com/IPA) to identify canonical pathways. Genes were selected by $p \leq 0.05$ and log-fold changes $-0.06 \leq$ or ≥ 0.06. As referenced from the IPA knowledge base, core analysis was filtered by human data and removed any cancer cell lines. Top 10 enriched canonical pathways were filtered by z-score $\geq |2|$, an IPA measure of pathway directionality, and ordered by p-value adjusted by BH corrections.

Gene Set Enrichment Analysis

We used MAGMA 1.10 (de Leeuw *et al.*, 2015) to test whether genes differentially regulated in the analysed models overlapped with genes enriched with GWAS-supported risk variants. Briefly, MAGMA calculates gene-level enrichment by generating a gene-wide statistic from summary statistics, adjusting associations for gene size, variant density, and linkage disequilibrium using the 1000 Genomes Phase 3 European reference panel. Summary statistics from three GWAS studies from individuals with SZ, BD and ASC (Grove *et al.*, 2019; Mullins *et al.*, 2021; Trubetskoy *et al.*, 2022) were downloaded from the Psychiatric Genomics Consortium website. In order to reduce complexity and ease computational processing, only biallelic single nucleotide polymorphisms were analysed with minor allele frequency set at > 5% to remove rare, ungeneralisable variants. The imputation score was set at > 0.80 to ensure accuracy on the imputation of linked variants. We excluded from this analysis all genes and variants that were located within the extended MHC locus on chromosome 6, between 25 and

34 Mb (Watanabe *et al.*, 2017). SNPs from GWASs were assigned to genes using an annotation window of 10 kb upstream and downstream of each gene, using the gene annotation provided by the authors.

2.2.5 Protein extraction

Cells for protein extraction were scraped, pelleted by centrifugation 300 x *g* for 2 minutes at RT and resuspended in ice cold RIPA buffer (Table 2.9). Then, the cell suspension was sonicated at 40% for 10 pulses, centrifuged to pellet out insoluble materials at 20,000 x *g* for 15 min at 4 ºC and proteins were collected in the supernatant. Protein concentration was quantified using the Pierce™ BCA protein assay kit (Thermo-Fisher; 23227).

Table 2.9 – RIPA buffer constitution, diluted in ddH2O.

Reagent	Final Concentration
Tris pH 7.2	20mM
NaCl	150mM
Triton X-100	1.0%
EDTA pH 8	5mM
SDS	0.1%
Sodium Deoxycholate	1%
AEBSF	1mM
Pepstatin A	1µg/ml
Leupeptin	10µg/ml
Aprotinin	10µg/ml
Ser/Thr phosphatase inhibitor cocktail	1:100
NaF	25mM

2.2.6 Immunoblotting

In preparation for SDS-PAGE separation, protein samples were denatured in 2x Laemmli Sample Buffer (BioRad; 1610737EDU) with 5% 2-Mercaptoethanol and boiled at 95ºC for 5min. 2 µg of each protein sample was loaded into 10% acrylamide gels, alongside 5 µl of the Dual Color (BioRad;1610374) standards marker. Gels were run at 20mA for approximately 20 min, then increased to 100V until the samples reached the bottom of the unit

(~90min). Separated samples were transferred to a PVDF membrane and run overnight at 78mA in 4ºC. Blots were blocked in 5% BSA TBS-T for 1 hour at RT with agitation. Antibodies (Table 2.10) were diluted in blocking buffer; primary antibody incubation occurred overnight at 4ºC with agitation, and secondary antibody incubation at RT for 1 hour with agitation. Washes between antibody probes occurred in TBS-T at three 15min intervals. For visualization, ECL Western Blotting Substrate (GE Healthcare; RPN2106) was incubated on the blot at RT for 5min before image capture by the Bio-Rad Molecular Imager® Gel Doc™ XR System. Blots were probed with antibodies directed towards phospho-(p)STAT3 first, then STAT3 and finally the loading control beta-actin (β-actin)(Table 2.10). Blots were stripped between each staining session by incubating the membrane in Restore™ Stripping Buffer (Thermo Fischer Scientific; 21059) for 20mins at RT, then rinsing with TBS-T three times before moving onto re-blocking with 5% BSA TBS-T to commence the next probing phase.

Blot signals were quantified using ImageStudioLite (LI-COR, version 5.2.5), by defining an identical rectangular region of interest around each signal band and measuring the median signal value. Background correction was then performed using the automatic background detection toolkit provided with the aforementioned software. All target protein signals were normalized to β-actin signal. Data for pSTAT3 was divided by the total STAT3 (tSTAT3) signal data within each lane, to give a pSTAT3/tSTAT3 ratio for each sample. Fold change was calculated by dividing pSTAT3/tSTAT3 of treated samples with the matching timepoint pSTAT3/tSTAT3 vehicle data from identical membranes, to reduce batch effects across donors on different membranes. For example, 15min IL-6 treated pSTAT3/tSTAT3 ratio was divided by the 15min IL-6 vehicle pSTAT3/tSTAT3 ratio to get a fold change from vehicle within timepoint.

Table 2.10 - List of antibodies used for immunoblotting

Epitope	Host	Dilution	Supplier
pSTAT3 (Y705)	Mouse	1:1000	Cell Signalling; 9138S
STAT3	Rabbit	1:1000	Cell Signalling; 30835S
Beta-actin	Mouse	1:5000	Invitrogen; MA5-15739
Anti-Rabbit HRP-conjugated	Goat	1:5000	Thermo Fischer Scientific; 31460
Anti-Mouse HRP-conjugated	Goat	1:5000	Thermo Fischer Scientific; 31430

2.3 Cell Specific Assays

2.3.1 Media cytokine profiling array

Media was taken from cells in culture and immediately spun at 300 x *g* for 2 minutes to remove cells and cellular debris from the supernatant, which was transferred to a new tube, snap frozen and stored at -80ºC until use. Cytokines in the cell culture media samples were profiled using a Proteome Profiler Human Cytokine Array kit (R&D Systems; ARY005B). Membranes were initially blocked with 2ml of Array Buffer 4 for 1 hour at RT with agitation. 0.5ml of array Buffer 5 and 15µl of reconstituted human cytokine antibody cocktail was added to 1ml of cell culture media. After blocking, the Array Buffer 4 was removed, and the prepared samples were added to corresponding membranes and incubated overnight at 4ºC with agitation. The following day, membranes were washed with 1X wash buffer for 3 x 10 minutes. Then, 2ml of Array Buffer 5 with streptavidin-HRP was added to each membrane and incubated at RT for 30 minutes with agitation. Finally, membranes were washed again with 1X wash buffer for 3 x 10minutes and taken for imaging with 1ml of Chemi-Reagent mix. Each membrane was imaged for 10 minutes using the Bio-Rad Molecular Imager® Gel Doc™ XR System. Dot blot signals were quantified using the Protein Array Analyzer Palette plug-in for ImageJ, and technical dot replicates averaged to one value. These values were then corrected for background staining by subtracting the mean negative reference value from each of the signals.

Each corrected value was then normalized mean positive reference value on the membrane by division.

2.3.2 Soluble IL-6 receptor quantification

The IL-6 Receptor (Soluble) Human ELISA Kit (Invitrogen; BMS214) was used to quantify soluble IL-6Ra expression in cell culture media. Media was collected from cultures and immediately centrifuged (300 x *g* for 2min) to remove cells in suspension. The resulting supernatant was transferred to a new Eppendorf and frozen at -80ºC until use. For the ELISA, media samples were used undiluted and measured in duplicate to provide technical replicates. Microwell strips were washed twice with wash buffer for about 15s each. 100µl of IL-6RA Assay Buffer (1X) was added to all standard wells, while leaving the first wells empty. 200µl of prepared standard was added into the first wells and standard dilutions were created by transferring 100µl from well to well and discarding 100µl from the last wells. IL-6RA Assay Buffer was used as a blank. 20µl of sample was added to designated wells and topped up to 100µl with IL-6Ra Assay Buffer. 50µl of HRP-Conjugate was added to each well and incubated for 2h at RT. After incubation, the microwells were washed 3 x 15s with wash buffer, taking care not the scratch the surface of the microwells. For visualization, 100µl of TMB Substrate was added to all wells and incubated at RT for 10min. To stop the reaction, 100µl of Stop Solution was added to all wells. Optical density (OD) of the microwells was blanked and measured at 450nm.

2.3.3 Immunocytochemistry

Cells were fixed with 4% formaldehyde (w/v; made in 4% sucrose PBS) for 20min at room temperature. Samples were then washed twice in PBS, then simultaneously permeabilized and blocked with 2% normalised goat serum (NGS) PBS + 0.1 % Triton X-100 for 2 hours at RT.

All antibodies were diluted in 2% NGS in PBS. Primary antibodies were incubated with cells overnight at 4ºC, and secondary antibodies were incubated with cells for 1 hour at RT, both in humidified chambers. Between incubations, cells were washed three times in PBS at 15min intervals. Finally, cells were incubated for 10min in PBS + DAPI (1:50,000). Coverslips were mounted onto glass slides with VECTASHIELD HardSet Antifade Mounting Medium (Vector Laboratories; H-1500-10), and 96-well Perkin Elmer plate wells left in 150µl/well PBS before imaging.

2.4 Figure Creation and Assembly

Throughout this thesis, the software used to create figures were as follows: BioRender.com was used to create any cartoon diagrams of processes such as those in figures 2.2 and 2.3; Prism 9 (version 9.4.1, GraphPad) was used to create bar charts and line graphs such as those in figures 3.2C and 3.6D; heatmaps, bubbleplots and principle component analysis plots such as those in figures 3.3 B and 4.3A-E were created in RStudio (version 2022.12.0+353); assembly of plots, diagrams and images into whole figure grids occurred in the Figma Desktop App (version 116.11.1).

Chapter 3

Microglia, Neural Progenitor Cells, and Their Differential Response to IL-6

NOTE: SOME OF THE RESULTS FROM THIS CHAPTER WERE FIRST PUBLISHED IN BRAIN, BEHAVIOR AND IMMUNITY, IN 2023, ENTITLED "ACUTE IL-6 EXPOSURE TRIGGERS CANONICAL IL-6RA SIGNALLING IN HIPSC MICROGLIA, BUT NOT NEURAL PROGENITOR CELLS" (COUCH *ET AL.*, 2023) (APPENDIX 1).

Chapter Summary

Background: The multitude of cell types in the developing cortex are likely to show differential responses and vulnerability to immune system stimulation. This depends on temporal factors, for example which cell is exposed first, but also on the cell's ability to sense different cytokines and chemokines. In building an *in vitro* model to examine the molecular effects of maternal immune activation (MIA) in a dish, it is therefore vital to first establish the intrinsic responses of the component cell types to the stimulus of choice. Hence, this chapter investigates the propensity of hiPSC-derived microglia-like cells (MGLs) and neural progenitor cells (NPCs) to respond to the chosen immune stimulus, IL-6.

Results: hiPSCs were successfully shown to differentiate into both MGLs and forebrain NPCs, that recapitulate patterns present in the human foetal neocortex at mid-gestation. The data suggest that forebrain NPCs monocultures do not respond to acute IL-6 exposure at both protein and transcript levels, due to the absence of IL6R expression and soluble (s)IL-6Ra secretion. By contrast, acute IL-6 exposure resulted in STAT3 phosphorylation and increased the mRNA expression of *IL6*, *JMJD3* and *IL10* in monocultures of MGLs, confirming activation of classical IL-6Ra signalling. The addition of sIL-6Ra to NPCs in monoculture facilitated STAT3 phosphorylation in response to IL-6 in a receptor dose-dependent manner, indicating that human forebrain NPCs are only capable of responding to IL-6 by trans-IL-6Ra signalling. MGLs were also shown to secrete the soluble IL-6 receptor.

Conclusion: These data indicate that MGLs respond to IL-6 when grown in monoculture, while NPCs may only do so when in culture with cell types that secrete sIL-6Ra, or when the latter is added exogenously. Hence, MGLs may facilitate an NPC response to IL-6 via trans-IL-6Ra signalling in a co-culture system.

3.1 Introduction

Single-cell investigations have revealed the human neocortex to possess an extremely complex array of unique cell types (Polioudakis *et al.*, 2019), each with differing transcriptomic, morphological, and electrical characteristics (Gouwens *et al.*, 2020; Scala *et al.*, 2021). Specific cells, such as astrocytes and microglia, even exhibit intra- and inter-regional heterogeneity (Böttcher *et al.*, 2019; Batiuk *et al.*, 2020; Lee, Kim and Kim, 2022). MIA-derived insults can influence the typical developmental patterns of these cell types, by repressing neurodevelopmental transcription pathways which influence key developmental functions (Lombardo *et al.*, 2018; Baines *et al.*, 2020). But, due to their individual characteristics, each unique cell type may be predicted to respond in a differential way to a single MIA-derived insult (Vasistha and Khodosevich, 2021). In other words, selective cell types likely possess susceptibility or resilience to MIA-derived insults (Figure 3.1) (Vasistha and Khodosevich, 2021). Adding an additional level of complexity, the constantly diverging landscape of functional characteristics of these cell types mean specific cell types can move in and out of susceptibility, with temporal and functional state dependency (Vasistha and Khodosevich, 2021).

As discussed in section 1.2.4, elevated maternal IL-6 serum concentrations have been linked to an increased risk for NDDs in the offspring. In the case of IL-6 signalling, cell types will either express or not the cell-surface components IL-6Ra and IL-6ST required to receive the IL-6 signal. This concept can be extended to additional MIA-implicated cytokines including IFN-γ, TNFα and IL-17, and their receptors IFNGR1/2, TNFRSF1A/B, and IL17Ra respectively. The ensuing insult effect and cell-specific response will result in molecule secretion or cellular function changes, which will target neighbouring cells and have downstream knock-on effects on their developmental programmes. It is conceivable as well

that neighbouring cells may lack the necessary transmembrane components needed to receive the original insult, rendering them only sensitive to MIA-derived insults through reliance on other cell types.

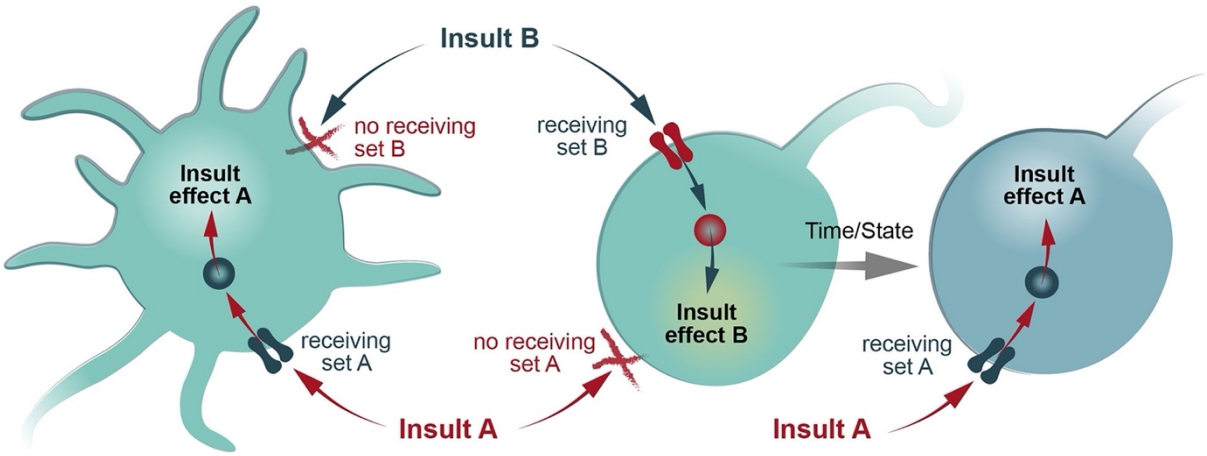

Figure 3.1 – The susceptibility and resilience of distinct cell types to MIA-derived insults. Cell types must express the necessary transmembrane receptors to receive, and therefore be sensitive to, specific MIA-derived insults. For example, the right-hand cell can receive Insult A via its receiving set A transmembrane receptors, which induces the insult effect A. This makes the right-hand cell susceptible to the MIA-derived insult A. On the other hand, the middle cell does not express the necessary receiving set A, making it resilient to Insult A. At the same time, the middle cell can express the correct receiving set B transmembrane receptors for Insult B, making it susceptible to Insult B, unlike the right-hand cell. Furthermore, the time or functional state of this middle cell can also make it susceptible or resilient to Insult A, since a change in either of those dependencies can cause it to express the receiving set A and force its susceptibility to Insult A. This figure was taken from the review by (Vasistha and Khodosevich, 2021).

Microglia play vital roles in the intricate process of cortical neurodevelopment, making them crucial entities to study in the context of NDDs, as discussed in section 1.2.2. Therefore, knowing how these hiPSC-derived microglial-like cells and neural progenitor cells react to any given stimulation relevant for MIA, is crucial when attempting to build an *in vitro* human cellular model. In particular, it is necessary to first characterise each component cells intrinsic and specific responses at the chosen developmental timepoint and functional state: early second trimester and basal functional state, respectively. NPCs and MGLs may react to IL-6 differently

within this chosen experimental design and hence, is important to investigate whether each cell type can respond to IL-6. To this end, this chapter aims to understand if, and how, hiPSC-derived microglia-like cells (MGLs) and neural progenitor cells (NPCs) respond in monocultures to acute IL-6 stimulation. The following three questions are addressed: (1) could hiPSC-derived MGLs and NPCs be generated, and do they represent human microglia and forebrain developing NPCs; (2) do the cells have the receptor machinery to respond to IL-6 and other cytokines; (3) do these cells respond to acute IL-6 by either cis- or trans-signalling, or both.

3.2 Methods

3.2.1 Cell Culture

A total of nine donor hiPSC lines from N = 3 healthy male donors (M3_CTR, 127_CTM and 014_CTM) were used to create *MYB*-independent macrophage/microglia progenitor factories (hereby referred to as factories) and terminally differentiated into MGLs according to the protocols described in section 2.1, with three clone factories per donor each (van Wilgenburg *et al.*, 2013; Haenseler *et al.*, 2017) (Table 2.1).

Likewise, the same nine hiPSC lines were neuralised to day 18 (D18) NPCs, from N = 3 healthy male donors (M3_CTR, 127_CTM, and 014_CTM) with three clones per donor (Table 2.1). The modified dual SMAD inhibition protocol outlined in section 2.1 was used (Shi, Kirwan and Livesey, 2012a), which has previously been demonstrated both externally and internally to our lab to generate a mix of excitatory and inhibitory forebrain neuronal subtypes (Warre-Cornish *et al.*, 2020; Adhya *et al.*, 2021; Bhat *et al.*, 2022; Couch *et al.*, 2023). Mouse BV2 cells, as used where indicated in the results, were cultured until confluent according to the

protocol described in section 2.1.5, and all cell culture treatment with 100ng/ml IL-6 was carried out in accordance with the protocol outlined in section 2.1.6.

3.2.2 RNA extraction and qPCR

RNA extraction, cDNA synthesis and qPCR protocols were carried as described in sections 2.2.1, 2.2.2 and 2.2.3 respectively. RNA for MGL quality control and receptor characterisation samples were taken at three stages: factory erythromyeloid progenitors (EMPs) on day 0 (D0) harvested immediately from each factory, after 1 day of terminal microglial differentiation (D1 MGL) and after 14 days of terminal microglial differentiation (D14 MGL). For the optimisation of IL-6 concentration to use as the stimulus, RNA was collected from both D1 MGL and D14 MGL. To carry out NPC quality control and receptor characterisation, RNA samples were collected at three stages: after 10, 14 and 18 days of differentiation from hiPSCs (D10, D14 and D18 respectively). RNA for NPC IL-6 stimulation optimisation was taken only from D18 NPCs. For receptor characterisation in 50-day terminal differentiation of mature cortical neurons, pre-extracted RNA using identical extraction methods was kindly provided by Lucía Dután Pólit. These samples were obtained from 3 independent male donor lines (M1_CTR, M2_CTR and M3_CTR), using a single clone for each donor.

3.2.3 Immunocytochemistry and Image Analysis

Slide Preparation and Image Acquisition

MGLs were stained on either D1 or D14 for TMEM119, PU.1 and DAPI for quality control following the protocol described in section 2.3.3 (Table 3.1). This was carried out over 3 donors, with 3 clone cultures each. Glass slides were prepared by mounting coverslips using VECTASHIELD HardSet Antifade Mounting Medium from Vector Laboratories (H-1500-10). One coverslip per cell line was stained, with three images taken per coverslip, chosen

randomly. Confocal images were captured by a Leica SP5 laser scanning confocal microscope, with 405/488/594nm lasers and a 63x oil immersion lens (Leica, Wetzlar, Germany).

Image Analysis

For image preparation, ImageJ software (version 1.53) was used (Abràmoff, Magalhães and Ram, 2004). To minimize observer bias, the image analysis was conducted in a blinded setting. Images were coded with randomly assigned letters, ensuring that the experimenters remained unaware of the source and conditions of the microglia-like cells throughout the analysis. The file names were decoded after the acquisition of datasets. For optimal visualization of the .lif image format, the Bio-Format Importer plugin was used. The lif hyperstack was imported using the default settings, and the colour mode was set to grayscale. The "split into separate windows" option was selected for splitting the channels. Each channel (Channel 0=DAPI, Channel 1=TMEM119, or Channel 2=PU.1) contained 12 slices of images, which were then projected into a single image by using the "max intensity" option under image, stack, Z project. Each resulting grayscale image was saved as an 8-bit .tiff file, and processed into CellProfiler (Stirling *et al.*, 2021) for counting.

Table 3.1 - List of antibodies used for immunocytochemistry in this chapter.

Epitope	Host	Dilution	Supplier
TMEM119	Rabbit	1:100	Abcam; ab185333
PU.1	Mouse	1:100	Santa Cruz; sc-390405
Anti-rabbit AlexaFluor 488	Goat	1:750	Thermo Fischer Scientific; A11034
Anti-mouse AlexaFluor 568	Goat	1:750	Thermo Fischer Scientific; A11031
Anti-chicken AlexaFluor 633	Goat	1:750	Thermo Fischer Scientific; A21103

3.2.4 Soluble IL-6Ra ELISA

As per the ELISA protocol described in section 2.3.2, soluble IL-6Ra was quantified in cell culture media from monoculture D14 MGL and D18 NPCs treated with vehicle or 100ng/ml IL-6 for 3h or 24h.

3.2.5 Immunoblotting

Protein was extracted and quantified by immunoblotting in accordance with the procedures described in sections 2.2.5 and 2.2.6 respectively.

3.3 Results

3.3.1 Confirmation of Cell Culture Identity

Microglia-like cell confirmation

We first confirmed that we could successfully generate MGLs from hiPSC using the published protocols in our laboratory. Consistent with data produced using the same protocol (Haenseler *et al.*, 2017; Hedegaard *et al.*, 2020; Vaughan-Jackson *et al.*, 2021), the mean macrophage/microglia progenitor cell concentration per weekly harvest on day 0 (D0) was 327,000 cells/ml and mean viability was 68.6% (Figure 3.2A). Using qPCR, after 14-days of differentiation, we observed increased expression of the microglial signature transcripts *P2RY12, MERTK, CX3CR1*, and *TMEM119* and decreased expression of the pluripotency transcript *Nanog*, as compared to hiPSC cells from the same donor line, indicating acquisition of a microglial fate consistent with previously published data (Haenseler *et al.*, 2017; Couch *et al.*, 2023) (Figure 3.2B, statistics in Table 3.2). By contrast, only after 14 days of terminal differentiation did *CX3CR1* expression significantly increase as compared to hiPSC and D1 MGLs from the same donor line (Figure 3.2B). Interestingly, *P2RY12* expression peaked in the

factory EMPs on differentiation D0 and decreased thereafter during terminal MGL differentiation, which has not previously been reported (Couch *et al.*, 2023) (Figure 3.2B). Expression of *MERTK* increased immediately after differentiation from the hiPSC stage and remained consistently expressed through day 0, 1 and 14 of MGL differentiation as did *TMEM119* mRNA expression (Figure 3.2B).

Table 3.2 - Two-way ANOVA of qPCR microglial marker gene expression with N=3 donors, each with N=3 clones.

Gene	Source of Variation	DF	F (DFn, DFd)	P value	P value summary
P2RY12	Interaction	6	F (6, 23) = 0.6872	P = 0.6620	ns
	Timepoint	3	F (3, 23) = 5.335	P = 0.0061	**
	Donor	2	F (2, 23) = 0.9417	P = 0.4045	ns
TMEM119	Interaction	6	F (6, 23) = 0.4903	P = 0.8089	ns
	Timepoint	3	F (3, 23) = 1.112	P = 0.3647	ns
	Donor	2	F (2, 23) = 2.905	P = 0.0750	ns
MERTK	Interaction	6	F (6, 23) = 1.302	P = 0.2957	ns
	Timepoint	3	F (3, 23) = 11.49	P < 0.0001	****
	Donor	2	F (2, 23) = 4.167	P = 0.0285	*
CX3CR1	Interaction	6	F (6, 23) = 0.2142	P = 0.9685	ns
	Timepoint	3	F (3, 23) = 3.398	P = 0.0349	*
	Donor	2	F (2, 23) = 0.5630	P = 0.5771	ns
Nanog	Interaction	6	F (6, 23) = 0.06092	P = 0.9989	ns
	Timepoint	3	F (3, 23) = 33.38	P < 0.0001	****
	Donor	2	F (2, 23) = 0.03520	P = 0.9655	ns

Cells were immunostained for the microglial markers PU.1 and TMEM119 to confirm protein-level microglial-marker expression to compare day 1 (D1) progenitor and day 14 (D14) phenotypes (Figure 3.2C). PU.1 is a crucial transcriptional factor that controls microglial fate determination (Kierdorf *et al.*, 2013), and transcriptome studies have identified the microglial marker TMEM119 to be a useful staining marker for discriminating residential microglia from similarly comparable cell types, such as blood-derived macrophages in the human brain (Satoh *et al.*, 2016; Bennett *et al.*, 2016). In our hands, the great majority of cells expressed both TMEM119 and PU.1 (D1 81.4%, D14 85.2%), which remained unchanged between D1 and D14 differentiation stages (PU1/TMEM119 expression $p < 0.0001$; Day $p = 0.9999$; Interaction

p = 0.8869; Two-way ANOVA) (Figure 3.2D). Each healthy male donor showed consistent mean expression of PU.1 and TMEM119 from 1 to 14 days of MGL differentiation from the factory (Figure 3.2E, statistics in Table 3.3).

Table 3.3 - Two-way ANOVA of ICC microglial marker TMEM119 and PU.1 protein expression with N=3 donors, each with N=3 clones.

Measurement	Source of Variation	DF	F (DFn, DFd)	P value	P value summary
PU.1 Mean Grey	Interaction	2	F (2, 12) = 0.8557	P = 0.4494	ns
	Time Factor	1	F (1, 12) = 1.506	P = 0.2432	ns
	Donor Factor	2	F (2, 12) = 0.6844	P = 0.5230	ns
TMEM119 Mean Grey	Interaction	2	F (2, 12) = 0.8489	P = 0.4520	ns
	Time Factor	1	F (1, 12) = 1.304	P = 0.2757	ns
	Donor Factor	2	F (2, 12) = 1.344	P = 0.2974	ns
Mean Whole Cell Area	Interaction	2	F (2, 12) = 0.3446	P = 0.7153	ns
	Time Factor	1	F (1, 12) = 0.9985	P = 0.3374	ns
	Donor Factor	2	F (2, 12) = 0.1248	P = 0.8838	ns

At day 1 in the MGL population (N = 338 cells from all donors and replicates combined), 81.4 ± 13.8% of cells expressed both TMEM119 and PU.1, and this percentage remained consistent until day 14 (N = 299), when 85.2 ± 9.8 % of cells expressed both markers (Figure 3.2E). Fewer cells expressed solely PU.1 (D1, 14.9%; D14, 10.8%), and even fewer cells displayed neither marker (D1, 3.72%; D14, 3.92%) (Figure 3.2E). No cells measured expressed only TMEM119, without PU.1 expression (Figure 3.2E). Overall, these data strongly suggest successful differentiation towards microglial-like cells from all nine hiPSC lines, distinct from peripheral macrophages as identified by TMEM119 expression. Prior work from the Vernon lab also confirms that these cells show the expected microglial functions, including phagocytosis (Solomon *et al.*, 2022).

Importantly, the donor source of the cells had no discernible impact on the expression of cell markers in both RNA and immunostaining analysis, and therefore, on MGL differentiation. This is with the exception of *MERTK* transcript expression which did exhibit a donor impact

but was not observed to interact significantly with the timepoint expression status in the two-way ANOVA (Table 3.2). Consequently, it was perceived that MGLs could be successfully generated from all three donors.

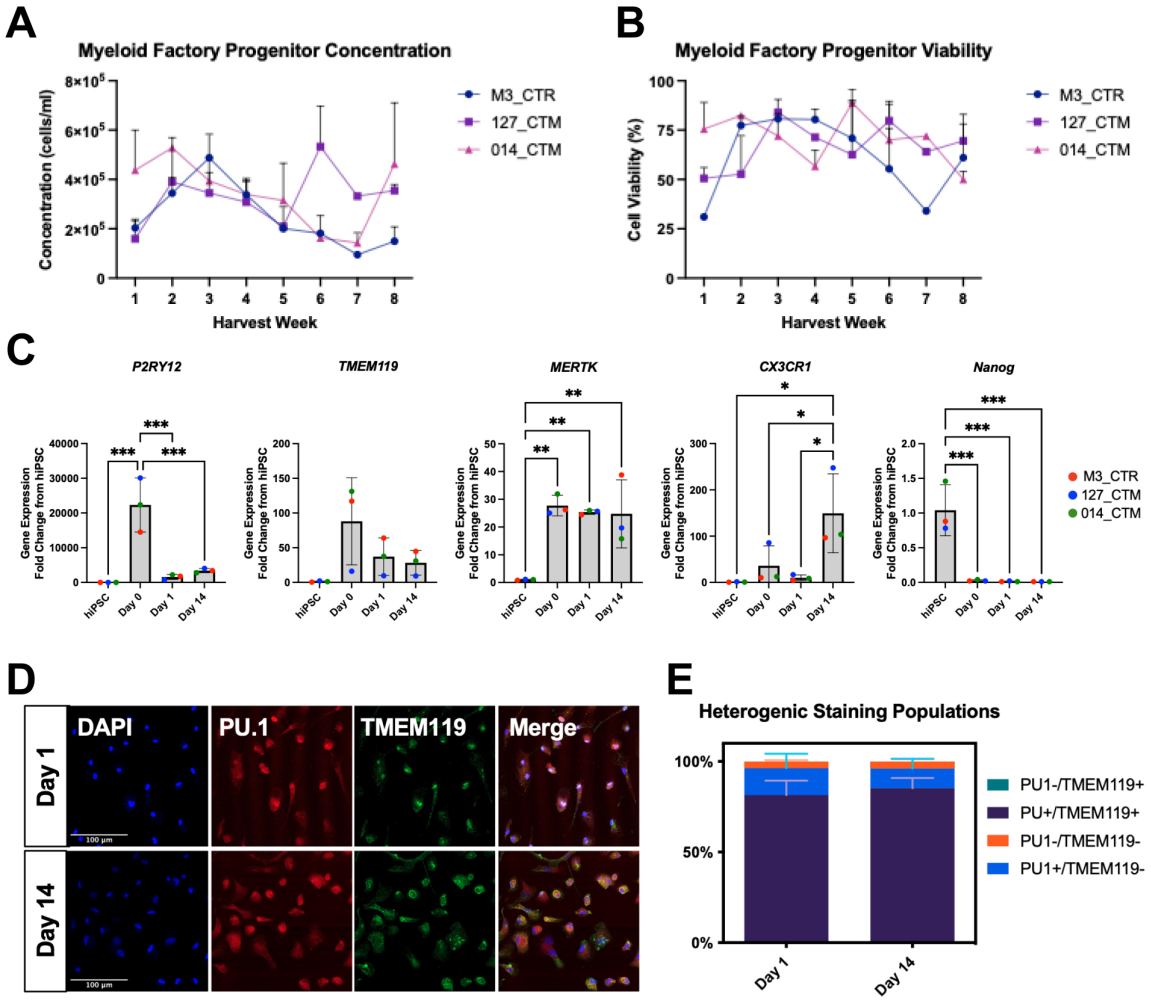

*Figure 3.2 - Expression of microglia and NPC markers in hiPSC derived MGLs and NPCs. Three male healthy control cell lines, averaged from three technical replicate clones per donor, unless stated otherwise. 5% FDR corrections formatted as follows: *p < 0.05, **p < 0.01, ***p < 0.001, and ****p < 0.0001; not significant not labelled. (**A**) Macrophage/microglia progenitors cell concentration in weekly factory harvests from each donor line, N=3 clones per donor. (**B**) Macrophage/microglia progenitors cell viability in weekly factory harvests from each donor line, N=3 clones per donor. (**C**) Differentiation time-course of microglial markers (TMEM119, MERTK, CX3CR1) and pluripotency marker (Nanog) by qPCR RNA samples at hiPSC, Macrophage/microglia progenitors (day 0), day 1 (D1) and day 14 (D14) MGL stages of differentiation. N=3 healthy male donors. 014_CTM Day 1 condition was averaged from N=2 clones only. (**D**) Representative confocal images of MGL progenitor (day 1) and MGL (day 14) collected by ICC, showing expression of both PU.1 (red) and*

*TMEM119 (green). 127_CTM_01 line presented in this figure only. (**E**) MGL D1 and D14 staining populations presented as the percentage of cells expressing either/or PU.1 and TMEM119.*

Neural progenitor cell confirmation

Prior work from the Srivastava and Vernon labs has both demonstrated successful replication of forebrain NPC differentiation from hiPSCs using the dual-SMAD inhibition protocol (Shi, Kirwan and Livesey, 2012a; Deans *et al.*, 2017; Kathuria *et al.*, 2018a; Warre-Cornish *et al.*, 2020; Adhya *et al.*, 2021; Pavlinek *et al.*, 2021; Bhat *et al.*, 2022; Couch *et al.*, 2023). Nonetheless, I verified that forebrain NPCs were generated in my hands via assessment of cell-specific marker transcript expression. Specifically, expression of key neural progenitor markers (*TBR1, Zeb2,* and *Pax6*) and pluripotency markers (*Nanog* and *Oct4*) were confirmed by qPCR (Figure 3.3A and statistics in Table 3.4) and their expression levels were validated against publicly available gene expression data from the human foetal neocortex (Figure 3.3B).

Both *Pax6* and *Zeb2* mRNA expression rose significantly during NPC differentiation from hiPSCs, whilst *Nanog* and *Oct4* mRNA expression declined significantly (Table 3.4). *TBR1* expression was the only marker to be statistically unchanged but demonstrated a numerical increase throughout differentiation to D18 NPCs from hiPSCs due to donor variance (Table 3.4). According to the human foetal neocortex bulk RNAseq datasets published by Fietz *et al.* (2012), *Zeb2* expression is found mainly in the cortical plate (CP) during gestation weeks 13-16 (Fietz *et al.*, 2012). Likewise, TBR1 expression is found earlier in gestation weeks 13-14, mainly in the CP and subventricular zone (SVZ). Additionally, PAX6 expression is found mainly in the ventricular zone (VZ), peaking between 14-15 weeks of gestation. Taken together, this suggests a view that the NPC population derived herein forms a heterogeneous population of progenitor cells that cover the CP, SVZ and VZ through gestational weeks that

cluster around the beginning of the second trimester; a key period of NDD risk from MIA. This is consistent with prior work from both inside and outside the group (Brennand and Gage, 2012; Brennand *et al.*, 2015; Kathuria *et al.*, 2018a; Shum *et al.*, 2020; Warre-Cornish *et al.*, 2020; Adhya *et al.*, 2021; Bhat *et al.*, 2022).

Table 3.4 - One-way ANOVA of qPCR NPC and pluripotent marker expression in hiPSC-derived NPC with N=3 donors, averaged to one point from three clones.

Gene	DF	F (DFn, DFd)	P value	P value summary
TBR1	3	F (3, 8) = 2.055	P = 0.1848	ns
Zeb2	3	F (3, 8) = 4.381	P = 0.0421	*
Pax6	3	F (3, 8) = 6.038	P = 0.0188	*
Nanog	3	F (3, 8) = 30.50	P < 0.0001	****
Oct4	3	F (3, 8) = 26.08	P = 0.0002	***

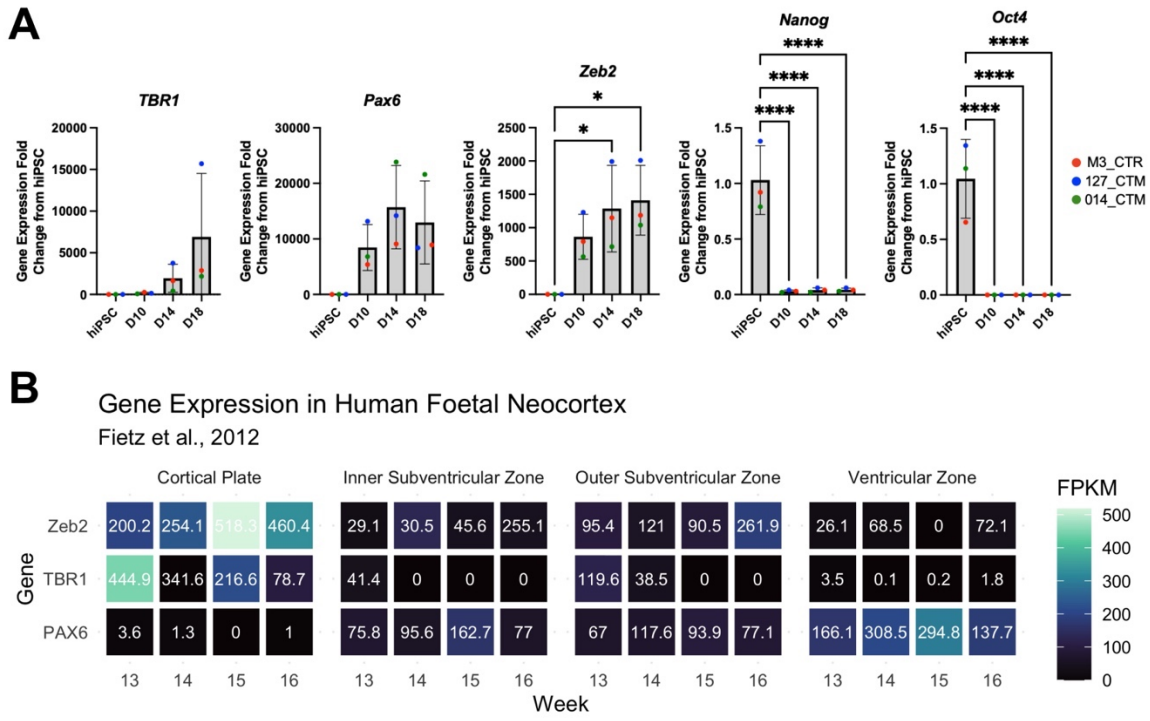

*Figure 3.3 – Neural progenitor cell quality control. (A) Differentiation time-course of neural progenitor cell markers (TBR1, Pax6, ZEB2) and pluripotency markers (Nanog, Oct4) by qPCR RNA samples at hiPSC, day 10, 14 and 18 of NPC differentiation. N=3 healthy male donors. In TBR1 measurement, 014_CTM hiPSC condition was averaged from N = 2 clones only. 5% false discovery rate (FDR) by Benjamini–Hochberg (BH) method corrections after one-way ANOVA formatted as follows: *q < 0.05, **q < 0.01, ***q < 0.001, and ****q < 0.0001; non-significant not labelled. Bar graphs plotted as mean*

*with standard deviation (SD) error bars, and points coloured by donor line as shown in key. (**B**) Human fetal neocortical bulk RNAseq (Fietz et al., 2012) dataset validate the NPC markers found in our hiPSC-derived NPC cultures at gestation timepoints 13-16 weeks, a gestational stage relevant to MIA risk.*

3.3.2 Microglial-like cells express necessary IL-6 signalling receptors, but neural progenitor cells do not

Having confirmed that we can successfully differentiate hiPSC into both MGLs and forebrain NPCs, we next measured the expression of cytokine receptors in both MGL and NPC monocultures by qPCR to determine each cell type's ability to respond *in vitro* to IL-6 and other key cytokines implicated in MIA, namely TNFα, IFN-γ and IL-17 (N = 3 neurotypical male donors (biological replicate) averaged from N = 3 separate clones per donor (technical replicate). During MGL differentiation from hiPSCs, mRNA expression *of IFNGR1/2, TNFARSF1A, IL17RA*, and both IL-6 signalling subunits, *IL6R* and *IL-6ST*, significantly increased (Figure 3.4A, statistics in Table 3.5). By contrast, *TNFRSF1B* expression did not change significantly from the hiPSC stage overall but was numerically enhanced at all time points after MGL differentiation, specifically 100-fold from hiPSC to D0, 50-fold from hiPSC to D1, and ~35-fold from hiPSC to D14 (Figure 3.4A). These findings suggest that MGLs are able to response to at least IL-6, IFN-γ, TNFα and IL-17 (Couch *et al.*, 2023).

Table 3.5 - One-way ANOVA of qPCR cytokine receptor expression in MGLs with N=3 donors, averaged to one point from three clones.

Gene	DF	F (DFn, DFd)	P value	P value summary
INFGR1	3	F (3, 8) = 48.40	P<0.0001	****
IFNGR2	3	F (3, 8) = 22.12	P=0.0003	***
TNFRSF1A	3	F (3, 8) = 12.41	P=0.0022	**
TNFRSF1B	3	F (3, 8) = 3.571	P=0.0666	ns
IL6R	3	F (3, 8) = 10.95	P=0.0033	**
IL-6ST	3	F (3, 8) = 10.06	P=0.0043	**
IL17RA	3	F (3, 8) = 3.008	P=0.0146	*

In contrast to MGLs, differentiation of hiPSCs to forebrain NPCs in monoculture resulted in exceptionally low levels of *IL6R* expression, although this did not achieve statistical significance overall, the expression was ~16-fold lower, as compared to the hiPSC stage (Figure 3.4B, statistics in Table 3.6). This reduction in *IL6R* expression observed during differentiation is consistent with prior evidence from human *post-mortem* foetal brain tissue (Fietz *et al.*, 2012; Florio *et al.*, 2015; Zhang *et al.*, 2016). These data suggest that *IL6R* is largely expressed by microglia and, to a lesser extent, astrocytes in the human brain, but not by neurons or their progenitors (Miller *et al.*, 2014; Zhang *et al.*, 2016) (Table 3.7). By contrast, *IFNGR1/2, IL-6ST,* and *IL17RA* transcripts were expressed in forebrain NPCs, with levels either staying constant or trending upward (albeit $p > 0.05$) during neuralisation (Figure 3.4B). Of note, *TNFRF1A* mRNA expression decreased relative to the hiPSC stage ($p > 0.05$), but *TNFRSF1B* mRNA expression increased significantly ($p = 0.0127$) (Figure 3.4B, statistics in Table 3.6). As previously stated, IL-6Ra must be present in its membrane bound form (cis-IL-6Ra signalling) or the soluble (s)IL-6Ra form (trans-IL-6Ra signalling) which is cleaved at the membrane surface of expressing cells for a cell to respond to IL-6 via either classical or trans-signalling (Wolf, Rose-John and Garbers, 2014). These findings suggest that when grown in monoculture, forebrain NPCs are unlikely to be responsive to IL-6 via classical-IL-6Ra signalling but would be receptive to IFN, as previously demonstrated (Warre-Cornish *et al.*, 2020; Bhat *et al.*, 2022).

Table 3.6 -One-way ANOVA of qPCR cytokine receptor expression in NPCs with N=3 donors, averaged to one point from three clones.

Gene	DF	F (DFn, DFd)	P value	P value summary
INFGR1	3	F (3, 8) = 0.4339	P=0.7346	ns
IFNGR2	3	F (3, 8) =0.6834	P=0.5867	ns
TNFRSF1A	3	F (3, 8) = 1.325	P=0.3324	ns
TNFRSF1B	3	F (3, 8) = 6.972	P=0.0127	*
IL6R	3	F (3, 8) = 3.008	P=0.0946	ns
IL-6ST	3	F (3, 8) = 2.464	P=0.1369	ns
IL17RA	3	F (3, 8) = 0.2049	P=0.8902	ns

Table 3.7 -Validation of IL6R and IL-6ST expression in previous transcriptomic datasets in comparison to our RNAseq.

Publication	Species	Age	Method	Sample	*IL6R*	*IL-6ST*
Zhang *et al.*, 2014	Human	Foetal /adult	RNAseq	Microglia/ macrophage	8.12 FPKM	80.06 FPKM
				Neurons	0.28 FPKM	18.59 FPKM
				Foetal Astrocytes	0.65 FPKM	9.20 FPKM
Miller *et al.*, 2014	Human	Midfoetal	Micro-array	Bulk	0.41 RPKM	5.35 RPKM
Fietz *et al.*, 2012	Human	Foetal	RNAseq	Cortical Plate	0 FPKM	1.6-5.9 FPKM
				Inner Subventricular Zone	0 FPKM	6.4-9.2 FPKM
				Outer Subventricular Zone	0-0.6 FPKM	9.0-16.1 FPKM
				Ventricular Zone	0 FPKM	16.4-36.1FPKM
Florio *et al.*, 2015	Human	Foetal	RNAseq	Neurons Neocortex	1.6 FPKM	6.3 FPKM
				Basal Radial Glia Neocortex	1.5 FPKM	6 FPKM
				Apical Radial Glia Neocortex	0.9 FPKM	9.5 FPKM

Of note, a recent study using a very similar differentiation protocol provides data to suggest that both transcriptional and morphological abnormalities relevant for neurodevelopmental disorders associated with MIA exposure can be produced in hiPSC-derived day 60 mature cortical pyramidal neurons after exposure to IL-6 (concentration) from days 25-27 of differentiation (Kathuria *et al.*, 2022). This suggests there may be a temporal difference in IL-6Ra expression with longer periods of differentiation. Hence, we next sought to replicate the finding of minimal *IL6R* expression in NPCs and extend this analysis to terminally differentiated mature cortical neurons. To do so, we performed qPCR analysis of RNA samples from NPCs up to 50 days of terminal cortical mature neuron differentiation in independent

male donor hiPSCs (N=3 cell lines, 1 clone per donor) and verified the relatively low expression of *IL6R* in forebrain NPCs at all time-points examined, including at least up to 50 days of differentiation, relative to the hiPSC stage (one-way ANOVA: $F(3,8) = 7.30$, $p = 0.0112$; Mean fold change from hiPSC: D7 = 0.03, D20 = 0.03, D50 = 0.12; Figure 3.4C). *IL-6ST* expression, on the other hand, increased across all phases of neural differentiation (one-way ANOVA: $F(3,8) = 19.87$, $p = 0.0005$; Mean fold change from hiPSC: D7 = 2.90, D20 = 6.54, D50 = 3.46; Figure 3.4C). These findings support our prior findings of low *IL6R* expression in forebrain NPCs and extend them to mature cortical neurons.

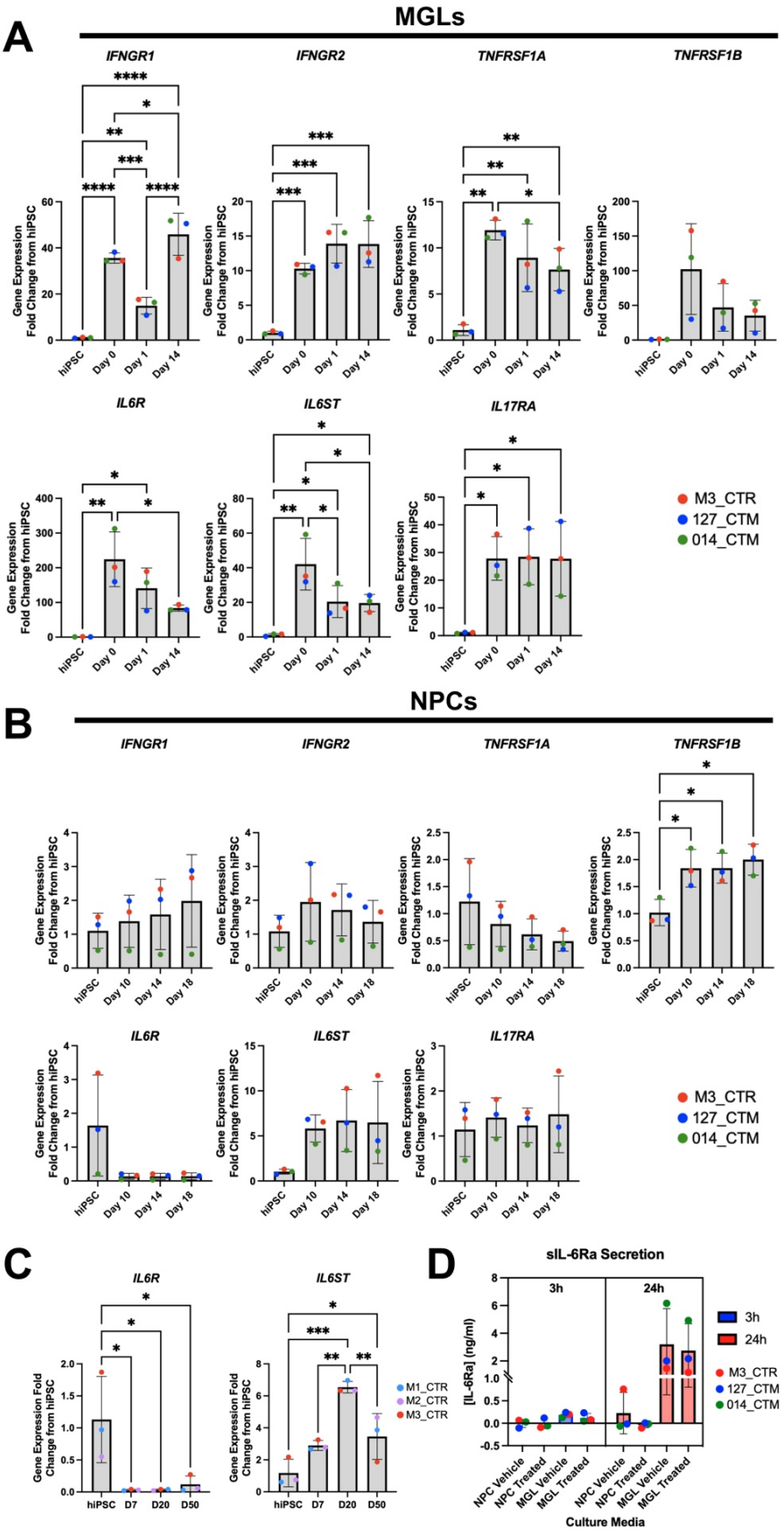

Figure 3.4 - Cytokine receptor transcript expression in MGL and NPCs. Data shown are from N=3 male neurotypical hiPSC cell lines, averaged from three technical replicate clones per donor, barring outlier removal where stated. 5% false discovery

*rate (FDR) by Benjamini–Hochberg (BH) method corrections after one-way ANOVA formatted as follows: *q < 0.05, **q < 0.01, ***q < 0.001, and ****q < 0.0001; non-significant not labelled. Bar graphs plotted as mean with standard deviation (SD) error bars, and points coloured by donor line as shown in key. (A) MGL differentiation time-course of cytokine receptors (IFNGR1, IFNGR2, TNFRSF1A, TNFRSF1B, IL6a, IL-6ST and IL17RA) gene expression at hiPSC, macrophage/microglia progenitors (day 0), MGL at day 1 and day 14 of differentiation. M3_CTR day 14 IL17RA data point averaged from N=2 clones only. (B) NPC differentiation time-course of the same cytokine receptors by qPCR RNA samples at hiPSC and days 10, 14 and 18 of neuralization to NPCs. 127_CTM day 14 TNFRSF1B data point was averaged form N=2 clones only. (C) qPCR of IL6R and IL-6ST transcript expression in N=3 different healthy male lines (M1_CTR, M2_CTR and M3_CTR, one technical repeat each) over a longer timeframe, from hiPSC to D50 mature neurons. (D) Protein concentrations quantified by ELISA of soluble IL-6Ra (ng/ml) in NPC (on D18) and MGL (on D14) culture media after 3h and 24h vehicle or IL-6 100ng/ml treatment exposure.*

Cleavage of the IL-6Ra transmembrane domain by protease ADAM17, and its subsequent secretion by a cell, indicates its capacity to facilitate trans-IL-6 signalling (Michalopoulou *et al.*, 2004; Campbell *et al.*, 2014; Wolf, Rose-John and Garbers, 2014). Considering the apparent minimal level of *IL6R* expression in forebrain NPCs under the tested conditions, we next examined the secretion of the soluble IL-6Ra protein using a specific ELISA kit with supernatants from both forebrain NPC and MGL monocultures following acute exposure to either vehicle or 100ng/ml IL-6 for either 3 or 24 hours. In accordance with the gene expression data, NPCs secreted a minimal quantity of sIL-6Ra protein into the culture media (Figure 3.4D). By contrast, MGL sIL-6Ra secretion, was detected in the culture media after both 3h and 24h but this was not altered by IL-6 stimulation under the conditions tested in either cell type (Figure 3.4D, Table 3.8). Nonetheless, the fact that MGLs release sIL-6Ra enables other cell types in their proximity to respond to IL-6 through soluble, non-membrane bound (trans-)IL-6Ra signalling. The absence of sIL-6Ra secretion from NPCs, on the other hand, confirms that they lack the soluble form of the IL-6 receptor and strongly suggests that forebrain NPCs are unlikely to be responsive to IL-6 in monoculture under the conditions examined.

Table 3.8 - Two-way ANOVAs comparing sIL-6Ra secretion from NPC or MGL (cell type factor) in monoculture media and whether IL-6 100ng/ml treatment alters this secretion (treatment factor), after both 3h and 24h.

Treatment Length	Source of Variation	DF	F (DFn, DFd)	P value	P value summary
3h	Interaction	1	F (1, 8) = 0.3499	P = 0.5705	ns
	Treatment Factor	1	F (1, 8) = 0.4969	P = 0.5009	ns
	Cell Type Factor	1	F (1, 8) = 9.349	P = 0.0156	*
24h	Interaction	1	F (1, 8) = 0.01056	P = 0.9207	ns
	Treatment Factor	1	F (1, 8) = 0.1467	P = 0.7116	ns
	Cell Type Factor	1	F (1, 8) = 9.392	P = 0.0155	*

3.3.3 IL-6 activates the STAT3 pathway in microglia-like cells but not neural progenitor cells in monoculture

We next confirmed that the expressed IL-6Ra and IL-6ST receptors were or were not functional in forebrain day 18 (D18) NPCs, D1 and D14 MGLs through examination of the canonical STAT-3 signalling pathway (Figure 3.5A). These early-stage optimisation experiments considered the two stages of MGL differentiation (D1 and D14) in order to establish the optimal timing for IL-6 stimulation and response. Initially, qPCR was used to quantify transcripts of relevant IL-6Ra and STAT3 downstream target genes *IL6*, *IL10*, tumour necrosis factor *α* (*TNF),* and Jumonji Domain-Containing Protein 3 (*JMJD3*) (Przanowski *et al.*, 2014). Following acute exposure for 3 hours to IL-6 (100 ng/ml) both D1 MGL and D14 MGL cells displayed increasing expression of *IL6* and *JMJD3*, relative to a vehicle control stimulation (Figure 3.5B, Table 3.9). Due to donor variance as a function of our small sample size (N = 3 donors), when comparing post-IL-6 stimulation statistical significance for *IL10* mRNA expression was unidentifiable in D1 MGLs (~5-fold) but significant in D14 MGLs (~3-fold) despite D1 MGLs having a greater fold change than D14 MGLs. Interestingly*, TNF* expression was unaffected by IL-6 exposure in either D1 or D14 MGLs at this time-point (Figure 3.5B, statistics in Table 3.9). By contrast, 24h following 100 ng/ml IL-6 treatment, the expression of all these genes was no longer statistically significant different from the vehicle control in both D1 and D14 MGLs (Figure 3.5B, Table 3.9). Given the similar comparability of D1 and D14

MGL responses, as well as their apparent greater functional maturity after 14 days of differentiation (Haenseler *et al.*, 2017), all further experiments used only MGLs differentiated for 14 days (Couch *et al.*, 2023).

Table 3.9 - Unpaired t-test statistics and 5% FDR BH corrected q-values of IL6, IL10, JMJD3 and TNF expression changes in D1 MGL and D14 MGL IL-6 treated samples over 3 and 24h.

Cell Type	Gene	3h t, df	3h P value	3h P value Summary	3h q value	24h t, df	24h P value	24h P value Summary	24h q value
D1 MGL	*IL6*	3.83, 4	0.0186	*	0.04	1.38, 4	0.2391	ns	0.40
	TNF	1.89, 4	0.1312	ns	0.15	1.45, 4	0.2202	ns	0.40
	JMJD3	3.00, 4	0.0401	*	0.06	1.00, 4	0.3748	ns	0.43
	IL10	1.93, 4	0.1264	ns	0.15	1.34, 4	0.2529	ns	0.40
D14 MGL	*IL6*	4.38, 4	0.0118	*	0.03	1.85, 4	0.1378	ns	0.40
	TNF	1.31, 4	0.2620	ns	0.26	0.69, 4	0.5259	ns	0.53
	JMJD3	5.04, 4	0.0073	**	0.03	1.18, 4	0.3004	ns	0.40
	IL10	4.36, 4	0.0120	*	0.03	1.37, 4	0.2419	ns	0.40

The D18 NPC response to 100 ng/ml IL-6 in monoculture was also quantified using qPCR to determine whether they could mount a response even with minimal IL-6Ra expression. NPCs did not significantly increase the expression of *IL6*, *JMJD3*, and *TNF* transcripts 3h after IL-6 treatment compared to vehicle controls (Figure 3.5C, statistics in Table 3.10). Furthermore, because *IL10* Ct values were undeterminable during qPCR, the *IL10* transcript was considered undetectable in all NPC samples regardless of treatment. To verify that the undetectable Ct values were not due to incorrectly designed primers, melt curves were evaluated and compared between MGL and NPC samples, revealing no flaw in the primer's capacity to amplify the target amplicon (Figure 3.5D). Taking these results together, forebrain NPCs at D18 *in vitro* do not demonstrate the same IL-6-induced IL6R signalling in monoculture that MGLs do.

Table 3.10 - Unpaired t-test statistics and 5% FDR BH corrected q-values for IL6, JMJD3 and TNF expression changes in NPC IL-6 treated samples over 3h.

Gene	3h t, df	3h P Value	P value summary	3h q value
IL6	0.712, 4	0.5161	ns	0.774
TNF	1.705, 4	0.1634	ns	0.490
JMJD3	0.097, 4	0.9275	ns	0.928

To complement our gene expression analysis, we looked at the acute time course of STAT3 phosphorylation after IL-6 receptor activation in both forebrain D18 NPCs and D14 MGLs. When the IL-6/IL-6Ra/IL-6ST complex forms on the cell surface membrane, the protein kinase JAK phosphorylates STAT3 (pSTAT3) at Y705, which then shuttles to the nucleus to allow further transcription of STAT3 target genes, such as *JMJD3* (Wolf, Rose-John and Garbers, 2014). Because of this, pSTAT3 is an excellent marker for determining the immediate presence of IL-6 signalling pathway activation at the protein level. Protein samples were therefore collected from either D18 NPCs or D14 MGLs at four time periods after acute 100ng/ml IL-6 exposure and Y705-pSTAT3 and total STAT3 protein levels measured by western blot (Figure 2E-G). Ratio quantification between Y705-pSTAT3 and total STAT3 (tSTAT3) revealed that in MGLs, IL-6 triggered a time-dependent increase in pSTAT3 relative to vehicle controls that peaked after 15 min, which was absent in D18 forebrain NPCs at any time-point (Figure 2E, two-way ANOVA: cell type $F(3,16) = 17.45$, $p = 0.0007$; time $F(3,16) = 5.486$, $p = 0.0089$; interaction $F(3,16) = 5.47$, $p = 0.0088$). These findings support the absence of an IL-6Ra-mediated response in forebrain D18 NPCs to 100ng/ml IL-6 in monoculture for at least 3 hours after exposure, in contrast to MGLs.

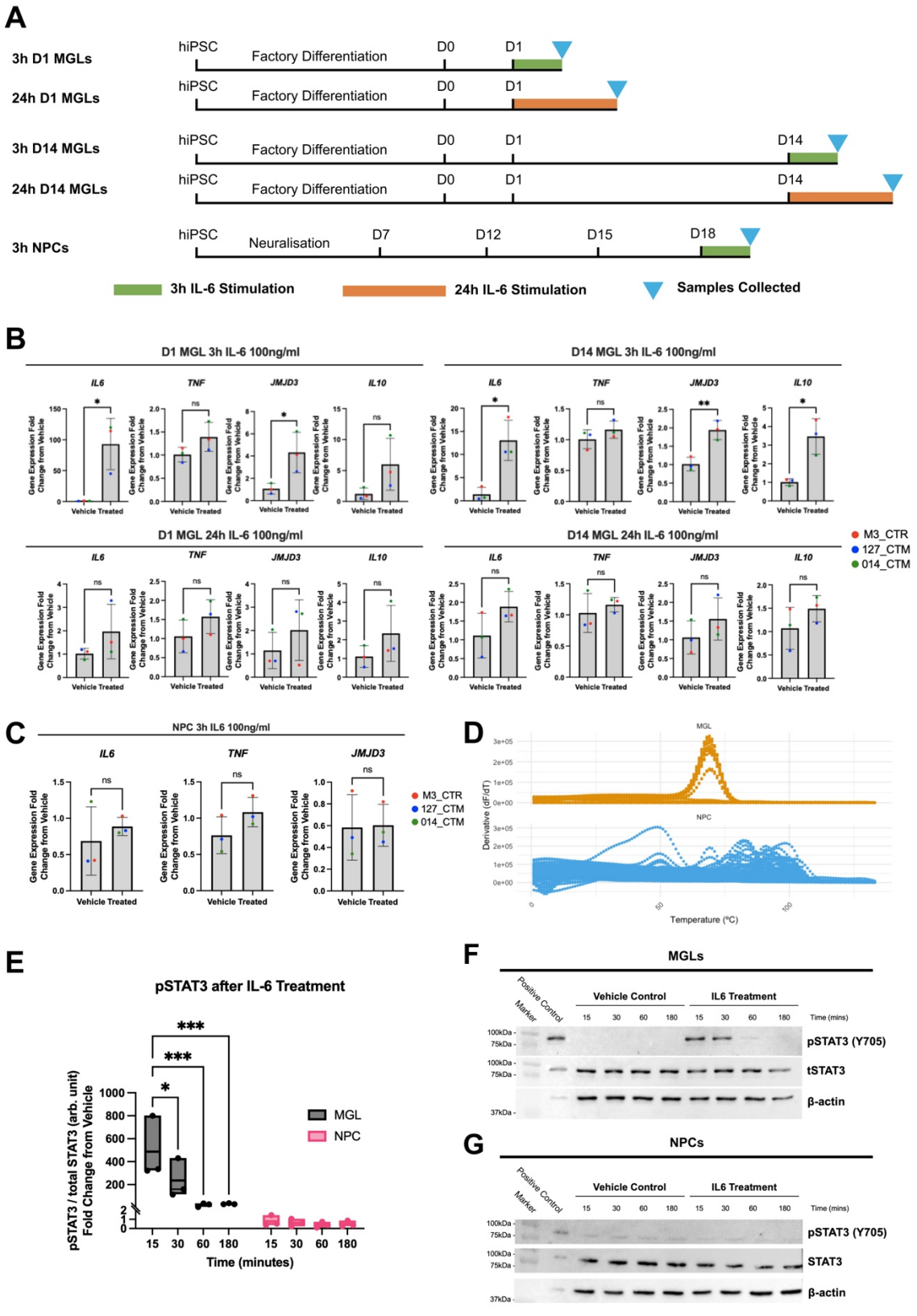

Figure 3.5 - MGL monocultures respond to IL-6 in a dose and time dependent manner, NPC monocultures do not respond at all. (A) Schematic of MGL and NPC cell culture and RNA sample collection. (B) Transcripts of downstream IL-6 pathway genes IL6, TNF, JMJD3 and IL10 were measured by qPCR in three male healthy control cell lines treated with 100ng/ml IL-

*6, averaged over three technical replicate clone cultures per donor unless stated otherwise, in the following conditions: D1 MGL treated for 3h; D14 MGLs treated for 3h; D1 MGL treated for 24h, 014_CTM treated condition averaged from N=2 clones only; MGLs treated for 24h. Unpaired test results formatted as follows: *p < 0.05, **p < 0.01, ***p < 0.001, and ****p < 0.0001; not significant (ns). Bar graphs plotted as means with standard deviation (SD) error bars, and points coloured by donor line: red (M3_CTR), blue (127_CTM) and green (014_CTM). (C) Transcripts of downstream IL-6 pathway genes IL6, TNF and JMJD3 in NPCs treated for 3h, with unpaired t-test results formatted as above. IL10 transcripts were undetectable in NPC samples so data is not shown. (D) Derivative melt curve of IL10 primer from both MGL and NPC samples from qPCR reactions presented in part 3.3.3. (E) Quantification of pSTAT3/tSTAT3 protein signal in arbitrary (arb.) units from blots F and G, shown as a fold change ratio from timepoint vehicle within cell type. Box plot presented with split y-axis at 2 arb. units to visualize variance in NPC data. (F-G) Immunoblotting for 88kDa pSTAT3/tSTAT3 in both vehicle and 100ng/ml IL-6 stimulated samples collected after 15, 30, 60 and 180mins, in MGL (E) and NPC (F) monocultures, with 3h IL-6 100ng/ml treated immortalized mouse microglia cells (BV2s) as a positive control.*

3.3.4 Neural progenitor cells respond to IL-6 by trans-signalling in the presence of sIL-6Ra in a dose-dependent manner

So far, the data suggest that IL-6Ra, and its soluble form sIL-6Ra, are absent from human forebrain NPC monocultures *in vitro*. Because both the IL-6Ra and IL-6RA subunits must be in complex with IL-6 before a cell can respond to the cytokine, forebrain NPCs alone are therefore insensitive to cis- or trans-signalling in monoculture. However, this does not necessarily imply that they are unable to respond to IL-6 even in the presence of sIL-6Ra from an alternative source. To test this hypothesis with human forebrain NPCs *in vitro*, recombinant human sIL-6Ra was added exogenously to the monocultures at D18 of differentiation from N = 3 healthy male donors (one clone per donor), to examine if this enabled them to respond to IL-6 as measured by pSTAT3 protein levels via western blotting. Upon addition of 100ng/ml recombinant sIL-6Ra (rIL-6Ra) in combination with 100ng/ml IL-6 (Figure 3.6A), STAT3 phosphorylation significantly increased in D18 NPCs after 15mins (one-way ANOVA $F(3, 8) = 1773$, $p < 0.0001$), which diminished but was still present by 3h (one-way ANOVA $F(3, 8) = 4.920$, $p = 0.0318$) (Figure 3.6B). Moreover, when the dose concentration of rIL-6Ra was

reduced, so too was the ratio of pSTAT3/tSTAT3 after 15mins of IL-6 treatment (two-way ANOVA: Interaction $F(4, 20) = 31.94$, $p < 0.0001$; [rIL-6Ra] Factor $F(4, 20) = 36.55$, $p < 0.0001$; Treatment Factor $F(1, 20) = 436.0$, $p < 0.001$) (Figure 3.6C and Figure 3.6D). Only at the lowest dose (1ng/ml rIL-6Ra) was pSTAT3/tSTAT3 in vehicle and IL-6 treated NPCs statistically indistinguishable (5% FDR = 0.371). These findings indicate that D18 NPCs may indeed respond to IL-6 stimulation, but only in the presence of sIL-6Ra from an alternate source via trans-signalling, and in a receptor dose-dependent manner.

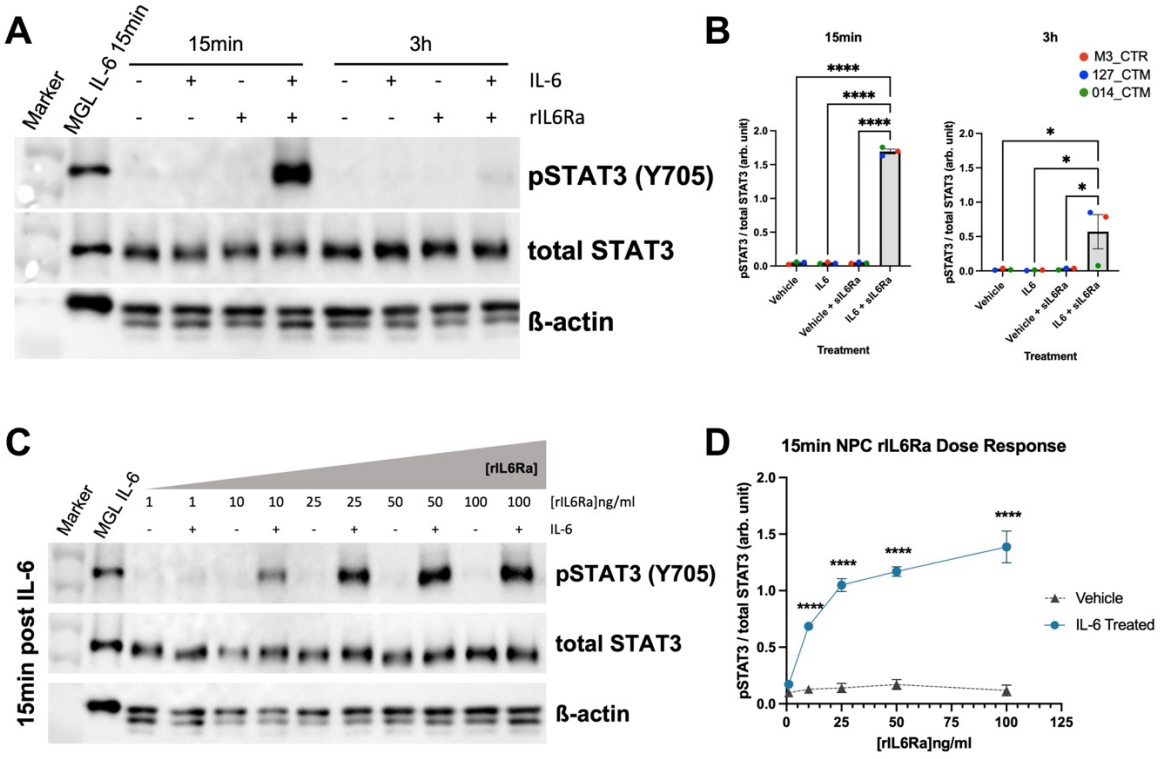

*Figure 3.6 - Human forebrain NPCs respond to IL-6 by trans-signalling only. Data shown are from N=3 male neurotypical hiPSC cell lines, one technical repeat each. 5% false discovery rate (FDR) by Benjamini–Hochberg (BH) method corrections after one-way (B) or two-way (D) ANOVA formatted as follows: * q < 0.05, ** q < 0.01, *** q < 0.001, and **** q < 0.0001; non-significant not labelled. (A) Immunoblotting for 88kDa pSTAT3/tSTAT3 and ß-Actin in both vehicle and 100ng/ml IL-6 stimulated samples in the presence or absence of rIL-6Ra collected after 15 and 3h in D18 NPC monocultures. (B) Quantification of pSTAT3/tSTAT3 protein signal after both 15min and 3h IL-6 stimulation in arbitrary (arb.) units from previous blot (A). Bar graph plotted as mean with standard deviation (SD) error bars, and points coloured by donor line: red (M3_CTR), blue (127_CTM) and green (014_CTM). (C) Immunoblotting for 88kDa pSTAT3/tSTAT3 and ß-Actin in both vehicle and 100ng/ml IL-6 stimulated samples in the presence of increasing rIL-6Ra concentrations (1, 10, 25, 50 and 100*

ng/ml) collected in RIPA after 15min stimulation in D18 NPC monocultures. (D) Quantification of pSTAT3/tSTAT3 protein signal after both 15min and 3h IL-6 stimulation in arbitrary (arb.) units from previous blot (A). Line graph plotted as mean with standard deviation (SD) error bars, and points coloured by treatment condition as shown in key. 5% FDR comparisons of treatment to corresponding vehicle annotated.

3.4 Discussion

This chapter describes how hiPSC lines derived from three male, neurotypical donors were differentiated into MGLs and cortical NPCs and used to characterise the cell-specific response to acute IL-6 exposure in monoculture. The data suggest three main conclusions: first, the MGL and NPCs in monoculture express markers with relevance for microglia and NPCs respectively in the human foetal neocortex at mid-gestation; second, that the cytokine receptor expression profiles of MGL and NPCs produced from hiPSCs clearly differ compared to one another, giving them unequal ability to respond to IL-6; and third, that these two distinct cell types demonstrate differential IL-6 response mechanisms. Specifically, human cortical NPCs are not capable of initiating the IL-6 cis-signalling pathway in monoculture but may become responsive when either grown together with other cell types that release sIL-6Ra, or if this protein is added exogenously.

3.4.1 hiPSC-derived MGL and NPC phenotype

Overall, hiPSC-derived MGLs and NPCs were successfully differentiated from nine hiPSC lines and transcripts of cell-specific markers were comparable to those from primary human foetal datasets at key gestational timepoints indicated in MIA literature as being at risk for NDDs in the offspring. Our data replicated findings from hiPSC-derived MGLs differentiated using the same technique (Haenseler *et al.*, 2017), in which the MGL transcriptome profile was confirmed as similar to that of primary foetal human microglia (Haenseler *et al.*, 2017). There

was little difference in microglial marker expression or cell area between 1 and 14 days of terminal differentiation from the progenitor factory, except for *CX3CR1* expression. Even though increased *CX3CR1* expression in microglia is considered to indicate greater neuron-glial signalling capacity, it was unclear if a longer terminal differentiation provided an increased microglial-functional capacity (Subbarayan *et al.*, 2021). Prior work in the Vernon lab confirms that 7-14 days of differentiation is sufficient to induce microglia marker expression and key functions such as phagocytosis (Solomon *et al.*, 2022). We therefore selected 14 days of differentiation for MGLs for all subsequent experiments in this thesis. Additionally, two-way ANOVA analysis of microglial markers at both RNA transcript (Table 3.2) and protein levels (Table 3.3), comparing each gene expression with donor and time point, revealed that donor had no effect on cell phenotype. To minimise batch and reprogramming variability, independent donors were considered as biological replicates. These replicates were averaged from N=3 technical replicates either from clone cultures or different MGL harvests, as stated in figure legends of optimisation experiments. This was extended to NPC optimisation experiments as well.

3.4.2 Cell-specific differences in IL-6 Receptor Machinery and STAT3 Signalling

Both hiPSC-derived forebrain NPCs and mature neurons had extremely low levels of *IL6R*, resulting in a restricted ability to respond to IL-6 treatment in monoculture, as indicated by the lack of STAT3-phosphorylation and changes in *IL6, JMJD3,* and *TNF* expression after IL-6 exposure. These results appear to contradict recent findings using hiPSC-derived mature neurons, produced via a similar differentiation protocol, in which IL-6 exposure resulted in changes to mitochondrial respiration and to the expression of genes that regulate extracellular matrix, actin cytoskeleton and TGF-β signalling (Kathuria *et al.*, 2022). One important distinction between this study and ours is the stage at which these cells were exposed to IL-6:

D18 NPCs in this study vs. D25-27 neurons (Kathuria *et al.*, 2022). Although *IL6R* expression is minimal in the D50 forebrain neurons derived in our hands, it is possible that *IL6R* mRNA is expressed transiently between days 25-50, or that only protein levels are present, which qPCR cannot detect. As a result, we cannot rule out the possibility that D25-27 neurons produced from our approach might elicit an IL-6 response and that changes in IL-6 exposure time may result in different outcomes (Estes and McAllister, 2016). With that being said, the extensive evidence obtained from both human foetal tissue and organoid studies strongly supports the conclusion drawn in this chapter, which indicate a notable absence of *IL6R* expression in NPCs throughout human foetal cortical development (Fietz *et al.*, 2012; Florio *et al.*, 2015; Zhang *et al.*, 2016; Sarieva *et al.*, 2023).

A second distinction from the study presented here and that of Kathuria *et al.*, (2022) is the amount and duration of IL-6 exposure for these cells: 3h and 24h of 100ng/ml IL-6 as opposed to 48h of 1µg/ml IL-6 (Kathuria *et al.*, 2022). It is important to emphasize that, as demonstrated in animal MIA models, differences in the degree and duration of immune activation in human cellular models will result in different outcomes. RNAseq was not carried out on our IL-6-exposed NPC RNA, so we cannot rule out a non-canonical IL-6 response that is independent of the IL-6Ra-STAT3 pathway at higher or more chronic IL-6 concentrations. Further experiments are required to answer these questions, whilst ensuring careful descriptions of protocols and replications between labs in order to avoid the same pitfalls observed in animal studies, where methodological variance can lead to heterogeneous results.

3.4.3 The Necessity for an MGL-NPC Co-culture

Furthermore, our findings indicate that MGLs in co-culture with NPCs is likely to be required to investigate the effect of IL-6 on NPC-specific development when utilising D18 forebrain

cortical NPCs under the conditions studied in this chapter. This is based on the observation that sIL-6Ra is secreted from MGLs but not NPCs, at two different time periods. Hence, sIL-6Ra secretion by MGLs may facilitate NPCs to respond to IL-6 *in vitro* via trans-signalling, given their incapacity for cis-signalling (Figure 3.7). Following this, NPCs were found to respond to IL-6, as measured by STAT3 phosphorylation in the presence of recombinant sIL-6Ra, in a dose-dependent manner. In support of this view, data from a transgenic mouse model show that inhibiting CNS trans-signalling via sIL-6Ra reduces several relevant neuropathological hallmarks previously associated with NDDs, such as impaired neurogenesis, blood brain barrier leakage, vascular proliferation, astrogliosis, and microgliosis (Campbell *et al.*, 2014). These findings support the hypothesis that sIL-6Ra trans-signalling has the propensity to be a detrimental mechanism of IL-6 signalling in both glial and non-glial cell types (Campbell *et al.*, 2014). In addition, sIL-6Ra is constitutively expressed irrespective of inflammatory condition in cerebrospinal fluid (CSF) at 1.92–3.03ng/ml (Hans *et al.*, 1999; Azuma *et al.*, 2000). This not only demonstrates that IL-6 trans-signalling is feasible in the human brain, but it also confirms the findings reported in this chapter, which show that MGL sIL-6Ra secretion in culture medium reaches concentrations comparable to human CSF after 24 hours and is independent of IL-6 stimulation (Sarieva *et al.*, 2023).

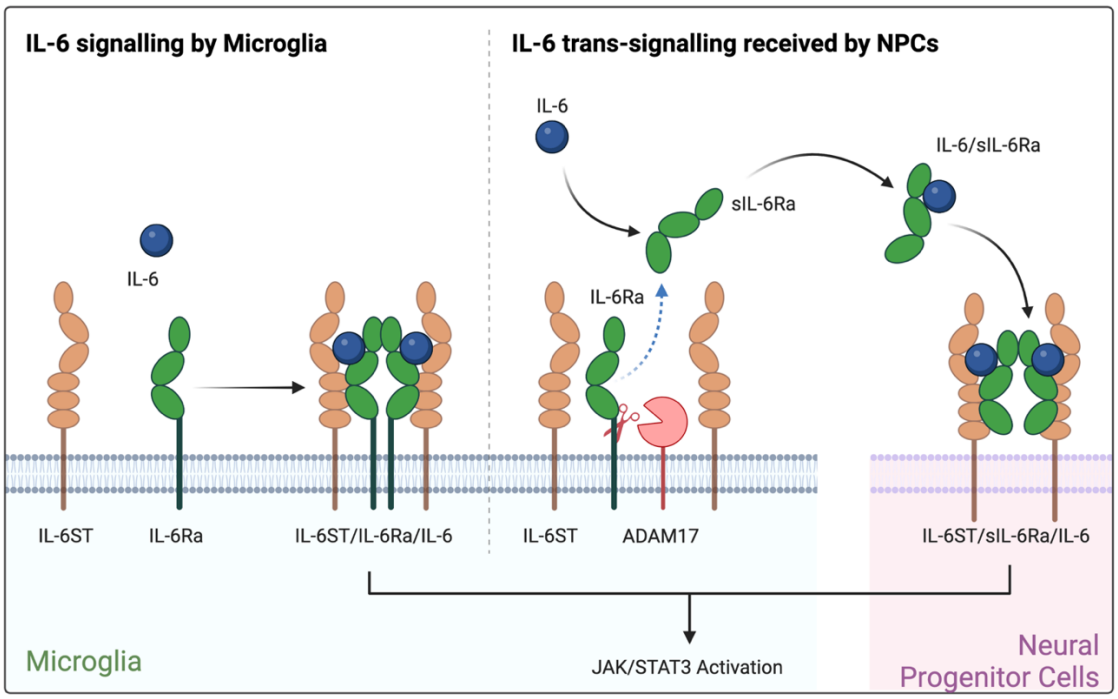

Figure 3.7 – Diagram illustrating the IL-6 signalling mechanism differences between microglia and neural progenitor cells. Microglia express both IL-6ST and IL-6Ra with which they can respond to IL-6 by either cis- or trans-signalling. The microglia can also cleave the sIL-6Ra on the cell surface membrane, which hypothetically will allow NPCs to respond to IL-6 via trans-signalling when in co-culture. This hypothesis requires testing.

3.5 Conclusion

In conclusion, hiPSC-derived MGLs can react to IL-6 via canonical IL-6Ra signalling pathway, but NPCs cannot, owing to low *IL6R* expression and sIL-6Ra secretion. sIL-6Ra, which is secreted by MGLs, assists the IL-6 response of NPCs by enabling trans-signalling. Therefore, human microglia can receive MIA-derived IL-6 insults, while human NPCs are only susceptible to this stimulus when exposed to sIL-6Ra secreted from other cell types. These findings give way to two logical steps in determining the effect of IL-6 on human NPC development: firstly, to characterise the MGL response to IL-6 more thoroughly to characterise additional form and function changes in response to the IL-6 insult that may target NPC development; and second, co-culture these two cell types together to allow microglia to secrete sIL-6Ra and facilitate NPC response to IL-6.

Chapter 4

Acute IL-6 Evokes Changes to Human Microglia-Like Cell Form and Function

---

NOTE: SOME OF THE RESULTS FROM THIS CHAPTER WERE FIRST PUBLISHED IN BRAIN, BEHAVIOR AND IMMUNITY, IN 2023, ENTITLED "ACUTE IL-6 EXPOSURE TRIGGERS CANONICAL IL-6RA SIGNALLING IN HIPSC MICROGLIA, BUT NOT NEURAL PROGENITOR CELLS" (COUCH *ET AL.*, 2023) (APPENDIX 1).

Chapter Summary

Background: IL-6 has the capacity to alter microglial activity through modifying their transcriptome, motility, and secreted signals including cytokines and chemokines. However, it is unclear how far microglial neurodevelopmental functions are affected by IL-6, and whether this microglial functional change is implicated in the mediation of MIA risk for NDDs.

Methods: This chapter combined RNAseq, live imaging, and secretome analysis by a proteome profiler kit to investigate how acute IL-6 affects the shape and function of MGLs in monocultures only.

Results: First it was discovered that 100 ng/ml was the lowest concentration of IL-6 to initiate up-regulation of genes downstream of JAK/STAT3 signalling (*IRF8*, *IL6*, *IL10* and *JMJD3*) by MGLs. Bulk RNAseq detected 156 up-regulated genes in MGL after acute IL-6 exposure and 22 down-regulated genes. The up-regulated gene set from this *in vitro* model significantly overlapped with an up-regulated gene set from human *post-mortem* brain tissue from schizophrenia patients, but not with GWAS-identified schizophrenia risk genes. Acute IL-6 stimulation markedly enhanced cytoplasmic MGL motility, and induced cytokine and chemokine secretion. The human MGL IL-6 response observations are consistent with key microglia findings in animal models of MIA. These include the new-born pup's microglial transcriptome, IRF8-dependent microglia motility, and maternal MIP-1 serum production.

Conclusion: These indicate the significance of microglia in human NDDs and provide clues for a potential mechanism by which IL-6 may influence NPC development.

4.1 Introduction

According to the findings in Chapter 3, in response to IL-6 we observed activation of canonical STAT-3 signalling in microglia-like cells (MGLs), but not neural progenitor cells (NPCs), unless these latter cells were exposed to soluble IL-6Ra to activate the IL-6 trans-signalling pathway. As mentioned in section 1.2.2, microglia play key roles typical neurodevelopment, including regulation of processes ranging from synaptogenesis, axon guidance, neurite migration, astrocyte growth and vasculature development (Paolicelli *et al.*, 2011; Cunningham, Martínez-Cerdeño and Noctor, 2013; Hanger *et al.*, 2020; Ferro, Auguste and Cheadle, 2021). Importantly, these neurodevelopmental processes involve both physical cell-to-cell contacts and the secretion of cytokine and chemokine signals from microglia (Shigemoto-Mogami *et al.*, 2014; Li and Barres, 2018; Chagas *et al.*, 2020). As such they are clearly dependent on the microglial functional state, which is dynamic and highly sensitive to environmental cues as mentioned in section 1.2.2 (Schafer *et al.*, 2012). Based on *in vitro* evidence from primary mouse microglia (Ozaki *et al.*, 2020), the microglial functional shift brought about in response to IL-6-driven canonical STAT-3 signalling is likely to result in a change to microglial motility and secretome, both microglial functions that play a role in development as discussed in the following sections (Paolicelli *et al.*, 2011; Cunningham, Martínez-Cerdeño and Noctor, 2013; Ozaki *et al.*, 2020; Pérez-Rodríguez, Blanco-Luquin and Mendioroz, 2021). Consistent with this view, there is circumstantial evidence from human genetics, brain *post-mortem* tissue research, neuroimaging, and peripheral biomarker studies that implicate microglia in the pathogenesis of NDDs, as presented in section 1.2.2 (Mondelli *et al.*, 2017; Coomey *et al.*, 2020). Therefore, acutely elevated maternal IL-6 during pregnancy, for example as a consequence of maternal infection, could be predicted to influence microglia to change their functional state. Even if this reflects a temporary state shift, it will therefore have the potential to influence the aforementioned normal neurodevelopmental process. This may occur either by

disrupting the normative functions microglia play in development, leading the development of a “latent” insult, or by influencing how microglia acquire their functions, which is thought to reflect a stepwise process of switching on different transcriptional programs (Matcovitch-Natan *et al.*, 2016). Our understanding of how IL-6 affects the development and functioning of human foetal microglia, and its knock-on effects on other cell types, is currently limited. In the subsequent sections, we will focus on discussing the microglial functions of motility and secretome to provide a rationale for this choice.

4.1.1 Microglial Motility

Microglia demonstrate a high degree of motility (Franco-Bocanegra *et al.*, 2019). They exhibit a steady continuous motility in which processes extend and retract without movement of the cell body (soma), which is known as "surveillance motility" (Nimmerjahn, Kirchhoff and Helmchen, 2005). This allows microglia to scan their surroundings, eliminate undesired cell debris, and connect with other cell types (Garden and Möller, 2006). Microglia appear to spread out across the brain, known as “tiling”, with each cell overseeing a specific functional area (Miller *et al.*, 2019). However, this arrangement is disrupted when microglia gather in clusters, such as when they migrate to a region of tissue damage or respond to other stimuli like changes in neural activity (Miller *et al.*, 2019). As a result, their usual surveillance function is compromised.

In order to gain direction on their movement, microglia will fluidly transfer through different functional states towards directed motility, or "chemotactic motility," in response to certain chemokines, directing microglial movement of the whole soma towards a source of damage or disease (Khurana *et al.*, 2002; Miller *et al.*, 2019). Monocyte chemotactic protein (MCP-1), macrophage inflammatory peptide-1 (MIP-1) and interleukin-8 (IL-8) are all well-known

chemotactic signalling molecules (Yao and Tsirka, 2010; Johnson *et al.*, 2011; McLarnon, 2012; Matsushima, Yang and Oppenheim, 2022). Nonetheless, reports of the existence of additional potential chemotactic agents, such as vascular endothelial growth factor (VEGF), have been published (Forstreuter, Lucius and Mentlein, 2002). Both surveillance and chemotactic motilities are mutually exclusive, with the latter having a putative pro-inflammatory phenotype (Madry and Attwell, 2015; Hefendehl *et al.*, 2014). Specifically, during neurodevelopment, a key function of microglia is to phagocytose various cargoes, for example, either to regulate the precise number of neural progenitors and neurons or shaping synaptic connections either through formation or elimination of synapses (Paolicelli *et al.*, 2011; Cunningham, Martínez-Cerdeño and Noctor, 2013; Sierra, Tremblay and Wake, 2014). This allows microglia to regulate precursor differentiation, which is an important aspect of cortical neurogenesis (Pérez-Rodríguez, Blanco-Luquin and Mendioroz, 2021). Understanding the impact of environmental stimuli on microglial motility during cortical development is therefore an important and plausible mechanism by which MIA (and by inference, IL-6) may contribute to elevated risk for NDDs in the offspring. In this context, cortical microglia exhibit enhanced microglial process velocity but not directionality, as revealed by *in vivo* 2-photon imaging of the cortex of mice exposed to MIA by systemic Poly I:C *in utero* compared to controls (Ozaki *et al.*, 2020). Acute exposure of primary foetal microglia to IL-6 *in vitro* replicated the *in vivo* data, suggesting a specific role for IL-6 in the regulation of microglial motility (Ozaki *et al.*, 2020). Nevertheless, a question arises regarding the extent to which these motility data can be extrapolated from rodent primary microglia to their human-derived counterparts.

4.1.2 Determining the Influence of IL-6 on hiPSC-derived Microglia Function

The results from the previous chapter left unanswered questions with regards to the hiPSC-derived MGL response to acute IL-6. First, the minimum concentration of IL-6 required to provide an increase of JAK/STAT3 targeted gene expression by the MGLs had not yet been established. Consequently, it is necessary to conduct a dose-response optimisation to ensure that the MGLs respond to IL-6 at a dose that is physiologically relevant, rather than using an excessively high dose that could result in a saturation point of the microglial response. Second, because the hiPSC-derived MGL IL-6 response is expected to extend beyond the few genes measured in chapter 3, it is critical to characterise a broader view of the impact of acute IL-6 on the MGL transcriptome, which will provide clues for future assay development and allow overlap testing to publicly available data from cases and controls from both animal and human data to provide a clue as to the potential relevance of our *in vitro* findings for NDD pathophysiology. Third, based on hypotheses developed from both the literature and the gene expression characterisations presented in section 3.3.3, it is necessary to identify IL-6-induced modifications to microglial function that are particular to neurodevelopment, such as microglial motility and their secretome. Exploring these questions could offer valuable insights and hypotheses to investigate further in a co-culture system involving hiPSC-derived MGLs and NPCs (Gonzalez, Gregory and Brennand, 2017; Russo *et al.*, 2018). Additionally, it serves as a proof of concept to initially examine the MGLs in a monoculture setting.

To this end, this chapter aims to evaluate how acute IL-6 alters the form or function of hiPSC-derived microglia-like cells (MGLs) in monocultures. The following three questions were considered: (1) what is the lowest dose of IL-6 that ensures an increase in transcript expression downstream of IL-6 pathway activation in MGLs; (2) does acute IL-6 induce a transcriptional profile shift and is this similar to that seen in the major NDDs (ASC, SZ and BD); and (3) how

does acute IL-6 impact the function of human MGLs, in terms of its motility state and secretome?

4.2 Methods

4.2.1 MGL Monoculture

As in section 3.2.1, hiPSCs from 3 healthy male donors, with 3 clones per donor, for a total of 9 lines were used to create *MYB*-independent macrophage/microglia progenitor factories and terminally differentiated into MGLs (M3_CTR, 127_CTM and 014_CTM) according to the protocols described in section 2.1 (van Wilgenburg *et al.*, 2013; Haenseler *et al.*, 2017) (Table 2.1). However, only two clone factories per donor were completed in time for the RNAseq experiment. Progenitors were terminally differentiated for 14 days from the factories before being treated with IL-6.

3.2.2 RNA extraction, qPCR and bulk RNAseq

RNA extraction, cDNA synthesis and qPCR protocols were carried as described in sections 2.2.1, 2.2.2 and 2.2.3 respectively. The RNA for the dose-response and RNAseq experiments were collected from vehicle/treated day 14 MGLs. For RNAseq, total RNA extracted from 3h IL-6 treated day 14 MGLs was pooled from two clones per healthy male donor (N = 3 samples per condition in total). RNAseq analysis, including gene ontology and MAGMA analysis was carried out as described in section 2.2.4.

3.2.3 MGL Motility Assay

The motility assay was performed as previously described (Solomon *et al.*, 2022; Couch *et al.*, 2023). In brief, hiPSC-derived microglia progenitor cells were seeded onto 100ng/ml PDL

coated Perkin Elmer CellCarrier Ultra 96-well flat glass bottom plates at a density of 30,000 cells/well. The cells were then differentiated to MGLs for 14 days, on which day the motility assay was carried out. Before imaging, the OperaPhenix High-Content Screening System microscope (PerkinElmer) temperature and CO_2 were controlled to 37ºC and 5% respectively. Cells were exposed to 3 conditions for 3h: unstimulated, IL-6 (100 ng/ml) or vehicle alone. Each condition had 6 technical replicate wells on each plate. Prior to imaging, for the 3h treatment conditions a complete media was performed, with microglia media containing either IL-6 (100 ng/ml) or vehicle (sterile water with 100 picomolar acetic acid). At 30 minutes before imaging, a complete media change was performed, with microglia media containing either IL-6 (100 ng/ml) or vehicle alone or neither (unstimulated). This media change also included the staining dye, meaning that all cells were stained for 30min with HCS NuclearMask™ Blue Stain (Invitrogen; H10325) and CellMask™ Orange Plasma membrane Stain (Invitrogen; C10045). Immediately before imaging, the media containing treatment and stain was removed and replaced with FluoroBrite™ DMEM (Gibco; A1896701) imaging media without phenol red. Cells were imaged for 120min (30 timepoints, 4 mins between each timepoint) on an OperaPhenix high throughput imaging system (Perkin Elmer) using a 20x objective over 5 consistent fields of view per well, and data was analysed for both cytoplasmic and nuclear properties using Harmony High-Content Image analysis software (PerkinElmer).

3.2.4 Media cytokine profiling array

Cytokine profiling of the culture media was carried out as described in section 2.3.1, using the Proteome Profiler Human Cytokine Array kit (R&D Systems; ARY005B) as per the manufacturer's instructions. Each kit contained four membranes with dots of 36 different immobilised cytokine antibodies (Table 4.1), dotted with two technical replicates each (Figure 4.1). Media from N=3 harvest replicates of 37S_CTR_M3 were pooled into one sample, with

which the membrane was stained for each condition: 3h vehicle, 3h 100 ng/ml IL-6, 24h vehicle and 24h 100 ng/ml IL-6.

Table 4.1 – List of cytokine targets or controls at each coordinate dot on membranes of the Proteome Profiler Human Cytokine Array kit.

Human Cytokine Array Coordinate	Target/Control
A1-2	Reference Spots
A3-4	CCL1/I-309
A5-6	CCL2/MCP-1
A7-8	MIP-1A/MIP-1B
A9-10	CCL5/RANTES
A11-12	CD40 Ligand/TNFSF5
A13-14	Complement Component C5/C5a
A15-16	CXCL1/GROa
A17-18	CXCL10/IP-10
A19-20	Reference Spots
B3-4	CXCL11/I-TAC
B5-6	CXCL12/SDF-1
B7-8	G-CSF
B9-10	GM-CSF
B11-12	ICAM-1/CD54
B13-14	IFN-y
B15-16	IL-1a
B17-18	IL-1b
C3-4	IL-1ra
C5-6	IL-2
C7-8	IL-4
C9-10	IL-5
C11-12	IL-6
C13-14	IL-8
C15-16	IL-10
C17-18	IL-12 p70
D3-4	IL-13
D5-6	IL-16
D7-8	IL-17A
D9-10	IL-17E
D11-12	IL-18/IL-1F4
D13-14	IL-21
D15-16	IL-27
D17-18	IL-32a
E1-2	Reference Spots
E3-4	MIF
E5-6	Serpin E1/PAI-1
E7-8	TNFa
E9-10	TREM-1
E19-20	Negative Control

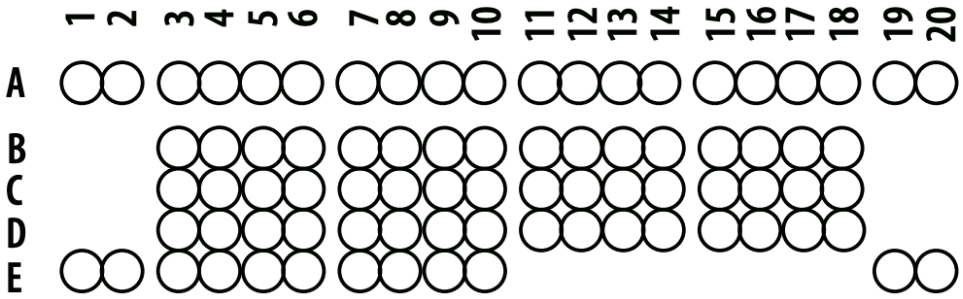

Figure 4.1 - Human cytokine array layout on each membrane of the small, 36 cytokine Proteome Profiler Human Cytokine Array kit from R&D systems.

3.2.5 Statistical Analysis

All statistical analyses were performed in Prism 9 for macOS version 9.3.1 (GraphPad Software LLC, California, USA), apart from all RNAseq analyses which were carried out using the research computing facility at King's College London, *Rosalind* and *CREATE,* and R version 4.0.2 (R Core Team, 2020). Each individual test performed is indicated in each associated figure legend and statistic data table, as is the number of replicate hiPSC lines that comprise each technical and biological replicate. One-way ANOVA was employed when comparing means for more than two groups, and in this chapter when comparing the area under the curve and specific motility phenotypes for different treatment groups during the MGL motility experiment (Table 4.5, Table 4.6). Two-way ANOVA was used to compare the mean for two separate conditions, which in this chapter was comparing transcript expression across different IL-6 dosage stimulations coupled with three different donors (Table 4.2). When significant differences between groups were found in these models, *post-hoc* testing was performed using the Benjamini technique with a 5% false discovery rate (FDR) to identify the individual groups with significant differences. P-values and adjusted p-values less than 0.05 were considered statistically significant. The 1% FDR cut off was used during RNAseq downstream GO

analysis to concentrate the number of significantly linked pathways. Statistics were not applied to the media cytokine array data because the sample power was insufficient.

4.3 Results

4.3.1 hiPSC-derived Microglia-like cells increase Gene Expression Linked to Canonical STAT-3 Signalling at doses ≥100 ng/ml *in vitro*

Having confirmed that MGLs activate canonical STAT-3 signalling in response to acute IL-6 challenge (see chapter 3), the minimum effective concentration of IL-6 in D14 MGLs was explored with a concentration-response experiment (Figure 4.2). To do so, qPCR was used to assess the mRNA expression of *IL6*, *IL10*, and *JMJD3* all of which were up-regulated after 3 hours exposure to 100 ng/ml IL-6. A range of IL-6 concentrations were tested, (range: 0.1 pg/ml to 100 ng/ml), in D14 MGLs from N = 3 male donors with 3 harvest replicates per donor. The average steady-state concentration of IL-6 found in maternal serum taken from second-trimester mothers in a recent birth cohort study was reported to be 0.98 ± 1.06 pg/ml, hence this was included in the concentration range as the starting point for the doses used in this experiment (Graham *et al.,* 2018). Furthermore, interferon regulatory factor 8 (IFR8), a transcription factor known to affect immunological function and myeloid cell development, was investigated to see if IRF8 may be regulated upstream by canonical IL-6 signalling (Tamura and Ozato, 2002; Masuda *et al.*, 2012; d'Errico *et al.*, 2021).

Consistent with our previous results, acute exposure (3hr) to 100 ng/ml IL-6 evoked a statistically significant increase in expression of *IL6*, *JMJD3*, *IL10*, and *IRF8* in D14 MGLs. Notably however, the mRNA expression of *IL6*, *JMJD3*, *IL10*, and *IRF8* was unaffected at all other concentration of IL-6 tested relative to vehicle controls (Figure 4.2, statistics in Table

4.2). In line with our previous data, the magnitude of the gene expression changes following stimulation with 100 ng/ml IL-6 varied by the donor (Table 4.2). For example, 014_CTM showed a minimal change to *IL10* expression after 3h 100 ng/ml IL-6 stimulation (~ 1.17 fold change from vehicle) in comparison to M3_CTR which showed the greatest change in transcript expression (~ 8.21 fold change from vehicle). There is no apparent pattern between the older 127_CTM aged line and the younger 014_CTM and M3_CTR lines, therefore this donor effect is unlikely to be attributable to differences in sex or age. Although the contribution of these variables needs to be confirmed in larger sample size, it is also conceivable this may reflect unmeasured genotype variations between the donors, which lead them to respond to immune stimuli differently (Table 4.2). Nonetheless, taking these data into account, 100 ng/ml IL-6 was pragmatically chosen for subsequent experiments, since it evoked a robust response in our MGLs that could be quantified at a single time-point.

Table 4.2 - Two-way ANOVA of qPCR dose response gene fold changes from vehicle, with N=3 donors averaged to one point from three clones, over 7 doses.

Gene	Source of Variation	DF	F (DFn, DFd)	P value	P value summary
IL6	Interaction	12	F (12, 42) = 4.782	P < 0.0001	****
	Dose Factor	6	F (6, 42) = 168.9	P < 0.0001	****
	Donor Factor	2	F (2, 42) = 4.685	P = 0.0146	*
IL10	Interaction	12	F (12, 41) = 13.21	P < 0.0001	****
	Dose Factor	6	F (6, 41) = 35.11	P < 0.0001	****
	Donor Factor	2	F (2, 41) = 11.48	P = 0.0001	***
JMJD3	Interaction	12	F (12, 42) = 0.9209	P = 0.5352	ns
	Dose Factor	6	F (6, 42) = 32.98	P < 0.0001	****
	Donor Factor	2	F (2, 42) = 0.4621	P = 0.6331	ns
IRF8	Interaction	12	F (12, 42) = 1.083	P = 0.3982	ns
	Dose Factor	6	F (6, 42) = 4.748	P = 0.0009	***
	Donor Factor	2	F (2, 42) = 1.666	P = 0.2013	ns

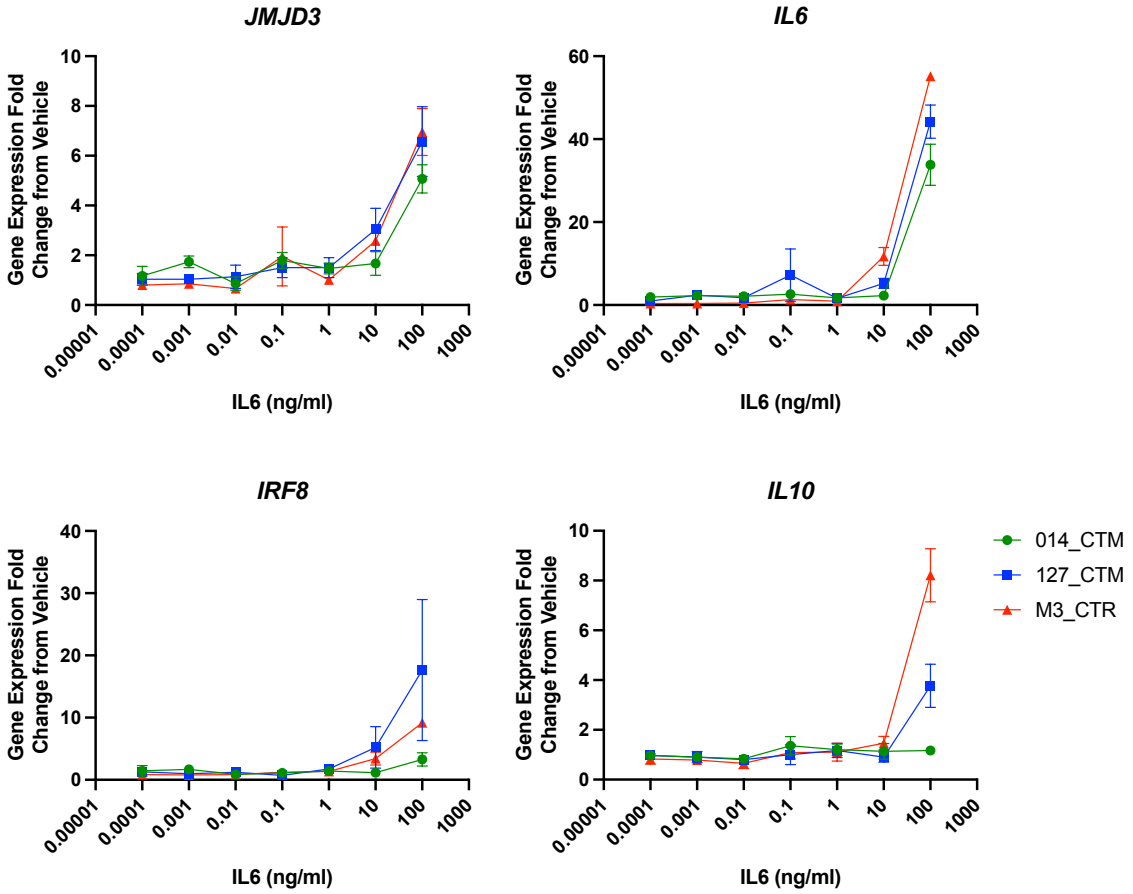

Figure 4.2 - Dose response of MGLs to 7 doses of a 10-fold serial dilution of IL-6 from 100ng/ml to 0.1pg/ml. Three healthy male donors with n=3 harvest replicates per donor. IL10 127_CTM_01 0.1ng/ml outlier removed and calculated form N=2 harvests. Fold change from vehicle calculated within line, but vehicle not plotted. No post-hoc tests were run on this data, given there were no interactions in the Two-way ANOVA model (results in previous table).

4.3.2 Transcriptional response to acute IL-6 exposure in human microglia-like cells

Having established the minimal IL-6 dose required in section 3.3.3, the transcriptional consequences and pathways affected were subsequently investigated. Bulk RNA-sequencing (RNAseq) was conducted in MGLs produced from N = 3 male neurotypical donor hiPSC lines, pooled from two clones each, 3 hours after IL-6 treatment (100 ng/ml) (Couch *et al.*, 2023). An average of 23.5 million 289-base pair paired-end reads per sample were obtained (Table 4.3). Principle Component Analysis (PCA) of gene expression data showed that samples

grouped by treatment (Figure 4.2A), which is consistent with a heatmap clustering of the top 25 differentially expressed genes (DEGs) (Figure 4.2B). Following 3 hours of IL-6 exposure, 156 and 22 genes were up- and down-regulated, respectively (FDR < 0.05) (B-C). Among the genes that were up-regulated, *IRF8* was noted to increase in expression, consistent with qPCR results (Figure 4.2). In addition, the NFkB subunit *REL*, heat shock proteins *HSPA1A/B*, and the oxytocin receptor (*OXTR*) were up-regulated (Figure 4.3B). Despite the fact that maternal IL-17 is thought to play a role in MIA-induced behavioural alterations in children that are relevant to ASC (Choi *et al.*, 2016), differential expression of *IL17* was insignificant at this timepoint.

Table 4.3 - Summary of read outputs per sample from RNAseq.

Sample	M3-Veh	M3-Treat	127-Veh	127-Treat	014-Veh	014-Treat
Unique read number	20379588	21394231	24408798	29440355	25250460	21251473
Average read length	292	279	295	285	292	292

To understand the overall pathways potentially regulated by IL-6 stimulation in MGLs, Webgestalt over representation analysis (ORA) on the 178 DEGs at 5% FDR was conducted by dividing them into up-regulated (156 genes) and down-regulated genes sets (22 genes) (Yuxing Liao *et al.*, 2019). The 156 up-regulated genes were most closely associated (FDR < 0.01) with 21 pathways across cellular components, biological processes, and molecular functions (Figure 4.3D). These included NFkB signalling (FE = 4.60, $p < 0.001$, FDR = 0.001), leukocyte differentiation (FE = 3.55, $p < 0.001$, FDR = 0.001), regulation of cell-cell adhesion (FE = 3.77, $p < 0.001$, FDR = 0.002), response to cytokine stimuli (FE = 5.57, $p < 0.001$, FDR = 0.002), production of IFN-γ (Figure 4.3D). The 22 down-regulated genes, however, were not substantially related with any pathways at either a 5% or 1% FDR correction.

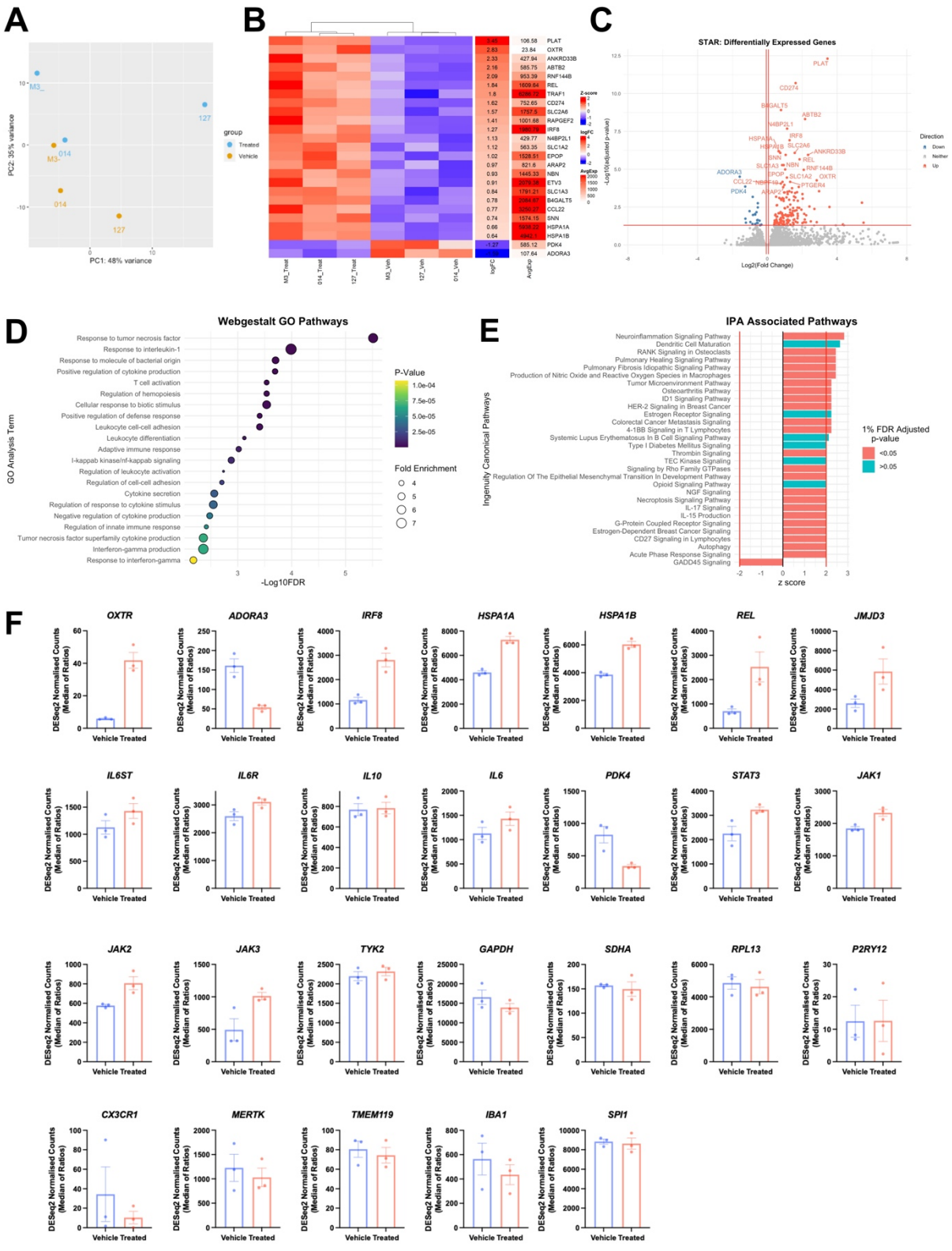

Figure 4.3 – hiPSC-derived MGLs illicit a strong transcriptomic shift in response to acute IL-6. RNA from MGLs differentiated from 3 healthy male donors, pooled from 2 clone cultures each, were exposed to IL-6 or vehicle for 3h and collected for RNAseq. (A) PCA analysis of all 6 samples, coloured by vehicle (orange) or IL-6 treated (blue) condition and labelled by donor line: M3_CTR as M3-, 014_CTM as 014 and 127_CTM as 127. (B) Heatmap of top 25 most differentially expressed

genes in the IL-6 3h MGL response, ranked by LogFC and clustering by treatment group. (C) Volcano plot of differentially expressed genes. Conditional axis set as follows: log2Foldchange > 0.06 and adjusted p-value < 0.05 coloured red; log2Foldchange < -0.06 and adjusted p-value < 0.05 coloured blue. The top 25 differentially expressed genes are labelled. (D) Webgestalt gene ontology analysis of up-regulated 156 gene set only with an adjusted 1% FDR. GO terms ordered by –log10FDR, coloured by adjusted p-value and sized by the fold enrichment within each dataset. (E) IPA associated pathways, ranked by z-score and coloured by 1% FDR adjusted p-value. Only pathways with z-score > |2| are shown, with z-score > |2| conditional axes labelled in red. (F) DESeq2 normalized counts of genes of interest after bulk RNAseq analysis. The DESeq2 median of ratios are calculated by dividing counts by sample-specific size factors that are determined by the median ratio of gene counts, relative to the geometric mean per gene. This accounts for sequencing depth and RNA composition. Bar graphs plotted as mean with standard error of the mean (SEM) error bars, with N=3 donor replicates.

The QIAGEN Ingenuity Pathway Analysis (IPA) software (Krämer *et al.*, 2014) was used in conjunction with the previous ORA analysis to discover 30 linked pathways at a z-score threshold of > |2| to find projected activation or inhibition of a pathway, 24 of which passed 1% FDR correction (Figure 4.3E). The top activated pathways included "neuroinflammation signalling" (Ratio = 0.035, $p < 0.001$, FDR <0.001), nitric oxide and reactive oxygen species (ROS) in macrophages (Ratio = 0.037, $p < 0.001$, FDR <0.001), TNFRSF signalling in lymphocytes (4-1BB: Ratio = 0.176, $p < 0.001$, FDR <0.001; CD27: Ratio = 0.088, $p < 0.001$,FDR < 0.001), epithelial-mesenchymal transition in development (Ratio = 0.058, $p < 0.001$, FDR = 0.001), G-protein coupled receptor signalling (Ratio = 0.023, $p < 0.001$, FDR <0.001), IL-17 signalling (Ratio = 0.021, $p < 0.001$, FDR =0.034) and a down-regulation of GADD45 signalling (Ratio = 0.067, $p < 0.001$, FDR =0.002). The involvement of the IL-17 signalling pathway in this reaction is interesting, considering that *IL17* itself showed no differential expression. This might imply that, while *IL17* was not altered at the moment of experiment, the components of its signalling pathway were still implicated in the MGL response to IL-6. In any case, under the conditions tested, the transcriptional response

encompasses downstream pathway modifications to ROS, cell adhesion, cytokine release, and TNFRSF signalling as well as activation of the NFkB pathway.

Finally, the median of ratios approach was used to construct the DESeq2 normalised counts for *IL6R* and *IL6ST*, which showed that the expression of these receptors is unaffected by the 3h IL-6 exposure (Figure 4.3F). Furthermore, to supplement the data that shows STAT3 phosphorylation after IL-6 stimulation in MGLs (Couch *et al.*, 2023), DESeq2 normalised counts demonstrated increasing trends of components of the JAK/STAT3 signalling pathway after IL-6 stimulation (BH FDR 5% > 0.05), including *STAT3*, *JAK1*, *JAK2*, and *JAK3* transcripts, except for *TYK2* (Figure 4.3F). Finally, counts revealed the presence of microglial markers, and IL-6 had no influence on these important markers (Figure 4.3F).

4.3.3 The transcriptomic changes associated with exposure of MGLs to IL-6 overlap with those observed in post-mortem brain tissue from schizophrenia cases

Multiple psychiatric disorders with a putative neurodevelopmental origin, including SZ, ASC, BD, and MDD, are associated with higher levels of IL-6 protein and/or gene expression in human blood, CSF, and in *post-mortem* brain tissue (Sasayama *et al.*, 2013; Khandaker *et al.*, 2014; Schwieler *et al.*, 2015; Gandal *et al.*, 2018; Lu *et al.*, 2019; Perry *et al.*, 2021; Zhao *et al.*, 2021). Of note, this has been reported throughout life, ranging from maternal serum (Allswede *et al.*, 2020), in 9-year-old children (Khandaker *et al.*, 2014) and in young adulthood at ages 18 to 25 (Schwieler *et al.*, 2015). This supports the idea that the aetiology of psychiatric diseases may include IL-6 related pathways through various stages of life. To test this hypothesis with the dataset produced in this chapter, the genes up- and down-regulated in MGLs after 3h IL-6 stimulation as measured by bulk RNAseq were compared with up- and down-regulated genes from *post-mortem* brain tissue from SZ, ASC, and BD patients (Gandal

et al., 2018) (two gene sets from the model vs. two gene sets from each disorder: 12 comparisons in total; Figure 4.4A). The up-regulated gene set in the MGL IL-6 model reached statistical significance for enrichment with the up-regulated gene sets in SZ (N genes in model = 156, N genes in cases = 2274, overlap size = 44 genes, P = 0.00022, odds ratio (OR) = 2.0), which survived correction for multiple comparisons (FDR q=0.003). For ASC, an overlap was also observed (N genes in model = 156, N genes in cases = 701, overlap size = 14 genes, P = 0.031, OR = 1.8), but this did not survive correction for multiple comparisons. The down-regulated gene set in the MGL IL-6 model and the gene set down-regulated in SZ also significantly overlapped (N genes in model = 22, N genes in cases = 2073, overlap size = 7 genes, P = 0.04, OR = 2.6), but neither survived correction for multiple comparisons.

We therefore focused on the 44 overlapping genes in the up-regulated gene set following IL-6 exposure to conduct additional pathway analysis. Webgestalt ORA suggested 10 related pathways (Figure 4.4B, overlap gene list in Table 4.4), including: Signalling response pathways (FE = 6.61, $p < 0.001$, FDR = 0.008), "leukocyte cell-cell adhesion" (FE = 7.81, $p < 0.001$, FDR = 0.009), "T-cell activation" (FE = 6.40, $p < 0.001$, FDR = 0.009) and apoptotic signalling (FE = 7.29, $p < 0.001$, FDR = 0.034). Of note, increased NFkB signalling was also observed as an output, though it just failed to survive a 5% FDR adjustment for multiple comparisons (FE = 11.4, p 0.001, FDR = 0.059). Together, these results demonstrate that IL-6 exposure induces transcriptional changes in human MGLs consistent with pathways affected in *post-mortem* brain tissue from adults with an *ante-mortem* diagnosis of schizophrenia. The results are not statistically robust enough however, with the current sample size to extend this conclusion to ASC and BD diagnoses.

Table 4.4 - Alphabetical list of the 44 genes found in both up-regulated IL-6 MGL response and SZ post-mortem up-regulated gene sets (Gandal et al., 2018).

SZ Overlap Genes
BCL2A1, BCL3, BIRC3, BTN2A2, CD83, CHI3L2, CPNE8, DRAM1, F3, FZD5, GADD45B, GFPT2, GRAMD1A, GRAMD2B, HSPA1A, HSPA1B, IRF1, LIMK2, MAFF, MAP3K5, MAP3K8, MCOLN2, MYO1G, NFKB2, OTUD4, OXTR, PLAGL2, PSTPIP2, RFX4, SBNO2, SDC4, SIX5, SLC1A2, SLC1A3, SOD2, STAT5A, STX11, TIFA, TNIP1, TRIP10, TUBB2B, ZBTB10, ZC3H12A, ZC3H12C

We next examined whether SZ, ASC and BD-associated risk genes were disproportionately altered in MGLs upon exposure to IL-6. Specifically, genes with SNPs linked to SZ, BD, and ASC risk from GWAS studies were compared with the differentially regulated genes in MGLs after 3 hours of IL-6 stimulation (Trubetskoy *et al.*, 2022; Mullins *et al.*, 2021; Grove *et al.*, 2019). MAGMA was used to perform gene-level enrichment analysis to identify risk gene variants linked with each condition and examined them for enrichment with the up- and down-regulated gene sets identified in IL-6 stimulated MGLs (de Leeuw *et al.*, 2015). When considering the genes that were differently regulated in our model, no statistically significant enrichment for SZ (or any condition) was seen (all comparisons $P > 0.05$) (Figure 4.4C). These findings imply that, under the conditions tested, the expression of genes linked to an elevated risk for SZ, BD, and ASC is not changed when human MGLs are exposed to IL-6.

Finally, the MGEnrichment tool was used to compare the MGL IL-6 model data with existing gene expression data from human and mouse microglia to examine the overlap of up- and down-regulated gene sets with microglia-specific module gene sets (Jao and Ciernia, 2021). After 5% FDR correction, 31 modules were linked with the up-regulated MGL IL-6 3h response gene set, and 12 with the down-regulated gene set. Important modules that overlapped with our up-regulated and down-regulated gene sets independently included the "SCZ, ASC

and Bipolar Disorder (BD) module" (Up: intersection size = 44 genes, FDR = 7.10e-29, OR = 13.5; Down: FDR = 5.69e-06, OR = 17.9, intersection size = 8 genes) (Gandal *et al.*, 2018), and the “core human microglial signatures module” (Up: intersection size = 26 genes, FDR = 3.29e-12, OR = 6.3. Down: intersection size = 10 genes, FDR = 4.47e-08, OR = 24.8) (Galatro *et al.*, 2017), both of which originate from bulk RNAseq datasets. Furthermore, these findings align with the formal overlap test conducted previously.

The same tool also suggested that the up- and down-regulated MGL IL-6 response gene sets were enriched for single-cell RNAseq microglial modules from a single published dataset (Olah *et al.*, 2020). These included enrichment for “Microglia anti-inflammatory responses” (intersection size = 18 genes, FDR < 0.0001, OR = 9.90), “Microglia cellular stress” (intersection size = 7 genes, FDR < 0.0001, OR = 11.7), “Microglia interferon response signalling pathway” (intersection size = 8 genes, FDR = 0.0007, OR = 5.39) and “Microglia homeostatic states” (intersection size = 7 genes, FDR = 0.009, OR = 3.96). The down-regulated gene set was enriched for “Microglia antigen presentation” (intersection size = 4 genes, FDR = 0.0003, OR = 29.2) and additionally “Microglia homeostatic states” (intersection size = 3 genes, FDR = 0.018, OR = 12.6).

The human MGL IL-6 response was compared with mouse data with the MGEnrichment tool, where 26 mouse modules were discovered to overlap with our up-regulated gene set and 4 mouse modules to overlap with our down-regulated gene set. The "MIA Poly I:C GD14 P0" module from Matcovitch-Natan *et al.* (2016), a microglial gene set obtained from newborn pups whose mothers were exposed to Poly I:C on gestational day 14, was the most pertinent module that overlapped with our up-regulated gene set (intersection size = 11 genes, FDR = 0.016, OR = 2.95) (Matcovitch-Natan *et al.*, 2016). It should be noted that a small number of

genes (11) make up the intersection of this comparison, which could be expected given the difference in MIA-derived insult (Poly I:C as opposed to IL-6), as well as the differing species and gestational time-points. Overall, these findings support the hypothesis that the transcriptomic IL-6 response from hiPSC-derived MGLs phenocopies key human microglia markers and has implications for human NDD states.

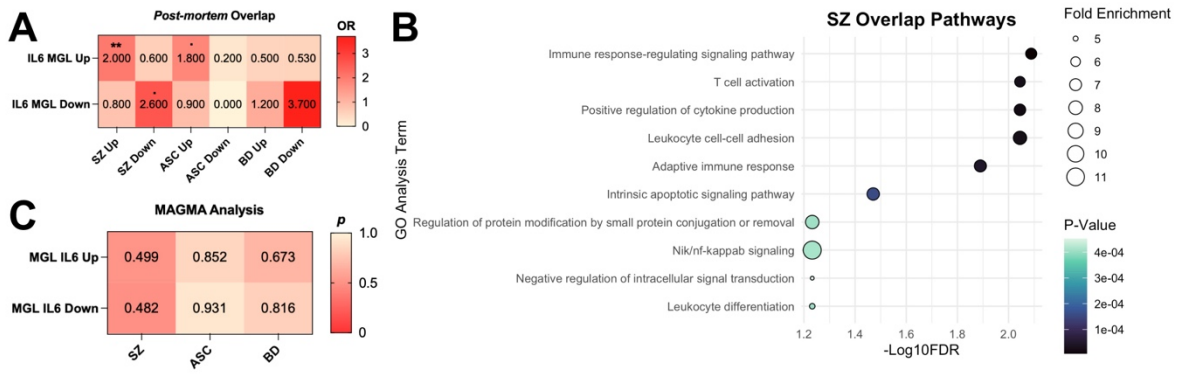

*Figure 4.4 – The hiPSC-derived MGL transcriptomic response to acute IL-6 has relevance for schizophrenia. (A) Fisher's exact test comparing gene sets from ASC, SZ and BD post-mortem human patient tissue (Gandal et al., 2018) with up- and down-regulated gene sets identified by RNAseq in this study. Odds ratios (OR) plotted in heatmap with significant 5% FDR corrections formatted as follows: . p < 0.1, *p < 0.05, **p < 0.01, ***p < 0.001, and ****p < 0.0001; not significant, not labelled. (B) Webgestalt gene ontology analysis of 44 genes overlapped from our up-regulated RNAseq dataset and SZ up-regulated genes from Gandal et a., 2018, with an adjusted 1% FDR. ORA terms ordered by –log10FDR, coloured by adjusted p-value and sized by the fold enrichment within each dataset. (C) MAGMA analysis comparing significant risk genes from SZ (Trubetskoy et al., 2022) , BD (Mullins et al., 2021) and ASC (Grove et al., 2019) GWAS studies with IL-6 MGL up and down DEGs obtained by RNAseq in this study. P-values plotted in heatmap.*

4.3.4 Acute IL-6 exposure increases microglia motility in monoculture

Two complementary analyses of gene expression suggest that acute IL-6 exposure results in an increase of *IFR8* expression, as demonstrated by the RNAseq (section 4.3.2) and qPCR (section 4.3.1) in these human MGLs. Of note, microglia-specific *IRF8* deletion in mice causes these cells to have fewer, shorter branches as well as reduced motility (d'Errico *et al.*, 2021).

Additionally, primary microglia from mice lacking *IRF8-/-* globally, show reduced ATP-induced chemotaxis when compared to wild type primary mouse microglia (Masuda *et al.*, 2014). Lastly, data from a mouse model of MIA suggests that acute IL-6 exposure promotes microglial mobility *in vivo* and *in vitro* (Ozaki *et al.*, 2020). Collectively, these findings suggest a testable hypothesis that IL-6 influences microglia motility. Given the importance of microglial motility during neurodevelopment (section 4.1.1), live cell imaging data were collected to observe how 3h exposure to 100 ng/ml IL-6 affected MGL morphology, whole cell (nuclear), and cytoplasmic specific (cytoplasm) motility. Data was collected from unstimulated, vehicle and treated conditions in N = 3 healthy male donors, each with technical replicates over 3 harvests (Figure 4.5A).

At a single cell level, it was observed that most cells had both mobile cytoplasm and nuclei (Figure 4.5B). The mobility of each individual cell was defined by its speed at each time point (non-motile = 0). Then, the percentages of mobile and non-mobile cells were then calculated from the total number of cells across each donor replicate, averaged to one mean percentage value of cell motility per donor and plotted at each timepoint (Figure 4.5B). To understand if the rates of change were different across each treatment group, the area under the curve (AUC) was calculated and compared across cytoplasm and nuclei motile datasets (Table 4.5). By one-way ANOVA, the percentages of cells with cytoplasm motility and nuclei motility were significantly different depending on the treatment group (Percentage cells with cytoplasm motility: $F(2, 180) = 3327293$, $p < 0.0001$. Percentage cells with nuclei motility: $F(2, 180) = 4390531$, $p < 0.0001$). According to the AUC, there were more cells with cytoplasmic motility in the unstimulated treatment group (AUC = 2850), followed by IL-6 treated cells (AUC = 2847) and then the vehicle treatment group (AUC = 2836). Likewise, the percentage of cells with nuclei motility was highest in the unstimulated group (AUC = 2750), then IL-6 (AUC =

2720) and vehicle (AUC = 2712) treatment groups (Table 4.5). This suggests that the cells were indeed alive and healthy, but that the acetic acid vehicle and IL-6 treatments did reduce the total percentages of cells with motility throughout the whole live imaging experiment, in comparison to the unstimulated control group.

Table 4.5 – Area under the curve (AUC) analysis to compare the percentages of cells with either cytoplasm or nuclei motility. One-way ANOVA used to compare the AUCs across each treatment group.

Motility Type	Treatment Group	AUC	Std. Error	F (DFn, DFd)	P value	P Summary
Cytoplasm	Unstimulated	2850	0.01910	F(2, 180) = 3327293	< 0.0001	****
	Vehicle	2836	0.04703			
	IL-6 Treated	2847	0.02029			
Nuclei	Unstimulated	2750	0.04691	F(2, 180) = 4390531	< 0.0001	****
	Vehicle	2712	0.1091			
	IL-6 Treated	2720	0.04675			

To draw out further sources of variation in the dataset, a qualitative principal component analysis (PCA) was used to visualise the similarities and variations in motility and morphology between each donor and treatment group (Figure 4.5B). To calculate the greatest sources of variance in the dataset, measurement inputs for the analysis included distance, speed, displacement from both nuclei and cytoplasm metrics, as well as cell duration, straightness, area, roundness, number, and length. When points were coloured by donor, it was evident that they clustered by their individual donor genetic background, regardless of treatment group (Figure 4.5B top panel). When the groups were coloured by treatment group, they clustered less closely than by donor effect, but the IL-6 treated group was still visually distinguishable from the untreated group (Figure 4.5B bottom panel). As a qualitative result, the greatest source of variance in this dataset is attributable to donor, followed by the treatment group.

One-way ANOVA was used to evaluate the means of morphological and motility phenotypes of the cytoplasm and nuclei from unstimulated, vehicle-, and IL-6-treated MGLs (Table 4.6).

The treatment factor was observed to change cytoplasmic distance, displacement, and cell roundness (one-way ANOVA $p < 0.05$). IL-6 increased mean cytoplasmic distance in contrast to the vehicle control after FDR 5% BH correction, indicating enhanced cytoplasmic ruffling function dIL-6 stimulation. (Figure 4.5D). Although cell roundness tended to decrease with IL-6 treatment (Table 4.6), none of the post-hoc corrections for the roundness phenotype passed FDR 5% testing. Importantly, it should be noted that the vehicle treatment alone was sufficient to impact MGLs motility, as shown by an increase in cytoplasmic distance and displacement in both vehicle- and IL-6-treated cells relative to untreated controls (Figure 4.5D). Neither the vehicle nor the IL-6 treatment modified the nuclear motility, cell area, or length (Figure 4.5D, statistics in Table 4.6). It was verified that neither the variation in cell numbers nor the migration of cells into or out of the field of vision (duration) was the cause of these effects (Figure 4.5D, statistics in Table 4.6). Given only the cytoplasmic motility increases rather than any movement of the cell body (Nimmerjahn, Kirchhoff and Helmchen, 2005), these data suggest an increase in microglial "surveillance" function in response to IL-6, that are consistent with previous results from rodent MIA-models (Ozaki *et al.*, 2020), an increase of *IRF8* expression (d'Errico *et al.*, 2021) and the ORA analysis from section 4.3.2.

Table 4.6 - One-way ANOVA of Motility Assay conditions, with N=3 male donors averaged each from N=3 separate MGL harvest technical replicates.

Measurement	DF	F (DFn, DFd)	P value	P value Summary
Cytoplasm Distance	2	F(2,6) = 17.35	0.0032	**
Cytoplasm Speed	2	F(2,6) = 0.9725	0.4307	ns
Cytoplasm Displacement	2	F(2,6) = 18.24	0.0028	**
Nuclear Distance	2	F(2,6) = 0.3008	0.7508	ns
Nuclear Speed	2	F(2,6) = 0.04809	0.9534	ns
Nuclear Displacement	2	F(2,6) = 0.8013	0.4915	ns
Area	2	F(2,6) = 2.191	0.1930	ns
Roundness	2	F(2,6) = 5.425	0.0451	*
Length	2	F(2,6) = 4.632	0.0607	ns
Cell Number	2	F(2,6) = 0.3693	0.7059	ns
Duration	2	F(2,6) = 0.02407	0.9763	ns

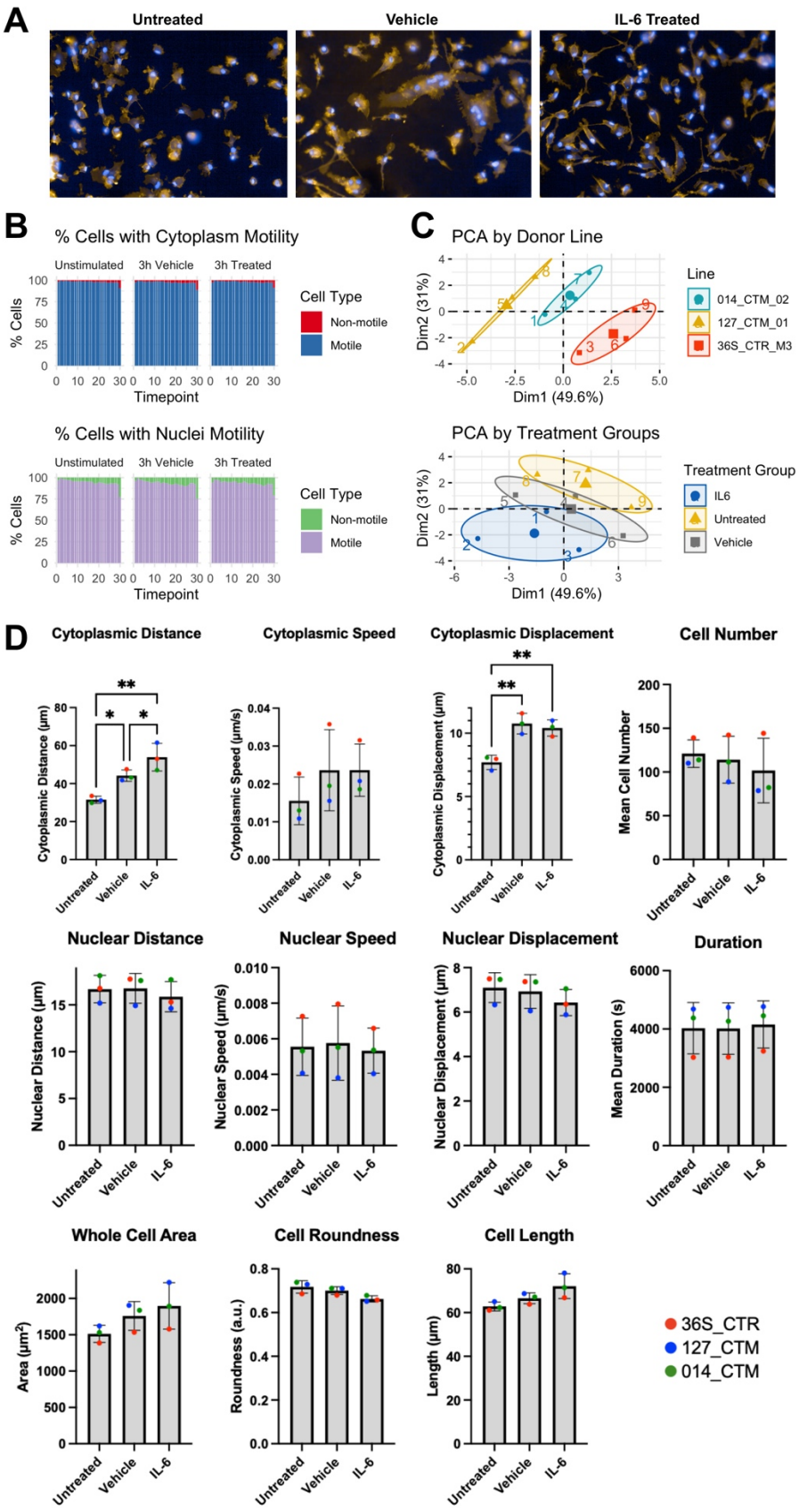

Figure 4.5 - MGL motility is altered in response to acute IL-6. (A) Representative images taken as stills from live imaging video .mp4 files that tracked MGL nuclear motility (Blue = HCS NuclearMask™ Blue Stain) and MGL cytoplasmic motility

*(Orange = CellMask™ Orange Plasma membrane stain). These are representative from one technical replicate form the 127_CTM_01 donor line. (B) Percentage of cell number with or without motility, split by cytoplasmic (top panel) or nuclear (bottom panel) motility, at each individual timepoint taken at 4min space intervals. (C) Principle component analysis (PCA) of all metrics found in (D). Top panel is coloured by donor line, and bottom panel is coloured by treatment group. Numbers indicate the biological replicate (1, 4, 7 = 014_CTM, 2, 5, 8 = 127_CTM and 3, 6, 9 = M3_CTR). (D) Metrics of MGL motility and morphology over 2h of live imaging, having been exposed to vehicle, IL-6 100ng/ml or untreated for 180 minutes. These include quality control metrics that showed the mean cell number per field of view and the mean duration of cells was unchanged by each condition. 5% FDR BH method corrections formatted as follows: *q < 0.05, **q < 0.01, ***q < 0.001, and ****q < 0.0001; not significant, not labelled. Bar graphs plotted as mean with standard deviation (SD) error bars, and points coloured by donor line: red (M3_CTR), blue (127_CTM) and green (014_CTM), all averaged from N=3 harvest replicates.*

4.3.5 Acute IL-6 exposure causes time-dependent changes in cytokine and chemokine secretion from human MGLs in monoculture

During RNAseq pathway analysis of the hiPSC-derived MGLs, several pathways related to cytokine release were discovered in response to IL-6 (Figure 4.6A). In addition to their traditional immunological function of attracting additional immune cells to regions of neuropathology, microglia release cytokines and chemokines that have a variety of effects on various cell types and their functions. Furthermore, cytokine measures in the blood, CSF and *post-mortem* brain tissue of SZ patients frequently differ significantly from controls (Morris *et al.*, 2018; Purves-Tyson *et al.*, 2020, 2021; Dawidowski *et al.*, 2021). As a result, a proteome profiler array kit was used to acquire an overview of cytokine secretion from IL-6 exposed MGLs as previously described (Garcia-Reitboeck *et al.*, 2018).

Chemokine and cytokine production is clearly influenced by acute IL-6 stimulation, either 3 or 24 hours after IL-6 (100 ng/ml) exposure relative to vehicle controls (Figure 4.6B-C and Table 4.7). Excluding IL-6, 12 of the 36 cytokines and chemokines detected in the experiment were

above the limit of detection (LOD) in the culture supernatant. We omitted IL-6 since it was injected into the medium ectopically when the cells were stimulated with IL-6 (Table 4.7). Since this protocol is semi-quantitative, changes in cytokine and chemokine production were described as fold changes from vehicle and no statistics were run on these data. Of the 12 cytokines above the LOD, MIP-1 and CXCL1 levels were higher in supernatants from IL-6-exposed MGLs at both time points, as compared to vehicle controls, although considerably less after 24 hours than 3 hours (Figure 4.6D). CCL1, Serpin-E1, MIF, and IL-18 levels increased only after 24 hours of IL-6 stimulation, with minimal difference after 3 hours (Figure 4.6D). IL-8 secretion was increased 3 hours after IL-6 simulation but was decreased in comparison to the vehicle 24 hours later (Figure 4.6D). Both time intervals saw a decrease in the anti-inflammatory cytokines IL-13 and IL-16 compared to vehicle controls (Figure 4.6D). Finally, following IL-6 exposure, IL-1Ra, CCL2, and ICAM were unaltered at both time periods (Figure 4.6D). These MGL secretome modifications show that IL-6 activation of human MGLs causes dynamic changes in particular inflammation-regulating chemokines and cytokines.

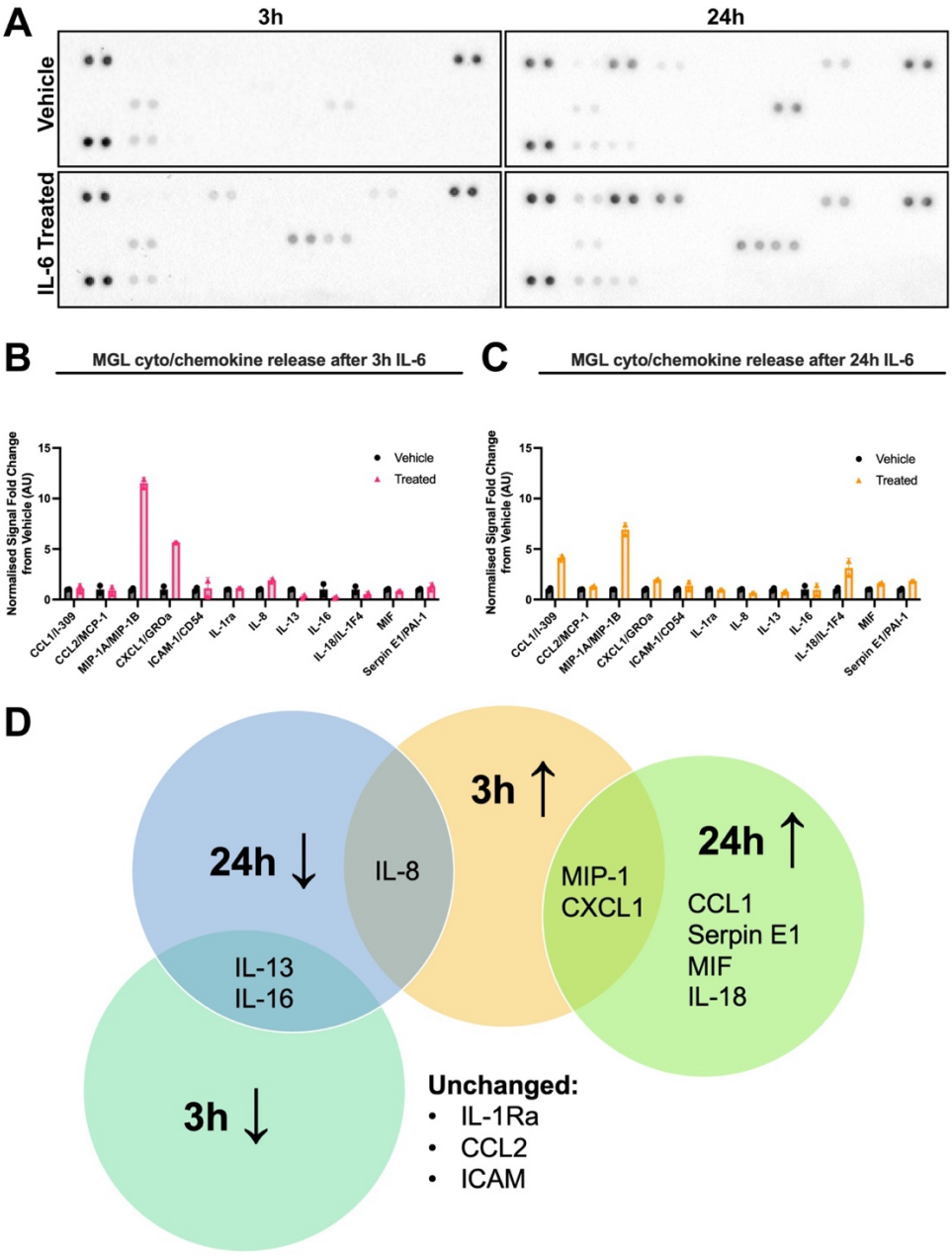

Figure 4.6 - Acute IL-6 increases time-dependent changes in cytokine and chemokine secretion from human MGLs in vitro. (A) Representative images of dot blot cytokine profiles secreted from vehicle and IL-6 stimulated MGLs analysed using the human cytokine array. N=3 separate harvest media samples were pooled into one sample per condition from M3_CTR_37S. Corresponding cytokine and chemokine coordinate labels are available in supplementary table 22 and supplementary figure 5. (B-C) Signal quantification of cytokine signals from dot blots presented in A, shortlisted for detectable cytokines and chemokines and split into 3h (B) and 24h (C) datasets. IL-6 not shown since it was artificially spiked by treatment. Each point represents a technical replicate of each signal point in arbitrary units, which were normalised to positive control reference spots and fold change calculated from averaged vehicle value within each time point. (D) Venn diagram categorising the twelve cytokines measured above the limit of detection. Cytokines are categorised into their direction of change from the vehicle at both 3h and 24h timepoints: ↓ indicates decrease and ↑ an increase.

*Table 4.7 - Mean signal values from cytokine profiler dot blots, including all 36 cytokines, averaged from two replicate dots that were then backgrounded to negative reference dots and normalised to positive control reference dots. Table cells are coloured on gradient from low (white) to high (red). * Cytokines that were measured above the lowest detectable signal level. # IL-6 spiked in treatment groups. Grid coordinate corresponds to grid in Figure 4.1 and blot images in Figure 4.6A*

Cytokine	Array Coordinate	3h Vehicle	3h Treated	24h Vehicle	24h Treated
CCL1/I-309 *	**A3-4**	0.01	0.01	0.05	0.22
CCL2/MCP-1 *	**A5-6**	0.02	0.02	0.75	0.98
MIP-1A/MIP-1B *	**A7-8**	0.01	0.15	0.09	0.65
CCL5/RANTES	**A9-10**	0.01	0	0	0
TNFSF5	**A11-12**	0.01	0	0	0
C5a	**A13-14**	0	0	0	-0.01
CXCL1/GROa *	**A15-16**	0.01	0.08	0.22	0.44
CXCL10/IP-10	**A17-18**	0.01	0	0.01	0
CXCL11/I-TAC	**B3-4**	0	0	0.01	0
CXCL12/SDF-1	**B5-6**	0	0	0	0
G-CSF	**B7-8**	0	0	0	0
GM-CSF	**B9-10**	0.01	0.01	0	0
ICAM-1/CD54 *	**B11-12**	0.01	0.01	0.01	0.01
IFN-y	**B13-14**	0	0	0.01	0
IL-1a	**B15-16**	0	0	0	0
IL-1b	**B17-18**	0	0	0	0
IL-1ra *	**C3-4**	0.19	0.22	0.09	0.09
IL-2	**C5-6**	0	0	0	0
IL-4	**C7-8**	0.01	0	0	0
IL-5	**C9-10**	0.01	0	0	-0.01
IL-6 *#	**C11-12**	0	0.53	0.01	0.55
IL-8 *	**C13-14**	0.11	0.21	0.73	0.47
IL-10	**C15-16**	0	0	0	0
IL-12 p70	**C17-18**	0	0	0	0
IL-13 *	**D3-4**	0.01	0	0.01	0
IL-16 *	**D5-6**	0.01	0	0	0
IL-17A	**D7-8**	0.01	-0.01	0	0
IL-17E	**D9-10**	0.01	0	0	0.01
IL-18/IL-1F4 *	**D11-12**	0.01	0.01	0.01	0.02
IL-21	**D13-14**	0	0	0.01	0.01
IL-27	**D15-16**	0	0	0	0.01
IL-32a	**D17-18**	0	0	0	0.01
MIF *	**E3-4**	0.19	0.16	0.11	0.19
Serpin E1/PAI-1 *	**E5-6**	0.02	0.02	0.07	0.13
TNFa	**E7-8**	0	0	0	0.01
TREM-1	**E9-10**	0	0	0	0.01

4.4 Discussion

This chapter defines the changes in form and function of hiPSC-derived MGLs from three male, neurotypical donors in response to an acute IL-6 challenge. These outcomes are distinguished into three main findings, addressing the questions outlined in section 4.1.2. First, the lowest concentration of IL-6 that resulted in an increase in transcript expression downstream of STAT3 pathway activation in MGLs was 100ng/ml. Second, the acute IL-6 stimulation induced a transcriptional profile shift that is relevant for molecular pathways identified in *post-mortem* tissue from individuals with SZ, but did not influence the expression of risk genes identified by GWAS for SZ, ASC or BD. Third, acute IL-6 impacted the function of human MGLs by changing their cytoplasmic motility and secretome, both of which would be predicted to have downstream functions that have the potential to be non-neuroprotective and target chemotaxis of additional cell types to the origin of secretion. These findings provide novel leads for IL-6 how may act on human foetal MGLs and potentially mediate the risk for SZ with elevated levels of this cytokine, as demonstrated previously in genetic (Perry *et al.*, 2021), blood biomarker (Allswede *et al.*, 2020) and animal models (Smith *et al.*, 2007).

4.4.1 Selecting the concentration of IL-6 to stimulate MGLs

Based on the seven concentrations tested, 100 ng/ml of IL-6 was chosen as the stimulation dosage for further characterisation studies because it was the lowest concentration that elicited an MGL response that could be quantified at an acute time-point within the genes studied. Consistent with this view, exposure of the MGLs for 3h to 100ng/ml IL-6 resulted in a robust transcriptional response, as measured by RNAseq. It should be emphasised, however, that this concentration was determined based on the specified STAT3 signalling genes. It is therefore unknown whether other pathways are active at different IL-6 concentrations or at other time-points.

As may be expected, 100 ng/ml IL-6 is significantly higher than the reported concentration of IL-6 in maternal serum at steady state (0.98 ± 1.06 pg/ml) (Graham *et al.,* 2018). This concentration is more likely to be representative of a spike in IL-6 concentration that would occur in maternal serum as an acute response to infection (Hsiao and Patterson, 2011; Wu *et al.*, 2017; Ozaki *et al.*, 2020; Matelski *et al.*, 2021). For example, adult patients with community-acquired pneumonia have a mean serum IL-6 concentration of 477 pg/ml (Antunes *et al.*, 2002), while COVID-19 patients with delirium have a mean serum IL-6 concentration of 229.9 pg/ml (Borsini *et al.*, 2022). It is important to note however, that these results only discuss peripheral IL-6 concentrations and do not account for variations that occur in other compartments, for example between maternal plasma, foetal brain and blood and the placenta. IL-6 passes from the maternal serum to the foetus via the placenta in MIA rodent models, and the transfer rate is greater in mid-gestation compared to late-gestation (Jarskog *et al.*, 2005; Dahlgren *et al.*, 2006). Although the *in vitro* model described in this chapter cannot account for placental-induced concentration variations, it is possible that local concentrations of IL-6 may be higher in the CNS (Ozaki *et al.*, 2020). As a result, the response of MGLs to 100 ng/ml IL-6 may reflect a realistic dose.

Finally, the dose optimisation presented in this chapter only accounts for the acute effects of IL-6 and does not account for chronic, low-dose IL-6 exposure to the developing cortex, which is more likely to be associated with a separate source of NDD risk and may even produce different results than the type of stimulus presented in this thesis. Although the IL-6 dose described in this chapter is sufficient for modelling acute infection-related events, it would be intriguing to determine whether we observe a similar response by the MGLs, whether heightened or blunted, with repeated exposure to IL-6 compared to the acute exposure scenario.

4.4.2 The MGL IL-6 transcriptional response recapitulates SZ-relevant pathways.

The second main finding is that the set of up-regulated genes by acute IL-6 exposure in our hiPSC-derived MGLs overlapped significantly with those up-regulated in *post-mortem* brain tissue from SZ patients. Despite the fact that there was no statistically significant overlap with gene sets from ASC or BD patients (Gandal *et al.*, 2018), the increased risk for psychiatric disorders with putative neurodevelopmental origin following MIA and, therefore potentially IL-6 elevation is non-specific. Put another way, our sample size was most likely underpowered to detect this overlap after a conservative correction for multiple comparisons. Consistent with this view, genes up-regulated in ASC cases *post-mortem* did overlap with those up-regulated in MGLs by IL-6, at $p<0.05$ uncorrected, but this did not survive FDR correction. In any case, a link between IL-6 exposure, key microglial pathways, and SZ pathogenesis is suggested by the observed overlap with up-regulated SZ gene sets. For example, both *HSPA1A/B* and *NFKB2* were found in the overlapping gene set (Volk *et al.*, 2019; Murphy, Walker and Weickert, 2021). These genes, as well as *Rel* and *IRF8*, all of which were up-regulated in MGLs by acute IL-6 exposure, are involved in the regulation of microglial homeostasis, core microglial signatures, and responses to stress (Gosselin *et al.*, 2017; Galatro *et al.*, 2017; Olah *et al.*, 2020). In addition, transcripts of NFkB are found elevated in prefrontal cortex *post-mortem* tissue of patients with SZ, as well as in adult mice that received Poly I:C injections, but not in their offspring who were exposed *in utero* (Volk *et al.*, 2019). This implies that IL-6 may induce a functional shift in microglia via changing the expression of these genes that may be relevant for SZ pathogenesis, that can inform functional assays *in vitro* and stimulate further cellular modelling studies using CRISPR/Cas9 engineering.

Furthermore, the lack of overlap with GWAS-identified risk gene sets for all the SZ, ASC, and BD diagnoses might imply that the observed link between IL-6 and these disorders is due to environmental variables that result in elevated IL-6 levels, such as infection (Allswede *et al.*, 2020; Careaga *et al.*, 2017; Graham *et al.*, 2018; Meyer, 2014; Mueller *et al.*, 2021; Potter *et al.*, 2023; Rasmussen *et al.*, 2021, 2019; Rudolph *et al.*, 2018). Therefore, it appears that IL-6 impacts common molecular pathways associated with SZ and potentially ASC, but it does not seem to modify the expression of risk genes identified through GWAS. This finding contrasts with previous research conducted by the group, which revealed that SZ genes overlapped with genes that were down-regulated upon exposure to IFN-γ in NPCs and neurons (Warre-Cornish *et al.*, 2020). It is important to note however, that genetics cannot be ruled out as a potential mediator of this relationship because all variants and genes located within the histocompatibility complex (MHC) locus are excluded from the MAGMA analysis due to the complex linkage disequilibrium structure in this region, despite the fact that many IL-6 response genes are in this locus. The development of novel approaches for translating MHC results into neurobiological risk pathways for complex illnesses may therefore increase our understanding of the MHC's role in psychiatric disorders.

Moreover, since the *post-mortem* gene expression data used for these comparisons is based on non-cell specific bulk RNAseq, our findings suggest microglia are at least one essential cell type to investigate further. Although single cell RNAseq data does not exist for microglia from patients with SZ, there is however an interesting divergence in the data on this topic. Specifically, using human cortical *post-mortem* brain tissue from patients with SZ, Gandal and colleagues (2018) reported that microglia genes were *down-regulated* using as measured by RNAseq and replicated in qPCR studies by Snijders and colleagues (2021) (Snijders *et al.*, 2021; Gandal *et al.*, 2018). Providing an example that is specifically pertinent to this work,

IRF8 expression is reported to be *down-regulated* in *post-mortem* human cortical brain tissue from patients with SZ (Snijders *et al.*, 2021; Gandal *et al.*, 2018). Contrary to these findings, we found that after 3 hours of acute IL-6 exposure, *IRF8* expression increased, along with cytoplasmic motility and time-dependent increases in chemokines and cytokines. These results are in line with the known function of IRF8 in promoting the adoption of a pro-inflammatory gene signature in diseased microglia (Ransohoff and Engelhardt, 2012). Interestingly, in line with our data, Ormel and colleagues performed mass cytometry to find two clusters of induced microglia (iM) cells that were enriched primarily in donors with a diagnosis of SZ using PBMCs that had been transdifferentiated to induced microglia (iM)(Ormel *et al.*, 2020). One of these clusters was distinguished by increased amounts of the proteins CD68, Cx3cr1, HLA-DR, P2RY12, TGF-1, and, most crucially, IRF-8 (Ormel *et al.*, 2020). These findings highlight the potential for confounding factors, such as prolonged antipsychotic exposure (Chan *et al.*, 2011) and illness chronicity following a long-term disease on tissue, to affect the interpretation of microglial gene expression changes in *post-mortem* brain tissue from individuals with schizophrenia (Mccullumsmith *et al.*, 2014). Another possibility to consider is that the disparity in findings could be attributed to the difference between living samples and deceased tissue. To gain more insights, it is crucial to acquire additional data from "living tissue" samples, such as resections obtained from patients with epilepsy or traumatic brain injury (TBI), both with and without comorbid psychiatric conditions (Wilson-Genderson *et al.*, 2018). Therefore, more research is needed to describe how IL-6 affects certain microglia states relevant to SZ and potentially other psychiatric disorders, utilising either mass cytometry or single-cell techniques that employ both hiPSC cellular models, donated living tissue and *post-mortem* brain tissue.

The finding that acute IL-6 stimulation increases OXT receptor (OXTR) expression, plus its overlap with the up-regulated SZ gene set (Gandal *et al.*, 2018) is however consistent with

evidence linking OXTR gene polymorphisms to the pathogenesis of both SZ (Nakata *et al.*, 2021; Broniarczyk-Czarniak *et al.*, 2022) and ASC (Francis *et al.*, 2016; de Oliveira Pereira Ribeiro *et al.*, 2018). Of note, findings in mouse primary microglia suggest OXT inhibits transition to a pro-inflammatory microglia state after LPS stimulation *in vitro* (Inoue *et al.*, 2019). Additionally, an OXT receptor agonist, carbetocin, ameliorates perinatal brain injury induced by a gestational low protein diet in mice by alleviating changes to microglial function (Mairesse *et al.*, 2019). Therefore, additional research including investigations using patient-derived cell lines, are warranted to ascertain the function of OXTR signalling in controlling MGL responses to IL-6 in our human model system.

4.4.3 IL-6 evokes a MGL secretome with similarities to that seen in rodent MIA model serum

After both 3 and 24 hours, IL-6 qualitatively decreased the secretion of anti-inflammatory cytokines IL-13 and IL-16, and increased secretion of MIP-1 and CXCL1 in comparison to the vehicle in hiPSC-derived MGLs. Importantly, the increase of MIP-1 release from this cell model confirms previous results that MIP-1 is strongly up-regulated in the maternal serum of rodent MIA models (Arrode-Brusés and Brusés, 2012; Brown *et al.*, 2022; Osborne *et al.*, 2019). Both MIP-1 and CXCL1 chemokines have been demonstrated to precede neutrophil infiltration to the brain in a rat seizure model (Johnson *et al.*, 2011). This chemoattractant function is also attributed to IL-8 (Cross and Woodroofe, 1999; Matsushima, Yang and Oppenheim, 2022), which in this model was secreted after 3h, but resolved after 24h. Although IL-16 was first identified as a CD4+ immune cell attractant in the periphery (Cruikshank, Kornfeld and Center, 2000), it has been shown in rats to be neuroprotective against kainite-induced excitotoxicity and neuronal death, as well as lowering neuronal excitability and synaptic activity (Shrestha *et al.*, 2014), as well as reducing neuronal excitability and synaptic

activity (Hridi *et al.*, 2019). Furthermore, IL-13 showed anti-inflammatory effects in a mouse model of traumatic brain injury (TBI), improving TBI impacts by modifying microglial phenotypes to promote phagocytosis of injured neurons and decreasing production of pro-inflammatory cytokines (Miao *et al.*, 2020).

On the other hand, changes to CCL1, Serpin E1, MIF and IL-18 secretion were seen only after 24h and indicate a delayed release of these signals by the MGLs, which are nonetheless associated with chemotaxis of cells towards the site of secretion (Miyoshi *et al.*, 2008; N. Akimoto *et al.*, 2013; Nasiri *et al.*, 2020; Huang *et al.*, 2021). Interestingly, CCL1 has also been shown in primary cultured mouse microglia to increase microglial motility and expression of additional pro-inflammatory cytokines such as IL-6 itself (Nozomi Akimoto *et al.*, 2013), in line with our motility results from section 4.3.4 and qPCR results from section 3.3.3 respectively. Taken together, the secretome function change evoked by IL-6 on these MGLs within 24 hours may target chemotaxis of non-neuronal cells to areas of pathology, which can be tested with *in vitro* migration assays. However, it should be mentioned that none of the twelve identified cytokines and chemokines' corresponding gene transcripts were found to be differently expressed in the 3h RNAseq analysis described in section 4.3.2. This may reflect the qualitative nature of the proteome profiler kit study, the chance that protein expression and transcript level will differ, or the simple reality that these genes failed to pass FDR correction.

4.4.4 Chapter Limitations

The present chapter's limitations should also be mentioned. As previously stated, each cell type's reaction is described here in the setting of an acute IL-6 administration in a monoculture, in the absence of a genetic background for a relevant psychiatric and neurodevelopmental disorder. Within this context, birth cohort studies describe the influence of cumulative IL-6

exposure on brain and behaviour phenotypes by reporting the correlation between mean IL-6 exposure across gestation (Graham *et al.,* 2018). Furthermore, it has been previously documented that acute IFN-γ exposure has a distinct impact on gene expression in hiPSC-derived forebrain NPCs when the experiments are performed using donors with a diagnosis of SZ, as compared to neurotypical controls (Warre-Cornish *et al.*, 2020; Bhat *et al.*, 2022). It will be be important therefore, to explore both chronic IL-6 exposure and incorporate patient-derived hiPSC lines from SZ (and potentially ASC) in future investigations. Although *in vitro* cultures are an artificial system, they are a useful reductionist system with which to investigating the interactions between certain cell types and specific cytokines, which is the motivation for their use in the present study. To extend the findings presented in this chapter, there is a necessity for the use of more complicated 3D culture techniques, such as microglia-containing organoids, to explore the effects of IL-6 on microglial motility within a cortical structured tissue and it's downstream effects on NPC and neuron migration through such tissue (Fagerlund *et al.*, 2022; Pașca *et al.*, 2022; Zhang *et al.*, 2022; Schafer *et al.*, 2023).

4.5 Conclusion

Building on the findings of Chapter 3, which highlighted the importance of cell-specific responses, this chapter defined the MGL response to acute IL-6 in further depth, demonstrating its relevance at multiple levels to NDDs. MGLs were demonstrated to phenocopy transcriptional alterations relevant for SZ in response to 100 ng/ml IL-6, expanding the reported connections between raised IL-6 levels and increased risk for NDDs. Furthermore, human MGL data matches critical microglia results from animal models of MIA, such as the microglial transcriptome of new-born pups from a Poly I:C MIA model, IRF8-dependent microglia motility, and maternal MIP-1 serum secretion. These findings support the role of microglia in the mediation of NDDs and aid in the formation of future hypotheses based on the characteristics of the responses that MGLs generate when exposed to IL-6, which may influence NPC development.

Chapter 5

The interaction between IL-6 and the 22q11.2 Deletion Genotype on Neural Progenitor Cell Development: A Gene-Environment hiPSC Co-Culture Study

Chapter Summary

Background: There is a requirement for a greater understanding of gene-environment interactions in the aetiology of neurodevelopmental disorders at a molecular level using human model systems. Combining bulk RNAseq, cytokine profiling and ELISA, the data in this chapter describes the transcriptional and secretome alterations in hiPSC-derived MGLs and cortical NPCs following acute stimulation with 100ng/ml interleukin-6 (IL-6) in co-culture. To extend this pilot study to investigate the interaction between IL-6 exposure and a relevant genotype, hiPSC lines from individuals with 22q11.2 deletion syndrome (22q11.2DS; N = 2) and healthy control donors (N = 4) were used.

Results: The data suggest that: (1) MGLs responded similarly to IL-6 stimulation irrespective of genotype; (2) NPCs did not appear to respond by trans-signalling in response to IL-6 stimulation in co-culture with MGLs at the timepoint measured; (3) the 22q11.2 deletion genotype triggered changes to transcriptional pathways that involve vasculature and extracellular matrix remodelling that still need to be functionally confirmed in both NPCs and MGLs; (4) the cytokine milieu measured in the co-culture media replicates to some extent that measured in the serum of pregnant rodent dams exposed to immune challenges *in vivo*.

Conclusion: These data suggest that the co-culture model serves as a simplified *in vitro* approach for studying the effect of IL-6 on relevant combinations of cell types using both control and patient derived cell lines to capture potential genotype differences. For example, the data suggest that the effect of IL-6 stimulation on microglia would likely extend to other cell types, such as endothelial cells, leading to indirect impacts on NPCs. The *in vitro* model presented here provides a methodological framework to test this hypothesis in future studies.

5.1 Introduction

The molecular neurobiology of neurodevelopmental disorders (NDDs), including schizophrenia (SZ) remains incompletely understood, yet it is clear that NDDs are highly heritable, with a complex polygenic genetic risk architecture (McDonald-McGinn *et al.*, 2001; Morrow *et al.*, 2018; Du, de la Morena and van Oers, 2020). There is strong evidence from epidemiological studies for associations between numerous environmental risk factors, including exposure to immune activation early in life and increased risk for NDDs in the offspring (Hilker *et al.*, 2018; Meyer, 2019). As such, an intricate interplay between genetic and environmental factors likely contributes to the development of NDDs, highlighting the need for a greater understanding of gene-environment (GxE) interactions at the cellular and molecular level (Meyer, 2019). As previously stated in section 1.1.2, genetic risk for NDDs including SZ is characterised predominantly by a variable burden of many low-penetrance, common, single nucleotide polymorphisms (SNPs), thereby classifying them as polygenic diseases (CNVs) that have larger effect sizes, thereby classifying them as polygenic diseases (McDonald-McGinn *et al.*, 2015; Ma *et al.*, 2018; Khan *et al.*, 2020). In parallel, genetic risk for NDDs (including SZ) are also associated well rarer, but much more penetrant copy number variation (CNVs), which may also interact with underlying polygenic risk. Recapitulating these complex genetic risk profiles in animal models remains challenging, hence development of human model systems is important to enable studies of GxE risk factors. One example of a highly penetrant CNV is 22q11.2DS carriers of which, have a substantial risk for developing a psychiatric disorder, including psychosis, autism and depression (McGuffin, Owen and Farmer, 1995; Hilker *et al.*, 2018; Khan *et al.*, 2020). Therefore, having characterised the response of both hiPSC-derived MGLs and NPCs from neurotypical donors, without any history of psychiatric illness in the preceding chapters, the next logical step is to study how the effects of IL-6 exposure may vary on a background of elevated genetic risk for NDDs. Based

on the aforementioned discussion of psychiatric genetics and informed by our previous work with hiPSC lines from individuals with 22q11.2DS (Reid *et al.*, 2022), we pragmatically choose to focus on 22q11.2DS to develop a simple, flexible human *in vitro* model to study GxE interactions, in order to begin determining the contribution of different cell types and the molecular pathways involved.

The importance of comparing cytokine responses on different genetic backgrounds is highlighted by previous work from the Srivastava and Vernon laboratories. Specifically, Bhat and colleagues (2022) reported an attenuated transcriptional response to acute interferon-gamma (IFN-γ) stimulation when using hiPSC-derived NPCs from individuals with idiopathic SZ, as compared to that observed in neurotypical controls (Warre-Cornish *et al.*, 2020; Bhat *et al.*, 2022). Specifically, Bhat and colleagues (2022) identified nearly 3000 genes that exhibit distinct responses to acute IFN-γ stimulation in the SZ donor lines, thereby highlighting that early developing NPCs may respond differently to acute cytokine stimulation when comparing donor lines from individuals with psychiatric disorders that have a neurodevelopmental origin to neurotypical controls. These findings underscore the value of hiPSC-based models, as they retain the genetic risk background in a manner that is not feasible in animal models, as already stated. Aside from the genetic risk for NDDs, conclusions from previous chapter's data have hinted at the possibility that the nature of the microglia-like cell's (MGL) interleukin-6 (IL-6) response could generate downstream effects on nearby developing neural progenitor cells (NPCs) after stimulation of these two cell types in co-culture. This is due to the secretion of cytokines, chemokines, and necessary IL-6 signalling receptors such as the soluble (s)IL-6Ra by the MGLs. Taken together, we can employ a straightforward co-culture system involving microglia and developing cortical NPCs to investigate the interplay between donor genotype (22q11.2DS) and acute exposure to IL-6.

One challenge to studying such interactions within an MGL-NPC co-culture however lies in minimizing any confounding results that may arise from microglial activation as a consequence of experimental manipulations. When building the 22q11.2DS and IL-6 GxE model presented in this chapter, a similar approach to that reported by Park and colleagues (2020) was considered. In this study, BV2 mouse microglia were grown on-top of mesh inserts and stimulated with a combination of LPS and Poly I:C 24 hours prior to adding the inserts to a trans-well co-culture system, in which hiPSC-derived cortical interneurons (cINs) donated from both control and SZ diagnosed patients were grown on the base of the well in the plate. Their results showed that co-culture of cINs with these previously simulated BV2s disturbed for 2 hours metabolic pathways, arborization, synapse formation, and synaptic GABA release (Park *et al.*, 2020). These alterations were of a greater magnitude and duration in the cINs from the SZ donor lines as compared to controls, suggestive of an "additive" interaction between the SZ genetic background and the cytokines released by the stimulated microglia (Park *et al.*, 2020). These findings are however limited, not only by the use of non-human (mouse) immortalized BV2 cells, but also by the non-specific immune response of microglia induced by LPS and Poly I:C stimulation. Importantly, BV2 cells may also exhibit different responses as compared to rodent or human primary microglia, including a limited and less robust response to LPS and IL-4, as measured by proteomics (Luan *et al.*, 2022). As a result, *in vitro* BV2 cells are unlikely to fully replicate the complexity of a human microglial response. Moreover, in this experimental design, the effects may be exaggerated as any impact of basal cytokine release on the cINs prior to the stimulation is not captured, in other words these cultures are not equilibrated with other. Nonetheless, the work of Park and colleagues is important, since it also provides proof-of-principle that stimulation of microglia is sufficient to cause an exaggerated phenotype in the patient-derived cells (Park *et al.*, 2020).

Taking into account the limitations associated with the study of Park and colleagues (2020), in this chapter we use hiPSC-derived MGLs and NPCs from the same donor, thus on the same genetic background (healthy controls or 22q11.2DS donors) and expose them acutely to IL-6, after 24h in co-culture. The aim of this chapter was to determine the cellular and molecular phenotype of both NPCs and MGLs on each genetic background after co-culture. Based on the findings of the previous chapter, and the findings of Park and colleagues (2020), we hypothesised that (1) co-culture with MGLs would enable the NPCs to respond acutely to IL-6 by via secretion of soluble the sIL-6Ra and via other cytokines secreted by MGLs, which (2) will alter the NPC transcriptome as measured by bulk RNAseq, used to identify relevant molecular pathways and (3) any such effects will be exacerbated in the 22q11.2DS cultures as compared to controls. Importantly, using a separated trans-well co-culture approach allows for examination of soluble factors vs. physical contact and minimises the risk of confounding effects from experimental manipulation of the microglia since it is not necessary to mechanically sort the individual cell types, for example by fluorescence-activated cell sorting (FACS).

5.2 Methods

5.2.1 Cell Culture and Sample Collection

Microglia like cells (MGLs) and neural progenitor cells (NPCs) were differentiated separately from hiPSCs as described in sections 2.1.2 and 2.1.3 respectively. A total of 7 hiPSC donor lines were used: N = 4 Control (M3_CTR_36S, 069_CTF_01, 014_CTM_02 and 127_CTM_01) and N= 3 22q11.2DS donors (509_CXF_05, 191_SZF_05 and 287_SZM_01) (Table 2.1). The 22q11.2DS hiPSC line 191_SZM_05, despite previously reported to generate

ventral midbrain NPCs and dopaminergic neurons (Reid *et al.* 2022), in our hands could not be made to successfully generate forebrain NPCs despite N=4 independent attempts. This line therefore had to be excluded for reasons of time, resulting in only N=2 22q11.2DS donor lines to be included in this dataset. At the present time, no additional 22q11.2DS donor lines were available in the Vernon and Srivastava laboratory that undergone sufficient quality control to replace 191_SZM_05 in this study. Information on the demographics of each 22q11.2DS donor can be found in Table 2.2. In this chapter, biological replicates were considered to be N=1 clone from each donor line; in other words, the donor is the biological replicate. Each donor line was matched for age and sex across the genotype comparisons insofar as possible (Table 2.1). MGL progenitors were seeded directly from the factory onto 0.4 μm Transparent PET Membrane Permeable Support Cell Culture Inserts (Falcon®; 353090) and allowed to differentiate for 12 days, after which they were assembled on top of the NPCs that had been differentiating in parallel for 16 days without their physical contact (Figure 5.1). This permitted the NPCs to settle after neural passaging the day before on day 15 of their differentiation. Both cell types were then cultured together for 48h in co-culture media (1X N2 supplement, 2mM Glutamax, 100ng/ml IL-34 and 10ng/ml GM-CSF), to allow the two cell types to "equilibrate" (Figure 5.1). In addition, the B27 supplement was left out of the co-culture medium. Specifically, during their initial optimization trials for establishing the hiPSC to MGL differentiation method, Haenseler *et al.* (2017) raised concerns regarding the presence of corticosterone, superoxide dismutase, and catalase compounds in the B27 supplement (Haenseler *et al.*, 2017). Therefore, B27 was removed from their medium, and therefore from this chapter, to guarantee compatibility with iPSC-derived cortical neurons while preserving microglial function (Haenseler *et al.*, 2017). The co-cultures were then exposed to 100ng/ml IL-6 or vehicle control (sterile water with 100 picomolar acetic acid) in fresh media, for 24h (Figure 5.1). This meant stimulation on the microglial differentiation day 14, and neural

progenitor differentiation day 18, as optimised in previous chapters. Following the period of 24h stimulation, the cell types were separated again, and RNA samples were collected as described in section 2.2.1. Media from both cell-type compartments were pooled, spun down to remove cell debris and frozen for secretome analysis (Figure 5.1).

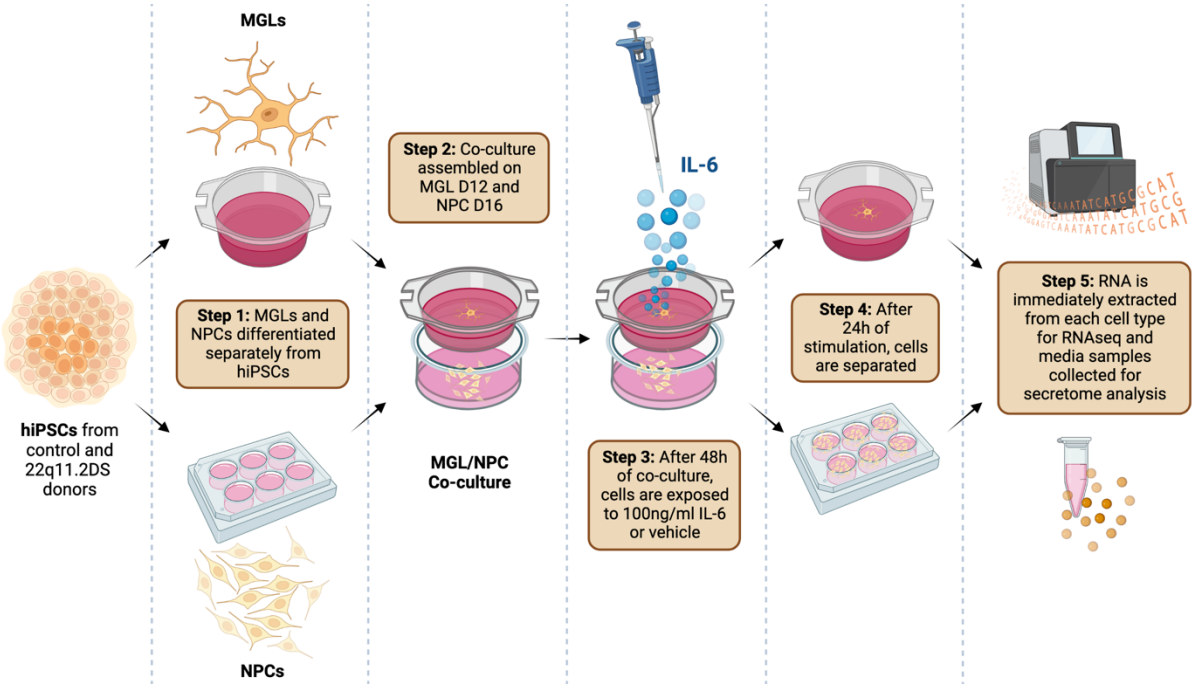

Figure 5.1 - Scheme for exposing co-cultured hiPSC-derived neural progenitor cells (NPCs) and microglial like cells (MGLs) with 100ng/ml IL-6 in both control and 22q11.2DS genotypes. Day 12 MGLs and day 16 NPCs were derived separately on cell culture inserts and 6-well plates respectively (step 1). They were then co-cultured for 48h (step 2) before stimulation with 100ng/ml IL-6 or acetic acid vehicle for 24h (step 3). MGL and NPC RNA and media samples were then collected after compartment separation (step 4) and extracted for analysis (step 5).

5.2.2 RNAseq

RNAseq, gene ontology and gene set enrichment analyses were carried out as described in section 2.2.4, in a total of 24 samples (Table 5.1).

Table 5.1 – The 24 samples from co-culture sent for RNAseq analysis. Of the control genotype samples, lines M3_CTR_36S, 069_CTF_01, 014_CTM_02 and 127_CTM_01 were used. Of the 22q11.2DS genotype, 509_CXF_05 and 287_SZM_01 were used. Individual donor was therefore used as a biological replicate in downstream analyses.

Cell Type	Treatment	Control Genotype	22q11.2DS Genotype
MGL	Vehicle	N=4 (3 ♂, 1 ♀)	N=2 (1 ♂, 1 ♀)
	IL-6	N=4 (3 ♂, 1 ♀)	N=2 (1 ♂, 1 ♀)
NPC	Vehicle	N=4 (3 ♂, 1 ♀)	N=2 (1 ♂, 1 ♀)
	IL-6	N=4 (3 ♂, 1 ♀)	N=2 (1 ♂, 1 ♀)

5.2.3 Media cytokine profiling array

Cytokine profiling was carried out as described in section 2.3.1, following the manufactures instructions using the Proteome Profiler Human XL Cytokine Array Kit **(**R&D Systems; ARY022B). Each kit contained four membranes with dots of 105 different immobilised cytokine antibodies (Appendix Table 1), dotted with two technical replicates each (Appendix Figure 1). Co-culture media samples were grouped and pooled by treatment condition and genotype, with which the four membranes were stained: Control Vehicle, Control IL-6, 22q11.2DS Vehicle, 22q11.2DS IL-6.

5.2.4 Multiplex Cytokine Assay

The concentrations of MIP-1a, TNFα, IL-8, and VEGF-A in vehicle/IL-6 treated co-culture, plus 24h treated NPC and MGL monoculture media (N = 3 healthy male donors M3_CTR, 014_CTM and 127_CTM) was measured using a custom U-Plex Biomarker Group 1 (Human) Multiplex Assay (K15067M-1, Meso Scale Discovery), following the manufacturer's instructions. Antibodies for each of the four analytes were cross-linked to a unique spot in each well of a 96-well plate. Each sample was incubated for 2 hours on the plate in technical

triplicate, in addition to a seven-point standard curve. A secondary detection antibody was then added and incubated for 2 hours. The plate was read on an MESO QuickPlex SQ 120MM Imager, and data was obtained using Discovery Workbench 4.0 (Meso Scale Discovery).

5.2.5 Soluble IL-6Ra ELISA

As per the ELISA protocol described in section 2.3.2, soluble IL-6Ra was quantified in MGL/NPC co-culture media from N = 4 Control and N = 2 22q11.2DS donors treated with vehicle or 100ng/ml IL-6 for 24h.

5.2.6 Statistical Analysis

All statistical analyses were conducted using Prism 9 for macOS version 9.3.1 (GraphPad Software LLC, California, USA), except for the RNAseq analyses which were carried out using the research computing facility at King's College London, Rosalind, and CREATE, along with R version 4.0.2 (R Core Team, 2020). Each specific test performed is described in the corresponding figure legend and statistical data table, providing the number of replicate hiPSC lines included in each technical and biological replicate, as specified in the relevant method section above. To compare the concentrations of cytokines and sIL-6Ra in control and IL-6 treated co-culture media from control and 22q11.2DS donors, an unpaired two-tailed t-test was employed (Figure 5.6 and Figure 5.7C). This decision was made due to the unequal number of replicates in the control (N = 4) and 22q11.2DS (N = 2) groups, hence, comparison of the treatment effect within each genotype was considered appropriate. When comparing the mean between two distinct conditions, such as the concentrations of cytokines in control and IL-6 treated monoculture media from NPCs and MGLs, a two-way ANOVA was employed in this chapter. This choice was made because the sample sizes were equal (Figure 5.7D).

In cases where significant differences were observed between groups in these models, post-hoc testing was conducted using the Benjamini-Hochberg (BH) method with a false discovery rate (FDR) of 5% to identify the individual groups with significant differences. Adjusted p-values (q-values) less than 0.05 were considered statistically significant, and relevant significant q-values are quoted. The BH correction method with a 5% FDR threshold was also employed when deciphering the differentially expressed genes from each transcriptome signature, and during the RNAseq downstream over representation analysis. No statistical analysis was applied to the media cytokine array data due to insufficient sample power.

5.3 Results

5.3.1 hiPSC-derived MGLs show subtly different transcriptional responses to acute IL-6, depending on the donor genotype

To characterise the transcriptional response to IL-6 of MGLs in co-culture with NPCs, and whether the 22q11.2DS genotype influences this, bulk RNAseq analysis of DEGs was conducted using RNA samples from both control and 22q11.2DS donor-derived MGLs after 24h exposure to either 100ng/ml of IL-6 or vehicle in co-culture. Given the technical constraints of the DESeq2 package and the unequal genotype donor replicates, it was not possible to run a two-way ANOVA analysis on differentiation expression to understand an interaction effect. Instead, the following four DESeq2 comparison signatures were created to examine similarities and differences as a function of genotype and treatment.

- **Signature A:** IL-6-treated vs vehicle-treated control MGLs from control donors (i.e., the effect of IL-6 stimulation on gene expression in the control cells).
- **Signature B:** IL-6-treated 22q11.2DS vs vehicle-treated 22q11.2DS MGLs (i.e., the effect of IL-6 stimulation on gene expression in the 22q11.2DS donors).

- **Signature C:** Vehicle-treated 22q11.2DS vs vehicle-treated control MGLs (i.e., the differences in MGL transcriptome as a function of genotype only).
- **Signature D:** The Gene by Environment effect of IL-6 treatment in 22q11.2DS vs in control MGLs (i.e., how the transcriptional response to IL-6 stimulation differs in 22q11.2DS MGLs compared to control MGLs).

When comparing differentially expressed genes (DEG) between vehicle and IL-6 treated samples, it was clear that MGLs responded to the IL-6 stimulus irrespective of their genotype (Healthy control signature A: 72 DEGs [$q < 0.05$], 22q11.2DS signature B: 27 DEGs [$q < 0.05$]). When comparing genotypes within the same treatment samples however, subtle genotype differences in DEGs were detectable (vehicle signature C: 28 DEGs [$q < 0.05$], IL-6 signature D: 15 DEGs [$q < 0.05$]) (Table 5.2). A principal component analysis (PCA) was carried out to identify the top two sources of variation within the MGL dataset, by comparing all RPKM gene counts in all 12 samples and plotting principal component (PC)1 against PC2 (Figure 5.2A). The greatest source of variation in the MGL dataset was sex, as seen with both female lines 069_CTF and 509_CXF clustering to the right of the male donor lines (PC1 = 35.68% variance explained), then IL-6 treatment (PC2 = 19.64% variance explained) (Figure 5.2A). With only N = 1 female hiPSC line per genotype and treatment group however, analysis of sex as a biological variable was not pursued further. To check successful that the 22q11.2DS genotype did not influence the differentiation of the hiPSC to MGLs, DESeq2 normalised counts from the vehicle-treated samples were plotted for each genotype, comprising human microglia and monocyte marker genes (Figure 5.2B). These were based on a list of genes created by the protocol's original publishers (Haenseler *et al.*, 2017), which included genes highly expressed in human microglia (Melief *et al.*, 2012), genes enriched in microglia over blood monocytes (Butovsky *et al.*, 2014), and TMEM119, a putative microglia-specific gene (Bennett *et al.*,

2016). This analysis suggests that the hiPSC-derived MGLs used in this chapter express these microglial marker or "signature" genes in a manner similar to that shown by the original publishers of the MGL differentiation protocol (Haenseler *et al.*, 2017). This profile did not cluster based on genotype, indicative that the 22q11.2DS genotype did not appear to impact on differentiation to MGL from hiPSC cells, at least insofar as gene expression is concerned (Figure 5.2B). In support of this, unpublished evidence from the Vernon lab shows 22q11.2DS MGLs from the same donor lines as those used in this chapter show no differences in the protein expression of Iba1 or TMEM119 (Hanger B, personal communications, unpublished data.)

Table 5.2 – Summary of transcriptional analyses signatures from MGLs, and the subsequent differentially expressed genes (DEGs) that were either increased or decreased and passed 5% FDR correction.

Signature	Description	Increased DEGs	Decreased DEGs	Total DEGs
A	The effect of IL-6 stimulation on gene expression in control MGLs	43	29	72
B	The effect of IL-6 stimulation on gene expression in 22q11.2DS MGLs	18	9	27
C	The effect of genotype on gene expression between 22q11.2DS and control MGLs treated with vehicle only	12	16	28
D	The effect of genotype on gene expression between 22q11.2DS and control MGLs treated with IL-6	7	8	15

Transcriptional response of neurotypical and 22q11.2DS MGLs to acute IL-6 exposure

MGLs differentiated from neurotypical control hiPSCs (N=4 donors) showed differential expression of 72 genes (out of 16820 genes measured) after FDR correction (5%) in response to IL-6 (100 ng/ml) relative to vehicle-treated samples after 24 hr exposure (Signature A; Table 5.2). As expected, genes involved in IL-6 receptor signal transduction, such as *JAK3* (q = 0.000253; log2FC = 1.745) and *STAT3* (q = 0.0254; log2FC = 0.505) were significantly up-

regulated by IL-6 signalling (Figure 5.2C). The top up-regulated gene was the Epstein-Barr virus-induced gene 3 (*EBI3,* q = 0.00001481; Log2FC = 4.360), which is known to also mediate IL-6 trans-signalling in the same way as sIL-6Ra, but with less efficiency (Chehboun *et al.*, 2017) (Figure 5.2C). In addition, *IDO1* which encodes the enzyme indoleamine 2,3-dioxygenase 1 (IDO) was increased in expression after IL-6 stimulation (q = 0.00444; Log2FC = 5.535) (Figure 5.2C). Of note, elevated serum concentrations of IDO are linked with first-episode psychosis and positively correlate with negative symptoms when compared against the Positive and Negative Syndrome Scale (PANSS) scores of schizophrenia patients (Y. Zhang *et al.*, 2021). Together, the up-regulation of these genes is consistent with successful IL-6 stimulation in these control MGLs in co-culture, which could potentially induce a response that mediates IL-6 trans-signalling in other cell types.

In comparison, MGLs differentiated from 22q11.2 donor hiPSC (N=2) also showed a transcriptional response to 24h 100ng/ml IL-6 exposure, relative to vehicle-treated MGLs on the same genetic background, with differential expression of 27 genes (out of 16752 genes measured) (Signature B; Table 5.2). The smaller number of DEGSs in comparison to signature A (27 vs. 72 DEGs), is most likely due to the reduced experimental power (signature A N = 4, signature B N = 2). In support of this view, similar to signature A, *JAK3* (q = 0.00452; log2FC = 1.558) and *EBI3* (q = 0.0186; log2FC = 2.872) were also significantly up-regulated by IL-6 signalling (Figure 5.2D). There were however some differential results, for example, *VEGFA* expression was increased in the 22q11.2DS MGLs (q = 0.0127; log2FC = 1.238) but not in the neurotypical control signature A analysis (q = 1; log2FC = 0.784). *VEGFA* encodes for vascular endothelial growth factor A, which is essential for angiogenesis during embryonic development (Carmeliet *et al.*, 1996) and *Vegf*^{164} isoform absence in mice triggers birth defects similar to those found in 22q11.DS patients (Stalmans *et al.*, 2003). Furthermore, it is currently being

investigated as a prognostic marker for cognitive impairment in SZ patients (Chukaew *et al.*, 2022), and elevated vascular endothelial biomarkers, specifically those involved in both inflammatory responses and vascular changes, are known to correlate with SZ diagnosis (Nguyen *et al.*, 2018). Also of note, *C3* was up-regulated in the signature B 22q11.2DS MGL response to IL-6 (q = 0.00630; log2FC = 1.246) (Figure 5.2D), but not the control MGL response in signature A (q = 0.0842; log2FC = 1.279) (Figure 5.2C). This is consistent with findings that individuals with 22q11.2DS have significantly elevated plasma levels of C3bc (Grinde *et al.*, 2020) and the evidence linking increased levels of complement pathway proteins in individuals with SZ (Kopczynska *et al.*, 2019; Grinde *et al.*, 2020). These data suggest that MGLs differentiated from both hiPSC of both genotypes show the expected transcriptional response to IL-6 stimulation in co-culture. Furthermore, although preliminary the data suggests subtle differences in the 22q11.2DS response to IL-6, which are of relevance to schizophrenia and affective disorders.

The impact of 22q11.2DS genotype on the hiPSC-derived MGL transcriptome

To investigate the basal transcriptional differences of MGLs differentiated from the 22q11.2DS donors to the neurotypical controls, vehicle-treated samples of each genotype were compared in signature C (Table 5.2). In total, 28 DEGs were found to be statistically significant (12 DEGs increased, 16 DEGs decreased after 5% FDR) (Figure 5.2E). Of the 16 genes with decreased expression, 8 were located in the 22q11.2 deletion region itself (Table 5.3) (Khan *et al.*, 2020). The reduced expression of these genes in the 22q11.2DS donor lines therefore confirms that the genotype difference between these 22q11.2DS and control experimental donor groups, even at an N = 2 of 22q11.2DS replicates, is quantifiable in the hiPSC-derived MGLs. Regarding the genes with increased expression, we noted increased expression of *HLA-DRB5* (q = 0.00543, Log2FC = 3.034) in 22q11.2DS MGLs relative to control donors, which is consistent

with findings from GWAS studies that implicate the MHC locus as the major genetic determinant of risk for schizophrenia and autism (Sekar *et al.*, 2016; Gandal *et al.*, 2018; Pardiñas *et al.*, 2018; Grove *et al.*, 2019)(Figure 5.2F). Although preliminary, these data highlight some potentially important genotype differences in the MGLs driven by the 22q11.2DS genotype.

Table 5.3 – The 8 down-regulated genes from signature C that are found in the 22q11.2 region.

Gene	q-value	Log2FC
HIRA	2.72×10^{-9}	-1.127
ZDHHC8	2.05×10^{-6}	-1.057
TANGO2	2.65×10^{-6}	-1.34
TRMT2A	6.88×10^{-4}	-1.237
C22orf39	9.73×10^{-5}	-1.329
UFD1L	0.0076	-0.955
RTL10	0.00902	-1.152
DGCR6L	0.0214	-1.0946
TXNRD2	0.041	-1.204

Finally, to begin to understand whether the transcriptomic response to IL-6 differed in the 22q11.2DS MGLs relative to the neurotypical controls, we compared the IL-6-treated samples from each genotype (signature D; Table 5.2). We observed only 15 statistically significant DEGs ($q < 0.05$ with 7 DEGs increased, 8 DEGs decreased) (Figure 5.2F As seen in signature C, 6 out of the 8 down-regulated genes were also found in the 22q11.2 deletion region in signature D, confirming the expected result that IL-6 treatment does not change the intrinsic genotype difference. The following few sections provide a more detailed discussion of the 7 up-regulated DEGs, focusing on their relevance to the overlapping interaction effect between IL-6 and the 22q11.2DS genotype (Table 5.5). We therefore proceeded to carry out secondary analysis to identify potential molecular pathways associated with these DEGs.

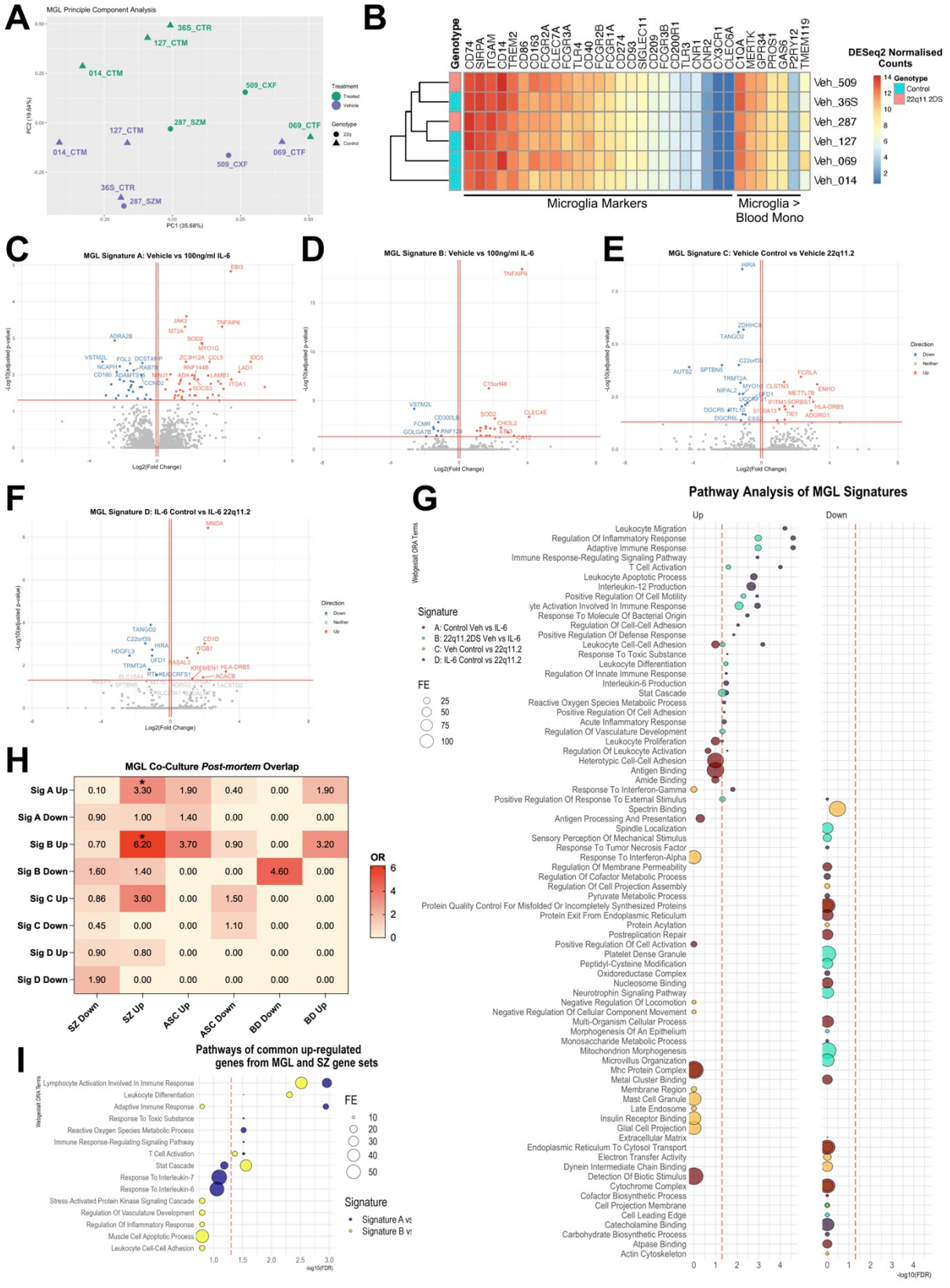

Figure 5.2 – The MGL Response to IL-6 in Co-Culture. (A) PCA analysis from all RPKM gene counts in the 12 samples, coloured by vehicle (purple) or IL-6 treated (green) condition, shaped by genotype (triangle = control, circle = 22q11.2DS) and labelled by donor line. (B) DESeq2 normalised (median of ratios) counts taken from vehicle-treated MGL samples from

*both genotypes, of consensus cell-specific markers and plotted into a heatmap. These consisted of genes highly expressed in human microglia (Melief et al., 2012), and genes that were significantly expressed in microglia when compared with blood monocytes (Butovsky et al., 2014), plus TMEM119 (Bennett et al., 2016). (C-F) Volcano plots of differentially expressed genes from Signatures A (C), B (D), C (E) and D (F). Conditional axis set as follows: log2Foldchange > 0.06 and adjusted p-value < 0.05 coloured red; log2Foldchange < -0.06 and adjusted p-value < 0.05 coloured blue. The top 25 differentially expressed genes are labelled. (G) Webgestalt gene ontology analysis of differentially expressed genes in all four MGL Signatures and corrected with 5% FDR. ORA terms ordered by –log10FDR, coloured by adjusted p-value and sized by the fold enrichment. Plots are split by pathway sets generated from up-regulated genes (left) and down-regulated genes (right). Red dashed line set as 5% FDR threshold. (H) Fisher's exact test comparing gene sets from ASC, SZ and BD post-mortem human patient tissue (Gandal et al., 2018) with up- and down-regulated gene sets identified by RNAseq in all signatures. Odds ratios (OR) plotted in heatmap with significant 5% FDR corrections formatted as follows: . q < 0.1, * q < 0.05, ** q < 0.01, *** q < 0.001, and **** q < 0.0001; not significant, not labelled. (I) Webgestalt gene ontology analysis of the 17 (up-regulated genes in signature A and SZ sets) and 10 (up-regulated genes in signature B and SZ sets) common genes found after Fischer's overlap tests between the signature gene sets from this study and those from the human post-mortem gene sets (Gandal et al., 2018). ORA terms ordered by –log10FDR, coloured by Signature (blue = Signature A vs SZ, yellow = Signature B vs SZ) and sized by the fold enrichment within each dataset.*

Over Representation Analysis of MGL Transcriptomes

To gain insight into the molecular pathways regulated by IL-6 receptor signalling in the aforementioned MGL transcriptional signatures, Webgestalt ORA was carried out separately using the up- and down-regulated gene sets for each individual signature (Yuxing Liao *et al.*, 2019) (Figure 5.2G). Concerning decreased genes, none of the down-regulated gene sets from any MGL signature were substantially related with any ORA pathways after FDR correction ($q > 0.05$) (Figure 5.2G). By contrast, for genes that were up-regulated, 24 ORA pathways were significantly associated with the signature A in response to IL-6 (24 pathways; $q < 0.05$). These included some expected pathways consistent with an IL-6 receptor signal response, namely "STAT cascade" (FE = 10.91, $p < 0.001$, $q = 0.032$), "Interleukin-6 production" (FE = 10.83, $p < 0.001$, $q = 0.032$) and "acute inflammatory response" (FE = 9.94, $p < 0.001$, $q = 0.040$) (Figure 5.2G). The pathway of "positive regulation of cell motility" (FE = 6.49, $p < 0.001$, q =

0.0012) was also significantly associated with the up-regulated gene set, supporting the increase in cytoplasmic motility noted in the live imaging results from section 4.3.4 and verifying that co-culture of MGLs with NPCs does not affect this.

Considering signature B, 10 ORA pathways were significantly associated with the up-regulated gene set (10 pathways $q < 0.05$). Consistent with signature A, the top 3 up-regulated pathways were “regulation of inflammatory Response” (FE = 15.38, q = 0.001), “adaptive inflammatory response” (FE = 9.94, q = 0.040) and “positive regulation of cell motility” (FE = 6.49, q = 0.0012) (Figure 5.2G). Concerning an IL-6 signalling response, “STAT cascade” (FE = 10.91, q = 0.032) was also up-regulated (Figure 5.2G). In contrast to signature A however, signature B up-regulated genes also associated with the “regulation of vasculature development” (FE = 11.36, q = 0.0477), consistent with the upregulation of *VEGFA* expression.

Signatures C and D, comparing genotypes in MGLs under both vehicle and IL-6 treated conditions respectively, yielded no significant pathway enrichments (5% FDR), likely due to the low experimental power (Figure 5.2G). However, the “MHC Protein Complex” had high fold enrichment in both signature C and D up-regulated gene sets, although this did not survive FDR correction (Signature C FE = 66.12, p = 0.015, q = 1; Signature D FE = 105.89, p = 0.009, q = 1). MHC molecules influence adaptive immune regulation particularly in response to interferons via antigen presentation, so the differential expression of this MHC class II molecule by the 22q11.2DS donors could indicate that the 22q11.2DS MGLs may regulate their immune responses to stimuli in a distinctive way to the control donors.

Gene Set Enrichment Analysis of MGL Transcriptome Signatures

In section 4.3.3, it was observed that up-regulated genes in MGL MGLs differentiated from neurotypical controls and stimulated for 3 h with IL-6 significantly overlapped with genes that were up-regulated in *post-mortem* brain tissue from SZ patients, but not with genes identified by genome-wide association studies (GWAS) after MAGMA analysis. To investigate whether this correlation remained after 24h IL-6 stimulation in co-culture with NPCs, gene set enrichment analysis (GSEA) was carried out by overlapping each signature up- and down-regulated gene set with those from *post-mortem* brain tissue from individuals with SZ, ASC, and BD; a corresponding analysis to that from the preceding chapter (Gandal *et al.*, 2018) (eight gene sets from the model vs. two gene sets from each disorder: 48 Fischer's test comparisons in total; Figure 5.2H). Based on the absence of GWAS risk gene enrichment in the IL-6-induced differentially expressed gene set from monoculture MGLs found in the previous chapter, it was determined that MAGMA analysis would not be conducted on the datasets in this chapter to maintain simplicity. Both the up-regulated gene sets from signatures A and B were significantly enriched for the up-regulated gene set from SZ patients (Signature A, N genes in model = 43, N genes in cases = 2274, overlap size = 17 genes, p = 0.00031, odds ratio (OR) = 3.3, q = 0.00372; Signature B, N genes in model = 18, N genes in cases = 2274, overlap size = 10 genes, p = 0.0002, OR = 6.2, q = 0.0024) (Figure 5.2H, Table 5.4). Of note, the odds ratio for the signature B overlap with the up-regulated SZ gene set was almost twice as much than that of signature A. This suggests that the up-regulated gene set from 22q11.2DS MGLs in response to IL-6 overlaps with greater specificity with the SZ up-regulated gene set than that from control MGLs in response to IL-6. Webgestalt ORA of the overlapping Signature A and SZ gene set identified 7 enriched pathways; "lymphocyte activation involved in immune response" (FE = 26.71, q = 0.001), "adaptive immune response" (FE = 14.78, q = 0.001), "T cell activation" (FE = 9.89, q = 0.03), "response to toxic substance" (FE = 9.81, p < 0.001, q =

0.03), “immune response-regulating signalling pathway” (FE = 9.16, q = 0.03), “reactive oxygen species metabolic process” (FE = 14.06, q = 0.03) and “leukocyte differentiation” (FE = 9.00, q = 0.03) (Figure 5.2I). Concerning the 22q11.2DS MGL overlap with the SZ gene set, Webgestalt ORA of Signature B and the SZ up-regulated gene set found 4 enriched pathways; “lymphocyte activation involved in immune response” (FE = 38.09, q = 0.003), “leukocyte differentiation” (FE = 15.52, q = 0.004), “STAT cascade” (FE = 36.27, q = 0.028) and “T cell activation” (FE = 13.66, q = 0.043) (Figure 5.2I). Of note, the STAT3 cascade was significantly enriched in the 22q11.2DS MGL response to IL-6 to a greater extent as compared to the control donors (22q11.2DS FE = 36.27, q = 0.028; control FE = 10.92, q = 0.0321) (Figure 5.2I). When considering these findings collectively, they suggest that the co-culture of MGLs and NPCs does not alter the IL-6 response of MGLs observed in monocultures. Furthermore, the molecular processes implicated in SZ *post-mortem* brain tissue can be identified in our developmental *in vitro* model, as detected in the monoculture MGL response. These data also suggest that the IL-6 signalling cascade through STAT3 may be particularly enriched in cells from donors with 22q11.2DS when compared with control donors.

On the other hand, both signatures C and D were not enriched (5% FDR) with any gene set from patient *post-mortem* datasets (Figure 5.2H) (Gandal *et al.*, 2018). This indicates that the genotype-dependent 22q11.2DS MGL transcriptome is not the sole predisposing factor contributing to end-stage NDD disease states. The response of MGLs to environmental stimuli may also therefore plays a role in NDD risk. However, drawing definitive conclusions can be challenging due to the low statistical power used in this study and the comparison of results to idiopathic diseases rather than patients with the specific 22q11.2DS genotype.

Table 5.4 - Alphabetical list of the 17 (up-regulated genes in signature A and SZ sets) and 10 (up-regulated genes in signature B and SZ sets) common genes found after Fischer's overlap tests between the signature gene sets from this study and those from the human post-mortem gene sets (Gandal et al., 2018).

Gene Sets	Common Genes in Both Sets
Signature A and SZ Upregulated Genes	BATF, CA12, CHI3L2, CLEC4E, FPR2, GK, GRAMD1A, JAK3, KREMEN1, MCOLN2, MT2A, MYO1G, S100A8, SOCS3, SOD2, STAT3, ZC3H12A
Signature B and SZ Upregulated Genes	CA12, CHI3L2, CLEC4E, GADD45B, JAK3, NFKBIZ, SOCS3, SOD2, VEGFA, ZC3H12A

The Gene by Environment Interaction of 22q11.2DS with acute IL-6 stimulation in MGLs

To explore putative gene by environment effect of 22q11.2DS and IL-6, up- and down-regulated gene sets from signatures C and D were compared for overlapping genes in each gene set (Figure 5.3A-B). This made it possible to identify the genes that exhibit differential expression in samples that received both IL-6 treatment and vehicle (in both signatures C and D), clearly attributing their genotype as the cause. As expected, 6 of the 7 down-regulated genes present in both signature C and D and whose down-regulated status was unaffected by IL-6 stimulation were found in the 22q11.2 deletion region (Khan *et al.*, 2020) (Figure 5.3A). The only gene that was down-regulated in the 22q11.2DS MGL response to IL-6 and not found in the 22q11.2 deletion region was *HDGFL3* (q = 0.00352; Log2FC = -2.361) (Figure 5.3A, Table 5.5), which codes for hepatoma-derived growth factor-related protein 3 (HRP-3) and is shown to function in proliferation and cell survival in the CNS of rodent models (El-Tahir *et al.*, 2006). The fact that three of the 22q11.2 deletion region genes down-regulated in signature C were not found in signature D (*DGCR6L* q = 0.416, Log2FC = -0.974; *TXNRD2* q = 0.913, Log2FC = -0.991; *ZDHHC8* q = 0.248, Log2FC = -1.026) could be explained by the fact only N = 2

22q11.2DS donors were used, influencing the statistical power of these comparisons (Figure 5.3A).

On the other hand, *HLA-DRB5* was the only gene to be up-regulated in both vehicle and IL-6 treated 22q11.2DS cells in comparison to the vehicle (signature D q = 0.0193; Log2FC = 3.215), indicating that the increase of this gene's expression is not linked with the MGL IL-6 response status, but likely due to the 22q11.2DS genotype (Figure 5.3B). There were 6 up-regulated 22q11.2DS genes and influenced by IL-6 exposure (Figure 5.3B, Table 5.5). Although not enough genes were found in this set to run robust pathway analysis, and STRING analysis identified no connections between any of the mentioned genes, the function of these genes is consistent with internal cellular signalling regulation (*RASAL3, ACACB, KREMEN1*), response to interferon (*MNDA*), antigen presentation (*CD1D*) or extracellular matrix signalling (*ITGB7*) (Table 5.5) (Sayers *et al.*, 2022). A combination of a small number of biological replicates and multiple sources of experimental variance such as individual donor genetic background and sex may have led to these genes passing multiple correction, and further studies are required with more donor lines

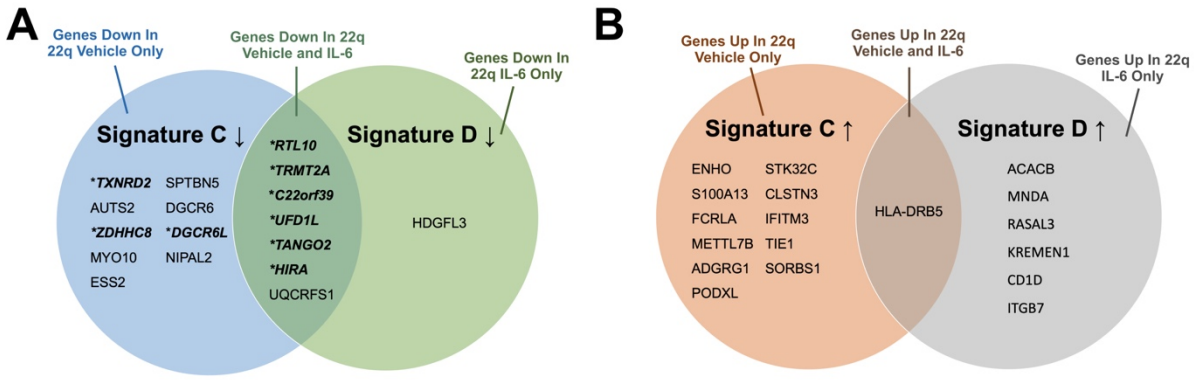

Figure 5.3 – Identifying the gene by environment interaction gene sets in MGLs. (A) Venn diagram that shows the overlap between the genes that are differentially decreased in expression in response to IL-6 in control cells and in 22q11.2DS MGLs. Of the 17 genes that were down-regulated in the 22q11.2DS vehicle and IL-6 treated samples in relation to the control donors, only 7 genes are in common and their 22q11.2DS-associated downregulation is not affected by IL-6 stimulation, meaning that

*there are 10 genes that appear differentially decreased because of genotype and treatment status. Genes in bold and marked with an * are genes found in the 22q11.2 deletion region. (B) Venn diagram that shows the overlap between the genes that are differentially increased in expression in response to IL-6 in control cells and in 22q11.2DS MGLs. Of the 18 genes that were up-regulated in the 22q11.2DS vehicle and IL-6 treated samples in relation to the control donors, only HLA-DRB5 was in common and its 22q11.2DS-associated upregulation is not affected by IL-6 stimulation, meaning that there are 17 genes that appear differentially increased because of genotype and treatment status. Genes in bold and marked with an * are genes found in the 22q11.2 deletion region.*

Table 5.5 – Genes up- or down-regulated as a result of the interaction effect between the 22q11.2DS genotype and IL-6 stimulation, and their functions, i.e. the only genes to be differentially expressed in IL-6 treated 22q11.2DS donors, not their vehicle or control genotypes. Function definitions have been taken from the NCBI Gene summary for each gene.

Gene	Protein Name	q-value	Log2FC	Expression Direction vs. Control Genotype	Function Summary
HDGFL3	HDGF like 3	0.00352	-2.361	Decreased	Predicted to enable double-strand DNA, microtubule binding and transcription coregulator activity, in several processes: microtubule polymerization, negative regulation of microtubule depolymerization, and neuron projection development. Proliferation and cell survival in the CNS.
ACACB	Acetyl-CoA carboxylase 2	0.0360	1.896	Increased	Enzyme that catalyses the carboxylation of acetyl-CoA to malonyl-CoA.
MNDA	Myeloid cell nuclear differentiation antigen	3.64×10^{-9}	2.185		Expected to participate in blood cell-specific responses to interferons.
RASAL3	RAS protein activator like 3	0.0044	0.978		Expected to negatively regulate Ras signalling pathway.
KREMEN1	Kringle containing transmembrane protein 1	0.0422	1.278		DKK1 transmembrane receptor which, when in complex with DKK1, blocks WNT-signalling.
CD1D	CD1d molecule	9.44×10^{-4}	1.983		Member of the CD1 transmembrane glycoprotein family which are structurally related to MHCs. CD1s mediate presentation of primarily lipid or glycolipid antigens to T-cells.
ITGB7	Integrin subunit beta 7	0.0027	1.601		Adhesion receptor that signals to cell from the extracellular matrix.

Collectively, the bulk RNAseq analysis of MGL signatures A to D provides several preliminary insights that will inform future studies in larger sample sizes. Firstly, it indicates that the MGL response to IL-6 in co-culture with NPCs is comparable to that observed in monoculture. Secondly, it suggests that the 22q11.2DS genotype does not exert influence on MGL differentiation, at least not at the level of gene expression of signature markers. Thirdly, there is evidence of overlap with disease-relevant processes, with a higher degree observed in the 22q11.2DS context. Lastly, intriguing differences in response to IL-6 based on genotype are observed, albeit in a highly preliminary manner, which include interactions with vasculature and MHC pathways.

5.3.2 The transcriptional response to IL-6 in NPCs differentiated from neurotypical control and 22q11.2DS hiPSC lines

In parallel to the analysis of the MGLs, bulk RNAseq was conducted in both control and 22q11.2DS donor-derived NPCs 24h after the co-cultures with MGLs were exposed to either vehicle or IL-6. This enables us to examine first, transcriptional changes induced in the NPCs as a consequence of the MGL exposure to IL-6 and second, whether the 22q11.2DS genotype exacerbates this response in a manner that may have relevance for neurodevelopmental disorders. As with the MGLs, the four DESeq2 comparison signatures were created to tease out similarities and differences between the NPC IL-6 responses across the two genotypes.

- **Signature E:** IL-6-treated vs. vehicle-treated neurotypical control NPCs (i.e., the effect of IL-6 stimulation on gene expression in the neurotypical control cells).
- **Signature F:** IL-6-treated vs vehicle-treated 22q11.2DS NPCs (i.e., the effect of IL-6 stimulation on gene expression in the 22q11.2DS cells).
- **Signature G:** Vehicle-treated 22q11.2DS vs vehicle-treated control NPCs (i.e., the effect of the 22q11.2DS genotype).

- **Signature H:** Interaction effect of IL-6 treatment in 22q11.2DS vs in control (i.e., how the transcriptional response to IL-6 stimulation differs in 22q11.2DS NPCs compared to neurotypical control NPCs).

When comparing differentially expressed genes in vehicle and IL-6 treated samples, it was clear that NPCs from both genotypes gave a negligible transcriptional response to the IL-6 stimulus of the MGLs (control signature E: 2 DEGs passing 5% FDR, 22q11.2DS signature F: 0 DEGs passing 5% FDR). By contrast, genotype differences were detectable in NPCs and even more so than MGLs, as evidenced by the comparison of NPCs from each genotype within the same treatment samples (vehicle signature G: 343 DEGs passing 5% FDR, IL-6 signature H: 261 DEGs passing 5% FDR) (Table 5.6). Principle component analysis (PCA) was also carried out to identify the top two sources of variation within the NPC dataset, by comparing all RPKM gene counts in all 12 samples and plotting PC1 against PC2 (Figure 5.4A) suggested that the greatest source of variation in the NPC dataset was due to the 287_SZM donor, which clustered away from the control lines (PC1 = 63.59% variance explained), then by the 509_CXF donor (PC2 = 10.19% variance explained) (Figure 5.4A). This demonstrates the 22q11.2DS genotype exerts a great proportion of variation within the NPC transcriptome relative to a control genotype. As shown in Table 2.2, the characteristics of the 22q11.2 region for each of the donors varied hugely by the number of deleted genes, furthermore the total number of copy number variations in each donor differed (287_SZM_01 CNVs = 1; 509_CXF_05 CNVs = 3) indicating substantial genetic variation between these individuals. Moreover, the donor's differential clinical status is displayed to emphasize the variability observed in these lines. It is therefore unsurprising to see that their transcriptomes lead them to cluster away from each other within the PCA analysis (Figure 5.4A), and reinforces the point made in Reid *et al.* (2022), that it is essential to know the genetics of the hiPSC donors prior

to their use in study. Vehicle and IL-6 treated samples of each donor clustered very closely with each other in the PCA, consistent with our observation of minimal transcriptional differences between control NPCs treated with vehicle or 100ng/ml IL-6 for 24h in co-culture, irrespective of genotype. Interestingly, the control male lines (127_CTM, M3_CTR and 014_CTM) showed slightly more separation between vehicle and treated samples. However, these data are not sufficiently powered to study sex differences, but this will be important to examine in the future. The results from each of these four signatures are described in detail in the subsections that follow.

Table 5.6 – Summary of transcriptional analyses signatures from NPCs, and the subsequent differentially expressed genes (DEGs) that were either increased or decreased and passed 5% FDR correction.

Signature	Description	Increased DEGs	Decreased DEGs	Total DEGs
E	The effect of IL-6 stimulation on gene expression in control NPCs	2	0	2
F	The effect of IL-6 stimulation on gene expression in 22q11.2DS NPCs	0	0	0
G	The effect of genotype on gene expression between 22q11.2DS and control NPCs treated with vehicle only	251	92	343
H	The effect of genotype on gene expression between 22q11.2DS and control NPCs treated with IL-6	165	96	261

Unlike the protocol to derive MGLs from hiPSCs which is considered to make only microglia-like cells and their subtypes, dual SMAD inhibition can derive cell-types other than neurons (Adhya *et al.*, 2021). Taking into account the increased number of DEGs from NPC signature G and H analysis compared to the number found in MGL signature C and D, the effect of genotype on cell type heterogeneity in the NPC RNAseq dataset was considered. For example, neural stem cells with the ASC-related *NRXN1-alpha* deletion have been shown to shift

towards a more radial glia-like cell identity and have subsequent higher proportion of astroglia after terminal differentiation (Lam *et al.*, 2019). Therefore, to test the hypothesis that the 22q11.2 deletion could develop a similar effect on the heterogeneity of the cultures and to validate the successful differentiation of NPCs, the DESeq2 normalised counts from vehicle-treated NPC samples for markers of neural progenitor, pan-neuronal, dorsal forebrain, ventral forebrain, midbrain, hindbrain, upper layer and deep layer cells were plotted for comparison. The strongest expression was noted in genes related to neural progenitor cells, as to be expected from this timepoint of this protocol's differentiation. There was no hierarchical clustering based on genotype, indicating that genotype did not affect the cell population make up at this stage of culture (Figure 5.4B).

The absence of a transcriptional response to MGL stimulation with IL-6 in NPCs irrespective of genotype

NPCs differentiated from neurotypical controls showed increased expression of only 2 genes and expression of no genes was decreased (out of 17225 genes measured) when comparing MGL-NPC co-cultures stimulated with either IL-6 (100 ng/ml) or vehicle for 24 hrs (Table 5.6). The two genes to increase were TNF-Alpha-Induced Protein 3 (*TNFAIP3*: q = 0.0282, Log2FC = 1.545) and Poly(A) Binding Protein Cytoplasmic 1 (*PABPC1*: q = 0.0282, Log2FC = 0.1874). *TNFAIP3* is involved in cytokine-mediated immune responses and interestingly; expression of this gene has been previously reported to be up-regulated in human foetal neural stem cells infected with ZIKA virus (McGrath *et al.*, 2017). In contrast, *PABPC1* is involved in ribosomal recruitment and protein synthesis promotion (Kawahara *et al.*, 2008). It is possible that the sample size of this study was insufficient to detect additional differentially expressed genes. Of note however, JAK/STAT pathway genes did not exhibit differential expression following 24 hours of IL-6 stimulation in co-culture with MGLs (*STAT3* Log2FC = 0.0997, p

= 0.543, q = 0.9998; *JAK3* Log2FC = 0.584, p = 0.0396, q = 0.9998). These findings suggest that IL-6-receptor signal transduction pathways may not be activated, in contrast to what is observed in the MGL transcriptome at the same experimental time-point. Furthermore, these data encompass the cumulative events occurring over 24 hours of IL-6 exposure, which could involve both direct effects of IL-6 (via trans signalling) and indirect effects resulting from the production of other cytokines and chemokines by the MGLs or NPCs during the exposure period. In the absence of specific IL-6 signalling pathway blocking studies, it is difficult however to separate and distinguish these effects. Nonetheless, the virtual absence of any significant DEGs (as compared to the genotype effect) in NPCs during this time frame would suggest that whatever cytokine signalling events have occurred, they were either insufficient to activate the appropriate signalling pathways in the NPCs (for example, the NPCs lacked the correct receptors to respond as demonstrated for classical IL-6 receptor signalling in Chapter 3), or the timeframe examined in the current study was not well-matched to any potential transcriptional effects. Overall, however, in contrast to MGLs, NPCs appear to exhibit minimal activity in response to IL-6 stimulation of the co-culture system. Overall, these data suggest that NPCs differentiated from neurotypical control donors have a negligible or limited response to 24-hour IL-6 exposure in co-culture with MGLs under the conditions tested.

Likewise, the 22q11.2 genotype NPCs in signature F had no DEGs in response to IL-6 (out of 16954 genes measured) compared with vehicle-treated samples (Table 5.2). No genes passed FDR correction (5% FDR), and only three genes (*MUC5B* q = 0.99998, p = 0.01; *PHKG1* q = 0.99998, p = 0.027; *SPDYE5* q = 0.99998, p = 0.049) were differentially expressed without FDR correction ($p < 0.05$) (Figure 5.4C). Like signature E, signature F also exhibited no alterations in *JAK3* (Log2FC = -0.1813, p = 0.8380, q = 0.99998) and *STAT3* (Log2FC = 0.1010, p = 0.6898, q = 0.99998) expression. These findings further reinforce the idea that the

cells are not directly responding to IL-6 or any potential indirect effects resulting from the MGL cell's secretions. Neither signatures E and F provided enough DEGs to run further GSEA or over representation analysis. As well as the control NPCs, these data also confirm an insignificant transcriptional response by the 22q11.2DS NPCs after 24h IL-6 100ng/ml co-culture exposure.

The impact of the 22q11.2DS genotype effect on the NPC transcriptome

As with the MGL analyses, vehicle-treated NPCs from 22q11.2DS and control donors were compared to investigate gene expression differences as a function of genotype. Interestingly, there was a much greater difference in the number of DEGs by basal NPCs (Signature G DEG total = 343; up-regulated = 251 and down-regulated = 92) in comparison to basal MGLs (Signature C DEG total = 28) (Table 5.2). 15 of the 251 differentially decreased genes are genes located in the 22q11.2 deletion region (Khan *et al.*, 2020) (Figure 5.4D), confirming the genotype difference between these 22q11.2DS and control experimental donor groups is similarly quantifiable in the hiPSC-derived NPCs as it is in the MGLs, but more noticeable in the NPC cell type. Furthermore, to understand the IL-6-specific differential transcriptome of 22q11.2DS NPCs from control NPCs, the final interaction transcriptomic Signature H was investigated. 261 DEGs were statistically significant (165 DEGs increased and 96 DEGs decreased after 5% FDR, 16 of those decreased were found in 22q11.2 deletion region), demonstrating the differences between 22q11.2DS and control genotypes were still recognisable in NPCs after IL-6 treatment (Figure 5.4E).

Over Representation Analysis of NPC Transcriptomes

Signatures E and F did not provide enough DEGs for downstream ORA testing. Irrespective of this, the pathways associated with genotype differences across control and 22q11.2DS NPCs

can still be compared in basal and IL-6 exposed conditions. Webgestalt ORA analysis found 42 pathways enriched in the up-regulated DEGs from signature G (vehicle control vs vehicle-22q11.2DS) and one pathway in the down-regulated DEGs, while signature H (IL-6-exposed control vs IL-6-exposed 22q11.2DS) ORA identified 50 pathways associated with the up-regulated gene set, but none with the down-regulated gene set (Figure 5.4G). Specifically, the "Extracellular Matrix" pathway (signature G - FE = 3.85, p = $9.64x10^{-10}$, q = $1.26x10^{-6}$; signature H - FE = 4.69, p = $6.24x10^{-10}$, q = $6.69x10^{-7}$), which includes genes like *APOE*, *SERPINE1*, and ADAM proteases (*ADAMTS9, ADAM11, ADAM19,* and *ADAMTS15*), was the most significant pathway enriched in up-regulated gene sets after FDR correction and common to both signatures (Figure 5.4G). The extracellular matrix (ECM) is known to play a role in human neurodevelopment, modulating NPC proliferation and differentiation, plus axonal and dendritic elongation, and cortical folding (Barros, Franco and Müller, 2011; Fietz *et al.*, 2012; Long *et al.*, 2016; Long and Huttner, 2019; Amin and Borrell, 2020). These data suggest a testable difference in how developing NPCs regulate the ECM as a function of the 22q11.2 deletion over the control genotype, irrespective of IL-6 signalling. Additionally common to both signatures was “Regulation of Vasculature Development” (signature G - FE = 3.48, p = $1.59x10^{-5}$, q = 0.0045; signature H - FE = 4.23, p = $1.29x10^{-5}$, q = 0.0034) and “Angiogenesis” (signature G - FE = 2.76, p = $4.09x10^{-5}$, q = 0.0067; signature H - FE = 3.29, p = $2.96x10^{-5}$, q = 0.0055). These data suggest another testable hypothesis that 22q11.2DS may cause abnormal development of the endothelium (Okuda and Hogan, 2020), a pathway also enriched in the 22q11.2DS NPC up-regulated gene set in comparison to control NPCs (“Endothelium Development”: signature G - FE = 4.89, p = $9.45x10^{-5}$, q = 0.0088; signature H - FE = 4.84, p = 0.0015, q = 0. 0449). A handful of studies have drawn attention to the impairment of the blood-brain barrier (BBB) in individuals with 22q11.2DS (Crockett *et al.*, 2021; Y. Li *et al.*, 2021; Li *et al.*, 2023). Through transcriptome analysis of a BBB model derived from hiPSCs

obtained from 22q11.2DS donors, these studies have identified abnormalities in the cell-to-cell junctions of the compromised BBB and thereby implicating abnormal BBB function as a phenotype of 22q11.2DS (Y. Li *et al.*, 2021; Li *et al.*, 2023).

The only down-regulated pathway enriched in the vehicle-treated 22q11.2DS NPC transcriptome with relation to control after FDR correction was “Replication Fork” (FE = -13.69, p = $3.13x10^{-5}$, q = 0.041), including genes *CDC45, UHRF1, PRPF19, XRCC2* and *PCNA* which form a network of linked molecules at and around the replication fork to regulate it (Boehm, Gildenberg and Washington, 2016; Yadav *et al.*, 2020). Reduction of this pathway by decreased expression of these genes may inhibit replication fork elongation and thus DNA integrity and replication in 22q11.2DS NPCs in comparison to control NPCs. Regarding the up-regulated pathways specific to the vehicle-treated 22q11.2DS NPCs, the "Presynapse" pathway (FE = 2.49, p-value = 2.41x10-4, q-value = 0.016) was exclusively associated with signature G. This finding supports the previously identified dysregulation of presynaptic gene products in hiPSC-derived cortical neurons from individuals with 22q11.2DS, as reported by Nehme *et al.* (2022). In their study, 22q11.2DS neurons exhibited a distinct enrichment of transcripts related to presynaptic functions in synaptic vesicle cycles (Nehme *et al.*, 2022). Neither of these pathway findings were replicated in the signature H IL-6 control vs 22q11.2DS dataset.

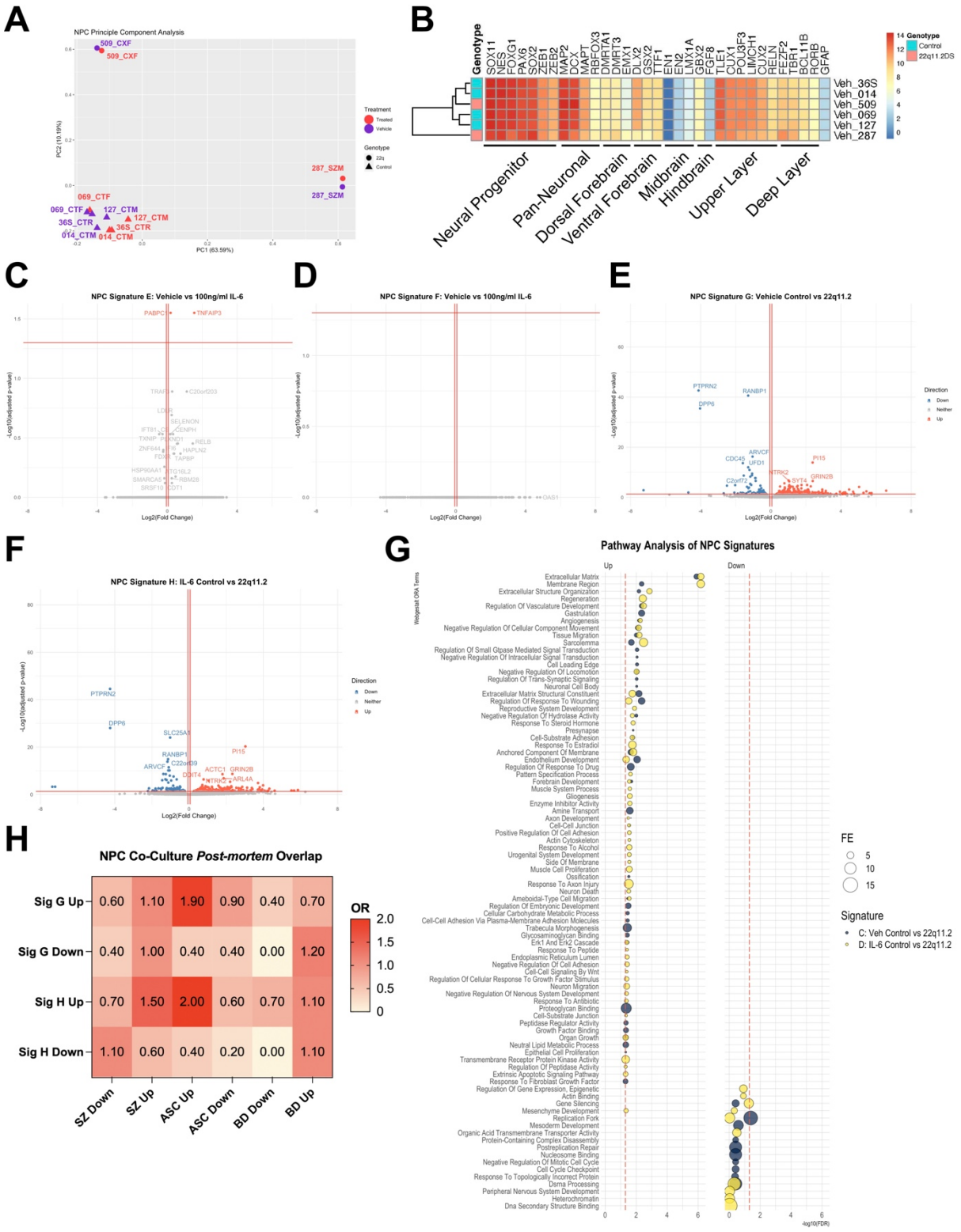

Figure 5.4 – The NPC Response to IL-6 in Co-Culture: (A) PCA analysis from all RPKM gene counts in the 12 samples, coloured by vehicle (purple) or IL-6 treated (pink) condition, shaped by genotype (triangle = control, circle = 22q11.2DS) and labelled by donor line. (B) DESeq2 normalised (median of ratios) counts taken from vehicle-treated NPC samples from both genotypes, of cell-specific markers plotted into a heatmap. (C-F) Volcano plots of differentially expressed genes from Signatures E (C), F (D), G (E) and H (F). Conditional axis set as follows: log2Foldchange > 0.06 and adjusted p-value <

0.05 coloured red; log2Foldchange < -0.06 and adjusted p-value < 0.05 coloured blue. The top 25 differentially expressed genes are labelled. (G) Webgestalt gene ontology analysis of differentially expressed genes in all four NPC Signatures and corrected with 5% FDR. ORA terms ordered by –log10FDR, coloured by adjusted p-value and sized by the fold enrichment. Plots are split by pathway sets generated from up-regulated genes (left) and down-regulated genes (right). Red dashed line set as 5% FDR threshold. (H) Fisher's exact test comparing gene sets from ASC, SZ and BD post-mortem human patient tissue (Gandal et al., 2018) with up- and down-regulated gene sets identified by RNAseq in all NPC signatures. Odds ratios (OR) plotted in heatmap with all comparisons not significant (5% FDR), so not labelled.

Gene Set Enrichment Analysis of NPC Transcriptomes

Lastly, GSEA was carried out by overlapping each signature's up- and down-regulated gene sets with those from *post-mortem* brain tissue from SZ, ASC, and BD patients (Gandal *et al.*, 2018) (four gene sets from the model vs. two gene sets from each disorder: 24 Fischer's test comparisons in total; Figure 5.4G). GSEA indicated neither up-regulated nor down-regulated gene sets signature G or H are enriched (5% FDR) with any gene set from NDD patient *post-mortem* datasets (Figure 5.4G) (Gandal *et al.*, 2018).

The Interaction of 22q11.2 deletion with IL-6 stimulation in NPCs

To examine the interaction in NPCs between 22q11.2DS genotype and IL-6 stimulation of the NPC-MGL co-cultures, overlapping genes in the up- and down-regulated gene sets from signatures G and H were examined (Figure 5.5A-B). Consequently, as with the MGL analysis, it was possible to pinpoint the genes that display differential expression in samples that received both IL-6 therapy and vehicle (in both signatures G and H), linking the differential expression cause to the donor genotype. Genes from the 22q11.2 deletion region accounted for 15 of the 46 down-regulated genes found in both signatures G and H (Khan *et al.*, 2020) (Figure 5.5A). The same analysis was carried out with up-regulated genes from signatures G and H (Figure 5.5B). Of the 311 genes that were up-regulated in both the 22q11.2DS vehicle and IL-

6 treated samples in comparison to the control donors, 105 were shared, leaving 206 genes that are differentially increased based on genotype and IL-6 treatment status.

To understand which pathways are associated with the groups of overlaps, a final Webgestalt ORA analysis was carried out on: (1) genes that overlapped in both up- and down-regulated G and H gene sets, and therefore enriched in the 22q11.2DS genotype irrespective of IL-6 exposure (Figure 5.5C); (2) genes that were either up- or down-regulated in signature G only, indicating their enrichment in the vehicle-treated 22q11.2DS genotype (Figure 5.5D); and (3) genes that were up- or down-regulated in signature H only, indicating their enrichment in the IL-6 treated 22q11.2DS genotype and therefore those that are termed as the "interaction" genes between the environment IL-6 stimulus and the 22q11.2DS genotype (Figure 5.5E). Firstly, ORA found 12 pathways associated with the overlapping up-regulated genes, and none with the down-regulated overlapping genes (Figure 5.5C). The enriched pathways supported the independent ORA analysis from signatures G and H, with "extracellular matrix" (FE = 5.87, p = $1.27x10^{-9}$, q = $1.65x10^{-6}$), plus vasculature pathways "angiogenesis" (FE = 4.65, p = $1.73x10^{-6}$, q = 0.0008) and "regulation of vasculature development" (FE = 5.87, p = $3.67x10^{-6}$, q = 0.0012) being significantly enriched with the 22q11.2DS genotype independent of IL-6 treatment (Figure 5.5C). Furthermore, pathways associated with cell growth and development were also enriched in the 22q11.2DS ("Tissue migration": FE = 5.14, p = $6.42x10^{-5}$, q = 0.012. "Cell-cell signalling by WNT": FE = 3.87, p = $1.25x10^{-4}$, q = 0.016. "Regulation of embryonic development": FE = 7.75, p = $1.25x10^{-4}$, q = 0.016), indicative that the 22q11.2DS genotype has the potential to alter neurodevelopmental pathways of NPCs *per se*. This is consistent with data from previous hiPSC-derived *in vitro* models studying the impact of 22q11.2DS genotype on neuronal cells in either 3D or 2D (Li *et al.*, 2019; Khan *et al.*, 2020; Reid *et al.*, 2022).

Secondly, in regards to the genes that were exclusive to the vehicle-treated NPCs and did not overlap between the vehicle- and IL-6-treated NPCs, no statistically significant pathways were associated with either up- or down-regulated genes compared to control donors (Figure 5.5D). Yet, the 22q11.2DS and IL-6 overlap genes that were up-regulated in 22q11.2DS IL-6 treated NPCs, but not found in vehicle-treated 22q11.2DS NPCs were enriched for two pathways: "regeneration" (FE = 9.04, $p = 5.01x10^{-5}$, q = 0.033) and "reproductive system development" (FE = 5.84, $p = 1.97x10^{-5}$, q = 0.026) (Figure 5.5E). It is possible that the reproductive system development pathway became significant in the IL-6 22q11.2DS-specific transcriptome due to a sex imbalance during the analyses, with 50% of the 22q11.2DS genotype replicates being female (22q11.2DS female N = 1, male N = 1) compared to only 25% of the control genotype replicates (control male N = 3, female N = 1), bringing through inherent sex differences that permits this pathway to be disregarded. However, the QuickGO EMBL search engine reports that the "regeneration" ontology definition refers to the regrowth of tissue and contains the related child terms: "neuron projection regeneration" and "axon extension involved in regeneration" (Binns *et al.*, 2009). These data indicate that axon projection and extension during neuron regeneration is a possible interaction mechanism associated with the 22q11.2DS NPC response to IL-6 and/or other cytokines produced as a consequence of MGL IL-6 response.

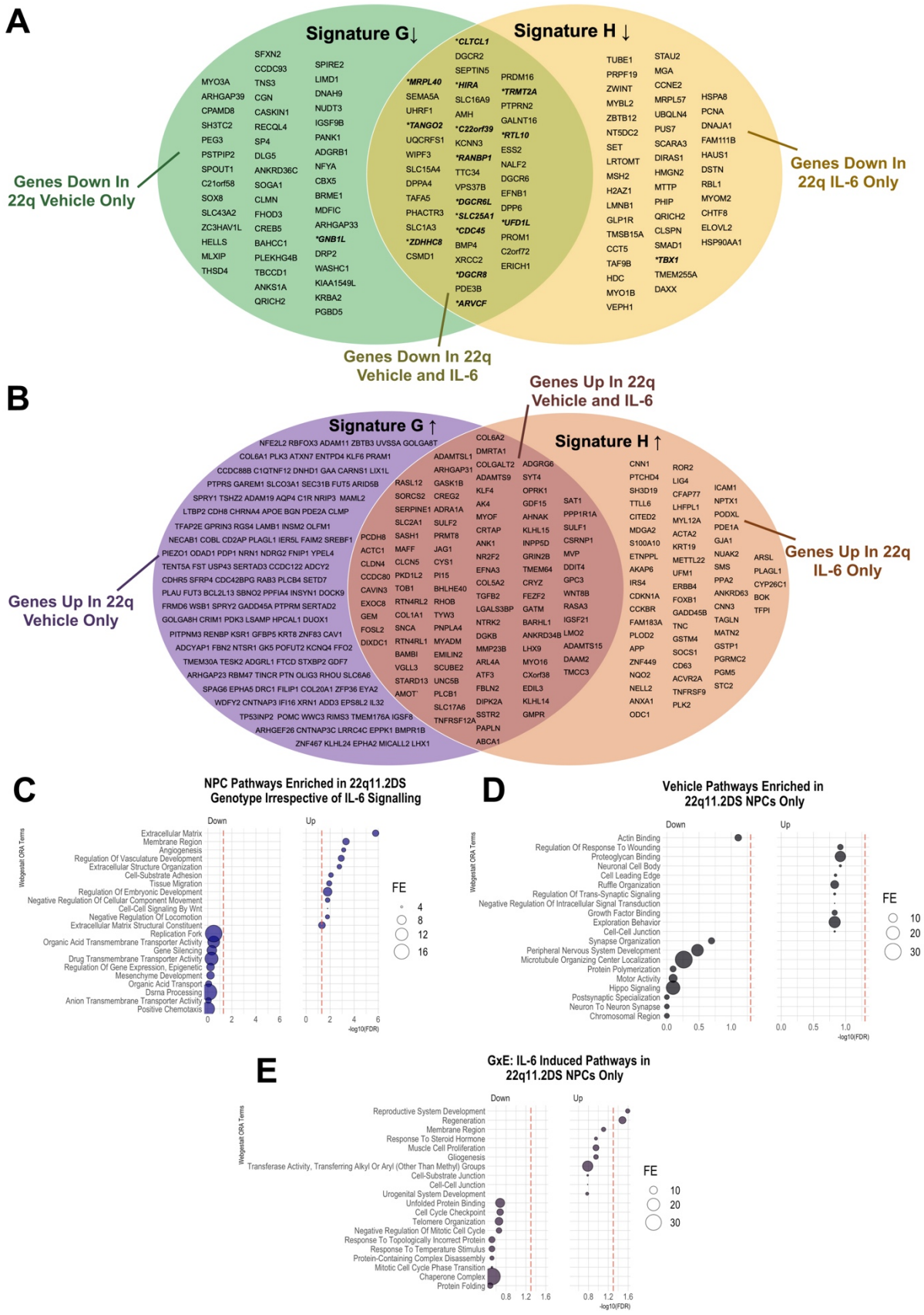

Figure 5.5 - The Gene by Environment Interaction of 22q11.2 deletion with IL-6 stimulation in NPCs (A) Venn diagram that shows the overlap between the genes that are differentially decreased in expression in response to IL-6 in control cells and in

*22q11.2DS NPCs. Of the 142 genes that were down-regulated in both 22q11.2DS vehicle and IL-6 treated samples in relation to the control donors, 46 genes are in common, meaning that there are 96 genes that appear differentially decreased because of genotype and treatment status. Genes in bold and marked with an * are genes found in the 22q11.2 deletion region. (B) Venn diagram that shows the overlap between the genes that are differentially increased in expression in response to IL-6 in control cells and in 22q11.2DS NPCs. Of the 311 genes that were up-regulated in the 22q11.2DS vehicle and IL-6 treated samples in relation to the control donors, 105 were in common, meaning that there are 206 genes that appear differentially increased because of genotype and treatment status. Genes in bold and marked with an * are genes found in the 22q11.2 deletion region. (C) Webgestalt gene ontology analysis of differentially expressed genes in both signature G and H up- and down-regulated gene sets, thereby defining the pathways common to the 22q11.2DS genotype in NPCs irrespective of IL-6 treatment. Signatures and corrected with 5% FDR. ORA terms ordered by –log10FDR, coloured by adjusted p-value and sized by the fold enrichment. Plots are split by pathway sets generated from up-regulated genes (left) and down-regulated genes (right). Red dashed line set as 5% FDR threshold. (D) Webgestalt gene ontology analysis of differentially expressed genes in signature G up- and down-regulated gene sets only, thereby defining the pathways specific to 22q11.2DS genotype in NPCs in a vehicle-treated state only. Signatures and corrected with 5% FDR. ORA terms ordered by –log10FDR, coloured by adjusted p-value and sized by the fold enrichment. Plots are split by pathway sets generated from up-regulated genes (left) and down-regulated genes (right). Red dashed line set as 5% FDR threshold. (E) Webgestalt gene ontology analysis of differentially expressed genes in signature H up- and down-regulated gene sets only, thereby defining the GxE interaction pathways specific to 22q11.2DS genotype in NPCs in an IL-6-treated state only. Signatures and corrected with 5% FDR. ORA terms ordered by –log10FDR, coloured by adjusted p-value and sized by the fold enrichment. Plots are split by pathway sets generated from up-regulated genes (left) and down-regulated genes (right). Red dashed line set as 5% FDR threshold.*

5.3.3 sIL-6Ra secretion into the co-culture is unaffected by IL-6 exposure

The fact that transcriptional effects in NPCs were mainly driven by genotype, with apparent negligible contributions within the co-culture system of IL-6 stimulation of the MGLs, suggests the hypothesis that IL-6 may activate trans-Il-6 signalling in the NPCs via soluble IL6 receptor (sIL-6Ra) secreted by the MGLs may not be correct. For example, it may that the levels of sIL-6Ra secretion by the MGLs within the co-culture were insufficient to trigger trans-signalling in the NPCs. We therefore proceeded to confirm the extent to which MGLs secrete the sIL-6Ra within this co-culture system, to establish whether it was at a concentration that was sufficient for NPCs to mount an IL-6 trans-signalling response. To quantify the concentration

of sIL-6Ra in MGL-NPC co-culture, an ELISA was performed on co-culture media. The sIL-6Ra concentration did not vary after 24h IL-6 exposure in either genotype (unpaired two-tailed t-test: neurotypical control $t(6) = 0.180$, $R^2 = 0.005$, $p = 0.863$; 22q11.2DS $t(2) = 0.154$, $R^2 = 0.012$, $p = 0.892$). The mean sIL-6Ra concentration in all 12 samples was 0.322 ng/ml ± 0.323, and had a range of 0.0238 to 0.847 ng/ml. This concentration of sIL-6Ra, although detectable in the co-culture media, is below the concentration range required for NPCs to mount a response to exogenously added recombinant sIL-6Ra protein ([sIL-6Ra] < 1 ng/ml in culture media), as presented in section 3.3.4. If this minimal receptor concentration was maintained through the entire 24h stimulation period, these data would support a view that insufficient sIL-6Ra is present for the NPCs to initiate trans-signalling within this co-culture system. Alternatively, these data may highlight its internalisation and breakdown by the NPC and MGLs after 24h of culture.

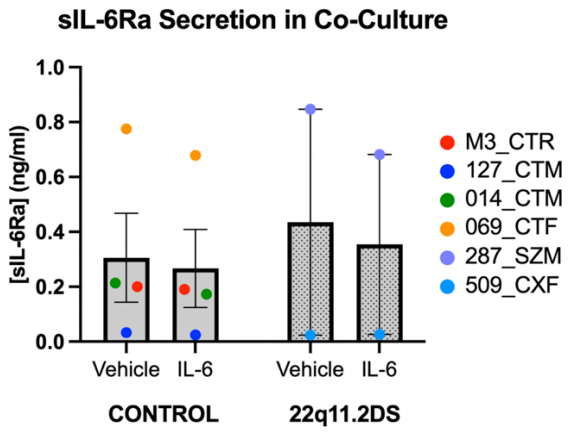

Figure 5.6 – sIL-6Ra secretion in co-culture. Co-culture media sIL-6Ra concentration (ng/ml) varied according to donor, with no notable effect of IL-6 treatment or 22q11.2DS genotype on the sIL-6Ra secretion into media. Different donors are represented with different coloured points, and data is presented as mean ± SD.

5.3.4 The cytokine milleu in co-cultures 24 hr post exposure to IL-6 or vehicle

Based on the hypothesis discussed in section 3.1, that individual cell types will have a differential response to cytokines, which will depend on (a) the cytokine milieu induced downstream of the initial stimulus and (b) to what extent individual cell types do or not express the corresponding cytokine/chemokine receptors. Put another way, it is plausible that NPCs might respond to the cytokines generated by MGLs in response to IL-6, irrespectively of NPCs receiving the IL-6 signal directly. To explore this question, a qualitative cytokine profiler was used to characterise the overall cytokine and chemokine milleu in the co-culture media after 24 hr exposure to either IL-6 or vehicle, for both genotypes. This consisted of a panel of 105 cytokines and chemokines (Appendix Table 1). The molecules with the greatest abundance in co-culture media for both 22q11.2DS and control genotypes were osteopontin, IL-8 and MMP-9 (Figure 5.7A). Initially, cytokine compositions were compared in the vehicle samples (Figure 5.7A), which identified 96 molecules as qualitatively higher in NPC-MGL co-cultures from 22q11.2DS donors as compared to control donors, while 8 were found to be lower. These sets exclude the exogenously spiked IL-6. Under vehicle-treated conditions, notably reduced signal of ENA-78 was observed in 22q11.2DS cultures compared to control donor cultures, a leukocyte attractant that is significantly decreased in plasma of MDD patients (Li *et al.*, 2017). On the other hand, the top ten molecules with a greater signal in the vehicle-treated 22q11.2DS genotype over the control genotype included Pentraxin-3, VEGF, MMP-9, VCAM-1, IGFBP-2, Chitinase3-like-1, IL-1β, IGFBP-3 and GDF-15 (Figure 5.7A).

Differential patterns were detected when evaluating the impact of acute IL-6 exposure within genotypes. We first calculated the fold change of cytokines in the IL-6 exposed culture medium from each genotype's vehicle treated control cultures. This revealed that in co-culture media from neurotypical control donors, 78 molecules were up-regulated and 26 down-regulated as a

consequence of IL-6 exposure. In contrast, 18 molecules were up-regulated and 86 down-regulated in co-culture media of 22q11.2DS donors as a consequence of IL-6 exposure (Figure 5.7B). In the media from the neurotypical controls, the top five up-regulated molecules were MIP-1α/MIP-1β (control FC = 4.153), RANTES (control FC = 2.118), GROα (control FC = 2.105), TNFα (control FC = 1.689) and PF4 (control FC = 1.593) (Figure 5.7B). In comparison, in the 22q11.2DS donors, the top 5 were: MIP-1α/MIP-1β (22q11.2DS FC = 3.252), ENA-78 (22q11.2DS FC = 3.041), MIP-3α (22q11.2DS FC = 1.608), MCP-3 (22q11.2DS FC = 1.368), and GROα (22q11.2DS FC = 1.329) (Figure 5.7B). Despite therefore being increased in both genotypes, ENA-78 secretion was notably higher in 22q11.2DS co-cultures (22q11.2DS FC = 3.041) than control co-cultures (control FC = 1.246) as a consequence of IL-6 exposure (Figure 5.7B). Interestingly, RANTES, TNFα, PF4, VCAM-1 and Resistin were all up-regulated in the neurotypical control co-culture media in response to IL-6, but down-regulated in the 22q11.2DS medium in response to IL-6 (Figure 5.7B). On the other hand, IL-34 and Osteopontin were both up-regulated in the 22q11.2DS co-culture response to IL-6 but down-regulated in control co-cultures (Figure 5.7B). Given that IL-34 is present in the co-culture media, it's differential expression could be confounded and therefore this result will be disregarded.

To verify data from the proteome profiler assay, four cytokine candidates were subsequently measured using a more sensitive and quantifiable multiplex cytokine ELISA assay (Figure 5.7C). MIP-1α was chosen since it was strongly up-regulated by both genotypes in response to IL-6, while TNFα and VEGF were chosen due to their differential secretion in response to IL-6 as a function of genotype, and finally IL-8 was chosen as a negative control given its strong and unchanging secretion in both genotypes in vehicle-treated media (Figure 5.7C). As expected, levels of IL-8 were unchanged with IL-6 treatment in both genotypes (unpaired two-

tailed t-test: control t(6) = 1.603, R^2 = 0.30, p = 0.160; 22q11.2DS t(2) = 0.1706, R^2 = 0.014, p = 0.880) (Figure 5.7C). There was a notable increase in MIP-1α after IL-6 treatment compared to vehicle in both genotypes, although this did not reach statistical significance (unpaired two-tailed t-test: control FC = 2.48, t(6) = 2.220, R^2 = 0.451, p = 0.0682; 22q11.2DS FC = 19.61, t(2) = 1.744, R^2 = 0.603, p = 0.223) (Figure 5.7C). Similarly, levels of TNFα were increased with IL-6 exposure in the control genotype media (unpaired two-tailed t-test: control FC = 13.75, t(6) = 2.628, R^2 = 0.535, p = 0.039), which also increased in 22q11.2DS genotype media but failed to reach statistical significance (unpaired two-tailed t-test: control FC = 6.55; t(2) = 0.996, R^2 = 0.332, p = 0.424) (Figure 5.7C). Finally, levels of VEGF-A were unchanged with IL-6 exposure in both genotypes (unpaired two-tailed t-test: control FC = 1.155, t(6) = 0.202, R^2 = 0.007, p = 0.0.847; 22q11.2DS FC = 0.689, t(2) = 1.085, R^2 = 0.370, p = 0.392) (Figure 5.7C). Importantly, VEGF was the only cytokine of the four candidates that was notably higher in 22q11.2DS co-culture media in comparison to control media (FC = 3.63) (Figure 5.7C). Overall, the expression patterns of all four cytokines reflected those qualitatively determined from the proteome profiler.

Finally, the same candidates were assessed in 24h IL-6 treated D14 MGL and D18 NPC monocultures from N = 3 control male cultures to determine which cell type may be responsible for the co-culture cytokine secretion (Figure 5.7D, two-way ANOVA statistics in Table 5.7). The data suggest that MGLs were responsible for the majority of IL-8, MIP-1α and TNFα secretion, while VEGF was mainly secreted from NPCs (Figure 5.7D, statistics in Table 5.7). TNFα was the only cytokine to show a statistically significant increase after IL-6 treatment in MGLs (MGL Veh vs IL-6 5% q = 0.0154), and not in NPCs, confirming the fact that NPCs do not respond to IL-6 in monoculture in the absence of exogenous sIL-6Ra (Figure 5.7D). These data identify cell-specific secretome patterns that implicate NPCs, as well as MGLs, in the

influence of vasculature remodelling and endothelial dysregulation given their significant secretion of VEGF over MGLs.

Table 5.7 - Two-way ANOVA of MSD quantified IL-8, MIP-1α, TNF α and VEGF secretion from D14 MGLs and D18 NPCs from N=3 donors in monoculture treated for 24h with 100ng/ml IL-6.

Cytokine	Source of Variation	DF	F (DFn, DFd)	P Value	P Value Summary
IL-8	Interaction	1	F (1, 8) = 1.119	0.3211	ns
	Treatment Factor	1	F (1, 8) = 1.140	0.3169	ns
	Cell Factor	1	F (1, 8) = 4845	<0.0001	****
MIP-1α	Interaction	1	F (1, 8) = 0.1479	0.7106	ns
	Treatment Factor	1	F (1, 8) = 0.1479	0.7106	ns
	Cell Factor	1	F (1, 8) = 11.55	0.0094	**
VEGF	Interaction	1	F (1, 8) = 0.1200	0.7379	ns
	Treatment Factor	1	F (1, 8) = 0.1258	0.7320	ns
	Cell Factor	1	F (1, 8) = 33.52	0.0004	***
TNFα	Interaction	1	F (1, 8) = 6.255	0.0369	*
	Treatment Factor	1	F (1, 8) = 6.212	0.0374	*
	Cell Factor	1	F (1, 8) = 49.03	0.0001	***

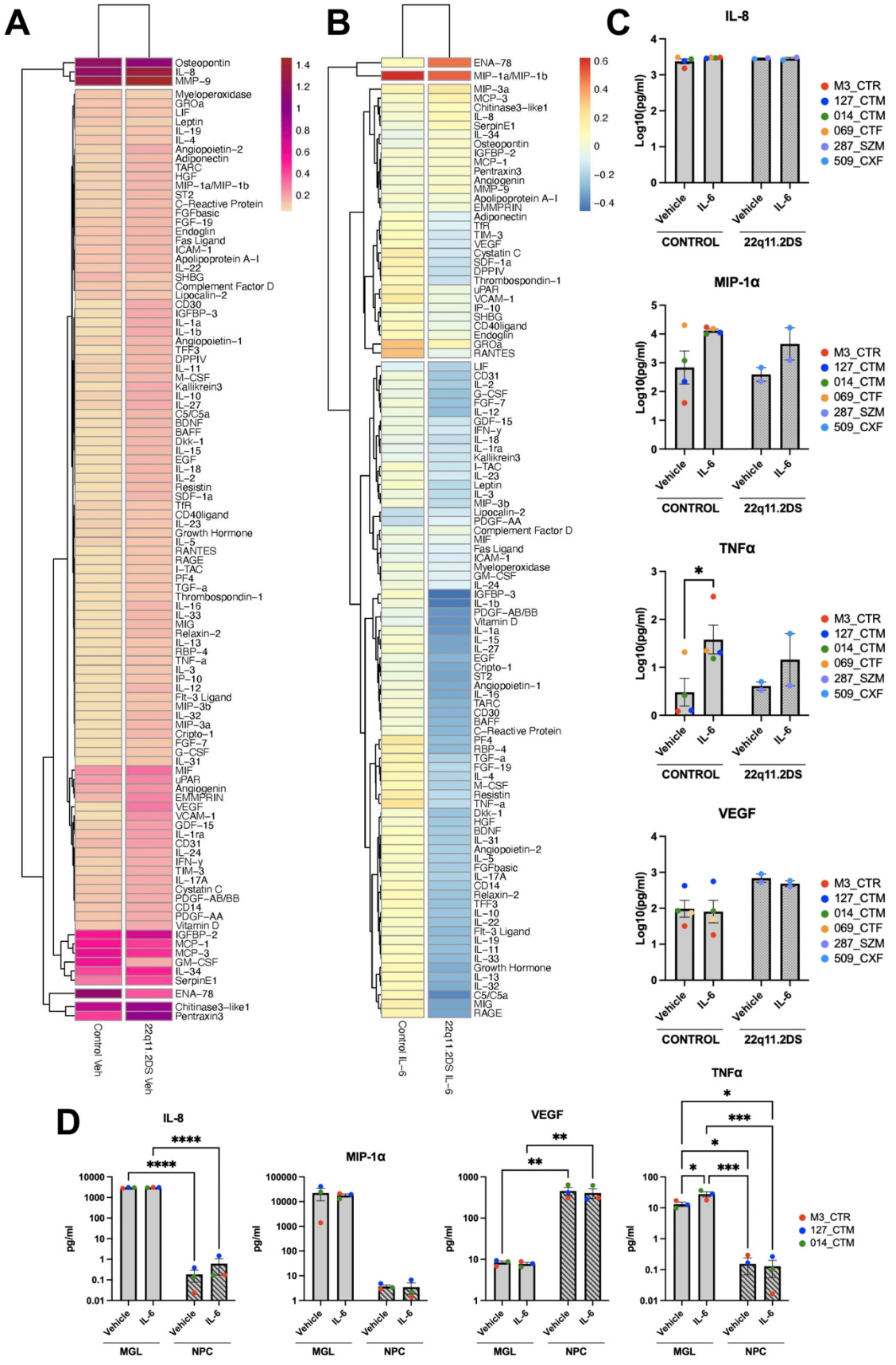

Figure 5.7 – Differential Cytokine Response to IL-6 by control and 22q11.2DS co-culture. (A) Clustered heatmap of raw signal values, averaged from 2 technical replicate dots, from a Proteome Profiler Human XL Cytokine Array Kit (R&D Systems)

*measuring 104 cytokines in vehicle-treated media samples from control (N = 4 pooled) and 22q11.2DS (N = 2 pooled) genotype co-cultures. IL-6 was excluded since it was spiked during treatment. (B) Clustered heatmap of Log10FoldChange values comparing IL-6 treated co-culture culture media to vehicle-treated media within control (N = 4 pooled) and 22q11.2DS genotypes (N = 2 pooled), using a Proteome Profiler Human XL Cytokine Array Kit (R&D Systems). IL-6 was excluded since it was spiked during treatment. Red indicates up-regulation, blue indicates down-regulation and white represents an unchanged signal of each molecule after IL-6 treatment in comparison to vehicle. (C) Multiplex Cytokine Assay data measuring the concentration (plotted as Log10(pg/ml)) of MIP-1a, TNFa, IL-8, and VEGF-A in 24h vehicle and 100ng/ml IL-6 treated co-culture media, from both control (N = 4, solid grey bars) and 22q11.2DS (N = 2, dotted grey bars) genotypes. P-values from unpaired two-tailed t-test comparing vehicle to treated concentrations within genotype are formatted as follows: *p < 0.05, ** p < 0.01, *** p < 0.001, and **** p < 0.0001; non-significant not labelled. Bar graphs plotted as mean with standard deviation (SD) error bars, and points coloured by donor line as shown in key. (D) Multiplex Cytokine Assay data measuring the concentration (plotted as pg/ml on a log scale) of MIP-1a, TNFa, IL-8, and VEGF-A in control donor (N = 3 males) derived D14 MGLs and D18 NPCs in monoculture media treated for 24h vehicle or 100ng/ml IL-6. 5% false discovery rate (FDR) by Benjamini–Hochberg (BH) method corrections after two-way ANOVA formatted as follows: *q < 0.05, ** q < 0.01, *** q < 0.001, and **** q < 0.0001; non-significant not labelled. Bar graphs plotted as mean with standard deviation (SD) error bars, and points coloured by donor line as shown in key.*

5.4 Discussion

In this chapter hiPSC-derived MGLs and forebrain cortical NPCs from both 22q11.2DS and control donors were exposed to exogenous IL-6 or vehicle stimulation which resulted in four key findings. First, MGLs responded to a 24h 100ng/ml IL-6 stimulation in co-culture with comparative results to those characterised in the previous chapter, with only subtle differences between 22q11.2DS and control genotype responses. Second, the hypothesis that NPCs would harness MGL-secreted sIL-6Ra to respond to IL-6 by trans-signalling after a 24h stimulation may not be accepted, since virtually no transcriptional response was identified in either control or 22q11.2DS genotypes in response to exogenous IL-6, which requires further investigation. Third, in NPCs the 22q11.2 deletion genotype was associated with transcriptional changes that suggest the potential for abnormal extracellular matrix remodelling and potentially with

enhanced neurite outgrowth and projection growth propensity. Fourth, the cytokine milieu as quantified in the co-culture media was similar to that measured in animal models of MIA, indicating that this co-culture model is an alternative method of modelling the interaction between the immune response and the foetal neural environment, since it recapitulates some key changes observed *in vivo*. Since most cytokines and chemokines found in the co-culture media specifically target non-NPC cell types, however, suggests that additional cell types, such as endothelial cells, are required to model this interaction more closely. It is important to note that the significant variability observed among donors of the same genotype, along with the limited statistical power of this study's dataset, does however impose constraints on our interpretation of the data. Therefore, any conclusions drawn from these findings necessitate further investigation to ensure their validity. This is particularly true for the data concerning the 22q11.2DS donors, which must be considered highly preliminary.

5.4.1 No statistically significant changes in the NPC transcriptome in response to IL-6 after 24-hours in co-culture with MGLs

The bulk RNAseq data suggests that MGLs in co-culture responded similarly to IL-6 stimulation without an effect of 22q11.2DS genotype. For example, increases in both *JAK3* and *STAT3* transcripts were found following IL-6 stimulation of MGLs in both genotypes (Figure 5.2C and Figure 5.2D). Of note, in co-culture with NPCs, MGLs from both genotypes responded to 24 hours of IL-6 exposure in a manner comparable to MGL monocultures despite the differences in stimulation lengths (3h IL-6 stimulation; data in chapter 4), recapitulating pathways and gene sets relevant to SZ. The overlapping gene sets from *post-mortem* brain tissue associated with a schizophrenia diagnosis were not only found to exhibit a stronger overlap in the 22q11.2DS MGLs exposed to IL-6, as compared to neurotypical control donor cells, but there were also subtle genotype differences. These differences included the

enrichment of ORA terms related to MHC molecules, the vasculature and endothelium in the 22q11.2DS MGLs, regardless of IL-6 stimulation (Figure 5.8). Yet despite this and the fact both MGLs and NPCs were in shared medium, we observed essentially no transcriptional response in the NPCs at 24 hr following exposure to IL-6, irrespective of genotype.

The relative lack of transcriptional changes in response to IL-6 treatment in NPCs suggests that, in contrast to monocultured NPCs treated exogenously with sIL-6Ra shown in section 3.3.4, co-cultured NPCs may not exhibit a direct response to IL-6 stimulation through the cleavage of soluble IL-6 receptor, as hypothesised. Just two transcripts were altered in NPCs from control co-cultures, and none in NPCs from 22q11.2DS co-cultures after 5% FDR correction. Notably, at the level of this analysis, no alterations were found in the JAK/STAT transcripts in NPCs. Given the small and uneven sample size, the biological significance of these genotype variations remains uncertain. Although the neurotypical control group with N=4 is in line with the minimum power requirements as outlined in a recent consensus paper (Dutan Polit *et al.*, 2023), there is still an absence of IL-6 response at least transcriptionally, by NPCs within this genotype group. However, it is important to note that in studies with limited sample sizes, the lack of statistical significance after multiple corrections may not necessarily indicate the absence of a biological effect (Nehme *et al.*, 2022). This is particularly relevant when the false discovery rate (FDR) is conservative at 5%. Therefore, this study may be underpowered to detect any effects. This may be similar to the lack of any transcriptional response reported by Bhat *et al.* (2022) in NPCs stimulated with IL-1β as compared to IFN-γ (Bhat *et al.*, 2022).

Under the conditions tested, the low levels of soluble IL-6Ra (<1ng/mL) found in the co-culture system did not seem to trigger STAT3 phosphorylation as per section 3.3.4, at least at the level of gene expression. Interestingly however, the levels of sIL6R in co-culture are similar to those

reported in the cerebrospinal fluid of MS patients (Frieling *et al.*, 1994; Padberg *et al.*, 1999; Stelmasiak *et al.*, 2001), and logically, these levels are likely to change depending on the disease state (Padberg *et al.*, 1999). These data suggest we may have a biologically relevant amount of sIL-6Ra in our co-culture system. Other cell types like endothelial cells, peripheral leukocytes and astrocytes, which are present *in vivo* and might be able to respond to microglia-induced cellular cues not only by altering their own secretome but also by increasing extracellular concentrations of sIL-6Ra are absent in our co-culture system, thus amplification signals may be lacking (Rose-John, 2012; Müllberg *et al.*, 1992) (Figure 5.8). Additionally, as sIL-6Ra may already be bound to cells, the quantities of sIL6R in supernatant may not accurately represent the levels secreted in co-culture. Moreover, it is worth nothing the variance in sIL-6Ra concentration observed among donors within the same genotype. These variations potentially indicate differences in receptor levels associated with genotype (Tvedt *et al.*, 2018), which could confound the presented results. Finally, a cellular response to IL-6 that occurs outside of the temporal dynamics of this investigation cannot be ruled out because a more precise marker of IL-6 activation, such STAT3 phosphorylation, was not assessed in the co-culture NPCs. To further understand the cellular response in both MGLs and NPCs to IL-6 stimulation, more studies using the pan-IL-6Ra antibody tocilizumab, which both cis and trans IL-6 signalling (Sebba, 2008), and soluble gp130, which can disrupt only the trans-signalling route (Rose-John, 2012), are needed.

By contrast, transcriptional differences as a function of genotype (22q11.2DS vs. control donors) were much more pronounced in NPCs than in MGLs. Pathways including extracellular matrix remodelling were significantly enriched in the 22q11.2DS NPC transcriptome, supported increased secretion of key molecules involved in this process in the 22q11.2DS co-culture media. In particular, Chitinase3-like-1 and MMP-9 exhibited elevated levels in

22q11.2DS cells. These proteins play a role in remodelling the ECM and contribute to CNS development and plasticity, particularly during crucial early postnatal stages (Bednarek *et al.*, 2009; Aujla and Huntley, 2014). Furthermore, increased levels of these proteins have been associated with SZ-relevant phenotypes, such as modifications in hippocampal synaptic circuitry, the plasticity of retinotectal projections, and the dysregulation of synaptogenesis, axonal pathfinding, and myelination (Vaillant *et al.*, 1999; Oliveira-Silva *et al.*, 2007; Yang *et al.*, 2008; Bednarek *et al.*, 2009; Aujla and Huntley, 2014; Reinhard, Razak and Ethell, 2015).

Pentraxin-3, VEGF, and VCAM-1, proteins that exhibited a comparatively higher secretion in 22q11.2DS co-culture media compared to control donor media, play essential roles in vasculature remodelling, endothelial dysfunction, and leukocyte-vasculature migration (Mancuso, Kuhnert and Kuo, 2008; Kong *et al.*, 2018; Domínguez-Vivero *et al.*, 2020). These proteins have downstream effects on various processes, including neurogenesis, neuronal migration, neuronal survival, and axon guidance (Mackenzie and Ruhrberg, 2012). These findings are consistent with the ORA pathway analysis hinting at an enhanced propensity for neurite outgrowth and projection growth in this sample set (Giulio *et al.*, 2010) (Figure 5.8). Interestingly, increased neurite outgrowth has been previously observed in hiPSC-derived neurons from ASC patients, an effect mimicked by exposure of NPCs to IFN-γ (Schafer *et al.*, 2012; Deshpande *et al.*, 2017; Kathuria *et al.*, 2018; Warre-Cornish *et al.*, 2020). It may be that the NPCs did respond to IL-6, with a transcriptional effect that may have peaked earlier that the 24-hour time point measured in the current study, which had resolved by 24h. Although this remains to be confirmed in future work, it would suggest that it would be worth investigating whether IL-6 leads to increased neurite outgrowth in the control donors and if this is exacerbated in the NPCs from the 22q11.2DS donors similar to that seen with IFN-γ and recapitulating a relevant NDD phenotype (Figure 5.8).

Importantly, osteopontin was qualitatively found up-regulated by 22q11.2DS cultures after IL-6 stimulation but down-regulated by control donor cultures. This molecule is thought to play a role in autoimmune neuropathology by exacerbating the production of IL-17 from T-helper 17 lymphocytes. Its serum concentration is also significantly higher in children with ASC (AL-ayadhi and Mostafa, 2011), which correlates with symptom severity (AL-ayadhi and Mostafa, 2011), is up-regulated in poorly myelinating brains (Holloway *et al.*, 2023), and is expressed in a sex-dependent manner with an increased expression in males (Bjelobaba *et al.*, 2019). Further to this argument, osteopontin has also been shown to characterise a disease-associated functional cluster of microglia after single cell RNAseq analysis of hiPSC-derived microglia (Dräger *et al.*, 2022). These data suggest the secretion of osteopontin by either MGLs or NPCs in response to IL-6 is exacerbated by the 22q11.2DS genotype and is relevant to the pathogenesis of ASC, in a sex-dependent manner.

Finally, it is worth noting that participant 287_SZM_01 has been diagnosed with SZ, while participant 509_CXF_05 has been diagnosed with ASC (Table 2.2). Therefore, it is crucial to acknowledge the potential impact of the diagnosis, and to consider the variable penetrance of SZ. It is therefore necessary to conduct future studies to compare individuals with 22q11.2 deletion syndrome who have and have not received a diagnosis. Previous research utilizing hiPSC differentiated into neurons and lymphoblastoid cells has indicated significant differences based on diagnosis, which could be attributed to additional genetic risk factors beyond the chromosomal copy number variation (CNV), known as "variable penetrance" (J. Li *et al.*, 2021).

5.4.2 The co-culture cytokine and chemokine secretome targets non-NPC cell types, except for TNFα

Irrespective of JAK/STAT signalling in NPCs induced by IL-6, it was also possible that NPCs could have responded to other cytokines and chemokines secreted by the MGLs in response to IL-6, or the NPCs themselves in an autocrine or paracrine manner. As already stated, any such a response will be governed by (a) the cytokine and chemokine milleu resulting from the upstream initial immune stimulus and (b) whether the cell types present express the corresponding receptors. In our co-cultures we observed a quantitative increase of MIP-1α and TNFα following IL-6 treatment. The patterns of these effects were quite consistent between genotypes in direction and magnitude, although they did not always reach statistical significance in the 22q11.2DS donor culture due to the low N. We also observed with qualitative increases in many other cytokines, some of which have already been discussed and require confirmation by ELISA. Importantly, at least in the neurotypical control donor lines, MGLs, but not NPCs, were shown to be the primary cellular source of both MIP-1α and TNFα at least in monoculture. Furthermore, as per the Brain RNAseq database (Zhang *et al.*, 2016), chemokine receptors, including those responsible for MIP-1α signalling, are not significantly expressed in NPCs. It is therefore unlikely that elevated levels of MIP-1α would influence NPCs. Although our present results cannot completely exclude this possibility, it is perhaps more likely that the role of MIP-1α would be to recruit additional immune cells to the site of inflammation via signalling to endothelial cells, which needs to be tested in future work. By contrast, NPCs do express receptors for TNFα, as shown in chapter 3 and by others (Sheng *et al.*, 2005). Of note then, *TNFAIP3*, which is associated with the cellular response to TNFα (Antonia *et al.*, 2022), was one of only two DEGs observed in the control NPCs' signature E after correction for multiple comparisons. This suggests that production of TNFα by MGLs in

response to IL-6 may lead to downstream effects on the NPCs consistent with some *in vivo* findings from a rodent model of MIA (Potter *et al.*, 2023)(Figure 5.8).

Although the NPCs possess the machinery to respond to TNFα we still observed a relatively limited transcriptional response, which might be attributed to a variety of other factors. First, there is naturally variation in how individual donor lines may respond as a function of their genetic background, biological sex, as well as the variable size of the 22q11.2 deleted region (see PCA plot in Figure 5.4A). Hence, within our small sample size (N=4 neurotypical control donors, N=2 22q11.2DS donors) subtle biological effects may be masked. Second, RNA for sequencing was collected at 24h after IL-6 stimulation of the MGLs, which could either be too late to detect a specific response to TNFα by the NPCs, or too early such that TNFα has not amounted to a sufficient concentration in co-culture media to initiate any such response by the NPCs. To validate the impact of TNFα on these NPCs, it is recommended to incorporate multiple sample collection time-points, including those dedicated to proteomic analysis, in the presented experiment. This approach will help ensure that any potential transcriptomic and proteomic responses are not overlooked due to temporal limitations. Additionally, conducting monoculture stimulation experiments with TNFα, like those performed with IL-6 in chapters 3 and 4, can be employed to assess the NPCs' ability to respond to TNFα.

Third, cell types other than microglia and neural progenitor cells are missing, to which most chemokines and cytokines found in the co-culture media specifically target. The responses of these cell types, such as endothelial cells are therefore not captured in the model presented here, which if they were present, would have the potential to influence NPCs, in a subsequent chain reaction of responses initiated by the MGL response to IL-6. Nevertheless, in control and 22q11.2DS co-culture medium, comparable patterns of cytokine expression were identified,

characterised by overexpression of cytokines and chemokines such MIP-1α/MIP-1β, GRO-α, RANTES, and MIP-3α with IL-6 treatment. It is reassuring to note that these cytokines replicate findings from studies measuring the maternal immune response in animal models of MIA (Arrode-Brusés and Brusés, 2012) as well as microglial and cytokine response in offspring's foetal brain (Jarskog *et al.*, 2005; Garay *et al.*, 2013; Fernández de Cossío *et al.*, 2021).

Taken together, these findings emphasise future work to investigate the cocktail of cytokines and chemokines secreted by microglia in response to an MIA-derived IL-6 response during vulnerable key prenatal timepoints, that have the potential to affect multiple cell types and not just NPCs (Figure 5.8). These findings also highlight the potential role of microglia as a crucial "first" responder to elevations in IL-6 within the brain. Microglia likely initiate a coordinated set of changes in other cell types, resulting in cumulative effects on NPCs and other cells through feedback mechanisms. The data presented in this chapter highlight a strength of our simple 2D co-culture model to identify which cell types can or cannot respond to specific stimuli. The data however also highlight a limitation in that it would be desirable to build a more complex model that incorporates more cell types to better approach the complexity of the *in vivo* environment when investigating the effects of IL-6 in the context of NDDs (Figure 5.8). This becomes especially important when comparing it to other cytokine factors, such as IFN-γ, to which NPCs exhibit a robust response without the requirement for additional cell types to be present (Warre-Cornish *et al.*, 2020; Bhat *et al.*, 2022). One cell type in particular that our data suggest would be key to investigate are endothelial cells.

5.4.3 Endothelial cells should be included when modelling the interaction of IL-6 with 22q11.2DS and their combined risk for neurodevelopmental disorder.

Angiogenesis-related pathways were enriched in the 22q11.2DS transcriptional signatures for both MGLs and NPCs, specifically in signature B (the 22q11.2DS MGL response to IL-6). Consistent with this, VEGF-A levels in the co-culture medium were numerically higher in 22q11.2DS donor cultures, regardless of IL-6 treatment, suggesting a genetic difference that may result in constitutive overexpression (Roscoe *et al.*, 2009; Brauer *et al.*, 2011). IL-6 increases vasculature leakage by initiating VEGF production which facilitates the cadherin disassembly of vasculature endothelial cells (Kang and Kishimoto, 2021). Moreover, as mentioned earlier in the section discussing the ORA of NPC transcriptomes, research has detected transcriptomic irregularities in the cell-to-cell junctions of impaired BBBs derived from hiPSCs of individuals with 22q11.2DS, thereby pointing inferences towards the abnormal BBB function as a characteristic phenotype of 22q11.2DS (Crockett *et al.*, 2021; Y. Li *et al.*, 2021; Li *et al.*, 2023). This implies a unique BBB endothelial-targeted role for microglia in response to IL-6, which may be more potent in the context of 22q11.2DS, particularly given the increase in *VEGFA* gene expression after IL-6 exposure in the 22q11.2DS genotype co-cultures only (Figure 5.8).

Interestingly, despite the lack of endothelial cells in our model, the results of the monoculture experiment appear to show that NPCs are the principal producers of VEGF-A, indicating that an *in vivo* response to IL-6 may entail interaction between MGLs, NPCs, and endothelial cells. Given that endothelial cells are predicted to respond to IL-6 via trans-signalling (Zhang *et al.*, 2016; Kang and Kishimoto, 2021), it would be interesting to investigate the notion that the atypical vasculature signalling noted in 22q11.2 and psychosis patients could be as a result of an IL-6-directed dysregulation of the vasculogenesis and angiogenesis developmental function

that microglia poses during foetal neurodevelopment (Checchin *et al.*, 2006; Pont-Lezica *et al.*, 2011; Rymo *et al.*, 2011; Nguyen *et al.*, 2018; L. Zhang *et al.*, 2021). Therefore, to further understand the effect 22q11.2DS has on neurodevelopment, endothelial cells should be considered when modelling potential pathological mechanisms (Figure 5.8).

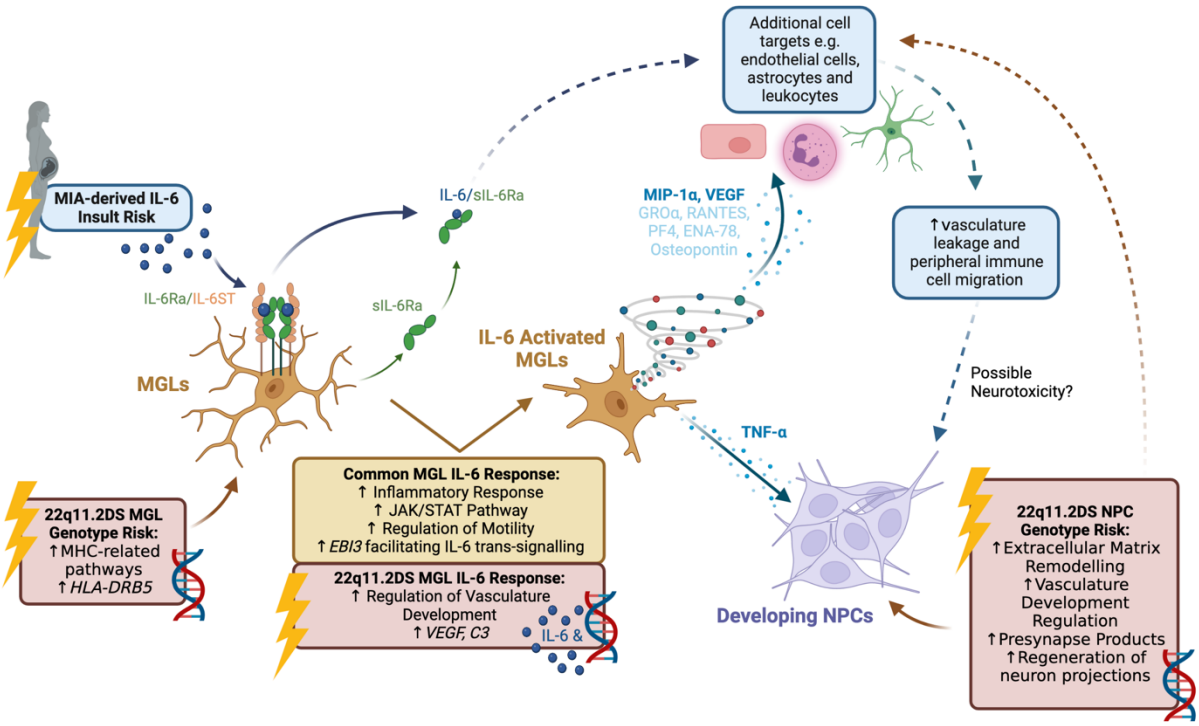

Figure 5.8 – The acute effects of the 22q11.2DS genotype and an MIA-derived IL-6 insult on microglia-like cells and developing neural progenitor cells, and how they interact to exacerbate the risk of atypical neurodevelopment at a vulnerable prenatal stage. This figure summarises the chapter's results. Sources of risk are signalled with a lightning-bolt; 22q11.2DS genetic risk labelled with a DNA helix and MIA-derived IL-6 risk with blue spheres. Dotted lines indicate results that have not been studied in this chapter but are hypothesised to take place and require further investigation.

5.5 Conclusion

In conclusion, this chapter aimed to investigate the interaction between genetic and IL-6 on developing cortical neural progenitor cells, using 22q11.2DS as our genetic model. A separated co-culture approach of hiPSC-derived MGLs and NPCs was used to reduce the risk of confounding results from cell sorting and to provide a nexus of causality as to which cell type is driving the effects. The data suggest that acute IL-6 stimulation and 22q11.2DS both influence cortical neural progenitor cell transcriptome, if not secretome, and that microglial release of additional cytokines after IL-6 stimulation is likely to contribute to these effects. Theoretically, there appears to be a threshold at which atypical neurodevelopmental phenotypes precipitate, to which risk factors contribute. The more risk factors present, whether genetic or environmental, the more likely the precipitation of NDDs. In this model, the NDD-associated risk from 22q11.2DS and IL-6 stimulation intercept at vasculature and extracellular matrix remodelling pathways in MGLs and NPCs. However, the limitations of the chapter did not permit any sturdier conclusions on their direct interactions. Experiments including additional cell types, increased experimental power, and longer chronic IL-6 exposure are needed to further investigate this interaction.

Chapter 6

Gene and IL-6 Priming of Atypical Cortical Neuron Development

Chapter Summary

Background: Throughout cortical development, neural progenitor cells (NPCs) are tightly regulated in their proliferation, migration, maturation, and differentiation into mature neuron types. Disruptions to these processes are thought to contribute to the pathophysiology of neurodevelopmental disorders (NDDs) such as autism spectrum condition (ASC) and schizophrenia (SZ). Both genetic and environmental factors have been shown to alter cell fate differentiation and synapse development in neurons, including maternal IL-6 concentrations and the 22q11.2DS genotype. This chapter discusses the priming effects of the 22q11.2 deletion and acute exposure to IL-6 on the cortical differentiation trajectories of neural progenitor cells (NPCs) while in culture with microglia-like cells (MGLs).

Methods: Cell-type specific, pre- and post-synaptic markers were visualised by immunocytochemistry to assess terminally differentiated cortical neurons from NPCs with and without the 22q11.2 deletion, that had either been exposed acutely to vehicle or IL-6 treatment as NPCs.

Results: There was an increase in the population of TUJ1+/Pax6-/GFAP+ cells in 22q11.2DS donors compared to controls, irrespective of IL-6 treatment, specifically driven by an increase in the number of GFAP expressing cells and not the loss of Pax6 expression. A combination of NPC exposure to IL-6 and the 22q11.2DS genotype reduced vGlut1 puncta density in mature neurons. These findings converge with evidence for dysregulated astrocyte function and abnormalities of the presynapse, in line with published data from 22q11.2DS neurons *in vitro*. Overall, the chapter provides additional insights into the effects of genetic and IL-6 on cortical differentiation and has implications for understanding neurodevelopmental disorders.

6.1 Introduction

6.1.1 Typical neurodevelopment of cortical neuroepithelial cells to mature cell types

Cerebral cortex development is characterised by the progressive proliferation and differentiation of neuroepithelial cells, first into neural progenitor cells (NPCs) and then into specialised mature cell types including upper and deeper layer cortical neurons and astrocytes (Okano and Temple, 2009; Bergström and Forsberg-Nilsson, 2012; Franco and Müller, 2013). Neuroepithelial cells divide symmetrically in the prenatal early stages of development to increase the pool of progenitor cells before transforming into radial glial cells (RGCs) (Smart, 1973; Miyata *et al.*, 2001; Noctor *et al.*, 2002) (Figure 6.1). RGCs are the most common form of NPC in the developing cortex, dividing asymmetrically into either one neuroblast or intermediate progenitor cell (IPC), and one new RGC to maintain the population of RGCs (Franco and Müller, 2013) (Figure 6.1).

Neuroblasts migrate along radial glial processes to reach the cortical plate, as directed by a complex interplay of molecular signals, including chemokines and growth factors that guide their movement along radial glial fibres (Noctor *et al.*, 2002; Bergström and Forsberg-Nilsson, 2012) (Figure 6.1). As the neuroblasts migrate, they undergo a series of morphological changes and differentiate into mature neurons (Hatten, 1999; Ayala, Shu and Tsai, 2007). This process involves the extension of neurites and the formation of synapses with other neurons, which ultimately results in the formation of functional neural circuits. In contrast, IPCs divide symmetrically to produce either a pair of migrating neurons or new IPCs that eventually develop into neurons themselves (Vasistha *et al.*, 2015; Mihalas and Hevner, 2017) (Figure 6.1).

Basal RGCs (bRGCs) are a form of neural progenitor cell that has certain characteristics in common with RGCs, such as a basal attachment at the pial basement membrane (Figure 6.1). But, bRGCs do not have an apical process and their cell bodies are positioned on the outer subventricular zone (oSVZ). bRGCs can self-renew and can also produce both IPCs and neurons. In addition, RGCs and bRGCs differentiate into foetal astrocytes towards the end of neocortical formation, which can then develop into mature astrocytes (Kageyama, Shimojo and Imayoshi, 2015) (Figure 6.1). Importantly, early cortical neuro-development exhibits an interesting pattern of intrinsic timing from the inside out, where deep layer neurons are formed before those in the outer layers (Webb, 2008). There is a delayed emergence of astrocytes compared to other neuronal cell types, despite originating from the same population of NPCs. These observations suggest the existence of mechanisms that regulate the cell fate acquisition of NPCs, ensuring the precise orchestration of cortical development (Webb, 2008). This process of "restricting" the fate of NPCs to follow the appropriate developmental sequence appears to be conserved not only in early cortical neuro-development but also in the hiPSC-derived cortical neuron differentiation protocol, making it a suitable model (Gaspard *et al.*, 2008; Shi *et al.*, 2012b). The intricate and tightly governed process of cell proliferation, maturation, migration, and differentiation is crucial in the creation of the cerebral cortex, and the construction of neuronal networks that underpin typical brain function (Nowakowski *et al.*, 2017). Understanding these mechanisms can provide valuable insights into the fundamental processes governing cell fate determination and the intricate regulation of neurodevelopment.

Hence, it is not surprising that when crucial prenatal developmental processes and the acquisition of cell fate are disrupted by genetic or environmental factors, or a combination of both, the likelihood of developing a neurodevelopmental psychiatric disorder such as autism spectrum condition (ASC) or schizophrenia (SZ) is significantly increased (Courchesne,

Gazestani and Lewis, 2020; Adhya *et al.*, 2021). However, the limited accessibility of human foetal tissue, especially during mid- to late-gestation, has hindered our understanding of human foetal developmental processes. This creates a compelling justification for the employment of human-induced pluripotent stem cells (hiPSCs) as a valuable tool to bridge this gap in knowledge. By differentiating hiPSCs to more specialised cells at different stages of development, we can investigate and simulate human foetal development in a controlled setting, offering insights into the molecular processes that occur during this critical period (Adhya *et al.*, 2021; Gaspard *et al.*, 2008; Shi *et al.*, 2012b, 2012a). For example, a single-cell transcriptomic study of human foetal developing tissues revealed significant differences in the early-stage cortex development of humans and rodents (Eze *et al.*, 2021). Specifically, there are specific cell populations and gene regulatory networks that are absent in mouse models but present in humans (Eze *et al.*, 2021). This leads to a lack of understanding for the governance of these developmental processes at a human molecular level, and an explicit call for human-based hiPSC models to be used when studying these developmental timepoints in conjunction with *in vivo* rodent models (Eze *et al.*, 2021).

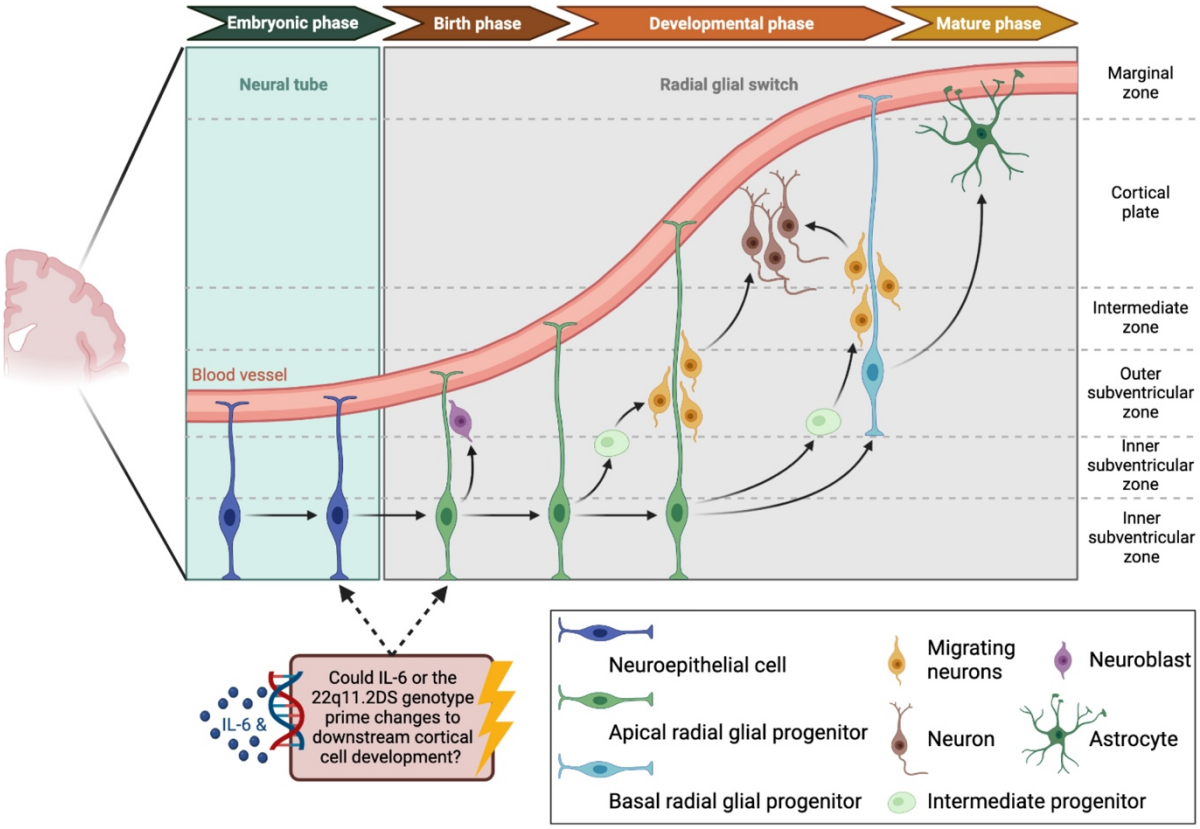

Figure 6.1 – Prenatal developmental trajectory of cortical neuroepithelial cells into mature cortical neurons and astrocytes. Neuroepithelial cells differentiate into radial glial cells (RGCs), which either symmetrically divide and self-renew to maintain their population or asymmetrically divide into one RGC and one neuroblast or intermediate progenitor cell (IPC). Likewise, IPCs self-renew or asymmetrically divide into one neuron and one IPC. Neuroblasts and migrating neurons then migrate along RBC fibres to the cortical plate, maturing along the way to specialised neurons. RGCs and basal RGCs (bRGCs) also have the propensity to differentiate into astrocytes at later stages of cortical development. This chapter investigates whether the 22q11.2DS genotype, acute early-stage IL-6 exposure to neuroepithelial and neural progenitor cells, or their interaction, has the ability to prime alterations in the conventional developmental trajectories of these cell types.

6.1.2 Exposure to elevated IL-6 levels in early life and 22q11.2DS are associated with disruption of cortical synaptogenesis and cell fate

Elevations in serum IL-6 levels, as a consequence of either infectious or non-infectious stimuli during pregnancy and genetic risk factors, such as the copy number variation (CNV) 22q11.2 deletion syndrome (DS) have been independently associated with atypical development of

NPCs towards mature neurons (Brennand *et al.*, 2015; Toyoshima *et al.*, 2016; Khan *et al.*, 2020; Nehme *et al.*, 2022; Reid *et al.*, 2022). Specifically, birth cohort studies have linked elevated maternal IL-6 concentrations across gestation with aberrant structural and functional brain connectivity (as measured by MRI) including key limbic and cognitive circuits, which in turn are associated with abnormal cognitive development and increased externalising behaviours in the offspring (Graham *et al.*, 2018; Rasmussen *et al.*, 2019; Rudolph *et al.*, 2018). These macro-level data however do not provide any insight in the cellular and molecular processes involved in these associations, nor can they establish the direction of causality. At a molecular level, the development of the correct number, organisation and input of synapses onto a cell is essential during typical cortical development (Bayés *et al.*, 2011; Südhof, 2017; Kuljis *et al.*, 2019). Mouse models can therefore be informative in unravelling the links from macro- to micro-scale.

In this particular context, Mirabella and colleagues (2021) employed both *in vivo* and *in vitro* methods to propose that administering a single intraperitoneal injection of 5µg of IL-6 on gestational day 15, which corresponds to the second trimester of pregnancy in humans (Patten, Fontaine and Christie, 2014), results in increased vGlut1 puncta area and PSD95-vGlut1 colocalization in both cultured primary hippocampus (HPC) neurons and in mouse hippocampus taken in adulthood (postnatal day (PND) 15-60) (Mirabella *et al.*, 2021). These findings suggest heightened excitatory synaptogenesis in response to acute IL-6 exposure during specific gestational period (Mirabella *et al.*, 2021). Consistent with this view, in this study, IL-6 exposure resulted in the activation of transcriptional programs the drive synaptogenesis in glutamatergic neurons (Mirabella *et al.*, 2021). At the macro-scale, this resulted in a hyperconnectivity phenotype in adulthood (PND 15-60), as measured by functional MRI and behavioural deficits of relevance for neurodevelopmental disorders. These

data indicate that a single early life exposure of IL-6 is sufficient to induce a long-lasting phenotype into adulthood (Mirabella *et al.*, 2021). Interestingly, in this study, IL-6 exposure resulted in the activation of transcriptional programs the drive synaptogenesis in glutamatergic neurons (Mirabella *et al.*, 2021). Furthermore, activation of STAT3 signalling and expression of the RGS4 gene were shown to be necessary and sufficient for these changes (Mirabella *et al.*, 2021). Collectively, these data suggest a view that elevation of IL-6, even acutely, during early neurodevelopmental of the mouse brain exerts a long-lasting effect on glutamatergic synaptogenesis and brain connectivity, establishing a potential mechanistic link for the association between prenatal IL-6 exposure and subsequently increased risk for neurodevelopmental disorders (Mirabella *et al.*, 2021). The data presented by Mirabella and colleagues (2021) however were exclusively obtained from experiments conducted on the mouse brain, which, as previously mentioned, undergoes distinct developmental processes compared to the human brain. Consequently, it remains uncertain whether these findings can be extrapolated to humans. However, the objective of the study discussed in this chapter is to investigate these findings within a human-relevant model, aiming to determine if the conclusions drawn from mouse studies hold true in the context of human neurodevelopment.

In parallel, there is convergent evidence that connects the CNV 22q11.2DS, one of the most highly penetrant genetic risk factors for ASC and SZ, with atypical synaptogenesis and neuronal differentiation trajectories. For instance, Nehme and colleagues (2022) utilized a hiPSC-derived isogenic model *in vitro* system featuring a CRISPR/Cas9 heterozygous 22q11.2 deletion in a control donor line. Their study demonstrated a reduction in the puncta intensity of the pre-synaptic protein synaptic vesicle glycoprotein 2A (SV2A) within maturing neurons derived from 22q11.2DS individuals, a decrease that was replicated in hiPSC lines from donors with 22q11.2 deletions (Nehme *et al.*, 2022). These findings not only suggest that the synaptic

differences are attributed to the deletion itself but also imply that one potential underlying mechanism of neurodevelopmental risk is the alteration of typical NPC fate trajectories caused by the 22q11.2DS genotype. Such alteration could lead to an imbalance in the functions of neurons (Toyoshima *et al.*, 2016).

Together, these studies highlight the importance of prenatal inflammatory events driven by IL-6 and specific genetic risk factors, that are independently associated with atypical neurodevelopment in terms of cell fate and synaptic development, which in turn may create a "latent insult" and shape a person's vulnerability to develop psychopathology in later life. What is unclear however, is the extent to which these factors may *interact* to define an individual's risk for psychopathology. For example, susceptibility to psychopathology following exposure to prenatal inflammatory events may be different depending on the presence or absence of risk factors such as those arising from individual genetic differences, including 22q11.2DS (Meyer, 2019). The communication between the internal physiological and biochemical processes and the external environment, which might later influence neuron and synapse development, is facilitated by the immune system (Rook, 2013). Prenatal programming as a consequence of prenatal inflammatory events, for example related to elevations in IL-6, would therefore be predicted to interact with an individual's inbuilt genetic susceptibility for psychopathology, mediated by atypical neuron fate or synapse development. Animal models combining prenatal immune activation with the presence of CNVs linked to psychiatric disorders such as *DISC1* provide important proof-of-concept for the idea that NDD phenotypes are only present when multiple risk factors are combined (Abazyan *et al.*, 2010). To date however, whilst there is data to suggest that IL-6 and 22q11.2DS may independently cause atypical neurodevelopment, studies addressing any interactions between these risk factors in relevant human cellular models of neurodevelopment are lacking. Of note, our preliminary transcriptional profiling of

NPCs from 22q11.2DS carriers show that synaptogenesis pathways were up-regulated in the absence of any IL-6 stimulation (q = 0.016; see section 5.3.2). Hence, in this chapter we aimed to use our hiPSC co-culture model to provide a preliminary examination of (1) the long-term effects of a 22q11.2DS genotype on NPC cell fate and synaptogenesis in mature cortical neurons; (2) the impact of IL-6 on the same phenotypes and (3) to what extent these risk factors may interact.

6.2 Materials and Methods

6.2.1 Mature Cortical Neuron Culture and ICC

NPCs were differentiated using the dual SMAD inhibition protocol (Shi *et al.*, 2012b), as described in section 2.1.3 from N=4 healthy control donors and N=2 22q11.2DS donors, with one clone per donor. As described in Chapter 5, cell culture inserts containing hiPSC-derived microglia like cells (MGLs) on D12 of their differentiation protocol were added to the same well as the NPCs on D16 of their differentiation protocol, and allowed to adapt to each other in culture for 48h. D18 of the NPC differentiation protocol, co-cultures were exposed to either 100ng/ml IL-6 or acetic acid vehicle for 24h (Table 6.1). The cell types were then separated, and mature cortical neurons were subsequently terminally differentiated until D50 from these NPCs following the protocol described in section 2.1.4. Details of the 22q11.2 region variants can be found in chapter 2, section 2.1.1, table 2.2. As in chapter 5, three donor lines with the 22q11.2DS genotype were initially intended for differentiation. However, one of the lines consistently failed to undergo neural differentiation, despite three separate attempts. This further emphasizes the challenge of working with iPSC lines, as their behaviour can often be unpredictable and stochastic in nature.

Table 6.1 – 12 cultures differentiated for phenotypic assay. Each donor was plated onto one 96-well plate, with N=4 technical replicate wells per condition, with N=2 primary negative and N=2 secondary negative wells per conditions. Of the control genotype samples, lines M3_CTR_36S, 069_CTF_01, 014_CTM_02 and 127_CTM_01 were used. Of the 22q11.2DS genotype, 509_CXF_05 and 287_SZM_01 were used. Individual donor was therefore used as a biological replicate in downstream analyses.

Treatment	Control Genotype	22q11.2DS Genotype
Vehicle	N=4 (3 ♂, 1 ♀)	N=2 (1 ♂, 1 ♀)
IL-6	N=4 (3 ♂, 1 ♀)	N=2 (1 ♂, 1 ♀)

6.2.2 Immunocytochemistry of Cortical Neurons

On day 50 of neural differentiation, 29 days after seeding at a density of $0.3x10^5$ cells/well into 96-well Perkin Elmer CellCarrier Ultra plates, cells were fixed and stained for immunocytochemistry as described in section 2.3.3 (Table 6.2, Table 6.3). After the final DAPI stain however, cells were left in 150µl/well PBS ready for imaging. Cells from the 22q11.2DS and control genotypes were stained in the same batch as to reduce possible batch staining effects. For example, both 509_CXF and 069_CTF donors were stained at the same time, as well as 287_SZM and 127_CTM. For the healthy controls, the final two donors M3_CTR and 014_CTM were also stained simultaneously.

Table 6.2 - List of antibodies used for immunocytochemistry in this chapter.

Epitope	Host	Dilution	Supplier
MAP2	Chicken	1:1000	Abcam; ab92434
GluN1 (NMDAR1)	Mouse	1:500	Biolegend; 818601
vGlut1	Rabbit	1:500	Synaptic Systems; 135302
PSD95	Mouse	1:500	Biolegend; 810401
Gephyrin	Rabbit	1:500	Millipore; AB5725
GAD67	Mouse	1:500	Abcam; ab26116
SV2A	Rabbit	1:500	Abcam; ab32942
GFAP	Chicken	1:500	Abcam; ab4674
TUJ1	Mouse	1:500	Biolegend; 801201
Pax6	Rabbit	1:500	Biolegend; 901301
Anti-rabbit AlexaFluor 568	Goat	1:750	Thermo Fischer Scientific; A11011
Anti-mouse AlexaFluor 488	Goat	1:750	Thermo Fischer Scientific; A11001
Anti-chicken AlexaFluor 633	Goat	1:750	Thermo Fischer Scientific; A21103

Table 6.3 - Plate map for 96-well Perkin Elmer CellCarrier Ultra plates used for OperaPhoenix image acquisition of ICC-stained mature neurons exposed to co-culture IL-6 treatment with MGLs. Each treatment condition was stained for four different combinations of markers. In rows columns 1-2, cells were stained with a combination of MAP2, PSD-95, vGlut1 and DAPI. In columns 4 and 5, cells were stained for MAP2, GluN1, SV2A and DAPI. In columns 7 and 8, cells were stained for MAP2, Gephyrin, GAD67 and DAPI. Finally, columns 10 and 11 were stained for TUJ1, GFAP, Pax6 and DAPI. As negative staining controls, rows E and F contained primary only antibodies (secondary negative) and rows G and H contained only secondary antibodies (primary negative). Data not shown for columns 3, 6, 9 and 12. Secondary antibody abbreviations: chicken raised (chk), mouse raised (ms) and rabbit raised (rb).

<table>
<tr><th></th><th>1: Vehicle</th><th>2: IL6</th><th>3</th><th>4: Vehicle</th><th>5: IL6</th><th>6</th><th>7: Vehicle</th><th>8: IL6</th><th>9</th><th>10: Vehicle</th><th>11: IL6</th><th>12</th></tr>
<tr><td>A</td><td colspan="2" rowspan="4">MAP2 (chk) + PSD-95 (ms) + vGlut1 (rb) + DAPI</td><td></td><td colspan="2" rowspan="4">MAP2 (chk) + GluN1 (ms) + SV2A (rb) + DAPI</td><td></td><td colspan="2" rowspan="4">MAP2 (ck) + Gephyrin(rb) + GAD67 (ms) + DAPI</td><td></td><td colspan="2" rowspan="4">TUJ1 (chk) + GFAP (ms) + Pax6 (rb) + DAPI</td><td></td></tr>
<tr><td>B</td><td></td><td></td><td></td><td></td></tr>
<tr><td>C</td><td></td><td></td><td></td><td></td></tr>
<tr><td>D</td><td></td><td></td><td></td><td></td></tr>
<tr><td>E</td><td>Primary Only</td><td>Primary Only</td><td></td><td>Primary Only</td><td>Primary Only</td><td></td><td>Primary Only</td><td>Primary Only</td><td></td><td>Primary Only</td><td>Primary Only</td><td></td></tr>
<tr><td>F</td><td>Primary Only</td><td>Primary Only</td><td></td><td>Primary Only</td><td>Primary Only</td><td></td><td>Primary Only</td><td>Primary Only</td><td></td><td>Primary Only</td><td>Primary Only</td><td></td></tr>
<tr><td>G</td><td>Secondary Only</td><td>Secondary Only</td><td></td><td>Secondary Only</td><td>Secondary Only</td><td></td><td>Secondary Only</td><td>Secondary Only</td><td></td><td>Secondary Only</td><td>Secondary Only</td><td></td></tr>
<tr><td>H</td><td>Secondary Only</td><td>Secondary Only</td><td></td><td>Secondary Only</td><td>Secondary Only</td><td></td><td>Secondary Only</td><td>Secondary Only</td><td></td><td>Secondary Only</td><td>Secondary Only</td><td></td></tr>
</table>

Cell Identity Assay

Using the antibodies listed in section 2.3.3, cortical neurons were stained with DAPI and TUJ1 to identify morphological boundaries, alongside GFAP and Pax6 to identify astrocytes and immature neurons respectively (Table 3.1, Table 6.3). The protein β-tubulin III (TUJ1) is present in the neurite filaments of mature developed cortical neurons and foetal astrocytes, enabling their visualization through morphological staining (Dráberová *et al.*, 2008). However, while TUJ1 is an excellent marker for identifying neurons, it does not provide the ability to differentiate between axons and dendrites in this particular analysis. Pax6, known as a marker for forebrain progenitor cells, is anticipated to be present in the nucleus of NPCs but not in post-mitotic neurons (Adhya *et al.*, 2021; Shi *et al.*, 2012a; Zhang *et al.*, 2016). Consequently,

Pax6 was selected as a marker to identify undifferentiated NPCs, as well as immature astrocytes and radial glia, as it is expected to be expressed in these cell types (Götz, Stoykova and Gruss, 1998; Zhang *et al.*, 2016). GFAP-expression in adult *post-mortem* tissue (Laurence and Fatemi, 2005; Crawford *et al.*, 2015; Toyoshima *et al.*, 2016), infant plasma (Vergine *et al.*, 2021) and adult cerebrospinal fluid (Michel *et al.*, 2021) correlates with psychiatric disorders in humans. Through the assessment of GFAP levels in this *in vitro* model, a marker known to be expressed by astrocytes and radial glia, we can explore whether either the genotype or IL-6 influences the ratio of these cell types to neurons.

Using the DAPI stain for PAX6 given it's expected expression in the nucleus, and TUJ1 stain for GFAP given it's expected expression in the cytoplasm, the number of cells positive for each marker per well was defined by the intensity of marker being above the background (see subsequent section). The number of PAX6+, MAP2+ and TUJ1+ cells per well were collated, and relative populations within each donor were calculated as a percentage of total cells counted.

Synapse Counting Assay

In order to identify nuclei and neurite sections on which synapsis lie in cortical neurons, DAPI and MAP2 staining was performed respectively. In addition, a combination of specific pre- and post-synaptic proteins was utilized for staining, including the pre-synaptic protein, vesicular glutamate transporter 1 (vGlut1) and post-synaptic protein, postsynaptic density protein 95 (PSD95), or SV2A (pre-synaptic) and the NMDA receptor subunit GluN1(post-synaptic) (Table 3.1, Table 6.3). Furthermore, the staining also involved a combination of inhibitory synaptic proteins, Gephyrin (post-synaptic) and glutamate decarboxylase (GAD67; pre-synaptic) (Table 3.1, Table 6.3). The selection of each puncta marker was guided by the

following rationale: PSD95, GluN1, and vGlut1 are all involved in glutamatergic neurotransmission, which, when atypically expressed, is thought to be relevant to SZ and ASC onset (Oni-Orisan *et al.*, 2008; Bitanihirwe *et al.*, 2009; Moghaddam and Javitt, 2012; Holloway *et al.*, 2013; De Bartolomeis *et al.*, 2014; Grunwald *et al.*, 2019; Mirabella *et al.*, 2021). SV2A has been found to be decreased in patients with 22q11.2DS (Nehme *et al.*, 2022). GAD67 expression consistently shows decreased levels in the brains of individuals with psychiatric disorders such as SZ, BD, and MDD (Miyata *et al.*, 2021; Karolewicz *et al.*, 2010; Hashimoto *et al.*, 2008; Guidotti *et al.*, 2000). Moreover, Gephyrin has been linked to hemizygous microdeletions in the genetic sequence related to the G-domain, observed in unrelated individuals affected by ASC and SZ (Lionel *et al.*, 2013). The antibodies used for each of these markers were readily available within the group and had been previously quality controlled by the Srivastava lab (Table 3.1) (Deans *et al.*, 2017; Adhya *et al.*, 2021; Bhat *et al.*, 2022).

Initially, MAP2+ cells were identified automatically by the software (Figure 6.2). Then, dendrites were automatically identified using the MAP2+ cell masks (Figure 6.2). Along each dendrite, synaptic puncta were then identified separately from either the 568nm or 488nm imaging channel depending on the secondary antibodies used (Figure 6.2). Synaptic puncta were thresholded by two characteristics: size and intensity. Synaptic puncta sizes were considered to be between 0.8-5μm^2 (Glynn and McAllister, 2006), which equated to between 27-170 pixels. To calculate the lowest intensity limit, the intensity of each channel's background florescence was taken and averaged from 5 random locations from the primary negative wells. To identify maximum intensity, fluorescence intensity from 5 clear artefacts in the primary negative wells were averaged. The dendrite length of MAP2+ cells was measured and averaged per well, to normalise the number of puncta for culture and dendrite outgrowth.

This gave two outputs for each puncta channel: intensity and puncta number/dendrite length (density) (Figure 6.2). Finally, positively identified puncta were masked on top of each other, to count those that co-colocalised (overlapped). For each donor, synaptic puncta metrics were averaged from all replicate images for each condition. To reduce the possibility of confounding results caused by staining differences across donor replicate plates, all IL-6 treated puncta metrics were normalised to the vehicle average to create a fold change value from vehicle. Then, to assess the effect of IL-6 on each synaptic metric measured, Welch's t-test was used due to the unequal variances between each group (all vehicle donor points = 1).

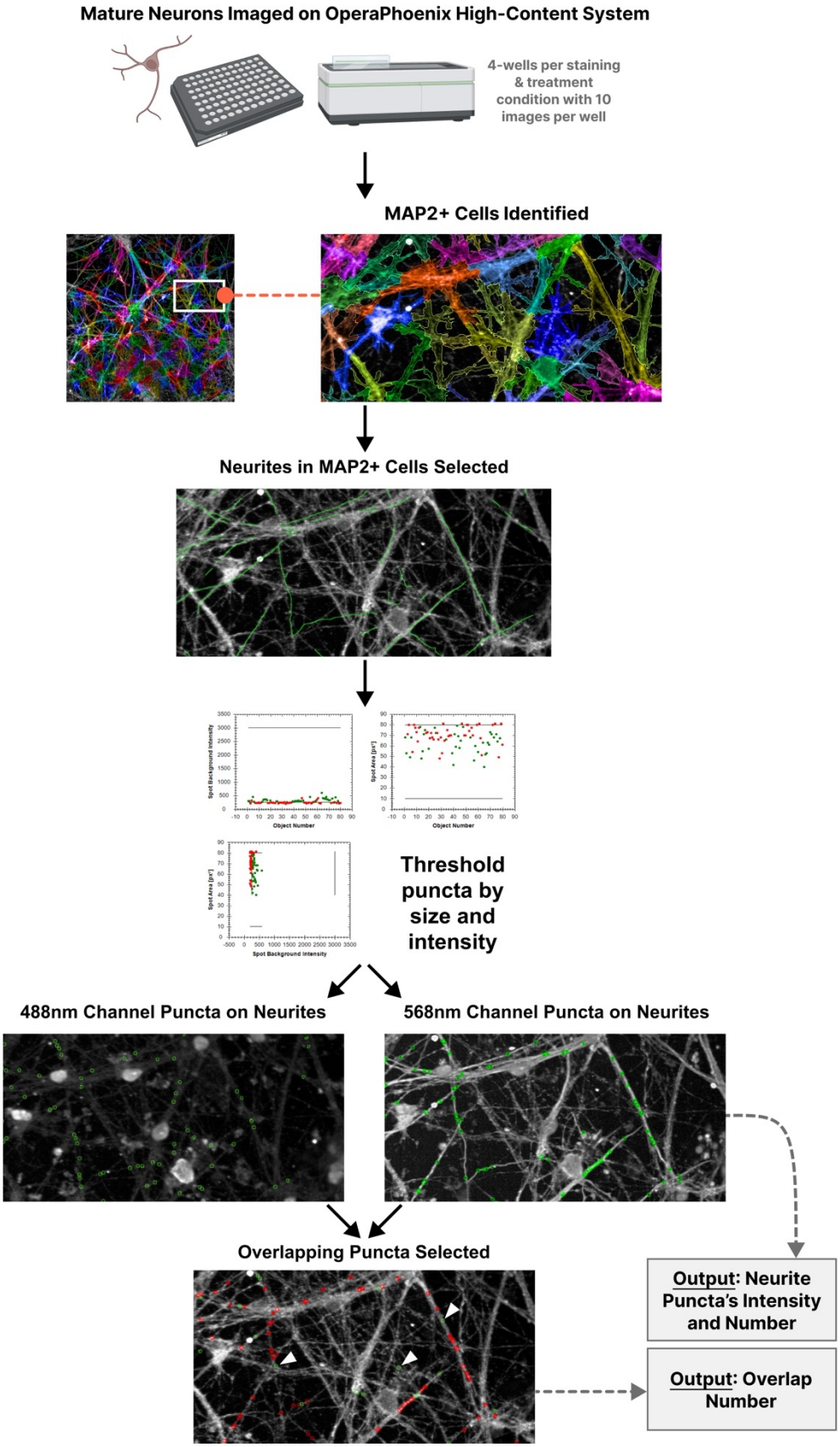

Figure 6.2 – Schematic for Synapse Counting. Mature cortical neurons from control and 22q11.2DS donors that had been exposed to acute IL-6 treatment in co-culture with MGLs at an NPC stage were seeded into a 96-well plate. MAP2+, DAPI

and combinations of synaptic puncta were imaged on the OperaPhenix high-content screening system. Following this, images were analysed on Harmony software to identify Map2+ cells, and subsequent neurites indicated by green lines. Puncta along these neurites were found by thresholding between size and intensity limits. Positively identified puncta were indicated by the software with a green circle, counted, and their fluorescence intensity measured. Finally, co-localisation of puncta in both channels were counted, with positive co-localisation targets identified with a green circle and white arrow.

6.3 Results

6.3.1 Impact of 22q11.2DS and IL-6 alone and in combination on NPC cell fate

The relative proportions of cell-specific markers were first investigated to establish whether the differentiation trajectories of forebrain NPCs were affected by either 22q11.2DS or IL-6 exposure, alone or in combination, at D18 (NPC stage) at which time-point the NPCs were in co-culture with MGLs. As described in the preceding chapter, the NPCs from which the terminal differentiation occurred were in co-culture via a trans-well system with MGLs on the same genetic background, and exposed acutely to either IL-6 (100 ng/ml) or a vehicle control for 24 hrs. After this time, the MGLs were removed to collect mRNA and culture supernatant as reported in Chapter 5 of this thesis and the NPCs allowed to terminally differentiate to day 50. The numbers of cells immunopositive for combinations of β-tubulin III (TUJ1+), a neuronal marker, glial fibrillary acidic protein (GFAP+), an astrocyte marker, and paired box protein (Pax6+), a forebrain progenitor marker were assessed in terminally differentiated cortical neurons (day 50) using both health donor lines (N=4) and carriers of the 22q11.2 deletion with psychiatric diagnoses (N=2) (Figure 6.3A).

The majority of cells in culture expressed TUJ1 (mean across vehicle and treated cultures: control 96.66% ; 22q11.2DS 95.68%), but not Pax6 (control 6.38% ; 22q11.2DS 8.27%) or GFAP (control 17.27% ; 22q11.2DS 4.36%), indicating a predominance of neurons (Figure

6.3B). The next highest percentage of cells in the culture expressed both TUJ1 and GFAP, indicating foetal astrocytes or radial glia (Dráberová *et al.*, 2008) (Figure 6.3B). Pax6 expression was found in a limited population of cells, with minimal co-expression with TUJ1, indicating the presence of undifferentiated NPCs (Figure 6.3B). The percentage of total cells expressing GFAP were significantly higher in 22q11.2DS lines, as compared to healthy controls, irrespective of their Pax6 or TUJ1 expression and again unaffected by IL-6 exposure (Figure 6.3B and C, two-way ANOVA: treatment $F(1,8) = 0.819$, $p = 0.392$; genotype $F(1,8) = 10.30$, $p = 0.0124$; interaction $F(1,8) = 0.0934$; $p = 0.768$). This relationship was not the same for the percentage of total cells that also expressed Pax6, inferring that the 22q11.2DS-influenced increase in TUJ1+/Pax6-/GFAP+ cells is driven by an increase in GFAP expression and not Pax6 (Figure 6.3D, two-way ANOVA: treatment $F(1,8) = 0.005$, $p = 0.945$; genotype $F(1,8) = 0.071$, $p = 0.797$; interaction $F(1,8) = 0.177$; $p = 0.685$). The genotype 22q11.2DS results in a consistent observation in *post-mortem* data from people with SZ, ASC, and depression, indicating that this happens early in development (Laurence and Fatemi, 2005; Crawford *et al.*, 2015; Toyoshima *et al.*, 2016; Michel *et al.*, 2021). Qualitatively, there was a clear increase in the population of TUJ1+/Pax6-/GFAP+ cells in the cell lines from the 22q11.2DS donors (N=2) as compared to healthy controls (N=4), in the absence of IL-6 exposure (Figure 6.3B). Indeed, there were significantly more TUJ1+/Pax6-/GFAP+ cells in the 22q11.2DS donor lines than the healthy control lines, which was unchanged by IL-6 exposure (Figure 6.3E, two-way ANOVA: treatment $F(1,8) = 1.379$, $p = 0.274$; genotype $F(1,8) = 14.11$, $p = 0.0056$; interaction $F(1,8) = 0.331$; $p = 0.5811$). In summary, the data suggest that IL-6 did not result in a significant impact on the differentiation towards different cell fates and/or populations.

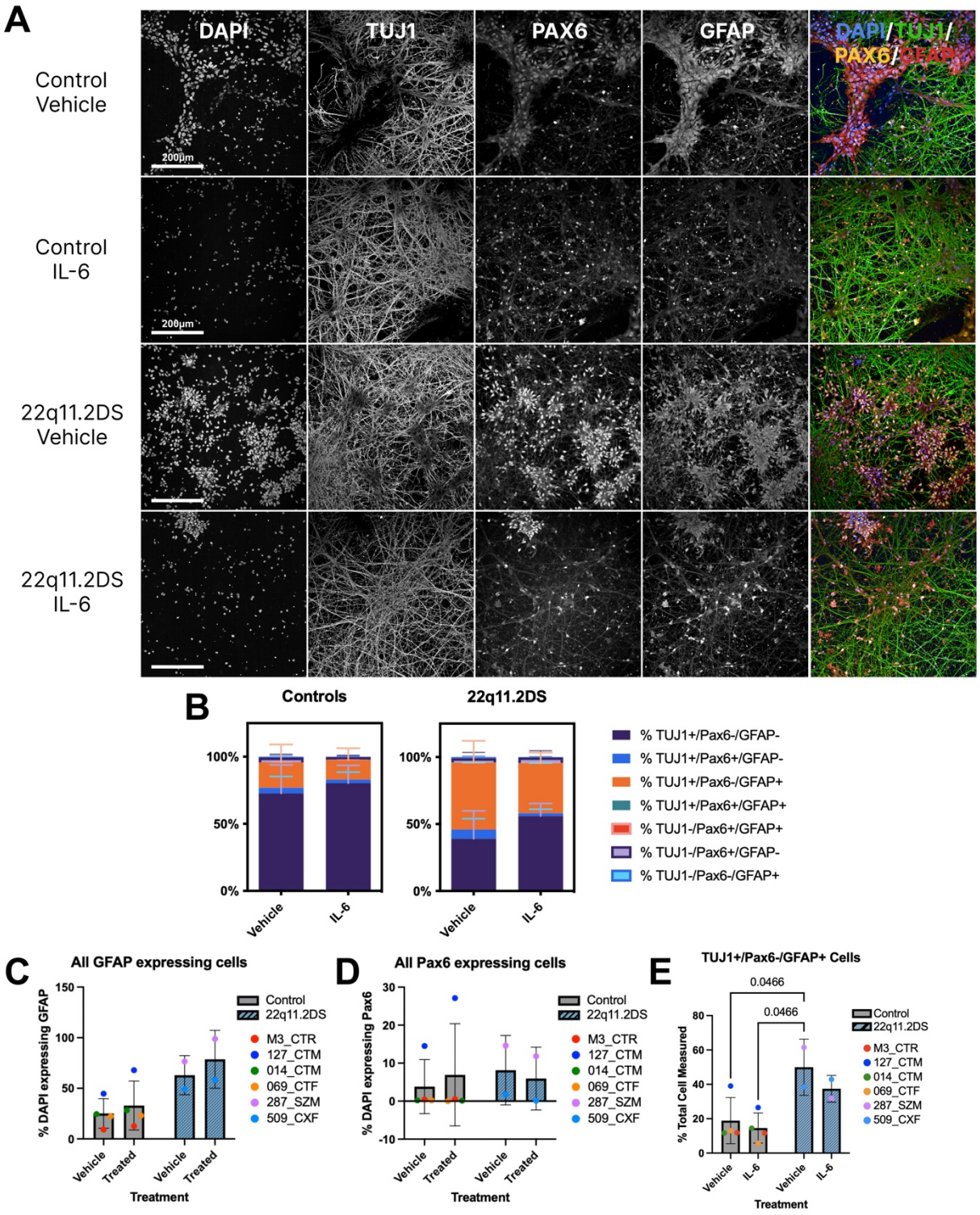

Figure 6.3 – IL-6 primed changes to cell fate and morphological phenotypes of hiPSC-derived cortical neurons from healthy and 22q11.2DS genotype. (A) Representative images of cortical neurons from healthy control donor 127_CTM_01 and 22q11.2DS donor 287_SZM_01, exposed to vehicle or IL-6 in co-culture with MGLs at their NPC stage. Cells were stained for DAPI (column 1), TUJ1 (column 2), PAX6 (column 3) and GFAP (column 4). Channels were overlayed in column 5. Scale bar represents 200µm. (B) Cell populations as a percentage of total number of cells counted within each donor, averaged across all images to one single data point per donor. N=4 control donors, N=2 22q11.2DS donors. (C) TUJ1+/Pax6-/GFAP+

cells as a percentage of total cells measured. Significant (<0.05) 5% false discovery rate (FDR) by Benjamini–Hochberg (BH) method corrections after two-way ANOVA formatted on graph. Bar graphs plotted as mean with standard deviation (SD) error bars, and points coloured by donor line as shown in key. N=4 control donors, N=2 22q11.2DS donors. (D) Percentages of all cells expressing GFAP, irrespective of other markers, as a percentage of the total number of cells measured. Bar graphs plotted as mean with standard deviation (SD) error bars, and points coloured by donor line as shown in key. N=4 control donors, N=2 22q11.2DS donors. (E) Percentages of all cells expressing Pax6, irrespective of other markers, as a percentage of the total number of cells measured. Bar graphs plotted as mean with standard deviation (SD) error bars, and points coloured by donor line as shown in key. N=4 control donors, N=2 22q11.2DS donors.

6.3.2 Effects of 22q11.2DS genotype and early acute IL-6 exposure on synaptic marker immunostaining in cortical neurons

As previously mentioned, the arrangement, quantity, and input identity of synapses onto a nerve cell are important drivers of neuronal activity (Kuljis *et al.*, 2019). Moreover, dysregulation of these drivers is a key pathological mechanism implicated in NDDs (Südhof, 2017; Bayés *et al.*, 2011). Given the results of the previous chapter which demonstrated that the transcriptome of NPCs and MGLs is greatly affected by genotype and IL-6 respectively, we assessed whether dysregulations in synaptogenesis could be influenced by IL-6 during the NPC stage, or by the 22q11.2DS genotype. Both inhibitory and excitatory synaptic puncta density and intensity was measured in 22q11.2DS and control MAP2+ neurons that had been exposed at their NPC stage to vehicle or IL-6 in co-culture with MGLs. Firstly, the density and intensity of the pre- and post-synaptic excitatory markers vGlut1 and PSD95 were quantified along MAP2+ neurites. vGlut1 puncta density was reduced by half in the 22q112DS donor lines after acute exposure to IL-6 at NPC stage in co-culture with MGLs in comparison to those treated vehicle (Figure 6.4B-C, FC = 0.561, Welch's t-test: t = 15.03, df = 1, p = 0.0423). Of note, decreases in vGlut1 protein expression, which functions to fill synaptic vesicles with glutamate (Edwards, 2007), have been previously reported in *post-mortem* cortical brain tissue from individuals with SZ (Eastwood and Harrison, 2005; Oni-Orisan *et al.*, 2008; Mirabella *et*

al., 2021). Yet, no differences were found in either PSD95 puncta density and intensity, nor vGlut1 puncta intensity as a function of genotype or IL-6 exposure (Figure 6.4B). These findings are consistent with those from human *post-mortem* data and indicate that a microglial response to IL-6 during the NPC stage may interact with the 22q11.DS genotype to influence synaptic pathology based on decreased vGlut1 puncta in 22q11.2DS, IL-6 treated neurons only.

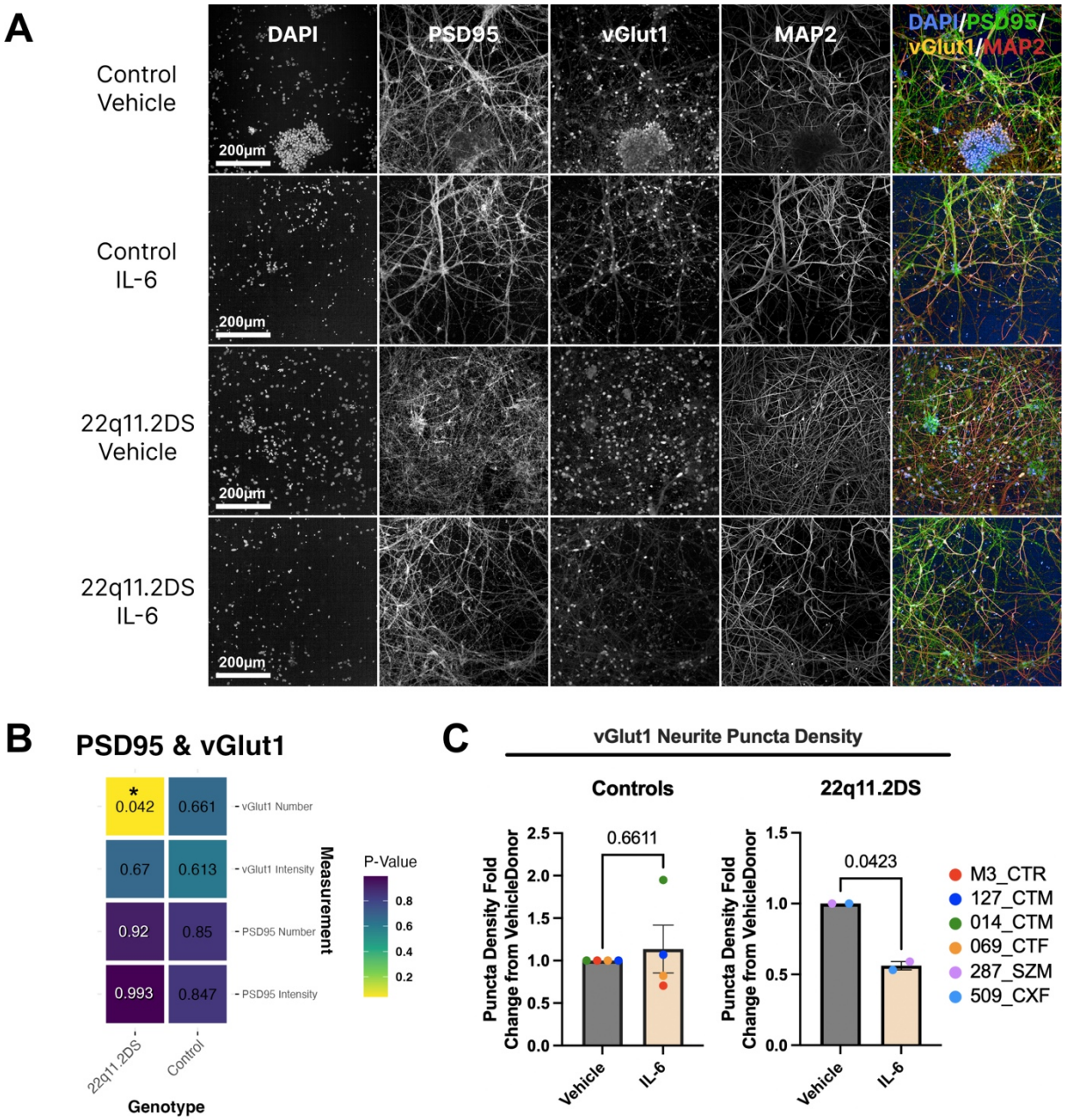

Figure 6.4 - IL-6 primed changes to vGlu1 synapse puncta development of hiPSC-derived cortical neurons from healthy and 22q11.2DS genotype. (A) Representative images of cortical neurons from healthy control donor 127_CTM_01 and 22q11.2DS

*donor 287_SZM_01, exposed to vehicle or IL-6 in co-culture with MGLs at their NPC stage. Scale bar represents 200µm. Cells were stained for DAPI (column 1), PSD95 (column 2), vGlut1 (column 3) and MAP2 (column 4). Channels were overlayed in column 5. (B) Heatmap of two-tailed unpaired t-test p-values comparing neurite PSD95 and vGlut1 protein puncta intensity and number from vehicle and IL-6 treated cultures. Metrics were averaged to give one data point per donor and then IL-6 treated culture values were calculated as a fold change from each donor's vehicle. * $p < 0.05$. (B) Fold change from vehicle-treated conditions within each donor of neurite vGlut1 puncta number normalised by neurite length, plotted for both control and 22q11.2DS genotypes. P-value of two-tailed unpaired t-test comparison formatted on graph. Bar graphs plotted as mean with standard deviation (SD) error bars, and points coloured by donor line as shown in key. N=4 control donors, N=2 22q11.2DS donors.*

Further to vGlut1 and PSD95 puncta staining, additional excitatory synaptic markers were investigated. This included SV2A which has been found to be decreased in patients with 22q11.2DS (Nehme *et al.*, 2022), and the excitatory marker GluN1 (Figure 6.5A). In addition, expression of both inhibitory markers GAD67 and Gephyrin were investigated (Figure 6.5C). Although the protocol used to differentiate the forebrain cortical neurons from hiPSCs is expected to produce primarily excitatory neurons (Shi *et al.*, 2012a), staining for synaptic proteins associated with inhibitory neurons was noted and this was similar in magnitude to GAD67 staining from neurons derived using the same protocol in prior work from the Srivastava lab (Adhya *et al.*, 2021) (Figure 6.5C). However, neither the densities nor intensities of GluN1, SV2A, Gephryin and GAD67 puncta were affected either by early IL-6 exposure or the 22q11.2DS genotype alone under the conditions tested and with the caveat of a small sample size (Figure 6.5B and D). Alternatively, the presence of excessive variance in our 22q11.2DS donor lines could account for this discrepancy.

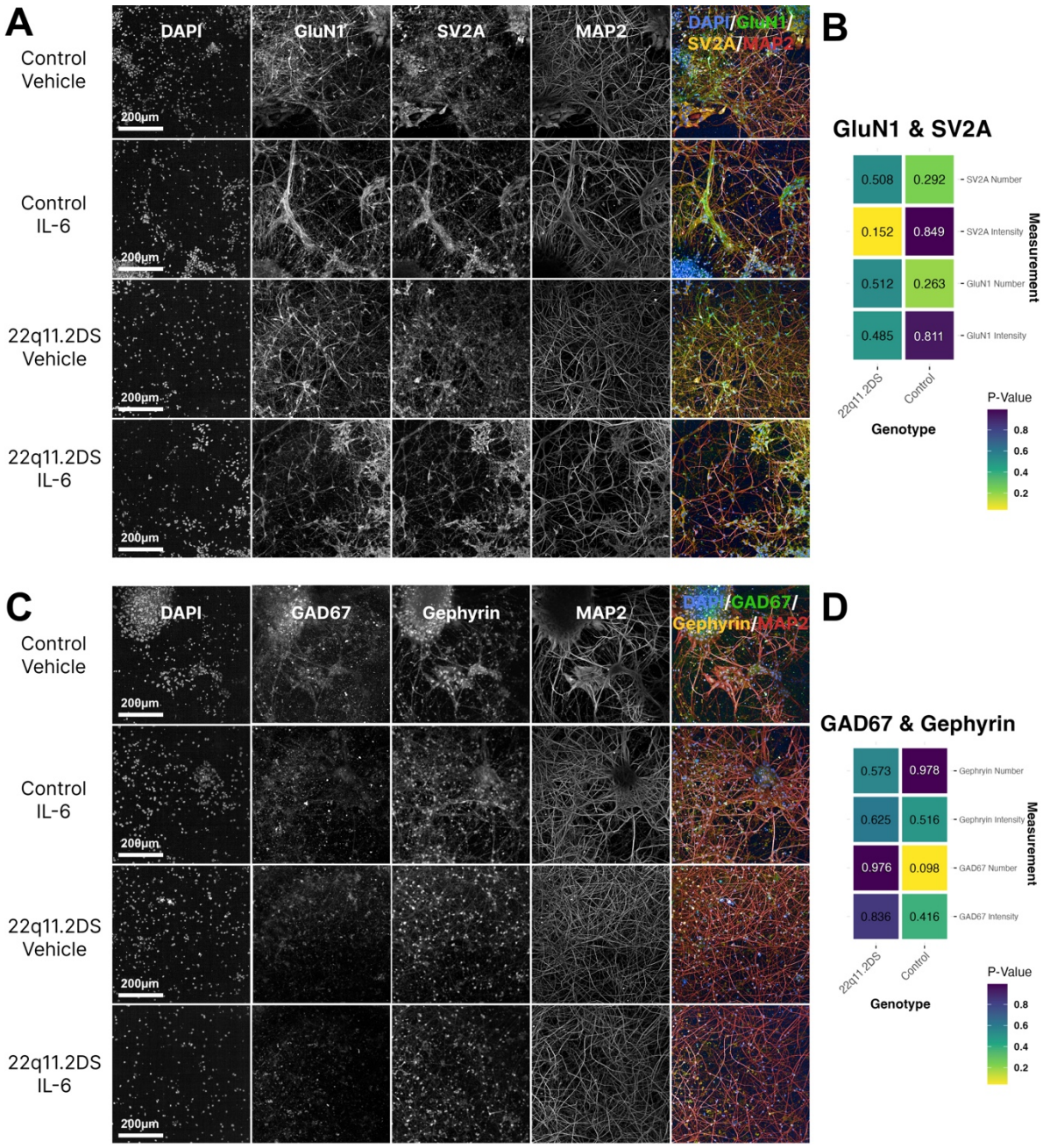

Figure 6.5 – IL-6 or 22q11.2DS did not prime changes to GluN1, SV2A, GAD67 or Gephyrin puncta development. (A) Representative images of cortical neurons from healthy control donor 127_CTM_01 and 22q11.2DS donor 287_SZM_01, exposed to vehicle or IL-6 in co-culture with MGLs at their NPC stage. Scale bar represents 200µm. Cells were stained for DAPI (column 1), GluN1 (column 2), SV2A (column 3) and MAP2 (column 4). Channels were overlayed in column 5. (B) Heatmap of two-tailed unpaired t-test p-values comparing neurite GluN1 and SV2A protein puncta intensity and number from vehicle and IL-6 treated cultures. Metrics were averaged to give one data point per donor and then IL-6 treated culture values were calculated as a fold change from each donor's vehicle. (C) Representative images of cortical neurons from healthy control donor 127_CTM_01 and 22q11.2DS donor 287_SZM_01, exposed to vehicle or IL-6 in co-culture with MGLs at their NPC stage. Scale bar represents 200µm. Cells were stained for DAPI (column 1), Gephyrin (column 2), GAD67 (column 3)

and MAP2 (column 4). Channels were overlayed in column 5. (D) Heatmap of two-tailed unpaired t-test p-values comparing neurite GAD67 and Gephyrin protein puncta intensity and number from vehicle and IL-6 treated cultures. Metrics were averaged to give one data point per donor and then IL-6 treated culture values were calculated as a fold change from each donor's vehicle.

Finally, the co-localisation for each pair of pre- and post-synaptic protein was investigated: PSD95 with vGlut; GluN1 with SV2A; and Gephyrin with GAD67. This meant identifying regions of interest where positively identified puncta overlapped with the other paired puncta other along MAP2+ neurites. Areas of overlapping puncta stains are considered to be a possible pre- and post-synaptic point of connection. The overlap density fold change from vehicle-treated neurons to those having been exposed to IL-6 were compared with a Welch's t-test (Figure 6.6). Puncta co-localisation was found to be independent of the early acute IL-6 exposure in both control and 22q11.2DS genotypes, suggestive that the formation of such synaptic connections was not influenced by IL-6 exposure in both genotypes (Figure 6.6).

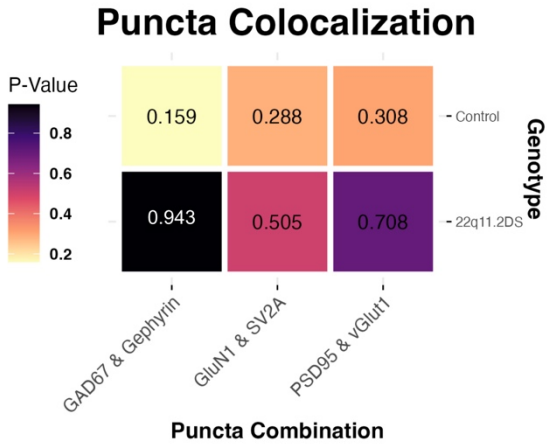

Figure 6.6 - Heatmap of two-tailed unpaired t-test p-values comparing colocalising puncta number in neurites from vehicle and IL-6 treated cultures. Metrics were averaged to give one data point per donor and then IL-6 treated culture values were calculated as a fold change from each donor's vehicle.

6.4 Discussion

This chapter focussed on examining (1) the long-term differentiation of neural progenitor cells (NPCs) in terms of cell fate and synaptic density in individuals with 22q11.2DS (N=2) compared to healthy control cells (N=4); and (2) how exposure to IL-6 in co-culture with microglia may interact with genetic background to influence the same parameters. The data suggest two main findings, although these should be considered preliminary due to the low sample size. First, the expression of GFAP was significantly higher in cultures from 22q11.2DS individuals than in healthy control-derived donor cultures and this did not seem to be affected by IL-6. Second, acute exposure to IL-6 during the NPC differentiation stage, when in co-culture with MGLs on the same genetic background, reduced the density of vGlut1 puncta in MAP2+ neurites by 50% *only* in the 22q11.2DS donor lines, with no effect of IL-6 observed in the healthy donor lines, suggestive of an interaction.

6.4.1 Increased GFAP expression in the hiPSC-derived 22q11.2DS cortical cell cultures

The increased staining for GFAP suggests that the 22q11.2DS genotype significantly influences cell fate differentiation during cortical neurodevelopment, and under the conditions tested, does so irrespective of IL-6 exposure. These data are consistent with findings of increased GFAP protein expression from previous studies using human adult *post-mortem* cortical brain tissue donated by from patients with ASC or SZ (Laurence and Fatemi, 2005; Crawford *et al.*, 2015; Toyoshima *et al.*, 2016). Although these studies utilised material from idiopathic cases and thus do not suggest a clear correlative link between the 22q11.2DS genotype and increased GFAP expression *per se*, the data from our *in vitro* model suggests this observation is potentially relevant for the link between 22q11.2DS and increased risk for ASC or SZ and that this may occur early in neurodevelopment. Astrocytes play crucial roles in both

the developing and adult brain including the regulation of synaptic development (Singh *et al.*, 2016) and transmission (Yang *et al.*, 2003; Ma *et al.*, 2016; Wang *et al.*, 2021). An increase of GFAP expression observed both in this chapter and NDD *post-mortem* tissue, caused either by an increased number of astrocytes in the developing brain or increased astrogliosis at a later disease stage, could support the notion that dysregulated astrocyte function may contribute as a mechanism for the precipitation of NDD symptoms. Furthermore, the 22q11.2DS genotype may prime these changes at an early stage of development, further contributing to this mechanism. Additional investigations are needed to comprehensively comprehend the molecular and functional implications of 22q11.2DS on astrocytes. Importantly, astrocytes also contribute to the production of complement C4, thereby establishing a connection to synaptic pruning and alterations to synaptogenesis (Yilmaz *et al.*, 2021). This concept underscores yet again the importance of examining the influence of genetic risk variants not only on neuronal cells but also on non-neuronal cells. Therefore, studying the impact of these variants on both neuronal and non-neuronal cells is crucial for a comprehensive understanding of their effects. Future investigations should aim to expand the sample size and perform more comprehensive analyses utilizing single-cell RNA sequencing techniques.

Moreover, through single-cell sequencing analysis of human organoids, it has been discovered that radial glia cells exhibit heightened responsiveness and susceptibility to IL-6 stimulation (Sarieva *et al.*, 2023). This heightened responsiveness is attributed to their increased immune response, reduced protein translation, and increased STAT3 phosphorylation (Sarieva *et al.*, 2023). Cells that express both TUJ1 and GFAP could either be considered as prenatal RGCs or foetal astrocytes. Given its essential role in both neuron and astrocyte development (Johnson *et al.*, 2016; Dráberová *et al.*, 2008), GFAP is expressed in RGCs (Sanai *et al.*, 2004; Middeldorp *et al.*, 2010). RGCs also express TUJ1, but then so do foetal astrocytes which also

express GFAP (Dráberová *et al.*, 2008; Toyoshima *et al.*, 2016). However, Pax6 is known to control radial-glia differentiation (Götz, Stoykova and Gruss, 1998), so it's lack of expression in these cell types suggest that they are post-radial glial and more foetal astrocyte specific. Therefore, it is not completely clear, under the conditions tested, precisely what cell type the increased subpopulation of cells directly belongs to. Nonetheless, it is possible that more radial glia cells that are transitioning towards an astrocyte fate could arise as a result of the 22q11.2DS genotype and thus present as a vulnerable cell type for the genetic and environmental interaction between the IL-6 and 22q11.2DS risk factors. To address the limited understanding of cell-specific vulnerability, more detailed insights can be obtained by conducting experiments using single-cell sequencing, which can provide results with greater granularity.

6.4.2 IL-6 and the 22q11.2 deletion may interact in NPCs to promote neuron differentiation with decreased vGlut1 density on neurites

Dysfunction in the regulation of glutamatergic neurotransmission is implicated in the development of schizophrenia (Moghaddam and Javitt, 2012). In brief, it is hypothesised that decreased activity of N-methyl-D-aspartate receptors (NMDARs) on inhibitory neurons can lead to glutamate neuron disinhibition, resulting in increased glutamate synaptic activity, particularly in the prefrontal cortex, because NMDAR antagonists can induce SZ-like symptoms (Moghaddam and Javitt, 2012). This also implies that excitatory and inhibitory signalling imbalances could result in altered neuronal circuitry and SZ-like symptoms (Adhya *et al.*, 2021). Furthermore, anomalies in NMDAR receptor function are thought to result in altered synaptic plasticity, poor information processing, and probable changes in brain network development and maturation, ultimately contributing to schizophrenia symptoms and pathophysiology (Moghaddam and Javitt, 2012). Hence, GluN1, the NMDAR subunit was chosen as a candidate for investigation by ICC. Interestingly however, there was no evidence

to suggest the expression of this synaptic protein was altered by either IL-6 or the 22q11.2DS genotype in this study. On the other hand, vesicular glutamate transporters (vGluts) have been identified as a strong candidate target to investigate the molecular basis of SZ, since the presynaptic transport of glutamate into vesicles via vGluts is a crucial point of control for normal synaptic activity, as it enables subsequent release into the synaptic cleft (Takamori *et al.*, 2000). Reduced presynaptic vGlut1 expression in 22q11.2DS neurites following IL-6 exposure during the NPC stage is a key finding of this chapter and supports the notion of a dysregulated of glutamatergic transmission as a priming mechanism for the putative neurodevelopmental origin of NDDs such as SZ. However, these findings both mimic and contradict similar studies presented in the following paragraph, in terms of the individual effects of IL-6 and genetic risk for NDDs.

In one such study, exposure of mouse neurons to IL-6 at an early stage of development led to an increase in vGlut1 puncta density and PSD95-vGlut1 colocalization (Mirabella *et al.*, 2021). The main difference between that study and this one is the species involved and the timing of IL-6 exposure, specifically the species difference from mouse to human. Conversely, in human *post-mortem* tissue from individuals with SZ, vGlut1 protein expression is decreased in the anterior cingulate cortex and therefore aligns with the results of this chapter (Oni-Orisan *et al.*, 2008). It was also found that haloperidol treatment did not affect vGlut1 expression in rats, suggesting that antipsychotic treatment is not a confounding factor of vGlut1 expression (Oni-Orisan *et al.*, 2008). This is similarly observed with SV2A expression suggesting no effect from antipsychotic treatment (Onwordi *et al.*, 2020; Halff *et al.*, 2021). Finally, in a study conducted by Kathuria *et al.* (2022), it was revealed that hiPSC-derived neurons exhibited a substantial decrease in dendritic spine density following a 3-day exposure to 25ng/ml IFN-γ during the differentiation process (Kathuria *et al.*, 2022). However, when exposed for an equal

duration to 1µg/ml IL-6, no significant reduction in dendritic spine density was observed (Kathuria *et al.*, 2022). Hence, it is plausible that the impacts of IL-6 and genetic risk factors for NDDs are specific to certain brain regions, the type of exposure, or even the species under investigation.

Finally in section 5.3.2 of the previous chapter, which discussed enriched transcriptome pathways found in NPCs after IL-6 stimulation, it was observed that the "Presynapse" pathway (FE = 2.49, p = 2.41x10-4, FDR = 0.016) was up-regulated in the basal 22q11.2DS NPC transcriptome (signature G). This dysregulation of presynapse-associated gene products was also previously identified in 22q11.2DS hiPSC-derived cortical neurons (Nehme *et al.*, 2022). One piece of imaging data presented in this chapter supports the notion that presynapse products are dysregulated during development in 22q11.2DS donor cells. According to the data presented here, the dysregulation effect becomes evident only once NPCs differentiate into mature neurons and their synapses develop along neurites, whose length appears to be affected by early IL-6 stimulation. Thus, it is possible to speculate that presynapse dysregulation, influenced by the 22q11.2DS genotype, leading to decreased density of vGlut1 expression in IL-6 treated 22q11.2DS mature neurons.

The experiments of this chapter are the first to demonstrate a potential interaction of both 22q11.2DS and IL-6 in priming an early change in vGlut1 expression in human mature differentiated neurons. In future experiments within this context, there are several promising directions to explore based on the current observations. Firstly, expanding the sample size would enhance statistical power and ensure a more representative sample of the population, enabling a more robust analysis of the underlying mechanisms driving the observed findings. Furthermore, delving into the potential involvement of synaptic pruning mechanisms by

investigating the expression of complement proteins on the neurons and the engulfment of synaptic material by astrocytes could provide a clearer understanding of synaptic remodelling in relation to the increased GFAP+ expression observed here. It is important to note, however, that the presence of more GFAP+ cells and lower vGlut1 synaptic puncta does not necessarily indicate a reduction in synapse density. Rather, these findings may suggest the presence of a specific glutamatergic dysfunction that merits further investigation and characterisation. To obtain a more comprehensive understanding of overall changes, proteomics could be employed to quantitatively measure synaptic proteins in an unbiased manner. Additionally, functional readouts such as multi-electrode array (MEA) or electrophysiological recordings could be employed to assess the functional consequences of altered presynaptic products after IL-6 stimulation or 22q11.2 region deletion. These approaches are particularly relevant considering the findings of Khan and colleagues (2020), who reported evidence of defects in calcium signalling in neurons derived from donors with 22q11.2DS (Khan *et al.*, 2020).

6.4.3 Chapter Limitations

The results from the previous chapter suggest that neither IL-6 nor other cytokines produced by microglia in response to IL-6 were shown to alter the transcriptional profile of NPCs after 24 hours of co-culture. As a result, it is challenging to conclude that exposure to IL-6 during the NPC stage is responsible for the reduction of vGlut1 density and increased neurite outgrowth in 22q11.2DS cells. However, changes at the protein level may indicate that NPCs did respond to IL-6, but the 24-hour timepoint was too late to detect a change in the NPC's profile. Overall, based on the metrics measured in this chapter, a single acute exposure of IL-6 to NPCs in co-culture with microglia does not appear to be sufficient to cause significant differences in synaptic development in mature neurons from either genotype. In order to address this issue, future studies should strive to employ proteomics techniques to

quantitatively assess synaptic proteins in an unbiased manner, which would provide a more comprehensive view of changes within the synaptic proteome.

There were several limitations to the imaging process and experimental setup that restricted downstream analysis. The magnification used (20X) did not provide enough detail for each synapse but allowed for more images to be obtained for high-throughput analysis. The plating density also made it difficult for the software to identify neurites, and although all cells were seeded at the same density, cell migration during differentiation resulted in denser areas with more processes, which could affect the results. To mitigate this problem, 10 images were taken per well, but inherent migration differences between genotypes could still confound the results. Lastly, it is important to mention that while donors were plated individually on separate plates, the staining process was conducted in batches consisting of donor pairs. Consequently, discernible variations were observed in the data between different staining batches. To mitigate the influence of these batch effects, it was imperative to calculate fold change values for each donor's vehicle condition as a means of normalization. This made it inappropriate to compare metrics across genotypes directly, and comparisons had to be inferred through t-tests. In future experiments, multiple donors should be plated on one plate to allow for a comparison between excitatory and inhibitory neurons across genotypes. This is particularly relevant given the hypothesis that an imbalance of these neuron types is a hallmark of NDD pathology (Adhya *et al.*, 2021). Regarding sample sizes, it's worth noting that our study only involved a small number of donor lines and a very brief exposure to IL-6. This limited the opportunity for microglia and neurons to secrete cytokines and chemokines that could potentially influence the differentiation of NPCs, such as TNFα, VEGF, and others. To gain a deeper understanding, it may be necessary to extend the duration of exposure to IL-6 or consider leaving the cells

together for a longer period, allowing for more significant interactions and potential impacts on NPC differentiation.

6.5 Conclusion

The development of the cerebral cortex is a highly regulated process involving the proliferation, differentiation, and migration of neural progenitor cells into specialized mature cell types such as cortical neurons and astrocytes. This process is vital for the formation of functional neural circuits, and disruptions from genetic or environmental factors can increase the risk of neurodevelopmental disorders. The study investigated the effect of the 22q11.2DS deletion and IL-6 exposure when in co-culture with MGLs at the neural progenitor cell (NPC) stage on subsequent cortical differentiation trajectories by analysing the expression of cell-specific markers in terminally differentiated cortical neurons. The results showed the number of GFAP+ cells were significantly higher in cultures from 22q11.2DS individuals than in control-derived donor cultures, mimicking a molecular phenotype of NDDs for which 22q11.2 is a highly penetrant genetic risk factor. Acute exposure to IL-6 during the NPC differentiation stage, when in co-culture with MGLs also appeared to reduce the density of vGlut1 puncta in MAP2+ neurites by 50% in 22q11.2DS cells, while control cells did not show this reduction, although overall synaptic density *per se* did not appear to be affected. To gain a deeper understanding of potential glutamatergic neuron dysfunction in these cells at the protein level, it is necessary to investigate the synaptic proteome by mass-spectrometry, super-resolution microscopy thereby enabling the examination of protein distribution with high resolution, and functional readouts using methods like MEA or electrophysiology. Overall, these findings provide a methodological framework in which one can use hiPSC co-culture models to explore the interactions between genetic risk factors and prenatal inflammatory events mediated at least in part by IL-6.

Chapter 7

General Discussion and Conclusion

Neurodevelopmental disorders encompass a range of conditions that cause developmental deficits in areas such as communication, social interaction, cognition, and externalising and internalising behaviours in the affected offspring. These are lifelong conditions, which significantly affect an individual's quality of life. Whilst there is evidence to suggest that both genetic and environmental factors combine to determine the risk of developing an NDD, our understanding of their molecular basis and the specific cellular contributions involved remains limited, especially in the context of human-led models. Specifically, research into associations between genetic and environmental risk factors is focussed on epidemiological studies, with animal models contributing important causal evidence and clues to the cellular and molecular basis. Critically however, there are important distinctions between rodent and human neurodevelopment, which naturally raise concerns about the extent to which findings from animal models may translate to humans. To address this gap in our knowledge, researchers are increasingly employing human induced pluripotent stem cells as a human-led *in vitro* model to explore the neurobiology of NDDs. These investigations have however predominantly focussed on genetic risk factors, overlooking the potential influence and/or interaction with environmental factors that can be modelled, from a reductionist point of view *in vitro*. Moreover, the emphasis remains on studying neurons, thus neglecting the potentially crucial role of glial cells. This is relevant, since several lines of evidence implicate microglia for example, the pathophysiology of NDDs. Hence, developing human *in vitro* models to study gene by environment interactions, using hiPSC, which incorporate microglia is necessary to advance our knowledge of proximal cellular and molecular mechanisms of NDDs.

The overall aim of this project is therefore to develop, validate, and test a hiPSC model to study the pathophysiology of NDDs that captures gene by environment interactions in neurons and microglia within a human relevant context. In the case presented in this thesis, we chose IL-6

as the environmental insult, and the 22q11.2 deletion genotype as our genetic risk. The initial objective was to create and characterise a 2D multi-cell type hiPSC model (neural progenitor cells and microglia) to examine the signalling mechanisms of IL-6. During this process as presented in chapter 3 and 4, the dosage, timing, and duration of IL-6 cytokine treatment were optimised first in hiPSC-derived neuronal and microglial progenitor monocultures. This was subsequently replicated in an NPC-MGL co-culture in chapters 5 and 6, where the objective was to determine the immediate and long-term effects of IL-6 exposure on co-cultures that had undergone terminal differentiation into neural and microglial cells. This evaluation was conducted at both the molecular level using RNA sequencing and at the cellular level by examining the expression of GABAergic and glutamatergic synaptic markers by immunocytochemistry and high-content imaging. A key focus of this objective was to test the potential for this hiPSC model to evaluate gene-environment interactions. This was accomplished in chapters 5 and 6, by comparing the above-mentioned outcomes between hiPSC-derived co-cultures from healthy donors and those with a known genetic risk for neurodevelopmental abnormalities, in this case the 22q11.2 deletion, when exposed to IL-6. It was first hypothesised that exposing forebrain neuronal cultures to IL-6 would result in decreases and increases in the expression of GABAergic and glutamatergic synaptic markers respectively, as well as gene expression signatures in both neurons and microglia that would overlap with similar data from ASC and SZ brain *post-mortem* tissue since IL-6 is implicated in these disorders from both human and animal model studies. It was additionally predicted that IL-6 would interact with the pre-existing 22q11.2DS genetic risk to increase the severity and spectrum of cellular and molecular abnormalities in our hiPSC-derived model. The upcoming discussion will focus on the obtained results in relation to the stated objectives, assessing whether these findings have provided insights into the proposed hypotheses, and

explore potential avenues for expanding this study to address additional questions that could not be answered by the data presented in this thesis.

7.1 Acute IL-6 Stimulation Results in a SZ-Relevant Response from hiPSC derived Microglia, but not Neural Progenitor Cells

7.1.1 hiPSC-derived NPCs from neurotypical donors cannot respond to exogenous IL-6 via cis-signalling

In developing the multi-cell hiPSC-derived model, cell-specific responses of microglia and neural progenitor cells to exogenously added IL-6 were uncovered. Specifically, the hiPSC-derived microglia in monoculture were found to respond to IL-6 via the canonical IL-6Ra signalling pathway, with a clear increase in STAT3 phosphorylation (Couch *et al.,* 2023). In contrast, neural progenitor cells in monoculture no STAT3 phosphorylation was observed, due to very low *IL6R* gene expression and very low to no secretion of the soluble IL6 receptor (sIL-6Ra) (Couch *et al.*, 2023). The sIL-6Ra was however secreted by the microglia in response to IL-6 and when this protein was added exogenously to NPC monocultures in combination with IL-6 in chapter 3, STAT3 phosphorylation was observed in NPCs consistent with IL-6 trans-signalling. These data suggest that, under the conditions tested microglia are the cell types that will respond directly to changes in local levels of IL-6, while human NPCs will only do so when in combination with sIL-6Ra secreted from other cell types, or will respond indirectly via other cytokine and chemokines, released from the microglia in response to the initial IL-6 stimulus. Consistent with this view, Sarieva *et al.* (2023) exposed hiPSC-derived dorsal forebrain organoids to a constitutively active form of IL-6 called Hyper-IL-6 (Sarieva *et al.*, 2023). Although microglia were absent from these cultures, Hyper-IL6 which represents a cross-linking of IL-6 and sIL-6Ra, was sufficient to cause activation of JAK/STAT3 signalling

pathways in the organoid cultures that did not contain microglia (Sarieva *et al.*, 2023). This study also confirmed the absence of human IL-6Ra protein expression in neural progenitor cells using human foetal *post-mortem* brain tissue, demonstrating consistency between our hiPSC model and human primary tissue (Sarieva *et al.*, 2023; Couch *et al.*, 2023). Interestingly, radial glia cells were the cell type which showed the largest response to the Hyper-IL-6 signalling by having the greatest number of DEGs in single-cell RNAseq, plus was there an additional difference in their cortical layering as measured by immunostaining and microscopy (Sarieva *et al.*, 2023). These findings provide further evidence to support our claim that the activation of JAK/STAT3 pathway signalling in NPCs and cortical neurons requires the presence of both sIL-6Ra and IL-6, yet it is not clear to the extent radial glial cells would be present in the NPC monocultures. Combined with the data presented in this thesis (Couch *et al.*, 2023), the findings of Sarieva *et al.* (2023) contradict the findings of a recent paper by Kathuria and colleagues (2022), in they propose a response to exogenous IL-6 in monocultures of cortical neurons derived from hiPSC. The authors did not however explicitly confirm that IL-6 led to activation of canonical IL-6Ra signalling, nor did they address the presence or absence of sIL-6Ra, as discussed in section 3.4.2 (Kathuria *et al.*, 2022). Taken together, these findings supported the ensuing chapter 4's goal of characterising the IL-6-induced response in microglial cells more thoroughly, to investigate the effects of IL-6 on changes in the structure and function of microglia.

7.1.2 Acute IL-6 stimulation of hiPSC-derived microglia from neurotypical donors recapitulates cellular and molecular phenotypes relevant for schizophrenia

During the characterisation in chapter 4, the response of microglia to 100 ng/ml exogenous IL-6 for 3 hours was found to induce transcriptional changes that overlapped with gene expression data from SZ *post-mortem* brain tissue but did not alter the expression of genes associated with

SZ risk, as measured by GWAS. These data are consistent with the known associations between elevated IL-6 levels and increased risk for SZ in humans, as demonstrated at multiple stages through life, including in maternal serum (Allswede *et al.*, 2020), in children aged 9 (Khandaker *et al.*, 2014) and young adulthood at ages 18-25 (Schwieler *et al.*, 2015). Furthermore, our data regarding the microglial response to IL-6 replicated some key findings from rodent models of MIA, with respect to microglia form and function. Specifically, first, the transcriptional response of the hiPSC-derived microglia at 3h to exogenous IL-6 overlapped significantly with the transcriptome of microglia isolated from the brain of new-born pups (PND0) exposed to MIA on GD15 *in utero* using Poly I:C, in section 4.3.3 (Matcovitch-Natan *et al.*, 2016). Second, we observed increases in both *IRF8* expression and increased cytoplasmic motility in section 4.3.4, consistent with IRF8-dependent microglia motility observed in mice and increased microglia motility observed both *in vivo* and *in vitro* in response to Poly I:C stimulation, an effect shown to be mediated via IL-6 signalling (Ransohoff and Engelhardt, 2012; Ormel *et al.*, 2020; Ozaki *et al.*, 2020). Third microglia and co-cultures secreted MIP-1α in response to IL-6 in both sections 4.3.5 and 5.3.4, which is also strongly up-regulated in the maternal serum of rodent MIA models and the foetal brain (Meyer *et al.*, 2006; Arrode-Brusés and Brusés, 2012; Osborne *et al.*, 2019; Brown *et al.*, 2022). Finally, Hyper-IL-6 stimulated organoids also revealed the upregulation of genes associated with ASC (Sarieva *et al.*, 2023), supporting the transcriptome overlaps presented in sections 4.3.3 and 5.3.1. The data presented in chapter 4 and 5, which drew upon similarities observed in animal models of MIA, *post-mortem* data from patients with SZ, and *in vitro* models using primary cells, provides a strong rationale for the involvement of both IL-6 and microglia in the molecular mechanisms underlying the risk of NDDs. Taken together, these data demonstrated the nature of the microglial response generated when exposed to IL-6, which, if tested, could influence neural progenitor cells after stimulation of these two cell types in co-culture.

Taking these data together, a reasonable assumption is that Microglia that secrete sIL-6Ra, (independently of IL-6 exposure) when in co-culture with NPCs would enable the NPCs to respond to IL-6 via trans-signalling. After characterising the impact of IL-6 exposure in NPC-microglia co-cultures however (chapter 5) the data suggested that the chosen experimental set-up might not, in fact, be optimal. Specifically, we were unable to demonstrate convincing changes to the neural progenitor cell transcriptome within 24h of acute IL-6 stimulation to the co-culture, despite data suggesting a robust transcriptional response and altered secretome of the hiPSC-derived microglia. A pragmatic interpretation of these data is that our model requires either additional cell types, such as astrocytes and endothelial cells, in combination with developing neurons and microglia (as discussed in section 5.4.3). Such an experiment has been outlined in later sections. Or, that the duration of IL-6 exposure was insufficient in this model to generate a response.

7.2 The Use of hiPSCs to Model the Gene-Environment Interactions relevant for NDD pathophysiology

The hiPSC model characterized in this thesis served as a valuable tool for investigating the interplay between genetic and environmental factors in the development of cortical NPCs. The cortex was specifically chosen as the focus brain region of the model due to the presence of abnormal cortical neuron organization observed in *post-mortem* studies of individuals with ASC and SZ (Kulkarni and Firestein, 2012; Schafer *et al.*, 2019). Additionally, prenatal exposure of offspring to Poly I:C, mimicking MIA has been shown to alter cortical development and raise cytokine levels in the prefrontal cortex (Garay *et al.*, 2013; Meyer, 2014; Li *et al.*, 2018). Moreover, the Srivastava and Vernon labs had established and quality-

controlled protocols for generating hiPSC-derived cortical neurons as demonstrated in section 3.3.1, making them suitable for this investigation (Warre-Cornish *et al.*, 2020; Adhya *et al.*, 2021; Bhat *et al.*, 2022; Couch *et al.*, 2023). Although it should be noted that it is not unexpected for gene-environment interactions to affect other brain regions, such as dopaminergic (DA) neurons in the ventral midbrain which have also been identified as an affected population by MIA (Vuillermot *et al.*, 2010; Purves-Tyson *et al.*, 2021). Yet, as a practical first step, it was decided to start with cortical neurons, but there is clearly room to expand this to other cell types, such hiPSC-derived DA neurons (Reid *et al.*, 2022), in future studies.

7.2.1 The interaction between IL-6 and the 22q11.2 deletion region genotype in NPCs and MGLs

To explore the impact of acute IL-6 exposure on cortical NPCs, co-cultures derived from both healthy donors and individuals with a 22q11.2 deletion were subjected to this stimulation. Transcriptomic analysis was conducted to examine the molecular effects. The results revealed the presence of the 22q11.2 deletion influenced the developmental transcriptome of NPCs in the cortical region. Acute stimulation with IL-6 seemed to have little impact on the NPC transcriptome but induced a robust response from hiPSC-derived MGLs. In chapter 5, the patterns of differentially expressed genes and secreted proteins in the MGL-NPC co-culture samples suggest alterations to the vasculature and extracellular matrix are important mechanisms to investigate in future studies. In this context it is worth noting that serum levels of vascular endothelial cytokines (VEGF, ICAM-1 and VCAM-1) have been identified as elevated in individuals with SZ (Nguyen *et al.*, 2018). Furthermore, the 22q11.2DS genotype is associated with endothelial and brain barrier disruption, as discussed in section 5.3.2 (Crockett *et al.*, 2021; Y. Li *et al.*, 2021; Li *et al.*, 2023). Separately, as covered in section

1.2.2, Matcovitch-Natan *et al.* (2016) demonstrated that MIA negatively affected the developmental programming of microglia, compromising their intended developmental function (Matcovitch-Natan *et al.*, 2016). Combining this, with the transcriptome and secretion data from Chapter 5, as well as the fact that microglia are thought to play important roles in guiding angiogenesis and vasculature development in the foetal brain (Greenberg and Jin, 2005; Checchin *et al.*, 2006; Fantin *et al.*, 2010; Rigato *et al.*, 2011; Yang *et al.*, 2020), leads us to the conclusion that signals originating from the microglial IL-6 response and the 22q11.2DS would lead to a shift in typical microglial function aimed at developing vasculature, compromising vasculature development and endothelial function. This notion gains further support in its role in NDD pathogenesis, from the transcriptomic analysis conducted in chapter 4 and 5, where the response of microglia to IL-6 demonstrated significant overlap with gene expression patterns observed in *post-mortem* tissue from SZ patients, and that therefore the same microglial-IL-6 response transcriptome that has altered vasculature regulation pathways, also hold relevance to the transcriptome of adults with SZ.

Importantly, our model also permitted investigation of the downstream effects on long term neural progenitor differentiation into specialized mature cell types in chapter 6, in this case upper- and lower-layer cortical neurons and astrocytes. The results suggest that cultures from 22q11.2DS individuals had significantly higher numbers of GFAP+ cells that was unaffected by IL-6 stimulation, mimicking a relevant cellular phenotype associated with NDDs, as demonstrated by data from both rodent MIA models and *post-mortem* tissues from individuals diagnosed with ASC and SZ (Kiehl *et al.*, 2009; Crawford *et al.*, 2015; Mariani *et al.*, 2015; Toyoshima *et al.*, 2016; Marchetto *et al.*, 2017; Velmeshev *et al.*, 2019; Michel *et al.*, 2021; Price, Jaffe and Weinberger, 2021). Of note however, only neurons derived from donors with 22q11.2DS did acute exposure to IL-6 during the differentiation stage of NPCs result in a 50%

reduction in the density of vGlut1 puncta in MAP2+ neurites, which was not observed in the neurotypical control donor neurons. This finding supports the notion discussed in section 6.4.2 that the glutamatergic transmission abnormalities found in NDDs such as SZ (Oni-Orisan *et al.*, 2008), may be influenced by both IL-6 signalling and the presence of the 22q11.2DS genotype.

Overall, these findings suggest that both IL-6 exposure and the 22q11.2 deletion contribute as risk factors to the threshold at which atypical neurodevelopmental phenotypes precipitate. The more risk factors present, whether genetic or environmental, the more likely the precipitation of NDDs. However, the limitations of the experimental design of both RNAseq and high-throughput imaging did not permit any sturdier conclusions on their direct interactions. Therefore, further experiments are required to overcome these limitations, which are further outlined in the following sections.

7.3 Overall Study Strengths and Weaknesses

7.3.1 The Advantages and Disadvantages of a 2D co-culture system

The use of a 2D culture system in this thesis was advantageous for analysing the cell-specific responses of NPCs and MGLs. Significantly, the protocol utilized for obtaining microglia-like cells from hiPSCs effectively mirrors, to the best extent achievable in a laboratory setting, the *MYB*-independent developmental process of microglia (van Wilgenburg *et al.*, 2013; Hoeffel and Ginhoux, 2015; Haenseler *et al.*, 2017). Furthermore, the positive identification of microglia-like cells through protein staining (as described in Chapter 3) and transcriptomic analysis (as presented in Chapter 5), which specifically indicate the expression of microglia-specific markers, strongly supports the successful independent replication of this protocol

(Haenseler *et al.*, 2017; Couch *et al.*, 2023). However, the 2D co-culture culture system also highlighted the necessity of incorporating other cell kinds to make our model more complicated. Expanding upon the findings of this study and the research conducted by Sarieva *et al.* (2023), it becomes evident that a promising approach for further investigation would be to integrate their organoid model grafted with microglia (Fagerlund *et al.*, 2022; Schafer *et al.*, 2023). This combination offers a viable pathway to examine whether the release of sIL6R from microglia can indeed have an impact or not. It would also deepen our understanding of the specific cell types involved in mediating the IL-6 risk for NDDs at a cellular signalling level and is discussed in the subsequent section regarding future experiments. To gain a comprehensive understanding of the true nature of NDD molecular and cellular phenotypes, further development of hiPSC-derived models that include microglial cells is necessary. Such experiments are discussed in section 7.4.2.

7.3.2 Harnessing the heterogeneity of hiPSC-derived model systems

The genetic and experimental heterogeneity of an hiPSC-derived system resulted in large variations within our dataset, calling for a cleaner experiment by implementing a combination of isogenic, diagnoses-based and population-based approaches to reduce this variability (Nehme *et al.*, 2022). The implementation of an isogenic system would provide valuable insights by confirming the specific effects associated with a 22q11.2 deletion of a known size compared to the absence of such a deletion on the same genetic background and thereby reducing the variation in results induced by the 22q11.2 region differences across 22q11.2DS donors (Table 2.2). This approach would ensure genetic uniformity, as demonstrated by Nehme and colleagues in their CRISPR-mediated deletion of the 22q11.2 region (Nehme *et al.*, 2022). Here, Nehme and colleagues were able to showcase that the SZ-related phenotypes seen in their hiPSC-derived models was in fact to do with the deletion itself, rather than other areas of

the genome, by comparing the CRIPSR-mediated lines to those derived from patients with 22q11.2DS. Following on from this therefore, an important aspect to consider is the impact of diagnosis. It is well-established that the penetrance of SZ can vary within individuals with 22q11.2DS, and there is evidence suggesting differences between individuals with 22q11.2DS who have been diagnosed with SZ and those without such a diagnosis (Li *et al.*, 2019; J. Li *et al.*, 2021). Therefore, in order to examine the influence of SZ penetrance, it is necessary to expand upon the research conducted by Nehme *et al.* (2022) by including donors who possess the 22q11.2DS genotype, both with and without diagnoses, for instance. Finally, to compliment this type of analysis, the research conducted by Wells and colleagues (2023) showcases the implementation of a "cell village" system, which can be used to assess the generalizability of results obtained from isogenic experiments. In a cell village system, thousands of cells from numerous donors are pooled together in a shared *in vitro* environment and subsequently analysed simultaneously through single-cell RNA sequencing (Wells *et al.*, 2023). This approach allows for the preservation of individual donor genetic variations while multiplexing them into a single experiment for comprehensive analysis. Therefore, using hiPSC-derived models in a combination of isogenic, diagnoses-based and population-based approaches is necessary to complement each other.

In addition, enhanced experimental design within familial contexts should be considered, due to the adverse consequences of heightened genetic variation from un-related donors. It must be considered that gene expression results can significantly vary among individual donors in hiPSC studies. Therefore, the modest sample sizes used through this thesis may influence the ability to detect statistically significant differences from the data presented throughout. For instance, *IL10* expression in 3h IL-6 treated D1 MGLs was not statistically significant but exhibited a higher fold change (~5-fold) compared to 3h IL-6 treated D14 MGLs (~3-fold),

which did in-fact pass statistical significance thresholding (Figure 3.5B). Therefore, although statistical significance may not be reached for certain experiments in this thesis, it does not negate the potential biological significance to be present, and vice versa. Notably, robust fold change differences were observed in receptor expression changes, such as *IL6R* and *IL6ST* expression in NPCs (hiPSC vs D18 NPC: *IL6R* = 0.137-fold change, *IL6ST* = 6.50-fold change), despite the lack of statistical significance. Confirming or disproving our findings would necessitate replication studies with larger sample sizes. Evidently, the smaller the sample size the more likely we will see variation from the true population effect. The number of donor lines required to achieve a specific level of statistical power for the detection of biologically relevant gene expression fold changes can be calculated using the R package "PROspective Power Evaluation for RNAseq" (PROPER, v1.0.0) (Wu, Wang and Wu, 2015), as demonstrated by Khan *et al.* (2020) using their RNAseq dataset acquired from hiPSC-derived neurons of 22q11.2DS patients (Khan *et al.*, 2020). Simulating this study would provide the minimum number of hiPSC lines required to detect relevant changes in the gene expressions of RNAseq datasets presented in this thesis.

Furthermore, evidence from rodent models suggests sex-specific microglial differences at functional, structural, and transcriptional levels (Guneykaya *et al.*, 2018; Villa *et al.*, 2018; Han *et al.*, 2021). While the optimisation experiments in chapters 3 and 4 were conducted using three individual clones per donor from N=3 male donor lines, we cannot discount the possibility of genotype- or sex-specific IL-6 responses based on the select few donors included in these experiments. Nevertheless, the sample sizes used in the original optimisation experiments in chapters 3 and 4 aligned with existing studies investigating the impact of IL-6 on neurodevelopment using hiPSC models (Kathuria *et al.*, 2022; Sarieva *et al.*, 2023). This highlights the need of the hiPSC field to develop superior methods for selecting the optimal

number of hiPSC donor lines to use. It has been more recently recommended that a higher number of donors be included as biological replicates rather than focusing simply on the number of clones per donor, as this method improves statistical power (Dutan Polit *et al.*, 2023). Furthermore, the selection of control hiPSCs should be carefully considered, with the recommended practise of using sex-matched family members or individuals matched for age, sex, and ethnicity to account for key biological characteristics (Dutan Polit *et al.*, 2023).

Finally, given the variations in differentiation and cytokine exposure protocols across different laboratories, there is a substantial risk that reproducibility and the validity of mechanistic data from hiPSC models could be compromised (McNeill *et al.*, 2020; Dutan Polit *et al.*, 2023). Therefore, multiple replication experiments by multiple research groups to reproduce the results presented here, as well as including a comparison to common hiPSC reference line such as the corrected KOLF2.1 line, will be a crucial advancement for the field to increase reproducibility across different groups (Volpato and Webber, 2020; Pantazis *et al.*, 2022).

7.3.3 Confounding microglial reactions to experimental effects

To begin with, it is important to consider the potential impact of using acetic acid as a vehicle and the disturbance caused by media exchange during the experimental procedures conducted in this thesis. These factors may have affected the response of MGLs since they are particularly sensitive to their surrounding environment. Consequently, these influences have the potential to introduce confounding factors that could influence the response of microglial cells to IL-6. The clearest example of this is in the MGL motility experiment from chapter 4 when, following a 3-hour treatment, the addition of the acetic acid vehicle alone significantly enhanced the cells' cytoplasmic distance and displacement (Figure 4.5D). To reduce the confounding of acetic acid activation in the data, a comparative approach was used in statistical analysis, which compared

the IL-6 treatment group to the acetic acid treatment group as a fold change. However, the fact that acetic acid is fundamentally altering the MGLs' functionality and producing a different response to IL-6 cannot be discounted. To ensure comprehensive analysis, future experiments that stimulate MGLs with any agent should incorporate an additional untreated control condition to properly address the potential impact of the vehicle used in the experimental procedures.

7.4 Future Experiments

Future experiments aimed at investigating the complex interplay between genetic factors, environmental influences, and neural development in individuals with 22q11.2DS could incorporate the following various approaches to gain a deeper understanding of the underlying cellular and molecular mechanisms.

7.4.1 Do microglia respond to the IL-6 signal through cis- or trans-signalling, and could these have different outcomes on the developing NPCs?

First, investigating the specific effects of cis- and trans-signalling of IL-6 on NPCs could provide insights into the distinct mechanisms through which IL-6 influences neural development. By differentiating between these signalling pathways, researchers will be able to gain a more comprehensive understanding of the molecular pathways involved, whether cis- or trans-signalling is deemed more pathological than the other, and potentially identify therapeutic targets specific to each type of signalling. To provide an example, it would be beneficial to understand whether the MGLs primarily respond to IL-6 through cis- or trans-signalling when grown individually, as this remains unclear based on the results presented in this thesis. Furthermore, it is unclear what causes MGLs to release sIL-6Ra, since this was

unaffected by IL-6 signalling itself. To differentiate between the two pathways, the use of soluble IL-6RA (sgp130) as an inhibitor of the sIL-6Ra:IL-6 complex can be added to the *in vitro* model presented in this thesis (Jostock *et al.*, 2001). This inhibition would specifically block trans-signalling, allowing for the identification of differences in the IL-6 response generated by MGLs after cis- and trans-signalling, and thereby highlighting which type of signalling could be more pathogenic. However, it should be noted that there are currently no approved drugs targeting sgp130. Nevertheless, a recent trial has reported promising outcomes for the sgp130 fusion protein, olamkicept, in treating active inflammatory bowel disease (Schreiber *et al.*, 2021). In addition, tocilizumab, a humanized monoclonal antibody targeting IL-6Ra, inhibits both trans- and cis-IL-6 signalling (Foley *et al.*, 2023). Tocilizumab has been licensed in the UK for the treatment of rheumatoid arthritis and currently, a randomized, double-blind, placebo-controlled trial is being conducted to investigate the effects of tocilizumab in patients with psychosis (Foley *et al.*, 2023). The goal of this trial is to determine whether IL-6 can contribute to the onset of first-episode psychosis and to identify the underlying molecular mechanisms involved (Foley *et al.*, 2023). Hence, if future studies confirm the involvement of IL-6 trans-signalling in the development of NDDs, drugs like olamkicept and tocilizumab could be considered as valuable treatment options to reduce the risk of NDD onset in high-risk patients. To further enhance the findings of Foley *et al.*'s (2023) study, it would be interesting to generate hiPSC lines from the trial participants and subsequently differentiate them into NPCs and MGLs, to allow for a direct investigation into the specific mechanisms through which this drug may exert its effects.

7.4.2 Advancing the MGL and NPC co-culture: how can we expand to additional cell types without complicating the results?

Second, to gain a more comprehensive understanding of the cellular interactions involved, it is suggested that future experiments expand beyond 2D co-cultures and embrace more complex multicellular models, depending on the specific research question. For example, if the objective is to investigate the impact of the microglial response to IL-6 on various cell types beyond developing NPCs, it will be necessary to incorporate other cell types, including astrocytes, oligodendrocytes and the endothelial vasculature. This approach could provide valuable insights into their contributions to the findings presented in this thesis, as discussed in section 5.4.3. In order to maintain a more cell-specific examination of the expected outcomes, incorporation of these cell types could be achieved in a 2D setup assembled into a multi-culture configuration using an on-a-chip platform, enabling their interaction while maintaining physical separation (Pașca *et al.*, 2022). Notably, Liu *et al.* (2022) have successfully implemented a brain-on-a-chip model that combines hiPSC-derived neurons and astrocytes (Liu *et al.*, 2020; L. Liu *et al.*, 2022). This technology was used by Liu and colleagues been utilized for neurotoxicity screening, and holds potential for personalized medicine and disease modelling, serving as an alternative to animal testing for drug screening (Liu *et al.*, 2020; L. Liu *et al.*, 2022). In addition, vessel-on-chip technology exists for hiPSC-derived endothelial cells and their influence on other cell types such as vascular smooth muscle cells (Vila Cuenca *et al.*, 2021). Therefore, this type of technology could be employed to address the question of whether the microglial response to IL-6 influences NPC development via vasculature remodelling, by integrating developing neurons, microglia, and endothelial cells through the brain-on-a-chip fluidics system. This approach would enable the study of the combined influence of IL-6 and NDD genetic risk on vasculature development.

Separately, incorporating microglial cells into 3D organoid cultures could also provide a representative model of the neural and non-neural environment affected in 22q11.2DS. However, it is important to consider the diversity of organoids, as emphasized in a recent consensus paper by prominent researchers in the field (Pașca *et al.*, 2022). This leads us to question which type of organoid would best suit our specific research objectives. While incorporating multiple cell types is valuable, it is crucial to identify the research question that requires additional complexity in the experimental model. Simply introducing more cell types does not guarantee a comprehensive understanding of the underlying mechanisms (Pașca *et al.*, 2022; Couch *et al.*, 2023). By clarifying our research objectives and considering the inherent complexities of the biological processes under investigation, we can determine the most appropriate organoid system to employ (Pașca *et al.*, 2022). Based on the findings from chapter 5, which demonstrated changes to transcriptional pathways and secreted molecules involved in extracellular matrix (ECM) remodelling after co-culture exposure to IL-6 and the presence of the 22q11.2DS deletion, it would be valuable to investigate whether the microglial response to environmental factors can influence cortical neuronal migration in individuals with the 22q11.2DS genotype. In this context, the incorporation of microglia-grafted cerebral cortex organoids offers distinct advantages, as demonstrated by the work of Fargerlund *et al.* (2022). These organoids not only exhibit cortex-like structural formations and capable of action potential firing, like non-microglial-containing cerebral organoids, but they also display more mature and diverse neuronal phenotypes compared to organoids without microglia (Fagerlund *et al.*, 2022). Advancing the utilization of these microglia-grafted organoids, Schafer *et al.* (2023) have recently introduced an innovative *in vivo* neuroimmune organoid model for investigating human microglial phenotypes (Schafer *et al.*, 2023). In their study, the microglia-grafted organoids were xenotransplanted into mouse brains, enabling Schafer and colleagues to observe specific morphological differences in the microglia that resembled more closely

those from human *in vivo* developing tissue (Schafer *et al.*, 2023). Notably, they found enhanced soma size, increased thickness of primary processes, and a higher number of filopodia on each process in microglia of the organoids derived from individuals with ASC compared to those from control donors (Schafer *et al.*, 2023). Building upon this technology and applying it to the research question addressed in this thesis, we could generate organoids from 22q11.2DS donor lines, stimulate them with IL-6, and subsequently perform xenotransplantation. This approach would additionally build on the work by Sarieva *et al.* (2023) with Hyper-IL6 stimulated organoids that did not contain microglia, and enable us to investigate the combined effects of the IL-6 microglial response, the 22q11.2DS genotype, and their impact on neural migration and network development.

7.4.3 Statistical power: is more, more?

Third, enhancing the experimental power by increasing the sample size or using advanced techniques such as single-cell sequencing could offer more precise and detailed information about the cellular and molecular changes occurring in individuals with 22q11.2DS. For instance, by utilizing transcriptional data to cluster microglia into subtypes, we can examine if any specific subtypes are overrepresented or underrepresented in the 22q11.2DS model, or after IL-6 exposure. Utilising additional cell lines derived from individuals with 22q11.2DS, including different genetic backgrounds yet with similar types of 22q11.2 region deletions, would enable researchers to investigate the effects of specific genetic factors on cellular and molecular mechanisms, thereby overcoming the limitations observed in chapters 5 and 6. Comparing multiple lines after power analysis and careful donor consideration as aforementioned in section 7.3.2 could help differentiate common pathological features from those specific to certain individuals or genetic subgroups.

7.4.4 Does chronic IL-6 signalling have a different effect on the developing NPCs rather than a single, acute shot of IL-6?

Finally, investigating the effects of prolonged IL-6 exposure on neural development and potential long-term consequences could provide valuable insights. The model presented in this thesis focuses on the acute response to IL-6, which serves as an illustrative example of maternal prenatal infection, as discussed in section 4.4.1. However, it is important to recognize that the risk associated with IL-6 for NDD is not limited to maternal prenatal infection alone; it is also evident in blood biomarker and genetic studies that span into adulthood (Graham *et al.*, 2018; Perry *et al.*, 2021; Rasmussen *et al.*, 2021; Rudolph *et al.*, 2018; Schwieler *et al.*, 2015). Therefore, it is plausible that chronic exposure to elevated levels of IL-6 may also contribute to the onset of NDDs via different mechanisms. This is an additional topic that present animal MIA models are constrained by (Smith *et al.*, 2007), since a single dose of MIA-associated immune-stimulation has little physiological significance. For example, there are non-infectious factors, such as maternal stress, anaemia, drug use, and gestational diabetes, which are inherently chronic and lead to prolonged elevation of IL-6 across gestation (Meyer, 2019). As a result, in certain circumstances, predicting the effect of low grade, chronic inflammation would be of relevance, although animal MIA models have left this question unsolved to date. Addressing this question using an *in vitro* model represents a logical next step, wherein hiPSC-derived systems could be exposed to IL-6-containing media daily, simulating a sustained rather than an acute burst of exposure. In order to accomplish this objective, a potential approach could involve the utilization of microglia that are loaded with nanoparticles capable of controlled release of IL-6 over multiple days of culture differentiation.

By incorporating these experimental strategies, researchers can build upon the existing knowledge to unravel the intricate interactions between genetic factors, environmental

influences, and neural development in individuals with 22q11.2DS. These investigations would ultimately lead to a deeper understanding of the disorder's pathogenesis and potentially guide the development of targeted interventions and treatments.

Overall, the continuing use of hiPSC to model NDDs will not entirely close the gap between animal and human adult brains, but it can be more adapted to offer answers to the developmental impacts of NDD risk factors rather than the typical endpoints of many animal MIA models. However, *in vitro* MIA model observations still require confirmation in animals, where organ interactions may be studied. As a result, investigating pathophysiological pathways in both *in vivo* animal models and *in vitro* hiPSC-derived models in tandem, demonstrated well by Schafer *et al.* (2023) with their xenotransplanted mouse brain microglia-containing organoids, might accelerate disease understanding to more clinically relevant levels and identify opportunities to develop novel therapeutics.

7.4 Concluding Remarks

The aim of this project was to develop and use an hiPSC model to study NDD pathophysiology and gene-environment interactions, with both objectives achieved during the project. The acute IL-6-induced response in MGLs exhibited associations with NDDs at various levels, resembling transcriptional changes related to SZ and aligning with data from animal models of MIA. These findings provide support for the idea of reducing the use of animal MIA models for studying NDD aetiologies by conducting more molecular and cellular investigations using hiPSC-derived models. These findings also provide support for the involvement of microglia in mediating NDDs, and contribute to the development of future hypotheses regarding MGL responses that may influence NPC development through IL-6 trans-signalling, alterations in

microglial motility, and changes in other cell types within the CNS via cytokine and chemokine signalling. Yet, it remains unclear if IL-6 alone could disrupt NPC development without the presence of other cell types. MGLs responded to IL-6 through the IL-6Ra signalling pathway, while NPCs lacked sufficient IL6R expression and relied on secreted sIL-6Ra from other cell types for response. High-risk genetic variations were found to exacerbate cellular and molecular abnormalities of NPCs in response to IL-6, when grown in co-culture with microglia-like cells. Both acute IL-6 stimulation and 22q11.2DS posed risks to neurodevelopment in NPCs, implicating both vasculature and extracellular matrix remodelling pathways, whilst involving microglial cytokine release. Notably, GFAP+ cell numbers were significantly higher in 22q11.2DS neuron cultures, resembling the molecular phenotype of NDDs. Together, these findings confirm and enhance understanding of the complex interplay between genetic factors, prenatal elevated IL-6 influence, and neural development. While hiPSC models offer insights into the developmental impacts of neurodevelopmental disorder risk factors whilst simultaneously reducing the use of animals in scientific research, confirmation of these observations in animal models is still necessary, particularly when studying multiple organ interactions. Combining *in vivo* animal models with *in vitro* hiPSC-derived models will accelerate disease understanding and identify opportunities for developing new therapeutics at clinically relevant levels.

References

Aasen, T. *et al.* (2008) 'Efficient and rapid generation of induced pluripotent stem cells from human keratinocytes', *Nature Biotechnology*, 26(11), pp. 1276–1284. doi: 10.1038/nbt.1503.

Abazyan, B. *et al.* (2010) 'Prenatal interaction of mutant DISC1 and immune activation produces adult psychopathology', *Biological Psychiatry*, 68(12), pp. 1172–1181. doi: 10.1016/j.biopsych.2010.09.022.

Abràmoff, M. D., Magalhães, P. J. and Ram, S. J. (2004) 'Image processing with imageJ', *Biophotonics International*, pp. 36–41. doi: 10.1201/9781420005615.ax4.

Adam, M. P. (2012) 'The all-or-none phenomenon revisited', *Birth Defects Research Part A - Clinical and Molecular Teratology*, pp. 664–669. doi: 10.1002/bdra.23029.

Adhya, D. *et al.* (2021) 'Atypical Neurogenesis in Induced Pluripotent Stem Cells From Autistic Individuals', *Biological Psychiatry*, 89(5), pp. 486–496. doi: 10.1016/j.biopsych.2020.06.014.

Akimoto, N. *et al.* (2013) 'CCL-1 in the spinal cord contributes to neuropathic pain induced by nerve injury', *Cell Death and Disease*, 4(6). doi: 10.1038/cddis.2013.198.

Akimoto, Nozomi *et al.* (2013) 'Effects of chemokine (C-C motif) ligand 1 on microglial function', *Biochemical and Biophysical Research Communications*, 436(3), pp. 455–461. doi: 10.1016/j.bbrc.2013.05.126.

AL-ayadhi, L. Y. and Mostafa, G. A. (2011) 'Increased serum osteopontin levels in autistic children: Relation to the disease severity', *Brain, Behavior, and Immunity*, 25(7), pp. 1393–1398. doi: 10.1016/j.bbi.2011.04.006.

Allswede, D. M. *et al.* (2020) 'Cytokine concentrations throughout pregnancy and risk for psychosis in adult offspring: a longitudinal case-control study', *The Lancet Psychiatry*, 7(3), pp. 254–261. doi: 10.1016/S2215-0366(20)30006-7.

American Psychiatric Association (2022) *Diagnostic and Statistical Manual of Mental Disorders*, *Diagnostic and Statistical Manual of Mental Disorders*. American Psychiatric Association Publishing. doi: 10.1176/appi.books.9780890425787.

Amin, S. and Borrell, V. (2020) 'The Extracellular Matrix in the Evolution of Cortical Development and Folding', *Frontiers in Cell and Developmental Biology*. Front Cell Dev Biol. doi: 10.3389/fcell.2020.604448.

Anderson, N. C. *et al.* (2021) 'Balancing serendipity and reproducibility: Pluripotent stem cells as experimental systems for intellectual and developmental disorders', *Stem Cell Reports*, pp. 1446–1457. doi: 10.1016/j.stemcr.2021.03.025.

Anholt, G. E. *et al.* (2010) 'Autism and adhd symptoms in patients with ocd: Are they associated with specific oc symptom dimensions or oc symptom severity', *Journal of Autism and Developmental Disorders*, 40(5), pp. 580–589. doi: 10.1007/s10803-009-0922-1.

Antonia, R. J. *et al.* (2022) 'STAT3 regulates inflammatory cytokine production downstream of TNFR1 by inducing expression of TNFAIP3/A20', *Journal of Cellular and Molecular Medicine*, 26(16), pp. 4591–4601. doi: 10.1111/jcmm.17489.

Antunes, G. *et al.* (2002) 'Systemic cytokine levels in community-acquired pneumonia and their association with disease severity', *European Respiratory Journal*, 20(4), pp. 990–995. doi: 10.1183/09031936.02.00295102.

Arinami, T. (2006) ‘Analyses of the associations between the genes of 22q11 deletion syndrome and schizophrenia’, *Journal of Human Genetics*. Nature Publishing Group, pp. 1037–1045. doi: 10.1007/s10038-006-0058-5.

Arrode-Brusés, G. and Brusés, J. L. (2012) ‘Maternal immune activation by poly(I:C) induces expression of cytokines IL-1β and IL-13, chemokine MCP-1 and colony stimulating factor VEGF in fetal mouse brain’, *Journal of Neuroinflammation*, 9. doi: 10.1186/1742-2094-9-83.

Aujla, P. K. and Huntley, G. W. (2014) ‘Early postnatal expression and localization of matrix metalloproteinases-2 and -9 during establishment of rat hippocampal synaptic circuitry’, *Journal of Comparative Neurology*, 522(6), pp. 1249–1263. doi: 10.1002/cne.23468.

Ayala, R., Shu, T. and Tsai, L. H. (2007) ‘Trekking across the Brain: The Journey of Neuronal Migration’, *Cell*. Elsevier B.V., pp. 29–43. doi: 10.1016/j.cell.2006.12.021.

Azuma, H. *et al.* (2000) ‘Analysis of soluble interleukin 6 receptor in cerebprospinal fluid in inflammatory and non-inflammatory conditions’, *Cytokine*, 12(2), pp. 160–164. doi: 10.1006/cyto.1999.0534.

Baines, K. J. *et al.* (2020) ‘Maternal Immune Activation Alters Fetal Brain Development and Enhances Proliferation of Neural Precursor Cells in Rats’, *Frontiers in Immunology*, 11, p. 1145. doi: 10.3389/fimmu.2020.01145.

Barros, C. S., Franco, S. J. and Müller, U. (2011) ‘Extracellular Matrix: Functions in the nervous system’, *Cold Spring Harbor Perspectives in Biology*, 3(1), pp. 1–24. doi: 10.1101/cshperspect.a005108.

De Bartolomeis, A. *et al.* (2014) ‘Glutamatergic postsynaptic density protein dysfunctions in synaptic plasticity and dendritic spines morphology: Relevance to schizophrenia and other

behavioral disorders pathophysiology, and implications for novel therapeutic approaches', *Molecular Neurobiology*, pp. 484–511. doi: 10.1007/s12035-013-8534-3.

Basil, P. *et al.* (2018) 'Prenatal immune activation alters the adult neural epigenome but can be partly stabilised by a n-3 polyunsaturated fatty acid diet', *Translational Psychiatry*, 8(1), pp. 1–12. doi: 10.1038/s41398-018-0167-x.

Bassett, A. S. and Chow, E. W. C. (2008) 'Schizophrenia and 22q11.2 deletion syndrome', *Current Psychiatry Reports*. doi: 10.1007/s11920-008-0026-1.

Batiuk, M. Y. *et al.* (2020) 'Identification of region-specific astrocyte subtypes at single cell resolution', *Nature Communications*, 11(1), pp. 1–15. doi: 10.1038/s41467-019-14198-8.

Bayer, T. A., Falkai, P. and Maier, W. (1999) 'Genetic and non-genetic vulnerability factors in schizophrenia: The basis of the "Two hit hypothesis"', *Journal of Psychiatric Research*, 33(6). doi: 10.1016/S0022-3956(99)00039-4.

Bayés, Á. *et al.* (2011) 'Characterization of the proteome, diseases and evolution of the human postsynaptic density', *Nature Neuroscience*, 14(1), pp. 19–21. doi: 10.1038/nn.2719.

Bednarek, N. *et al.* (2009) 'Ontogeny of MMPs and TIMPs in the murine neocortex', *Pediatric Research*, 65(3), pp. 296–300. doi: 10.1203/PDR.0b013e3181973aee.

Beilen, M. *et al.* (2002) 'Low IQ scores in schizophrenia: primary or secondary deficit?', *Acta Neuropsychiatry,* 14(3), pp. 106-110. doi: 10.1034/j.1601-5215.2002.140302.x.

Bennett, M. L. *et al.* (2016) 'New tools for studying microglia in the mouse and human CNS', *Proceedings of the National Academy of Sciences of the United States of America*, 113(12), pp. E1738–E1746. doi: 10.1073/pnas.1525528113.

Ben-Reuven, L. and Reiner, O. (2021) 'Dynamics of cortical progenitors and production of subcerebral neurons are altered in embryos of a maternal inflammation model for autism', *Molecular Psychiatry*, 26(5), pp. 1535–1550. doi: 10.1038/s41380-019-0594-y.

Benros, M. E. *et al.* (2011) 'Autoimmune diseases and severe infections as risk factors for schizophrenia: A 30-year population-based register study', *American Journal of Psychiatry*, 168(12), pp. 1303–1310. doi: 10.1176/appi.ajp.2011.11030516.

Bergström, T. and Forsberg-Nilsson, K. (2012) 'Neural stem cells: Brain building blocks and beyond', *Upsala Journal of Medical Sciences*. Ups J Med Sci, pp. 132–142. doi: 10.3109/03009734.2012.665096.

Bhat, A. *et al.* (2022) 'Attenuated transcriptional response to pro-inflammatory cytokines in schizophrenia hiPSC-derived neural progenitor cells', *Brain, Behavior, and Immunity*, 105, pp. 82–97. doi: 10.1016/j.bbi.2022.06.010.

Binns, D. *et al.* (2009) 'QuickGO: A web-based tool for Gene Ontology searching', *Bioinformatics*, 25(22), pp. 3045–3046. doi: 10.1093/bioinformatics/btp536.

Bitanihirwe, B. K. Y. *et al.* (2009) 'Glutamatergic deficits and parvalbumin-containing inhibitory neurons in the prefrontal cortex in schizophrenia', *BMC Psychiatry*, 9. doi: 10.1186/1471-244X-9-71.

Bjelobaba, I. *et al.* (2019) 'Distinct expression patterns of osteopontin and dentin matrix protein 1 genes in pituitary gonadotrophs', *Frontiers in Endocrinology*, 10(MAR). doi: 10.3389/fendo.2019.00248.

Bloom, W. and Bartelmez, G. W. (1940) 'Hematopoiesis in young human embryos', *American Journal of Anatomy*, 67(1), pp. 21–53. doi: 10.1002/aja.1000670103.

Boehm, E. M., Gildenberg, M. S. and Washington, M. T. (2016) 'The Many Roles of PCNA in Eukaryotic DNA Replication', in *Enzymes*, pp. 231–254. doi: 10.1016/bs.enz.2016.03.003.

Borçoi, A. R. *et al.* (2015) 'Effects of prenatal immune activation on amphetamine-induced addictive behaviors: Contributions from animal models', *Progress in Neuro-Psychopharmacology and Biological Psychiatry*, 63, pp. 63–69. doi: 10.1016/j.pnpbp.2015.05.015.

Borsini, A. *et al.* (2022) 'Neurogenesis is disrupted in human hippocampal progenitor cells upon exposure to serum samples from hospitalized COVID-19 patients with neurological symptoms', *Molecular Psychiatry*, pp. 1–13. doi: 10.1038/s41380-022-01741-1.

Böttcher, C. *et al.* (2019) 'Human microglia regional heterogeneity and phenotypes determined by multiplexed single-cell mass cytometry', *Nature Neuroscience*, 22(1), pp. 78–90. doi: 10.1038/s41593-018-0290-2.

Botto, L. D. *et al.* (2003) 'A population-based study of the 22q11.2 Deletion: Phenotype, incidence, and contribution to major birth defects in the population', *Pediatrics*, 112(1 I), pp. 101–107. doi: 10.1542/peds.112.1.101.

Brauer, R. *et al.* (2011) 'Matrix metalloproteinase-19 inhibits growth of endothelial cells by generating angiostatin-like fragments from plasminogen', *BMC Biochemistry*, 12(1). doi: 10.1186/1471-2091-12-38.

Breitmeyer, R. *et al.* (2023) 'Regulation of synaptic connectivity in schizophrenia spectrum by mutual neuron-microglia interaction', *Communications Biology*, 6(1), pp. 1–16. Available at: https://www.nature.com/articles/s42003-023-04852-9.

Brennand, K. *et al.* (2015) 'Phenotypic differences in hiPSC NPCs derived from patients with schizophrenia', *Molecular Psychiatry*, 20(3), pp. 361–368. doi: 10.1038/mp.2014.22.

Brennand, K. J. and Gage, F. H. (2012) 'Modeling psychiatric disorders through reprogramming', *DMM Disease Models and Mechanisms*, pp. 26–32. doi: 10.1242/dmm.008268.

Broniarczyk-Czarniak, M. *et al.* (2022) 'The Role of OXT, OXTR, AVP, and AVPR1a Gene Expression in the Course of Schizophrenia', *Current Issues in Molecular Biology*, 44(1), pp. 336–349. doi: 10.3390/cimb44010025.

Brown, A. M. *et al.* (2022) 'Maternal immune activation with high molecular weight poly(I:C) in Wistar rats leads to elevated immune cell chemoattractants', *Journal of Neuroimmunology*, 364. doi: 10.1016/j.jneuroim.2022.577813.

Brown, A. S. and Conway, F. (2019) 'Maternal immune activation and related factors in the risk of offspring psychiatric disorders', *Frontiers in Psychiatry*, 10(MAY). doi: 10.3389/fpsyt.2019.00430.

Brown, A. S. and Meyer, U. (2018) 'Maternal immune activation and neuropsychiatric illness: A translational research perspective', *American Journal of Psychiatry*, 175(11), pp. 1073–1083. doi: 10.1176/appi.ajp.2018.17121311.

Brynge, M. *et al.,* (2022) 'Maternal infection during pregnancy and likelihood of autism and intellectual disability in children in Sweden: a negative control and sibling comparison cohort study', *The Lancet,* 9(10), pp. 781-791. doi: 10.1016/S2215-0366(22)00264-4.

Butovsky, O. *et al.* (2014) 'Identification of a unique TGF-β-dependent molecular and functional signature in microglia', *Nature Neuroscience*, 17(1), pp. 131–143. doi: 10.1038/nn.3599.

Cameron, D. *et al.* (2023) 'Single-Nuclei RNA Sequencing of 5 Regions of the Human Prenatal Brain Implicates Developing Neuron Populations in Genetic Risk for Schizophrenia', *Biological Psychiatry*, 93(2), pp. 157–166. doi: 10.1016/j.biopsych.2022.06.033.

Campbell, I. L. *et al.* (2014) 'Trans-signaling is a dominant mechanism for the pathogenic actions of interleukin-6 in the brain', *Journal of Neuroscience*, 34(7), pp. 2503–2513. doi: 10.1523/JNEUROSCI.2830-13.2014.

Canetta, S. *et al.* (2016) 'Maternal immune activation leads to selective functional deficits in offspring parvalbumin interneurons', *Molecular Psychiatry*, 21(7), pp. 956–968. doi: 10.1038/mp.2015.222.

Careaga, M., Murai, T. and Bauman, M. D. (2017) 'Maternal Immune Activation and Autism Spectrum Disorder: From Rodents to Nonhuman and Human Primates', *Biological Psychiatry*, 81(5), pp. 391–401. doi: 10.1016/j.biopsych.2016.10.020.

Carmeliet, P. *et al.* (1996) 'Abnormal blood vessel development and lethality in embryos lacking a single VEGF allele', *Nature*, 380(6573), pp. 435–439. doi: 10.1038/380435a0.

Carvey, P. M. *et al.* (2003) 'Prenatal exposure to the bacteriotoxin lipopolysaccharide leads to long-term losses of dopamine neurons in offspring: A potential, new model of Parkinson's disease', *Frontiers in Bioscience*. Bioscience Research Institute, pp. 826–837. doi: 10.2741/1158.

Cattane, N., Richetto, J. and Cattaneo, A. (2020) 'Prenatal exposure to environmental insults and enhanced risk of developing Schizophrenia and Autism Spectrum Disorder: focus on biological pathways and epigenetic mechanisms', *Neuroscience and Biobehavioral Reviews*, 117, pp. 253–278. doi: 10.1016/j.neubiorev.2018.07.001.

Chagas, L. da S. *et al.* (2020) 'Environmental signals on microglial function during brain development, neuroplasticity, and disease', *International Journal of Molecular Sciences*. doi: 10.3390/ijms21062111.

Chahal, R. *et al.* (2021) 'Greater age-related changes in white matter morphometry following early life stress: Associations with internalizing problems in adolescence', *Developmental Cognitive Neuroscience*, 47. doi: 10.1016/j.dcn.2020.100899.

Chan, M. K. *et al.* (2011) 'Evidence for disease and antipsychotic medication effects in post-mortem brain from schizophrenia patients', *Molecular Psychiatry*, 16(12), pp. 1189–1202. doi: 10.1038/mp.2010.100.

Checchin, D. *et al.* (2006) 'Potential role of microglia in retinal blood vessel formation', *Investigative Ophthalmology and Visual Science*, 47(8), pp. 3595–3602. doi: 10.1167/iovs.05-1522.

Chehboun, S. *et al.* (2017) 'Epstein-Barr virus-induced gene 3 (EBI3) can mediate IL-6 trans-signaling', *Journal of Biological Chemistry*, 292(16), pp. 6644–6656. doi: 10.1074/jbc.M116.762021.

Cho, K. H. *et al.* (2013) 'Site-specific distribution of CD68-positive microglial cells in the brains of human midterm fetuses: A topographical relationship with growing axons', *BioMed Research International*, 2013. doi: 10.1155/2013/762303.

Choi, B. H. and Lapham, L. W. (1978) 'Radial glia in the human fetal cerebrum: A combined golgi, immunofluorescent and electron microscopic study', *Brain Research*, 148(2), pp. 295–311. doi: 10.1016/0006-8993(78)90721-7.

Choi, G. B. *et al.* (2016) 'The maternal interleukin-17a pathway in mice promotes autism-like phenotypes in offspring', *Science*, 351(6276), pp. 933–939. doi: 10.1126/science.aad0314.

Chukaew, P. *et al.* (2022) 'Correlation of BDNF, VEGF, TNF-α, and S100B with cognitive impairments in chronic, medicated schizophrenia patients', *Neuropsychopharmacology Reports*, 42(3), pp. 281–287. doi: 10.1002/npr2.12261.

Claus, C., Jung, M. and Hübschen, J. M. (2020) 'Pluripotent Stem Cell-Based Models: A Peephole into Virus Infections during Early Pregnancy', *Cells*, 9(3). doi: 10.3390/cells9030542.

Clemente, A. *et al.,* (2015) 'Bipolar disorder prevalence: a systematic review and meta-analysis of the literature', *Braz J Psychiatry,* 37(2), pp.155-61. doi: 10.1590/1516-4446-2012-1693.

Coiro, P. *et al.* (2015) 'Impaired synaptic development in a maternal immune activation mouse model of neurodevelopmental disorders', *Brain, Behavior, and Immunity*, 50, pp. 249–258. doi: 10.1016/j.bbi.2015.07.022.

Coomey, R. *et al.* (2020) 'The Role of Microglia in Neurodevelopmental Disorders and their Therapeutics', *Current Topics in Medicinal Chemistry*, 20(4), pp. 272–276. doi: 10.2174/1568026620666200221172619.

Cotel, M. C. *et al.* (2015) 'Microglial activation in the rat brain following chronic antipsychotic treatment at clinically relevant doses', *European Neuropsychopharmacology*. doi: 10.1016/j.euroneuro.2015.08.004.

Couch, A. C. M. *et al.* (2021) 'Maternal immune activation primes deficiencies in adult hippocampal neurogenesis', *Brain, behavior, and immunity*, 97, pp. 410–422. doi: 10.1016/J.BBI.2021.07.021.

Couch, A. C. M. *et al.* (2023) 'Acute IL-6 exposure triggers canonical IL6Ra signaling in hiPSC microglia, but not neural progenitor cells', *Brain, Behavior, and Immunity*, 110, pp. 43–59. doi: 10.1016/j.bbi.2023.02.007.

Courchesne, E., Gazestani, V. H. and Lewis, N. E. (2020) 'Prenatal Origins of ASD: The When, What, and How of ASD Development', *Trends in Neurosciences*, pp. 326–342. doi: 10.1016/j.tins.2020.03.005.

Crawford, J. D. *et al.* (2015) 'Elevated GFAP Protein in Anterior Cingulate Cortical White Matter in Males With Autism Spectrum Disorder', *Autism Research*, 8(6), pp. 649–657. doi: 10.1002/aur.1480.

Crockett, A. M. *et al.* (2021) 'Disruption of the blood-brain barrier in 22q11.2 deletion syndrome', *Brain*, 144(5), pp. 1351–1360. doi: 10.1093/brain/awab055.

Cross, A. K. and Woodroofe, M. N. (1999) 'Chemokine modulation of matrix metalloproteinase and TIMP production in adult rat brain microglia and a human microglial cell line in vitro', *GLIA*, 28(3), pp. 183–189. doi: 10.1002/(SICI)1098-1136(199912)28:3<183::AID-GLIA2>3.0.CO;2-3.

Cruikshank, W. W., Kornfeld, H. and Center, D. M. (2000) 'Interleukin-16', *Journal of Leukocyte Biology*, 67(6), pp. 757–766. doi: 10.1002/jlb.67.6.757.

Crum, W. R. *et al.* (2017) 'Evolution of structural abnormalities in the rat brain following in utero exposure to maternal immune activation: A longitudinal in vivo MRI study', *Brain, Behavior, and Immunity*, 63. doi: 10.1016/j.bbi.2016.12.008.

Cullen, A. E. *et al.* (2019) 'Associations Between Non-neurological Autoimmune Disorders and Psychosis: A Meta-analysis', *Biological Psychiatry*, 85(1), pp. 35–48. doi: 10.1016/j.biopsych.2018.06.016.

Cunningham, C. L., Martínez-Cerdeño, V. and Noctor, S. C. (2013) 'Microglia regulate the number of neural precursor cells in the developing cerebral cortex', *The Journal of neuroscience : the official journal of the Society for Neuroscience*, 33(10), pp. 4216–4233. doi: 10.1523/JNEUROSCI.3441-12.2013.

Dahlgren, J. *et al.* (2006) 'Interleukin-6 in the maternal circulation reaches the rat fetus in mid-gestation', *Pediatric Research*, 60(2). doi: 10.1203/01.pdr.0000230026.74139.18.

Dang, J. *et al.* (2016) 'Zika Virus Depletes Neural Progenitors in Human Cerebral Organoids through Activation of the Innate Immune Receptor TLR3', *Cell Stem Cell*, 19(2), pp. 258–265. doi: 10.1016/j.stem.2016.04.014.

Dawidowski, B. *et al.* (2021) 'The role of cytokines in the pathogenesis of schizophrenia', *Journal of Clinical Medicine*, 10(17). doi: 10.3390/jcm10173849.

Deans, P. J. M. *et al.* (2017) 'Psychosis Risk Candidate ZNF804A Localizes to Synapses and Regulates Neurite Formation and Dendritic Spine Structure', *Biological Psychiatry*, 82(1), pp. 49–61. doi: 10.1016/j.biopsych.2016.08.038.

Deglincerti, A. *et al.* (2016) 'Self-organization of the in vitro attached human embryo', *Nature*, 533(7602), pp. 251–254. doi: 10.1038/nature17948.

Deng, M. Y. *et al.* (2011) 'Frontal-subcortical protein expression following prenatal exposure to maternal inflammation', *PLoS ONE*, 6(2), p. e16638. doi: 10.1371/journal.pone.0016638.

d'Errico, P. *et al.* (2021) 'Microglia contribute to the propagation of Aβ into unaffected brain tissue', *Nature Neuroscience 2021*, pp. 1–6. doi: 10.1038/s41593-021-00951-0.

Deshpande, A. *et al.* (2017) 'Cellular Phenotypes in Human iPSC-Derived Neurons from a Genetic Model of Autism Spectrum Disorder', *Cell Reports*, 21(10), pp. 2678–2687. doi: 10.1016/j.celrep.2017.11.037.

Ding, S. *et al.* (2019) 'Age-related changes in neuroinflammation and prepulse inhibition in offspring of rats treated with Poly I:C in early gestation', *Behavioral and Brain Functions*, 15(1), pp. 1–10. doi: 10.1186/s12993-019-0154-2.

Dobin, A. *et al.* (2013) 'STAR: Ultrafast universal RNA-seq aligner', *Bioinformatics*, 29(1), pp. 15–21. doi: 10.1093/bioinformatics/bts635.

Domínguez-Vivero, C. *et al.* (2020) 'Pentraxin 3 (PTX3): A molecular marker of endothelial dysfunction in chronic migraine', *Journal of Clinical Medicine*, 9(3). doi: 10.3390/jcm9030849.

Dráberová, E. *et al.* (2008) 'Class III β-tubulin is constitutively coexpressed with glial fibrillary acidic protein and nestin in midgestational human fetal astrocytes: Implications for phenotypic identity', *Journal of Neuropathology and Experimental Neurology*, 67(4), pp. 341–354. doi: 10.1097/NEN.0b013e31816a686d.

Dräger, N. M. *et al.* (2022) 'A CRISPRi/a platform in human iPSC-derived microglia uncovers regulators of disease states', *Nature Neuroscience*, 25(9), pp. 1149–1162. doi: 10.1038/s41593-022-01131-4.

Druart, M. *et al.* (2021) 'Elevated expression of complement C4 in the mouse prefrontal cortex causes schizophrenia-associated phenotypes', *Molecular psychiatry*, 26(7), pp. 3489–3501. Available at: https://pubmed.ncbi.nlm.nih.gov/33837272/.

Du, Q., de la Morena, M. T. and van Oers, N. S. C. (2020) 'The Genetics and Epigenetics of 22q11.2 Deletion Syndrome', *Frontiers in Genetics*, 10. doi: 10.3389/fgene.2019.01365.

Dubois, J. *et al.* (2014) 'The early development of brain white matter: A review of imaging studies in fetuses, newborns and infants', *Neuroscience*, 276, pp. 48–71. doi: 10.1016/j.neuroscience.2013.12.044.

Dutan Polit, L. *et al.* (2023) 'Recommendations, guidelines, and best practice for the use of human induced pluripotent stem cells for neuropharmacological studies of neuropsychiatric disorders', *Neuroscience Applied*, 2, p. 101125. doi: 10.1016/J.NSA.2023.101125.

Eastwood, S. L. and Harrison, P. J. (2005) 'Decreased expression of vesicular glutamate transporter 1 and complexin II mRNAs in schizophrenia: Further evidence for a synaptic pathology affecting glutamate neurons', *Schizophrenia Research*, 73(2–3), pp. 159–172. doi: 10.1016/j.schres.2004.05.010.

Edlow, A. G. *et al.* (2023) 'Sex-Specific Neurodevelopmental Outcomes Among Offspring of Mothers With SARS-CoV-2 Infection During Pregnancy.', *JAMA network open*, 6(3), p. e234415. doi: 10.1001/jamanetworkopen.2023.4415.

Edmonson, C., Ziats, M. N. and Rennert, O. M. (2014) 'Altered glial marker expression in autistic post-mortem prefrontal cortex and cerebellum', *Molecular Autism*, 5(1), pp. 1–9. doi: 10.1186/2040-2392-5-3.

Edwards, R. H. (2007) ‘The Neurotransmitter Cycle and Quantal Size’, *Neuron*, 55(6), pp. 835–858. doi: 10.1016/j.neuron.2007.09.001.

Eggen, B. J. L., Boddeke, E. W. G. M. and Kooistra, S. M. (2019) ‘Regulation of Microglia Identity from an Epigenetic and Transcriptomic Point of View’, *Neuroscience*, pp. 3–13. doi: 10.1016/j.neuroscience.2017.12.010.

El-Tahir, H. M. *et al.* (2006) ‘Expression of hepatoma-derived growth factor family members in the adult central nervous system’, *BMC Neuroscience*, 7(6). doi: 10.1186/1471-2202-7-6.

Estes, M. L. and McAllister, A. K. (2016) ‘Maternal immune activation: Implications for neuropsychiatric disorders’, *Science*, 353(6301), pp. 772–777. doi: 10.1126/science.aag3194.

Eze, U. C. *et al.* (2021) ‘Single-cell atlas of early human brain development highlights heterogeneity of human neuroepithelial cells and early radial glia’, *Nature Neuroscience*, 24(4), pp. 584–594. doi: 10.1038/s41593-020-00794-1.

Fagerlund, I. *et al.* (2022) ‘Microglia-like cells promote neuronal functions in cerebral organoids’, *Cells*, 11(1). doi: 10.3390/cells11010124.

Fantin, A. *et al.* (2010) ‘Tissue macrophages act as cellular chaperones for vascular anastomosis downstream of VEGF-mediated endothelial tip cell induction’, *Blood*, 116(5), pp. 829–840. doi: 10.1182/blood-2009-12-257832.

Fatemi, S. H. *et al.* (1999) ‘Defective corticogenesis and reduction in Reelin immunoreactivity in cortex and hippocampus of prenatally infected neonatal mice’, *Molecular Psychiatry*, 4(2), pp. 145–154. doi: 10.1038/sj.mp.4000520.

Fatemi, S. H. *et al.* (2008) 'Maternal infection leads to abnormal gene regulation and brain atrophy in mouse offspring: Implications for genesis of neurodevelopmental disorders', *Schizophrenia Research*, 99(1–3), pp. 56–70. doi: 10.1016/j.schres.2007.11.018.

Fatemi, S. H. *et al.* (2012) 'The viral theory of schizophrenia revisited: Abnormal placental gene expression and structural changes with lack of evidence for H1N1 viral presence in placentae of infected mice or brains of exposed offspring', *Neuropharmacology*, 62(3), pp. 1290–1298. doi: 10.1016/j.neuropharm.2011.01.011.

Faber, N. (2003) 'The NMDA receptor hypofunction model of psychosis', *Ann N Y Acad Sci.,* 1003, pp. 119-30. doi: 10.1196/annals.1300.008.

Fernández de Cossío, L. *et al.* (2021) 'Lipopolysaccharide-induced maternal immune activation modulates microglial CX3CR1 protein expression and morphological phenotype in the hippocampus and dentate gyrus, resulting in cognitive inflexibility during late adolescence', *Brain, Behavior, and Immunity*, 97. doi: 10.1016/j.bbi.2021.07.025.

Ferro, A., Auguste, Y. S. S. and Cheadle, L. (2021) 'Microglia, Cytokines, and Neural Activity: Unexpected Interactions in Brain Development and Function', *Frontiers in Immunology*, 12. doi: 10.3389/fimmu.2021.703527.

Fietz, S. A. *et al.* (2012) 'Transcriptomes of germinal zones of human and mouse fetal neocortex suggest a role of extracellular matrix in progenitor self-renewal', *Proceedings of the National Academy of Sciences of the United States of America*, 109(29), pp. 11836–11841. doi: 10.1073/pnas.1209647109.

Florio, M. *et al.* (2015) 'Human-specific gene ARHGAP11B promotes basal progenitor amplification and neocortex expansion', *Science*, 347(6229), pp. 1465–1470. doi: 10.1126/science.aaa1975.

Foley, É. M. *et al.* (2023) 'Protocol for the Psychosis Immune Mechanism Stratified Medicine (PIMS) trial: a randomised double-blind placebo-controlled trial of single-dose tocilizumab in patients with psychosis', *BMJ open*, 13(3), p. e067944. doi: 10.1136/bmjopen-2022-067944.

Forstreuter, F., Lucius, R. and Mentlein, R. (2002) 'Vascular endothelial growth factor induces chemotaxis and proliferation of microglial cells', *Journal of Neuroimmunology*, 132(1–2), pp. 93–98. doi: 10.1016/S0165-5728(02)00315-6.

Fougerousse, F. *et al.* (2000) 'Human-mouse differences in the embryonic expression patterns of developmental control genes and disease genes', *Human Molecular Genetics*, 9(2), pp. 165–173. doi: 10.1093/hmg/9.2.165.

Francés, L. *et al.* (2022) 'Current state of knowledge on the prevalence of neurodevelopmental disorders in childhood according to the DSM-5: a systematic review in accordance with the PRISMA criteria', *Child and Adolescent Psychiatry and Mental Health*, 16(1), pp. 1–15. doi: 10.1186/s13034-022-00462-1.

Francis, S. M. *et al.* (2016) 'ASD and genetic associations with receptors for oxytocin and vasopressin-AVPR1A, AVPR1B, and OXTR', *Frontiers in Neuroscience*, 10(NOV). doi: 10.3389/fnins.2016.00516.

Franco, S. J. and Müller, U. (2013) 'Shaping Our Minds: Stem and Progenitor Cell Diversity in the Mammalian Neocortex', *Neuron*. Cell Press, pp. 19–34. doi: 10.1016/j.neuron.2012.12.022.

Franco-Bocanegra, D. K. *et al.* (2019) 'Molecular mechanisms of microglial motility: Changes in ageing and Alzheimer's disease', *Cells*, 8(6). doi: 10.3390/cells8060639.

Frieling, J. T. M. *et al.* (1994) 'Soluble interleukin 6 receptor in biological fluids from human origin', *Cytokine*, 6(4), pp. 376–381. doi: 10.1016/1043-4666(94)90061-2.

Galatro, T. F. *et al.* (2017) 'Transcriptomic analysis of purified human cortical microglia reveals age-associated changes', *Nature Neuroscience*, 20(8), pp. 1162–1171. doi: 10.1038/nn.4597.

Gandal, M. J. *et al.* (2018) 'Transcriptome-wide isoform-level dysregulation in ASD, schizophrenia, and bipolar disorder', *Science*, 362(6420). doi: 10.1126/science.aat8127.

Garay, P. A. *et al.* (2013) 'Maternal immune activation causes age- and region-specific changes in brain cytokines in offspring throughout development', *Brain, Behavior, and Immunity*, 31, pp. 54–68. doi: 10.1016/j.bbi.2012.07.008.

Garcia-Reitboeck, P. *et al.* (2018) 'Human Induced Pluripotent Stem Cell-Derived Microglia-Like Cells Harboring TREM2 Missense Mutations Show Specific Deficits in Phagocytosis', *Cell Reports*, 24(9), pp. 2300–2311. doi: 10.1016/j.celrep.2018.07.094.

Garden, G. A. and Möller, T. (2006) 'Microglia biology in health and disease', *Journal of Neuroimmune Pharmacology*, 1(2), pp. 127–137. doi: 10.1007/s11481-006-9015-5.

Garrido-Torres, N. *et al.* (2022) 'Examining the immune signatures of SARS-CoV-2 infection in pregnancy and the impact on neurodevelopment: Protocol of the SIGNATURE longitudinal study', *Frontiers in Pediatrics*, 10. doi: 10.3389/fped.2022.899445.

Gaspard, N. *et al.* (2008) 'An intrinsic mechanism of corticogenesis from embryonic stem cells', *Nature*, 455(7211), pp. 351–357. doi: 10.1038/nature07287.

Gilman, S. E. *et al.* (2017) 'Socioeconomic disadvantage, gestational immune activity, and neurodevelopment in early childhood', *Proceedings of the National Academy of Sciences of the United States of America*, 114(26). doi: 10.1073/pnas.1617698114.

Gilmore, J. H. and Jarskog, L. F. (1997) 'Exposure to infection and brain development: cytokines in the pathogenesis of schizophrenia.', *Schizophrenia research*, 24(3), pp. 365–367. doi: 10.1016/s0920-9964(96)00123-5.

Gilmore, J. H., Jarskog, L. F. and Vadlamudi, S. (2005) 'Maternal poly I:C exposure during pregnancy regulates TNFa, BDNF, and NGF expression in neonatal brain and the maternal-fetal unit of the rat', *Journal of Neuroimmunology*, 159, pp. 106–112.

Ginhoux, F. *et al.* (2010) 'Fate mapping analysis reveals that adult microglia derive from primitive macrophages', *Science*. doi: 10.1126/science.1194637.

Giovanoli, S. *et al.* (2013) 'Stress in puberty unmasks latent neuropathological consequences of prenatal immune activation in mice', *Science*, 339(6123), pp. 1100–1102. doi: 10.1126/science.1228261.

Giovanoli, S. *et al.* (2015) 'Late prenatal immune activation causes hippocampal deficits in the absence of persistent inflammation across aging.', *Journal of neuroinflammation*, 12(1), p. 221. doi: 10.1186/s12974-015-0437-y.

Girard, S. *et al.* (2010) 'IL-1 Receptor Antagonist Protects against Placental and Neurodevelopmental Defects Induced by Maternal Inflammation', *The Journal of Immunology*, 184(7), pp. 3997–4005. doi: 10.4049/jimmunol.0903349.

Giulio, S. T. *et al.* (2010) 'Development and regeneration of projection neuron subtypes of the cerebral cortex', *Science Progress*, 93(2), pp. 151–169. doi: 10.3184/003685010X12705764469952.

Glantz, L. A. and Lewis, D. A. (2000) 'Decreased dendritic spine density on prefrontal cortical pyramidal neurons in schizophrenia', *Archives of General Psychiatry*, 57(1), pp. 65–73. doi: 10.1001/archpsyc.57.1.65.

Glynn, M. W. and McAllister, A. K. (2006) 'Immunocytochemistry and quantification of protein colocalization in cultured neurons', *Nature Protocols*, 1(3), pp. 1287–1296. doi: 10.1038/nprot.2006.220.

Gomez Perdiguero, E. *et al.* (2015) 'Tissue-resident macrophages originate from yolk-sac-derived erythro-myeloid progenitors', *Nature*. doi: 10.1038/nature13989.

Gonzalez, D. M., Gregory, J. and Brennand, K. J. (2017) 'The importance of non-neuronal cell types in hiPSC-based disease modeling and drug screening', *Frontiers in Cell and Developmental Biology*. Frontiers Media S.A., p. 117. doi: 10.3389/fcell.2017.00117.

Gosselin, D. *et al.* (2017) 'An environment-dependent transcriptional network specifies human microglia identity', *Science*, 356(6344), pp. 1248–1259. doi: 10.1126/science.aal3222.

Götz, M., Stoykova, A. and Gruss, P. (1998) 'Pax6 controls radial glia differentiation in the cerebral cortex', *Neuron*, 21(5), pp. 1031–1044. doi: 10.1016/S0896-6273(00)80621-2.

Gouwens, N. W. *et al.* (2020) 'Integrated Morphoelectric and Transcriptomic Classification of Cortical GABAergic Cells', *Cell*, 183(4), pp. 935-953.e19. doi: 10.1016/j.cell.2020.09.057.

Grabert, K. *et al.* (2016) 'Microglial brain regionâ 'dependent diversity and selective regional sensitivities to aging', *Nature Neuroscience*, 19(3), pp. 504–516. doi: 10.1038/nn.4222.

Graham, *et al.* (2018) 'Maternal Systemic Interleukin-6 During Pregnancy Is Associated With Newborn Amygdala Phenotypes and Subsequent Behavior at 2 Years of Age', *Biological Psychiatry*, 83(2), pp. 109–119. doi: 10.1016/j.biopsych.2017.05.027.

Graus, F., Saiz, A. and Dalmau, J. (2010) 'Antibodies and neuronal autoimmune disorders of the CNS', *Journal of Neurology*. J Neurol, pp. 509–517. doi: 10.1007/s00415-009-5431-9.

Greenberg, D. A. and Jin, K. (2005) 'From angiogenesis to neuropathology', *Nature*, pp. 954–959. doi: 10.1038/nature04481.

Grinde, D. *et al.* (2020) 'Complement Activation in 22q11.2 Deletion Syndrome', *Journal of Clinical Immunology*, 40(3), pp. 515–523. doi: 10.1007/s10875-020-00766-x.

Grove, J. *et al.* (2019) 'Identification of common genetic risk variants for autism spectrum disorder', *Nature Genetics*, 51(3), pp. 431–444. doi: 10.1038/s41588-019-0344-8.

Grunwald, L. M. *et al.* (2019) 'Comparative characterization of human induced pluripotent stem cells (hiPSC) derived from patients with schizophrenia and autism', *Translational Psychiatry*, 9(1). doi: 10.1038/s41398-019-0517-3.

Guidotti, A. *et al.* (2000) 'Decrease in reelin and glutamic acid decarboxylase67 (GAD67) expression in schizophrenia and bipolar disorder: A postmortem brain study', *Archives of General Psychiatry*, 57(11), pp. 1061–1069. doi: 10.1001/archpsyc.57.11.1061.

Guneykaya, D. *et al.* (2018) 'Transcriptional and Translational Differences of Microglia from Male and Female Brains', *Cell Reports*, 24(10), pp. 2773-2783.e6. doi: 10.1016/j.celrep.2018.08.001.

Haenseler, W. *et al.* (2017) 'A Highly Efficient Human Pluripotent Stem Cell Microglia Model Displays a Neuronal-Co-culture-Specific Expression Profile and Inflammatory Response', *Stem Cell Reports*, 8(6), pp. 1727–1742. doi: 10.1016/j.stemcr.2017.05.017.

Halff, E. F. *et al.* (2021) 'Effects of chronic exposure to haloperidol, olanzapine or lithium on SV2A and NLGN synaptic puncta in the rat frontal cortex', *Behavioural Brain Research*, 405. doi: 10.1016/j.bbr.2021.113203.

Han, J. *et al.* (2021) 'Uncovering sex differences of rodent microglia', *Journal of Neuroinflammation*, 18(1), pp. 1–11. doi: 10.1186/S12974-021-02124-Z/TABLES/2.

Hanger, B. *et al.* (2020) 'Emerging Developments in Human Induced Pluripotent Stem Cell-Derived Microglia: Implications for Modelling Psychiatric Disorders With a Neurodevelopmental Origin', *Frontiers in Psychiatry*, 11, p. 789. doi: 10.3389/fpsyt.2020.00789.

Hans, V. H. J. *et al.* (1999) 'Interleukin-6 and its soluble receptor in serum and cerebrospinal fluid after cerebral trauma', *NeuroReport*, 10(2), pp. 409–412. doi: 10.1097/00001756-199902050-00036.

Hansen, D. V. *et al.* (2010) 'Neurogenic radial glia in the outer subventricular zone of human neocortex', *Nature*, 464(7288), pp. 554–561. doi: 10.1038/nature08845.

Hashimoto, T. *et al.* (2008) 'Alterations in GABA-related transcriptome in the dorsolateral prefrontal cortex of subjects with schizophrenia', *Molecular Psychiatry*, 13(2), pp. 147–161. doi: 10.1038/sj.mp.4002011.

Hatten, M. E. (1999) 'Central nervous system neuronal migration', *Annual Review of Neuroscience*. Annu Rev Neurosci, pp. 511–539. doi: 10.1146/annurev.neuro.22.1.511.

Havdahl, K. A. *et al.* (2016) 'Utility of the Child Behavior Checklist as a Screener for Autism Spectrum Disorder', *Autism Research*, 9(1), pp. 33–42. doi: 10.1002/aur.1515.

Hayes, L. N. *et al.* (2022) 'Prenatal immune stress blunts microglia reactivity, impairing neurocircuitry', *Nature*, 610(7931), pp. 327–334. doi: 10.1038/s41586-022-05274-z.

Hedegaard, A. *et al.* (2020) 'Honing the Double-Edged Sword: Improving Human iPSC-Microglia Models', *Frontiers in Immunology*. doi: 10.3389/fimmu.2020.614972.

Hefendehl, J. K. *et al.* (2014) 'Homeostatic and injury-induced microglia behavior in the aging brain', *Aging Cell*, 13(1), pp. 60–69. doi: 10.1111/acel.12149.

Helms, J. *et al.* (2020) 'Neurologic Features in Severe SARS-CoV-2 Infection', *New England Journal of Medicine*, 382(23), pp. 2268–2270. doi: 10.1056/nejmc2008597.

Hilker, R. *et al.* (2018) 'Heritability of Schizophrenia and Schizophrenia Spectrum Based on the Nationwide Danish Twin Register', *Biological Psychiatry*, 83(6), pp. 492–498. doi: 10.1016/j.biopsych.2017.08.017.

Hoeffel, G. and Ginhoux, F. (2015) 'Ontogeny of tissue-resident macrophages', *Frontiers in Immunology*, 6(SEP), p. 1. doi: 10.3389/fimmu.2015.00486.

Hoffman, G. E. *et al.* (2019) 'New considerations for hiPSC-based models of neuropsychiatric disorders', *Molecular Psychiatry*, 24(1), pp. 49–66. doi: 10.1038/s41380-018-0029-1.

Holloway, R. K. *et al.* (2023) 'Localized microglia dysregulation impairs central nervous system myelination in development', *Acta neuropathologica communications*, 11(1), p. 49. doi: 10.1186/s40478-023-01543-8.

Holloway, T. *et al.* (2013) 'Prenatal stress induces schizophrenia-like alterations of serotonin 2A and metabotropic glutamate 2 receptors in the adult offspring: Role of maternal immune system', *Journal of Neuroscience*, 33(3), pp. 1088–1098. doi: 10.1523/JNEUROSCI.2331-12.2013.

Howard, R. *et al.* (2000) 'Late-Onset Schizophrenia and Very-Late-Onset Schizophrenia-Like Psychosis: An International Consensus', *The American Journal of Psychiatry*, 157(2), pp. 172-178. doi: 10.1176/appi.ajp.157.2.172.

Hridi, S. U. *et al.* (2019) 'Interleukin-16 inhibits sodium channel function and GluA1 phosphorylation via CD4- and CD9-independent mechanisms to reduce hippocampal neuronal excitability and synaptic activity', *Molecular and Cellular Neuroscience*, 95, pp. 71–78. doi: 10.1016/j.mcn.2019.01.002.

Hsiao, E. Y. and Patterson, P. H. (2011) 'Activation of the maternal immune system induces endocrine changes in the placenta via IL-6', *Brain, Behavior, and Immunity*, 25(4), pp. 604–615. doi: 10.1016/j.bbi.2010.12.017.

Huang, X. *et al.* (2021) 'Immune-Related Gene SERPINE1 Is a Novel Biomarker for Diffuse Lower-Grade Gliomas via Large-Scale Analysis', *Frontiers in Oncology*, 11. doi: 10.3389/fonc.2021.646060.

Huhn, M. *et al.* (2019) 'Comparative efficacy and tolerability of 32 oral antipsychotics for the acute treatment of adults with multi-episode schizophrenia: a systematic review and network meta-analysis', *The Lancet*, 394(10202), pp. 939–951. doi: 10.1016/S0140-6736(19)31135-3.

Hunter, C. A. and Jones, S. A. (2015) 'IL-6 as a keystone cytokine in health and disease', *Nature Immunology*. Nat Immunol, pp. 448–457. doi: 10.1038/ni.3153.

Huttunen, M. O. and Niskanen, P. (1978) 'Prenatal Loss of Father and Psychiatric Disorders', *Archives of General Psychiatry*, 35(4). doi: 10.1001/archpsyc.1978.01770280039004.

Inoue, T. *et al.* (2019) 'Oxytocin suppresses inflammatory responses induced by lipopolysaccharide through inhibition of the eIF-2α–ATF4 pathway in mouse microglia', *Cells*, 8(6). doi: 10.3390/cells8060527.

Ishii, S. and Hashimoto-Torii, K. (2015) 'Impact of prenatal environmental stress on cortical development', *Frontiers in Cellular Neuroscience*. Frontiers Research Foundation, p. 207. doi: 10.3389/fncel.2015.00207.

Jansen, A. G. *et al.* (2020) 'Psychiatric Polygenic Risk Scores as Predictor for Attention Deficit/Hyperactivity Disorder and Autism Spectrum Disorder in a Clinical Child and Adolescent Sample', *Behavior Genetics*, 50(4), pp. 203–212. doi: 10.1007/s10519-019-09965-8.

Jao, J. and Ciernia, A. V. (2021) 'MGEnrichment: A web application for microglia gene list enrichment analysis', *PLoS Computational Biology*, 17(11), p. e1009160. doi: 10.1371/journal.pcbi.1009160.

Jarskog, L. F. *et al.* (2005) 'Apoptotic mechanisms in the pathophysiology of schizophrenia', *Progress in Neuro-Psychopharmacology and Biological Psychiatry*, pp. 846–858. doi: 10.1016/j.pnpbp.2005.03.010.

Johnson, E. A. *et al.* (2011) 'Increased expression of the chemokines CXCL1 and MIP-1α by resident brain cells precedes neutrophil infiltration in the brain following prolonged soman-induced status epilepticus in rats', *Journal of Neuroinflammation*, 8(1), pp. 1–10. doi: 10.1186/1742-2094-8-41.

Johnson, K. *et al.* (2016) 'Gfap-positive radial glial cells are an essential progenitor population for later-born neurons and glia in the zebrafish spinal cord', *GLIA*, 64(7), pp. 1170–1189. doi: 10.1002/glia.22990.

Jones, H. J. *et al.* (2016) 'Phenotypic Manifestation of Genetic Risk for Schizophrenia During Adolescence in the General Population', *Jama Psychiatry,* 73(3), pp. 221-228. doi: 10.1001/jamapsychiatry.2015.3058.

Jones, K. L. *et al.* (2017) 'Autism with intellectual disability is associated with increased levels of maternal cytokines and chemokines during gestation', *Molecular Psychiatry*, 22(2), pp. 273–279. doi: 10.1038/mp.2016.77.

Jostock, T. *et al.* (2001) 'Soluble gp130 is the natural inhibitor of soluble interleukin-6 receptor transsignaling responses', *European Journal of Biochemistry*, 268(1), pp. 160–167. doi: 10.1046/j.1432-1327.2001.01867.x.

Kageyama, R., Shimojo, H. and Imayoshi, I. (2015) 'Dynamic expression and roles of Hes factors in neural development', *Cell and Tissue Research*, 359(1), pp. 125–133. doi: 10.1007/s00441-014-1888-7.

Kahn, R. S. *et al.* (2015) 'Schizophrenia', *Nature Reviews Disease Primers*, 1(1), pp. 1–23. doi: 10.1038/nrdp.2015.67.

Kang, S. and Kishimoto, T. (2021) 'Interplay between interleukin-6 signaling and the vascular endothelium in cytokine storms', *Experimental and Molecular Medicine*, 53(7). doi: 10.1038/s12276-021-00649-0.

Karolewicz, B. *et al.* (2010) 'Reduced level of glutamic acid decarboxylase-67 kDa in the prefrontal cortex in major depression', *International Journal of Neuropsychopharmacology*, 13(4), pp. 411–420. doi: 10.1017/S1461145709990587.

Kathuria, A. *et al.* (2018a) 'Stem cell-derived neurons from autistic individuals with SHANK3 mutation show morphogenetic abnormalities during early development', *Molecular Psychiatry*, 23(3), pp. 735–746. doi: 10.1038/mp.2017.185.

Kathuria, A. *et al.* (2018b) 'Stem cell-derived neurons from autistic individuals with SHANK3 mutation show morphogenetic abnormalities during early development', *Molecular Psychiatry*, 23(3), pp. 735–746. doi: 10.1038/mp.2017.185.

Kathuria, A. *et al.* (2022) 'Distinct effects of interleukin-6 and interferon-γ on differentiating human cortical neurons', *Brain, Behavior, and Immunity*, 103, pp. 97–108. doi: 10.1016/j.bbi.2022.04.007.

Kawahara, H. *et al.* (2008) 'Neural RNA-binding protein Musashi1 inhibits translation initiation by competing with eIF4G for PABP', *Journal of Cell Biology*, 181(4), pp. 639–653. doi: 10.1083/jcb.200708004.

Kendler, K. S. and Jablensky, A. (2011) 'Kraepelin's concept of psychiatric illness', *Psychological Medicine*, pp. 1119–1126. doi: 10.1017/S0033291710001509.

Kenk, M. *et al.,* 2015 'Imaging neuroinflammation in gray and white matter in schizophrenia: An in-vivo PET study with [18 F]-FEPPA', *Schizophrenia Bulletin,* 41(1) pp. 85-93. doi: 10.1093/schbul/sbu157.

Kentner, A. C. *et al.* (2019) 'Maternal immune activation: reporting guidelines to improve the rigor, reproducibility, and transparency of the model', *Neuropsychopharmacology*, 44(2), pp. 245–258. doi: 10.1038/s41386-018-0185-7.

Kępińska, A. P. *et al.* (2020) 'Schizophrenia and Influenza at the Centenary of the 1918-1919 Spanish Influenza Pandemic: Mechanisms of Psychosis Risk', *Frontiers in Psychiatry*, p. 72. doi: 10.3389/fpsyt.2020.00072.

Khan, T. A. *et al.* (2020) 'Neuronal defects in a human cellular model of 22q11.2 deletion syndrome', *Nature Medicine*, 26(12), pp. 1888–1898. doi: 10.1038/s41591-020-1043-9.

Khandaker, G. M. *et al.* (2014) 'Association of serum interleukin 6 and C-reactive protein in childhood with depression and psychosis in young adult life a population-based longitudinal study', *JAMA Psychiatry*, 71(10), pp. 1121–1128. doi: 10.1001/jamapsychiatry.2014.1332.

Khodosevich, K. and Sellgren, C. M. (2023) 'Neurodevelopmental disorders—high-resolution rethinking of disease modeling', *Molecular Psychiatry*, 28(1), pp. 34–43. doi: 10.1038/s41380-022-01876-1.

Khurana, B. *et al.* (2002) 'Functions of LIM proteins in cell polarity and chemotactic motility', *EMBO Journal*, 21(20), pp. 5331–5342. doi: 10.1093/emboj/cdf550.

Kiehl, T. R. *et al.* (2009) 'Neuropathologic features in adults with 22q11.2 deletion syndrome', *Cerebral Cortex*, 19(1), pp. 153–164. doi: 10.1093/cercor/bhn066.

Kierdorf, K. *et al.* (2013) 'Microglia emerge from erythromyeloid precursors via Pu.1-and Irf8-dependent pathways', *Nature Neuroscience*, 16(3), pp. 273–280. doi: 10.1038/nn.3318.

Kierdorf, K. and Prinz, M. (2013) 'Factors regulating microglia activation', *Frontiers in Cellular Neuroscience*. Frontiers, p. 44. doi: 10.3389/fncel.2013.00044.

Kirov, G. *et al.* (2014) 'The penetrance of copy number variations for schizophrenia and developmental delay', *Biol Psychiatry*, 75(5), pp. 378-85. doi: 10.1016/j.biopsych.2013.07.022.

Knuesel, I. *et al.* (2014) 'Maternal immune activation and abnormal brain development across CNS disorders', *Nature Reviews Neurology*, pp. 643–660. doi: 10.1038/nrneurol.2014.187.

Koga, K. *et al.* (2009) 'Activation of TLR3 in the trophoblast is associated with preterm delivery', *American Journal of Reproductive Immunology*, 61(3), pp. 196–212. doi: 10.1111/j.1600-0897.2008.00682.x.

Kong, D. H. *et al.* (2018) 'Emerging roles of vascular cell adhesion molecule-1 (VCAM-1) in immunological disorders and cancer', *International Journal of Molecular Sciences*. doi: 10.3390/ijms19041057.

Kopczynska, M. *et al.* (2019) 'Complement system biomarkers in first episode psychosis', *Schizophrenia Research*, 204, pp. 16–22. doi: 10.1016/j.schres.2017.12.012.

Kowash, H. M. *et al.* (2019) 'Poly(I:C) source, molecular weight and endotoxin contamination affect dam and prenatal outcomes, implications for models of maternal immune activation', *Brain, Behavior, and Immunity*, 82, pp. 160–166. doi: 10.1016/j.bbi.2019.08.006.

Kraepelin, E. (1890) 'Ueber Psychosen nach Influenza', *Deutsche Medizinische Wochenschrift*, 16(11), pp. 209–212. doi: 10.1055/s-0029-1207083.

Krämer, A. *et al.* (2014) 'Causal analysis approaches in ingenuity pathway analysis', *Bioinformatics*, 30(4), pp. 523–530. doi: 10.1093/bioinformatics/btt703.

Kuljis, D. A. *et al.* (2019) 'Fluorescence-based quantitative synapse analysis for cell type-specific connectomics', *eNeuro*, 6(5). doi: 10.1523/ENEURO.0193-19.2019.

Kulkarni, V. A. and Firestein, B. L. (2012) 'The dendritic tree and brain disorders', *Molecular and Cellular Neuroscience*, pp. 10–20. doi: 10.1016/j.mcn.2012.03.005.

Lam, M. *et al.* (2019) 'Single cell analysis of autism patient with bi-allelic NRXN1-alpha deletion reveals skewed fate choice in neural progenitors and impaired neuronal functionality', *Experimental Cell Research*, 383(1), p. 111469. doi: 10.1016/j.yexcr.2019.06.014.

Lauber, E., Filice, F. and Schwaller, B. (2018) 'Parvalbumin neurons as a hub in autism spectrum disorders', *Journal of Neuroscience Research*, 96(3), pp. 360–361. doi: 10.1002/jnr.24204.

Laurence, J. A. and Fatemi, S. H. (2005) 'Glial fibrillary acidic protein is elevated in superior frontal, parietal and cerebellar cortices of autistic subjects', *Cerebellum*, 4(3), pp. 206–210. doi: 10.1080/14734220500208846.

Lawson, L. J. *et al.* (1990) 'Heterogeneity in the distribution and morphology of microglia in the normal adult mouse brain', *Neuroscience*, 39(1), pp. 151–170. doi: 10.1016/0306-4522(90)90229-W.

Lee, H. *et al.* (2018) 'BBOX1 is down-regulated in maternal immune-activated mice and implicated in genetic susceptibility to human schizophrenia', *Psychiatry Research*, 259, pp. 197–202. doi: 10.1016/j.psychres.2017.10.018.

Lee, J., Kim, S. W. and Kim, K. T. (2022) 'Region-Specific Characteristics of Astrocytes and Microglia: A Possible Involvement in Aging and Diseases', *Cells*. Cells. doi: 10.3390/cells11121902.

Lee, Y. *et al.* (2012) 'Induction and molecular signature of pathogenic T H 17 cells', *Nature Immunology*, 13(10), pp. 991–999. doi: 10.1038/ni.2416.

de Leeuw, C. A. *et al.* (2015) 'MAGMA: Generalized Gene-Set Analysis of GWAS Data', *PLoS Computational Biology*, 11(4). doi: 10.1371/journal.pcbi.1004219.

Li, H. *et al.* (2009) 'The Sequence Alignment/Map format and SAMtools', *Bioinformatics*, 25(16), pp. 2078–2079. doi: 10.1093/bioinformatics/btp352.

Li, J. *et al.* (2019) 'Mitochondrial deficits in human iPSC-derived neurons from patients with 22q11.2 deletion syndrome and schizophrenia', *Translational Psychiatry 2019 9:1*, 9(1), pp. 1–10. doi: 10.1038/s41398-019-0643-y.

Li, J. *et al.* (2021) 'Association of Mitochondrial Biogenesis with Variable Penetrance of Schizophrenia', *JAMA Psychiatry*, 78(8), pp. 911–921. doi: 10.1001/jamapsychiatry.2021.0762.

Li, Q. and Barres, B. A. (2018) 'Microglia and macrophages in brain homeostasis and disease', *Nature Reviews Immunology*, pp. 225–242. doi: 10.1038/nri.2017.125.

Li, Y. *et al.* (2018) 'Maternal and early postnatal immune activation produce dissociable effects on neurotransmission in mPFC–amygdala circuits', *Journal of Neuroscience*, 38(13), pp. 3358–3372. doi: 10.1523/JNEUROSCI.3642-17.2018.

Li, Y. *et al.* (2021) 'Investigation of neurodevelopmental deficits of 22 q11.2 deletion syndrome with a patient-ipsc-derived blood–brain barrier model', *Cells*, 10(10). doi: 10.3390/cells10102576.

Li, Y. *et al.* (2023) 'Inhibition of Abl Kinase by Imatinib Can Rescue the Compromised Barrier Function of 22q11.2DS Patient-iPSC-Derived Blood–Brain Barriers', *Cells*, 12(3). doi: 10.3390/cells12030422.

Li, Z. *et al.* (2017) 'Reduced ENA78 levels as novel biomarker for major depressive disorder and venlafaxine efficiency: Result from a prospective longitudinal study', *Psychoneuroendocrinology*, 81, pp. 113–121. doi: 10.1016/j.psyneuen.2017.03.015.

Liao, Y. *et al.* (2019) 'WebGestalt 2019: gene set analysis toolkit with revamped UIs and APIs', *Nucleic Acids Research*, 47(W1), pp. W199–W205. doi: 10.1093/nar/gkz401.

Liao, Y., Smyth, G. K. and Shi, W. (2019) 'The R package Rsubread is easier, faster, cheaper and better for alignment and quantification of RNA sequencing reads', *Nucleic Acids Research*, 47(8), p. e47. doi: 10.1093/nar/gkz114.

Lionel, A. C. *et al.* (2013) 'Rare exonic deletions implicate the synaptic organizer gephyrin (GPHN) in risk for autism, schizophrenia and seizures', *Human Molecular Genetics*, 22(10), pp. 2055–2066. doi: 10.1093/hmg/ddt056.

Liu, D. *et al.* (2022) 'Impact of schizophrenia GWAS loci converge onto distinct pathways in cortical interneurons vs glutamatergic neurons during development', *Molecular Psychiatry*, 27(10), pp. 4218–4233. doi: 10.1038/s41380-022-01654-z.

Liu, L. *et al.* (2019) 'Protection of ZIKV infection-induced neuropathy by abrogation of acute antiviral response in human neural progenitors', *Cell Death and Differentiation*, 26(12), pp. 2607–2621. doi: 10.1038/s41418-019-0324-7.

Liu, L. *et al.* (2020) 'Three-dimensional brain-on-chip model using human iPSC-derived GABAergic neurons and astrocytes: Butyrylcholinesterase posttreatment for acute malathion exposure', *PLoS ONE*, 15(3). doi: 10.1371/journal.pone.0230335.

Liu, L. *et al.* (2022) 'A Three-Dimensional Brain-on-a-Chip Using Human iPSC-Derived GABAergic Neurons and Astrocytes', in *Methods in Molecular Biology*, pp. 117–128. doi: 10.1007/978-1-0716-2289-6_6.

Livak, K. J. and Schmittgen, T. D. (2001) 'Analysis of relative gene expression data using real-time quantitative PCR and the 2-ΔΔCT method', *Methods*, 25(4), pp. 402–408. doi: 10.1006/meth.2001.1262.

Loh, Y. H. *et al.* (2009) 'Generation of induced pluripotent stem cells from human blood', *Blood*, 113(22), pp. 5476–5479. doi: 10.1182/blood-2009-02-204800.

Lombardo, M. V. *et al.* (2018) 'Maternal immune activation dysregulation of the fetal brain transcriptome and relevance to the pathophysiology of autism spectrum disorder', *Molecular Psychiatry*, 23(4), pp. 1001–1013. doi: 10.1038/mp.2017.15.

Long, K. *et al.* (2016) 'Integrin signalling regulates the expansion of neuroepithelial progenitors and neurogenesis via Wnt7a and Decorin', *Nature Communications*, 7(1), p. 10354. doi: 10.1038/ncomms10354.

Long, K. R. and Huttner, W. B. (2019) 'How the extracellular matrix shapes neural development', *Open Biology*, 9(1). doi: 10.1098/rsob.180216.

Love, M. I., Huber, W. and Anders, S. (2014) 'Moderated estimation of fold change and dispersion for RNA-seq data with DESeq2', *Genome Biology*, 15(12), pp. 1–21. doi: 10.1186/s13059-014-0550-8.

Lu, Y. R. *et al.* (2019) 'High concentrations of serum interleukin-6 and interleukin-8 in patients with bipolar disorder', *Medicine (United States)*, 98(7). doi: 10.1097/MD.0000000000014419.

Luan, W. *et al.* (2022) 'Proteomic dissimilarities of primary microglia and BV2 cells under stimuli', *European Journal of Neuroscience*, 55(7), pp. 1709–1723. doi: 10.1111/ejn.15637.

Lydholm, C. N. *et al.* (2019) 'Parental Infections Before, During, and After Pregnancy as Risk Factors for Mental Disorders in Childhood and Adolescence: A Nationwide Danish Study', *Biological Psychiatry*, 85(4), pp. 317–325. doi: 10.1016/j.biopsych.2018.09.013.

Ma, C. *et al.* (2018) 'The integrated landscape of causal genes and pathways in schizophrenia', *Translational Psychiatry*. doi: 10.1038/s41398-018-0114-x.

Ma, Z. *et al.* (2016) 'Neuromodulators signal through astrocytes to alter neural circuit activity and behaviour', *Nature*, 539(7629), pp. 428–432. doi: 10.1038/NATURE20145.

Mackenzie, F. and Ruhrberg, C. (2012) 'Diverse roles for VEGF-A in the nervous system', *Development*. The Company of Biologists, pp. 1371–1380. doi: 10.1242/dev.072348.

Madry, C. and Attwell, D. (2015) 'Receptors, ion channels, and signaling mechanisms underlying Microglial dynamics', *Journal of Biological Chemistry*, 290(20), pp. 12443–12450. doi: 10.1074/jbc.R115.637157.

Mahic, M. *et al.* (2017) 'Epidemiological and Serological Investigation into the Role of Gestational Maternal Influenza Virus Infection and Autism Spectrum Disorders', *ASM Journals,* 2(3), doi: 10.1128/msphere.00159-17.

Mairesse, J. *et al.* (2019) 'Oxytocin receptor agonist reduces perinatal brain damage by targeting microglia', *GLIA*, 67(2), pp. 345–359. doi: 10.1002/glia.23546.

Malaspina, D. *et al.* (2008) 'Acute maternal stress in pregnancy and schizophrenia in offspring: A cohort prospective study', *BMC Psychiatry*, 8. doi: 10.1186/1471-244X-8-71.

Mancuso, M. R., Kuhnert, F. and Kuo, C. J. (2008) 'Developmental angiogenesis of the central nervous system', *Lymphatic Research and Biology*, 6(3–4), pp. 173–180. doi: 10.1089/lrb.2008.1014.

Mao, L. *et al.* (2020) 'Neurologic Manifestations of Hospitalized Patients with Coronavirus Disease 2019 in Wuhan, China', *JAMA Neurology*, 77(6), pp. 683–690. doi: 10.1001/jamaneurol.2020.1127.

Marchetto, M. C. *et al.* (2017) 'Altered proliferation and networks in neural cells derived from idiopathic autistic individuals', *Molecular Psychiatry*, 22(6), pp. 820–835. doi: 10.1038/mp.2016.95.

Mariani, J. *et al.* (2015) 'FOXG1-Dependent Dysregulation of GABA/Glutamate Neuron Differentiation in Autism Spectrum Disorders', *Cell*, 162(2), pp. 375–390. doi: 10.1016/j.cell.2015.06.034.

Marin Navarro, A. *et al.* (2018) 'Modeling cancer using patient-derived induced pluripotent stem cells to understand development of childhood malignancies', *Cell Death Discovery*. Nature Publishing Group, pp. 1–9. doi: 10.1038/s41420-017-0009-2.

Martínez-Cerdeño, V. (2017) 'Dendrite and spine modifications in autism and related neurodevelopmental disorders in patients and animal models', *Developmental Neurobiology*, pp. 393–404. doi: 10.1002/dneu.22417.

Masuda, T. *et al.* (2012) 'IRF8 Is a Critical Transcription Factor for Transforming Microglia into a Reactive Phenotype', *Cell Reports*, 1(4), pp. 334–340. doi: 10.1016/j.celrep.2012.02.014.

Masuda, T. *et al.* (2014) 'IRF8 is a transcriptional determinant for microglial motility', *Purinergic Signalling*, 10(3), pp. 515–521. doi: 10.1007/s11302-014-9413-8.

Matcovitch-Natan, O. *et al.* (2016) 'Microglia development follows a stepwise program to regulate brain homeostasis', *Science*, 353(6301). doi: 10.1126/science.aad8670.

Matelski, L. *et al.* (2021) 'Effects of cytokines on nuclear factor-kappa B, cell viability, and synaptic connectivity in a human neuronal cell line', *Molecular Psychiatry*, 26(3), pp. 875–887. doi: 10.1038/s41380-020-0647-2.

Matias, I., Morgado, J. and Gomes, F. C. A. (2019) 'Astrocyte Heterogeneity: Impact to Brain Aging and Disease', *Frontiers in Aging Neuroscience*, 11. doi: 10.3389/fnagi.2019.00059.

Matsushima, K., Yang, D. and Oppenheim, J. J. (2022) 'Interleukin-8: An evolving chemokine', *Cytokine*. doi: 10.1016/j.cyto.2022.155828.

Matuleviciute, R. *et al.* (2023) 'Microglial contribution to the pathology of neurodevelopmental disorders in humans', *Acta Neuropathologic.* doi: 10.1007/s00401-023-02629-2.

Mccullumsmith, R. E. *et al.* (2014) 'Postmortem brain: An underutilized substrate for studying severe mental illness', *Neuropsychopharmacology*, 39(1), pp. 65–87. doi: 10.1038/npp.2013.239.

McDonald-McGinn, D. M. *et al.* (2001) 'Phenotype of the 22q11.2 deletion in individuals identified through an affected relative: Cast a wide FISHing net!', *Genetics in Medicine*, 3(1), pp. 23–29. doi: 10.1097/00125817-200101000-00006.

McDonald-McGinn, D. M. *et al.* (2015) '22q11.2 deletion syndrome', *Nature Reviews Disease Primers*, 1(1), pp. 1–19. doi: 10.1038/nrdp.2015.71.

McGrath, E. L. *et al.* (2017) 'Differential Responses of Human Fetal Brain Neural Stem Cells to Zika Virus Infection', *Stem Cell Reports*, 8(3), pp. 715–727. doi: 10.1016/j.stemcr.2017.01.008.

McGuffin, P., Owen, M. J. and Farmer, A. E. (1995) 'Genetic basis of schizophrenia', *The Lancet*, 346(8976), pp. 678–682. doi: 10.1016/S0140-6736(95)92285-7.

McLarnon, J. G. (2012) 'Microglial chemotactic signaling factors in Alzheimer's disease', *American Journal of Neurodegenerative Diseases*, pp. 199–204.

McNeill, R. V. *et al.* (2020) 'Mental health dished up—the use of iPSC models in neuropsychiatric research', *Journal of Neural Transmission*. Springer, pp. 1547–1568. doi: 10.1007/s00702-020-02197-9.

Melief, J. *et al.* (2012) 'Phenotyping primary human microglia: Tight regulation of LPS responsiveness', *GLIA*, 60(10), pp. 1506–1517. doi: 10.1002/glia.22370.

Menassa, D. A. *et al.* (2022) 'The spatiotemporal dynamics of microglia across the human lifespan', *Developmental Cell*, 57(17), pp. 2127-2139.e6. doi: 10.1016/j.devcel.2022.07.015.

Menninger, K. A. (1919) 'Psychoses associated with influenza: I. general data: Statistical analysis', *Journal of the American Medical Association*, 72(4), pp. 235–241. doi: 10.1001/jama.1919.02610040001001.

Meyer, U. *et al.* (2006) 'The time of prenatal immune challenge determines the specificity of inflammation-mediated brain and behavioral pathology', *Journal of Neuroscience*, 26(18), pp. 4752–4762. doi: 10.1523/JNEUROSCI.0099-06.2006.

Meyer, U. *et al.* (2008) 'Preliminary evidence for a modulation of fetal dopaminergic development by maternal immune activation during pregnancy', *Neuroscience*, 154(2), pp. 701–709. doi: 10.1016/j.neuroscience.2008.04.031.

Meyer, Urs *et al.* (2008) 'Relative prenatal and postnatal maternal contributions to schizophrenia-related neurochemical dysfunction after in utero immune challenge', *Neuropsychopharmacology*, 33(2), pp. 441–456. doi: 10.1038/sj.npp.1301413.

Meyer, U. (2014) 'Prenatal Poly(I:C) exposure and other developmental immune activation models in rodent systems', *Biological Psychiatry*, 75(4), pp. 307–315. doi: 10.1016/j.biopsych.2013.07.011.

Meyer, U. (2019) 'Neurodevelopmental Resilience and Susceptibility to Maternal Immune Activation', *Trends in Neurosciences*, pp. 793–806. doi: 10.1016/j.tins.2019.08.001.

Meyer, U. and Feldon, J. (2010) 'Epidemiology-driven neurodevelopmental animal models of schizophrenia', *Progress in Neurobiology*. doi: 10.1016/j.pneurobio.2009.10.018.

Miao, W. *et al.* (2020) 'IL-13 Ameliorates Neuroinflammation and Promotes Functional Recovery after Traumatic Brain Injury', *The Journal of Immunology*, 204(6), pp. 1486–1498. doi: 10.4049/jimmunol.1900909.

Michalopoulou, M. *et al.* (2004) 'Soluble interleukin-6 receptor (sIL-6R) in cerebrospinal fluid of patients with inflammatory and non inflammatory neurological diseases', *Immunology Letters*, 94(3), pp. 183–189. doi: 10.1016/j.imlet.2004.04.018.

Michel, M. *et al.* (2021) 'Increased GFAP concentrations in the cerebrospinal fluid of patients with unipolar depression', *Translational Psychiatry*, 11(1), pp. 1–9. doi: 10.1038/s41398-021-01423-6.

Middeldorp, J. *et al.* (2010) 'GFAPdelta in radial glia and subventricular zone progenitors in the developing human cortex', *Development (Cambridge, England)*, 137(2), pp. 313–321. doi: 10.1242/DEV.041632.

Mihalas, A. B. and Hevner, R. F. (2017) 'Control of Neuronal Development by T-Box Genes in the Brain', in *Current Topics in Developmental Biology*. Curr Top Dev Biol, pp. 279–312. doi: 10.1016/bs.ctdb.2016.08.001.

Miller, E. B. *et al.* (2019) 'In vivo imaging reveals transient microglia recruitment and functional recovery of photoreceptor signaling after injury', *Proceedings of the National Academy of Sciences of the United States of America*, 116(33), pp. 16603–16612. doi: 10.1073/pnas.1903336116.

Miller, J. A. *et al.* (2014) 'Transcriptional landscape of the prenatal human brain', *Nature*, 508(7495), pp. 199–206. doi: 10.1038/nature13185.

Mirabella, F. *et al.* (2021) 'Prenatal interleukin 6 elevation increases glutamatergic synapse density and disrupts hippocampal connectivity in offspring', *Immunity*, 54(11), pp. 2611-2631.e8. doi: 10.1016/j.immuni.2021.10.006.

Miyata, S. *et al.* (2021) 'Global knockdown of glutamate decarboxylase 67 elicits emotional abnormality in mice', *Molecular Brain*, 14(1). doi: 10.1186/s13041-020-00713-2.

Miyata, T. *et al.* (2001) 'Asymmetric inheritance of radial glial fibers by cortical neurons', *Neuron*, 31(5), pp. 727–741. doi: 10.1016/S0896-6273(01)00420-2.

Miyoshi, K. *et al.* (2008) 'Interleukin-18-mediated microglia/astrocyte interaction in the spinal cord enhances neuropathic pain processing after nerve injury', *Journal of Neuroscience*, 28(48), pp. 12775–12787. doi: 10.1523/JNEUROSCI.3512-08.2008.

Moghaddam, B. and Javitt, D. (2012) 'From revolution to evolution: The glutamate hypothesis of schizophrenia and its implication for treatment', *Neuropsychopharmacology*, 37(1), pp. 4–15. doi: 10.1038/npp.2011.181.

Mokhtari, R. and Lachman, H. M. (2016) 'The Major Histocompatibility Complex (MHC) in Schizophrenia: A Review', *Journal of Clinical & Cellular Immunology*. doi: 10.4172/2155-9899.1000479.

Mondelli, V. *et al.* (2017) 'Brain microglia in psychiatric disorders', *The Lancet Psychiatry*, 4(7), pp. 563–572. doi: 10.1016/S2215-0366(17)30101-3.

Monks, S. *et al.* (2014) 'Further evidence for high rates of schizophrenia in 22q11.2 deletion syndrome', *Schizophrenia Research*, 153(1–3), pp. 231–236. doi: 10.1016/j.schres.2014.01.020.

Du Montcel, S. T. *et al.* (1996) 'Prevalence of 22q11 microdeletion [1]', *Journal of Medical Genetics*. J Med Genet, p. 719. doi: 10.1136/jmg.33.8.719.

Morris, G. *et al.* (2018) 'Leaky brain in neurological and psychiatric disorders: Drivers and consequences', *Australian and New Zealand Journal of Psychiatry*, 52(10), pp. 924–948. doi: 10.1177/0004867418796955.

Morrow, B. E. *et al.* (2018) 'Molecular genetics of 22q11.2 deletion syndrome', *American Journal of Medical Genetics, Part A*, pp. 2070–2081. doi: 10.1002/ajmg.a.40504.

Mueller, F. S. *et al.* (2018) 'Mouse models of maternal immune activation: Mind your caging system!', *Brain, Behavior, and Immunity*, 73, pp. 643–660. doi: 10.1016/j.bbi.2018.07.014.

Mueller, F. S. *et al.* (2019) 'Influence of poly(I:C) variability on thermoregulation, immune responses and pregnancy outcomes in mouse models of maternal immune activation', *Brain, Behavior, and Immunity*, 80, pp. 406–418. doi: 10.1016/j.bbi.2019.04.019.

Mueller, F. S. *et al.* (2020) 'Behavioral, neuroanatomical, and molecular correlates of resilience and susceptibility to maternal immune activation', *Molecular Psychiatry*. doi: 10.1038/s41380-020-00952-8.

Mueller, F. S. *et al.* (2021) 'Behavioral, neuroanatomical, and molecular correlates of resilience and susceptibility to maternal immune activation', *Molecular Psychiatry*, 26, pp. 396–410. doi: 10.1038/s41380-020-00952-8.

Müllberg, J. *et al.* (1992) 'Protein kinase C activity is rate limiting for shedding of the interleukin-6 receptor', *Biochemical and Biophysical Research Communications*, 189(2), pp. 794–800. doi: 10.1016/0006-291X(92)92272-Y.

Müllberg, J. *et al.* (1999) 'Generation and function of the soluble interleukin-6 receptor', *Biochemical Society Transactions*, 27(2), pp. 211–219. doi: 10.1042/bst0270211.

Mullins, N. *et al.* (2021) 'Genome-wide association study of more than 40,000 bipolar disorder cases provides new insights into the underlying biology', *Nature Genetics*, 53(6). doi: 10.1038/s41588-021-00857-4.

Murphy, C. E., Walker, A. K. and Weickert, C. S. (2021) 'Neuroinflammation in schizophrenia: the role of nuclear factor kappa B', *Translational Psychiatry*. doi: 10.1038/s41398-021-01607-0.

Murphy, K. C., Jones, L. A. and Owen, M. J. (1999) 'High rates of schizophrenia in adults with velo-cardio-facial syndrome', *Archives of general psychiatry*, 56(10), pp. 940–945. doi: 10.1001/ARCHPSYC.56.10.940.

Murray, R. M. *et al.* (2022) 'Schizophrenia: A developmental disorder with a risk of non-specific but avoidable decline', *Schizophrenia Research*, 243, pp. 181–186. doi: 10.1016/j.schres.2022.03.005.

Nakamura, J. P. *et al.* (2019) 'The maternal immune activation model uncovers a role for the Arx gene in GABAergic dysfunction in schizophrenia', *Brain, Behavior, and Immunity*. doi: 10.1016/j.bbi.2019.06.009.

Nakata, Y. *et al.* (2021) 'Oxytocin system dysfunction in patients with treatment-resistant schizophrenia: Alterations of blood oxytocin levels and effect of a genetic variant of OXTR', *Journal of Psychiatric Research*, 138, pp. 219–227. doi: 10.1016/j.jpsychires.2021.03.053.

Nakua, H. *et al.* (2022) 'Cortico-amygdalar connectivity and externalizing/internalizing behavior in children with neurodevelopmental disorders', *Brain Structure and Function*, 227(6), pp. 1963–1979. doi: 10.1007/s00429-022-02483-0.

Nasiri, E. *et al.* (2020) 'Key role of MIF-related neuroinflammation in neurodegeneration and cognitive impairment in Alzheimer's disease', *Molecular Medicine*, 26(1). doi: 10.1186/s10020-020-00163-5.

Nehme, R. *et al.* (2022) 'The 22q11.2 region regulates presynaptic gene-products linked to schizophrenia', *Nature Communications*, 13(1), pp. 1–21. doi: 10.1038/s41467-022-31436-8.

Newcomer, J *et al.,* (1999) 'Ketamine-Induced NMDA Receptor Hypofunction as a Model of Memory Impairment and Psychosis', *Neuropsychopharmacology*, 20, pp. 106-118. doi: 10.1016/S0893-133X(98)00067-0.

Nguyen, T. T. *et al.* (2018) 'Abnormal levels of vascular endothelial biomarkers in schizophrenia', *European Archives of Psychiatry and Clinical Neuroscience*, 268(8), pp. 849–860. doi: 10.1007/s00406-017-0842-6.

Nielsen, P. R., Benros, M. E. and Mortensen, P. B. (2014) 'Hospital contacts with infection and risk of schizophrenia: A population-based cohort study with linkage of danish national registers', *Schizophrenia Bulletin*, 40(6), pp. 1526–1532. doi: 10.1093/schbul/sbt200.

Nimmerjahn, A., Kirchhoff, F. and Helmchen, F. (2005) 'Neuroscience: Resting microglial cells are highly dynamic surveillants of brain parenchyma in vivo', *Science*, 308(5726), pp. 1314–1318. doi: 10.1126/science.1110647.

Noctor, S. C. *et al.* (2002) 'Dividing precursor cells of the embryonic cortical ventricular zone have morphological and molecular characteristics of radial glia', *Journal of Neuroscience*, 22(8), pp. 3161–3173. doi: 10.1523/jneurosci.22-08-03161.2002.

Notter, T. *et al.* (2018) 'Reconceptualization of translocator protein as a biomarker of neuroinflammation in psychiatry', *Molecular Psychiatry*, pp. 36–47. doi: 10.1038/mp.2017.232.

Nowakowski, T. J. *et al.* (2017) 'Spatiotemporal gene expression trajectories reveal developmental hierarchies of the human cortex', *Science*, 358(6368), pp. 1318–1323. doi: 10.1126/science.aap8809.

Nutma, E. *et al.* (2023) ‘Translocator protein is a marker of activated microglia in rodent models but not human neurodegenerative diseases’, *Nat Commun.,* 14(1):5247. Doi: 10.1038/s41467-023-40937-z.

Nyffeler, M. *et al.* (2006) ‘Maternal immune activation during pregnancy increases limbic GABAA receptor immunoreactivity in the adult offspring: Implications for schizophrenia’, *Neuroscience*, 143(1), pp. 51–62. doi: 10.1016/j.neuroscience.2006.07.029.

O’Brien, H. E. *et al.* (2018) ‘Sex differences in gene expression in the human fetal brain’, *bioRxiv*. doi: 10.1101/483636.

Okahisa, Y. *et al.* (2010) ‘Leukemia inhibitory factor gene is associated with schizophrenia and working memory function’, *Progress in Neuro-Psychopharmacology and Biological Psychiatry*. doi: 10.1016/j.pnpbp.2009.10.020.

Okano, H. and Temple, S. (2009) ‘Cell types to order: temporal specification of CNS stem cells’, *Current Opinion in Neurobiology*. Curr Opin Neurobiol, pp. 112–119. doi: 10.1016/j.conb.2009.04.003.

Okuda, K. S. and Hogan, B. M. (2020) ‘Endothelial Cell Dynamics in Vascular Development: Insights From Live-Imaging in Zebrafish’, *Frontiers in Physiology*. doi: 10.3389/fphys.2020.00842.

Olah, M. *et al.* (2020) ‘Single cell RNA sequencing of human microglia uncovers a subset associated with Alzheimer’s disease’, *Nature Communications*, 11(1), pp. 1–18. doi: 10.1038/s41467-020-19737-2.

de Oliveira Pereira Ribeiro, L. *et al.* (2018) 'Evidence for Association Between OXTR Gene and ASD Clinical Phenotypes', *Journal of Molecular Neuroscience*, 65(2), pp. 213–221. doi: 10.1007/s12031-018-1088-0.

Oliveira-Silva, P. *et al.* (2007) 'Matrix metalloproteinase-9 is involved in the development and plasticity of retinotectal projections in rats', in *NeuroImmunoModulation*. Neuroimmunomodulation, pp. 144–149. doi: 10.1159/000110638.

Olsen, L. *et al.* (2018) 'Prevalence of rearrangements in the 22q11.2 region and population-based risk of neuropsychiatric and developmental disorders in a Danish population: a case-cohort study', *The Lancet Psychiatry*, 5(7), pp. 573–580. doi: 10.1016/S2215-0366(18)30168-8.

Oni-Orisan, A. *et al.* (2008) 'Altered Vesicular Glutamate Transporter Expression in the Anterior Cingulate Cortex in Schizophrenia', *Biological Psychiatry*, 63(8), pp. 766–775. doi: 10.1016/j.biopsych.2007.10.020.

Onwordi, E. C. *et al.* (2020) 'Synaptic density marker SV2A is reduced in schizophrenia patients and unaffected by antipsychotics in rats', *Nature Communications*, 11(1). doi: 10.1038/s41467-019-14122-0.

Ormel, P. R. *et al.* (2020) 'A characterization of the molecular phenotype and inflammatory response of schizophrenia patient-derived microglia-like cells', *Brain, Behavior, and Immunity*, 90, pp. 196–207. doi: 10.1016/j.bbi.2020.08.012.

Osborne, B. F. *et al.* (2019) 'Sex- and region-specific differences in microglia phenotype and characterization of the peripheral immune response following early-life infection in neonatal male and female rats', *Neuroscience Letters*, 692, pp. 1–9. doi: 10.1016/j.neulet.2018.10.044.

Óskarsdóttir, S., Vujic, M. and Fasth, A. (2004) 'Incidence and prevalence of the 22q11 deletion syndrome: A population-based study in Western Sweden', *Archives of Disease in Childhood*, 89(2), pp. 148–151. doi: 10.1136/adc.2003.026880.

Ozaki, K. *et al.* (2020) 'Maternal immune activation induces sustained changes in fetal microglia motility', *Scientific Reports*, 10(1), pp. 1–19. doi: 10.1038/s41598-020-78294-2.

Padberg, F. *et al.* (1999) 'CSF and serum levels of soluble interleukin-6 receptors (sIL-6R and sgp130), but not of interleukin-6 are altered in multiple sclerosis', *Journal of Neuroimmunology*, 99(2), pp. 218–223. doi: 10.1016/S0165-5728(99)00120-4.

Pantazis, C. B. *et al.* (2022) 'A reference human induced pluripotent stem cell line for large-scale collaborative studies', *Cell Stem Cell*, 29(12). doi: 10.1016/j.stem.2022.11.004.

Paolicelli, R. C. *et al.* (2011) 'Synaptic pruning by microglia is necessary for normal brain development', *Science*, 333(6048), pp. 1456–1458. doi: 10.1126/science.1202529.

Paolicelli, R. C. *et al.* (2022) 'Microglia states and nomenclature: A field at its crossroads', *Neuron*, pp. 3458–3483. doi: 10.1016/j.neuron.2022.10.020.

Pardiñas, A. F. *et al.* (2018) 'Common schizophrenia alleles are enriched in mutation-intolerant genes and in regions under strong background selection', *Nature Genetics*, 50(3), pp. 381–389. doi: 10.1038/s41588-018-0059-2.

Park, G. H. *et al.* (2020) 'Activated microglia cause metabolic disruptions in developmental cortical interneurons that persist in interneurons from individuals with schizophrenia', *Nature Neuroscience*, 23(11), pp. 1352–1364. doi: 10.1038/s41593-020-00724-1.

Pașca, S. P. *et al.* (2022) 'A nomenclature consensus for nervous system organoids and assembloids', *Nature*, 609(7929), pp. 907–910. doi: 10.1038/s41586-022-05219-6.

Patten, A. R., Fontaine, C. J. and Christie, B. R. (2014) 'A comparison of the different animal models of fetal alcohol spectrum disorders and their use in studying complex behaviors', *Frontiers in Pediatrics*. doi: 10.3389/fped.2014.00093.

Pavlinek, A. *et al.* (2021) 'Interferon-y Exposure of Human iPSC-derived Neurons Alters Major Histocompatibility Complex I and Synapsin I Protein Expression', *bioRxiv*, p. 2021.12.15.472810. doi: 10.1101/2021.12.15.472810.

Pera, M. F. (2017) 'Human embryo research and the 14-day rule', *Development (Cambridge)*, 144(11), pp. 1923–1925. doi: 10.1242/dev.151191.

Perälä, J. *et al.* (2007) 'Lifetime prevalence of psychotic and bipolar I disorders in a general population', *Archives of General Psychiatry*, 64(1), pp. 19–28. doi: 10.1001/archpsyc.64.1.19.

Pérez-Rodríguez, D. R., Blanco-Luquin, I. and Mendioroz, M. (2021) 'The Participation of Microglia in Neurogenesis: A Review', *Brain Sciences*, 11(5). doi: 10.3390/BRAINSCI11050658.

Perry, B. I. *et al.* (2021) 'Associations of immunological proteins/traits with schizophrenia, major depression and bipolar disorder: A bi-directional two-sample mendelian randomization study', *Brain, Behavior, and Immunity*, 97, pp. 176–185. doi: 10.1016/j.bbi.2021.07.009.

Peters, M. *et al.* (1997) 'Extramedullary expansion of hematopoietic progenitor cells in interleukin (IL)-6-sIL-6R double transgenic mice', *Journal of Experimental Medicine*, 185(4), pp. 755–766. doi: 10.1084/jem.185.4.755.

Polioudakis, D. *et al.* (2019) 'A Single-Cell Transcriptomic Atlas of Human Neocortical Development during Mid-gestation', *Neuron*, 103(5), pp. 785-801.e8. doi: 10.1016/j.neuron.2019.06.011.

Pont-Lezica, L. *et al.* (2011) 'Physiological roles of microglia during development', *Journal of Neurochemistry*, pp. 901–908. doi: 10.1111/j.1471-4159.2011.07504.x.

Potter, H. G. *et al.* (2023) 'Maternal behaviours and adult offspring behavioural deficits are predicted by maternal TNFα concentration in a rat model of neurodevelopmental disorders', *Brain, Behavior, and Immunity*, 108, pp. 162–175. doi: 10.1016/J.BBI.2022.12.003.

Price, A. J., Jaffe, A. E. and Weinberger, D. R. (2021) 'Cortical cellular diversity and development in schizophrenia', *Molecular Psychiatry*. NIH Public Access, pp. 203–217. doi: 10.1038/s41380-020-0775-8.

Przanowski, P. *et al.* (2014) 'The signal transducers Stat1 and Stat3 and their novel target Jmjd3 drive the expression of inflammatory genes in microglia', *Journal of Molecular Medicine*, 92(3), pp. 239–254. doi: 10.1007/s00109-013-1090-5.

Purves-Tyson, T. D. *et al.* (2020) 'Increased Macrophages and C1qA, C3, C4 Transcripts in the Midbrain of People With Schizophrenia', *Frontiers in Immunology*, 11. doi: 10.3389/fimmu.2020.02002.

Purves-Tyson, T. D. *et al.* (2021) 'Increased levels of midbrain immune-related transcripts in schizophrenia and in murine offspring after maternal immune activation', *Molecular Psychiatry*, 26(3), pp. 849–863. doi: 10.1038/s41380-019-0434-0.

Qi, H. and Pei, D. (2007) 'The magic of four: Induction of pluripotent stem cells from somatic cells by Oct4, Sox2, Myc and Klf4', *Cell Research*, 17(7), pp. 578–580. doi: 10.1038/cr.2007.59.

R Core Team (2020) 'R: A language and environment for statistical'. R Foundation for Statistical Computing, Vienna, Austria.

Rahman, T. *et al.* (2020) 'Effect of Immune Activation during Early Gestation or Late Gestation on Inhibitory Markers in Adult Male Rats', *Scientific Reports*, 10(1), p. 77. doi: 10.1038/s41598-020-58449-x.

Ransohoff, R. M. (2016) 'How neuroinflammation contributes to neurodegeneration', *Science*, 353(6301), pp. 777–783. doi: 10.1126/science.aag2590.

Ransohoff, R. M. and Engelhardt, B. (2012) 'The anatomical and cellular basis of immune surveillance in the central nervous system', *Nature Reviews Immunology 2012 12:9*, 12(9), pp. 623–635. doi: 10.1038/nri3265.

Rasmussen, J. M. *et al.* (2019) 'Maternal Interleukin-6 concentration during pregnancy is associated with variation in frontolimbic white matter and cognitive development in early life', *NeuroImage*, 185, pp. 825–835. doi: 10.1016/j.neuroimage.2018.04.020.

Rasmussen, J. M. *et al.* (2021) 'Neuroanatomical Correlates Underlying the Association Between Maternal Interleukin 6 Concentration During Pregnancy and Offspring Fluid Reasoning Performance in Early Childhood', *Biological Psychiatry: Cognitive Neuroscience and Neuroimaging*. doi: 10.1016/j.bpsc.2021.03.007.

Reeh, H. *et al.* (2019) 'Response to IL-6 trans- A nd IL-6 classic signalling is determined by the ratio of the IL-6 receptor α to gp130 expression: Fusing experimental insights and dynamic modelling', *Cell Communication and Signaling*, 17(1), pp. 1–21. doi: 10.1186/s12964-019-0356-0.

Reid, M. J. *et al.* (2022) 'Cell line specific alterations in genes associated with dopamine metabolism and signaling in midbrain dopaminergic neurons derived from 22q11.2 deletion carriers with elevated dopamine synthesis capacity', *Schizophrenia Research*. doi: 10.1016/j.schres.2022.05.010.

Reinhard, S. M., Razak, K. and Ethell, I. M. (2015) 'A delicate balance: Role of MMP-9 in brain development and pathophysiology of neurodevelopmental disorders', *Frontiers in Cellular Neuroscience*, 9(JULY). doi: 10.3389/fncel.2015.00280.

Richetto, J. *et al.* (2014) 'Prenatal immune activation induces maturation-dependent alterations in the prefrontal GABAergic transcriptome', *Schizophrenia Bulletin*, 40(2), pp. 351–361. doi: 10.1093/schbul/sbs195.

Richetto, J. *et al.* (2017) 'Genome-wide DNA Methylation Changes in a Mouse Model of Infection-Mediated Neurodevelopmental Disorders', *Biological Psychiatry*, 81(3), pp. 265–276. doi: 10.1016/j.biopsych.2016.08.010.

Rigato, C. *et al.* (2011) 'Pattern of invasion of the embryonic mouse spinal cord by microglial cells at the time of the onset of functional neuronal networks', *GLIA*, 59(4), pp. 675–695. doi: 10.1002/glia.21140.

Ripke, S. *et al.* (2014) 'Biological insights from 108 schizophrenia-associated genetic loci', *Nature*, 511(7510), pp. 421–427. doi: 10.1038/nature13595.

Ritchie, L. *et al.* (2018) 'Toll-like receptor 3 activation impairs excitability and synaptic activity via TRIF signalling in immature rat and human neurons', *Neuropharmacology*, 135, pp. 1–10. doi: 10.1016/j.neuropharm.2018.02.025.

Rockowitz, S. and Zheng, D. (2015) 'Significant expansion of the REST/NRSF cistrome in human versus mouse embryonic stem cells: Potential implications for neural development', *Nucleic Acids Research*, 43(12), pp. 5730–5743. doi: 10.1093/nar/gkv514.

Rook, G. A. (2013) 'Regulation of the immune system by biodiversity from the natural environment: An ecosystem service essential to health', *Proceedings of the National Academy*

of Sciences of the United States of America, 110(46), pp. 18360–18367. doi: 10.1073/pnas.1313731110.

Roscoe, W. A. *et al.* (2009) 'VEGF and angiogenesis in acute and chronic MOG(35-55) peptide induced EAE', *Journal of Neuroimmunology*, 209(1–2), pp. 6–15. doi: 10.1016/j.jneuroim.2009.01.009.

Rose-John, S. (2001) 'Coordination of interleukin-6 biology by membrane bound and soluble receptors', in *Advances in Experimental Medicine and Biology*. Kluwer Academic/Plenum Publishers, pp. 145–151. doi: 10.1007/978-1-4615-0685-0_19.

Rose-John, S. *et al.* (2009) 'Interleukin-6 Trans-Signaling and Colonic Cancer Associated with Inflammatory Bowel Disease', *Current Pharmaceutical Design*, 15(18), pp. 2095–2103. doi: 10.2174/138161209788489140.

Rose-John, S. (2012) 'Il-6 trans-signaling via the soluble IL-6 receptor: Importance for the proinflammatory activities of IL-6', *International Journal of Biological Sciences*, 8(9), pp. 1237–1247. doi: 10.7150/ijbs.4989.

Rudolph, M. D. *et al.* (2018) 'Maternal IL-6 during pregnancy can be estimated from newborn brain connectivity and predicts future working memory in offspring', *Nature Neuroscience*, 21(5), pp. 765–772. doi: 10.1038/s41593-018-0128-y.

Russo, F. B. *et al.* (2018) 'Modeling the Interplay Between Neurons and Astrocytes in Autism Using Human Induced Pluripotent Stem Cells', *Biological Psychiatry*, 83(7), pp. 569–578. doi: 10.1016/j.biopsych.2017.09.021.

Rymo, S. F. *et al.* (2011) 'A two-way communication between microglial cells and angiogenic sprouts regulates angiogenesis in aortic ring cultures', *PLoS ONE*, 6(1). doi: 10.1371/journal.pone.0015846.

Samuelsson, A. M. *et al.* (2006) 'Prenatal exposure to interleukin-6 results in inflammatory neurodegeneration in hippocampus with NMDA/GABAA dysregulation and impaired spatial learning', *American Journal of Physiology - Regulatory Integrative and Comparative Physiology*, 290(5), pp. 1345–1356. doi: 10.1152/ajpregu.00268.2005.

Sanai, H. *et al.* (2004) 'Unique astrocyte ribbon in adult human brain contains neural stem cells but lacks chain migration', *Nature*, 427(6976), pp. 740–744. doi: 10.1038/nature02301.

Saporta, M. A., Grskovic, M. and Dimos, J. T. (2011) 'Induced pluripotent stem cells in the study of neurological diseases', *Stem Cell Research and Therapy*, 2(5), pp. 1–9. doi: 10.1186/scrt78.

Sarieva, K. *et al.* (2023) 'Human brain organoid model of maternal immune activation identifies radial glia cells as selectively vulnerable', *Molecular Psychiatry*, pp. 1–13. doi: 10.1038/s41380-023-01997-1.

Sasayama, D. *et al.* (2013) 'Increased cerebrospinal fluid interleukin-6 levels in patients with schizophrenia and those with major depressive disorder', *Journal of Psychiatric Research*, 47(3), pp. 401–406. doi: 10.1016/j.jpsychires.2012.12.001.

Satoh, J. ichi *et al.* (2016) 'TMEM119 marks a subset of microglia in the human brain', *Neuropathology*, 36(1), pp. 39–49. doi: 10.1111/neup.12235.

Sayers, E. W. *et al.* (2022) 'Database resources of the national center for biotechnology information', *Nucleic Acids Research*, 50(D1), pp. D20–D26. doi: 10.1093/nar/gkab1112.

Scala, F. *et al.* (2021) 'Phenotypic variation of transcriptomic cell types in mouse motor cortex', *Nature*, 598(7879), pp. 144–150. doi: 10.1038/s41586-020-2907-3.

Scambler, P. J. *et al.* (1991) 'Microdeletions within 22q11 associated with sporadic and familial DiGeorge syndrome', *Genomics*, 10(1), pp. 201–206. doi: 10.1016/0888-7543(91)90501-5.

Scambler, P. J. (2000) 'The 22q11 deletion syndromes', *Human Molecular Genetics*. Hum Mol Genet, pp. 2421–2426. doi: 10.1093/hmg/9.16.2421.

Schaafsma, W. *et al.* (2017) 'Maternal inflammation induces immune activation of fetal microglia and leads to disrupted microglia immune responses, behavior, and learning performance in adulthood', *Neurobiology of Disease*, 106, pp. 291–300. doi: 10.1016/J.NBD.2017.07.017.

Schafer, D. P. *et al.* (2012) 'Microglia Sculpt Postnatal Neural Circuits in an Activity and Complement-Dependent Manner', *Neuron*, 74(4), pp. 691–705. doi: 10.1016/j.neuron.2012.03.026.

Schafer, S. T. *et al.* (2019) 'Pathological priming causes developmental gene network heterochronicity in autistic subject-derived neurons', *Nature Neuroscience*, 22(2), pp. 243–255. doi: 10.1038/s41593-018-0295-x.

Schafer, S. T. *et al.* (2023) 'An in vivo neuroimmune organoid model to study human microglia phenotypes', *Cell*, 186(10), pp. 2111-2126.e20. doi: 10.1016/J.CELL.2023.04.022.

Schalbetter, S. M. *et al.* (2022) 'Adolescence is a sensitive period for prefrontal microglia to act on cognitive development', *Science Advances*, 8(9). doi: 10.1126/sciadv.abi6672.

Scheller, J. *et al.* (2011) 'The pro- and anti-inflammatory properties of the cytokine interleukin-6', *Biochimica et Biophysica Acta - Molecular Cell Research*, 1813(5), pp. 878–888. doi: 10.1016/j.bbamcr.2011.01.034.

Schepanski, S. *et al.* (2018) 'Prenatal Immune and Endocrine Modulators of Offspring's Brain Development and Cognitive Functions Later in Life', *Frontiers in Immunology*. Frontiers Media S.A., p. 2186. doi: 10.3389/fimmu.2018.02186.

Schneider, M. *et al.* (2014) 'Psychiatric disorders from childhood to adulthood in 22q11.2 deletion syndrome: Results from the international consortium on brain and behavior in 22q11.2 deletion syndrome', *American Journal of Psychiatry*. Am J Psychiatry, pp. 627–639. doi: 10.1176/appi.ajp.2013.13070864.

Scholz, D. *et al.* (2011) 'Rapid, complete and large-scale generation of post-mitotic neurons from the human LUHMES cell line', *Journal of Neurochemistry*, 119(5), pp. 957–971. doi: 10.1111/j.1471-4159.2011.07255.x.

Schreiber, S. *et al.* (2021) 'Therapeutic Interleukin-6 Trans-signaling Inhibition by Olamkicept (sgp130Fc) in Patients With Active Inflammatory Bowel Disease', *Gastroenterology*, 160(7), pp. 2354-2366.e11. doi: 10.1053/j.gastro.2021.02.062.

Schulz, C. *et al.* (2012) 'A lineage of myeloid cells independent of myb and hematopoietic stem cells', *Science*, 335(6077), pp. 86–90. doi: 10.1126/science.1219179.

Schwieler, L. *et al.* (2015) 'Increased levels of IL-6 in the cerebrospinal fluid of patients with chronic schizophrenia - Significance for activation of the kynurenine pathway', *Journal of Psychiatry and Neuroscience*, 40(2), pp. 126–133. doi: 10.1503/jpn.140126.

Sebba, A. (2008) ‘Tocilizumab: The first interleukin-6-receptor inhibitor’, *American Journal of Health-System Pharmacy*, 65(15), pp. 1413–1418. doi: 10.2146/ajhp070449.

Sekar, A. *et al.* (2016) ‘Schizophrenia risk from complex variation of complement component 4’, *Nature*. doi: 10.1038/nature16549.

Sellgren, C. M. *et al.* (2019) ‘Increased synapse elimination by microglia in schizophrenia patient-derived models of synaptic pruning’, *Nature Neuroscience*. doi: 10.1038/s41593-018-0334-7.

Sharma, K. and Tremblay, M. E. (2020) ‘Microglia: Multiple states and multiple roles in the normal and diseased brain and spinal cord’, *Neuroscience Letters*, 729, p. 135019. doi: 10.1016/j.neulet.2020.135019.

Sheng, W. S. *et al.* (2005) ‘TNF-α-induced chemokine production and apoptosis in human neural precursor cells’, *Journal of Leukocyte Biology*, 78(6), pp. 1233–1241. doi: 10.1189/jlb.0405221.

Shi, Y. *et al.* (2012) ‘Human cerebral cortex development from pluripotent stem cells to functional excitatory synapses’, *Nature Neuroscience*, 15(3), pp. 477–486. doi: 10.1038/nn.3041.

Shi, Y., Kirwan, P. and Livesey, F. J. (2012a) ‘Directed differentiation of human pluripotent stem cells to cerebral cortex neurons and neural networks’, *Nature Protocols*, 7(10), pp. 1836–1846. doi: 10.1038/nprot.2012.116.

Shi, Y., Kirwan, P. and Livesey, F. J. (2012b) ‘Directed differentiation of human pluripotent stem cells to cerebral cortex neurons and neural networks’, *Nature Protocols*, 7(10), pp. 1836–1846. doi: 10.1038/nprot.2012.116.

Shigemoto-Mogami, Y. *et al.* (2014) 'Microglia enhance neurogenesis and oligodendrogenesis in the early postnatal subventricular zone', *Journal of Neuroscience*, 34(6), pp. 2231–2243. doi: 10.1523/JNEUROSCI.1619-13.2014.

Shrestha, R. *et al.* (2014) 'Lymphocyte-mediated neuroprotection in in vitro models of excitotoxicity involves astrocytic activation and the inhibition of MAP kinase signalling pathways', *Neuropharmacology*, 76(PART A), pp. 184–193. doi: 10.1016/j.neuropharm.2013.06.025.

Shum, C. *et al.* (2015) 'Utilizing induced pluripotent stem cells (iPSCs) to understand the actions of estrogens in human neurons', *Hormones and Behavior*, 74, pp. 228–242. doi: 10.1016/J.YHBEH.2015.06.014.

Shum, C. *et al.* (2020) 'Δ9-tetrahydrocannabinol and 2-AG decreases neurite outgrowth and differentially affects ERK1/2 and Akt signaling in hiPSC-derived cortical neurons', *Molecular and Cellular Neuroscience*, 103. doi: 10.1016/j.mcn.2019.103463.

Sierra, A., Tremblay, M. È. and Wake, H. (2014) 'Never-resting microglia: Physiological roles in the healthy brain and pathological implications', *Frontiers in Cellular Neuroscience*. doi: 10.3389/fncel.2014.00240.

da Silveira, V. T. *et al.* (2017) 'Effects of early or late prenatal immune activation in mice on behavioral and neuroanatomical abnormalities relevant to schizophrenia in the adulthood', *International Journal of Developmental Neuroscience*, 58(1), pp. 1–8. doi: 10.1016/j.ijdevneu.2017.01.009.

Singh, S. K. *et al.* (2016) 'Astrocytes Assemble Thalamocortical Synapses by Bridging NRX1α and NL1 via Hevin', *Cell*, 164(1–2), pp. 183–196. doi: 10.1016/j.cell.2015.11.034.

Singh, T. *et al.* (2022) 'Rare coding variants in ten genes confer substantial risk for schizophrenia', *Nature*, 604(7906), pp. 509–516. doi: 10.1038/s41586-022-04556-w.

Skene, N. G. *et al.* (2018) 'Genetic identification of brain cell types underlying schizophrenia', *Nature Genetics*. doi: 10.1038/s41588-018-0129-5.

Smart, I. H. (1973) 'Proliferative characteristics of the ependymal layer during the early development of the mouse neocortex: a pilot study based on recording the number, location and plane of cleavage of mitotic figures.', *Journal of anatomy*, 116(Pt 1), pp. 67–91. Available at: https://www.ncbi.nlm.nih.gov/pmc/articles/PMC1271551/ (Accessed: 29 March 2023).

Smith, S. E. P. *et al.* (2007) 'Maternal immune activation alters fetal brain development through interleukin-6', *Journal of Neuroscience*, 27(40), pp. 10695–10702. doi: 10.1523/JNEUROSCI.2178-07.2007.

Smolders, S. *et al.* (2018) 'Controversies and prospects about microglia in maternal immune activation models for neurodevelopmental disorders', *Brain, Behavior, and Immunity*, 73, pp. 51–65. doi: 10.1016/j.bbi.2018.06.001.

Snijders, G. J. L. J. *et al.* (2021) 'A loss of mature microglial markers without immune activation in schizophrenia', *GLIA*, 69(5), pp. 1251–1267. doi: 10.1002/glia.23962.

Solomon, S. *et al.* (2022) 'Heterozygous expression of the Alzheimer's disease-protective PLCγ2 P522R variant enhances Aβ clearance while preserving synapses', *Cellular and Molecular Life Sciences*, 79(8). doi: 10.1007/s00018-022-04473-1.

Squarzoni, P. *et al.* (2014) 'Microglia Modulate Wiring of the Embryonic Forebrain', *Cell Reports*, 8(5), pp. 1271–1279. doi: 10.1016/j.celrep.2014.07.042.

Stalmans, I. *et al.* (2003) 'VEGF: A modifier of the de122q11 (DiGeorge) syndrome?', *Nature Medicine*, 9(2), pp. 173–182. doi: 10.1038/nm819.

Steiner, J. *et al.* (2006) 'Distribution of HLA-DR-positive microglia in schizophrenia reflects impaired cerebral lateralization', *Acta Neuropathologica,* 112(3), pp. 305-316. doi: 10.1007/s00401-006-0090-8

Steiner, J. *et al.* (2008) 'Immunological aspects in the neurobiology of suicide: Elevated microglial density in schizophrenia and depression is associated with suicide', *Journal of Psychiatric Research,* 42(2), pp. 151-157. doi: 10.1016/j.jpsychires.2006.10.013

Stelmasiak, Z. *et al.* (2001) 'IL-6 and sIL-6R concentration in the cerebrospinal fluid and serum of MS patients', *Medical Science Monitor*, 7(5), pp. 914–918.

Stirling, D. R. *et al.* (2021) 'CellProfiler 4: improvements in speed, utility and usability', *BMC Bioinformatics*, 22(1). doi: 10.1186/s12859-021-04344-9.

Stone, W. *et al.,* (2022) 'Neurodegenerative model of schizophrenia: Growing evidence to support a revisit', *Schizophrenia Research,* 243, p. 154-162. doi: 10.1015/j.schres.2022.03.004.

Subbarayan, M. S. *et al.* (2021) 'CX3CL1/CX3CR1 signaling targets for the treatment of neurodegenerative diseases', *Pharmacology and Therapeutics*, p. 107989. doi: 10.1016/j.pharmthera.2021.107989.

Südhof, T. C. (2017) 'Synaptic Neurexin Complexes: A Molecular Code for the Logic of Neural Circuits', *Cell*. Cell, pp. 745–769. doi: 10.1016/j.cell.2017.10.024.

Takahashi, K. *et al.* (2007) 'Induction of Pluripotent Stem Cells from Adult Human Fibroblasts by Defined Factors', *Cell*, 131(5), pp. 861–872. doi: 10.1016/j.cell.2007.11.019.

Takahashi, K. and Yamanaka, S. (2006) 'Induction of Pluripotent Stem Cells from Mouse Embryonic and Adult Fibroblast Cultures by Defined Factors', *Cell*, 126(4), pp. 663–676. doi: 10.1016/j.cell.2006.07.024.

Takamori, S. *et al.* (2000) 'Identification of a vesicular glutamate transporter that defines a glutamatergic phenotype in neurons', *Nature*, 407(6801), pp. 189–194. doi: 10.1038/35025070.

Tamura, T. and Ozato, K. (2002) 'ICSBP/IRF-8: its regulatory roles in the development of myeloid cells', *Journal of interferon & cytokine research : the official journal of the International Society for Interferon and Cytokine Research*, 22(1), pp. 145–152. doi: 10.1089/107999002753452755.

Tang, B. *et al.* (2013) 'Epigenetic changes at gene promoters in response to immune activation in utero', *Brain, Behavior, and Immunity*, 30, pp. 168–175. doi: 10.1016/j.bbi.2013.01.086.

Thion, M. S. *et al.* (2019) 'Biphasic Impact of Prenatal Inflammation and Macrophage Depletion on the Wiring of Neocortical Inhibitory Circuits', *Cell Reports*, 28(5), pp. 1119-1126.e4. doi: 10.1016/j.celrep.2019.06.086.

Torrey, E. F. and Peterson, M. R. (1976) 'The viral hypothesis of schizophrenia', *Schizophrenia Bulletin*, 2(1), pp. 136–146. doi: 10.1093/schbul/2.1.136.

Toyoshima, M. *et al.* (2016) 'Analysis of induced pluripotent stem cells carrying 22q11.2 deletion', *Translational Psychiatry*, 6(11), pp. e934–e934. doi: 10.1038/tp.2016.206.

Traglia, M. *et al.* (2018) 'Cross-genetic determination of maternal and neonatal immune mediators during pregnancy', *Genome Medicine*, 10(1). doi: 10.1186/s13073-018-0576-8.

Trubetskoy, V. *et al.* (2022) ‘Mapping genomic loci implicates genes and synaptic biology in schizophrenia’, *Nature 2022 604:7906*, 604(7906), pp. 502–508. doi: 10.1038/s41586-022-04434-5.

Tvedt, T. H. A. *et al.* (2018) ‘A pilot study of single nucleotide polymorphisms in the interleukin-6 receptor and their effects on pre- and post-transplant serum mediator level and outcome after allogeneic stem cell transplantation’, *Clinical and Experimental Immunology*, 193(1), pp. 130–141. doi: 10.1111/cei.13124.

Umbach, R. H. and Tottenham, N. (2021) ‘Callous-unemotional traits and reduced default mode network connectivity within a community sample of children’, *Development and Psychopathology*, 33(4), pp. 1170–1183. doi: 10.1017/S0954579420000401.

Vaillant, C. *et al.* (1999) ‘Spatiotemporal expression patterns of metalloproteinases and their inhibitors in the postnatal developing rat cerebellum’, *Journal of Neuroscience*, 19(12), pp. 4994–5004. doi: 10.1523/jneurosci.19-12-04994.1999.

Vasistha, N. A. *et al.* (2015) ‘Cortical and clonal contribution of Tbr2 expressing progenitors in the developing mouse brain’, *Cerebral Cortex*, 25(10), pp. 3290–3302. doi: 10.1093/cercor/bhu125.

Vasistha, N. A. *et al.* (2020) ‘Maternal inflammation has a profound effect on cortical interneuron development in a stage and subtype-specific manner’, *Molecular Psychiatry*, 25(10), pp. 2313–2329. doi: 10.1038/s41380-019-0539-5.

Vasistha, N. A. and Khodosevich, K. (2021) ‘The impact of (ab)normal maternal environment on cortical development’, *Progress in Neurobiology*, 202. doi: 10.1016/j.pneurobio.2021.102054.

Vaughan-Jackson, A. *et al.* (2021) 'Differentiation of human induced pluripotent stem cells to authentic macrophages using a defined, serum-free, open-source medium', *Stem Cell Reports*, 16(7), pp. 1735–1748. doi: 10.1016/j.stemcr.2021.05.018.

Velmeshev, D. *et al.* (2019) 'Single-cell genomics identifies cell type–specific molecular changes in autism', *Science*, 364(6441), pp. 685–689. doi: 10.1126/science.aav8130.

Vergine, M. *et al.* (2021) 'Perioperative glial fibrillary acidic protein is associated with long-term neurodevelopment outcome of infants with congenital heart disease', *Children*, 8(8). doi: 10.3390/children8080655.

Vijayakumar, N. *et al.* (2017) 'Cortico-amygdalar maturational coupling is associated with depressive symptom trajectories during adolescence', *NeuroImage*, 156. doi: 10.1016/j.neuroimage.2017.05.051.

Vila Cuenca, M. *et al.* (2021) 'Engineered 3D vessel-on-chip using hiPSC-derived endothelial- and vascular smooth muscle cells', *Stem Cell Reports*, 16(9), pp. 2159–2168. doi: 10.1016/j.stemcr.2021.08.003.

Villa, A. *et al.* (2018) 'Sex-Specific Features of Microglia from Adult Mice', *Cell Reports*, 23(12), pp. 3501–3511. doi: 10.1016/j.celrep.2018.05.048.

Volk, D. W. *et al.* (2019) 'The Role of the Nuclear Factor-κB Transcriptional Complex in Cortical Immune Activation in Schizophrenia', *Biological Psychiatry*, 85(1), pp. 25–34. doi: 10.1016/j.biopsych.2018.06.015.

Volpato, V. and Webber, C. (2020) 'Addressing variability in iPSC-derived models of human disease: Guidelines to promote reproducibility', *DMM Disease Models and Mechanisms*. Company of Biologists Ltd. doi: 10.1242/dmm.042317.

Vorstman, J. A. S. *et al.* (2006) 'The 22q11.2 deletion in children: High rate of autistic disorders and early onset of psychotic symptoms', *Journal of the American Academy of Child and Adolescent Psychiatry*, 45(9), pp. 1104–1113. doi: 10.1097/01.chi.0000228131.56956.c1.

Vuillermot, S. *et al.* (2010) 'A longitudinal examination of the neurodevelopmental impact of prenatal immune activation in mice reveals primary defects in dopaminergic development relevant to schizophrenia', *Journal of Neuroscience*, 30(4), pp. 1270–1287. doi: 10.1523/JNEUROSCI.5408-09.2010.

Wang, Q. *et al.* (2021) 'Impaired calcium signaling in astrocytes modulates autism spectrum disorder-like behaviors in mice', *Nature Communications*, 12(1), pp. 1–13. doi: 10.1038/s41467-021-23843-0.

Warre-Cornish, K. *et al.* (2020) 'Interferon-γ signaling in human iPSC–derived neurons recapitulates neurodevelopmental disorder phenotypes', *Science Advances*, 6(34). doi: 10.1126/sciadv.aay9506.

Washer, S. J. *et al.* (2022) 'Single-cell transcriptomics defines an improved, validated monoculture protocol for differentiation of human iPSC to microglia', *Scientific Reports*, 12(1). doi: 10.1038/s41598-022-23477-2.

Webb, S. (2008) 'An intrinsic program of brain development', *Nature Reports Stem Cells*. doi: 10.1038/stemcells.2008.120.

Wells, M. F. *et al.* (2023) 'Natural variation in gene expression and viral susceptibility revealed by neural progenitor cell villages', *Cell Stem Cell*, 30(3), pp. 312-332.e13. doi: 10.1016/j.stem.2023.01.010.

van Wilgenburg, B. *et al.* (2013) 'Efficient, Long Term Production of Monocyte-Derived Macrophages from Human Pluripotent Stem Cells under Partly-Defined and Fully-Defined Conditions', *PLoS ONE*, 8(8). doi: 10.1371/journal.pone.0071098.

Willette, A. A. *et al.* (2011) 'Brain enlargement and increased behavioral and cytokine reactivity in infant monkeys following acute prenatal endotoxemia', *Behavioural Brain Research*, 219(1), pp. 108–115. doi: 10.1016/j.bbr.2010.12.023.

Wilson-Genderson, M. *et al.* (2018) 'Authorization of tissues from deceased patients for genetic research', *Human Genetics*, 137(1), pp. 63–71. doi: 10.1007/s00439-017-1855-y.

Wingett, S. W. and Andrews, S. (2018) 'FastQ Screen: A tool for multi-genome mapping and quality control', *F1000Research*, 7, p. 1338. doi: 10.12688/f1000research.15931.2.

Wolf, J., Rose-John, S. and Garbers, C. (2014) 'Interleukin-6 and its receptors: a highly regulated and dynamic system', *Cytokine*, 70(1), pp. 11–20. doi: 10.1016/j.cyto.2014.05.024.

Wright-Jin, E. C. and Gutmann, D. H. (2019) 'Microglia as Dynamic Cellular Mediators of Brain Function', *Trends in Molecular Medicine*. Elsevier BV, pp. 967–979. doi: 10.1016/j.molmed.2019.08.013.

Wu, H., Wang, C. and Wu, Z. (2015) 'PROPER: Comprehensive power evaluation for differential expression using RNA-seq', *Bioinformatics*, 31(2), pp. 233–241. doi: 10.1093/bioinformatics/btu640.

Wu, W. L. *et al.* (2017) 'The placental interleukin-6 signaling controls fetal brain development and behavior', *Brain, Behavior, and Immunity*, 62, pp. 11–23. doi: 10.1016/j.bbi.2016.11.007.

Yadav, A. *et al.* (2020) 'DNA replication protein Cdc45 directly interacts with PCNA via its PIP box in Leishmania donovani and the Cdc45 PIP box is essential for cell survival', *PLoS Pathogens*, 16(5). doi: 10.1371/journal.ppat.1008190.

Yamanaka, S. (2012) 'Induced pluripotent stem cells: Past, present, and future', *Cell Stem Cell*. Cell Press, pp. 678–684. doi: 10.1016/j.stem.2012.05.005.

Yamasaki, A. E., Panopoulos, A. D. and Belmonte, J. C. I. (2017) 'Understanding the genetics behind complex human disease with large-scale iPSC collections', *Genome Biology*, 18(1), pp. 1–3. doi: 10.1186/s13059-017-1276-1.

Yang, M. S. *et al.* (2008) 'Chitinase-3-Like 1 (CHI3L1) Gene and Schizophrenia: Genetic Association and a Potential Functional Mechanism', *Biological Psychiatry*, 64(2), pp. 98–103. doi: 10.1016/j.biopsych.2007.12.012.

Yang, X. *et al.* (2020) 'CSF1R blockade induces macrophage ablation and results in mouse choroidal vascular atrophy and RPE disorganization', *eLife*, 9. doi: 10.7554/eLife.55564.

Yang, Y. *et al.* (2003) 'Contribution of astrocytes to hippocampal long-term potentiation through release of D-serine', *Proceedings of the National Academy of Sciences of the United States of America*, 100(25), pp. 15194–15199. doi: 10.1073/PNAS.2431073100.

Yao, Y. and Tsirka, S. E. (2010) 'The C terminus of Mouse Monocyte Chemoattractant Protein 1 (MCP1) mediates MCP1 dimerization while blocking its chemotactic potency', *Journal of Biological Chemistry*, 285(41), pp. 31509–31516. doi: 10.1074/jbc.M110.124891.

Yilmaz, M. *et al.* (2021) 'Overexpression of schizophrenia susceptibility factor human complement C4A promotes excessive synaptic loss and behavioral changes in mice', *Nature Neuroscience*, 24(2), pp. 214–224. doi: 10.1038/s41593-020-00763-8.

Yokoyama, K. D., Zhang, Y. and Ma, J. (2014) 'Tracing the Evolution of Lineage-Specific Transcription Factor Binding Sites in a Birth-Death Framework', *PLoS Computational Biology*, 10(8). doi: 10.1371/journal.pcbi.1003771.

Zandi, M. S. *et al.* (2011) 'Disease-relevant autoantibodies in first episode schizophrenia', *Journal of Neurology*. Springer, pp. 686–688. doi: 10.1007/s00415-010-5788-9.

Zaretsky, M. v. *et al.* (2004) 'Transfer of inflammatory cytokines across the placenta', *Obstetrics and Gynecology*, 103(3). doi: 10.1097/01.AOG.0000114980.40445.83.

Zeng, H. *et al.* (2012) 'Large-scale cellular-resolution gene profiling in human neocortex reveals species-specific molecular signatures', *Cell*, 149(2), pp. 483–496. doi: 10.1016/j.cell.2012.02.052.

Zhang, L. *et al.* (2021) 'Extracellular vesicles from hypoxia-preconditioned microglia promote angiogenesis and repress apoptosis in stroke mice via the TGF-β/Smad2/3 pathway', *Cell Death and Disease*, 12(11). doi: 10.1038/s41419-021-04363-7.

Zhang, W. *et al.* (2022) 'Microglia-containing human brain organoids for the study of brain development and pathology', *Molecular Psychiatry*, pp. 1–12. doi: 10.1038/s41380-022-01892-1.

Zhang, W. *et al.* (2023) 'Microglia-containing human brain organoids for the study of brain development and pathology', *Molecular Psychiatry*. Nature Publishing Group, pp. 96–107. doi: 10.1038/s41380-022-01892-1.

Zhang, Y. *et al.* (2016) 'Purification and Characterization of Progenitor and Mature Human Astrocytes Reveals Transcriptional and Functional Differences with Mouse', *Neuron*, 89(1), pp. 37–53. doi: 10.1016/j.neuron.2015.11.013.

Zhang, Y. *et al.* (2021) ‘Associations between expression of indoleamine 2, 3-dioxygenase enzyme and inflammatory cytokines in patients with first-episode drug-naive Schizophrenia’, *Translational Psychiatry*, 11(1). doi: 10.1038/s41398-021-01688-x.

Zhao, H. *et al.* (2021) ‘Association of Peripheral Blood Levels of Cytokines With Autism Spectrum Disorder: A Meta-Analysis’, *Frontiers in Psychiatry*. doi: 10.3389/fpsyt.2021.670200.

Zhao, X. and Bhattacharyya, A. (2018) ‘Human Models Are Needed for Studying Human Neurodevelopmental Disorders’, *American Journal of Human Genetics*. Cell Press, pp. 829–857. doi: 10.1016/j.ajhg.2018.10.009.

Zinkstok, J. R. *et al.* (2019) ‘Neurobiological perspective of 22q11.2 deletion syndrome’, *The Lancet Psychiatry*. Lancet Psychiatry, pp. 951–960. doi: 10.1016/S2215-0366(19)30076-8.

Zuiki, M. *et al.* (2017) ‘Luteolin attenuates interleukin-6-mediated astrogliosis in human iPSC-derived neural aggregates: A candidate preventive substance for maternal immune activation-induced abnormalities’, *Neuroscience Letters*, 653, pp. 296–301. doi: 10.1016/j.neulet.2017.06.004.

Appendix: Tables and Figures

*Appendix Table 1 - List of cytokine targets or controls at each coordinate dot on membranes of the Proteome Profiler Human XL Cytokine Array kit from R&D systems. Mean signal values from cytokine profiler dot blots, including all 105 cytokines, averaged from two replicate dots that were then backgrounded to negative reference dots and normalised to positive control reference dots. Table cells are coloured on gradient from low (white) to high (red). * IL-6 spiked in treatment groups. Grid coordinate corresponds to grid in Appendix Figure 1 and heatmaps in Figure 5.7A-B.*

Cytokine	Array Coordinate	Control Vehicle	Control IL-6	22q11.2DS Vehicle	22q11.2DS IL-6
Adiponectin	**A3-4**	0.108	0.131	0.162	0.130
Apolipoprotein A-I	**A5-6**	0.124	0.138	0.159	0.163
Angiogenin	**A7-8**	0.176	0.178	0.231	0.255
Angiopoietin-1	**A9-10**	0.085	0.087	0.165	0.078
Angiopoietin-2	**A11-12**	0.097	0.116	0.168	0.102
BAFF	**A13-14**	0.072	0.075	0.159	0.081
BDNF	**A15-16**	0.070	0.083	0.165	0.097
Complement Component C5/C5a	**A17-18**	0.055	0.072	0.163	0.065
CD14	**A19-20**	0.125	0.156	0.186	0.107
CD30	**A21-22**	0.065	0.068	0.178	0.089
CD40 ligand	**B3-4**	0.104	0.132	0.123	0.115
Chitinase 3-like 1	**B5-6**	0.773	0.840	0.901	1.092
Complement Factor D	**B7-8**	0.116	0.108	0.128	0.122
C-Reactive Protein	**B9-10**	0.099	0.103	0.154	0.078
Cripto-1	**B11-12**	0.079	0.078	0.140	0.067
Cystatin C	**B13-14**	0.118	0.172	0.179	0.136
Dkk-1	**B15-16**	0.070	0.078	0.158	0.089
DPPIV	**B17-18**	0.093	0.122	0.160	0.109
EGF	**B19-20**	0.067	0.064	0.155	0.078
EMMPRIN	**B21-22**	0.156	0.161	0.255	0.258
ENA-78	**C3-4**	1.135	1.414	0.367	1.117
Endoglin	**C5-6**	0.111	0.139	0.145	0.148
Fas Ligand	**C7-8**	0.113	0.099	0.140	0.113
FGF basic	**C9-10**	0.098	0.110	0.150	0.089
FGF-7	**C11-12**	0.080	0.081	0.138	0.076
FGF-19	**C13-14**	0.112	0.145	0.151	0.100
Flt-3 Ligand	**C15-16**	0.067	0.075	0.139	0.074
G-CSF	**C17-18**	0.071	0.067	0.134	0.075

GDF-15	**C19-20**	0.106	0.102	0.219	0.157
GM-CSF	**C21-22**	0.589	0.574	0.185	0.147
GROα	**D1-2**	0.115	0.241	0.121	0.161
Growth Hormone	**D3-4**	0.093	0.121	0.127	0.061
HGF	**D5-6**	0.101	0.111	0.149	0.085
ICAM-1	**D7-8**	0.130	0.118	0.146	0.115
IFN-γ	**D9-10**	0.097	0.094	0.193	0.146
IGFBP-2	**D11-12**	0.546	0.596	0.681	0.760
IGFBP-3	**D13-14**	0.064	0.075	0.185	0.064
IL-1α	**D15-16**	0.073	0.077	0.184	0.079
IL-1β	**D17-18**	0.070	0.069	0.192	0.071
IL-1ra	**D19-20**	0.120	0.107	0.217	0.157
IL-2	**D21-22**	0.077	0.074	0.150	0.089
IL-3	**D23-24**	0.063	0.061	0.138	0.092
IL-4	**E1-2**	0.111	0.145	0.112	0.072
IL-5	**E3-4**	0.098	0.114	0.128	0.078
IL-6*	**E5-6**	0.098	0.788	0.137	0.938
IL-8	**E7-8**	1.178	1.269	1.325	1.752
IL-10	**E9-10**	0.084	0.102	0.178	0.099
IL-11	**E11-12**	0.090	0.108	0.153	0.081
IL-12 p70	**E13-14**	0.072	0.071	0.141	0.076
IL-13	**E15-16**	0.059	0.072	0.138	0.070
IL-15	**E17-18**	0.066	0.073	0.151	0.070
IL-16	**E19-20**	0.060	0.063	0.147	0.069
IL-17A	**E21-22**	0.118	0.133	0.171	0.105
IL-18	**E23-24**	0.068	0.062	0.156	0.107
IL-19	**F1-2**	0.108	0.123	0.111	0.059
IL-22	**F3-4**	0.125	0.144	0.153	0.084
IL-23	**F5-6**	0.103	0.109	0.124	0.095
IL-24	**F7-8**	0.139	0.137	0.188	0.152
IL-27	**F9-10**	0.091	0.104	0.174	0.081
IL-31	**F11-12**	0.077	0.091	0.133	0.079
IL-32	**F13-14**	0.066	0.083	0.140	0.069
IL-33	**F15-16**	0.061	0.072	0.147	0.076
IL-34	**F17-18**	0.419	0.381	0.481	0.511
IP-10	**F19-20**	0.065	0.074	0.137	0.130
I-TAC	**F21-22**	0.063	0.071	0.131	0.096
Kallikrein 3	**F23-24**	0.077	0.068	0.174	0.127
Leptin	**G1-2**	0.115	0.129	0.107	0.070
LIF	**G3-4**	0.112	0.091	0.117	0.072

Lipocalin-2	**G5-6**	0.116	0.081	0.137	0.101
MCP-1	**G7-8**	0.538	0.575	0.440	0.497
MCP-3	**G9-10**	0.611	0.709	0.475	0.650
M-CSF	**G11-12**	0.085	0.111	0.156	0.098
MIF	**G13-14**	0.228	0.225	0.322	0.286
MIG	**G15-16**	0.060	0.084	0.144	0.066
MIP-1α/MIP-1β	**G17-18**	0.102	0.424	0.146	0.475
MIP-3α	**G19-20**	0.066	0.090	0.142	0.228
MIP-3β	**G21-22**	0.066	0.069	0.139	0.093
MMP-9	**G23-24**	1.301	1.341	1.461	1.692
Myeloperoxidase	**H1-2**	0.138	0.142	0.105	0.086
Osteopontin	**H3-4**	1.173	1.112	1.074	1.256
PDGF-AA	**H5-6**	0.128	0.089	0.177	0.141
PDGF-AB/BB	**H7-8**	0.114	0.103	0.175	0.074
Pentraxin 3	**H9-10**	0.444	0.477	0.930	1.035
PF4	**H11-12**	0.064	0.102	0.129	0.069
RAGE	**H13-14**	0.067	0.092	0.129	0.060
RANTES	**H15-16**	0.061	0.129	0.126	0.111
RBP-4	**H17-18**	0.057	0.082	0.136	0.072
Relaxin-2	**H19-20**	0.062	0.080	0.142	0.080
Resistin	**H21-22**	0.072	0.107	0.150	0.099
SDF-1α	**H23-24**	0.072	0.099	0.154	0.109
Serpin E1	**I1-2**	0.295	0.297	0.405	0.517
SHBG	**I3-4**	0.139	0.160	0.135	0.121
ST2	**I5-6**	0.101	0.098	0.146	0.068
TARC	**I7-8**	0.107	0.117	0.166	0.082
TFF3	**I9-10**	0.081	0.104	0.161	0.090
TfR	**I11-12**	0.084	0.100	0.114	0.091
TGF-α	**I13-14**	0.065	0.089	0.119	0.073
Thrombospondin-1	**I15-16**	0.059	0.076	0.111	0.078
TNFα	**I17-18**	0.062	0.105	0.136	0.091
uPAR	**I19-20**	0.205	0.292	0.265	0.258
VEGF	**I21-22**	0.074	0.093	0.288	0.221
VCAM-1	**J11-12**	0.080	0.125	0.231	0.221
Vitamin D	**J5-6**	0.129	0.114	0.182	0.076
CD31	**J7-8**	0.143	0.144	0.196	0.115
TIM-3	**J9-10**	0.100	0.127	0.183	0.136

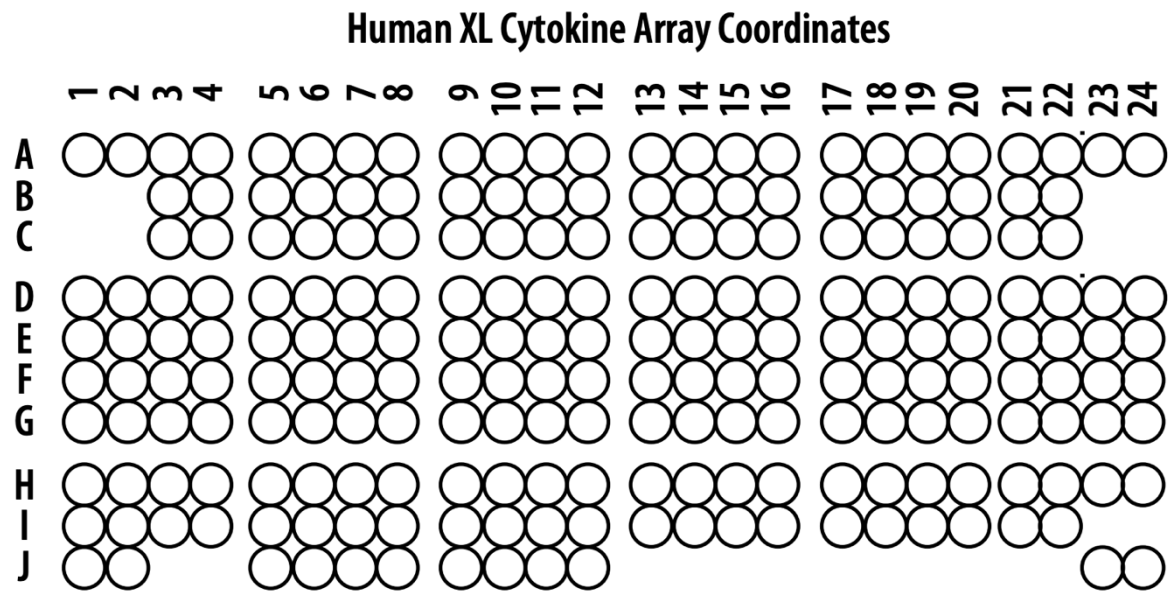

Appendix Figure 1 - Human cytokine array layout on each membrane of the small, 36 cytokine Proteome Profiler Human XL Cytokine Array kit from R&D systems.

Appendix 1: Couch *et al.* 2023

Brain, Behavior, and Immunity 110 (2023) 43–59

Contents lists available at ScienceDirect

Brain Behavior and Immunity

journal homepage: www.elsevier.com/locate/ybrbi

Acute IL-6 exposure triggers canonical IL6Ra signaling in hiPSC microglia, but not neural progenitor cells

Amalie C.M. Couch [a,b], Shiden Solomon [a], Rodrigo R.R. Duarte [c,d], Alessia Marrocu [a,e], Yiqing Sun [a], Laura Sichlinger [a,b], Rugile Matuleviciute [a,b], Lucia Dutan Polit [a], Bjørn Hanger [a,b], Amelia Brown [a,b], Shahram Kordasti [f], Deepak P. Srivastava [a,b,1], Anthony C. Vernon [a,b,*,1]

[a] Department of Basic and Clinical Neuroscience, Institute of Psychiatry, Psychology and Neuroscience, King's College London, London, UK
[b] MRC Centre for Neurodevelopmental Disorders, King's College London, London, UK
[c] Department of Social, Genetic & Developmental Psychiatry, Institute of Psychiatry, Psychology & Neuroscience, King's College London, London, UK
[d] Department of Medicine, Weill Cornell Medical College, Cornell University, NY, USA
[e] Division of Immunology, Infection and Inflammatory Disease, King's College London, London, UK
[f] Comprehensive Cancer Centre, School of Cancer and Pharmaceutical Sciences, Faculty of Life Sciences and Medicine, King's College London, London, UK

ARTICLE INFO

Keywords:
IL-6
Neurodevelopmental disorders
Human induced-pluripotent stem cells
Microglia
Neural progenitor cells

ABSTRACT

Background: Prenatal exposure to elevated interleukin (IL)-6 levels is associated with increased risk for psychiatric disorders with a putative neurodevelopmental origin, such as schizophrenia (SZ), autism spectrum condition (ASC) and bipolar disorder (BD). Although rodent models provide causal evidence for this association, we lack a detailed understanding of the cellular and molecular mechanisms in human model systems. To close this gap, we characterized the response of human induced pluripotent stem cell (hiPSC-)derived microglia-like cells (MGL) and neural progenitor cells (NPCs) to IL-6 in monoculture.

Results: We observed that human forebrain NPCs did not respond to acute IL-6 exposure in monoculture at both protein and transcript levels due to the absence of *IL6R* expression and soluble (s)IL6Ra secretion. By contrast, acute IL-6 exposure resulted in STAT3 phosphorylation and increased *IL6, JMJD3* and *IL10* expression in MGL, confirming activation of canonical IL6Ra signaling. Bulk RNAseq identified 156 up-regulated genes (FDR < 0.05) in MGL following acute IL-6 exposure, including *IRF8, REL, HSPA1A/B* and *OXTR*, which significantly overlapped with an up-regulated gene set from human *post-mortem* brain tissue from individuals with schizophrenia. Acute IL-6 stimulation significantly increased MGL motility, consistent with gene ontology pathways highlighted from the RNAseq data and replicating rodent model indications that IRF8 regulates microglial motility. Finally, IL-6 induces MGLs to secrete CCL1, CXCL1, MIP-1α/β, IL-8, IL-13, IL-16, IL-18, MIF and Serpin-E1 after 3 h and 24 h.

Conclusion: Our data provide evidence for cell specific effects of acute IL-6 exposure in a human model system, ultimately suggesting that microglia-NPC co-culture models are required to study how IL-6 influences human cortical neural progenitor cell development *in vitro*.

1. Introduction

Maternal immune activation (MIA) during pregnancy is associated with a generalized increased risk of the offspring developing psychopathology later in life, including schizophrenia (SZ), bipolar disorder (BD), depression and autism spectrum condition (ASC) (Estes and McAllister, 2016; Mondelli et al., 2017). MIA is a broad term that covers multiple risk sources, covering both infectious and non-infectious stimuli (Meyer, 2019). Human epidemiological studies suggest MIA acts to increase the risk for psychopathology equally during both prenatal and postnatal periods (Lydholm et al., 2019), findings given causal support by data from animal models of MIA (Meyer, 2019; Potter et al., 2023). The more an offspring is exposed to such scenarios, the higher the risk for psychopathology, suggesting an additive mechanism (Bayer

* Corresponding author at: Department of Basic and Clinical Neuroscience, Maurice Wohl Clinical Neuroscience Institute, Institute of Psychiatry, Psychology and Neuroscience, King's College London, London SE5 9RT, UK.
E-mail address: anthony.vernon@kcl.ac.uk (A.C. Vernon).
[1] These authors share senior authorship.

https://doi.org/10.1016/j.bbi.2023.02.007
Received 9 August 2022; Received in revised form 20 December 2022; Accepted 10 February 2023
Available online 11 February 2023

et al., 1999; Couch et al., 2021; Meyer, 2019). Fundamentally however, the mechanisms by which pre- and postnatal exposure confer disease risk are likely to be explained by distinct cellular and/or molecular mechanisms. Focusing specifically on *prenatal* MIA exposure, both human and rodent studies suggest that, at least in part, the maternal peripheral cytokine profile mediates the increased risk for psychopathology in the offspring (Allswede et al., 2020; Careaga et al., 2017; Graham et al., 2018; Meyer, 2014; Mueller et al., 2021; Potter et al., 2023; Rasmussen et al., 2021, 2019; Rudolph et al., 2018). Whilst data from human, rodent and *in vitro* models are not always consistent, there is accumulating evidence to suggest that interleukin (IL-)6 may act as a sensor, effector, and transducer of environmental risk factors on the prenatal brain. This view is consistent with evidence from genetic and blood biomarker studies that implicate IL-6 in the pathogenesis of multiple psychiatric disorders (Graham et al., 2018; Ozaki et al., 2020; Perry et al., 2021; Rasmussen et al., 2021, 2019; Rudolph et al., 2018; Smith et al., 2007).

Specifically, birth cohort data show that higher levels of maternal serum steady state IL-6 concentrations correlate with larger right amygdala volume and stronger bilateral amygdala connectivity in the offspring, which influence both cognitive development and some externalizing behaviors in the offspring (Graham et al., 2018; Rasmussen et al., 2021, 2019; Rudolph et al., 2018). In a mouse model based on maternal exposure to the viral mimetic Poly I:C, transcripts of *IL6* are shown to be consistently elevated in maternal liver, placenta, and primary fetal microglia (Ozaki et al., 2020). Furthermore, peripheral IL-6 levels remain elevated in adult mouse offspring which exhibit behavioral deficits relevant for SZ and ASC after MIA exposure compared to offspring who do not show any such deficits, despite exposure to MIA *in utero* (Mueller et al., 2021). Moreover, acute elevation of IL-6 by injection into pregnant mice or developing embryos enhances glutamatergic synapse development resulting in overall brain hyperconnectivity and behavioral deficits relevant for ASC in adult offspring (Mirabella et al., 2021). Finally, blocking IL-6R signaling either genetically or pharmacologically in the pregnant rodent dam, irrespective of the immune stimulation paradigm, eliminates the pathological effects of MIA in the fetal rodent brain and subsequent behavioral deficits in the adult animal (Smith et al., 2007).

Human epidemiological and neuroimaging studies cannot however establish the cellular or molecular basis underlying the effects of exposure to elevated levels of IL-6 prenatally. Whilst animal models address this gap, and have provided important causal mechanistic evidence, the extent to which data from such models may translate to humans remains unclear, due to the species-specific gene regulation networks that encompass human neurodevelopment (Yokoyama et al., 2014). This is compounded by heterogeneity between laboratories in the gestational timing, dose, frequency, and route of administration of the infectious challenge in rodents (Smolders et al., 2018) and batch-to-batch heterogeneity of infectious agents (Mueller et al., 2019). As such, conflicting findings exist in the animal MIA literature regarding cellular mechanisms (Kentner et al., 2019), exemplified by studies on the role of microglia (Smolders et al., 2018). Third, only a fraction of animal studies has investigated cellular or molecular phenotypes proximal to the MIA event in the developing brain. This is important as knowledge of the most proximal molecular events to MIA could reveal important therapeutic targets for prevention of downstream pathology.

Human induced pluripotent stem cells (hiPSC), which may be differentiated into multiple different neural and glial lineages, have the potential to address these gaps in our knowledge. Specifically, hiPSC directed towards neuronal fates have been utilized to investigate the pathological impact of Zika virus infection (Muffat et al., 2018), exposure to TLR3-agonists (Ritchie et al., 2018), and following direct exposure to cytokines, including interferon-gamma (Warre-Cornish et al., 2020) and IL-6 (Kathuria et al., 2022). Nonetheless, these studies have exclusively focused on neurons or astrocytes, at the expense of human microglia (Bhat et al., 2022; Park et al., 2020; Russo et al., 2018; Warre-Cornish et al., 2020). We therefore lack data on the impact of IL-6 on these critical immune-effector cells in a human–relevant model. Converging lines of evidence from human genetics, brain *post-mortem* tissue studies, neuroimaging and peripheral biomarker studies implicate microglia and the innate immune system in the pathophysiology of neurodevelopmental disorders (NDDs) (Coomey et al., 2020; Mondelli et al., 2017). Since microglia also play critical roles in shaping neurodevelopment and the central immune response to maintain homeostasis (Hanger et al., 2020; Paolicelli et al., 2011), incorporating human microglia into hiPSC models to study the effects of immune activation on development is vital (Gonzalez et al., 2017; Russo et al., 2018).

To this end, we evaluated whether, and how, hiPSC-derived microglia-like cells (MGLs) and neural progenitor cells (NPCs) respond to acute IL-6 stimulation in monocultures. We considered the following four questions: (1) do the cells have the receptor machinery to respond to IL-6 and other cytokines; (2) do these cells respond to acute IL-6; (3) does acute IL-6 induce a transcriptional profile similar to that seen in the major psychiatric disorders; and finally, (4) how does acute IL-6 impact the function of human MGLs?

2. Materials and methods

2.1. Cell culture

Participants were recruited and methods carried out in accordance with the 'Patient iPSCs for Neurodevelopmental Disorders (PiNDs) study' (REC No 13/LO/1218). Informed consent was obtained from all subjects for participation in the PiNDs study. Ethical approval for the PiNDs study was provided by the NHS Research Ethics Committee at the South London and Maudsley (SLaM) NHS R&D Office. HiPSCs were generated and characterized from a total of nine lines donated by three males with no history of neurodevelopmental or psychiatric disorders (Supplementary Table 1) as previously described (Adhya et al., 2021; Warre-Cornish et al., 2020) and grown in hypoxic conditions on Geltrex™ (Life Technologies; A1413302) coated 6-well NUNC™ plates in StemFlex medium (Gibco, A3349401) exchanged every 48 h. For passaging, cells were washed with HBSS (Invitrogen; 14170146) and then passaged by incubation with Versene (Lonza; BE17-711E), diluted in fresh StemFlex and plated onto fresh Geltrex-coated 6-well NUNC™ plates. For specifics on cell culture differentiation, see supplementary. Both cell types were differentiated from hiPSCs using an embryonic MYB-independent method (Haenseler et al., 2017; Shi et al., 2012). Day 14 MGL monocultures for dose response experiments were exposed for 3 h to 100 ng/ml, 10 ng/ml, 1 ng/ml, 100 pg/ml, 10 pg/ml, 1 pg/ml, 0.1 pg/ml IL-6 (Gibco; PHC0066) or 100 pM acetic acid vehicle and were collected immediately for analysis. MGL progenitor (D1) and MGL (D14) cultures for single, high dose IL-6 stimulation received 100 ng/ml IL-6 (Gibco; PHC0066) or 100 pM acetic acid vehicle stimulation for either 3- or 24-hours and were immediately collected for analysis. NPC cultures received 100 pM acetic acid vehicle or 100 ng/ml IL-6 (Gibco; PHC0066) on day 18 for 3 h, then were collected for analysis. Eighteen days after neural induction reflects early second trimester neurodevelopment, which corresponds to a known period of increased risk for offspring NDD in mothers with increased IL-6 serum concentrations (Estes and McAllister, 2016).

2.2. RNA extraction, cDNA synthesis and quantitative PCR

Cells cultured for RNA extraction were collected in room temperature TRI Reagent™ Solution (Invitrogen; AM9738) and stored at −80 °C. RNA was extracted as directed per manufacturer's instructions. Precipitation of RNA by 0.3 M Sodium-acetate and 100 % ethanol at −80 °C overnight was performed to clean samples further, before resuspension in RNAse-free water. Nucleic acid content was measured using NanoDrop™ One. Reverse transcription of RNA to complementary DNA was carried out according to manufacturer's instruction (SuperScript™ III

Reverse Transcriptase Invitrogen 18080093 and 40 U RNaseOUT Invitrogen 10777019). qPCR was carried out using Forget-Me-Not™ EvaGreen® qPCR Master Mix (Biotium; 31041-1) in the QuantStudio 7 Flex Real-Time PCR System (Fisher), according to cycling parameters described in Supplementary Table 6. Cycle threshold (Ct) data were normalized to an average of *GADPH*, *RPL13* and *SDHA* housekeeper expression Ct values, which were unchanged upon IL-6 stimulation according to bulk RNAseq normalized DESeq2 counts (unpaired *t*-test $p = 0.281$, $p = 0.718$ and $p = 0.653$ respectively) (Supplementary Fig. 3). Gene expression fold change analysis was calculated following the $2^{-}\Delta\Delta^{Ct}$ method (Livak and Schmittgen, 2001), using the following formulas:

$$Ct = Ct_{Gene\ of\ interest} - Ct_{Housekeeping\ gene\ average}$$

$$\Delta\Delta Ct = \Delta Ct_{Sample} - \Delta Ct_{Control\ average}$$

$$Fold\ change\ from\ control = 2^{-\Delta\Delta Ct}$$

2.3. Western blot

Cells were scraped on ice and collected in RIPA buffer (Supplementary Table 7), sonicated at 40 % for 10 pulses, pelleted for 15 min at 4 °C and proteins collected in supernatant. Protein concentration was quantified using the Pierce™ BCA protein assay kit (Thermo-Fisher; 23227). In preparation for SDS-PAGE separation, protein samples were denatured in Laemmli buffer and boiled at 95 °C for 5 min. 2 μg of each protein sample was loaded into self-made 10 % gels, alongside 5 μl of the Dual Color (BioRad #1610374) standards marker. Gels were run at 20 mA for approximately 20 min, then increased to 100 V until the samples reached the bottom of the unit (~90 min). Separated samples were transferred to a PVDF membrane and run overnight at 78 mA in 4 °C. Blots were blocked in 5 % BSA TBS-T for 1 h at RT with agitation. Antibodies were diluted in blocking buffer; primary antibody incubation occurred overnight at 4 °C with agitation, and secondary antibody incubation at RT for 1 h with agitation (Supplementary Table 4). Washes between antibody probes occurred in TBS-T at three 15 min intervals. For visualization, ECL Western Blotting Substrate (GE Healthcare; RPN2106) was incubated on the blot at RT for 5 min before image capture by the Bio-Rad Molecular Imager® Gel Doc™ XR System. Signals were quantified using ImageStudioLite (LI-COR, version 5.2.5), by defining an identical rectangular region of interest around each signal band and measuring the median signal value which was then backgrounded against the automatic background detection of the software. Signal data for pSTAT3 was divided by the tSTAT3 signal data within each lane, to give a pSTAT3/tSTAT3 ratio in both vehicle and treated samples across all four timepoints (15, 30, 60 and 180 min). Fold change was calculated by dividing pSTAT3/tSTAT3 of treated samples with the matching timepoint pSTAT3/tSTAT3 vehicle data from identical membranes, to reduce batch effects across donors on different membranes. For example, the 15 min IL-6 treated pSTAT3/tSTAT3 ratio was divided by the 15 min IL-6 vehicle pSTAT3/tSTAT3 ratio to get a fold change from vehicle within timepoint.

2.4. RNA Library preparation and NovaSeq sequencing

Total RNA extracted from 3 h IL-6 treated day 14 MGLs was pooled from two clones per healthy male donor (n = 3 in total). The samples were submitted for sequencing at Genewiz Inc (South Plainfield, NJ). Libraries were prepared using a polyA selection method using the NEBNext Ultra II RNA Library Prep Kit for Illumina following manufacturer's instructions (NEB, Ipswich, MA, USA) and quantified using Qubit 4.0 Fluorometer (Life Technologies, Carlsbad, CA, USA). RNA integrity was checked with RNA Kit on Agilent 5300 Fragment Analyzer (Agilent Technologies, Palo Alto, CA, USA). The sequencing libraries were multiplexed and loaded on the flowcell on the Illumina NovaSeq 6000 instrument according to manufacturer's instructions. The samples were sequenced using a 2x150 Pair-End (PE) configuration v1.5. Image analysis and base calling were conducted by the NovaSeq Control Software v1.7 on the NovaSeq instrument. We obtained an average of 23.5 million 289-base pair paired-end reads per sample (Supplementary Table 8). All downstream analyses were carried out in R version 4.0.2 (R Core Team, 2020). FASTQ files were quality controlled using Fastqc (Wingett and Andrews, 2018) and subsequently aligned to the human reference genome (GRCh38) with STAR (Dobin et al., 2013). A count table was prepared and filtered for counts ≥ 1 using featureCounts (Liao et al., 2014) from the Rsubread (Liao et al., 2019a) package, version 2.4.3. Differential gene expression analysis was carried out using DESeq2 (Love et al., 2014) version 1.30.1 and the default Wald test. Subsequently, using the Benjamini-Hochberg (BH) method, only genes with adjusted $P < 0.05$ were considered differentially expressed and submitted for downstream analyses.

2.5. Enrichment analyses

Gene ontology (GO) analysis was carried out using WebGestalt (Liao et al., 2019b), where differentially expressed genes were tested for over representation of non-redundant cellular component, biological process and molecular function GO terms. This analysis used as a background list all genes considered expressed in our model, according to DESeq2s's internal filtering criteria (i.e., adjusted $P \neq NA$). Enrichment P-values were corrected for multiple testing using the Benjamini-Hochberg (BH) method, and only terms with adjusted $P < 0.05$ were considered significant.

Outcomes from differential expression analysis were uploaded into the Qiagen Ingenuity Pathway Analysis (IPA) software (QIAGEN Inc., https://digitalinsights.qiagen.com/IPA) to identify canonical pathways. Analysis-ready genes were selected by $p \leq 0.05$ and logfold changes $-0.06 \leq$ or ≥ 0.06, resulting in 153 up-regulated and 22 down-regulated genes. Core analysis was filtered by human data and removed any cancer cell lines as reference from the IPA knowledge base (IPKB). Top 10 enriched canonical pathways were filtered by z-score $\geq |2|$, an IPA measure of pathway directionality, and ordered by p-value adjusted by Benjamini-Hochberg (BH) corrections.

To calculate the overlap significance between genes up- or down-regulated in our model with those up- or down-regulated in *post-mortem* brain samples from SZ, BD or ASC cases (Gandal et al., 2018), we performed Fisher's exact tests using the R package 'GeneOverlap' (Shen, 2021). We considered the number of genes expressed in our model according to DEseq2's internal filtering criteria as the genome size. We performed multiple testing correction using the false discovery rate (FDR) method and considered significant results under the FDR of 0.01 (FDR < 1 %). We used MAGMA 1.10 (de Leeuw et al., 2015) to test whether genes differentially regulated in the IL-6 model overlapped with genes enriched with GWAS-supported risk variants. Briefly, MAGMA calculates gene-level enrichment by generating a gene-wide statistic from summary statistics, adjusting associations for gene size, variant density, and linkage disequilibrium using the 1000 Genomes Phase 3 European reference panel. Summary statistics from three GWAS studies (Grove et al., 2019; Mullins et al., 2021; Trubetskoy et al., 2022) were downloaded from the Psychiatric Genomics Consortium website. We analyzed only biallelic single nucleotide polymorphisms with minor allele frequency > 5 % and imputation score > 0.80. We excluded from this analysis all genes and variants that were located within the extended MHC locus on chromosome 6, between 25 and 34 Mb (Watanabe et al., 2017). SNPs from GWASs were assigned to genes using an annotation window of 10 kb upstream and downstream of each gene, using the gene annotation provided by the authors.

2.6. Motility assay

The motility of MGLs from donors M3_CTR_36S, 127_CTM_01 and

014_CTM_02, averaged from three harvests was measured by live imaging, with 6 technical repeat wells per condition. D0 macrophage/microglia progenitors were seeded onto a glass bottom 96 well plate (PerkinElmer) precoated with Poly-D-Lysine (Gibco; A3890401) at 22,000 cells/well and matured in MGL media for 14 days. On the day of imaging cells were exposed to 3 conditions: unstimulated, 100 pM acetic acid vehicle or 100 ng/ml IL-6 for 3 h. A complete media change was performed with microglia media containing either 100 ng/ml IL-6 or 100 pM acetic acid vehicle. Thirty min before imaging, a second complete media change was performed on all wells with microglia media containing either 100 ng/ml IL-6, 100 pM acetic acid vehicle or neither (unstimulated) in order to stain all cells for 30 min with HCS NuclearMask™ Blue Stain (Invitrogen; H10325) and CellMask™ Orange Plasma membrane Stain (Invitrogen; C10045). Immediately before imaging, the media containing treatment and stain was removed and replaced with FluoroBrite™ DMEM (Gibco; A1896701) imaging media without phenol. Cells were imaged for 2 h on an Opera Phoenix high throughput imaging system (Perkin Elmer) using a 20× objective over 5 consistent fields of view per well, and data was analyzed using Harmony High-Content Image analysis software (PerkinElmer).

2.7. Media cytokine array

Day 14 MGL media samples collected after 3 and 24 h of IL-6 exposure and pooled from one donor over 3 harvests were incubated with Proteome Profiler Human Cytokine antibody array membranes (R&D Systems; ARY005B), as per the manufacturers instructions. Dot blot signals were quantified using the Protein Array Analyzer Palette plug-in for ImageJ, and technical dot replicates averaged to one value. These values were backgrounded and normalized to positive reference controls on the dot blot.

2.8. sIL6Ra ELISA

The IL-6 Receptor (Soluble) Human ELISA Kit (Invitrogen; BMS214) was used as per the manufactures instructions to quantify soluble IL6Ra expression in day 14 MGL and day 18 NPC vehicle/treated cell culture media. Optical density (OD) was blanked and measured at 450 nm.

2.9. Statistical analysis

To account for variability between cultures, three distinct male donors considered as biological replicates, averaged from three technical replicate clone cultures per donor unless stated otherwise (Supplementary Table 1). The use of multiple clones per line enhanced reproducibility and ensured validation of results in each donor line. All statistical analyses were performed in Prism 9 for macOS version 9.3.1 (GraphPad Software LLC, California, USA), apart from RNAseq analyses which were carried out using the research computing facility at King's College London, *Rosalind*, and R version 4.0.2 (R Core Team, 2020). Each specific test carried out is described in each corresponding figure legend, as well as the number of replicates hiPSC lines that make up each technical and biological replicates. Statistical summary tables can be found in the Supplementary. When comparing means for more than 2 groups (Supplementary Tables 11, 14, 15 and 20), one-way ANOVA was used. To test whether transcript expression changed after treating cells with IL-6, we performed unpaired t-tests (Supplementary Tables 17 and 19). When comparing means for two separate conditions (Supplementary Tables 9, 10 and 18), two-way ANOVA was used. *Post-hoc* testing was carried out using Benjamini method 5 % or 1 % FDR. P- and adjusted P-values < 0.05 were considered as statistically significant. During GO analysis, 1 % FDR cut off was chosen to concentrate the number of significantly associated pathways. During MGL quality control (Supplementary Fig. 1), two-way ANOVAs comparing each gene expression with donor and time point demonstrated cell phenotype was not influenced by donor line (Supplementary Tables 9 and 10). Therefore, to reduce batch and reprogramming variability, biological replicates were considered as separate male donors which were averaged from N = 3 technical replicates from either clone cultures of the same donor or separate MGL harvests, as described in figure legends. Statistics were not applied to media cytokine array data since the sample power was too low.

3. Results

3.1. Human iPSC-derived microglial-like cells express IL-6 signaling receptors, but cortical neural progenitor cells do not

Successful differentiation of hiPSCs to MGLs and forebrain NPCs was confirmed by expression of key signature genes and proteins for each cell type (Supplementary Fig. 1). We then profiled human iPSC-derived MGL and NPC monocultures (N = 3 neurotypical male donors with N = 3 separate clones per donor) for cytokine receptor expression by qPCR to establish the potential of each cell type to respond to IL-6, and other cytokines, *in vitro* (ΔCt values available in Supplementary Tables 12 and 13). Transcript expression of *IFNGR1/2, TNFARSF1A, IL17RA*, and both subunits required for IL-6 signaling, *IL6R* and *IL6ST*, all significantly increased with longer differentiation of MGLs *in vitro* relative to the hiPSC state (Fig. 1A, statistics in Supplementary Table 14). Expression of *TNFRSF1B* was not significantly different from the hiPSC stage overall, but was numerically increased at all time points after MGL differentiation, namely ~100-fold from hiPSC to D0, then ~50-fold from hiPSC to D1 and ~35-fold hiPSC to D14 (Fig. 1A). These data indicate that MGLs would be responsive to at least IL-6, IFNγ, TNFα and IL-17.

In contrast to MGLs, differentiation of hiPSCs to forebrain NPCs in monoculture led to extremely low levels of *IL6R* expression, reduced by ~16-fold relative to the hiPSC stage, although this failed to reach statistical significance overall (Fig. 1B statistics in Supplementary Table 15). This observed reduction of *IL6R* expression upon differentiation is in agreement with previously reported data from human *post-mortem* fetal brain tissue (Fietz et al., 2012; Florio et al., 2015; Zhang et al., 2016) (Supplementary Fig. 2). Specifically, these data demonstrate *IL6R* is primarily expressed by microglia and in part by astrocytes in the human brain, but not in neurons (Miller et al., 2014; Zhang et al., 2016) (Supplementary Table 16). Transcripts for *IFNGR1/2, IL6ST* and *IL17RA* were expressed in forebrain NPCs, with expression levels either remaining constant or trended to increase ($p > 0.05$) throughout neuralization (Fig. 1B). *TNFRF1A* trended to decrease from hiPSC ($p > 0.05$) and *TNFRSF1B* increased significantly ($p = 0.0127$) relative to the hiPSC state (Fig. 1B, statistics in Supplementary Table 15). For a cell to respond to IL-6, the IL6Ra must be present in its membrane bound form along with IL-6ST (*cis*-IL6Ra signaling), or the soluble (s)IL6Ra form (*trans*-IL6Ra signaling), which is cleaved at the membrane surface of expressing cells is required (Wolf et al., 2014). These data indicate forebrain NPCs are likely to be unresponsive to IL-6 via *cis*-IL6Ra signaling when grown in monoculture, but responsive to IFNγ, as shown previously (Bhat et al., 2022; Warre-Cornish et al., 2020).

Contrary to this view, a recent study provides data to suggest that transcriptional and morphological phenotypes may be induced in hiPSC-derived D60 mature cortical pyramidal neurons following exposure to IL-6 at D25-27 of differentiation, using an identical protocol (Kathuria et al., 2022). We therefore sought to replicate our finding of very low *IL6R* expression and extend this analysis to longer differentiation times using an identical dual SMAD inhibition protocol, with N = 3 different hiPSC lines from male, neurotypical donors. Analysis of RNA samples by qPCR confirmed the very low expression of *IL6R* in forebrain NPCs and provides evidence to suggest this continues to be the case in mature neurons, at least at 50-days of differentiation *in vitro* (one-way ANOVA: $F(3,8) = 7.30$, $p = 0.0112$; Mean fold change from hiPSC: D7 = 0.03, D20 = 0.03, D50 = 0.12; Fig. 1C). By contrast, *IL6ST* expression increased throughout all stages of differentiation (one-way ANOVA: $F(3,8) = 19.87$, $p = 0.0005$; Mean fold change from hiPSC: D7 = 2.90, D20 = 6.54, D50 = 3.46; Fig. 1C). These data confirm our previous

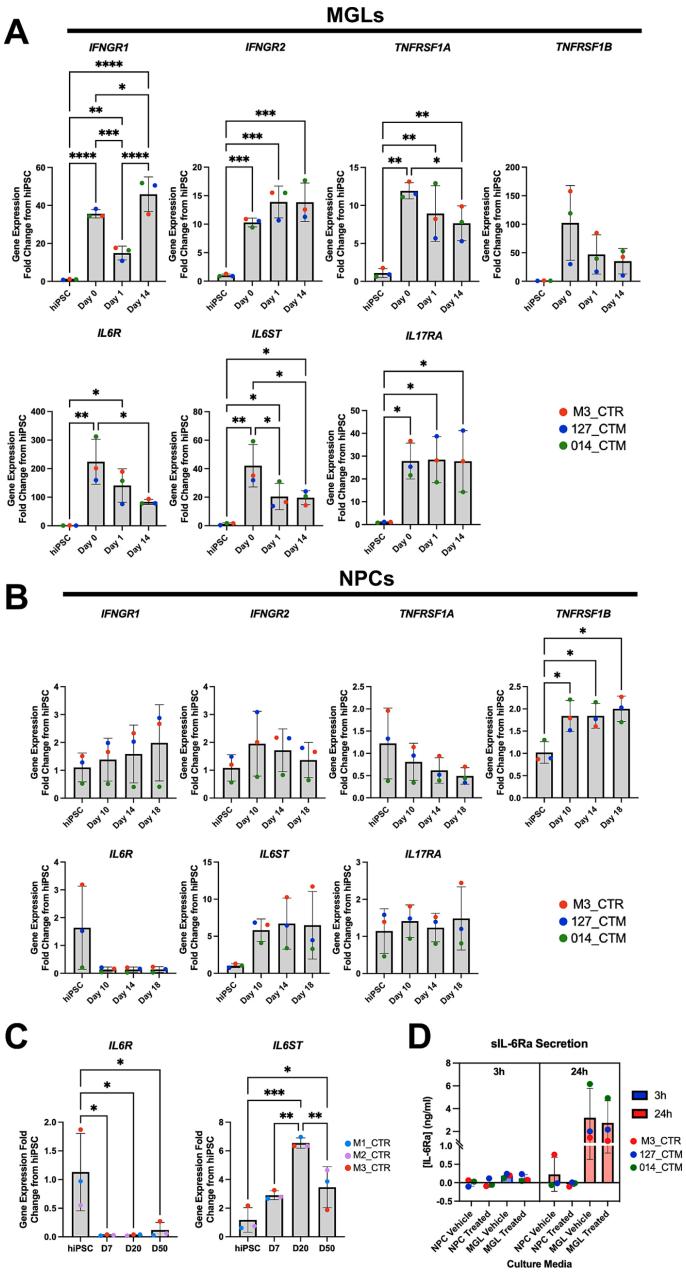

Fig. 1. Cytokine receptor transcript expression in MGL and NPCs. Data shown are from N = 3 male neurotypical hiPSC cell lines, averaged from three technical replicate clones per donor, barring outlier removal where stated. 5 % false discovery rate (FDR) by Benjamini–Hochberg (BH) method corrections after one-way ANOVA formatted as follows: *p < 0.05, **p < 0.01, ***p < 0.001, and ****p < 0.0001; non-significant not labelled. Bar graphs plotted as mean with standard deviation (SD) error bars, and points colored by donor line as shown in key. (A) MGL differentiation time-course of cytokine receptors (*IFNGR1, IFNGR2, TNFRSF1A, TNFRSF1B, IL6a, IL6ST and IL17RA*) gene expression at hiPSC, macrophage/microglia progenitors (day 0), MGL at day 1 and day 14 of differentiation. M3_CTR day 14 *IL17RA* data point averaged from N = 2 clones only. (B) NPC differentiation time-course of the same cytokine receptors by qPCR RNA samples at hiPSC and days 10, 14 and 18 of neuralization to NPCs. 127_CTM day 14 *TNFRSF1B* data point was averaged form N = 2 clones only. (C) qPCR of *IL6R* and *IL6ST* transcript expression in N = 3 different healthy male lines (M1_CTR, M2_CTR and M3_CTR, one technical repeat each) over a longer timeframe, from hiPSC to D50 mature neurons. (D) Protein concentrations quantified by ELISA of soluble IL-6R (ng/ml) in NPC (on D18) and MGL (on D14) culture media after 3 h and 24 h vehicle or IL-6 100 ng/ml treatment exposure.

observations of very low *IL6R* expression in forebrain NPCs and extend these to mature cortical neurons (D50).

Given the apparent very low level of *IL6R* transcript expression in forebrain NPCs under the conditions tested, we next examined the secretion of the soluble IL6Ra protein in both forebrain NPCs and MGLs after a 3 h exposure to IL-6, indicative of the ability to initiate *trans*-IL-6 signaling (Fig. 1D) (Campbell et al., 2014; Michalopoulou et al., 2004; Wolf et al., 2014). Using a sIL6Ra-ELISA kit in vehicle-treated cultures, we observed very limited secretion of sIL6Ra protein into the culture supernatant by forebrain NPCs (Fig. 1D). By contrast, sIL6Ra secretion was clearly present in vehicle-treated MGLs in the culture supernatant after both 3 h and 24 h (Fig. 1D). Both 3 h and 24 h exposure to IL-6 (100 ng/ml) did not increase the secretion of sIL6Ra protein in either cell type (two-way ANOVA 3 h: cell type $F(1,8) = 9.35$ $p = 0.0156$, treatment $F(1,8) = 0.497$ $p = 0.5009$, interaction $F(1,8) = 0.350$ $p = 0.5709$; 24 h: cell type $F(1,8) = 9.39$ $p = 0.0155$, treatment $F(1,8) = 0.147$ $p = 0.7116$, interaction $F(1,8) = 0.0106$ $p = 0.9207$). Nonetheless, the fact that MGLs secrete sIL6Ra provides an opportunity for other cell types within their vicinity to respond to IL-6 via soluble, non-membrane bound (*trans*-) IL6Ra signaling. By contrast, the lack of sIL6Ra secretion from NPCs confirms the fact that they do not express the soluble form of the IL-6 receptor and strongly suggests forebrain NPCs are unlikely to be responsive to IL-6 in monoculture under the conditions tested.

3.2. IL-6 activates the canonical STAT3 pathway in microglia-like cells but not forebrain neural progenitor cells

We next determined the functionality of the IL6Ra and IL6ST receptors in forebrain NPCs and in MGLs at day 1 (D1) and day 14 (D14) of differentiation (Fig. 2A). First, transcripts of relevant STAT3 downstream target genes *IL6, IL10,* tumor necrosis factor α (*TNF)* and Jumonji Domain-Containing Protein 3 *(JMJD3)* (Przanowski et al., 2014) were measured by qPCR (Fig. 2B, statistics in Supplementary Table 17). At 3 h after exposure to IL-6 (100 ng/ml), both D1 MGL and D14 MGL cells responded by increasing the expression of *IL6* itself and *JMJD3*, relative to the vehicle control. Our modest sample size (N = 3 donors) may have reduced our ability, however, to detect any statistical significance when comparing *IL10* expression after IL-6 stimulation. For example, D1 MGL stimulated with IL-6 for 3 hr increase *IL10* expression (~5-fold) more so than MGLs at the same time-point (~3-fold), but the former result is not statistically significant whilst the latter is. The expression of *TNF* was not affected in either D1 MGL or D14 MGLs by IL-6 exposure (Fig. 2B, statistics in Supplementary Table 17). By contrast, at 24 h after exposure to IL-6 (100 ng/ml), the expression of all these genes was no longer statistically significantly different relative to the vehicle control in both D1 MGL and D14 MGLs (Fig. 2B). Based on the apparent functional maturity of MGLs after 14 days of differentiation (Haenseler et al., 2017), and their response to IL-6 by significantly increasing *IL10*, only MGLs differentiated for 14 days were used in all subsequent experiments.

Having confirmed IL-6 triggers a transcriptional response associated with IL6R signaling in MGLs, we next sought to determine the minimal concentration of IL-6 that would induce this response from day 14 MGLs in monoculture (Fig. 2C). We exposed day 14 MGLs to several different IL-6 concentrations (range: 0.1 pg/ml to 100 ng/ml) and measured the expression of genes that were up-regulated after 3 h (*IL6, IL10* and *JMJD3*) by qPCR. Our concentration range included the average, steady state concentration of IL-6 present in maternal serum collected from second-trimester mothers in a recent birth cohort study, which was reported to be 0.98 ± 1.06 pg/ml (Graham et al., 2018). We also measured expression of interferon regulatory factor 8 (*IFR8)*, a transcription factor known to regulate immune function and myeloid cell development (d'Errico et al., 2021; Tamura and Ozato, 2002). Expression of *IL6*, *JMJD3*, *IL10* and *IRF8* were unaffected relative to vehicle control at all concentrations of IL-6 tested except 100 ng/ml, which elicited a clear increase in expression, which varied between donors as may be expected (Fig. 2C, statistics in Supplementary Table 18). This 100 ng/ml IL-6 concentration is much higher than observed in steady state maternal serum (Graham et al., 2018) yet it would be expected that IL-6 concentration increases in maternal serum during an acute response to infection (Hsiao and Patterson, 2011; Matelski et al., 2021; Ozaki et al., 2020; Wu et al., 2017). For instance, adult patients with community-acquired pneumonia have a mean serum IL-6 of 477 pg/ml (Antunes et al., 2002), and COVID-19 patients with delirium have a mean serum IL-6 of 229.9 pg/ml (Borsini et al., 2022). We therefore selected 100 ng/ml IL-6 for further experiments since this elicited a response in our MGLs that can be measured at a single time-point, allowing us to investigate the response to IL-6, a specific cytokine that plays a key role in MIA, as per our previous work on IFNγ (Bhat et al., 2022; Warre-Cornish et al., 2020). Whilst this concentration is still significantly higher than the data reported above, it should be remembered that both microglia (consistent with our own data herein) but also astrocytes in the fetal brain would produce IL-6 in response to infection, thus local levels of IL-6 may be considerably higher than those reported in the maternal serum.

Since forebrain NPCs, in contrast to MGLs, displayed a very low level of *IL6R* expression, we sought to confirm whether forebrain NPCs in monoculture show any response to 100 ng/ml IL-6. Three hours after IL-6 exposure, forebrain NPCs did not significantly increase the expression of *IL6*, *JMJD3* and *TNF* transcripts relative to vehicle controls (Fig. 2D, statistics in Supplementary Table 19). Furthermore, the *IL10* transcript was undetectable in all NPC samples irrespective of treatment, given no CT values were generated (data not shown). These data suggest that whilst IL-6 triggers IL6R signaling in MGLs, this is not the case for forebrain NPCs at D18 *in vitro*.

To complement our gene expression analysis, we next assessed the time-scale of canonical STAT3 signaling following IL-6 receptor stimulation at the protein level in both forebrain NPCs and MGLs. Formation of the IL-6/IL6Ra/IL6ST complex on the cell surface membrane results in phosphorylation of STAT3 (pSTAT3) by the protein kinase JAK, which shuttles to the nucleus to enable subsequent transcription of STAT3 target genes (Wolf et al., 2014). We therefore collected protein samples at multiple time points following acute IL-6 exposure (100 ng/ml) of either NPCs or MGLs and performed western blotting for Y705-pSTAT3 and total STAT3 (Fig. 2E-G). Quantification of the Y705-pSTAT3 ratio to total STAT3 (tSTAT3) indicated that IL-6 triggered a time-dependent increase in pSTAT3 relative to vehicle controls that peaked after 15 min in MGLs but was absent in D18 forebrain NPCs (Fig. 2E, two-way ANOVA: cell type $F(3,16) = 17.45$; $p = 0.0007$, $F(3,16) = 5.486$; time $p = 0.0089$, interaction $F(3,16) = 5.47$; $p = 0.0088$).

3.3. Transcriptional response in human microglia-like cells to acute IL-6 exposure

Our data thus far provide evidence suggesting that the canonical STAT-3 signaling pathway is activated in MGLs within 3hr of exposure to IL-6. To better characterize the transcriptional response of MGLs to this stimulus, we next performed bulk RNA-sequencing at 3hr post IL-6 exposure (100 ng/ml) in MGLs generated from N = 3 male neurotypical donor hiPSC lines. Principal component analysis (PCA) of the gene expression data reveals that samples clustered by treatment (Fig. 3A), consistent with the heatmap clustering of the top 25 differentially expressed genes (DEGs) (Fig. 3B). Overall, we found that 156 and 22 genes were up- and down-regulated, respectively, following 3 h IL-6 exposure (FDR < 0.05) (Fig. 3B-C). Up-regulated genes of note included *IRF8,* consistent with our qPCR data (Fig. 2C) the NFkB subunit *REL,* heat shock proteins *HSPA1A/B* and the oxytocin receptor (*OXTR)* (Supplementary Fig. 3). Although maternal IL-17 is suggested to be involved in MIA-induced behavioral changes in offspring with relevance to ASC (Choi et al., 2016), we found no evidence for its differential expression in our MGL 3 h IL-6 response. The DESeq2 normalized counts (calculated using the median of ratios method) for *IL6R* and *IL6ST* remained constant, confirming that the expression of these receptors is independent of the 3 h IL-6 exposure (Supplementary Fig. 3). Using

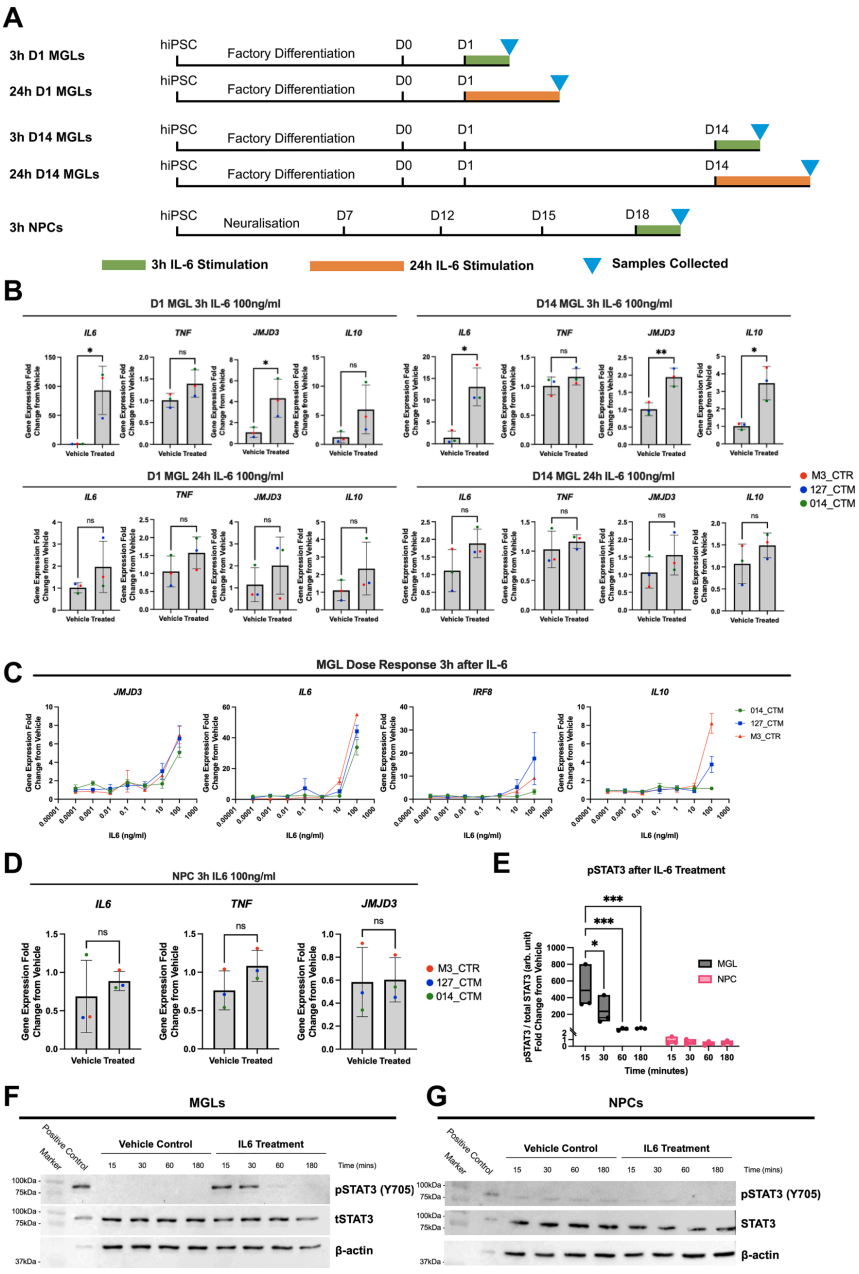

(caption on next page)

Fig. 2. MGL monocultures respond to IL-6 in a dose and time dependent manner, NPC monocultures do not respond at all. (A) Schematic of MGL and NPC cell culture and RNA sample collection. (B) Transcripts of downstream IL-6 pathway genes *IL6, TNF, JMJD3* and *IL10* were measured by qPCR in three male healthy control cell lines treated with 100 ng/ml IL-6, averaged over three technical replicate clone cultures per donor unless stated otherwise, in the following conditions: D1 MGL treated for 3 h; D14 MGLs treated for 3 h; D1 MGL treated for 24 h, 014_CTM treated condition averaged from N = 2 clones only; MGLs treated for 24 h. Unpaired test results formatted as follows: *p < 0.05, **p < 0.01, ***p < 0.001, and ****p < 0.0001; not significant (ns). Bar graphs plotted as means with standard deviation (SD) error bars, and points coloured by donor line: red (M3_CTR), blue (127_CTM) and green (014_CTM). (C) Dose response of MGLs to 7 doses of a 10-fold serial dilution of IL-6 from 100 ng/ml to 0.1 pg/ml. Three healthy male donors with n = 3 harvest replicates per donor. *IL10* 127_CTM_01 0.1 ng/ml outlier removed and calculated form N = 2 harvests. Fold change from vehicle calculated within line, but vehicle not plotted. (D) Transcripts of downstream IL-6 pathway genes *IL6, TNF* and *JMJD3* in NPCs treated for 3 h, with unpaired *t*-test results formatted as above. *IL10* transcripts were undetectable in NPC samples so data is not shown. (E) Quantification of pSTAT3/tSTAT3 protein signal in arbitrary (arb.) units from blots F and G, shown as a fold change ratio from timepoint vehicle within cell type. Box plot presented with split y-axis at 2 arb. units to visualize variance in NPC data. (F-G) Immunoblotting for 88 kDa pSTAT3/tSTAT3 in both vehicle and 100 ng/ml IL-6 stimulated samples collected after 15, 30, 60 and 180mins, in MGL (F) and NPC (G) monocultures, with 3 h IL-6 100 ng/ml treated immortalized mouse microglia cells (BV2s) as a positive control.

DESeq2 normalized counts we identified numerical increases in key IL-6 signaling transcripts, including STAT3, JAK1, JAK2, and JAK3, but not in tyrosine kinase 2 (TYK2), although none of these were statistically significant in the DESeq2 analysis (p > 0.05; BH 5 % FDR). Finally, the presence of microglial markers was confirmed in DESeq2 normalized counts, and no effects of IL-6 were observed on these markers (Supplementary Fig. 3).

Using only the 178 DEGs at 5 % FDR, we carried out Webgestalt GO analyses splitting these into either up-regulated (156) or down-regulated genes (22). Across cellular components, biological processes, and molecular functions, 21 GO pathways were significantly associated with the 156-up-regulated genes (1 % FDR) (Fig. 3D). These included the NFkB signaling (FE = 4.60, $p < 0.001$, FDR = 0.001), leukocyte differentiation (FE = 3.55, $p < 0.001$,FDR < 0.001), cell–cell adhesion regulation (FE = 3.77, $p < 0.001$, FDR = 0.002), response to cytokine stimuli (FE = 5.57, $p < 0.001$, FDR = 0.002), production of IFNγ (FE = 6.95, $p < 0.001$, FDR = 0.004) and TNF superfamily (FE = 5.87, $p < 0.001$, FDR = 0.004) cytokines (Fig. 3D). By contrast, no GO pathways at either 5 % or 1 % FDR correction were significantly associated with the 22 down-regulated genes. Complementary GO analysis using the QIAGEN Ingenuity Pathway Analysis (IPA) software (Krämer et al., 2014) identified 30 associated pathways at a z-score threshold of > 2 to identify predicted activation or inhibition of a pathway, of which 24 passed 1 % FDR correction (Fig. 3E). The top activated pathways were "neuroinflammation signaling" (Ratio = 0.035, $p < 0.001$, FDR < 0.001), nitric oxide and reactive oxygen species (ROS) in macrophages (Ratio = 0.037, $p < 0.001$, FDR < 0.001), TNFRSF signaling in lymphocytes (4-1BB: Ratio = 0.176, $p < 0.001$, FDR < 0.001; CD27: Ratio = 0.088, $p < 0.001$, FDR < 0.001), epithelial-mesenchymal transition in development (Ratio = 0.058, $p < 0.001$, FDR = 0.001), G-protein coupled receptor signaling (Ratio = 0.023, $p < 0.001$, FDR < 0.001), IL-17 signaling (Ratio = 0.021, $p < 0.001$, FDR = 0.034) and a down-regulation of GADD45 signaling (Ratio = 0.067, $p < 0.001$, FDR = 0.002). Overall, these complementary GO analyses provide evidence for a prototypical microglial cell response after 3 h of IL-6 stimulation, characterized by NFkB pathway activation and downstream pathway changes to ROS, cell adhesion, cytokine secretion and TNFRSF signaling.

3.4. The transcriptomic changes associated with IL-6 MGL exposure are associated with those observed in post-mortem brain tissue from schizophrenia cases

IL-6 is increased in human serum, cerebrospinal fluid (CSF) and *post-mortem* brain tissue in multiple psychiatric disorders including SZ, ASC, BD and major depressive disorder (MDD) (Gandal et al., 2018; Khandaker et al., 2014; Lu et al., 2019; Perry et al., 2021; Sasayama et al., 2013; Schwieler et al., 2015; Zhao et al., 2021). Furthermore, this association is demonstrated at multiple stages through life, including maternal serum (Allswede et al., 2020), in children aged 9 (Khandaker et al., 2014) and young adulthood at ages 18–25 (Schwieler et al., 2015). This is consistent with a view that IL-6 pathways are likely to be involved at different stages of the pathogenesis of psychiatric disorders.

To corroborate the role of IL-6 signalling in these disorders, we therefore investigated whether the genes up- and down-regulated in MGLs following 3 h IL-6 stimulation were enriched within genes up- and down-regulated in *post-mortem* brain tissue from SZ, ASC and BD patients, as identified by Gandal et al. (2018) (two gene sets from the model vs two gene sets from each disorder: 12 comparisons in total; Fig. 3F). We observed statistically significant enrichments between the up-regulated gene set in the IL-6 model and the gene sets up-regulated in SZ (N genes in model = 156, N genes in cases = 2274, overlap size = 44 genes, P = 0.00022, odds ratio (OR) = 2.0) and ASC (N genes in model = 156, N genes in cases = 701, overlap size = 14 genes, P = 0.031, OR = 1.8), and between the down-regulated gene set in the model and the gene set down-regulated in SZ (N genes in model = 22, N genes in cases = 2073, overlap size = 7 genes, P = 0.04, OR = 2.6). The only significant overlap observed after multiple testing correction (1 % FDR), was that between the up-regulated gene set in the IL-6 model and the up-regulated genes in SZ cases (FDR = 0.003). Using the 44 overlapping genes, Webgestalt GO analyses identified 10 associated pathways (Fig. 3G, overlap gene list in Supplementary Table 20). This included signaling response pathways (FE = 6.61, $p < 0.001$, FDR = 0.008), "leukocyte cell–cell adhesion" (FE = 7.81, $p < 0.001$, FDR = 0.009), "*T*-cell activation" (FE = 6.40, $p < 0.001$, FDR = 0.009) and apoptotic signaling (FE = 7.29, $p < 0.001$, FDR = 0.034). Importantly, although just failing to pass a 5 % FDR correction, increased NFkB signaling was also highlighted as an output (FE = 11.4, $p < 0.001$, FDR = 0.059), consistent with gene expression data in post-mortem brain tissue from SZ patients as compared to controls (Volk et al., 2019). These data suggest IL-6 signaling modifies gene expression in a manner consistent with the dysregulation observed in the brains of individuals with SZ.

To complement this analysis, we next tested whether the genes differentially regulated in MGLs after 3 h IL-6 stimulation were significantly enriched in genes identified as risk factors for SZ, BD, and ASC through genome-wide association (GWAS) studies (Grove et al., 2019; Mullins et al., 2021; Trubetskoy et al., 2022). To this end, we performed gene-level enrichment analyses to identify risk genes associated with each condition, and we tested these for enrichment with the up- and down-regulated gene sets observed in the IL-6 stimulated MGLs, using MAGMA (de Leeuw et al., 2015). We found no significant enrichment for SZ (or any disorder) considering the genes differentially regulated in our model (all comparisons P > 0.05) (Fig. 3H). These data suggest that exposure of human MGLs to IL-6 does not alter the expression of genes associated with increased risk for SZ, BD and ASC.

Finally, we investigated the overlap of up- and down-regulated gene sets with microglia-specific module gene sets using the MGEnrichment tool (https://ciernialab.shinyapps.io/MGEnrichmentApp/) to compare our data with published gene expression data in human and mouse microglia (Jao and Ciernia, 2021). When comparing our data to microglia gene sets derived from human tissue only, we found 31 modules were associated with the up-regulated gene set and 12 with the down-regulated gene set after 5 % FDR correction from MGLs exposed to IL-6 for 3 h. Notable modules that overlapped with our up and down-regulated gene sets separately were a "SCZ, ASD and Bipolar Disorder

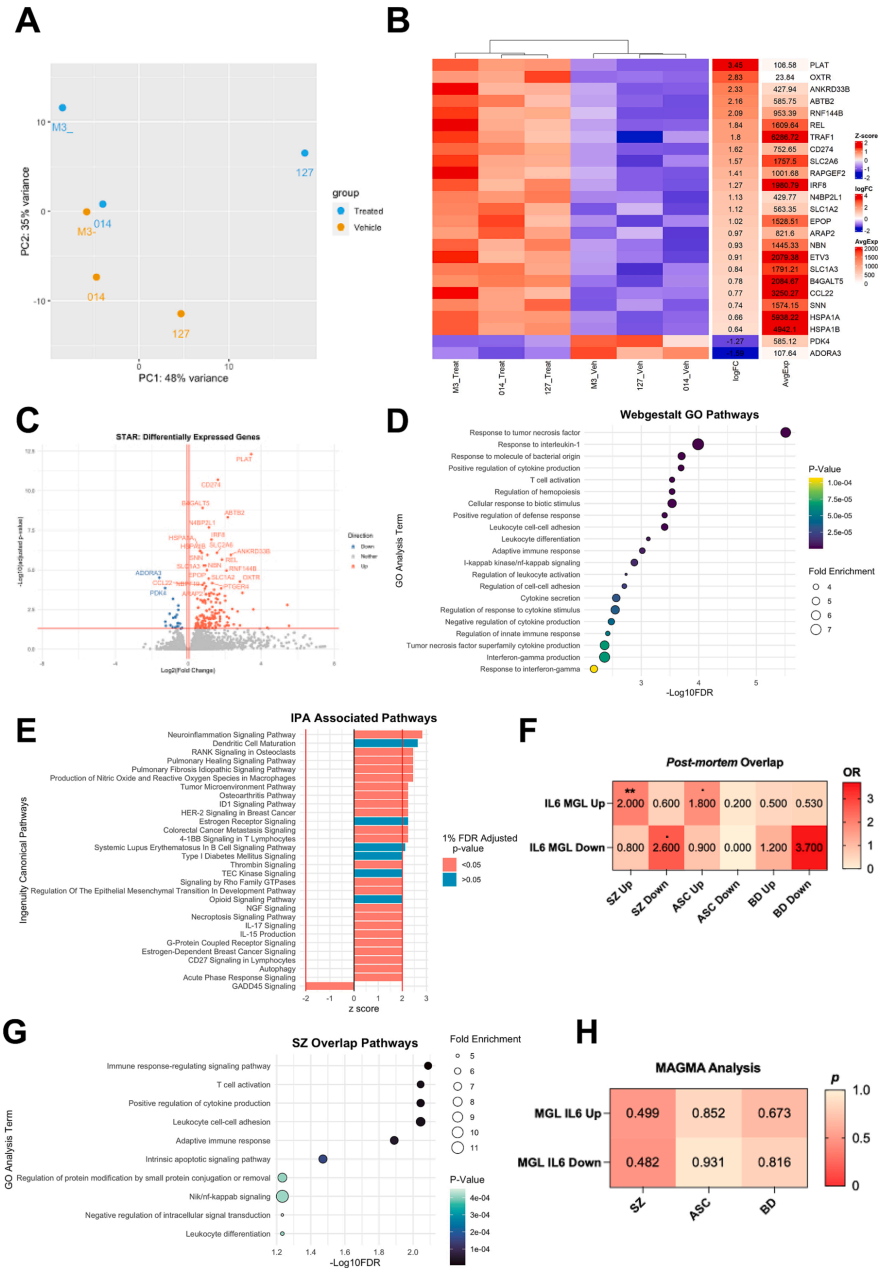

(caption on next page)

Fig. 3. Acute IL-6 exposure elicits a transcriptional response in human microglia-like cells of relevance for schizophrenia. MGLs from 3 healthy male donors, pooled from 2 clone cultures each, were exposed to IL-6 or vehicle for 3 h and collected for RNAseq. (A) PCA analysis of all 6 samples, colored by vehicle (orange) or IL-6 treated (blue) condition and labelled by donor line: M3_CTR as M3-, 014_CTM as 014 and 127_CTM as 127. (B) Heatmap of top 25 most differentially expressed genes in the IL-6 3 h MGL response, ranked by LogFC and clustering by treatment group. (C) Volcano plot of differentially expressed genes. Conditional axis set as follows: log2Foldchange > 0.06 and adjusted p-value < 0.05 colored red; log2Foldchange < −0.06 and adjusted p-value < 0.05 colored blue. The top 25 differentially expressed genes are labelled. (D) Webgestalt gene ontology analysis of up-regulated 156 gene set only with an adjusted 1 % FDR. GO terms ordered by –log10FDR, colored by adjusted p-value and sized by the fold enrichment within each dataset. (E) IPA associated pathways, ranked by z-score and colored by 1 % FDR adjusted p-value. Only pathways with z-score > |2| are shown, with z-score > |2| conditional axes labelled in red. (F) Fisher's exact test comparing gene sets from ASC,SZ and BD post-mortem human patient tissue (Gandal et al., 2018) with up- and down-regulated gene sets identified by RNAseq in this study. Odds ratios (OR) plotted in heatmap with significant 5 % FDR corrections formatted as follows: p < 0.1, *p < 0.05, **p < 0.01, ***p < 0.001, and ****p < 0.0001; not significant, not labelled. (G) Webgestalt gene ontology analysis of 44 genes overlapped from our up-regulated RNAseq dataset and SZ up-regulated genes from Gandal et al., 2018, with an adjusted 1 % FDR. GO terms ordered by −log10FDR, colored by adjusted p-value and sized by the fold enrichment within each dataset. (H) MAGMA analysis comparing significant risk genes from SZ (Trubetskoy et al., 2022), BD (Mullins et al., 2021) and ASD (Grove et al., 2019) GWAS studies with IL-6 MGL up and down DEGs obtained by RNAseq in this study. P-values plotted in heatmap.

(BD) module" (Up: intersection size = 44 genes, FDR = 7.10e-29, OR = 13.5. Down: intersection size = 8 genes, FDR = 5.69e-06, OR = 17.9) (Gandal et al., 2018), and a "core human microglial signatures module" (Up: intersection size = 26 genes, P = 3.29e-12, OR = 6.3. Down: intersection size = 10 genes, FDR = 4.47e-08, OR = 24.8) (Galatro et al., 2017), both of which originate from bulk RNAseq datasets. With the same tool, we additionally found both our up- and down-regulated gene set to be enriched for single-cell RNAseq microglial modules (Olah et al., 2020). These included up-regulation enrichment for "Microglia anti-inflammatory responses" (intersection size = 18 genes, FDR < 0.0001, OR = 9.90), "Microglia cellular stress" (intersection size = 7 genes, FDR < 0.0001, OR = 11.7), "Microglia interferon response signaling pathway" (intersection size = 8 genes, FDR = 0.0007, OR = 5.39) and "Microglia homeostatic states" (intersection size = 7 genes, FDR = 0.009, OR = 3.96). Our down-regulated gene set was enriched for "Microglia antigen presentation" (intersection size = 4 genes, FDR = 0.0003, OR = 29.2) and additionally "Microglia homeostatic states" (intersection size = 3 genes, FDR = 0.018, OR = 12.6). To assess the additional overlap with mouse data, we used the MGEnrichment tool and found 26 mouse modules to overlap with our up-regulated gene set and 4 mouse modules with our down-regulated gene set. The most relevant module that overlapped with our up-regulated gene set was "MIA Poly I:C GD14 P0" module (intersection size = 11 genes, FDR = 0.016, OR = 2.95) from Matcovitch-Natan et al. (2016), a microglial gene set taken from newborn pups whose mothers were exposed to Poly I:C on gestational day 14 (Matcovitch-Natan et al., 2016). Of note, the intersection size of this comparison is only 11 genes, which may be expected given the different stimuli involved (Poly IC as compared to IL-6), plus the different species and gestational time-points.

3.5. Acute 3 h IL-6 exposure increases microglia motility and chemokine secretion in vitro

Both our RNAseq and qPCR data provide evidence for an increase in *IFR8* expression after IL-6 exposure in human MGLs. In mice, microglia-specific deletion of *IRF8* results in cells with fewer, shorter branches and reduced motility, consistent with the regulatory role of *IRF8* in microglia state (d'Errico et al., 2021). Furthermore, primary microglia from an *IRF8*−/− mouse model demonstrated attenuated ATP-induced chemotaxis in comparison to wild type primary mouse microglia (Masuda et al., 2014). Finally, a recent data from a mouse model of MIA provides evidence that IL-6 increases microglial motility *in vivo* (Ozaki et al., 2020). Based on these data, we acquired live cell imaging data to record the effect of 3 h exposure to IL-6 (100 ng/ml) on MGL whole cell (nuclear) motility, cytoplasmic specific (cytoplasm) motility and morphology, another known correlate of microglial function (Hanger et al., 2020). We observed that vehicle treatment was by itself sufficient to influence MGLs motility, as evidenced by an increase in cytoplasmic distance and displacement in both vehicle- and IL-6 treated cultures relative to untreated controls (Fig. 4A, statistics in Supplementary Table 21). Critically however, IL-6 increased mean cytoplasmic distance relative to vehicle-treated controls, suggestive of increased cytoplasmic ruffling (Fig. 4A, statistics in Supplementary Table 21). Nuclear motility, cell area and length were unchanged by either vehicle or IL-6 treatment (Supplementary Fig. 4). We confirmed these effects were not due to differences in cell number or the movement of cells in or out of the field of view (statistics in Supplementary Table 21). These data are consistent with increased *IRF8* expression (d'Errico et al., 2021) and our GO analysis.

Microglia release cytokines and chemokines to recruit additional immune cells to sites of pathology in the brain and these signaling molecules are often indicated to be dysregulated in SZ patients (Dawidowski et al., 2021; Morris et al., 2018; Purves-Tyson et al., 2021, 2020). As several pathways related to cytokine secretion were specified during RNAseq GO analysis, we next aimed to gain an overview of cytokine secretion from IL to 6 exposed MGLs by using a proteome profiler array, as previously described (Garcia-Reitboeck et al., 2018) (Supplementary Table 22 and Supplementary Figure 5). Chemokine and cytokine release is clearly influenced by IL-6 stimulation at either 3 or 24 h after exposure to IL-6 (100 ng/ml) (Fig. 4C-D and Supplementary Table 23). Of the 36 cytokines and chemokines in the assay, 13 were above the limit of detection in culture supernatant. We excluded IL-6 since it was ectopically spiked into the media when the cells were stimulated with IL-6 (Fig. 4B). Although semi-quantitative, changes in cytokine and chemokine secretion may be represented as fold changes from vehicle. MIP-1α/β and CXCL1 were increased in supernatants from IL-6 exposed cultures at both time-points relative to vehicle-controls, although considerably less so after 24 h. This replicates findings that MIP-1α is robustly up-regulated in maternal serum of rodent MIA models (Brown et al., 2022; Osborne et al., 2019). CCL1/2, Serpin-E1, MIF and IL-18 were increased only after 24 h IL-6 stimulation with little difference observed at 3 h. IL-8 presented higher secretion 3 h after IL-6 simulation but not at 24 h. The anti-inflammatory cytokines IL-13 and IL-16 were reduced at both time-points relative to vehicle-controls. Finally, IL-1Ra, CCL2 and ICAM remained unchanged after IL-6 exposure at both time points. These alterations to the MGL secretome provide evidence that IL-6 stimulation of human MGLs leads to dynamic changes in specific inflammation-regulating chemokines and cytokines.

4. Discussion

We characterized the cell-specific responses of MGL and NPC to acute IL-6 exposure using hiPSC lines obtained from male, neurotypical donors (N = 3). Our data suggest two main findings; first, that hiPSC-derived MGL and NPC cells show clear differences in IL6Ra signaling capabilities and second, that exposure of MGLs to IL-6 recapitulates molecular and functional phenotypes of relevance for psychiatric disorders, particularly schizophrenia, consistent with evidence from genetic (Perry et al., 2021), blood biomarker (Allswede et al., 2020) and animal models (Smith et al., 2007) that link this cytokine with increased risk for schizophrenia.

We observed that both hiPSC-derived forebrain NPCs and mature

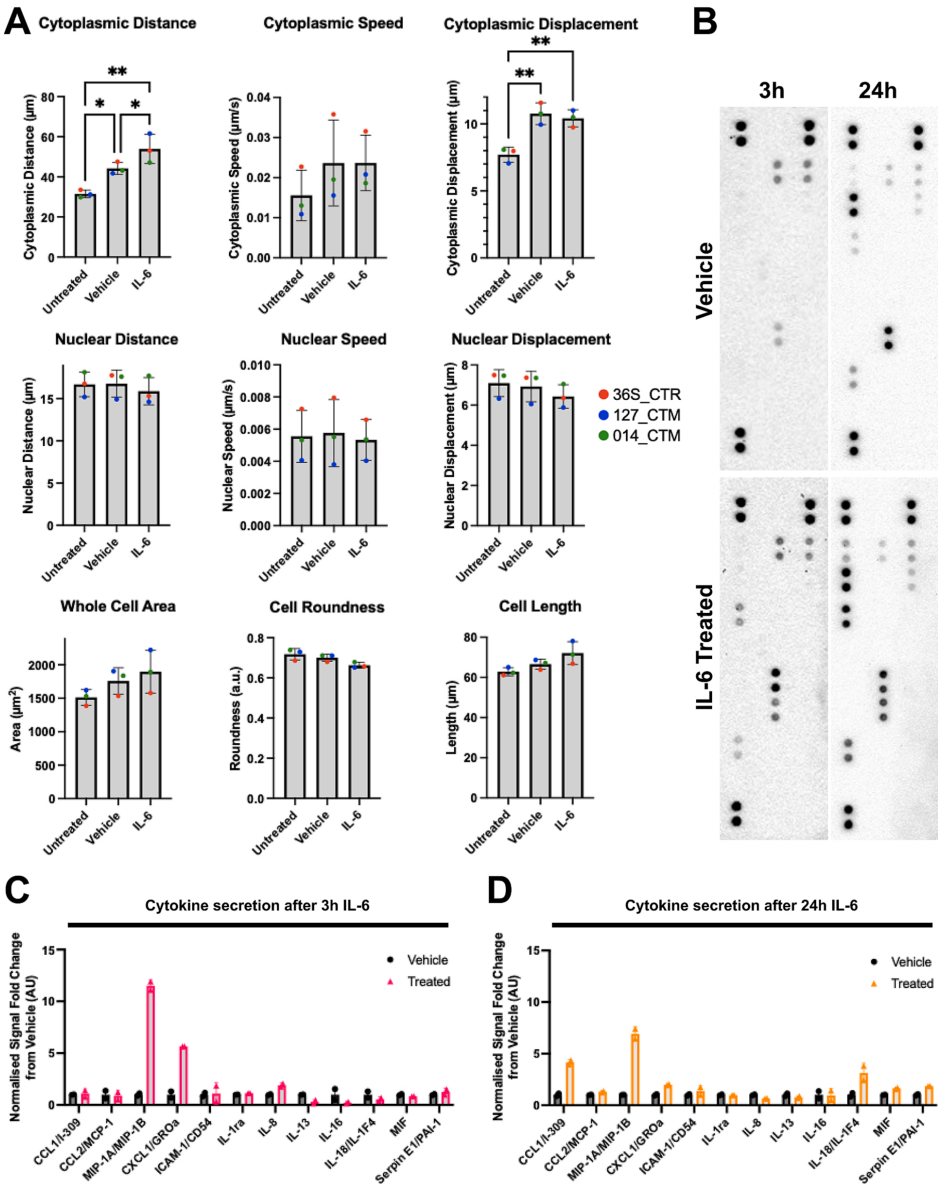

Fig. 4. Acute IL-6 increases time-dependent changes in cytokine and chemokine secretion from human MGLs *in vitro*. MGL motility and secretome is altered in response to IL-6. (A) Metrics of MGL motility and morphology over 2 h of live imaging, having been exposed to vehicle, IL-6 100 ng/ml or untreated for 180 min. 5 % FDR Benjamini method corrections formatted as follows: *p < 0.05, **p < 0.01, ***p < 0.001, and ****p < 0.0001; not significant, not labelled. Bar graphs plotted as mean with standard deviation (SD) error bars, and points coloured by donor line: red (M3_CTR), blue (127_CTM) and green (014_CTM), all averaged from N = 3 harvest replicates. (B) Representative images of dot blot cytokine profiles secreted from vehicle and IL-6 stimulated MGLs analysed using the human cytokine array. N = 3 separate harvest media samples were pooled into one sample per condition from M3_CTR_37S. Corresponding cytokine and chemokine coordinate labels are available in Supplementary Table 22 and supplementary Fig. 5. (C-D) Signal quantification of cytokine signals from dot blots presented in B, shortlisted for detectable cytokines and chemokines and split into 3 h (C) and 24 h (D) datasets. IL-6 not shown since it was artificially spiked by treatment. Each point represents a technical replicate of each signal point in arbitrary units, which were normalised to positive control reference spots and fold change calculated from averaged vehicle value within each time point.

neurons express very low levels of *IL6R*, resulting in their limited ability to respond to IL-6 treatment in monoculture, as evidenced by the absence of STAT3-phosphorylation and *IL6, JMJD3* and *TNF* expression changes post-IL-6 exposure. These data are seemingly at odds with those from hiPSC-derived mature neurons derived using a similar differentiation protocol, in which IL-6 exposure resulted in transcriptional and morphological phenotypes (Kathuria et al., 2022). One important difference between this work and our own is the age at which these cells were exposed to IL-6: specifically, D18 NPCs vs D25-27 neurons (Kathuria et al., 2022). Although we confirmed *IL6R* expression is absent in forebrain neurons at D50, it may be possible that *IL6R* mRNA is expressed transiently between days 25–50, or only protein levels are present, which is not detectable by RNAseq. Therefore, we cannot rule out that D25-27 neurons derived by this protocol can prompt an IL-6 response and that differences in the timing of IL-6 exposure may lead to differential results (Estes and McAllister, 2016). A second difference is the dose and length at which these cells were exposed to IL-6: 3 h and 24 h of 100 ng/ml IL-6 herein as compared to 48 h to 1 μg/ml IL-6 (Kathuria et al., 2022). It is important to note here that just as observed in animal MIA models, differences in the intensity and duration of immune activation will lead to variations in results. In this context we sought to find the minimum concentration of IL-6 that our cells would respond to *in vitro*, at least in monoculture, which is 100 ng/ml and the dose with which we continued to characterize the cell's IL-6 response. We did not carry out RNAseq on our IL-6 exposed NPC RNA, so we cannot discount a non-canonical response to IL-6 that is independent of the IL6Ra-STAT3 pathway at higher concentrations of IL-6. More experiments are necessary to address these questions.

Furthermore, our data strongly suggest MGLs in co-culture with neural progenitors and additional cell types are necessary to study the influence of IL-6 on NPC-specific development when using D18 NPCs under the conditions tested in our study. In this context, we observed secretion of sIL6Ra protein from MGLs but minimal sIL6Ra secretion from NPCs at two separate time points, suggesting that in a co-culture paradigm, secretion of the sIL6Ra by MGLs may enable NPCs to respond to IL-6 via *trans*-signaling *in vitro*. In support of this view, data from a transgenic mouse model provide evidence that targeted inhibition of CNS *trans*-signaling via sIL6Ra mitigates several relevant neuropathological hallmarks previously associated with NDDs, including impaired neurogenesis, blood brain barrier leakage, vascular proliferation, astrogliosis and microgliosis (Campbell et al., 2014). These data support the view that sIL6Ra *trans*-signaling may be a relevant pathogenic mechanism of IL-6 in both glial and non-glial cell types (Campbell et al., 2014). In addition, sIL6Ra is present (irrespective of inflammatory conditions) in human CSF at 1.92–3.03 ng/ml (Azuma et al., 2000; Hans et al., 1999). This not only indicates that IL-6 *trans*-signaling is possible in the human brain but also supports the data presented in this study, that MGL sIL6Ra secretion reaches concentrations relevant to human CSF in culture media after 24 h and is independent of IL-6 stimulation. Further studies are therefore now required to confirm in our system whether forebrain NPCs can activate *trans*-IL6 signaling in the presence of sIL6Ra protein.

Our second main observation is the genes up-regulated by acute IL-6 exposure in our hiPSC-derived MGLs significantly overlap with genes increased in *post-mortem* brain issue from SZ patients, but not ASC or BD (Gandal et al., 2018). However, these genes did not overlap with risk genes for SZ, ASC and BD, as identified by GWAS. This could suggest that the relationship observed between IL-6 and these disorders may be driven by environmental factors leading to abnormal levels of IL-6 (Allswede et al., 2020; Careaga et al., 2017; Graham et al., 2018; Meyer, 2014; Mueller et al., 2021; Potter et al., 2023; Rasmussen et al., 2021, 2019; Rudolph et al., 2018). We are unable however, to disregard the effect of genetics as a potential mediator of this relationship, as all variants and genes located within the histocompatibility complex (MHC) locus are excluded from the MAGMA analysis due to the complex linkage disequilibrium structure in this region, although many IL-6 response genes are in this locus. Ultimately, the development of new methods to translate findings from the MHC into neurobiological risk mechanisms for complex disorders could advance our understanding of the role of the MHC in psychiatric disorders.

Key up-regulated DEGs in this study, such as *HSPA1A/B*, *Rel* and *IRF8* are responsible for maintenance of microglial homeostasis, core microglial signatures and stress responses (Galatro et al., 2017; Gosselin et al., 2017; Olah et al., 2020), consistent with their differential expression after IL-6 stimulation. The observed overlap with up-regulated SZ gene sets, particularly with *HSPA1A/B* and *NFKB2* overlap genes (Supplementary Table 20), suggests a link between IL-6 exposure, microglial signature pathways and SZ pathogenesis consistent with *post-mortem* gene expression data in brain tissue from individuals with SZ (Murphy et al., 2021; Volk et al., 2019). Importantly, microglial genes are also reported to be down-regulated in both RNAseq and qPCR studies of human cortical *post-mortem* brain tissue from individuals with SZ (Gandal et al., 2018; Snijders et al., 2021). Taking an example directly relevant to our study, *IRF8* expression is down-regulated in *post-mortem* human cortical brain tissue from individuals with SZ (Gandal et al., 2018; Snijders et al., 2021). In contrast to these data, we observed an increase of *IRF8* expression after 3hr acute IL-6 exposure, accompanied by increased cytoplasmic motility and time-dependent increases in chemokines and cytokines, findings consistent with the documented role of IRF8 in enabling microglia to adopt a pro-inflammatory gene signature in disease (Ransohoff and Engelhardt, 2012). In contrast, Ormel and colleagues used PBMCs trans-differentiated to induced microglia (iM) to identify two clusters of iM cells using mass cytometry, that were enriched only in donors with a diagnosis of SZ (Ormel et al., 2020). Of these, one cluster was characterized by elevated protein levels of CD68, Cx3cr1, HLA-DR, P2RY12, TGF-β1 and importantly, IRF-8 (Ormel et al., 2020). These data illustrate the possibility of confounding factors in the interpretation of microglial gene expression changes in *post-mortem* brain tissue from individuals with schizophrenia, for example, prolonged antipsychotic exposure (Chan et al., 2011) plus the end-of-life effect after a long-term disease on tissue (Mccullumsmith et al., 2014). Further studies are therefore required to characterize how IL-6 impacts on specific microglia states of relevance to SZ via mass cytometry and/or single-cell sequencing approaches using both *post-mortem* brain tissue and hiPSC cellular models with appropriate functional assays.

Our observation that acute IL-6 stimulation is associated with up-regulation of the OXT receptor (*OXTR*) and it's overlap in the up-regulated SZ gene set (Gandal et al., 2018) (Supplementary Table 20), links with evidence that polymorphisms in the *OXTR* gene are linked to the pathogenesis of both SZ (Broniarczyk-Czarniak et al., 2022; Nakata et al., 2021), but also ASC (de Oliveira Pereira Ribeiro et al., 2018; Francis et al., 2016). Intriguingly, studies in rodent primary microglia suggest OXT suppresses inflammatory responses following LPS stimulation *in vitro* (Inoue et al., 2019). Furthermore, in mice, treatment with an OXTR agonist reduces perinatal brain damage by specifically acting on microglia (Mairesse et al., 2019). Further studies are therefore required to investigate the role of OXTR signaling in regulating MGL responses to IL-6 in our human model system, including studies in patient-derived cell lines.

Limitations of the current study should also be noted. As mentioned above, the response of each cell type presented here lies within the context of an acute IL-6 treatment in a monoculture, in the absence of a genetic background for a relevant psychiatric or neurodevelopmental disorder. In this context, birth cohort studies report the association between *average* IL-6 exposure across gestation, hence describing the impact of a cumulative exposure to IL-6 on brain and behavior phenotypes (Graham et al., 2018). Furthermore, we have previously reported differential effects of acute IFNγ exposure on gene expression in forebrain NPCs from individuals with or without a diagnosis of SZ (Bhat et al., 2022). It will therefore be important to investigate both chronic IL-6 exposure and include patient-derived hiPSC lines in future studies

to address these issues. Although, *in vitro* cultures are an artificial system, they are nonetheless a useful reductionist tool that permit the investigations of precise interactions between specific cell types, which is the rationale behind their use in this study. We acknowledge, however, the need for further studies using more complex 3D culture methods such as microglia-containing organoids to extend our observations herein (Zhang et al., 2022).

Gene expression results can vary significantly as a function of individual donors in hiPSC studies. As such, we acknowledge that the modest number of donors used in the present study (N = 3) may influence our ability to find statistically significant differences. For example, IL-10 expression in 3hr D1 MGLs is not statistically significant, but in fact has a fold change (~5-fold) higher than 3 h D14 MGLs (~3-fold). Therefore, although the results obtained in this study may not reach statistical significance, this does not necessarily mean an absence of biological significance, and vice versa. This is specifically important when discussing cases of receptor expression changes, such as *IL6R* and *IL6ST* expression in NPCs, which demonstrate robust fold change differences despite a lack of statistical significance (Fig. 1B: *IL6R* hiPSC vs D18 = 0.137 fold change, *IL6ST* hiPSC vs D18 = 6.50-fold change), and the effects of IL-6 treatment as mentioned previously. Replication studies with larger sample sizes will be required to confirm or disprove our findings. In addition, evidence from rodent models suggests functional, structural, and transcriptional sex-specific microglial differences (Guneykaya et al., 2018; Han et al., 2021; Villa et al., 2018). Our experiments were carried out using three individual clones per donor, from a total of N = 3 male donor lines, hence we cannot discount genotype- or sex-specific IL-6 responses by the select few donors chosen here. Our sample size is however consistent with existing studies of the impact of IL-6 on neurodevelopment using hiPSC models (Kathuria et al., 2022). Combined with unique differentiation and/or cytokine exposure protocols reported by different laboratories, there is substantial risk that the reproducibility and hence, validity of mechanistic data from hiPSC models will be compromised (McNeill et al., 2020). Replication of our results by multiple groups using common hiPSC reference lines (e.g. corrected KOLF92) will therefore be an important advance for this field (Volpato and Webber, 2020).

In conclusion, hiPSC-derived MGLs can respond to IL-6 via canonical IL6Ra signaling monoculture but monoculture NPCs cannot, due to their limited *IL6R* expression. The response of MGLs to IL-6 phenocopies molecular changes of relevance for SZ, consistent with the documented associations between IL-6 levels and risk for SZ (Khandaker et al., 2014; Perry et al., 2021; Schwieler et al., 2015). Our human model data also replicates key microglia findings from animal models of MIA, with relation to the microglial transcriptome of newborn pups from a PolyI:C MIA model (Matcovitch-Natan et al., 2016), IRF8-dependent microglia motility (d'Errico et al., 2021; Masuda et al., 2014) and maternal MIP-1α serum secretion (Brown et al., 2022; Osborne et al., 2019). Collectively, our data underline the importance of studying microglial cells to understand the influence of IL-6 on human neurodevelopment and to elucidate cellular and molecular mechanisms that link early life immune activation to increased risk for psychiatric disorders with a putative neurodevelopmental origin.

Declaration of Competing Interest

The authors declare that they have no known competing financial interests or personal relationships that could have appeared to influence the work reported in this paper.

Data availability

Data will be made available on request.

Acknowledgements

The authors acknowledge use of the research computing facility at King's College London, *Rosalind* (https://rosalind.kcl.ac.uk) and are thankful to George Chenell of the Wohl Cellular Imaging Centre at King's College London for technical support during live imaging. ACMC, DPS and ACV acknowledge financial support for this study from the National Centre for the Replacement, Refinement and Reduction of Animals in Research (NC/S001506/1). The work (at King's College, London) was also supported by the Medical Research Council (MRC) Centre grant (MR/N026063/1). AM, ACV and SK acknowledge support by the Neuro-Immune Interactions in Health & Disease Wellcome Trust PhD Training Programme (218452/Z/19/Z) at King's College London.

Appendix A. Supplementary data

Supplementary data to this article can be found online at https://doi.org/10.1016/j.bbi.2023.02.007.

References

Adhya, D., Swarup, V., Nagy, R., Dutan, L., Shum, C., Valencia-Alarcón, E.P., Jozwik, K. M., Mendez, M.A., Horder, J., Loth, E., Nowosiad, P., Lee, I., Skuse, D., Flinter, F.A., Murphy, D., McAlonan, G., Geschwind, D.H., Price, J., Carroll, J., Srivastava, D.P., Baron-Cohen, S., 2021. Atypical neurogenesis in induced pluripotent stem cells from autistic individuals. Biol. Psychiatry 89, 486–496. https://doi.org/10.1016/j.biopsych.2020.06.014.

Allswede, D.M., Yolken, R.H., Buka, S.L., Cannon, T.D., 2020. Cytokine concentrations throughout pregnancy and risk for psychosis in adult offspring: a longitudinal case-control study. Lancet Psychiatry 7, 254–261. https://doi.org/10.1016/S2215-0366(20)30006-7.

Antunes, G., Evans, S.A., Lordan, J.L., Frew, A.J., 2002. Systemic cytokine levels in community-acquired pneumonia and their association with disease severity. Eur. Respir. J. 20, 990–995. https://doi.org/10.1183/09031936.02.00295102.

Azuma, H., Moriyama, T., Ikeda, H., Oshima, M., Okuno, A., Sekiguchi, S., 2000. Analysis of soluble interleukin 6 receptor in cerebprospinal fluid in inflammatory and non-inflammatory conditions. Cytokine 12, 160–164. https://doi.org/10.1006/cyto.1999.0534.

Bayer, T.A., Falkai, P., Maier, W., 1999. Genetic and non-genetic vulnerability factors in schizophrenia: The basis of the "Two hit hypothesis". J. Psychiatr. Res. 33 https://doi.org/10.1016/S0022-3956(99)00039-4.

Bhat, A., Irizar, H., Couch, A., Raval, P., Duarte, R.R.R., Dutan Polit, L., Hanger, B., Powell, T., Michael Deans, P.J., Shum, C., Nagy, R., McAlonan, G., Iyegbe, C.O., Price, J., Bramon, E., Bhattacharyya, S., Vernon, A.C., Srivastava, D.P., 2022. Attenuated transcriptional response to pro-inflammatory cytokines in schizophrenia hiPSC-derived neural progenitor cells. Brain Behav. Immun. 105, 82–97. https://doi.org/10.1016/j.bbi.2022.06.010.

Borsini, A., Merrick, B., Edgeworth, J., Mandal, G., Srivastava, D.P., Vernon, A.C., Nebbia, G., Thuret, S., Pariante, C.M., 2022. Neurogenesis is disrupted in human hippocampal progenitor cells upon exposure to serum samples from hospitalized COVID-19 patients with neurological symptoms. Mol. Psychiatry 1–13. https://doi.org/10.1038/s41380-022-01741-1.

Broniarczyk-Czarniak, M., Szemraj, J., Śmigielski, J., Gałecki, P., 2022. The role of OXT, OXTR, AVP, and AVPR1a gene expression in the course of schizophrenia. Curr. Issues Mol. Biol. 44, 336–349. https://doi.org/10.3390/cimb44010025.

Brown, A.M., Conn, I., Boerrigter, D., Shannon Weickert, C., Purves-Tyson, T.D., 2022. Maternal immune activation with high molecular weight poly(I:C) in Wistar rats leads to elevated immune cell chemoattractants. J. Neuroimmunol. 364 https://doi.org/10.1016/j.jneuroim.2022.577813.

Campbell, I.L., Erta, M., Lim, S.L., Frausto, R., May, U., Rose-John, S., Scheller, J., Hidalgo, J., 2014. Trans-signaling is a dominant mechanism for the pathogenic actions of interleukin-6 in the brain. J. Neurosci. 34, 2503–2513. https://doi.org/10.1523/JNEUROSCI.2830-13.2014.

Careaga, M., Murai, T., Bauman, M.D., 2017. Maternal immune activation and autism spectrum disorder: from rodents to nonhuman and human primates. Biol. Psychiatry 81, 391–401. https://doi.org/10.1016/j.biopsych.2016.10.020.

Chan, M.K., Tsang, T.M., Harris, L.W., Guest, P.C., Holmes, E., Bahn, S., 2011. Evidence for disease and antipsychotic medication effects in post-mortem brain from schizophrenia patients. Mol. Psychiatry 16, 1189–1202. https://doi.org/10.1038/mp.2010.100.

Choi, G.B., Yim, Y.S., Wong, H., Kim, S., Kim, H., Kim, S.V., Hoeffer, C.A., Littman, D.R., Huh, J.R., 2016. The maternal interleukin-17a pathway in mice promotes autism-like phenotypes in offspring. Science 1979 (351), 933–939. https://doi.org/10.1126/science.aad0314.

Coomey, R., Stowell, R., Majewska, A., Tropea, D., 2020. The role of microglia in neurodevelopmental disorders and their therapeutics. Curr. Top. Med. Chem. 20, 272–276. https://doi.org/10.2174/1568026620666200221172619.

Couch, A.C.M., Berger, T., Hanger, B., Matuleviciute, R., Srivastava, D.P., Thuret, S., Vernon, A.C., 2021. Maternal immune activation primes deficiencies in adult

hippocampal neurogenesis. Brain Behav. Immun. 97, 410–422. https://doi.org/10.1016/J.BBI.2021.07.021.
d'Errico, P., Ziegler-Waldkirch, S., Aires, V., Hoffmann, P., Mezö, C., Erny, D., Monasor, L.S., Liebscher, S., Ravi, V.M., Joseph, K., Schnell, O., Kierdorf, K., Staszewski, O., Tahirovic, S., Prinz, M., Meyer-Luehmann, M., 2021. Microglia contribute to the propagation of Aβ into unaffected brain tissue. Nat. Neurosci. 1–6 https://doi.org/10.1038/s41593-021-00951-0.
Dawidowski, B., Górniak, A., Podwalski, P., Lebiecka, Z., Misiak, B., Samochowiec, J., 2021. The role of cytokines in the pathogenesis of schizophrenia. J. Clin. Med. 10 https://doi.org/10.3390/jcm10173849.
de Leeuw, C.A., Mooij, J.M., Heskes, T., Posthuma, D., 2015. MAGMA: generalized gene-set analysis of GWAS data. PLoS Comput. Biol. 11 https://doi.org/10.1371/journal.pcbi.1004219.
de Oliveira Pereira Ribeiro, L., Vargas-Pinilla, P., Kappel, D.B., Longo, D., Ranzan, J., Becker, M.M., dos Santos Riesgo, R., Schuler-Faccini, L., Roman, T., Schuch, J.B., 2018. Evidence for association between OXTR gene and ASD clinical phenotypes. J. Mol. Neurosci. 65, 213–221. https://doi.org/10.1007/s12031-018-1088-0.
Dobin, A., Davis, C.A., Schlesinger, F., Drenkow, J., Zaleski, C., Jha, S., Batut, P., Chaisson, M., Gingeras, T.R., 2013. STAR: Ultrafast universal RNA-seq aligner. Bioinformatics 29, 15–21. https://doi.org/10.1093/bioinformatics/bts635.
Estes, M.L., McAllister, A.K., 2016. Maternal immune activation: Implications for neuropsychiatric disorders. Science 1979 (353), 772–777. https://doi.org/10.1126/science.aag3194.
Fietz, S.A., Lachmann, R., Brandl, H., Kircher, M., Samusik, N., Schröer, R., Lakshmanaperumal, N., Henry, I., Vogt, J., Riehn, A., Distler, W., Nitsch, R., Enard, W., Paäbo, S., Huttner, W.B., 2012. Transcriptomes of germinal zones of human and mouse fetal neocortex suggest a role of extracellular matrix in progenitor self-renewal. Proc. Natl. Acad. Sci. U. S. A. 109, 11836–11841. https://doi.org/10.1073/pnas.1209647109.
Florio, M., Albert, M., Taverna, E., Namba, T., Brandl, H., Lewitus, E., Haffner, C., Sykes, A., Wong, F.K., Peters, J., Guhr, E., Klemroth, S., Prüfer, K., Kelso, J., Naumann, R., Nüsslein, I., Dahl, A., Lachmann, R., Pääbo, S., Huttner, W.B., 2015. Human-specific gene ARHGAP11B promotes basal progenitor amplification and neocortex expansion. Science (1979) 347, 1465–1470. https://doi.org/10.1126/science.aaa1975.
Francis, S.M., Kim, S.J., Kistner-Griffin, E., Guter, S., Cook, E.H., Jacob, S., 2016. ASD and genetic associations with receptors for oxytocin and vasopressin-AVPR1A, AVPR1B, and OXTR. Front. Neurosci. 10 https://doi.org/10.3389/fnins.2016.00516.
Galatro, T.F., Holtman, I.R., Lerario, A.M., Vainchtein, I.D., Brouwer, N., Sola, P.R., Veras, M.M., Pereira, T.F., Leite, R.E.P., Möller, T., Wes, P.D., Sogayar, M.C., Laman, J.D., den Dunnen, W., Pasqualucci, C.A., Oba-Shinjo, S.M., Boddeke, E.W.G. M., Marie, S.K.N., Eggen, B.J.L., 2017. Transcriptomic analysis of purified human cortical microglia reveals age-associated changes. Nat. Neurosci. 20, 1162–1171. https://doi.org/10.1038/nn.4597.
Gandal, M.J., Zhang, P., Hadjimichael, E., Walker, R.L., Chen, C., Liu, S., Won, H., van Bakel, H., Varghese, M., Wang, Y., Shieh, A.W., Haney, J., Parhami, S., Belmont, J., Kim, M., Losada, P.M., Khan, Z., Mleczko, J., Xia, Y., Dai, R., Wang, D., Yang, Y.T., Xu, M., Fish, K., Hof, P.R., Warrell, J., Fitzgerald, D., White, K., Jaffe, A.E., Peters, M. A., Gerstein, M., Liu, C., Iakoucheva, L.M., Pinto, D., Geschwind, D.H., 2018. Transcriptome-wide isoform-level dysregulation in ASD, schizophrenia, and bipolar disorder. Science (1979) 362. https://doi.org/10.1126/science.aat8127.
Garcia-Reitboeck, P., Phillips, A., Piers, T.M., Villegas-Llerena, C., Butler, M., Mallach, A., Rodrigues, C., Arber, C.E., Heslegrave, A., Zetterberg, H., Neumann, H., Neame, S., Houlden, H., Hardy, J., Pocock, J.M., 2018. Human induced pluripotent stem cell-derived microglia-like cells harboring TREM2 missense mutations show specific deficits in phagocytosis. Cell Rep. 24, 2300–2311. https://doi.org/10.1016/j.celrep.2018.07.094.
Gonzalez, D.M., Gregory, J., Brennand, K.J., 2017. The importance of non-neuronal cell types in hiPSC-based disease modeling and drug screening. Front. Cell Dev. Biol. https://doi.org/10.3389/fcell.2017.00117.
Gosselin, D., Skola, D., Coufal, N.G., Holtman, I.R., Schlachetzki, J.C.M., Sajti, E., Jaeger, B.N., O'Connor, C., Fitzpatrick, C., Pasillas, M.P., Pena, M., Adair, A., Gonda, D.D., Levy, M.L., Ransohoff, R.M., Gage, F.H., Glass, C.K., 2017. An environment-dependent transcriptional network specifies human microglia identity. Science (1979) 356, 1248–1259. https://doi.org/10.1126/science.aal3222.
Graham, A.M., Rasmussen, J.M., Rudolph, M.D., Heim, C.M., Gilmore, J.H., Styner, M., Potkin, S.G., Entringer, S., Wadhwa, P.D., Fair, D.A., Buss, C., 2018. Maternal systemic interleukin-6 during pregnancy is associated with newborn amygdala phenotypes and subsequent behavior at 2 years of age. Biol. Psychiatry 83, 109–119. https://doi.org/10.1016/j.biopsych.2017.05.027.
Grove, J., Ripke, S., Als, T.D., Mattheisen, M., Walters, R.K., Won, H., Pallesen, J., Agerbo, E., Andreassen, O.A., Anney, R., Awashti, S., Belliveau, R., Bettella, F., Buxbaum, J.D., Bybjerg-Grauholm, J., Bækvad-Hansen, M., Cerrato, F., Chambert, K., Christensen, J.H., Churchhouse, C., Dellenvall, K., Demontis, D., de Rubeis, S., Devlin, B., Djurovic, S., Dumont, A.L., Goldstein, J.I., Hansen, C.S., Hauberg, M.E., Hollegaard, M. v., Hope, S., Howrigan, D.P., Huang, H., Hultman, C.M., Klei, L., Maller, J., Martin, J., Martin, A.R., Moran, J.L., Nyegaard, M., Nærland, T., Palmer, D.S., Palotie, A., Pedersen, C.B., Pedersen, M.G., DPoterba, T., Poulsen, J.B., Pourcain, B.S., Qvist, P., Rehnström, K., Reichenberg, A., Reichert, J., Robinson, E. B., Roeder, K., Roussos, P., Saemundsen, E., Sandin, S., Satterstrom, F.K., Davey Smith, G., Stefansson, H., Steinberg, S., Stevens, C.R., Sullivan, P.F., Turley, P., Walters, G.B., Xu, X., Wray, N.R., Trzaskowski, M., Byrne, E.M., Abdellaoui, A., Adams, M.J., Air, T.M., Andlauer, T.F.M., Bacanu, S.A., Beekman, A.T.F., Bigdeli, T. B., Binder, E.B., Blackwood, D.H.R., Bryois, J., Buttenschøn, H.N., Cai, N., Castelao, E., Clarke, T.K., Coleman, J.R.I., Colodro-Conde, L., Couvy-Duchesne, B., Craddock, N., Crawford, G.E., Davies, G., Deary, I.J., Degenhardt, F., Derks, E.M., Direk, N., Dolan, C. v., Dunn, E.C., Eley, T.C., Escott-Price, V., Kiadeh, F.F.H., Finucane, H.K., Forstner, A.J., Frank, J., Gaspar, H.A., Gill, M., Goes, F.S., Gordon, S.D., Hall, L.S., Hansen, T.F., Herms, S., Hickie, I.B., Hoffmann, P., Homuth, G., Horn, C., Hottenga, J.J., Ising, M., Jansen, R., Jorgenson, E., Knowles, J.A., Kohane, I.S., Kraft, J., Kretzschmar, W.W., Krogh, J., Kutalik, Z., Li, Y., Lind, P.A., MacIntyre, D.J., MacKinnon, D.F., Maier, R.M., Maier, W., Marchini, J., Mbarek, H., McGrath, P., McGuffin, P., Medland, S.E., Mehta, D., Middeldorp, C.M., Mihailov, E., Milaneschi, Y., Milani, L., Mondimore, F.M., Montgomery, G.W., Mostafavi, S., Mullins, N., Nauck, M., Ng, B., Nivard, M.G., Nyholt, D.R., O'Reilly, P.F., Oskarsson, H., Owen, M.J., Painter, J.N., Peterson, R.E., Pettersson, E., Peyrot, W.J., Pistis, G., Posthuma, D., Quiroz, J.A., Rice, J.P., Riley, B.P., Rivera, M., Mirza, S.S., Schoevers, R., Schulte, E.C., Shen, L., Shi, J., Shyn, S.I., Sigurdsson, E., Sinnamon, G.C.B., Smit, J.H., Smith, D.J., Streit, F., Strohmaier, J., Tansey, K.E., Teismann, H., Teumer, A., Thompson, W., Thomson, P.A., Thorgeirsson, T.E., Traylor, M., Treutlein, J., Trubetskoy, V., Uitterlinden, A.G., Umbricht, D., van der Auwera, S., van Hemert, A.M., Viktorin, A., Visscher, P.M., Wang, Y., Webb, B.T., Weinsheimer, S.M., Wellmann, J., Willemsen, G., Witt, S.H., Wu, Y., Xi, H.S., Yang, J., Zhang, F., Arolt, V., Baune, B.T., Berger, K., Boomsma, D.I., Cichon, S., Dannlowski, U., de Geus, E.J.C., DePaulo, J.R., Domenici, E., Domschke, K., Esko, T., Grabe, H.J., Hamilton, S.P., Hayward, C., Heath, A.C., Kendler, K.S., Kloiber, S., Lewis, G., Li, Q.S., Lucae, S., Madden, P.A.F., Magnusson, P.K., Martin, N.G., McIntosh, A.M., Metspalu, A., Müller-Myhsok, B., Nöthen, M.M., O'Donovan, M.C., Paciga, S.A., Pedersen, N.L., Penninx, B.W.J.H., Perlis, R.H., Porteous, D.J., Potash, J.B., Preisig, M., Rietschel, M., Schaefer, C., Schulze, T.G., Smoller, J.W., Tiemeier, H., Uher, R., Völzke, H., Weissman, M.M., Lewis, C.M., Levinson, D.F., Breen, G., Agee, M., Alipanahi, B., Auton, A., Bell, R.K., Bryc, K., Elson, S.L., Fontanillas, P., Furlotte, N.A., Hromatka, B.S., Huber, K.E., Kleinman, A., Litterman, N.K., McIntyre, M.H., Mountain, J.L., Noblin, E.S., Northover, C.A.M., Pitts, S.J., Sathirapongsasuti, J.F., Sazonova, O. v., Shelton, J.F., Shringarpure, S., Tung, J.Y., Vacic, V., Wilson, C.H., Stefansson, K., Geschwind, D.H., Nordentoft, M., Hougaard, D.M., Werge, T., Mors, O., Mortensen, P.B., Neale, B.M., Daly, M.J., Børglum, A.D., 2019. Identification of common genetic risk variants for autism spectrum disorder. Nat. Genet. 51, 431–444. 10.1038/s41588-019-0344-8.
Haenseler, W., Sansom, S.N., Buchrieser, J., Newey, S.E., Moore, C.S., Nicholls, F.J., Chintawar, S., Schnell, C., Antel, J.P., Allen, N.D., Cader, M.Z., Wade-Martins, R., James, W.S., Cowley, S.A., 2017. A highly efficient human pluripotent stem cell microglia model displays a neuronal-co-culture-specific expression profile and inflammatory response. Stem Cell Rep. 8, 1727–1742. https://doi.org/10.1016/j.stemcr.2017.05.017.
Hanger, B., Couch, A., Rajendran, L., Srivastava, D.P., Vernon, A.C., 2020. Emerging developments in human induced pluripotent stem cell-derived microglia: implications for modelling psychiatric disorders with a neurodevelopmental origin. Front. Psychol. 11, 789. https://doi.org/10.3389/fpsyt.2020.00789.
Hans, V.H.J., Kossmann, T., Joller, H., Otto, V., Morganti-Kossmann, M.C., 1999. Interleukin-6 and its soluble receptor in serum and cerebrospinal fluid after cerebral trauma. NeuroReport 10, 409–412. https://doi.org/10.1097/00001756-199902050-00036.
Hsiao, E.Y., Patterson, P.H., 2011. Activation of the maternal immune system induces endocrine changes in the placenta via IL-6. Brain Behav. Immun. 25, 604–615. https://doi.org/10.1016/j.bbi.2010.12.017.
Inoue, T., Yamakage, H., Tanaka, M., Kusakabe, T., Shimatsu, A., Satoh-Asahara, N., 2019. Oxytocin suppresses inflammatory responses induced by lipopolysaccharide through inhibition of the eIF-2α–ATF4 pathway in mouse microglia. Cells 8. https://doi.org/10.3390/cells8060527.
Jao, J., Ciernia, A.V., 2021. MGEnrichment: A web application for microglia gene list enrichment analysis. PLoS Comput. Biol. 17, e1009160.
Kathuria, A., Lopez-Lengowski, K., Roffman, J.L., Karmacharya, R., 2022. Distinct effects of interleukin-6 and interferon-γ on differentiating human cortical neurons. Brain Behav. Immun. 103, 97–108. https://doi.org/10.1016/j.bbi.2022.04.007.
Kentner, A.C., Bilbo, S.D., Brown, A.S., Hsiao, E.Y., McAllister, A.K., Meyer, U., Pearce, B. D., Pletnikov, M.V., Yolken, R.H., Bauman, M.D., 2019. Maternal immune activation: reporting guidelines to improve the rigor, reproducibility, and transparency of the model. Neuropsychopharmacology 44, 245–258. https://doi.org/10.1038/s41386-018-0185-7.
Khandaker, G.M., Pearson, R.M., Zammit, S., Lewis, G., Jones, P.B., 2014. Association of serum interleukin 6 and C-reactive protein in childhood with depression and psychosis in young adult life a population-based longitudinal study. JAMA Psychiatry 71, 1121–1128. https://doi.org/10.1001/jamapsychiatry.2014.1332.
Krämer, A., Green, J., Pollard, J., Tugendreich, S., 2014. Causal analysis approaches in ingenuity pathway analysis. Bioinformatics 30, 523–530. https://doi.org/10.1093/bioinformatics/btt703.
Liao, Y., Smyth, G.K., Shi, W., 2014. FeatureCounts: An efficient general purpose program for assigning sequence reads to genomic features. Bioinformatics 30, 923–930. https://doi.org/10.1093/bioinformatics/btt656.
Liao, Y., Smyth, G.K., Shi, W., 2019a. The R package Rsubread is easier, faster, cheaper and better for alignment and quantification of RNA sequencing reads. Nucleic Acids Res. 47, e47.
Liao, Y., Wang, J., Jaehnig, E.J., Shi, Z., Zhang, B., 2019b. WebGestalt 2019: gene set analysis toolkit with revamped UIs and APIs. Nucleic Acids Res. 47, W199–W205. https://doi.org/10.1093/nar/gkz401.
Livak, K.J., Schmittgen, T.D., 2001 Dec. Analysis of relative gene expression data using real-time quantitative PCR and the 2(-Delta Delta C(T)) Method. Methods 25 (4), 402 – 8 . doi: 10.1006/meth.2001.1262.
Love, M.I., Huber, W., Anders, S., 2014. Moderated estimation of fold change and dispersion for RNA-seq data with DESeq2. Genome Biol. 15, 1–21. https://doi.org/10.1186/s13059-014-0550-8.

Lu, Y.R., Rao, Y.B., Mou, Y.J., Chen, Y., Lou, H.F., Zhang, Y., Zhang, D.X., Xie, H.Y., Hu, L.W., Fang, P., 2019. High concentrations of serum interleukin-6 and interleukin-8 in patients with bipolar disorder. Medicine (United States) 98. https://doi.org/10.1097/MD.0000000000014419.

Lydholm, C.N., Köhler-Forsberg, O., Nordentoft, M., Yolken, R.H., Mortensen, P.B., Petersen, L., Benros, M.E., 2019. Parental infections before, during, and after pregnancy as risk factors for mental disorders in childhood and adolescence: A Nationwide Danish Study. Biol. Psychiatry 85, 317–325. https://doi.org/10.1016/j.biopsych.2018.09.013.

Mairesse, J., Zinni, M., Pansiot, J., Hassan-Abdi, R., Demene, C., Colella, M., Charriaut-Marlangue, C., Rideau Batista Novais, A., Tanter, M., Maccari, S., Gressens, P., Vaiman, D., Soussi-Yanicostas, N., Baud, O., 2019. Oxytocin receptor agonist reduces perinatal brain damage by targeting microglia. Glia 67, 345–359. https://doi.org/10.1002/glia.23546.

Masuda, T., Nishimoto, N., Tomiyama, D., Matsuda, T., Tozaki-Saitoh, H., Tamura, T., Kohsaka, S., Tsuda, M., Inoue, K., 2014. IRF8 is a transcriptional determinant for microglial motility. Purinergic Signal 10, 515–521. https://doi.org/10.1007/s11302-014-9413-8.

Matcovitch-Natan, O., Winter, D.R., Giladi, A., Aguilar, S.V., Spinrad, A., Sarrazin, S., Ben-Yehuda, H., David, E., González, F.Z., Perrin, P., Keren-Shaul, H., Gury, M., Lara-Astaiso, D., Thaiss, C.A., Cohen, M., Halpern, K.B., Baruch, K., Deczkowska, A., Lorenzo-Vivas, E., Itzkovitz, S., Elinav, E., Sieweke, M.H., Schwartz, M., Amit, I., 2016. Microglia development follows a stepwise program to regulate brain homeostasis. Science (1979). 10.1126/science.aad8670.

Matelski, L., Morgan, R.K., Grodzki, A.C., van de Water, J., Lein, P.J., 2021. Effects of cytokines on nuclear factor-kappa B, cell viability, and synaptic connectivity in a human neuronal cell line. Mol. Psychiatry 26, 875–887. https://doi.org/10.1038/s41380-020-0647-2.

Mccullumsmith, R.E., Hammond, J.H., Shan, D., Meador-Woodruff, J.H., 2014. Postmortem brain: An underutilized substrate for studying severe mental illness. Neuropsychopharmacology 39, 65–87. https://doi.org/10.1038/npp.2013.239.

McNeill, R.V., Ziegler, G.C., Radtke, F., Nieberler, M., Lesch, K.P., Kittel-Schneider, S., 2020. Mental health dished up—the use of iPSC models in neuropsychiatric research. J. Neural Transm. https://doi.org/10.1007/s00702-020-02197-9.

Meyer, U., 2014. Prenatal Poly(I:C) exposure and other developmental immune activation models in rodent systems. Biol. Psychiatry 75, 307–315. https://doi.org/10.1016/j.biopsych.2013.07.011.

Meyer, U., 2019. Neurodevelopmental resilience and susceptibility to maternal immune activation. Trends Neurosci. 42, 793–806. https://doi.org/10.1016/j.tins.2019.08.001.

Michalopoulou, M., Nikolaou, C., Tavernarakis, A., Alexandri, N.M., Rentzos, M., Chatzipanagiotou, S., Cambouri, C., Vassilopoulos, D., 2004. Soluble interleukin-6 receptor (sIL-6R) in cerebrospinal fluid of patients with inflammatory and non inflammatory neurological diseases. Immunol. Lett. 94, 183–189. https://doi.org/10.1016/j.imlet.2004.04.018.

Miller, J.A., Ding, S.L., Sunkin, S.M., Smith, K.A., Ng, L., Szafer, A., Ebbert, A., Riley, Z.L., Royall, J.J., Aiona, K., Arnold, J.M., Bennet, C., Bertagnolli, D., Brouner, K., Butler, S., Caldejon, S., Carey, A., Cuhaciyan, C., Dalley, R.A., Dee, N., Dolbeare, T. A., Facer, B.A.C., Feng, D., Fliss, T.P., Gee, G., Goldy, J., Gourley, L., Gregor, B.W., Gu, G., Howard, R.E., Jochim, J.M., Kuan, C.L., Lau, C., Lee, C.K., Lee, F., Lemon, T. A., Lesnar, P., McMurray, B., Mastan, N., Mosqueda, N., Naluai-Cecchini, T., Ngo, N. K., Nyhus, J., Oldre, A., Olson, E., Parente, J., Parker, P.D., Parry, S.E., Stevens, A., Pletikos, M., Reding, M., Roll, K., Sandman, D., Sarreal, M., Shapouri, S., Shapovalova, N.V., Shen, E.H., Sjoquist, N., Slaughterbeck, C.R., Smith, M., Sodt, A. J., Williams, D., Zöllei, L., Fischl, B., Gerstein, M.B., Geschwind, D.H., Glass, I.A., Hawrylycz, M.J., Hevner, R.F., Huang, H., Jones, A.R., Knowles, J.A., Levitt, P., Phillips, J.W., Šestan, N., Wohnoutka, P., Dang, C., Bernard, A., Hohmann, J.G., Lein, E.S., 2014. Transcriptional landscape of the prenatal human brain. Nature 508, 199–206. https://doi.org/10.1038/nature13185.

Mirabella, F., Desiato, G., Mancinelli, S., Fossati, G., Rasile, M., Morini, R., Markicevic, M., Grimm, C., Amegandjin, C., Termanini, A., Peano, C., Kunderfranco, P., di Cristo, G., Zerbi, V., Menna, E., Lodato, S., Matteoli, M., Pozzi, D., 2021. Prenatal interleukin 6 elevation increases glutamatergic synapse density and disrupts hippocampal connectivity in offspring. Immunity 54, 2611–2631.e8. https://doi.org/10.1016/j.immuni.2021.10.006.

Mondelli, V., Vernon, A.C., Turkheimer, F., Dazzan, P., Pariante, C.M., 2017. Brain microglia in psychiatric disorders. Lancet Psychiatry 4, 563–572. https://doi.org/10.1016/S2215-0366(17)30101-3.

Morris, G., Fernandes, B.S., Puri, B.K., Walker, A.J., Carvalho, A.F., Berk, M., 2018. Leaky brain in neurological and psychiatric disorders: Drivers and consequences. Aust. N. Z. J. Psychiatry 52, 924–948. https://doi.org/10.1177/0004867418796955.

Mueller, F.S., Scarborough, J., Schalbetter, S.M., Richetto, J., Kim, E., Couch, A., Yee, Y., Lerch, J.P., Vernon, A.C., Weber-Stadlbauer, U., Meyer, U., Richetto, Juliet, Kim, E., Couch, A., Yee, Y., Lerch, J.P., Anthony, Vernon, C., Weber-Stadlbauer, U., Meyer, U., 2021. Behavioral, neuroanatomical, and molecular correlates of resilience and susceptibility to maternal immune activation. Mol. Psychiatry 26, 396–410. 10.1038/s41380-020-00952-8.

Mueller, F.S., Richetto, J., Hayes, L.N., Zambon, A., Pollak, D.D., Sawa, A., Meyer, U., Weber-Stadlbauer, U., 2019. Influence of poly(I:C) variability on thermoregulation, immune responses and pregnancy outcomes in mouse models of maternal immune activation. Brain Behav. Immun. 80, 406–418. https://doi.org/10.1016/j.bbi.2019.04.019.

Muffat, J., Li, Y., Omer, A., Durbin, A., Bosch, I., Bakiasi, G., Richards, E., Meyer, A., Gehrke, L., Jaenisch, R., 2018. Human induced pluripotent stem cell-derived glial cells and neural progenitors display divergent responses to Zika and dengue infections. Proc. Natl. Acad. Sci. U. S. A. 115, 7117–7122. https://doi.org/10.1073/pnas.1719266115.

Mullins, N., Forstner, A.J., O'Connell, K.S., Coombes, B., Coleman, J.R.I., Qiao, Z., Als, T. D., Bigdeli, T.B., Børte, S., Bryois, J., Charney, A.W., Drange, O.K., Gandal, M.J., Hagenaars, S.P., Ikeda, M., Kamitaki, N., Kim, M., Krebs, K., Panagiotaropoulou, G., Schilder, B.M., Sloofman, L.G., Steinberg, S., Trubetskoy, V., Winsvold, B.S., Won, H. H., Abramova, L., Adorjan, K., Agerbo, E., al Eissa, M., Albani, D., Alliey-Rodriguez, N., Anjorin, A., Antilla, V., Antoniou, A., Awasthi, S., Baek, J.H., Bækvad-Hansen, M., Bass, N., Bauer, M., Beins, E.C., Bergen, S.E., Birner, A., Bøcker Pedersen, C., Bøen, E., Boks, M.P., Bosch, R., Brum, M., Brumpton, B.M., Brunkhorst-Kanaan, N., Budde, M., Bybjerg-Grauholm, J., Byerley, W., Cairns, M., Casas, M., Cervantes, P., Clarke, T.K., Cruceanu, C., Cuellar-Barboza, A., Cunningham, J., Curtis, D., Czerski, P.M., Dale, A.M., Dalkner, N., David, F.S., Degenhardt, F., Djurovic, S., Dobbyn, A.L., Douzenis, A., Elvsåshagen, T., Escott-Price, V., Ferrier, I.N., Fiorentino, A., Foroud, T.M., Forty, L., Frank, J., Frei, O., Freimer, N.B., Frisén, L., Gade, K., Garnham, J., Gelernter, J., Giørtz Pedersen, M., Gizer, I.R., Gordon, S.D., Gordon-Smith, K., Greenwood, T.A., Grove, J., Guzman-Parra, J., Ha, K., Haraldsson, M., Hautzinger, M., Heilbronner, U., Hellgren, D., Herms, S., Hoffmann, P., Holmans, P.A., Huckins, L., Jamain, S., Johnson, J.S., Kalman, J.L., Kamatani, Y., Kennedy, J.L., Kittel-Schneider, S., Knowles, J.A., Kogevinas, M., Koromina, M., Kranz, T.M., Kranzler, H. R., Kubo, M., Kupka, R., Kushner, S.A., Lavebratt, C., Lawrence, J., Leber, M., Lee, H. J., Lee, P.H., Levy, S.E., Lewis, C., Liao, C., Lucae, S., Lundberg, M., MacIntyre, D.J., Magnusson, S.H., Maier, W., Maihofer, A., Malaspina, D., Maratou, E., Martinsson, L., Mattheisen, M., McCarroll, S.A., McGregor, N.W., McGuffin, P., McKay, J.D., Medeiros, H., Medland, S.E., Millischer, V., Montgomery, G.W., Moran, J.L., Morris, D.W., Mühleisen, T.W., O'Brien, N., O'Donovan, C., Olde Loohuis, L.M., Oruc, L., Papiol, S., Pardiñas, A.F., Perry, A., Pfennig, A., Porichi, E., Potash, J.B., Quested, D., Raj, T., Rapaport, M.H., DePaulo, J.R., Regeer, E.J., Rice, J.P., Rivas, F., Rivera, M., Roth, J., Roussos, P., Ruderfer, D.M., Sánchez-Mora, C., Schulte, E.C., Senner, F., Sharp, S., Shilling, P.D., Sigurdsson, E., Sirignano, L., Slaney, C., Smeland, O.B., Smith, D.J., Sobell, J.L., Søholm Hansen, C., Soler Artigas, M., Spijker, A.T., Stein, D. J., Strauss, J.S., Świątkowska, B., Terao, C., Thorgeirsson, T.E., Toma, C., Tooney, P., Tsermpini, E.E., Vawter, M.P., Vedder, H., Walters, J.T.R., Witt, S.H., Xi, S., Xu, W., Yang, J.M.K., Young, A.H., Young, H., Zandi, P.P., Zhou, H., Zillich, L., Adolfsson, R., Agartz, I., Alda, M., Alfredsson, L., Babadjanova, G., Backlund, L., Baune, B.T., Bellivier, F., Bengesser, S., Berrettini, W.H., Blackwood, D.H.R., Boehnke, M., Børglum, A.D., Breen, G., Carr, V.J., Catts, S., Corvin, A., Craddock, N., Dannlowski, U., Dikeos, D., Esko, T., Etain, B., Ferentinos, P., Frye, M., Fullerton, J.M., Gawlik, M., Gershon, E.S., Goes, F.S., Green, M.J., Grigoroiu-Serbanescu, M., Hauser, J., Henskens, F., Hillert, J., Hong, K.S., Hougaard, D.M., Hultman, C.M., Hveem, K., Iwata, N., Jablensky, A. v., Jones, I., Jones, L.A., Kahn, R.S., Kelsoe, J.R., Kirov, G., Landén, M., Leboyer, M., Lewis, C.M., Li, Q.S., Lissowska, J., Lochner, C., Loughland, C., Martin, N.G., Mathews, C.A., Mayoral, F., McElroy, S.L., McIntosh, A.M., McMahon, F.J., Melle, I., Michie, P., Milani, L., Mitchell, P.B., Morken, G., Mors, O., Mortensen, P.B., Mowry, B., Müller-Myhsok, B., Myers, R.M., Neale, B.M., Nievergelt, C.M., Nordentoft, M., Nöthen, M.M., O'Donovan, M.C., Oedegaard, K.J., Olsson, T., Owen, M.J., Paciga, S.A., Pantelis, C., Pato, C., Pato, M.T., Patrinos, G.P., Perlis, R.H., Posthuma, D., Ramos-Quiroga, J.A., Reif, A., Reininghaus, E.Z., Ribasés, M., Rietschel, M., Ripke, S., Rouleau, G.A., Saito, T., Schall, U., Schalling, M., Schofield, P.R., Schulze, T.G., Scott, L.J., Scott, R.J., Serretti, A., Shannon Weickert, C., Smoller, J.W., Stefansson, H., Stefansson, K., Stordal, E., Streit, F., Sullivan, P.F., Turecki, G., Vaaler, A.E., Vieta, E., Vincent, J.B., Waldman, I.D., Weickert, T.W., Werge, T., Wray, N.R., Zwart, J.A., Biernacka, J.M., Nurnberger, J.I., Cichon, S., Edenberg, H.J., Stahl, E.A., McQuillin, A., di Florio, A., Ophoff, R.A., Andreassen, O. A., 2021. Genome-wide association study of more than 40,000 bipolar disorder cases provides new insights into the underlying biology. Nat Genet 53. 10.1038/s41588-021-00857-4.

Murphy, C.E., Walker, A.K., Weickert, C.S., 2021. Neuroinflammation in schizophrenia: the role of nuclear factor kappa B. Transl. Psychiatry. https://doi.org/10.1038/s41398-021-01607-0.

Nakata, Y., Kanahara, N., Kimura, A., Niitsu, T., Komatsu, H., Oda, Y., Nakamura, M., Ishikawa, M., Hasegawa, T., Kamata, Y., Yamauchi, A., Inazumi, K., Kimura, H., Shiko, Y., Kawasaki, Y., Iyo, M., 2021. Oxytocin system dysfunction in patients with treatment-resistant schizophrenia: Alterations of blood oxytocin levels and effect of a genetic variant of OXTR. J. Psychiatr. Res. 138, 219–227. https://doi.org/10.1016/j.jpsychires.2021.03.053.

Olah, M., Menon, V., Habib, N., Taga, M.F., Ma, Y., Yung, C.J., Cimpean, M., Khairallah, A., Coronas-Samano, G., Sankowski, R., Grün, D., Kroshilina, A.A., Dionne, D., Sarkis, R.A., Cosgrove, G.R., Helgager, J., Golden, J.A., Pennell, P.B., Prinz, M., Vonsattel, J.P.G., Teich, A.F., Schneider, J.A., Bennett, D.A., Regev, A., Elyaman, W., Bradshaw, E.M., de Jager, P.L., 2020. Single cell RNA sequencing of human microglia uncovers a subset associated with Alzheimer's disease. Nat. Commun. 11, 1–18. https://doi.org/10.1038/s41467-020-19737-2.

Ormel, P.R., Böttcher, C., Gigase, F.A.J., Missall, R.D., van Zuiden, W., Fernández Zapata, M.C., Ilhan, D., de Goeij, M., Udine, E., Sommer, I.E.C., Priller, J., Raj, T., Kahn, R.S., Hol, E.M., de Witte, L.D., 2020. A characterization of the molecular phenotype and inflammatory response of schizophrenia patient-derived microglia-like cells. Brain Behav. Immun. 90, 196–207. https://doi.org/10.1016/j.bbi.2020.08.012.

Osborne, B.F., Turano, A., Caulfield, J.I., Schwarz, J.M., 2019. Sex- and region-specific differences in microglia phenotype and characterization of the peripheral immune response following early-life infection in neonatal male and female rats. Neurosci. Lett. 692, 1–9. https://doi.org/10.1016/j.neulet.2018.10.044.

Ozaki, K., Kato, D., Ikegami, A., Hashimoto, A., Sugio, S., Guo, Z., Shibushita, M., Tatematsu, T., Haruwaka, K., Moorhouse, A.J., Yamada, H., Wake, H., 2020.

Maternal immune activation induces sustained changes in fetal microglia motility. Sci. Rep. 10, 1–19. https://doi.org/10.1038/s41598-020-78294-2.
Paolicelli, R.C., Bolasco, G., Pagani, F., Maggi, L., Scianni, M., Panzanelli, P., Giustetto, M., Ferreira, T.A., Guiducci, E., Dumas, L., Ragozzino, D., Gross, C.T., 2011. Synaptic pruning by microglia is necessary for normal brain development. Science (1979) 333, 1456–1458. https://doi.org/10.1126/science.1202529.
Park, G.H., Noh, H., Shao, Z., Ni, P., Qin, Y., Liu, D., Beaudreault, C.P., Park, J.S., Abani, C.P., Park, J.M., Le, D.T., Gonzalez, S.Z., Guan, Y., Cohen, B.M., McPhie, D.L., Coyle, J.T., Lanz, T.A., Xi, H.S., Yin, C., Huang, W., Kim, H.Y., Chung, S., 2020. Activated microglia cause metabolic disruptions in developmental cortical interneurons that persist in interneurons from individuals with schizophrenia. Nat. Neurosci. 23, 1352–1364. https://doi.org/10.1038/s41593-020-00724-1.
Perry, B.I., Upthegrove, R., Kappelmann, N., Jones, P.B., Burgess, S., Khandaker, G.M., 2021. Associations of immunological proteins/traits with schizophrenia, major depression and bipolar disorder: A bi-directional two-sample Mendelian randomization study. Brain Behav. Immun. 97, 176–185. https://doi.org/10.1016/j.bbi.2021.07.009.
Potter, H.G., Kowash, H.M., Woods, R.M., Revill, G., Grime, A., Deeney, B., Burgess, M. A., Aarons, T., Glazier, J.D., Neill, J.C., Hager, R., 2023. Maternal behaviours and adult offspring behavioural deficits are predicted by maternal TNFα concentration in a rat model of neurodevelopmental disorders. Brain Behav. Immun. 108, 162–175. https://doi.org/10.1016/J.BBI.2022.12.003.
Przanowski, P., Dabrowski, M., Ellert-Miklaszewska, A., Kloss, M., Mieczkowski, J., Kaza, B., Ronowicz, A., Hu, F., Piotrowski, A., Kettenmann, H., Komorowski, J., Kaminska, B., 2014. The signal transducers Stat1 and Stat3 and their novel target Jmjd3 drive the expression of inflammatory genes in microglia. J. Mol. Med. 92, 239–254. https://doi.org/10.1007/s00109-013-1090-5.
Purves-Tyson, T.D., Robinson, K., Brown, A.M., Boerrigter, D., Cai, H.Q., Weissleder, C., Owens, S.J., Rothmond, D.A., Shannon Weickert, C., 2020. Increased macrophages and C1qA, C3, C4 transcripts in the midbrain of people with schizophrenia. Front. Immunol. 11 https://doi.org/10.3389/fimmu.2020.02002.
Purves-Tyson, T.D., Weber-Stadlbauer, U., Richetto, J., Rothmond, D.A., Labouesse, M. A., Polesel, M., Robinson, K., Shannon Weickert, C., Meyer, U., 2021. Increased levels of midbrain immune-related transcripts in schizophrenia and in murine offspring after maternal immune activation. Mol. Psychiatry 26, 849–863. https://doi.org/10.1038/s41380-019-0434-0.
R Core Team, 2020. R: A Language and Environment for Statistical.
Ransohoff, R.M., Engelhardt, B., 2012. The anatomical and cellular basis of immune surveillance in the central nervous system. Nat. Rev. Immunol. 12, 623–635. https://doi.org/10.1038/nri3265.
Rasmussen, J.M., Graham, A.M., Entringer, S., Gilmore, J.H., Styner, M., Fair, D.A., Wadhwa, P.D., Buss, C., 2019. Maternal Interleukin-6 concentration during pregnancy is associated with variation in frontolimbic white matter and cognitive development in early life. Neuroimage 185, 825–835. https://doi.org/10.1016/j.neuroimage.2018.04.020.
Rasmussen, J.M., Graham, A.M., Gyllenhammer, L.E., Entringer, S., Chow, D.S., O'Connor, T.G., Fair, D.A., Wadhwa, P.D., Buss, C., 2021. Neuroanatomical correlates underlying the association between maternal interleukin 6 concentration during pregnancy and offspring fluid reasoning performance in early childhood. Biol. Psychiatry Cogn. Neurosci. Neuroimaging. https://doi.org/10.1016/j.bpsc.2021.03.007.
Ritchie, L., Tate, R., Chamberlain, L.H., Robertson, G., Zagnoni, M., Sposito, T., Wray, S., Wright, J.A., Bryant, C.E., Gay, N.J., Bushell, T.J., 2018. Toll-like receptor 3 activation impairs excitability and synaptic activity via TRIF signalling in immature rat and human neurons. Neuropharmacology 135, 1–10. https://doi.org/10.1016/j.neuropharm.2018.02.025.
Rudolph, M.D., Graham, A.M., Feczko, E., Miranda-Dominguez, O., Rasmussen, J.M., Nardos, R., Entringer, S., Wadhwa, P.D., Buss, C., Fair, D.A., 2018. Maternal IL-6 during pregnancy can be estimated from newborn brain connectivity and predicts future working memory in offspring. Nat. Neurosci. 21, 765–772. https://doi.org/10.1038/s41593-018-0128-y.
Russo, F.B., Freitas, B.C., Pignatari, G.C., Fernandes, I.R., Sebat, J., Muotri, A.R., Beltrão-Braga, P.C.B., 2018. Modeling the interplay between neurons and astrocytes in autism using human induced pluripotent stem cells. Biol. Psychiatry 83, 569–578. https://doi.org/10.1016/j.biopsych.2017.09.021.
Sasayama, D., Hattori, K., Wakabayashi, C., Teraishi, T., Hori, H., Ota, M., Yoshida, S., Arima, K., Higuchi, T., Amano, N., Kunugi, H., 2013. Increased cerebrospinal fluid interleukin-6 levels in patients with schizophrenia and those with major depressive disorder. J. Psychiatry Res. 47, 401–406. https://doi.org/10.1016/j.jpsychires.2012.12.001.
Schwieler, L., Larsson, M.K., Skogh, E., Kegel, M.E., Orhan, F., Abdelmoaty, S., Finn, A., Bhat, M., Samuelsson, M., Lundberg, K., Dahl, M.L., Sellgren, C., Schuppe-Koistinen, I., Svensson, C.I., Erhardt, S., Engberg, G., 2015. Increased levels of IL-6 in the cerebrospinal fluid of patients with chronic schizophrenia - Significance for activation of the kynurenine pathway. J. Psychiatry Neurosci. 40, 126–133. https://doi.org/10.1503/jpn.140126.
Shen, L., 2021. GeneOverlap: Test and Visualize Gene Overlaps. R Package Version 1 (30).
Shi, Y., Kirwan, P., Livesey, F.J., 2012. Directed differentiation of human pluripotent stem cells to cerebral cortex neurons and neural networks. Nat. Protoc. 7, 1836–1846. https://doi.org/10.1038/nprot.2012.116.
Smith, S.E.P., Li, J., Garbett, K., Mirnics, K., Patterson, P.H., 2007. Maternal immune activation alters fetal brain development through interleukin-6. J. Neurosci. 27, 10695–10702. https://doi.org/10.1523/JNEUROSCI.2178-07.2007.
Smolders, S., Notter, T., Smolders, S.M.T., Rigo, J.M., Brône, B., 2018. Controversies and prospects about microglia in maternal immune activation models for neurodevelopmental disorders. Brain Behav. Immun. 73, 51–65. https://doi.org/10.1016/j.bbi.2018.06.001.
Snijders, G.J.L.J., van Zuiden, W., Sneeboer, M.A.M., Berdenis van Berlekom, A., van der Geest, A.T., Schnieder, T., MacIntyre, D.J., Hol, E.M., Kahn, R.S., de Witte, L.D., 2021. A loss of mature microglial markers without immune activation in schizophrenia. Glia 69, 1251–1267. https://doi.org/10.1002/glia.23962.
Tamura, T., Ozato, K., 2002. ICSBP/IRF-8: Its regulatory roles in the development of myeloid cells. J. Interferon Cytokine Res. 22, 145–152. https://doi.org/10.1089/107999002753452755.
Trubetskoy, V., Pardiñas, A.F., Qi, T., Panagiotaropoulou, G., Awasthi, S., Bigdeli, T.B., Bryois, J., Chen, C.Y., Dennison, C.A., Hall, L.S., Lam, M., Watanabe, K., Frei, O., Ge, T., Harwood, J.C., Koopmans, F., Magnusson, S., Richards, A.L., Sidorenko, J., Wu, Y., Zeng, J., Grove, J., Kim, M., Li, Z., Voloudakis, G., Zhang, W., Adams, M., Agartz, I., Atkinson, E.G., Agerbo, E., al Eissa, M., Albus, M., Alexander, M., Alizadeh, B.Z., Alptekin, K., Als, T.D., Amin, F., Arolt, V., Arrojo, M., Athanasiu, L., Azevedo, M.H., Bacanu, S.A., Bass, N.J., Begemann, M., Belliveau, R.A., Bene, J., Benyamin, B., Bergen, S.E., Blasi, G., Bobes, J., Bonassi, S., Braun, A., Bressan, R.A., Bromet, E.J., Bruggeman, R., Buckley, P.F., Buckner, R.L., Bybjerg-Grauholm, J., Cahn, W., Cairns, M.J., Calkins, M.E., Carr, V.J., Castle, D., Catts, S. v., Chambert, K.D., Chan, R.C.K., Chaumette, B., Cheng, W., Cheung, E.F.C., Chong, S.A., Cohen, D., Consoli, A., Cordeiro, Q., Costas, J., Curtis, C., Davidson, M., Davis, K.L., de Haan, L., Degenhardt, F., DeLisi, L.E., Demontis, D., Dickerson, F., Dikeos, D., Dinan, T., Djurovic, S., Duan, J., Ducci, G., Dudbridge, F., Eriksson, J.G., Fañanás, L., Faraone, S. v., Fiorentino, A., Forstner, A., Frank, J., Freimer, N.B., Fromer, M., Frustaci, A., Gadelha, A., Genovese, G., Gershon, E.S., Giannitelli, M., Giegling, I., Giusti-Rodríguez, P., Godard, S., Goldstein, J.I., González Peñas, J., González-Pinto, A., Gopal, S., Gratten, J., Green, M.F., Greenwood, T.A., Guillin, O., Gülöksüz, S., Gur, R. E., Gur, R.C., Gutiérrez, B., Hahn, E., Hakonarson, H., Haroutunian, V., Hartmann, A. M., Harvey, C., Hayward, C., Henskens, F.A., Herms, S., Hoffmann, P., Howrigan, D. P., Ikeda, M., Iyegbe, C., Joa, I., Julià, A., Kähler, A.K., Kam-Thong, T., Kamatani, Y., Karachanak-Yankova, S., Kebir, O., Keller, M.C., Kelly, B.J., Khrunin, A., Kim, S.W., Klovins, J., Kondratiev, N., Konte, B., Kraft, J., Kubo, M., Kučinskas, V., Kučinskiene, Z.A., Kusumawardhani, A., Kuzelova-Ptackova, H., Landi, S., Lazzeroni, L.C., Lee, P. H., Legge, S.E., Lehrer, D.S., Lencer, R., Lerer, B., Li, Miaoxin, Lieberman, J., Light, G.A., Limborska, S., Liu, C.M., Lönnqvist, J., Loughland, C.M., Lubinski, J., Luykx, J. J., Lynham, A., Macek, M., Mackinnon, A., Magnusson, P.K.E., Maher, B.S., Maier, W., Malaspina, D., Mallet, J., Marder, S.R., Marsal, S., Martin, A.R., Martorell, L., Mattheisen, M., McCarley, R.W., McDonald, C., McGrath, J.J., Medeiros, H., Meier, S., Melegh, B., Melle, I., Mesholam-Gately, R.I., Metspalu, A., Michie, P.T., Milani, L., Milanova, V., Mitjans, M., Molden, E., Molina, E., Molto, M.D., Mondelli, V., Moreno, C., Morley, C.P., Muntané, G., Murphy, K.C., Myin-Germeys, I., Nenadić, I., Nestadt, G., Nikitina-Zake, L., Noto, C., Nuechterlein, K.H., O'Brien, N.L., O'Neill, F.A., Oh, S. Y., Olincy, A., Ota, V.K., Pantelis, C., Papadimitriou, G.N., Parellada, M., Paunio, T., Pellegrino, R., Periyasamy, S., Perkins, D.O., Pfuhlmann, B., Pietiläinen, O., Pimm, J., Porteous, D., Powell, J.F., Quattrone, D., Quested, D., Radant, A.D., Rampino, A., Rapaport, M.H., Rautanen, A., Reichenberg, A., Roe, C., Roffman, J.L., Roth, J., Rothermundt, M., Rutten, B.P.F., Saker-Delye, S., Salomaa, V., Sanjuan, J., Santoro, M.L., Savitz, A., Schall, U., Scott, R.J., Seidman, L.J., Sharp, S.I., Shi, J., Siever, L.J., Sigurdsson, E., Sim, K., Skarabis, N., Slominsky, P., So, H.C., Sobell, J.L., Söderman, E., Stain, H.J., Steen, N.E., Steixner-Kumar, A.A., Stögmann, E., Stone, W.S., Straub, R.E., Streit, F., Strengman, E., Stroup, T.S., Subramaniam, M., Sugar, C.A., Suvisaari, J., Svrakic, D.M., Swerdlow, N.R., Szatkiewicz, J.P., Ta, T.M.T., Takahashi, A., Terao, C., Thibaut, F., Toncheva, D., Tooney, P.A., Torretta, S., Tosato, S., Tura, G.B., Turetsky, B.I., Üçok, A., Vaaler, A., van Amelsvoort, T., van Winkel, R., Veijola, J., Waddington, J., Walter, H., Waterreus, A., Webb, B.T., Weiser, M., Williams, N.M., Witt, S.H., Wormley, B.K., Wu, J.Q., Xu, Z., Yolken, R., Zai, C.C., Zhou, W., Zhu, F., Zimprich, F., Atbaşoğlu, E.C., Ayub, M., Benner, C., Bertolino, A., Black, D.W., Bray, N.J., Breen, G., Buccola, N.G., Byerley, W.F., Chen, W.J., Cloninger, C.R., Crespo-Facorro, B., Donohoe, G., Freedman, R., Galletly, C., Gandal, M.J., Gennarelli, M., Hougaard, D.M., Hwu, H.G., Jablensky, A. v., McCarroll, S.A., Moran, J.L., Mors, O., Mortensen, P.B., Müller-Myhsok, B., Neil, A.L., Nordentoft, M., Pato, M.T., Petryshen, T.L., Pirinen, M., Pulver, A.E., Schulze, T.G., Silverman, J.M., Smoller, J. W., Stahl, E.A., Tsuang, D.W., Vilella, E., Wang, S.H., Xu, S., Dai, N., Wenwen, Q., Wildenauer, D. B., Agiananda, F., Amir, N., Antoni, R., Arsianti, T., Asmarahadi, A., Diatri, H., Djatmiko, P., Irmansyah, I., Khalimah, S., Kusumadewi, I., Kusumaningrum, P., Lukman, P.R., Nasrun, M.W., Safyuni, N.S., Prasetyawan, P., Semen, G., Siste, K., Tobing, H., Widiasih, N., Wiguna, T., Wulandari, D., Evalina, N., Hananto, A.J., Ismoyo, J.H., Marini, T.M., Henuhili, S., Reza, M., Yusnadewi, S., Abyzov, A., Akbarian, S., Ashley-Koch, A., van Bakel, H., Breen, M., Brown, M., Bryois, J., Carlyle, B., Charney, A., Coetzee, G., Crawford, G., Dracheva, S., Emani, P., Farnham, P., Fromer, M., Galeev, T., Gandal, M., Gerstein, M., Giase, G., Girdhar, K., Goes, F., Grennan, K., Gu, M., Guerra, B., Gursoy, G., Hoffman, G., Hyde, T., Jaffe, A., Jiang, S., Jiang, Y., Kefi, A., Kim, Y., Kitchen, R., Knowles, J.A., Lay, F., Lee, D., Li, Mingfeng, Liu, C., Liu, S., Mattei, E., Navarro, F., Pan, X., Peters, M.A., Pinto, D., Pochareddy, S., Polioudakis, D., Purcaro, M., Purcell, S., Pratt, H., Reddy, T., Rhie, S., Roussos, Panagiotis, Rozowsky, J., Sanders, S., Sestan, N., Sethi, A., Shi, X., Shieh, A., Swarup, V., Szekely, A., Wang, D., Warrell, J., Weissman, S., Weng, Z., White, K., Wiseman, J., Witt, H., Won, H., Wood, S., Wu, F., Xu, X., Yao, L., Zandi, P., Arranz, M.J., Bakker, S., Bender, S., Bramon, E., Collier, D.A., Crepo-Facorro, B., Hall, J., Iyegbe, C., Kahn, R., Lawrie, S., Lewis, C., Lin, K., Linszen, D.H., Mata, I., McIntosh, A., Murray, R.M., van Os, J., Rujescu, D., Walshe, M., Weisbrod, M., Achsel, T., Andres-Alonso, M., Bagni, C., Bayés, À., Biederer, T., Brose, N., Brown, T.C., Chua, J. J.E., Coba, M.P., Cornelisse, L.N., de Jong, A.P.H., de Juan-Sanz, J., Dieterich, D.C., Feng, G., Goldschmidt, H.L., Gundelfinger, E.D., Hoogenraad, C., Huganir, R.L., Hyman, S.E., Imig, C., Jahn, R., Jung, H., Kaeser, P.S., Kim, E., Koopmans, F., Kreutz, M.R., Lipstein, N., MacGillavry, H.D., Malenka, R., McPherson, P.S., O'Connor, V.,

Pielot, R., Ryan, T.A., Sahasrabudhe, D., Sala, C., Sheng, M., Smalla, K.H., Smit, A.B., Südhof, T.C., Thomas, P.D., Toonen, R.F., van Weering, J.R.T., Verhage, M., Verpelli, C., Adolfsson, R., Arango, C., Baune, B.T., Belangero, S.I., Børglum, A.D., Braff, D., Bramon, E., Buxbaum, J.D., Campion, D., Cervilla, J.A., Cichon, S., Collier, D.A., Corvin, A., Curtis, D., Forti, M. di, Domenici, E., Ehrenreich, H., Escott-Price, V., Esko, T., Fanous, A.H., Gareeva, A., Gawlik, M., Gejman, P. v., Gill, M., Glatt, S.J., Golimbet, V., Hong, K.S., Hultman, C.M., Hyman, S.E., Iwata, N., Jönsson, E.G., Kahn, R.S., Kennedy, J.L., Khusnutdinova, E., Kirov, G., Knowles, J.A., Krebs, M.O., Laurent-Levinson, C., Lee, J., Lencz, T., Levinson, D.F., Li, Q.S., Liu, J., Malhotra, A. K., Malhotra, D., McIntosh, A., McQuillin, A., Menezes, P.R., Morgan, V.A., Morris, D.W., Mowry, B.J., Murray, R.M., Nimgaonkar, V., Nöthen, M.M., Ophoff, R.A., Paciga, S.A., Palotie, A., Pato, C.N., Qin, S., Rietschel, M., Riley, B.P., Rivera, M., Rujescu, D., Saka, M.C., Sanders, A.R., Schwab, S.G., Serretti, A., Sham, P.C., Shi, Y., St Clair, D., Stefánsson, H., Stefansson, K., Tsuang, M.T., van Os, J., Vawter, M.P., Weinberger, D.R., Werge, T., Wildenauer, Dieter B., Yu, X., Yue, W., Holmans, P.A., Pocklington, A.J., Roussos, Panos, Vassos, E., Verhage, M., Visscher, P.M., Yang, J., Posthuma, D., Andreassen, O.A., Kendler, K.S., Owen, M.J., Wray, N.R., Daly, M.J., Huang, H., Neale, B.M., Sullivan, P.F., Ripke, S., Walters, J.T.R., O'Donovan, M.C., de Haan, L., van Amelsvoort, T., van Winkel, R., Gareeva, A., Shi, Y., St Clair, D., van Os, J., 2022. Mapping genomic loci implicates genes and synaptic biology in schizophrenia. Nature 2022 604:7906 604, 502–508. 10.1038/s41586-022-04434-5.

Volk, D.W., Moroco, A.E., Roman, K.M., Edelson, J.R., Lewis, D.A., 2019. The role of the nuclear factor-κB transcriptional complex in cortical immune activation in schizophrenia. Biol. Psychiatry 85, 25–34. https://doi.org/10.1016/j.biopsych.2018.06.015.

Volpato, V., Webber, C., 2020. Addressing variability in iPSC-derived models of human disease: Guidelines to promote reproducibility. DMM Dis. Models Mech. https://doi.org/10.1242/dmm.042317.

Warre-Cornish, K., Perfect, L., Nagy, R., Duarte, R.R.R., Reid, M.J., Raval, P., Mueller, A., Evans, A.L., Couch, A., Ghevaert, C., McAlonan, G., Loth, E., Murphy, D., Powell, T. R., Vernon, A.C., Srivastava, D.P., Price, J., 2020. Interferon-γ signaling in human iPSC–derived neurons recapitulates neurodevelopmental disorder phenotypes. Sci. Adv. 6 https://doi.org/10.1126/sciadv.aay9506.

Watanabe, K., Taskesen, E., van Bochoven, A., Posthuma, D., 2017. Functional mapping and annotation of genetic associations with FUMA. Nat. Commun. 8 https://doi.org/10.1038/s41467-017-01261-5.

Wingett, S.W., Andrews, S., 2018. FastQ screen: A tool for multi-genome mapping and quality control. F1000Res 7, 1338. 10.12688/f1000research.15931.2.

Wolf, J., Rose-John, S., Garbers, C., 2014. Interleukin-6 and its receptors: a highly regulated and dynamic system. Cytokine 70, 11–20. https://doi.org/10.1016/j.cyto.2014.05.024.

Wu, W.L., Hsiao, E.Y., Yan, Z., Mazmanian, S.K., Patterson, P.H., 2017. The placental interleukin-6 signaling controls fetal brain development and behavior. Brain Behav. Immun. 62, 11–23. https://doi.org/10.1016/j.bbi.2016.11.007.

Yokoyama, K.D., Zhang, Y., Ma, J., 2014. Tracing the evolution of lineage-specific transcription factor binding sites in a birth-death framework. PLoS Comput. Biol. 10 https://doi.org/10.1371/journal.pcbi.1003771.

Zhang, W., Jiang, J., Xu, Z., Yan, H., Tang, B., Liu, C., Chen, C., Meng, Q., 2022. Microglia-containing human brain organoids for the study of brain development and pathology. Mol. Psychiatry 1–12. https://doi.org/10.1038/s41380-022-01892-1.

Zhang, Y., Sloan, S.A., Clarke, L.E., Caneda, C., Plaza, C.A., Blumenthal, P.D., Vogel, H., Steinberg, G.K., Edwards, M.S.B., Li, G., Duncan, J.A., Cheshier, S.H., Shuer, L.M., Chang, E.F., Grant, G.A., Gephart, M.G.H., Barres, B.A., 2016. Purification and characterization of progenitor and mature human astrocytes reveals transcriptional and functional differences with mouse. Neuron 89, 37–53. https://doi.org/10.1016/j.neuron.2015.11.013.

Zhao, H., Zhang, H., Liu, S., Luo, W., Jiang, Y., Gao, J., 2021. Association of peripheral blood levels of cytokines with autism spectrum disorder: A meta-analysis. Front. Psychol. https://doi.org/10.3389/fpsyt.2021.670200.

Guneykaya D, Ivanov A, Hernandez DP, Haage V, Wojtas B, Meyer N, Maricos M, Jordan P, Buonfiglioli A, Gielniewski B, Ochocka N, Cömert C, Friedrich C, Artiles LS, Kaminska B, Mertins P, Beule D, Kettenmann H, Wolf SA. Transcriptional and Translational Differences of **Microglia** from Male and Female Brains. Cell Rep. 2018 Sep 4;24(10):2773-2783.e6. doi: 10.1016/j.celrep.2018.08.001.

Han J, Fan Y, Zhou K, Blomgren K, Harris RA. Uncovering **sex** differences of rodent **microglia**. J Neuroinflammation. 2021 Mar 17;18(1):74. doi: 10.1186/s12974-021-02124-z.

Villa A, Gelosa P, Castiglioni L, Cimino M, Rizzi N, Pepe G, Lolli F, Marcello E, Sironi L, Vegeto E, Maggi A. **Sex**-Specific Features of **Microglia** from Adult Mice. Cell Rep. 2018 Jun 19;23(12):3501-3511. doi: 10.1016/j.celrep.2018.05.048.

Appendix 2: Couch *et al.* 2021

Brain, Behavior, and Immunity 97 (2021) 410–422

Contents lists available at ScienceDirect

Brain Behavior and Immunity

journal homepage: www.elsevier.com/locate/ybrbi

Maternal immune activation primes deficiencies in adult hippocampal neurogenesis

Amalie C.M. Couch [a,b], Thomas Berger [a], Bjørn Hanger [a,b], Rugile Matuleviciute [b], Deepak P. Srivastava [a,b], Sandrine Thuret [a,1], Anthony C. Vernon [a,b,*,1]

[a] Department of Basic and Clinical Neuroscience, Institute of Psychiatry, Psychology and Neuroscience, King's College London, London, UK
[b] MRC Centre for Neurodevelopmental Disorders, King's College London, London, UK

ARTICLE INFO

Keywords:
Maternal immune activation
Prenatal insult
Hippocampus
Neurogenesis
Stress
Psychiatric illness
Neurodevelopmental disorders
Human induced pluripotent stem cells

ABSTRACT

Neurogenesis, the process in which new neurons are generated, occurs throughout life in the mammalian hippocampus. Decreased adult hippocampal neurogenesis (AHN) is a common feature across psychiatric disorders, including schizophrenia, depression- and anxiety-related behaviours, and is highly regulated by environmental influences. Epidemiological studies have consistently implicated maternal immune activation (MIA) during neurodevelopment as a risk factor for psychiatric disorders in adulthood. The extent to which the reduction of hippocampal neurogenesis in adulthood may be driven by early life exposures, such as MIA, is however unclear. We therefore reviewed the literature for evidence of the involvement of MIA in disrupting AHN. Consistent with our hypothesis, data from both *in vivo* murine and *in vitro* human models of AHN provide evidence for key roles of specific cytokines induced by MIA in the foetal brain in disrupting hippocampal neural progenitor cell proliferation and differentiation early in development. The precise molecular mechanisms however remain unclear. Nonetheless, these data suggest a potential latent vulnerability mechanism, whereby MIA primes dysfunction in the unique hippocampal pool of neural stem/progenitor cells. This renders offspring potentially more susceptible to additional environmental exposures later in life, such as chronic stress, resulting in the unmasking of psychopathology. We highlight the need for studies to test this hypothesis using validated animal models of MIA, but also to test the relevance of such data for human pathology at a molecular basis through the use of patient-derived induced pluripotent stem cells (hiPSC) differentiated into hippocampal progenitor cells.

1. Introduction

Historically adult hippocampal neurogenesis (AHN) is a strongly contested topic. The concept of human AHN was first mooted in the mid-1960′s, with subsequent publications providing evidence for the generation of new neurons in the mammalian hippocampus that continues throughout adult life, but declines with age (Kuhn et al., 2018; Altman and Das, 1965). The first evidence for human AHN was provided by Eriksson et al. in 1998. Human brain tissue from patients which were administered the thymidine analog, bromodeoxyuridine (BrdU) was analysed. BrdU is incorporated into DNA during the S-phase. The authors identified neuronal cells that were positive for BrdU indicating that these must have originated from progenitors after the administration of BrdU, indicating the generation of new neurons in the adult hippocampus (Eriksson et al., 1998). Later, Spalding and colleagues used a carbon dating method to estimate the number of newly generated granule neurons at roughly 700 cells per day (Spalding et al., 2013). Recently, the existence of AHN in humans has been under debate after the publication of a study investigating *post-mortem* hippocampal tissue across a large age range. The authors reported that while they were able to detect newborn neurons in the tissue of young brains, their numbers drop to undetectable levels in adulthood, putting a large questionmark behind the role of AHN in humans (Sorrells et al., 2018). Shortly after this publication, several groups published results contrasting those of Sorrells and colleagues providing evidence for immature neurons and therefore AHN in post-mortem tissue of patients even in their 70 s and 80 s (Tobin et al., 2019; Moreno-Jiménez et al., 2019; Boldrini et al., 2018). These differences in observation of neurogenic markers may arise

* Corresponding author at: Department of Basic and Clinical Neuroscience, Institute of Psychiatry, Psychology and Neuroscience, King's College London, London, UK.
E-mail address: anthony.vernon@kcl.ac.uk (A.C. Vernon).
[1] Joint senior author.

https://doi.org/10.1016/j.bbi.2021.07.021
Received 3 March 2021; Received in revised form 25 June 2021; Accepted 28 July 2021
Available online 2 August 2021

from several factors, including differences in tissue preparation, or medical backgrounds of patients as summarised elsewhere (Kempermann et al., 2018). Most recently, another publication by Sorrells et al. systematically brought together data from existing studies and added experiments to show that common markers for immature neurons, such as doublecortin (DCX), may not necessarily only label immature neurons, concluding that AHN, if present at all, may be extremely rare in adults. In response María Llorens-Martín, one of the authors identifying AHN in tissue from older people, pointed out weaknesses in this study, questioning Sorrells claim of neglectable levels of AHN (Sorrells et al., 2021). Taken together, human adult AHN, is still under heavy debate. More studies and refined techniques may be needed to settle this debate once and for all (Lee and Thuret, 2018). Nevertheless, current evidence indicating the existence of adult human AHN outweighs evidence for a negligible role of newborn neurons in the hippocampus.

Accepting that debate still continues regarding adult human AHN, the mammalian hippocampus and AHN are critically involved in regulating several domains of human and animal behaviour (Abrous et al., 2021). The on-going shaping of hippocampal circuitry throughout life by the process of AHN has been attributed to different forms of learning and memory (Dupret et al., 2008; Sasaki et al., 2018), cognitive abilities such as pattern separation and cognitive flexibility, emotional regulation and response to stress (Toda et al., 2019; Bartsch and Wulff, 2015). Within the context of this review, stress is defined as the psychological and biochemical demands induced by environmental factors that evoke an individual's adaptive behaviour (Syed and Nemeroff, 2017). It is therefore not surprising to find evidence for the role that AHN plays in conferring risk or resilience to serious human mental illnesses (Fig. 1a), as previously reviewed elsewhere (Kempermann et al., 2008; Kang et al., 2016). Evidence from animal and human *post-mortem* brain tissue studies provide evidence for reductions in AHN and an immature dentate gyrus as one potentially causal basis for the increased risk of psychiatric disorders associated with exposure to stress, including depression, anxiety and schizophrenia (SZ) (Kang et al., 2016; Anacker, 2014; Yamasaki et al., 2008; Eliwa et al., 2021; Hagihara et al., 2013; Tunc-Ozcan et al., 2019). In support of this view, complementary evidence exists to suggest that AHN plays a key role in buffering against stress synthesising data from both animal models (Anacker et al., 2018; Yam et al., 2019) and human *post-mortem* studies (Boldrini et al., 2019). For example, using *in vivo* calcium imaging to record neuronal activity from large cell populations in the ventral DG (vDG), it was demonstrated that newborn neurons in this region act to decrease in the activity of other stress-responsive neurons that are preferentially active during social defeat attacks by aggressor mice or while mice explore anxiogenic environments (Anacker et al., 2018). These effects on AHN and thus DG activity are necessary and sufficient for stress resilience, as silencing of the vDG confers resilience whereas excitation promotes susceptibility (Anacker et al., 2018). These data also resonate with the substantial body of evidence linking exposure to stressful life events and increased risk for psychiatric illness (Syed and Nemeroff, 2017; Costello et al., 2003; Sarason et al., 1978; Heim, 2000; Andrews et al., 1978). Collectively, these data suggest that the degree of AHN may be one critical factor in determining an individual's level of either risk or resilience to developing psychopathology, particularly in the context of stress exposure.

It is also clear that AHN is remarkably sensitive to environmental influences, consistent with the evidence that 30–40% of neurodevelopmental disorder risk may be attributed to environmental factors (Cattane et al., 2020). Besides the aforementioned and well-documented impact of stress on AHN, human epidemiological studies have consistently reported associations between maternal immune activation (MIA, by either infectious or non-infectious stimuli) and increased risk for a

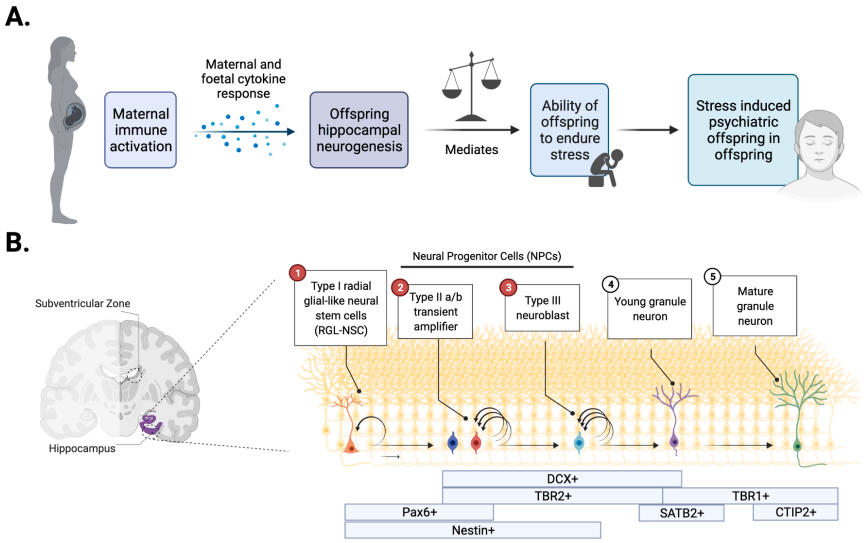

Fig. 1. Theoretical framework for understanding the interplay between AHN and MIA. A) The potential for MIA to increase susceptibility to psychiatric illness in offspring, as mediated by hippocampal neurogenesis. Each factor (maternal immune activation, hippocampal neurogenesis and stress) confers the offspring's resilience or susceptibility to the next B) Background and cell timeline adapted from (Berger et al., 2020) the molecular and cellular understanding of adult hippocampal neurogenesis, with the relevant cell marker expressions in boxes below. Stages 2 and 3, depicting type II a/b transient amplifier and type III neuroblasts are considered neural progenitor cells. Together with the first stage, type I radial glial-like neural stem cells, and denoted by the stages coloured red, these three neural stem / progenitor cell stages are particularly vulnerable to the effects of MIA-associated stimuli. Besides the subgranular zone, the subventricular zone is highlighted as well, representing the other well studied region of adult neurogenesis. Graphics created with BioRender.com. (For interpretation of the references to colour in this figure legend, the reader is referred to the web version of this article.)

range of psychiatric and potentially neurological disorders in the affected offsrping (Kępińska et al., 2020; Knuesel et al., 2014; Estes and McAllister, 2016). This has led to development of a whole field of research into prenatal programming, for example following MIA, which may "pre-set" an individual's risk for any subsequent differences in cognition, emotion or even psychiatric illness later in life (Bilbo and Schwarz, 2012; Kempermann, 2019). It is clear however that the impact of MIA is variable and a significant proportion of offspring exposed to MIA do not develop any overt behavioiural or psychological illness, That said, it is plausible that the absence of any such psychopathology could simply reflect a latent insult that may be unmasked by exposure to other environmental risk factors, including stress exposure during vulnerable periods of brain maturation such as adolescence. Regardless, of either possibility, the mechanisms underling either risk or resilience following MIA exposure remain unclear. Synthesising the aforementioned evidence that links reductions in AHN with increased risk, whislt boosting AHN may drive resilience for affective and non-affective psychiatric disorders, we hypothesised that a reduction in AHN following MIA during pregnancy might be one important driver of risk and resilience in the affected offspring. To address this, we first summarise the evidence linking AHN and MIA independently to increased risk for psychiatric disorders. We then consider the evidence supporting MIA-dependent disruption of AHN and how this relates to behaviour, including priming the response to stress exposure. Although we find evidence to support a link between MIA and disrupted AHN, we highlight the need for studies to directly test our hypothesis using validated animal models exposed to MIA in order to answer two key questions; First, does AHN differ between susceptible and resilient offspring? Second, does reduced AHN following MIA mediate susceptibility to a second risk exposure, such as stress (Mueller et al., 2021), even in apparently MIA-resilient offspring (Mueller et al., 2021; Ranaei et al., 2020; Giovanoli et al., 2013)? Finally, we highlight that to test the relevance of such data for human pathology, there is a need for complementary studies using human induced pluripotent stem cells (hiPSC) to understand how immune stimulation that results in MIA may impact upon AHN using a human cellular model system, which would also offers the potential to test gene * environment interactions using patient-derived material.

1.1. Adult hippocampal neurogenesis and behavioural disorder

Current evidence suggests there are only two brain regions in which adult neurogenesis may be detected in the human brain: the subgranular zone (SGZ) of the DG in the hippocampus, and the subventricular zone (SVZ) adjacent to the lateral ventricles (Spalding et al., 2013; Boldrini et al., 2018; Kempermann and Gage, 1999) (Fig. 1b). The proliferation of neural stem/progenitor cells (NSC/NPCs), as well as their differentiation into granule neurons and integration into existing circuits requires complex processes (Toda et al., 2019). Regulatory signals from the neurogenic niche direct neural stem cells to proliferate, migrate, extend neurites, form synapses and integrate into existing circuits (Fig. 1b).

Dysregulation of any these processes, particularly at the NSC/NPC stage, has the potential to permanently alter neuronal circuits within the hippocampus (Toda et al., 2019). The capability of NPCs to proliferate and differentiate is integral to the downstream quality of AHN. Conditional ablation of the miR-17–92 cluster in nestin + NPCs (stages 1–3 of Fig. 1b), known to regulate their function, significantly reduced proliferation and differentiation of NPCs in the DG which had a corresponding detrimental effect on hippocampus-dependent behaviour (Pan et al., 2019). On the other hand, the direct genetic-driven expansion of NSCs in the DG of mice by overexpressing Cdk4/cyclinD1 counteracts the age-related decline in AHN (Berdugo-Vega et al., 2020). Therefore, exposure to any entities, including MIA, capable of disturbing the essential function of the NSC/NPC pool has the potential to alter an individual's capacity for AHN (Fig. 1b). Hence, one potential mechanism contributing to the emergence of psychiatric disorders could be the disruption of AHN by MIA, which may by itself lead to increased risk for psychopathology later life, or create a "latent insult" that may be subsequently unmasked by additional second risk exposure, such as stress (Fig. 1) (Toda et al., 2019; Kang et al., 2016; Anacker, 2014; Gergues et al., 2018).

1.2. Maternal immune activation

Maternal immune activation (MIA) from both infectious and non-infectious sources contributes to a significant environmental risk to neurodevelopmental sequelae (Meyer, 2019). Epidemiological studies have consistently linked MIA and higher levels of inflammatory markers to increased risk for psychiatric disorders with a putative neurodevelopmental origin in the affected offspring, including schizophrenia (SZ) and autism spectrum disorder (ASD) (Kępińska et al., 2020; Knuesel et al., 2014; Estes and McAllister, 2016). Causality for these associations is provided by "one-hit" animal models for MIA in which a single immune challenge is administered to the pregnant dam at key stages of gestation. Data from such models confirms that such exposure to immune activation during critical periods of brain development in gestation leads to abnormal trajectories of brain development (Piontkewitz et al., 2011; Crum, 2017) and the emergence of behavioural disruption in adulthood, including deficits in social interaction, cognition and so on (Meyer, 2019; Meyer, 2014). As such, the biochemical prenatal maternal response to such environmental factors, both infectious and non-infectious, represents a risk factor capable of disrupting foetal neurodevelopment. Several birth cohort studies implicate increased psychiatric disorder risk in offspring with prenatal stress (Malaspina et al., 2008; Brown and Conway, 2019), such as bereavement (Huttunen, 1978) and socio-economic disadvantage (Gilman et al.,). Except for specific viral infections with maternal-foetus vertical transmission such as Zika, Rubella and Human Cytomegalovirus (HCMV) (Claus et al., 2020), it is now generally accepted that most infectious MIA cases do not confer psychiatric risk by direct infection of the foetus via the placenta, but rather a systemic maternal immune response influencing neurodevelopment (Meyer, 2014).

In order to identify which components of the maternal immune response are central to the effect of MIA, birth cohort studies have examined links between fluctuations in specific cytokines in maternal serum and the degree to which offspring experience any psychopathology. For example, Allswede and colleagues reported increased concentrations of the classical pro-inflammatory cytokines TNFα, IL-1β, and IL-6 in the maternal serum of offspring who developed psychosis, suggesting this effect is greatest when the elevations in these cytokines are present during the weeks 7–20 of pregnancy (Allswede et al., 2020). Hence, proxy markers of early prenatal infection may be associated with a greater risk for psychosis in the offspring, demonstrating the developing brain's increased sensitivity to environmental factors that can alter neurodevelopmental processes (Knuesel et al., 2014; Allswede et al., 2020; Adam, 2012). Further supporting this view, a recent human study by Goldstein and colleagues indicated that a higher ratio of TNFα: IL-10 in maternal serum correlated with sex-depedent increases in hippocampal activity and decreases in hypothalamus-hippocampus connectivity, as measured by functional magnetic resonance imaging (MRI) during response to stressful stimuli in the offspring even to the age of 45 years (Goldstein et al., 2021). Additionally, increased maternal IL-6 serum concentration correlated with decreased hippocampal acitivty in females only (Goldstein et al., 2021). These remarkable findings highlight that MIA can have long-lasting effects on stress circuitry in the brain, consistent with the idea of a "latent insult" such that MIA exposure may pre-set an increased sensitivity to negative stressful events in later life by disrupting the development of neural circuits linked to stress responses (Goldstein et al., 2021). In further support of this view, several recent studies have found a clear link between the concentration of circulating IL-6 in maternal serum with abnormal brain structural and functional connectivity, as measured by MRI and cognitive development and externalising behaviours in the offspring (Rasmussen et al., 2019;

Rudolph et al., 2018; Graham et al., 2018). Furthermore, the mean maternal concentration of IL-6 can be inferred from offspring functional connectivity patterns, derived from MRI data in the newborn brain (Rudolph et al., 2018).

In further support of maternal IL-6′s crucial role in foetal development, an *ex vivo* isolated cotyledon human placental perfusion model indicated IL-6 to transfer bidirectionally between mother and foetus, but not IL-1α or TNFα (Zaretsky et al., 2004). Furthermore, a single prenatal injection of IL-6 to pregnant rat dams on gestational day (GD) 12.5 leads to similar behavioural dysfunctions in the offspring as induced following exposure of pregnant dams to either influenza virus or the toll-like receptor 3 (TLR3) agonist Poly I:C, suggesting a key role for this cytokine (Smith et al., 2007). Behavioural and molecular phenotypes in this mouse model are also ameliorated by administration of IL-6 neutralising antibodies, or if Poly (I:C) is administered to dams lacking the IL-6 receptor, confirming the importance of this cytokine (Smith et al., 2007). One important pro-inflammatory function of IL-6 is the promotion of T_H17 cell differentiation, from which cells IL-17A is released (Lee et al., 2012). Notably, administration of IL-17 alone to pregnant mice also leads to behavioural deficits in the offspring which have relevance for both ASD and SZ (Choi et al., 2016). Finally, the response to MIA by maternal and neonatal cytokine serum concentrations is proposed to be genetically predetermined, after foetal loci for immune function were found to independently influence maternal immune mediators in a genome-wide association study (Traglia et al., 2018). Collectively, these data support the view that specific cytokines play a role in increasing risk for neurodevelopmental disorders by influencing neurodevelopment, as predetermined by genetic factors.

Nevertheless, epidemiology also provides evidence that prenatally exposed children can show resilience to neurodevelopmental deficits and remain healthy through adulthood (Meyer, 2019). Alternatively, consistent with the idea that exposure to MIA may predispose children to develop psychopathology in adulthood, that only emerges after additional environmental “hits” such as exposure to stress or drug abuse (Meyer, 2019; Bayer et al., 1999; Giovanoli et al., 2015). The interplay between offspring susceptibility and resilience to MIA is now being considered; under the notion that risk factors reach a threshold level within a vulnerable period of development, prior to precipitation of neurodevelopmental phenotypes (Meyer, 2019; Mueller et al., 2021).

These data raise important questions as to the mechanisms that define either susceptibility or resilience following exposure to pre- and post-natal environmental risk factors such as MIA and how this may prime suseceptibility to additional second hits such as stress. The immune system is known to play an essential role in the communication between the external environment and internal physiological and biochemical states (Rook, 2013). Hence, alterations to such physiological and biochemical states could subsequently mediate behavioural states via changes in the hippocampal neurogenic environmental niche. Given the evidence that AHN promotes resilience to stress (Anacker et al., 2018; Boldrini et al., 2019), it is reasonable to hypothesise that one mechanism by which MIA could prime offspring to be more sensitive to a post-natal stress exposure is through disruption of AHN, by creation of a “latent” insult. Such prenatal programming may therefore “pre-set” an individual’s risk for any subsequent behavioural disorder or psychiatric illness (Fig. 1a). But, what evidence is there that MIA disrupts AHN? In the following section, we will therefore consider the mechanisms by which MIA prenatally primes suppression of adult hippocampal neurogenesis, increasing susceptibility for psychopathology in adulthood.

2. Prenatal immune challenge alters hippocampal neurogenesis

Studies on adult hippocampal neurogenesis in the context of MIA have to date, largely been confined to “one-hit” animal models or *in vitro* cellular systems. Here we define a “one-hit” model as a single exposure to a pathogen, immunostimulant or specific cytokine. As previously reviewed (Brown and Meyer, 2018; Musaelyan et al., 2014), hippocampal neurogenesis in MIA models is usually investigated by exposing a pregnant animal or *in vitro* cultures to an immunostimulant, followed by assessment of behavioural, neurochemical, neuroanatomic, and neurophysiologic endophenotypes of relevance to brain disorders associated with impaired hippocampal neurogenesis in the offspring or using *in vitro* cell cultures (Musaelyan et al., 2014). Various immunostimulants have been used and include viral infection (e.g. Zika, human cytomegalovirus and porcine reproductive and respiratory syndrome virus (PRRSV) (Antonson et al., 2018; Dang et al., 2016; Meyer, 2006; Sun et al., 2020), viral or bacterial infection mimetics such as the toll-like receptor (TLR) 3 and 4 agonists Poly I:C and LPS respectively (Kępińska et al., 2020; Meyer, 2006; Musaelyan et al., 2014), or exposure to specific pro-inflammatory cytokines, such as IL-6, TNFα or IL-1β (Seguin et al., 2009). The following section will review recent works that incorporate such methods to investigate how MIA may supresses AHN either following the initial immue exposure, or as a consequence a “primed” response to subsequent immune activation following, for example, stress exposure.

2.1. The influence of MIA on AHN

There is evidence to suggest that a single, prenatal exposure to a “one-hit” single dose (5–20 mg/kg) Poly I:C, LPS or PRRSV exposure is sufficient to impair hippocampal neurogenesis in adulthood (Musaelyan et al., 2014). Test metrics used to quantify behaviour in animal MIA model offspring have been reported to correlate linearly with deficits in hippocampal neurogenesis in both adolescence and adulthood (Table 1). Both anxiety- and depression-related behaviours are commonly identified using Y-maze, prepulse inhibition (PPI), Morris water maze, open field, sensorimotor gating and motor coordination tests, in which MIA offspring perform significantly worse compared to control offspring (Depino, 2015; Li et al., 2020; Mattei et al., 2014; Sheu et al., 2019; Wolf et al., 2011; Zhang and van Praag, 2015; Zhao et al., 2019). Such deficits in fear-, anxiety-, and stress-related behaviour would be consistent with hippocampal dysfunction, including deficits in AHN, since the hippocampus is considered to be responsible, at least in part, for these behaviours (Bartsch and Wulff, 2015).

In this context, *post-mortem* studies in “one-hit” animal models of MIA provide evidence for reduced proliferation of hippocampal NSC/NPCs and impaired differentiation as indicated by reduction of cells expressing the proliferation marker BrdU and the immature neuron marker DCX (Mattei et al., 2014; Melnik et al., 2012; Mouihate, 2016; Piontkewitz et al., 2012; Sheu et al., 2019; Wolf et al., 2011; Zhao et al., 2019). These data confirm that the hippocampal pool of NSC/NPCs in adulthood is vulnerable to prenatal immune challenge, resulting in impaired proliferation and differentiation (Fig. 1b). The use of *post-mortem* animal studies at adolescent and adult timepoints alone, however, does not aid an understanding of the molecular basis by which MIA influences hippocampal neurogenesis at the point of prenatal exposure. Additional evidence from early, prenatal time-points relevant to prenatal risk exposure is needed to examine the acute, proximal effect of MIA on hippocampal neurogenesis.

2.1.1. Effects of MIA on AHN mediated by cytokines

The maternal cytokine-related immunological response to infection is one essential mechanism by which MIA confers increased psychiatric disorder risk in offspring (Allswede et al., 2020; GILMORE and FREDRIKJARSKOG, 1997). Various cytokines have been determined as essential in conferring the long-lasting negative impact of TLR4 and TLR3 prenatal activation in animal models (Mouihate, 2016; Smith et al., 2007). As already stated, LPS and Poly I:C do not cross the foetal-placental barrier, but pro-inflammatory cytokines transduce their effects in animal MIA models (Ashdown et al., 2006; Zaretsky et al., 2004). The systemic maternal cytokine response to MIA risk factors therefore has the potential to influence embryonic hippocampal neurogenesis.

Table 1
MIA reduces hippocampal neurogenesis correlating with behavioural deficits. Evidenced by animal models from the last decade updated from (Musaelyan et al., 2014).

Reference	Animal	Stimulation	Timing	Age of offspring	Behavioural Effect	Effect on Neurogenesis	Phenotype rescued by
(Li et al., 2020)	Rats	Poly I:C 10 mg/kg	GD9.5	PND40	No effect was seen.	No effect on ERK1/2 phosphorylation. Increased total NFM immunoreactivity.	N/A
				PND60	Deficiencies in Y-maze entries, time spent in novel arm and PPI performance.	Reduced ERK1/2 phosphorylation. No change in total NFM immunoreactivity, but distribution decreased in the CA3 region and increased in DG.	
(Sheu et al., 2019)	Mice	Poly I:C 5 mg/kg	GD17	PND42 PND63 PND84	No effect was seen. Decreased time in central zone, sucrose preference, increased immobility and latency to feed.	No effect seen. Reduced proliferation and aberrant dendritic development of newly generated neurons.	N/A
(Zhao et al., 2019)	Rats	Poly I:C 10 mg/kg	GD18	PND27-28	Abnormal behaviours in Morris water maze and elevated plus maze	Reduced proliferation and differentiation of SGZ cells.	PPARγ agonist Pioglitazone improved hippocampal-dependent spatial learning, memory and neurogenesis.
(Antonson et al., 2018)	Pigs	PRRSV	GD76	GD111 (3 days before suspected birth)	N/A	No change in the total number of hippocampal proliferative cells. Decreased brain weight and reduced neuronal number in DG. GFAP + density and expression increased.	N/A
(Mouihate, 2016)	Rats	LPS 100 μg/kg	GD15	PND45	N/A	Decreased newly born neurons in DG but not SVZ.	IL-6 blocking antibody and cortisone receptor blocker RU-486.
(Depino, 2015)	Mice	LPS 25 μg/kg	GD9	PND56-70	Increased anxiety- and depression-related behaviours	Decreased NA and 5-HT in the hippocampus. No difference in proliferation and differentiation in DG but decreased Reelin in the hippocampus.	N/A
(Zhang and van Praag, 2015)	Mice	Poly I:C 5 mg/kg	GD15	PND90	Deficiencies in PPI, spatial maze and motor coordination test plus increased depression-related behaviours	Reduced DG volume and PV + interneurons. Hippocampal neurons had increased input resistance, lower current threshold and decreased action potential number.	N/A
(Mattei et al., 2014)	Rats	Poly I:C 4 mg/kg	GD15	PND90-128	Deficient in PPI test	Decreased proliferation and net-neurogenesis in the DG. Decrease in microglia Iba1 reactivity.	Minocycline rescued both neurogenic and behavioural deficits, but not microglial.
(Melnik et al., 2012)	Mice	Poly I:C 16 kg/ml	GD15	PND60	N/A	Reduced proliferation of NPCs in DG.	N/A
(Piontkewitz et al., 2012)	Rats	Poly I:C 4 mg/kg	GD15	PND100	N/A	Decreased early (PND14-36) proliferation in DG but did not affect later (PND 77–79) differentiation of mature neurons in the DG.	Risperidone increased number of proliferating cells, percentage of differentiating cells and prevented a decrease in PV + HP interneurons.
(Wolf et al., 2011)	Mice	Poly I:C 5 mg/kg	GD15	PND60	Deficits in open field test and sensorimotor gating	Premature senescence, reduced telomere length and telomerase activity of NPCs in the DG.	Voluntary exercise increased telomerase activity but not telomere length, also rescuing behavioural and neurogenic phenotype.

Interferons (IFN) are produced by the innate immune system in response to environmental insults such as viral infection and are known to induce altered microglial phenotype and behavioural abnormalities Poly I:C induced MIA mice offspring (Ben-Yehuda et al., 2020). Using an immortalised human hippocampal progenitor cell line Borsini and colleagues demonstrated physiologically relevant concentrations of IFNα decreased neurogenesis and increased apoptosis at high concentrations (Borsini et al., 2018). Oxidative stress, immune response, neuronal formation and cell death regulation pathways were implicated in the action of IFNα on the human hippocampal cells (Borsini et al., 2018). Furthermore, chronic human IFNα treatment has been shown to reduce AHN and impair adaptive behaviour in adult common marmosets (Kaneko et al., 2020). MIA-dependent release of interferons can therefore acutely dysregulate neuronal maturation of NSC/NPCs in hippocampal regions.

Aside from interferons, maternal IL-6 is considered a sensor, effector and transducer of MIA (Seguin et al., 2009; Entringer et al., 2015) and also plays a key role in the regulation of neurogenesis (Erta et al., 2012). In the aforementioned study by Borsini and colleagues, dual administration of IFNα with IL-6 produced a synergistic effect on hippocampal progenitor cell death. Aquaporin 4 was downregulated, suggesting an imbalance in the cell's homeostatic capacity (Borsini et al., 2018). Offspring from LPS-challenged pregnant rat dams had a reduced number of newly born neurons in the DG in adulthood, as monitored by a decrease in the number of DCX and T-box brain protein-2 (TBR2) expressing NPCs (stages 2–4 of Fig. 1b) (Mouihate, 2016). Nevertheless, when LPS was co-administered with an IL-6 blocking antibody, the observed reduction of neurogenesis was salvaged suggesting an essential role for IL-6 in mediating changes in NSC/NPC differentiation in the DG (Mouihate, 2016). In a 3D neural differentiation model, referred to by the authors as "neural aggregates" that resembled neurospheres, IL-6 exposure did not affect neural aggregate size (Zuiki et al., 2017). Instead, it decreased the more mature $TBR1^+/CTIP2^+$ cell population's area ratio (stage 5 of Fig. 1b) without changing the proportion of latter born $SATB2^+$ neurons (stage 4 of Fig. 1b), suggesting a distorted cell fate differentiation or increased NPC-specific apoptosis (Zuiki et al., 2017). Besides IFN, IL-6 can therefore additionally acutely interfere with hippocampal neuron maturation.

Certainly, the influence of MIA on AHN is not as a result of the acute release of IFN and IL-6 alone. For example, IL-6 has the additional

potential to regulate DNA methylation in human-derived cells (Hodge et al., 2001), which itself has been shown to play a role in AHN (Jessop and Toledo-Rodriguez, 2018; Richetto et al., 2017; Zhang et al., 2013). Consequently, systemic cytokine signalling at an early vulnerable age of neurodevelopment provides MIA with a possibility to leave a dormant mark on neurogenic and cell survival programs, which in turn could alter neurodevelopmental and neurogenic trajectories to make an individual more or less susceptible to stressors in later life.

2.1.2. Effects of MIA on AHN mediated by changes in hippocampal neuron activity

Given that AHN is essential to the on-going formation and refinement of hippocampal neurocircuitry throughout adulthood, it is not surprising that the disruption of this process may result in the onset of atypical behaviours (Anacker and Hen, 2017). As reviewed elsewhere, new-born adult neurons generated by AHN inhibit the activity of mature granule cells in the DG, which contributes to information encoding (Anacker and Hen, 2017). Thus, AHN affects reversal learning and cognitive flexibility via the regulation of DG neuron activity (Anacker and Hen, 2017). As previously mentioned, inhibition of these new-born adult neurons in the vDG of rodent models increases the susceptibility to stressors in later life and vice versa to confer resilience to chronic stress (Tunc-Ozcan et al., 2019; Anacker et al., 2018). Therefore, the disruption of hippocampal neuron functioning by MIA could render an individual more susceptible to stress exposure as their adult born neurons are less capable of regulating a hippocampal stress circuit, which AHN directly regulates (Anacker et al., 2018; Patrich et al., 2016). Patrich and colleagues demonstrated in primary hippocampal culture from postnatal day (PND) 0–2 rodents that MIA exposed offspring had a considerably lower intrinsic excitability and stronger spike frequency adaptation (Patrich et al., 2016). In *post-mortem* brain tissue from the same study, two-weeks old MIA exposed rodent offspring had a lower intrinsic excitability in CA1 pyramidal neurons (Patrich et al., 2016). Hence, MIA has the potential to dysregulate hippocampal neuron function in early life (Patrich et al., 2016), potentially leaving an individual more susceptible to stress, given their reduced capacity to regulate a hippocampal stress circuit (Anacker and Hen, 2017; Patrich et al., 2016). The combination of reduced AHN plus the potential for MIA-dependent dysregulated hippocampal neuronal function may therefore leave an individual predisposed to behavioural disorder and/or psychiatric illness after stress exposure.

2.2. Effect of MIA on AHN via immune "priming"

Typically, the age of SZ onset is around late adolescence to early adulthood (Häfner et al., 1994). If such disorders were caused by MIA *per se*, the onset of psychiatric disorders in some cases is therefore latent rather than immediate. A handful of "one-hit" MIA models which investigated more than one postnatal timepoint reported that deficiencies in AHN post MIA occur in an age-dependent manner (Antonson et al., 2018; Depino, 2015; Li et al., 2020; Sheu et al., 2019). Sheu and colleagues determined gestation day (GD)17 Poly I:C exposed mice offspring at 6-weeks of age to have no behavioural phenotype or differences in AHN as compared to control offspring (Sheu et al., 2019). Nevertheless, after 9- and 12-weeks postpartum, the MIA offspring developed anxiety- and depressive-like behaviours that paralleled reduced proliferation and aberrant dendritic development of newly generated neurons in the DG, indicating a latent onset of these phenotypes in adulthood (Zhao et al., 2019). These data raise the question; by what means could the effects of MIA on AHN lie dormant until adolescence or adulthood? The latent onset of deficits in behaviour and AHN in adulthood suggests risk priming, whereby offspring may be more susceptible to future stress, which could unmask latent behavioural dysfunction and/or psychopathology. Conceivable mechanisms by which such immune priming following MIA exposure may affect AHN, and thus some behaviours, are presented as follows.

2.2.1. Microglia

Multiple lines of evidence from human genetics, *post-mortem*, neuroimaging and peripheral biomarker studies implicate the innate immune system and particularly microglia in the pathophysiology of neuropsychiatric disorders (Mondelli et al., 2017). As the resident CNS myeloid cells, microglia play critical roles in shaping the central immune response to maintain homeostasis (Hanger et al., 2020). The disturbance of healthy microglial function by MIA during foetal brain development could, in turn, disrupt essential processes required for healthy foetal or adult neurogenesis and neural circuit formation (Knuesel et al., 2014). Considering that MIA impacts microglial neurodevelopmental function most potently in early life (Matcovitch-Natan et al., 2016), but also primes the immune system to respond more strongly to stress (Giovanoli et al., 2013), dysfunctional microglia could cause abnormal AHN. The influence of MIA activated microglia could perhaps sensitise the individual to greater immune responses following stress exposure, thus leading to a latent effect on AHN to trigger pathology in later life.

Microglia are highly plastic cells, which can assume a range of functional and morphological states, resulting in significant intra- and inter-regional heterogeneity in the brain (Hanger et al., 2020; Sharma and Tremblay, 2020). Microglia polarised to a pro-inflammatory state release reactive oxygen species, complement proteins, proteinases and pro-inflammatory cytokines such as IL-6, TNFα, IL-1β, which attract other immune cells, such as macrophages, dendritic cells and lymphocytic T-cells, facilitating their entry into the brain across the blood–brain barrier and promoting phagocytosis of foreign agents or neurotoxic cellular debris (Barres, 2008; Hanger et al., 2020). These actions can impede the neurogenic cascade during chronic stress (Sierra et al., 2014). In contrast to a pro-inflammatory phenotype, microglia can also present anti-inflammatory phenotypes, secreting cytokines, chemokines and trophic factors to promote repair and re-establish homeostasis, essential for encouraging neurogenesis. A prolonged pro-inflammatory response can be detrimental to nearby neurons, given the molecules' potential cytotoxic nature. As a result, the damaging impact of pro-inflammatory microglia on neurogenesis is well supported (Ekdahl et al., 2009; Knuesel et al., 2014; Sierra et al., 2014). Importantly, microglia are strongly implicated in influencing AHN by regulating neuronal proliferation and differentiation, as well as synaptic connections, via phagocytosis of apoptotic new-born cells, secretion of neurotrophic factors and surveillance communication to nearby neurons by CX_3CR1/CX_3CL1 signalling (Gemma and Bachstetter, 2013). Therefore, microglia are important mediators in the modulation of cognitive and behavioural functions downstream of AHN.

Encouraging microglia towards an anti-inflammatory state benefits AHN (Han et al., 2019; Monje et al., 2003; Zhang et al., 2021). In the context of an immune response, Monje and colleagues revealed adult rodents exposed to LPS had an increased number of activated microglia in the DG and impaired AHN (Monje et al., 2003). The increase in activated microglia corresponded with increased cytokine levels, including IL-6. This immune response mediated AHN impairment as demonstrated by the fact that Indomethacin, a nonsteroidal anti-inflammatory, rescued the AHN deficit (Monje et al., 2003). Although the LPS stimulation during adulthood is not physiologically relevant to MIA, these data are consistent with a view that microglial function supports typical AHN. Furthermore, in a "two-hit" early adversity mouse model by Han and colleagues whereby male offspring were separated from their mothers for 3 h a day through PND1-14 and then a second stress 3 weeks after weaning, administration of the anti-inflammatory drug minocycline between stresses reversed the pro-inflammatory markers and microglia transition states that correlated with altered hippocampal neurogenesis (Han et al., 2019). Finally, Zhang and colleages identified the importance of anti-inflammatory microglia after knocking down the expression of the anti-inflammatory marker IL-4 receptor (IL4R) caused a reduction of hippocampal neurogenesis and increases susceptibility to chronic mild stress in mice, and vice versa when overexpressing IL-4 (Zhang et al., 2021). Interestingly, IL-4

expression in MIA-exposed offspring is reduced in the hippocampus up to PND7 compared to control offspring, meaning a potential for unchecked pro-inflammatory microglia to excert their effects on hippocampal neurogenesis during this time (Garay et al., 2013).

In recent work, Zhao and colleagues examined the potential beneficial effects of pioglitazone given on days PND21-27 to the offspring of pregnant rats exposed to Poly I:C or saline GD18 (Zhao et al., 2019). Pioglitazone activates the peroxisome proliferator-activated receptor gamma (PPARγ), which is expressed in human neurons, microglia, oligodendrocytes, endothelial cells and astrocytes (Zhang et al., 2016). Prepubescent MIA-offspring (PND28) subsequently presented abnormal learning and memory behaviours, the severity of which were positively associated with impairment of hippocampal neurogenesis and increased microglial, but not astrocytic density, in the DG (Zhao et al., 2019). Pioglitazone treatment improved both hippocampal neurogenesis and hippocampal-dependent spatial learning in the exposed offspring. Implicating microglial involvement in the DG, pioglitazone treatment also reduced total microglial population and the number of microglial processes (Zhao et al., 2019). Transcript levels of pro-inflammatory cytokines TNFα, IL-1β, IL-6, CD68, iNOS and IFNγ were increased in the hippocampus of MIA offspring, but returned to control levels upon pioglitazone administration (Zhao et al., 2019). Using immunofluorescence co-localisation, the source of IL-6 was determined by Zhao and colleagues to be microglial cells, indicating the involvement of a microglial phenotype in reduced neurogenesis in the hippocampus (Zhao et al., 2019). Hence, promoting microglia towards an anti-inflammatory phenotype by PPARγ, activation, IL-4 signalling, minocycline and Indomethacin demonstrates pro-neurogenic effects, ameliorating cognitive impairments, anxiety-related behaviours and reduced AHN caused by a prenatal immune challenge (Han et al., 2019; Monje et al., 2003; Zhang et al., 2021; Zhao et al., 2019).

Nevertheless, many studies suggest that at the point that neonatal and postnatal periods are reached, MIA-induced microglial activation is resolved (Antonson et al., 2018; Giovanoli et al., 2015; Missault et al., 2014). Therefore, an acute pro-inflammatory microglia phenotype is unlikely to be the main mechanism by which MIA results in neurogenic deficiencies that are observed in neuropsychiatric disorders. Instead, MIA might induce immune memory in microglia without the overt longstanding phenotypic expression. For example, neonatal infection altered microglia response to immune challenge after the reexposure to LPS in adulthood (Bilbo, 2005). The reexposed animals showed greater and more prolonged increase in microglial marker mRNA expression and faster IL-1β upregulation in the hippocampus and cortex (Bilbo, 2005). This suggests that adverse prenatal or early life experiences inform microglia response to such challenges in adulthood. Such priming effect could in part be mediated through epigenetic modifications. Although insights on the epigenetic mechanisms of immune memory formation in microglia remain limited, changes in histone deacetylase (HDAC) expression and activity as well as repressive (H3K27me3) and transcriptionally active (H3K4me3) histone marks have been implicated in studies, exploring microglia priming to such stimuli as LPS or glioma-conditioned medium (Cao et al., 2015; Maleszewska et al., 2021; Martins-Ferreira et al., 2021; Schaafsma et al., 2015). This way altered microglial state by prenatal MIA challenge might make an offspring more susceptible to future stress, which, unbalanced by AHN dependent mechanisms of stress resilience, could thus increase their risk for psychiatric illness (Giovanoli et al., 2013).

2.2.2. Telomeres

Telomere length has also long been associated with neurogenic disruption and SZ (Kempermann et al., 2008). Telomere length maintenance during mitosis is essential in cells with a high turnover rate, which NSCs and particularly NPCs have (Klapper et al., 2001). Mice deficient in telomerase (TERT), the enzyme that maintains telomere length, have shorter telomeres and disrupted SVZ neurogenesis with additional deficits in behaviour dependent on this part of the brain (Ferrón et al., 2004). Schizophrenic patients also have reduced TERT activity (Kempermann et al., 2008). Work by Wolf and colleagues identified premature NPC senescence in the DG correlated with reduced telomere length, telomerase activity and behavioural deficits in open field test and sensorimotor gating in offspring of a "one-hit" animal MIA model exposed to a single prenatal Poly I:C challenge on GD15 (Wolf et al., 2011). Except for telomerase activity, these phenotypes were rescued by voluntary exercise, a known hippocampal neurogenesis stimulant (Fabel and Kempermann, 2008; Wolf et al., 2011; Zang et al., 2017). This highlights the possibility that telomerase activity could be responsible for the disease-related decline of hippocampal neurogenesis. Telomere length is already reduced with age, irrespective of any atypical behaviour diagnosis or genetic risk for psychiatric disorders (Palmos et al., 2018, 2020). MIA's acceleration of this phenomenon only exacerbates the reduction of hippocampal neurogenesis with age. Nevertheless, the question remains; how does MIA exacerbate telomerase shortening to indirectly pre-set atypical AHN?

In summary, AHN is significantly reduced in MIA-exposed adolescent and adult offspring. MIA has the potential to pre-set an alternative trajectory of an individual's capacity for AHN, through numerous mechanisms, summarised in Fig. 2. The resulting AHN capacity of an individual may then mediate their resilience or susceptibility to a secondary stressor exposure, which in turn has the potential to precipitate behavioural disorder and psychiatric illness. It may be hypothesised that if this trajectory dips below a certain critical threshold, psychiatric illness becomes increasingly likely.

3. The knowledge gap, and how to bridge it

Integrating the aforementioned evidence, we can see MIA causes reduced AHN at adolescent and adult timepoints by numerous mechanisms. Evidence for whether MIA-disrupted AHN mediates either resilience or susceptibility in either the "one-hit" MIA model or, more likely, the "two-hit" MIA plus stress model is now needed. Very few, if any, studies have addressed AHN capacity after both initial prenatal MIA and secondary peripubertal stressor exposure. A complex interplay of multiple factors contributes to the susceptibility or resilience to behavioural disorder in MIA-exposed offspring (Meyer, 2019; Mueller et al., 2021). Mueller and colleagues recently demonstrated the metrics measuring behaviour, transcriptomics, brain networks and cytokine profiles in adult isogenic mice offspring exposed to Poly I:C prenatally on GD12 clustered into two groups of offspring that were either susceptible or resilient to behavioural disorder (Mueller et al., 2021). The fact that within-litter offspring were not equally affected by MIA holds particular relevance when concluding outcomes of "one-hit" MIA models.

Adult offspring defined as susceptible to MIA could also be characterised by increased circulating levels of pro-inflammatory cytokines, including TNFα, IL-1β, and IL-6 (Mueller et al., 2021). Whether these peripheral changes occur in the brain and if they are present from early development, however, remains to be determined. The impact, therefore, on an individual's capacity for AHN could be affected by cytokine response and additional mechanisms to leave an offspring more or less vulnerable to stress exposure. In order to confirm the hypothesis that resilience and susceptibility to psychiatric illness is mediated by AHN following MIA, "two-hit" MIA plus stress animal models are essential to fill the knowledge gap (Fig. 3). Furthermore, our understanding of the extent to which atypical neurogenesis is provoked by MIA at the point of prenatal exposure in the developing embryonic hippocampus is incomplete. The use of human induced pluripotent stem cells could be used to bridge this knowledge gap, as well as translating the pre-collected animal data to a human context (Fig. 3).

3.1. Upgrading from "one-hit" to "two-hit" MIA models

The age at which neurodevelopment is vulnerable to risk is not exclusive to a single prenatal period, but also adolescence and adulthood

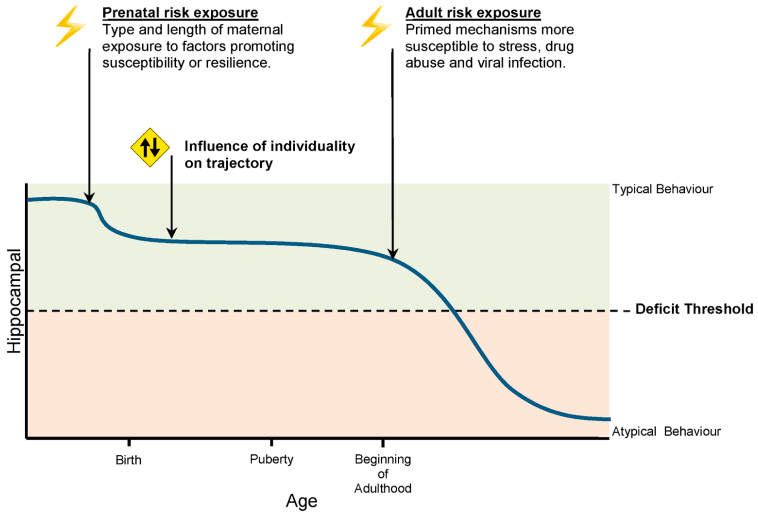

Fig. 2. The trajectory to atypical hippocampal neurogenesis. Once hippocampal neurogenesis surpasses a threshold, indicated by the dotted line, behavioural deficits are precipitated. Prenatal priming and individuality can influence the susceptibility to factors that cause neurogenesis trajectory to pass this threshold. Axes are not to scale. Graphics created with BioRender.com.

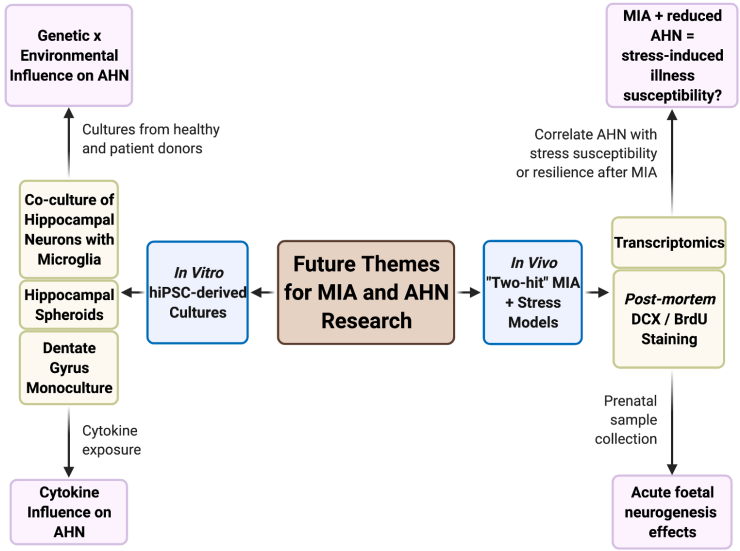

Fig. 3. Future themes for MIA and AHN research. To fill the knowledge gap in how AHN actually mediates susceptibility to stressors after prenatal MIA exposure, we suggest following two themes of modelling: *in vivo* "two-hit" animal models incorporating both MIA and stress exposure; and *in vitro* hiPSC-derived patient material to physiologically represent human hippocampal neurogenesis under the direct influence of cytokines or indirect microglia-released cytokines.

(Meyer, 2019). Postnatal exposure to secondary risk factors, such as drug abuse, systemic infection and stress, can result in the onset of psychiatric disorders (Kępińska et al., 2020; Giovanoli et al., 2013; Meyer, 2019; Bayer et al., 1999). This phenomenon, known as the "two-hit" hypothesis, may explain why some psychiatric illness precipitate in late adolescence or adulthood (Bayer et al., 1999). Animal MIA models exposed to repeated or chronic low dose immune stimulants may be more physiologically relevant to encapsulate the intricate interplay of exposure to the multiple risk factors experienced by humans, as well as post-natal stress exposure. It is important to understand whether AHN

plays a role in mediating the resilience or susceptibility to psychiatric illness onset after MIA exposure. Using "two-hit" animal models by incorporating both MIA prenatal insult with a secondary stressor, with subsequent investigation of potential differences in AHN, could aid in revealing the extent to which an individual's capacity for AHN dictates their susceptibility to psychiatric illness.

Correspondingly, "two-hit" models could reveal crucial time periods in which boosting AHN in high-risk patients could act as a prophylactic against psychiatric disorder onset. In fact, returning to existing *post-mortem* hippocampal sections and transcriptomic datasets from previous datasets using either a "two-hit" MIA plus stress approach or identification of MIA-resilient and -susceptible groups (Mueller et al., 2021; Ranaei et al., 2020) could immediately answer some of the following questions. Does an individual's capacity for AHN correlate with their susceptibility or resilience to behavioural disorder after prenatal MIA exposure? How would this kind of developmental design leave MIA models vulnerable to the risk of behavioural disorder in terms of risk priming? What are the implications for adult hippocampal neurogenic functionality after the combination of these types of stimuli?

3.2. hiPSC-Derived MIA models

Crucially, disparities in timing and dose of prenatal stimulation across comparative studies could be responsible for varying conclusions reached by animal MIA models. Variability in response to prenatal challenge originates from different rodent strains, gestational timing, dose, frequency, route of administration and batch of TLR3 or TLR4 agonists from different vendors (Mueller et al., 2019; Smolders et al., 2018). The molecular weight of Poly I:C can predict rat maternal IL-6 response and litter size, placental weight and male-specific reduction in foetal brain weights (Kowash et al., 2019). It is also vital to take into account both the timing of prenatal exposure and subsequent age of analysis, as variations in developmental timing can provide varying results since distinctive phases of pregnancy are susceptible to an assortment of environmental inputs at any one time (Allswede et al., 2020; Meyer, 2006). Consequently, questions surrounding the comparison of animal MIA models from multiple labs are raised, highlighting the importance of stimulant quality control for successful animal MIA models and accurate reporting of all model parameters, including housing and other variables (Kentner et al., 2019; Mueller et al., 2019).

Despite these caveats, it is striking to note the convergence of data across studies in MIA animal models providing converging evidence that AHN is reduced in adulthood following prenatal MIA exposure. Nevertheless, even though AHN is conserved across species, there are species-related differences that have to be taken into account (Kuhn et al., 2018). Animal brain development differs significantly from humans in terms of gene regulation networks and cellular proliferation pathways (Rockowitz and Zheng, 2015; Yokoyama et al., 2014). Hence, it cannot be assumed that the conclusions reached in animal MIA models will directly translate to human physiology. It is therefore important to complement this evidence base from animal models by using human based cellular models. Cell culture models are valuable tools to study biological mechanisms underlying health and disease in a controlled environment. It is important to keep in mind however, that cellular genotype plays a major role in the phenotypes observed *in vitro*, including, in the context of this review, shaping the cellular response to immune stimuluation *in vitro*. Of note then, the prevalence of subtle genetic variations in cell lines are not routinley characterised and taken into account when interpreting the data from *in vitro* studies of the effects of immune activation on neurogenesis. For example, the human hippocampal progenitor cell line (HPC0A07/03C) is frequently used as an *in vitro* model to study hippocampal neurogenesis (HN) (Borsini et al., 2018). A recent analysis of single nucleotide polymorphisms (SNPs) relevant to inflammation-related genes suggests that all stages of hippocampal neurogenesis may be negatively affected due to the genetic makeup of HPC0A07/03C cells following immune stimulation (Lee, 2021). Whilst these findings remain to be tested and validated experimentally, these data suggest a view that *in vitro* studies using such progenitor cell lines need to control for the genetic background of the cell line, since this could either mask or exacerbate findings (Lee, 2021). Taking this into account, we make the case for using human patient-derived material as a *complement* to animal and other cellular MIA modelling, specifically, hiPSCs. These cells offer many possibilities, as they can be differentiated into hippocampal granule neuron-like cells *in vitro* (Yu et al., 2014), as well as into different other neural or glial lineages and may be studied under either normal conditions or the influence of disease-causing immune exposure (Hoffman et al., 2019). Critically, the use of patient-derived material confers the important advantage of incorporating the various levels of polygenic risk in addition to environmental risk to further model the molecular mechanisms of MIA, particularly since many psychiatric illnesses share common genetic risk variants (O'Donovan and Owen, 2016). Importantly, in addition to using patient-derived cell lines, the use of genome editing may allow to investigate the role of specific genes in the effect of MIA on AHN on an isogenic background. Elucidating the genetic background of hiPSC lines is however still an important and necessary control.

As discussed in previous sections, epigenetic modifications might mediate the long-term effects of MIA and likely shape the cellular responses following subsequent exposures later in life, in line with "two-hit" hypothesis. Importantly, reservations do exist as to whether hiPSCs are a suitable model to assess epigenetic effects due to major epigenetic remodelling involved in their generation (Perrera and Martello, 2019). During differentiation, hiPSC-derived cells do undergo epigenetic remodelling (Bachmann et al., 2021; Su et al., 2021), and genome-wide DNA methylation patterns and gene expression patterns are preserved between neurons, derived from hiPSCs and human embryonic stem cells (de Boni, 2018). This provides confidence that hiPSC-derived cells would undergo MIA-associated epigenetic changes in similar manner as seen in *in vivo* models, thus making them a potentially useful model to investigate this. However, care should be taken to establish the baseline epigenetic signatures of the derived cell types to ensure valid like-with-like comparisons upon exposure to environmental stimuli.

A key barrier to the success of hiPSC modelling however, is the need to be able differentiate thse cells successfully into the relevant cell types, but also have the ability to capture interactions between such immature neurons with non-neuronal cells, such as microglia and/or endothelial and ependymal cells which form brain barriers *in vivo*, in a dish. Recently, Pomeshchik and colleagues have published a novel method of deriving hippocampal spheroids (HS) from hiPSCs which allows investigation of not only hippocampal neurons but also multiple stages of AHN, as well as other cell types within the neurogenic niche at a cellular and molecular level (Pomeshchik et al., 2020). While these hiPSC-derived HS have the advantage of incorporating multiple cell types, including both glia and neurons, the subsequent advancement would be to develop a model that features regional organisation of the hippocampus which has been attempted in part by a 2D model culturing both DG neurons and CA3 neurons in microfluidic chambers (Sarkar, 2018). To uncover the molecular effect of immune challenge on developing foetal hippocampal neurons, hiPSC-derived HS or NPC cultures could be exposed to an immune challenge from infectious viral particles, non-infectious mimic or cytokines as mirrored by studies (Claus et al., 2020; Dang et al., 2016; Sun et al., 2020; Warre-Cornish et al., 2020). As a further proof of concept investigated in hiPSC-derived cortical cultures, treatment of developing cortical NPCs with IFNγ induced widespread transcriptional changes that overlap with gene expression signatures measured in human *post-mortem* brain tissue from ASD and SZ patients, as well as increased neurite outgrowth, a hallmark phenotype of hiPSC-neurons derived from donors with genetic risk factors for ASD such as Shank-3 deletion (Schafer et al., 2019; Warre-Cornish et al., 2020).

The detrimental direct and indirect effects of cytokines released from activated microglia on AHN are clearly important to the mechanism by

which an individual becomes predisposed to psychiatric illness after MIA exposure. These mechanisms can be adequately modelled at a cellular and molecular level either using organoids or co-culture of hiPSC-derived hippocampal neurons or NPCs and microglia. The interaction of microglia with hippocampal neurogenesis *in vitro* could be modelled in a number of ways, including monoculture conditioned media experiments, co-culture by physical separation, 2D, 3D-scaffold or even 3D-organoid culture (Hedegaard et al., 2020; Pellegrini et al., 2020). Such organoid cultures are becoming so complex, that they are able to derive the correct morphology, maturation and function of the choroid plexus (Pellegrini et al., 2020). Similar to the aforementioned studies, cultures could then be exposed to a singular or mixtures of cytokines to reveal the molecular mechanisms by which microglia exert a direct or indirect effect on hippocampal neurogenesis. Yet, clearly, different hiPSC model systems will be required to address the complex interactions between MIA and AHN *in vitro*, depending on the experimental question.

While hiPSC-derived models are highly suitable to study developmental effects, the relative immaturity characteristics of hiPSC-derived cultures make it difficult to assess the molecular effect of MIA on hippocampal neurogenesis during adulthood. To overcome this technical issue, it might be worth artificially ageing the *in vitro* model (Mertens et al., 2018). This can be done using various strategies; by manipulation of age-related genes or telomerases (Cozzi et al., 2019; Liang, 2020; Miller et al., 2013; Vera et al., 2016), by exposure to x-ray irradiation (Carlessi et al., 2009; Schneider et al., 2013; Schneider and Zheng, 2014; Zhu et al., 2019; Limbad et al., 2020), hydroxyurea (Daniele et al., 2016; de Lucia et al., 2020; Dong et al., 2014), repeated passaging (de Lucia et al., 2020; Han et al., 2021; Liu et al., 2012; Zhu et al., 2019) or long term culture (Daniele et al., 2020; Bigagli et al., 2016) to induce senescence-like changes into the hiPSC-derived cultures for a more aged-like phenotype.

4. Conclusion

Reduced AHN is linked closely to risk and resilience for psychiatric illness. Animal and *in vitro* MIA models indicate prenatal immune exposure reduces AHN through multiple mechanisms. We advance the hypothesis that, mediated by AHN, MIA renders an individual susceptible to additional "hits" such as stress. Combined this may be one important mechanism by which prenatal programming predisposes an individual's risk for psychiatric illnesses. Once the accumulation of risk factors promoting susceptibility to hippocampal neurogenic deficits reaches a threshold, atypical behaviour ensues. However, the exact molecular mechanism and timing by which MIA primes latent dysfunction in hippocampal neurogenesis, plus the role of genetic interaction, remains to be found. Complementary research lines exposing animals to a "two-hit" MIA plus stressor experience and complimentary studies using relevant hiPSC-derived cultures exposed to cytokines are required to confirm or refute this hypothesis. Such studies have the potential to also uncover the mechanisms by which MIA confers susceptibility or resilience to psychiatric disorders, and the extent to which AHN mediates this risk.

Declaration of Competing Interest

The authors declare that they have no known competing financial interests or personal relationships that could have appeared to influence the work reported in this paper.

Acknowledgements

AC: conception and design, literature searching, manuscript writing. TB, BH and RM: manuscript writing and editing. DPS and ST: manuscript writing, editing and financial support. AV: conception and design, manuscript writing, financial support, final approval of manuscript. AC, DPS and ACV acknowledge financial support for this study from the National Centre for the Replacement, Refinement and Reduction of Animals in Research (NC/S001506/1). The work (at King's College, London) was also supported by the Medical Research Council (MRC) Centre grant (MR/N026063/1). TB is in receipt of a PhD studentship funded by the National Institute for Health Research (NIHR) Biomedical Research Centre at South London and Maudsley NHS Foundation Trust and King's College London. ST's lab is partly funded by MRC research grants MR/N030087/1 and MR/S00484X/1. RM is in receipt of the MRC-Sackler PhD Programme studentship as part of the MRC Centre for Neurodevelopmental Disorders (Medical Research Council MR/P502108/1).

References

Kuhn, H.G., Toda, T., Gage, F.H., 2018. Adult hippocampal neurogenesis: A coming-of-age story. J. Neurosci. 38 (49), 10401–10410.
Altman, J., Das, G.D., 1965. Autoradiographic and histological evidence of postnatal hippocampal neurogenesis in rats. Journal of Comparative Neurology 124 (3), 319–335.
Eriksson, P.S., Perfilieva, E., Björk-Eriksson, T., Alborn, A.-M., Nordborg, C., Peterson, D. A., Gage, F.H., 1998. Neurogenesis in the adult human hippocampus. Nat. Med. 4 (11), 1313–1317.
Spalding, K., Bergmann, O., Alkass, K., Bernard, S., Salehpour, M., Huttner, H., Boström, E., Westerlund, I., Vial, C., Buchholz, B., Possnert, G., Mash, D., Druid, H., Frisén, J., 2013. Dynamics of hippocampal neurogenesis in adult humans. Cell 153 (6), 1219–1227.
Sorrells, S.F., Paredes, M.F., Cebrian-Silla, A., Sandoval, K., Qi, D., Kelley, K.W., James, D., Mayer, S., Chang, J., Auguste, K.I., Chang, E.F., Gutierrez, A.J., Kriegstein, A.R., Mathern, G.W., Oldham, M.C., Huang, E.J., Garcia-Verdugo, J.M., Yang, Z., Alvarez-Buylla, A., 2018. Human hippocampal neurogenesis drops sharply in children to undetectable levels in adults. Nature 555 (7696), 377–381.
Tobin, M.K., Musaraca, K., Disouky, A., Shetti, A., Bheri, A., Honer, W.G., Kim, N., Dawe, R.J., Bennett, D.A., Arfanakis, K., Lazarov, O., 2019. Human Hippocampal Neurogenesis Persists in Aged Adults and Alzheimer's Disease Patients. Cell Stem Cell 24 (6), 974–982.e3.
Moreno-Jiménez, E.P., Flor-García, M., Terreros-Roncal, J., Rábano, A., Cafini, F., Pallas-Bazarra, N., Ávila, J., Llorens-Martín, M., 2019. Adult hippocampal neurogenesis is abundant in neurologically healthy subjects and drops sharply in patients with Alzheimer's disease. Nat. Med. 25 (4), 554–560.
Boldrini, M., Fulmore, C.A., Tartt, A.N., Simeon, L.R., Pavlova, I., Poposka, V., Rosoklija, G.B., Stankov, A., Arango, V., Dwork, A.J., Hen, R., Mann, J.J., 2018. Human Hippocampal Neurogenesis Persists throughout Aging. Cell Stem Cell 22 (4), 589–599.e5.
Kempermann, G., Gage, F.H., Aigner, L., Song, H., Curtis, M.A., Thuret, S., Kuhn, H.G., Jessberger, S., Frankland, P.W., Cameron, H.A., Gould, E., Hen, R., Abrous, D.N., Toni, N., Schinder, A.F., Zhao, X., Lucassen, P.J., Frisén, J., 2018. Human Adult Neurogenesis: Evidence and Remaining Questions. Cell Stem Cell 23 (1), 25–30.
Sorrells, S.F., Paredes, M.F., Zhang, Z., Kang, G., Pastor-Alonso, O., Biagiotti, S., Page, C. E., Sandoval, K., Knox, A., Connolly, A., Huang, E.J., Garcia-Verdugo, J.M., Oldham, M.C., Yang, Z., Alvarez-Buylla, A., 2021. Positive controls in adults and children support that very few, if any, new neurons are born in the adult human hippocampus. J. Neurosci. 41 (12), 2554–2565.
Lee, H., Thuret, S., 2018. Adult Human Hippocampal Neurogenesis: Controversy and Evidence. Trends Mol. Med. 24 (6), 521–522.
Abrous, D.N., Koehl, M., Lemoine, M., 2021. A Baldwin interpretation of adult hippocampal neurogenesis: from functional relevance to physiopathology. Mol. Psychiatry 1–20. https://doi.org/10.1038/s41380-021-01172-4.
Dupret, D. et al. Spatial relational memory requires hippocampal adult neurogenesis. PLoS ONE 3, 1959 (2008).
Sasaki, T., Piatti, V.C., Hwaun, E., Ahmadi, S., Lisman, J.E., Leutgeb, S., Leutgeb, J.K., 2018. Dentate network activity is necessary for spatial working memory by supporting CA3 sharp-wave ripple generation and prospective firing of CA3 neurons. Nat. Neurosci. 21 (2), 258–269.
Toda, T., Parylak, S.L., Linker, S.B., Gage, F.H., 2019. The role of adult hippocampal neurogenesis in brain health and disease. Mol. Psychiatry 24 (1), 67–87.
Bartsch, T., Wulff, P., 2015. The hippocampus in aging and disease: From plasticity to vulnerability. Neuroscience 309, 1–16.
Syed, S.A., Nemeroff, C.B., 2017. Early Life Stress, Mood, and Anxiety Disorders. Chronic Stress 1, 1–16.
Kempermann, G., Krebs, J., Fabel, K., 2008. The contribution of failing adult hippocampal neurogenesis to psychiatric disorders. Current Opinion in Psychiatry 21, 290–295.
Kang, E., Wen, Z., Song, H., Christian, K.M., Ming, G.-l., 2016. Adult neurogenesis and psychiatric disorders. Cold Spring Harbor Perspect. Biol. 8 (9), a019026. https://doi.org/10.1101/cshperspect.a019026.
Anacker, C., 2014. Adult hippocampal neurogenesis in depression: Behavioral implications and regulation by the stress system. Current Topics in Behavioral Neurosciences 18, 25–43.
Yamasaki, N., Maekawa, M., Kobayashi, K., Kajii, Y., Maeda, J., Soma, M., Takao, K., Tanda, K., Ohira, K., Toyama, K., Kanzaki, K., Fukunaga, K., Sudo, Y., Ichinose, H., Ikeda, M., Iwata, N., Ozaki, N., Suzuki, H., Higuchi, M., Suhara, T., Yuasa, S.,

Miyakawa, T., 2008. Alpha-CaMKII deficiency causes immature dentate gyrus, a novel candidate endophenotype of psychiatric disorders. Molecular brain 1 (1), 6. https://doi.org/10.1186/1756-6606-1-6.
Eliwa, H., Brizard, B., Le Guisquet, A.-M., Hen, R., Belzung, C., Surget, A., 2021. Adult neurogenesis augmentation attenuates anhedonia and HPA axis dysregulation in a mouse model of chronic stress and depression. Psychoneuroendocrinology 124, 105097. https://doi.org/10.1016/j.psyneuen.2020.105097.
Hagihara, H., Takao, K., Walton, N.M., Matsumoto, M., Miyakawa, T., 2013. Immature dentate gyrus: An endophenotype of neuropsychiatric disorders. Neural Plasticity 2013, 1–24.
Tunc-Ozcan, E., Peng, C.-Y., Zhu, Y., Dunlop, S.R., Contractor, A., Kessler, J.A., 2019. Activating newborn neurons suppresses depression and anxiety-like behaviors. Nat. Commun. 10 (1) https://doi.org/10.1038/s41467-019-11641-8.
Anacker, C., Luna, V.M., Stevens, G.S., Millette, A., Shores, R., Jimenez, J.C., Chen, B., Hen, R., 2018. Hippocampal neurogenesis confers stress resilience by inhibiting the ventral dentate gyrus. Nature 559 (7712), 98–102.
Yam, K.-Y., Schipper, L., Reemst, K., Ruigrok, S.R., Abbink, M.R., Hoeijmakers, L., Naninck, E.F.G., Zarekiani, P., Oosting, A., Van Der Beek, E.M., Lucassen, P.J., Korosi, A., 2019. Increasing availability of ω-3 fatty acid in the early-life diet prevents the early-life stress-induced cognitive impairments without affecting metabolic alterations. FASEB J. 33 (4), 5729–5740.
Boldrini, M., Galfalvy, H., Dwork, A.J., Rosoklija, G.B., Trencevska-Ivanovska, I., Pavlovski, G., Hen, R., Arango, V., Mann, J.J., 2019. Resilience Is Associated With Larger Dentate Gyrus, While Suicide Decedents With Major Depressive Disorder Have Fewer Granule Neurons. Biol. Psychiatry 85 (10), 850–862.
Costello, E.J., Compton, S.N., Keeler, G., Angold, A., 2003. Relationships between Poverty and Psychopathology: A Natural Experiment. J. Am. Med. Assoc. 290 (15), 2023. https://doi.org/10.1001/jama.290.15.2023.
Sarason, I.G., Johnson, J.H., Siegel, J.M., 1978. Assessing the impact of life changes: Development of the Life Experiences Survey. J. Consult. Clin. Psychol. 46 (5), 932–946.
Heim, C., et al., 2000. Pituitary-adrenal and automatic responses to stress in women after sexual and physical abuse in childhood. J. Am. Med. Assoc. 284, 592–597.
Andrews, J.G., Andrews, G., Tennant, C., 1978. Editorial: Life event stress and psychiatric illness. Psychol. Med. 8, 545–549.
Cattane, N., Richetto, J., Cattaneo, A., 2020. Prenatal exposure to environmental insults and enhanced risk of developing Schizophrenia and Autism Spectrum Disorder: focus on biological pathways and epigenetic mechanisms. Neurosci. Biobehav. Rev. 117, 253–278.
Kępińska, A.P., Iyegbe, C.O., Vernon, A.C., Yolken, R., Murray, R.M., Pollak, T.A., 2020. Schizophrenia and Influenza at the Centenary of the 1918–1919 Spanish Influenza Pandemic: Mechanisms of Psychosis Risk. Front. Psychiatry 11. https://doi.org/10.3389/fpsyt.2020.00072.
Knuesel, I., Chicha, L., Britschgi, M., Schobel, S.A., Bodmer, M., Hellings, J.A., Toovey, S., Prinssen, E.P., 2014. Maternal immune activation and abnormal brain development across CNS disorders. Nature Reviews Neurology 10 (11), 643–660.
Estes, M.L., McAllister, A.K., 2016. Maternal immune activation: Implications for neuropsychiatric disorders. Science 353 (6301), 772–777.
Bilbo, S.D., Schwarz, J.M., 2012. The immune system and developmental programming of brain and behavior. Front. Neuroendocrinol. 33 (3), 267–286.
Kempermann, G., 2019. Environmental enrichment, new neurons and the neurobiology of individuality. Nat. Rev. Neurosci. 20 (4), 235–245.
Mueller, F.S., Scarborough, J., Schalbetter, S.M., Richetto, J., Kim, E., Couch, A., Yee, Y., Lerch, J.P., Vernon, A.C., Weber-Stadlbauer, U., Meyer, U., 2021. Behavioral, neuroanatomical, and molecular correlates of resilience and susceptibility to maternal immune activation. Mol. Psychiatry 26 (2), 396–410.
Ranaei, E., Torshizi, S., Amini, A., Heidari, M.H., Namvarpour, Z., Fathabady, F.F., Salari, A.-A., 2020. Peripubertal stress following maternal immune activation sex-dependently alters depression-like behaviors in offspring. Behav. Brain Res. 393, 112800. https://doi.org/10.1016/j.bbr.2020.112800.
Giovanoli, S., Engler, H., Engler, A., Richetto, J., Voget, M., Willi, R., Winter, C., Riva, M. A., Mortensen, P.B., Feldon, J., Schedlowski, M., Meyer, U., 2013. Stress in puberty unmasks latent neuropathological consequences of prenatal immune activation in mice. Science 339 (6123), 1095–1099.
Kempermann, G., Gage, F.H., 1999. New nerve cells for the adult brain. Sci. Am. 280 (5), 48–53.
Pan, W.L., Chopp, M., Fan, B., Zhang, R., Wang, X., Hu, J., Zhang, X.M., Zhang, Z.G., Liu, X.S., 2019. Ablation of the microRNA-17-92 cluster in neural stem cells diminishes adult hippocampal neurogenesis and cognitive function. FASEB J. 33 (4), 5257–5267.
Berdugo-Vega, G., Arias-Gil, G., López-Fernández, A., Artegiani, B., Wasielewska, J.M., Lee, C.-C., Lippert, M.T., Kempermann, G., Takagaki, K., Calegari, F., 2020. Increasing neurogenesis refines hippocampal activity rejuvenating navigational learning strategies and contextual memory throughout life. Nat. Commun. 11 (1) https://doi.org/10.1038/s41467-019-14026-z.
Gergues, M. M., Yohn, C. N., Levinstein, M. R. & Samuels, B. A. Dentate gyrus activin signaling mediates the antidepressant treatment response. bioRxiv 491613 (2018) doi:10.1101/491613.
Meyer, U., 2019. Neurodevelopmental Resilience and Susceptibility to Maternal Immune Activation. Trends Neurosci. 42 (11), 793–806.
Piontkewitz, Y., Arad, M., Weiner, I., 2011. Abnormal trajectories of neurodevelopment and behavior following in utero insult in the rat. Biol. Psychiatry 70 (9), 842–851.
Crum, W.R., et al., 2017. Evolution of structural abnormalities in the rat brain following in utero exposure to maternal immune activation: A longitudinal in vivo MRI study. Brain Behav. Immun. 63.
Meyer, U., 2014. Prenatal Poly(I:C) exposure and other developmental immune activation models in rodent systems. Biol. Psychiatry 75 (4), 307–315.
Malaspina, D., Corcoran, C., Kleinhaus, K.R., Perrin, M.C., Fennig, S., Nahon, D., Friedlander, Y., Harlap, S., 2008. Acute maternal stress in pregnancy and schizophrenia in offspring: A cohort prospective study. BMC Psychiatry 8 (1). https://doi.org/10.1186/1471-244X-8-71.
Brown, A.S., Conway, F., 2019. Maternal immune activation and related factors in the risk of offspring psychiatric disorders. Front. Psychiatry 10.
Huttunen, M.O., 1978. Prenatal Loss of Father and Psychiatric Disorders. Arch. Gen. Psychiatry 35 (4), 429. https://doi.org/10.1001/archpsyc.1978.01770280039004.
Gilman, S. E. et al. Socioeconomic disadvantage, gestational immune activity, and neurodevelopment in early childhood. Proceedings of the National Academy of Sciences of the United States of America 114, (2017).
Claus, C., Jung, M., Hübschen, J.M., 2020. Pluripotent Stem Cell-Based Models: A Peephole into Virus Infections during Early Pregnancy. Cells 9 (3), 542. https://doi.org/10.3390/cells9030542.
Allswede, D.M., Yolken, R.H., Buka, S.L., Cannon, T.D., 2020. Cytokine concentrations throughout pregnancy and risk for psychosis in adult offspring: a longitudinal case-control study. The Lancet Psychiatry 7 (3), 254–261.
Adam, M.P., 2012. The all-or-none phenomenon revisited. Birth Defects Research Part A - Clinical and Molecular Teratology 94, 664–669.
Goldstein, J. M. et al. Impact of prenatal maternal cytokine exposure on sex differences in brain circuitry regulating stress in offspring 45 years later. Proceedings of the National Academy of Sciences of the United States of America 118, (2021).
Rasmussen, J.M., Graham, A.M., Entringer, S., Gilmore, J.H., Styner, M., Fair, D.A., Wadhwa, P.D., Buss, C., 2019. Maternal Interleukin-6 concentration during pregnancy is associated with variation in frontolimbic white matter and cognitive development in early life. NeuroImage 185, 825–835.
Rudolph, M.D., Graham, A.M., Feczko, E., Miranda-Dominguez, O., Rasmussen, J.M., Nardos, R., Entringer, S., Wadhwa, P.D., Buss, C., Fair, D.A., 2018. Maternal IL-6 during pregnancy can be estimated from newborn brain connectivity and predicts future working memory in offspring. Nat. Neurosci. 21 (5), 765–772.
Graham, A.M., Rasmussen, J.M., Rudolph, M.D., Heim, C.M., Gilmore, J.H., Styner, M., Potkin, S.G., Entringer, S., Wadhwa, P.D., Fair, D.A., Buss, C., 2018. Maternal Systemic Interleukin-6 During Pregnancy Is Associated With Newborn Amygdala Phenotypes and Subsequent Behavior at 2 Years of Age. Biol. Psychiatry 83 (2), 109–119.
Zaretsky, M.V., Alexander, J.M., Byrd, W., Bawdon, R.E., 2004. Transfer of inflammatory cytokines across the placenta. Obstet. Gynecol. 103 (3), 546–550.
Smith, S.E.P., Li, J., Garbett, K., Mirnics, K., Patterson, P.H., 2007. Maternal immune activation alters fetal brain development through interleukin-6. J. Neurosci. 27 (40), 10695–10702.
Lee, Y., Awasthi, A., Yosef, N., Quintana, F.J., Xiao, S., Peters, A., Wu, C., Kleinewietfeld, M., Kunder, S., Hafler, D.A., Sobel, R.A., Regev, A., Kuchroo, V.K., 2012. Induction and molecular signature of pathogenic T H 17 cells. Nat. Immunol. 13 (10), 991–999.
Choi, G.B., Yim, Y.S., Wong, H., Kim, S., Kim, H., Kim, S.V., Hoeffer, C.A., Littman, D.R., Huh, J.R., 2016. The maternal interleukin-17a pathway in mice promotes autism-like phenotypes in offspring. Science 351 (6276), 933–939.
Traglia, M., Croen, L.A., Jones, K.L., Heuer, L.S., Yolken, R., Kharrazi, M., DeLorenze, G. N., Ashwood, P., Van de Water, J., Weiss, L.A., 2018. Cross-genetic determination of maternal and neonatal immune mediators during pregnancy. Genome Med. 10 (1) https://doi.org/10.1186/s13073-018-0576-8.
Bayer, T.A., Falkai, P., Maier, W., 1999. Genetic and non-genetic vulnerability factors in schizophrenia: The basis of the "Two hit hypothesis". J. Psychiatr. Res. 33 (6), 543–548.
Giovanoli, S., Notter, T., Richetto, J., Labouesse, M.A., Vuillermot, S., Riva, M.A., Meyer, U., 2015. Late prenatal immune activation causes hippocampal deficits in the absence of persistent inflammation across aging. Journal of Neuroinflammation 12 (1). https://doi.org/10.1186/s12974-015-0437-y.
Rook, G.A., 2013. Regulation of the immune system by biodiversity from the natural environment: An ecosystem service essential to health. PNAS 110 (46), 18360–18367.
Berger, T., Lee, H., Young, A. H., Aarsland, D. & Thuret, S. Adult Hippocampal Neurogenesis in Major Depressive Disorder and Alzheimer's Disease. Trends in Molecular Medicine 26, 803–818 (2020).
Brown, A.S., Meyer, U., 2018. Maternal immune activation and neuropsychiatric illness: A translational research perspective. Am. J. Psychiatry 175 (11), 1073–1083.
Musaelyan, K., Egeland, M., Fernandes, C., Pariante, C.M., Zunszain, P.A., Thuret, S., 2014. Modulation of adult hippocampal neurogenesis by early-life environmental challenges triggering immune activation. Neural Plasticity 2014, 1–10.
Antonson, A., Balakrishnan, B., Radlowski, E., Petr, G., Johnson, R., 2018. Altered hippocampal gene expression and morphology in fetal piglets following maternal respiratory viral infection. Dev. Neurosci. 40 (2), 104–119.
Dang, J., Tiwari, S.K., Lichinchi, G., Qin, Y., Patil, V., Eroshkin, A., Rana, T., 2016. Zika Virus Depletes Neural Progenitors in Human Cerebral Organoids through Activation of the Innate Immune Receptor TLR3. Cell Stem Cell 19 (2), 258–265.
Sun, G., Chiuppesi, F., Chen, X., Wang, C., Tian, E., Nguyen, J., Kha, M., Trinh, D., Zhang, H., Marchetto, M.C., Song, H., Ming, G.-L., Gage, F.H., Diamond, D.J., Wussow, F., Shi, Y., 2020. Modeling Human Cytomegalovirus-Induced Microcephaly in Human iPSC-Derived Brain Organoids. Cell Reports Medicine 1 (1), 100002. https://doi.org/10.1016/j.xcrm.2020.100002.
Meyer, U., 2006. The time of prenatal immune challenge determines the specificity of inflammation-mediated brain and behavioral pathology. J. Neurosci. 26 (18), 4752–4762.

Seguin, J.A., Brennan, J., Mangano, E., Hayley, S., 2009. Proinflammatory cytokines differentially influence adult hippocampal cell proliferation depending upon the route and chronicity of administration. Neuropsychiatr. Dis. Treat. 5, 5–14.

Li, W., Sun, F., Guo, X., Hu, Y., Ding, S., Ding, M., Song, M., Shao, M., Yang, Y., Guo, W., Zhang, L., Zhang, Y., Wang, X., Su, X.i., Lv, L., 2020. Behavioral abnormalities and phosphorylation deficits of extracellular signal-regulated kinases 1 and 2 in rat offspring of the maternal immune activation model. Physiol. Behav. 217, 112805. https://doi.org/10.1016/j.physbeh.2020.112805.

Sheu, J.-R., Hsieh, C.-Y., Jayakumar, T., Tseng, M.-F., Lee, H.-N., Huang, S.-W., Manubolu, M., Yang, C.-H., 2019. A critical period for the development of schizophrenia-like pathology by aberrant postnatal neurogenesis. Front. Neurosci. 13 https://doi.org/10.3389/fnins.2019.00635.

Zhao, Q., Wang, Q., Wang, J., Tang, M., Huang, S., Peng, K.e., Han, Y., Zhang, J., Liu, G., Fang, Q.i., You, Z., 2019. Maternal immune activation-induced PPARγ-dependent dysfunction of microglia associated with neurogenic impairment and aberrant postnatal behaviors in offspring. Neurobiology of Disease 125, 1–13.

Depino, A.M., 2015. Early prenatal exposure to LPS results in anxiety- and depression-related behaviors in adulthood. Neuroscience 299, 56–65.

Zhang, Z., van Praag, H., 2015. Maternal immune activation differentially impacts mature and adult-born hippocampal neurons in male mice. Brain Behav. Immun. 45, 60–70.

Mattei, D., Djodari-Irani, A., Hadar, R., Pelz, A., de Cossío, L.F., Goetz, T., Matyash, M., Kettenmann, H., Winter, C., Wolf, S.A., 2014. Minocycline rescues decrease in neurogenesis, increase in microglia cytokines and deficits in sensorimotor gating in an animal model of schizophrenia. Brain Behav. Immun. 38, 175–184.

Wolf, S.A., Melnik, A., Kempermann, G., 2011. Physical exercise increases adult neurogenesis and telomerase activity, and improves behavioral deficits in a mouse model of schizophrenia. Brain Behav. Immun. 25 (5), 971–980.

Mouihate, A., 2016. Prenatal activation of toll-like receptor-4 dampens adult hippocampal neurogenesis in an IL-6 dependent manner. Front. Cell. Neurosci. 10.

Melnik, A., Tauber, S., Dumrese, C., Ullrich, O., Wolf, S.A., 2012. Murine adult neural progenitor cells alter their proliferative behavior and gene expression after the activation of toll-like-receptor 3. European Journal of Microbiology and Immunology 2 (3), 239–248.

Piontkewitz, Y., Bernstein, H.-G., Dobrowolny, H., Bogerts, B., Weiner, I., Keilhoff, G., 2012. Effects of risperidone treatment in adolescence on hippocampal neurogenesis, parvalbumin expression, and vascularization following prenatal immune activation in rats. Brain Behav. Immun. 26 (2), 353–363.

GILMORE, J., FREDRIKJARSKOG, L., 1997. Exposure to infection and brain development: cytokines in the pathogenesis of schizophrenia. Schizophr. Res. 24 (3), 365–367.

Ashdown, H., Dumont, Y., Ng, M., Poole, S., Boksa, P., Luheshi, G.N., 2006. The role of cytokines in mediating effects of prenatal infection on the fetus: Implications for schizophrenia. Mol. Psychiatry 11 (1), 47–55.

Ben-Yehuda, H., Matcovitch-Natan, O., Kertser, A., Spinrad, A., Prinz, M., Amit, I., Schwartz, M., 2020. Maternal Type-I interferon signaling adversely affects the microglia and the behavior of the offspring accompanied by increased sensitivity to stress. Mol. Psychiatry 25 (5), 1050–1067.

Borsini, A. et al. Interferon-alpha reduces human hippocampal neurogenesis and increases apoptosis via activation of distinct STAT1-dependent mechanisms. International Journal of Neuropsychopharmacology 21, 187–200 (2018).

Kaneko, N., Nakamura, S., Sawamoto, K., 2020. Effects of interferon-alpha on hippocampal neurogenesis and behavior in common marmosets. Molecular Brain 13 (1). https://doi.org/10.1186/s13041-020-00639-9.

Entringer, S., Buss, C. & Wadhwa, P. D. Prenatal stress, development, health and disease risk: A psychobiological perspective-2015. Psychoneuroendocrinology 62, 366–75 (2015).

Erta, M., Quintana, A., Hidalgo, J., 2012. Interleukin-6, a major cytokine in the central nervous system. International Journal of Biological Sciences 8 (9), 1254–1266.

Zuiki, M., Chiyonobu, T., Yoshida, M., Maeda, H., Yamashita, S., Kidowaki, S., Hasegawa, T., Gotoh, H., Nomura, T., Ono, K., Hosoi, H., Morimoto, M., 2017. Luteolin attenuates interleukin-6-mediated astrogliosis in human iPSC-derived neural aggregates: A candidate preventive substance for maternal immune activation-induced abnormalities. Neurosci. Lett. 653, 296–301.

Hodge, D.R., Xiao, W., Clausen, P.A., Heidecker, G., Szyf, M., Farrar, W.L., 2001. Interleukin-6 Regulation of the Human DNA Methyltransferase (HDNMT) Gene in Human Erythroleukemia Cells. J. Biol. Chem. 276 (43), 39508–39511.

Zhang, R.-R., Cui, Q.-Y., Murai, K., Lim, Y., Smith, Z., Jin, S., Ye, P., Rosa, L., Lee, Y., Wu, H.-P., Liu, W., Xu, Z.-M., Yang, L.u., Ding, Y.-Q., Tang, F., Meissner, A., Ding, C., Shi, Y., Xu, G.-L., 2013. Tet1 regulates adult hippocampal neurogenesis and cognition. Cell Stem Cell 13 (2), 237–245.

Jessop, P., Toledo-Rodriguez, M., 2018. Hippocampal TET1 and TET2 expression and DNA hydroxymethylation are affected by physical exercise in aged mice. Front. Cell Dev. Biol. 6.

Richetto, J., Massart, R., Weber-Stadlbauer, U., Szyf, M., Riva, M.A., Meyer, U., 2017. Genome-wide DNA Methylation Changes in a Mouse Model of Infection-Mediated Neurodevelopmental Disorders. Biol. Psychiatry 81 (3), 265–276.

Anacker, C., Hen, R., 2017. Adult hippocampal neurogenesis and cognitive flexibility-linking memory and mood. Nat. Rev. Neurosci. 18 (6), 335–346.

Patrich, E., Piontkewitz, Y., Peretz, A., Weiner, I., Attali, B., 2016. Maternal immune activation produces neonatal excitability defects in offspring hippocampal neurons from pregnant rats treated with poly I:C. Sci. Rep. 6 (1) https://doi.org/10.1038/srep19106.

Häfner, H., Maurer, K., Löffler, W., Fätkenheuer, B., Heiden, W.A.D., Riecher-Rössler, A., Behrens, S., Gattaz, W.F., 1994. The epidemiology of early schizophrenia. Influence of age and gender on onset and early course. Br. J. Psychiatry 164 (S23), 29–38.

Mondelli, V., Vernon, A.C., Turkheimer, F., Dazzan, P., Pariante, C.M., 2017. Brain microglia in psychiatric disorders. The Lancet Psychiatry 4 (7), 563–572.

Hanger, B., Couch, A., Rajendran, L., Srivastava, D.P., Vernon, A.C., 2020. Emerging Developments in Human Induced Pluripotent Stem Cell-Derived Microglia: Implications for Modelling Psychiatric Disorders With a Neurodevelopmental Origin. Front. Psychiatry 11, 789.

Matcovitch-Natan, O. et al. Microglia development follows a stepwise program to regulate brain homeostasis. Science (2016) doi:10.1126/science.aad8670.

Sharma, K., Tremblay, M.-E., 2020. Microglia: Multiple states and multiple roles in the normal and diseased brain and spinal cord. Neurosci. Lett. 729, 135019. https://doi.org/10.1016/j.neulet.2020.135019.

Barres, B.A., 2008. The Mystery and Magic of Glia: A Perspective on Their Roles in Health and Disease. Neuron 60 (3), 430–440.

Sierra, A., Beccari, S., Diaz-Aparicio, I., Encinas, J.M., Comeau, S., Tremblay, M.-È., 2014. Surveillance, phagocytosis, and inflammation: How never-resting microglia influence adult hippocampal neurogenesis. Neural Plasticity 2014, 1–15.

Ekdahl, C.T., Kokaia, Z., Lindvall, O., 2009. Brain inflammation and adult neurogenesis: The dual role of microglia. Neuroscience 158 (3), 1021–1029.

Gemma, C., Bachstetter, A.D., 2013. The role of microglia in adult hippocampal neurogenesis. Front. Cell. Neurosci. 7.

Monje, M.L., Toda, H., Palmer, T.D., 2003. Inflammatory Blockade Restores Adult Hippocampal Neurogenesis. Science 302, 1760–1765.

Han, Y., Zhang, L., Wang, Q., Zhang, D., Zhao, Q., Zhang, J., Xie, L., Liu, G., You, Z., 2019. Minocycline inhibits microglial activation and alleviates depressive-like behaviors in male adolescent mice subjected to maternal separation. Psychoneuroendocrinology 107, 37–45.

Zhang, J., Rong, P., Zhang, L., He, H., Zhou, T., Fan, Y., Mo, L.i., Zhao, Q., Han, Y., Li, S., Wang, Y., Yan, W., Chen, H., You, Z., 2021. IL4-driven microglia modulate stress resilience through BDNF-dependent neurogenesis. Sci. Adv. 7 (12), eabb9888. https://doi.org/10.1126/sciadv.abb9888.

Garay, P.A., Hsiao, E.Y., Patterson, P.H., McAllister, A.K., 2013. Maternal immune activation causes age- and region-specific changes in brain cytokines in offspring throughout development. Brain Behav. Immun. 31, 54–68.

Zhang, Y.e., Sloan, S., Clarke, L., Caneda, C., Plaza, C., Blumenthal, P., Vogel, H., Steinberg, G., Edwards, M.B., Li, G., Duncan, J., Cheshier, S., Shuer, L., Chang, E., Grant, G., Gephart, M.H., Barres, B., 2016. Purification and Characterization of Progenitor and Mature Human Astrocytes Reveals Transcriptional and Functional Differences with Mouse. Neuron 89 (1), 37–53.

Missault, S., Van den Eynde, K., Vanden Berghe, W., Fransen, E., Weeren, A., Timmermans, J.P., Kumar-Singh, S., Dedeurwaerdere, S., 2014. The risk for behavioural deficits is determined by the maternal immune response to prenatal immune challenge in a neurodevelopmental model. Brain Behav. Immun. 42, 138–146.

Bilbo, S.D., 2005. Neonatal infection-induced memory impairment after lipopolysaccharide in adulthood is prevented via caspase-1 inhibition. J. Neurosci. 25 (35), 8000–8009.

Maleszewska, M., Steranka, A., Smiech, M., Kaza, B., Pilanc, P., Dabrowski, M., Kaminska, B., 2021. Sequential changes in histone modifications shape transcriptional responses underlying microglia polarization by glioma. GLIA 69 (1), 109–123.

Schaafsma, W., Zhang, X., van Zomeren, K.C., Jacobs, S., Georgieva, P.B., Wolf, S.A., Kettenmann, H., Janova, H., Saiepour, N., Hanisch, U.-K., Meerlo, P., van den Elsen, P.J., Brouwer, N., Boddeke, H.W.G.M., Eggen, B.J.L., 2015. Long-lasting pro-inflammatory suppression of microglia by LPS-preconditioning is mediated by RelB-dependent epigenetic silencing. Brain Behav. Immun. 48, 205–221.

Cao, M., Cortes, M., Moore, C.S., Leong, S.Y., Durosier, L.D., Burns, P., Fecteau, G., Desrochers, A., Auer, R.N., Barreiro, L.B., Antel, J.P., Frasch, M.G., 2015. Fetal microglial phenotype in vitro carries memory of prior in vivo exposure to inflammation. Front. Cell. Neurosci. 9 https://doi.org/10.3389/fncel.2015.00294.

Martins-Ferreira, R., Leal, B., Costa, P.P., Ballestar, E., 2021. Microglial innate memory and epigenetic reprogramming in neurological disorders. Prog. Neurobiol. 200, 101971. https://doi.org/10.1016/j.pneurobio.2020.101971.

Klapper, W., Shin, T., Mattson, M.P., 2001. Differential regulation of telomerase activity and TERT expression during brain development in mice. J. Neurosci. Res. 64 (3), 252–260.

S. Ferrón H. Mira S. Franco Marifé Cano-Jaimez E. Bellmunt C. Ramírez I. Fariñas M.A. Blasco Telomere shortening and chromosomal instability abrogates proliferation of adult but not embryonic neural stem cells 131 16 2004 4059 4070.

Zang, J., Liu, Y., Li, W., Xiao, D.i., Zhang, Y., Luo, Y., Liang, W., Liu, F., Wei, W., 2017. Voluntary exercise increases adult hippocampal neurogenesis by increasing GSK-3β activity in mice. Neuroscience 354, 122–135.

Fabel, K., Kempermann, G., 2008. Physical activity and the regulation of neurogenesis in the adult and aging brain. NeuroMol. Med. 10 (2), 59–66.

Palmos, A.B., Duarte, R.R.R., Smeeth, D.M., Hedges, E.C., Nixon, D.F., Thuret, S., Powell, T.R., 2020. Telomere length and human hippocampal neurogenesis. Neuropsychopharmacology 45 (13), 2239–2247.

Palmos, A.B., Breen, G., Goodwin, L., Frissa, S., Hatch, S.L., Hotopf, M., Thuret, S., Lewis, C.M., Powell, T.R., 2018. Genetic risk for psychiatric disorders and telomere length. Front. Genet. 9 https://doi.org/10.3389/fgene.2018.0046810.3389/fgene.2018.00468.s00110.3389/fgene.2018.00468.s002.

Mueller, F.S., Richetto, J., Hayes, L.N., Zambon, A., Pollak, D.D., Sawa, A., Meyer, U., Weber-Stadlbauer, U., 2019. Influence of poly(I:C) variability on thermoregulation, immune responses and pregnancy outcomes in mouse models of maternal immune activation. Brain Behav. Immun. 80, 406–418.

Smolders, S., Notter, T., Smolders, S.M.T., Rigo, J.-M., Brône, B., 2018. Controversies and prospects about microglia in maternal immune activation models for neurodevelopmental disorders. Brain Behav. Immun. 73, 51–65.
Kowash, H.M., Potter, H.G., Edye, M.E., Prinssen, E.P., Bandinelli, S., Neill, J.C., Hager, R., Glazier, J.D., 2019. Poly(I:C) source, molecular weight and endotoxin contamination affect dam and prenatal outcomes, implications for models of maternal immune activation. Brain Behav. Immun. 82, 160–166.
Kentner, A.C., Bilbo, S.D., Brown, A.S., Hsiao, E.Y., McAllister, A.K., Meyer, U., Pearce, B. D., Pletnikov, M.V., Yolken, R.H., Bauman, M.D., 2019. Maternal immune activation: reporting guidelines to improve the rigor, reproducibility, and transparency of the model. Neuropsychopharmacology 44 (2), 245–258.
Yokoyama, K.D., Zhang, Y., Ma, J., Zhong, S., 2014. Tracing the Evolution of Lineage-Specific Transcription Factor Binding Sites in a Birth-Death Framework. PLoS Comput. Biol. 10 (8).
Rockowitz, S., Zheng, D., 2015. Significant expansion of the REST/NRSF cistrome in human versus mouse embryonic stem cells: Potential implications for neural development. Nucleic Acids Res. 43 (12), 5730–5743.
Lee, H., et al., 2021. The Effects of Genotype on Inflammatory Response in Hippocampal Progenitor Cells: A Computational Approach. Brain, Behavior, & Immunity - Health 15, 100286.
Yu, D., Di Giorgio, F., Yao, J., Marchetto, M., Brennand, K., Wright, R., Mei, A., Mchenry, L., Lisuk, D., Grasmick, J., Silberman, P., Silberman, G., Jappelli, R., Gage, F., 2014. Modeling hippocampal neurogenesis using human pluripotent stem cells. Stem Cell Rep. 2 (3), 295–310.
Hoffman, G.E., Schrode, N., Flaherty, E., Brennand, K.J., 2019. New considerations for hiPSC-based models of neuropsychiatric disorders. Mol. Psychiatry 24 (1), 49–66.
O'Donovan, M.C., Owen, M.J., 2016. The implications of the shared genetics of psychiatric disorders. Nat. Med. 22 (11), 1214–1219.
Perrera, V., Martello, G., 2019. How does reprogramming to pluripotency affect genomic imprinting? Front. Cell Dev. Biol. 7, 76.
Su, C., Argenziano, M., Lu, S., Pippin, J.A., Pahl, M.C., Leonard, M.E., Cousminer, D.L., Johnson, M.E., Lasconi, C., Wells, A.D., Chesi, A., Grant, S.F.A., 2021. 3D promoter architecture re-organization during iPSC-derived neuronal cell differentiation implicates target genes for neurodevelopmental disorders. Prog. Neurobiol. 201, 102000. https://doi.org/10.1016/j.pneurobio.2021.102000.
Bachmann, S., Linde, J., Bell, M., Spehr, M., Zempel, H., Zimmer-Bensch, G., 2021. DNA methyltransferase 1 (Dnmt1) shapes neuronal activity of human ipsc-derived glutamatergic cortical neurons. Int. J. Mol. Sci. 22 (4), 2034. https://doi.org/10.3390/ijms22042034.
de Boni, L., et al., 2018. DNA methylation alterations in iPSC- and hESC-derived neurons: Potential implications for neurological disease modeling. Clinical Epigenetics 10, 1–13.
Pomeshchik, Y., Klementieva, O., Gil, J., Martinsson, I., Hansen, M.G., de Vries, T., Sancho-Balsells, A., Russ, K., Savchenko, E., Collin, A., Vaz, A.R., Bagnoli, S., Nacmias, B., Rampon, C., Sorbi, S., Brites, D., Marko-Varga, G., Kokaia, Z., Rezeli, M., Gouras, G.K., Roybon, L., 2020. Human iPSC-Derived Hippocampal Spheroids: An Innovative Tool for Stratifying Alzheimer Disease Patient-Specific Cellular Phenotypes and Developing Therapies. Stem Cell Rep. 15 (1), 256–273.
Sarkar, A., et al., 2018. Efficient Generation of CA3 Neurons from Human Pluripotent Stem Cells Enables Modeling of Hippocampal Connectivity In Vitro. Cell Stem Cell 22, 684–697.e9.
Warre-Cornish, K., Perfect, L., Nagy, R., Duarte, R.R.R., Reid, M.J., Raval, P., Mueller, A., Evans, A.L., Couch, A., Ghevaert, C., McAlonan, G., Loth, E., Murphy, D., Powell, T. R., Vernon, A.C., Srivastava, D.P., Price, J., 2020. Interferon-γ signaling in human iPSC–derived neurons recapitulates neurodevelopmental disorder phenotypes. Sci. Adv. 6 (34), eaay9506. https://doi.org/10.1126/sciadv.aay9506.
Schafer, S.T., Paquola, A.C.M., Stern, S., Gosselin, D., Ku, M., Pena, M., Kuret, T.J.M., Liyanage, M., Mansour, A.A., Jaeger, B.N., Marchetto, M.C., Glass, C.K., Mertens, J., Gage, F.H., 2019. Pathological priming causes developmental gene network heterochronicity in autistic subject-derived neurons. Nat. Neurosci. 22 (2), 243–255.
Hedegaard, A., Stodolak, S., James, W.S., Cowley, S.A., 2020. Honing the Double-Edged Sword: Improving Human iPSC-Microglia Models. Front. Immunol. 11.
Pellegrini, L., Bonfio, C., Chadwick, J., Begum, F., Skehel, M., Lancaster, M.A., 2020. Human CNS barrier-forming organoids with cerebrospinal fluid production. Science 369 (6500), eaaz5626. https://doi.org/10.1126/science:aaz5626.
Mertens, J., Reid, D., Lau, S., Kim, Y., Gage, F.H., 2018. Aging in a dish: IPSC-derived and directly induced neurons for studying brain aging and age-related neurodegenerative diseases. Annu. Rev. Genet. 52 (1), 271–293.
Liang, K.X., et al., 2020. Disease-specific phenotypes in iPSC -derived neural stem cells with POLG mutations. EMBO Mol. Med. 12, e12146.
Miller, J., Ganat, Y., Kishinevsky, S., Bowman, R., Liu, B., Tu, E., Mandal, P.K., Vera, E., Shim, J.-W., Kriks, S., Taldone, T., Fusaki, N., Tomishima, M., Krainc, D., Milner, T., Rossi, D., Studer, L., 2013. Human iPSC-based modeling of late-onset disease via progerin-induced aging. Cell Stem Cell 13 (6), 691–705.
Cozzi, A., Orellana, D.I., Santambrogio, P., Rubio, A., Cancellieri, C., Giannelli, S., Ripamonti, M., Taverna, S., Di Lullo, G., Rovida, E., Ferrari, M., Forni, G.L., Fiorillo, C., Broccoli, V., Levi, S., 2019. Stem Cell Modeling of Neuroferritinopathy Reveals Iron as a Determinant of Senescence and Ferroptosis during Neuronal Aging. Stem Cell Rep. 13 (5), 832–846.
Vera, E., Bosco, N., Studer, L., 2016. Generating Late-Onset Human iPSC-Based Disease Models by Inducing Neuronal Age-Related Phenotypes through Telomerase Manipulation. Cell Reports 17 (4), 1184–1192.
Schneider, L., Zheng, J.C., 2014. Survival of neural stem cells undergoing DNA damage-induced astrocytic differentiation in self-renewal-promoting conditions in vitro. PLoS ONE 9 (1), e87228. https://doi.org/10.1371/journal.pone.008722810.1371/journal.pone.0087228.g00110.1371/journal.pone.0087228.g00210.1371/journal.pone.0087228.g003.
Schneider, L., Pellegatta, S., Favaro, R., Pisati, F., Roncaglia, P., Testa, G., Nicolis, S., Finocchiaro, G., d'Adda di Fagagna, F., 2013. DNA damage in mammalian neural stem cells leads to astrocytic differentiation mediated by BMP2 signaling through JAK-STAT. Stem Cell Rep. 1 (2), 123–138.
Carlessi, L., De Filippis, L., Lecis, D., Vescovi, A., Delia, D., 2009. DNA-damage response, survival and differentiation in vitro of a human neural stem cell line in relation to ATM expression. Cell Death Differ. 16 (6), 795–806.
Zhu, L., Sun, C., Ren, J., Wang, G., Ma, R., Sun, L., Yang, D., Gao, S., Ning, K.e., Wang, Z., Chen, X.u., Chen, S., Zhu, H., Gao, Z., Xu, J., 2019. Stress-induced precocious aging in PD-patient iPSC-derived NSCs may underlie the pathophysiology of Parkinson's disease. Cell Death Dis. 10 (2) https://doi.org/10.1038/s41419-019-1313-y.
Limbad, C. et al. Astrocyte senescence promotes glutamate toxicity in cortical neurons. Plos One 15, e0227887 (2020).
Dong, C. M. et al. A stress-induced cellular aging model with postnatal neural stem cells. Cell Death and Disease 5, e1116–e1116 (2014).
Daniele, S., Da Pozzo, E., Iofrida, C., Martini, C., 2016. Human Neural Stem Cell Aging Is Counteracted by α-Glycerylphosphorylethanolamine. ACS Chem. Neurosci. 7 (7), 952–963.
de Lucia, C., Murphy, T., Steves, C.J., Dobson, R.J.B., Proitsi, P., Thuret, S., 2020. Lifestyle mediates the role of nutrient-sensing pathways in cognitive aging: cellular and epidemiological evidence. Communications Biology 3 (1). https://doi.org/10.1038/s42003-020-0844-1.
Liu, G.-H., Ding, Z., Izpisua Belmonte, J.C., 2012. IPSC technology to study human aging and aging-related disorders. Curr. Opin. Cell Biol. 24 (6), 765–774.
Han, M.J., Lee, W.J., Choi, J., Hong, Y.J., Uhm, S.J., Choi, Y., Do, J.T., 2021. Inhibition of neural stem cell aging through the transient induction of reprogramming factors. J. Comp. Neurol. 529 (3), 595–604.
Daniele, S., Mangano, G., Durando, L., Ragni, L., Martini, C., 2020. The Nootropic Drug A-Glyceryl-Phosphoryl-Ethanolamine Exerts Neuroprotective Effects in Human Hippocampal Cells. Int. J. Mol. Sci. 21.
Bigagli, E. et al. Long-term neuroglial cocultures as a brain aging model: Hallmarks of senescence, microRNA expression profiles, and comparison with in vivo models. Journals of Gerontology - Series A Biological Sciences and Medical Sciences 71, 50–60 (2016).

"IF GOD HAD CONSULTED ME BEFORE EMBARKING ON THE CREATION, I WOULD HAVE SUGGESTED SOMETHING SIMPLER."

— ALFONSO X OF CASTILE